SAPIENZA
UNIVERSITÀ DI ROMA

Ph.D. in Environmental Engineering
Cycle XXIX

Department of Civil, Building and Environmental Engineering
Sapienza University of Rome

INNOVATIVE METHODOLOGY FOR QUANTITATIVE AND QUALITATIVE ASSESSMENT OF WATER RESOURCES IN KARST AQUIFERS: A CASE STUDY IN SOUTHERN LATIUM REGION, CENTRAL ITALY

Doctoral Dissertation of:
Flavia Ferranti

Tutor:
Prof. Giuseppe Sappa

Chair of the Doctoral Program:
Prof. Maria Rosaria Boni

September 2017

TABLE OF CONTENTS

LIST OF TABLES

LIST OF FIGURES

ABSTRACT

This paper outlines the results of a hydrogeological study carried on from July 2014 to November 2106 to assess quantitatively and qualitatively water resources (groundwater and surface water) emerging in the Upper Valley of the Aniene River (Latium Region, Central Italy). This work deals with the Environmental Monitoring Plan, related to the catchment project of the Pertuso Spring, which is going to be exploited to supply an important water network in the South part of Roma district. The study area is located in the Upper Valley of the Aniene River, in the outcrop of Triassic-Cenozoic carbonate rocks, and belong to an important karst aquifer. Pertuso Spring is the main outlet of this karst aquifer and is the one of the most important water resource in the southeast part of Latium Region, used for drinking, agriculture and hydroelectric supplies. This hydrogeological system is characterized by a strong local hydraulic connectivity between the Aniene River surface water and groundwater coming from the Pertuso Spring.

First at all, in this study, in order to estimate the vulnerability degree of the karst aquifer feeding the Pertuso Spring, the COP method has been applied and vulnerability maps are proposed. Thus, with the aim of highlighting the karst features key-role in the unsaturated zone, a new vulnerability approach has been set up, starting from two discretization approaches. The aim of this work is to compare both results of the intrinsic vulnerability mapping, in order to evaluate which one is the most suitable for the study area.

On the basis of the hydrogeochemical data and their interpretations for groundwater and surface water, monitored from July 2014 to November 2016, a hydrogeological study has been carried on to identify flowpaths and hydrogeochemical processes governing groundwater-surface water interactions in this region. To this end, discharge surveys were carried out on four monitoring sections along the Aniene River. The proposed conceptual model shows that the karst aquifer feeding the Pertuso Spring supplies the Aniene River, highlighting seasonal variability depending on the rainfall regime.

The analysis of solute contents in the monitoring points has suggested the identification of the Magnesium ion as a conservative tracer in this specific system and, consequently, to the development an indirect method for the evaluation of karst spring discharge based on discharge measurements and water geochemical data. This method is based on the elaboration of surface water discharge measurements in relationship with Mg^{2+} concentration values, determined as for groundwater, coming

from the Pertuso Spring, as for surface water samples, collected upstream and downstream the spring, along the Aniene River streamflow. This method has been validated by the comparison with discharge values obtained using the current meter method and by geochemical data.

This study suggests that the application of the Magnesium ion as an environmental tracer may provide a means to evaluate discharge of the Pertuso Spring, as it came up to be a marker of the mixing of surface water and groundwater. On the other hand, the Magnesium ion concentration provides information for the identification of groundwater flow systems and the main hydrogeochemical processes affecting the composition of water within the karst aquifer feeding the Pertuso Spring.

CHAPTER 1

INTRODUCTION

1.1 Overview

Water resources management is one of the most important challenges worldwide because water represents a vital resource for sustaining life and environment.

The latest United Nations World Water Development Report [1] outlines how the various global crises reported recently, in climate change, energy, food and economic recession, are related to each other and have impacts on water. In fact, although water is the most widely occurring substance on Earth, only 2.53% is freshwater while the remainder is saltwater. Some 2/3 of this freshwater is locked up in glaciers and permanent snow cover. In addition to the accessible freshwater in lakes, rivers and aquifers, man-made storage in reservoirs adds a further 8,000 km^3 [2]. We withdraw 8% of the total annual renewable freshwater, and appropriate 26% of annual evapotranspiration and 54% of accessible runoff [2].

Water resources are generally renewable, with great differences in availability from part to part in the world and wide variations in seasonal and annual precipitation in many places. Globally, water demand is expected to increase significantly over the coming decades. Accelerated urbanization and the expansion of municipal water supply and sanitation systems also contribute to the rising demand [3]. With better lifestyle, population is growing and per capita use is increasing. Together with spatial and temporal variations in available water, the consequence is that water for all our uses is becoming scarce and leading to a water crisis [4].

Climate change scenarios project an exacerbation of the spatial and temporal variations of water cycle dynamics, such that discrepancies between water supply and demand are becoming increasingly huge [3]. Last estimations suggest that climate change will account for about 20% of the increase in global water scarcity [2].

The availability of water resources is also intrinsically linked to water quality, as the pollution of water sources does not allow different types of uses. Increased discharges of untreated sewage, combined with agricultural runoff and inadequately treated wastewater from industry, have resulted in the degradation of water quality around the world. If current trends persist, water quality will continue to degrade over the coming decades, particularly in water resource-poor countries in arid areas, further endangering human health and ecosystems, contributing to water scarcity and constraining sustainable economic development [1].

Water is also an essential part of any ecosystem: water quantity and quality decreasing, both have serious negative impacts on ecosystems [2]. Thus, water resources assessment is an important tool to evaluate groundwater dynamics in the aim of maintaining high-quality water, in the framework of climate change effects [5].

Karst aquifers constitute more than 30 % of the EU land mass [6] and these groundwater resources are the most important source of water supply for worldwide, providing about the 25% of freshwater [7]. Most of part of groundwater in the southeast part of Latium Region, as in the whole Apennine Mountains chain is stored in karst aquifers [8]. The increasing of anthropogenic activities and the impacts of climate change are identified to be responsible of karst groundwater depletion [3,9].

Karst aquifers have complex and peculiar properties, which make them very different from other aquifers: high heterogeneity of the rock matrix, large voids, high flow velocities (up to several hundreds of m/h), and high flow rate springs (up to some tens of m^3/s) [10]. These aquifers are characterized by a heterogeneous distribution of permeability due to conduits and voids developed by the dissolution of carbonate rocks, frequently embedded in a less permeable fractured rock matrix [11]. Flow velocities into a well-developed karst system are extremely fast and contaminants can reach quickly the saturated zone [12]. Thus, groundwater exploitation in karst aquifers asks special management strategies to prevent their quality and quantity depletion and to support decision-making for water resources management [6].

The interest of researchers for better understanding the groundwater origin, the subsurface processes, and the factors controlling the residence time has gradually increased, and the investigation techniques evolved continuously [13], in the aim of better protecting these resources.

1.2 Study aims and objectives

This paper deals with the results of a hydrogeological study related to the activities of the Environmental Monitoring Plan of the Pertuso Spring, in the Upper Valley of the Aniene River (Central Italy), carry out from July 2014 to November 2016.

This complex hydrogeological system is characterized, on the one hand, by a well-developed karst network and, on the other hand, by a strong local hydraulic connectivity between groundwater and Aniene River surface water. This system receives localized inputs from karst features, responsible of the fast rainfall infiltration in the saturated zone and, consequently, of the high discharge rate of the Pertuso Spring. The water flow velocities into this well-developed karst system can be extremely fast and contaminants can quickly reach the saturated zone. For this reason, with the aim of highlighting the karst features key-role in the unsaturated zone, in this work, the vulnerability of karst aquifer feeding the Pertuso Spring was evaluated applying COP method, which focuses on the key role of karst features, responsible of the aquifer natural protection decreasing to pollution. With the aim of highlighting the presence of karst features, COP method was applied starting from two different discretization approaches of the hydrogeological basin: polygonal layers and Finite Square Elements (FSE). The polygonal layers are the result of an overlapping of two layers: the first one consists of the direct recharge area, related to the presence of karst features responsible of rainfall fast infiltration in the saturated zone, the second one coincides with the geology outcropping in the hydrogeological basin. The intrinsic vulnerability maps, produced using a GIS approach, were compared with those obtained using traditional vulnerability grid map discretization.

The strong local hydraulic connectivity between the Aniene River and the karst aquifer influences, directly and indirectly, the aquifer water budget and the chemical characteristics of groundwater and surface water. For this reason, an integrated approach based on the streamflow measurements and geochemical modeling, applied to groundwater and surface water, was carried on, with the aim of developing a conceptual model of aquifer-river interaction and achieving proper management and protection of this important hydrogeological system. Discharge surveys were carried out on four monitoring sections along the Aniene River by using the conventional current method. In one appropriate river section, the discharge measurement with salt dilution method was tested. These results were validated by the discharge values obtained with the current meter method, in the aim of defining a reliable methodology for discharge evaluation in mountain streams, where turbulent flows make difficult apply the conventional current meter method.

In this paper, it was applied the potentiality of Magnesium as a natural tracer in the karst system feeding the Pertuso Spring, to support a conceptual model for karst spring discharge evaluation. This method is based on the elaboration of surface water discharge measurements in relationship with Mg^{2+} concentration values, determined as for groundwater, coming from the Pertuso Spring, as for surface water samples, collected upstream and downstream the spring, along the Aniene River streamflow. This method was validated by the comparison with discharge values obtained using the current meter method and by geochemical data.

The purpose of this study is threefold. First, to evaluate the vulnerability degree of the karst aquifer feeding the Pertuso Spring using method using COP method, to improve sustainable management and protection of these water resources. Second, based on the results of the Environmental Monitoring, to define a hydrogeological framework that allows inferring the conceptual model of this karst aquifer. Third, to set up an inverse model, which allowed the evaluation of the Pertuso Spring discharge, using a combined approach based on discharge measurements and hydrogeochemical data.

1.3 Thesis outline

This thesis is presented in 9 chapters. The current chapter (Chapter 1) provides a general introduction and aims of the study. It also reviews aspects of water resources sustainable management and protection. In Chapter 2, an overview of the principal European and Italian environmental legislation about water resources and in particular concerning the Environmental Monitoring is given. Chapter 3 looks at the geological and hydrogeological setting of the study area. Chapter 4 reports a comparative evaluation of vulnerability assessment referred to the karst aquifer feeding the Pertuso Spring, through the COP method application and starting from two discretization approaches. Chapter 5 elaborates on the methodology employed in the study. Chapter 6 focus on the discussion of the environmental data obtained in the first three year of the Environmental Monitoring Plan of the Pertuso Spring. Chapters 7 deals with the results of the application in the study area of an inverse model, which allows estimation of groundwater flow coming out from the Pertuso Spring, starting from Aniene River discharge measurements and geochemical water characterization. Chapter 8 look at the remote monitoring system, which has been developed to monitor, and manages groundwater coming from the Pertuso Spring. Chapter 9 provides a conclusive discussion.

CHAPTER 2

ENVIRONMENTAL MONITORING REGULATORY REQUIREMENTS

2.1 Introduction

The present chapter deals with the design of a multi-disciplinary monitoring plan related to the catchment project of the Pertuso Spring, in the context of the "*Environmental Monitoring Plan in ante-operam phase according with the Environmental Impact Assessment process requirements, related to the realization of the catchment project from the Pertuso Spring to the Ceraso booster plant*".

According to the Legislative Decree 152/2006, as modified by D.M. 260/2010, any infrastructure design should take in consideration an Environmental Monitoring Plan (EMP) for the hydrogeological settings of the study area. Thus, the Environmental Monitoring combined with a hydrogeological characterization of the study area provides to evaluate the potential adverse environmental impacts due to the catchment works.

Rogedil Servizi S.r.l developed the Environmental Monitoring Plan, in 2009, according to the design project, following an analysis of the relevant environmental impacts related to the catchment project of the Pertuso Spring. According to the EMP, the environmental components for which environmental monitoring was required are:

- groundwater
- Aniene River surface water
- Aniene River ecosystem

The Environmental Monitoring Plan was structured in:

- Supervisory Monitoring (Ante Operam Monitoring), to define the initial level reference to which the results of the measurements in progress have to be compared.
- Operating Monitoring, to evaluate and measure the potential negative impact of work operations and assess the effectiveness of remedial measures.
- Survey Monitoring, to ensure adherence to regulatory and permit limits.

On 23/04/2014, Acea Ato2 S.p.A has commissioned the Environmental Monitoring to the Department of Civil, Building and Environmental Engineering (DICEA) of Sapienza University of Rome. The target of this part of the Environmental Monitoring Plan was to set up the background framework on the hydromorphological, physico-chemical and biological properties of water resources in the water basin influenced by any potential environmental impact due to the construction activities.

2.2 Water Framework Directive (2000/60/EC)

At now, the most important contribution of European water legislation is the Water Framework Directive 2000/60/EC (WFD). The European Union, by this directive, identifies the need to create a legal framework for sustainability and protection of all waters (surface water, groundwater, inland waters, transitional waters and coastal waters) and sets out specific objectives that must be achieved by specified dates. The Water Framework Directive aims to prevent further deterioration, to protect and to enhance all water resources and to sustain the natural ecosystems that depend on them.

The main purposes of the WFD are:

- the achievement of good status for all water bodies by 2015, and, if this is not possible, aim to achieve good status by 2021 or 2027;
- the sustainable use of all water resources throughout Europe.

To ensure the achievement of these targets and the application of the directive in all Member States and across borders, implementation is planned cyclically in a three-step process. The first step includes the preliminary characterization of water bodies, based upon existing geographical, hydrological and quality data. This activity drives to the identification of water bodies that are "at risk" (significant alteration in the ecological quality as a result of human pressures), "possibly at risk" (lack of sufficient information to decide or moderate alteration) and "not at risk" (no or slight alteration). This first assessment also includes economic analysis. The second step is to design the WFD compatible monitoring network. Based on the results of monitoring, the water body characterization might be refined, and the status assessment carried out by considering both biological and chemical quality elements. This should be carried out in order to classify the status of the water body as required by the Water Framework Directive. Finally, River Basin Management Plans should be drafted for all River Basins including specific programmes of measures. Before Management Plans are finalised and reported to the Commission, river basin authorities have to make sure that plans are presented and discussed openly with the public.

The most important target of the Water Framework Directive is the achievement of good status within 2015. Good status means good ecological status for surface waters up to one nautical mile from the coast; good chemical status for all territorial waters, good chemical and good quantitative status for groundwater and good ecological potential for heavily modified water bodies.

How "good ecological status" is defined is set out in Annex V of the WFD. Possible "high", "good" and "moderate" status for the various quality elements are listed here. Quality elements include:

- Biological elements, e.g. the composition and abundance of certain water plants (aquatic flora) or animals (benthic invertebrate fauna).
- Hydromorphological elements, e.g. quantity and dynamics of water flow, river continuity or morphological conditions like structure of the riparian zone.
- Chemical and physico-chemical elements supporting the biological elements, e.g. nutrient conditions (concentration of nitrogen and phosphorus), acidification status and pollution by hazardous substances.

In addition to the achievement of good status, the following objectives have also been set:

- No deterioration of status for surface and groundwater, and the protection, enhancement and restoration of all water bodies.

- Progressive reduction of pollution of priority substances and phase-out of priority hazardous substances in surface waters as well as the prevention and limitation of input of pollutants in groundwater.
- Reversal of any significant, upward trend of pollutants in groundwater.
- Achievement of standards and objectives set for protected areas in Community legislation.

The Water Framework Directive also applies to heavily modified and artificial water bodies. For these water categories, "specific objectives" are set. By 2015, only "good ecological potential" has to be achieved. The WFD also sets very strict criteria for the designation of these artificial or heavily modified water bodies.

The environmental objectives and the circumstances in which countries are allowed to deviate are set out in Article 4 of the Water Framework Directive. Exemptions are an integral part of the environmental objectives of the WFD. They give Member States the chance to deviate from the "good status" objective: these deviations range for small scale temporary exemptions like the extension of the deadline of 2015 to mid and long term deviations from the rule of "good status by 2015".

Parts of the WFD dealing with groundwater cover a number of different steps for achieving good quantitative and chemical status of groundwater by 2015. They ask Member States to:

- Define groundwater bodies within river basin districts to be designated and reported to the European Commission by Member States. They must classify them by analysing the pressures and impacts of human activity on the quality of groundwater, with a view to identifying groundwater bodies presenting a risk of not achieving WFD environmental objectives. Member States have been expected to carry out this classification between 2004 and 2005 and report the results back to the European Commission.
- Establish registers of protected areas within each river basin districts for those groundwater areas or habitats and species are directly dependent on water. These registers must include all bodies of water used for drinking water and all protected areas covered under the following directives: the Bathing Water Directive 76/160/EEC, the Nitrates Directive 91/676/EEC, the Urban Wastewater Directive 91/271/EEC, as well as areas identified for the protection of habitats and species including relevant Natura 2000 sites, designated under Directives 92/43/EEC and 79/409/EEC. Registers shall be reviewed under the River Basin Management Plan updates.
- Establish groundwater monitoring networks based on the results of the classification analysis so as to provide a comprehensive overview of groundwater chemical and quantitative status. Member States are also obliged to design a monitoring programme that had to be operational by the end of 2006.
- Set up a river basin management plan (RBMP) for each river basin district, which must include a summary of pressures and impacts of human activity on groundwater status, a presentation in map form of monitoring results, a summary of the economic analysis of water use, a summary of protection programmes, control or remediation measures etc. The updated RBMPs were due by the end of 2015 and their review is expected every six years thereafter.
- Take into account by 2010 the principle of recovery of costs for water services, including environmental and resource costs according to the polluter pays principle.
- Establish by the end of 2009 a programme of measures for achieving WFD environmental objectives (e.g. abstraction control, prevent or control pollution measures) that would be operational by the end of 2012. Basic measures include, in particular, controls of groundwater

extraction, controls of artificial recharge or augmentation of groundwater bodies (providing that it does not compromise the achievement of environmental objectives). Point source discharges and diffuse sources liable to cause pollution are also regulated under the basic measures. Direct discharges of pollutants into groundwater are prohibited subject to a range of provisions listed in the Article 11. The programme of measures has to be reviewed and if necessary updated by 2015 and every six years thereafter.

2.3 Groundwater Directive (2006/118/EC)

The Groundwater Directive 2006/118/EC sets groundwater quality standards and introduces measures to prevent or to limit inputs of pollutants into groundwater. The directive establishes quality criteria that takes in account local characteristics and allows further improvements to be made based on monitoring data and new scientific knowledge. The directive, thus, represents a proportionate and scientifically sound response to the requirements of the Water Framework Directive as it relates to assessments on chemical status of groundwater and the identification and reversal of significant and sustained upward trends in pollutant concentrations.

The Groundwater Directive requires:

- groundwater quality standards to be established by the end of 2008;
- pollution trend studies to be carried out by using existing data and data which is mandatory by the WFD (referred to as “baseline level” data obtained in 2007-2008);
- pollution trends to be reversed so that environmental objectives are achieved by 2015 by using the measures set out in the WFD;
- measures to prevent or limit inputs of pollutants into groundwater to be operational so that WFD environmental objectives can be achieved by 2015;
- reviews of technical provisions of the directive to be carried out in 2013 and every six years thereafter;
- compliance with good chemical status criteria (based on EU standards of nitrates and pesticides and on threshold values established by Member States).

Annexes I and II of the Groundwater Directive 2006/118/EC were reviewed in 2013 and are reflected under the Commission Directive 2014/80/EU of 20 June 2014. The review process included a call for evidence (to obtain information, studies and scientific reports among others) and a public consultation process.

2.4 Overview on the Environmental Monitoring

Most of European countries have water quality monitoring programmes for groundwater, rivers and lakes, where water quality is measured on a regular basis. Within the EU, water quality monitoring is currently being strengthened by the implementation of the Water Framework Directive.

The objective of water quality monitoring is to obtain quantitative information on the physical, chemical and biological characteristics of water via statistical sampling. The type of information investigated depends on the objectives and purposes of the monitoring programme, such as detection of drinking water standard violations or assessment of water quality trends.

The monitoring network is described by the water bodies (i.e. springs, brooks, streams, rivers, river systems, ponds, lakes, reservoirs, fjords, estuaries, coastal area, or open marine water) and the geographical area (e.g. country, river basin, etc.) it covers.

Two types of networks can be identified:

- an extensive network involving many sampling sites, few annual samples, analyses of a few determinants, and only one or few years of sampling;
- an intensive network including sampling sites with detailed investigation, many annual samples or measurement of substantial numbers of determinants, and many years of observations.

The number of parameters, which describe water quality, is continuously increasing. Moreover, parameters are constantly being modified, following the expanding uses to which water is withdrawn and according to the development of new technologies for measuring more substances at ever lower concentrations.

For many decades river basin management and water pollution control have relied on summary parameters, such as Biochemical Oxygen Demand (BOD) and Chemical Oxygen Demand (COD), to quantify sewage discharge and oxygen problems in rivers. For human consumption and public water supply, a set of microbiological indicator organisms (e.g. faecal coliform bacteria) have been identified and their enumeration is now commonly applied to determine the hygienic suitability for drinking water.

Parameters can be grouped into the following categories:

- Basic parameters (e.g. water temperature, pH, electrical conductivity, dissolved oxygen, and discharge, used for a general characterization of water quality).
- Suspended particulate matter (e.g. suspended solids, turbidity and TOC, BOD and COD.
- Indicators of pollution with oxygen consuming substances (e.g. dissolved oxygen, BOD, COD and ammonium).
- Indicators of pollution with nutrients and eutrophication effects (e.g. nitrogen and phosphorus, and various biological effect variables).
- Indicators of acidification (e.g. pH, alkalinity, electrical conductivity, sulphate, nitrate, aluminium, phytoplankton and diatom sampling).
- Specific major ions (e.g. chloride, sulphate, sodium, potassium, calcium and magnesium).
- Metals (e.g. cadmium, mercury, copper and zinc).
- Organic micro-pollutants (e.g. pesticides and the numerous chemical substances used in industrial processes, products and households).
- Indicators of radioactivity (e.g. total alpha and beta activity, ^{137}Cs, ^{90}Sr).
- Microbiological indicator organisms (e.g. total coliforms, faecal coliforms and faecal streptococci bacteria).
- Biological indicators of the ecological quality (e.g. phytoplankton, zooplankton, zoobenthos, fish and macrophytes).

The sampling frequency differs substantially depending on the purpose of the monitoring programme and the measured parameters. Generally, frequent samples are taken when the purpose of the monitoring programme is to observe trends. In cases where programmes aim to assess the general state of the water bodies, monitoring is based on low sampling frequency. Some monitoring programmes include continuous registration of a selection of parameters.

Investigation of ecological quality elements, such as macro-invertebrates in rivers, is usually based on a few annual samples. A large proportion of the costs of operating a monitoring programme are directly related to the sampling frequency.

2.5 Water Framework Directive and monitoring

Article 8 of the Water Framework Directive sets out the requirements for the monitoring of surface water status, groundwater status and protected areas: "*Monitoring programmes are required to establish a coherent and comprehensive overview of water status within each river basin district*".

The objective of monitoring is to establish an overview within each River Basin District.
Monitoring information requirements should include:

- Classification status of surface water.
- Chemical status of all groundwater bodies or groups of bodies determined to be at risk.
- Reliable assessment of quantitative status of all groundwater bodies or groups of bodies.
- Estimates of the direction and rate of flow in groundwater bodies that cross Member States boundaries. This should be used in the assessment of long-term trends, both as a result of changes in natural conditions and through anthropogenic activity.
- Estimates of pollutant loads transferred across international boundaries or discharged into seas.
- Assessments of changes in status of water bodies.
- Causes of water bodies failing to achieve environmental objectives.
- The magnitude and impacts of accidental pollution.
- Compliance assessments with the standards and objectives of Protected Areas.
- A quantification of reference conditions (where they exist) for surface water bodies.

Three types of monitoring for surface waters are described in Annex V of the WFD: surveillance, operational and investigative monitoring. In terms of groundwater chemical status, surveillance and operational monitoring are required. For groundwater, a water level monitoring network is required to provide a reliable assessment of the quantitative status of all groundwater bodies or groups of bodies including an assessment of the available groundwater resource.

The directive specifies quality elements for the classification of ecological status that include hydro-morphological, chemical and physico-chemical elements supporting the biological elements.

For surveillance monitoring, parameters indicative of all the biological, hydro-morphological and general as well as specific physico-chemical quality elements must be monitored. For operational monitoring, the parameters used should be those indicative of the biological and hydro-morphological quality elements most sensitive to the pressures to which the body is subject, as well as all priority substances discharged and other substances discharged in significant quantities. For surveillance monitoring of surface waters, Member States must monitor at least for a period of a year for parameters indicative of all biological, hydro-morphological and general physico-chemical quality elements. Those priority list substances discharged into the river basin or sub-basins must be monitored. Other pollutants also need to be monitored, if they are discharged in significant quantities in the river basin or sub-basin.

For operational monitoring of surface waters, Member States are required to monitor those biological and hydro-morphological quality elements most sensitive to the pressures to which the water body is subject.

EU Member States have re-designed over recent years their monitoring programmes, in order to meet the requirements of the WFD. The programmes had to be operational by 22 December 2006 at the latest, and Member States had to report their monitoring programmes to the Commission by 22 March 2007.

2.6 Italian Environmental Monitoring regulatory requirements

Italian law system (D.M. 260/2010), in agreement with the Water Framework Directive, establishes an Environmental Monitoring Plan both for protection and sustainability purposes of water resources. The D.M. 260/2010 identifies three categories of monitoring in the following: (i) Supervisory monitoring, to define the hydrogeological conceptual model of the aquifer; (ii) Operating monitoring, to measure the potential impact that could come out from project operations; (iii) Survey monitoring, to assess the effectiveness of remedial measures. The supervisory monitoring activities allow to carry out the environment characterization of the study area, including the definition of spatial and temporal trends in measured parameters. This monitoring is useful to set up the baseline values for environmental quality and quantity indicators so that long-term changes can be evaluated. The operating monitoring allows the existing physical and chemical characterization, the evaluation of the environmental parameters and the examination of the potential contamination sources due to the catchment project.

The monitoring plan aims to assess the status of water bodies, to check whether the environmental targets are being effectively achieved. This approach was needed to identify the environmental status of groundwater and surface water and to localize where management action is required to achieve the purposes of the WFD. The Environmental Monitoring Plan integrates water policy bridging together, within its framework, the actions that are required by all EU and national water legislation.

2.7 Purpose of the Environmental Monitoring Plan of the Pertuso Spring

Environmental monitoring is required to manage the effectiveness of the mitigation measures and to report to the regulatory authorities. The Environmental Monitoring Plan provides a delivery mechanism to address the negative environmental impacts of a project during its execution, to enhance project benefits, and to introduce standards of good practice to be adopted for all project works.

The EMP of the catchment project of the Pertuso Spring is important as it provides useful information and helps to:

- Define monitoring mechanism and identify monitoring parameters.
- Providing reliable measurements of environmental parameters.
- Collection, reporting and analysis of environmental data.
- Control and prevention of environment pollutions.
- Monitor any significant alteration of the physical, chemical or biological characteristics due to the project activities.
- Start mitigation measures before these changes alter the natural processes and turn it to irreversible processes.
- Evaluate the performance and effectiveness of mitigation measures and suggest improvements, if required.
- Report to the designated institutions

The Environmental Monitoring Plan and main features of the monitoring network will be presented in this study.

CHAPTER 3

GEOLOGICAL AND HYDROGEOLOGICAL SETTING OF THE KARST AQUIFER FEEDING THE PERTUSO SPRING

3.1 Geological and hydrogeological setting of the study area

The Latium region has several springs, under-lake springs and deep water tables. The most important groups of springs are in the outer ring (Upper Valley of the Aniene River and Monti Lucretili area), in the inner ring (Bracciano lake area, Genzano and Pomezia) and in the core (Cecchignola, Grottarossa and Castel Giubileo) [14].

The study area is located along the SW boundary of the Simbruini Mountains, characterized by the confluence of the Fiumata Valley and the Granara Valley from which originates the Aniene River Valley [15].

The lithological sequence outcropping in the Upper Valley of the Aniene River includes the North-West part of the Lower-Middle Miocene Latium-Abruzzi Carbonate Platform [16,17,18,19]. The stratigraphic succession of dolomite, dolomitic limestone and limestone is distributed homogeneously from North to South and from East to West in the Upper Valley of the Aniene River [20].

The bottom of the stratigraphic series (Triassic) is widely spread among Filettino, Aniene River Springs and Faito Plateau. Dolomite is the dominant lithofacies, characterized by white and grey crystalline dolomite, with some breccia levels. Over this geological formation, limestones and dolomites, of Upper Cretaceous age (Sinemurian) are present, and their immersion is concordant with the Triassic dolomite [20]. In fact, the Aniene basin is composed almost entirely of bare Mesozoic, highly fractured, karstified carbonate rocks of the central Apennine range [21].

This area is mostly made of highly permeable Cretaceous carbonate rocks, deeply fractured and mostly soluble. The base of the stratigraphic series is made of Upper Cretaceous carbonates, represented by the alternation of granular limestone and dolomites layers (Fig. 3.1). Above these ones Quaternary fluvial and alluvial deposits lie, downward pudding, and Miocene clay and shale [21,22].

The lithostratigraphy, detected in nearby Subiaco Station, confirms the presence of an extensive karst area, particularly limestones and dolomites (Latium-Abruzzi succession, Upper Triassic-Upper Miocene) [23]. The limestones outcropping in the Upper Valley of the Aniene River are very fractured and mostly soluble; karst erosion has occurred on a large scale on this area, assuming great importance in the modeling of the soil and also of the subsoil.

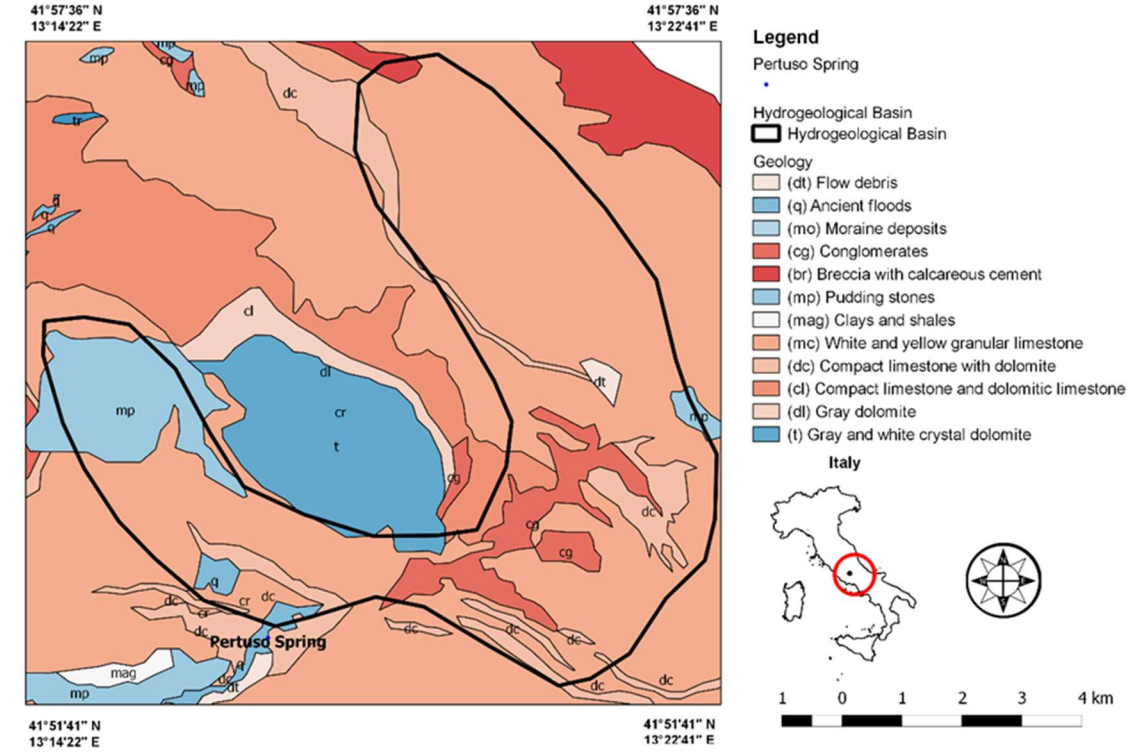

Figure 3.1 Simplified geological map the study area

Due to chemical weathering, distinctive surface and underground karst formations are developed in this area at small and large scales. The surface karst activity led to the formation of a typical karst landscape with rutted fields, sinkholes and flat filled by red soils, while the underground activity has given rise to cavities, ponor and cave systems [19,20]. The karst surface is very permeable and enables the rapid infiltration of rainfall into the underground system, where the carbonate dissolution makes cavities [19,20]. Dissolution conduits strongly influence groundwater flow and evolve into complex networks, often crossing several kilometers throughout the limestone matrix [11,24,25].

Karst aquifers are very much complex systems due to the development of secondary porosity made by the rock dissolution [7]. The presence of large conduits in karst aquifers, which lead to the duality of flow system with rapid flow in the conduit network and relatively slow permeability in the fissured rock matrix [27]. Additionally, may be present a highly weathered layer (epikarst) with higher porosity and permeability beneath the land surface, which divides the autogenic recharge on the saturated zone into diffuse and point infiltration [28].

The hydrogeological framework is therefore closely related to the karst nature of carbonate rocks constituting the reliefs strongly shaped by surface and underground karst activities. The alternation of carbonate rocks, limestone and dolomite, together with the epikarst, made of residual of karst activity, and some marl layers, dating back to the Miocene age, are the main responsible for the hydrogeological setting of this area [22]. Physical and chemical variations, that occur during storm events indicate the complex dynamic processes in the karst aquifer and the role undertaken by the epikarst as perched water reservoir, and by the major conduits that develop through the vadose and saturated zones of the karst system [23].

Thus, the abundance of water is due to the permeability of the limestone, which stores a significant quantity of rainwater feeding perennial springs located in the Upper Valley of the Aniene River, close to the boundary of the carbonate hydrogeological system [29].

Karst springs are many, along the upper part of the Aniene River and they have occurred in the Triassic dolomitic formations (Fig. 3.1). This karst system is characterized by one main outlet, Pertuso Spring, and several springs which inflow into the Aniene River, at different points (Tab. 3.1).

Table 3.1 Elevation and average annual discharge of the major karst springs in the Upper Valley of theAniene River [29]

Spring	Altitude (m a.s.l.)	Average Annual Discharge (l/s)
Acqua Santa	900	65
Acqua Nera	1030	80
Fonte del Forno	950	164
Cesa degli Angeli	940	200
Radica	1110	250
Pertuso	**698**	**1400**

The study area belongs to the Special Area of Conservation (SAC) of the Aniene River Springs (EC Site Code IT6050029) established under Directive 92/43/EEC (Fig. 3.2).

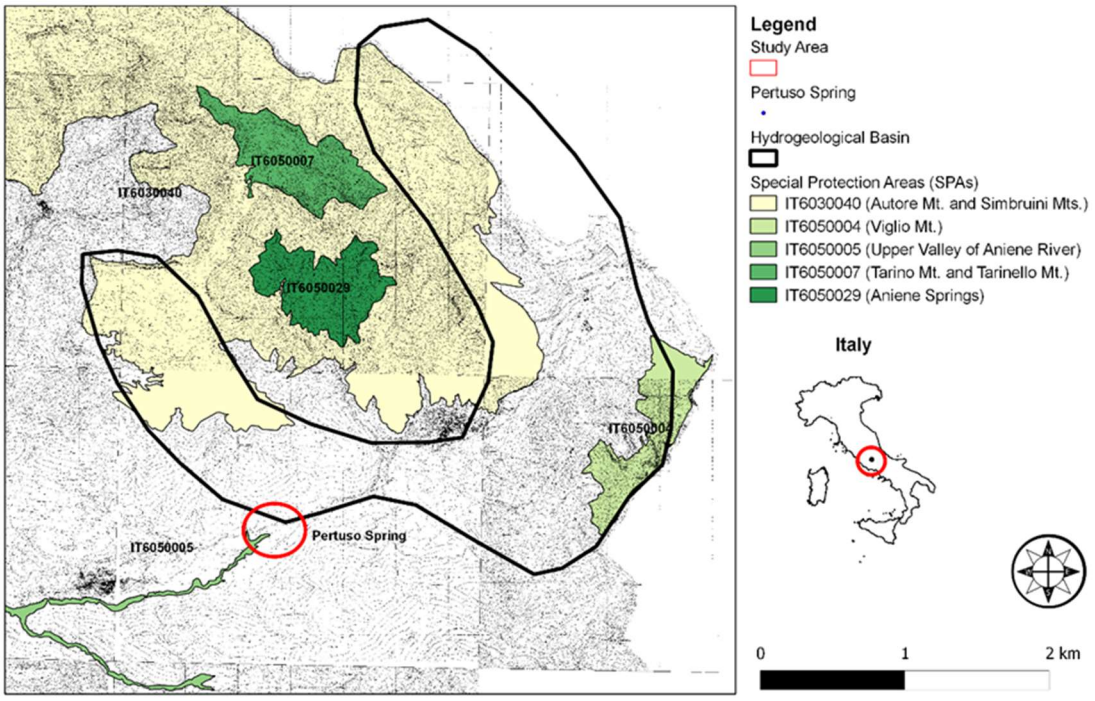

Figure 3.2 Map of the Special Areas of Conservation (SACs) in the Upper Valley of the Aniene River

This area is located within the Regional Natural Park of the Simbruini Mountains, bordered on the West and North-West from the Valley of the Aniene River, South-West from the Sacco River, East of the border of Abruzzo Region (Abruzzo and Simbruini Carseolani Mountains), to the South-East by Ernici Mountains. It covers about 30,000 hectares and its size is the largest protected area of Latium Region (Tab. 3.2).

Table 3.2 Natura 2000 sites inside the Regional Natural Park of the Simbruini Mountains

Typology	Code	Name	Area (ha)
SIC	IT6030040	Monte Autore e Monti Simbruini centrali	6684.9
SIC	IT6050004	Monte Virgilio (area sommitale)	291.7
SIC	IT6050005	Alta Valle del Fiume Aniene	281.6
SIC	IT6050007	Monte Tarino e Tarinello (area sommitale)	341.9
SIC	IT6050009	Campo Catino	132.9
SIC	IT6050029	Sorgenti dell'Aniene	234.3
ZPS	**IT6050008**	**Monti Simbruini ed Ernici**	**52098.8**

The Park is part of the Apennines, it is one of the most significant orographic formations of this area, and it falls within the territory of the Mountain Community Aniene (X) and Ernici (XII), including the territories of the seven municipalities in the provinces of Rome and Frosinone:

- Trevi nel Lazio and Filettino
- Vallepietra
- Jenne and Subiaco
- Cervara di Roma and Camerata

3.2 The Pertuso Spring

The Aniene River, close to Trevi nel Lazio (FR), receives an important contribution on the right side by the Pertuso spring, which is the largest karst spring in this area [22], which is located in the Upper Valley of the Aniene River, about 1 km from the confluence of the Fiumata Valley and the Granara Valley [15].

The Pertuso Spring (elevation of 696 m a.s.l.), the largest karst spring in South-East part of Latium Region, is located between Filettino and Trevi nel Lazio (FR). The outflow of this spring is located in alluvial sediments, which cover a very thick layer made of Cretaceous limestone (Fig. 3.3).

The karst aquifer feeding the Pertuso Spring underlies an area of about 50 km^2 in the Upper Valley of the Aniene River [30]. This aquifer is one of the most productive aquifer systems in the south part of Latium Region, suppling drinking water to the city of Rome and feeding the Comunacqua hydroelectric power plant, owned by ENEL group [29].

The Pertuso Spring hydrogeological basin is located between latitude 41°51' to 41°56'N and longitude 13°13' to 13°21'E and collect groundwater coming from catchment area bounded by the Triassic dolomite to the NE (Fig. 3.1).

Rainfall is the primary source of recharge to this karst aquifer. Dissolution of the limestone has produced small to large conduits at different levels in this aquifer system. These factors produce local variability in the lithology and the permeability of the aquifer system. For this reason, most of the recharge of the Pertuso Spring occurs through karst features such as sinkhole, dolines, swallows holes and fractures, which allow fast flow across the recharge zone.

The Pertuso Spring is the natural outlet of groundwater discharging from karst conduits and it outcrops when this aquifer made of this high enhanced karst network, matches topographic surface.

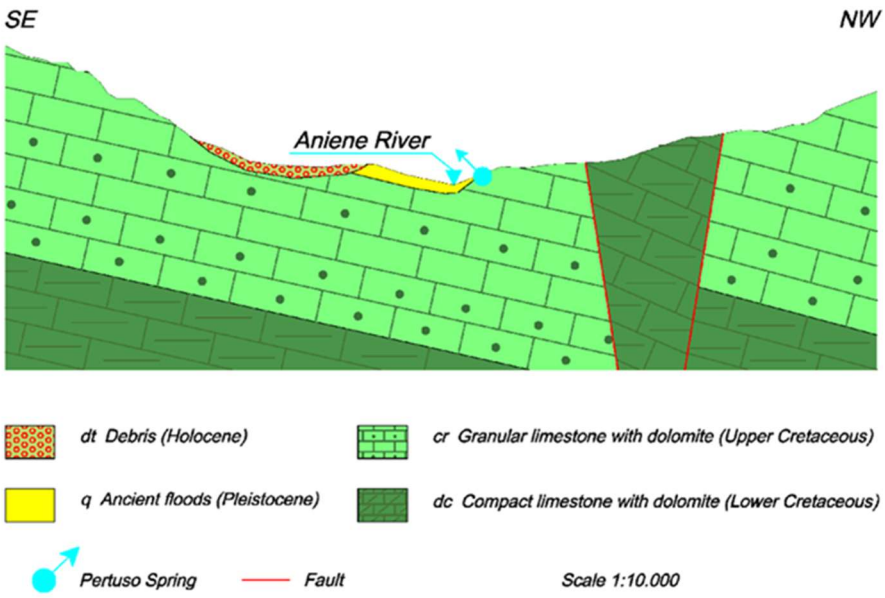

Figure 3.3 Geological cross section showing the aquifer in the Cretaceous limestone and the location of the Pertuso Spring

The Pertuso Spring drainage gallery contains interesting features as a result of the physical and chemical processes which form it. Among these features there are breakdown blocks of rock, formed by collapse of cave ceilings, sediments deposited from water flowing in and through conduits, stalactites that hang from cave ceiling and stalagmites protruding from the gallery floor (Figs. 3.4 and 3.5).

Figure 3.4 Stalactites and stalagmites in the Pertuso Spring drainage gallery

Figure 3.5 Stalactites and stalagmites in the Pertuso Spring drainage gallery

The most distinctive feature of the Pertuso karst spring is the branching network of conduits that increase in size in the downstream direction (Fig. 3.6). The largest active conduit drains the groundwater flow coming from the surrounding aquifer matrix, the adjoining fractures and the smaller nearby conduits [11, 24, 31].

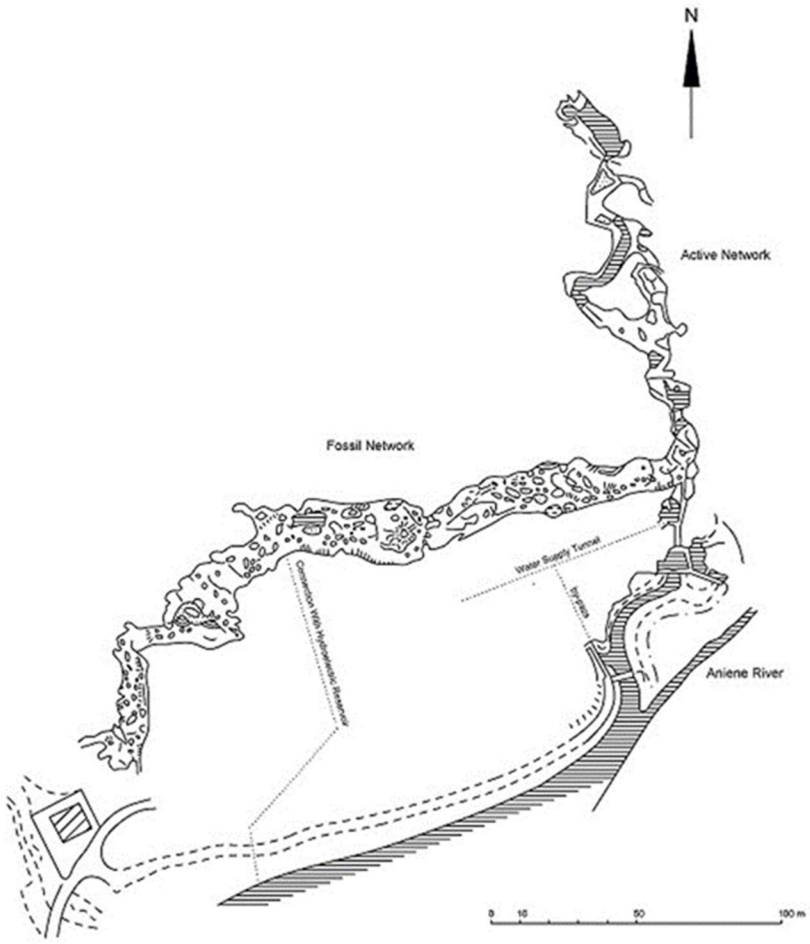

Figure 3.6 Pertuso Spring drainage gallery with plan view of the development of karst network (modified from [29])

The Pertuso Spring discharges has an annual average rate of 1400 l/s, based on the record from 1990 to 1999 [29] and reacts, rapidly, to precipitation events, with significant increases in discharge rates which are proportional to the intensity of rainfalls (Fig. 3.7). Unfortunately, they are not available data referred to groundwater discharge more than ones represented in Figure 3.7. These peculiar properties heighten the vulnerability of karstic aquifers and the groundwater emerging from them.

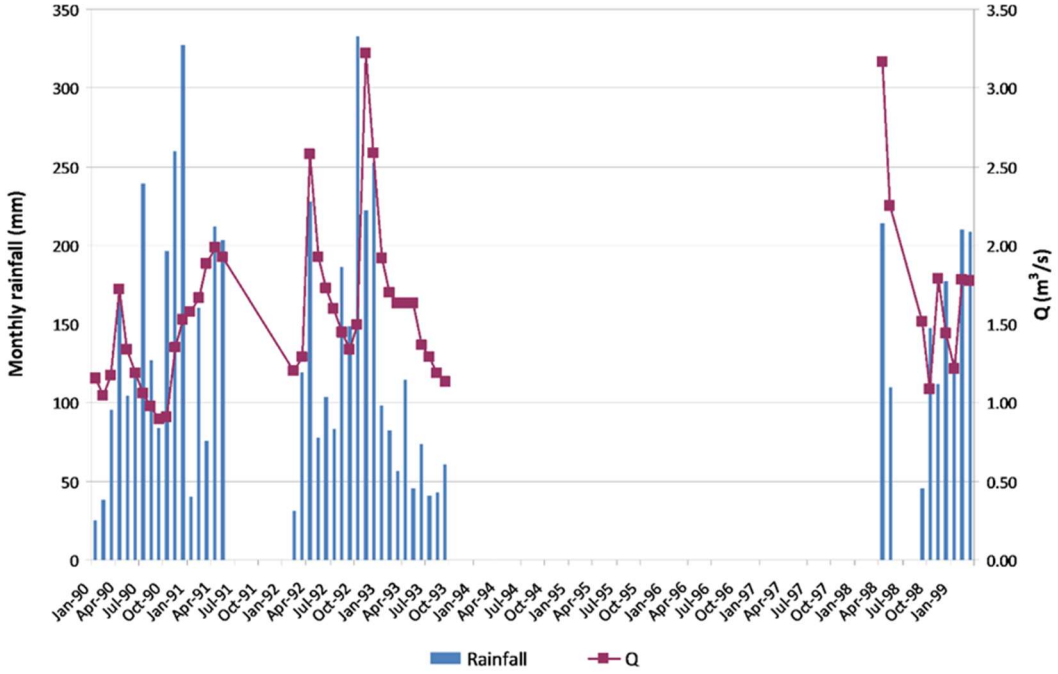

Figure 3.7 Monthly rainfall and Pertuso Spring average rate in the 1990 - 1999 period (Filettino meteorological station)

3.3 Hydrogeological water budget of the karst aquifer feeding the Pertuso Spring

Groundwater budgets are carried on by the estimation of all inflows (recharge and lateral groundwater inflow), all outflows of the system (discharge, evapotranspiration and extraction) and the storage changes over a clearly defined period of time which can be a water year, a season, the duration of a single storm, or any other period [25].

In karst aquifers, direct water budget may be evaluate using climatic, hydrogeological and geological data, but it requires a detailed description of karst networks geometry, which is not measurable with reliability in most of the cases [33]. The annual active recharge of the karst aquifer feeding the Pertuso Spring was calculated by using the inverse hydrogeological water budget method of Civita [34]. This method has been applied discretizing the hydrogeological basin in grid cells (FSE), 250 m each one, by the application of an open source GIS [35].

Rainfall data corresponds to the precipitation of Vallepietra (RM), Filettino (FR), Subiaco Santa Scolastica (RM) and Carsoli (AQ) stations (1992-2012 period) (Tab. 3.3), which may be considered rappresentative of the elevation of the study area. Temperature data were obtained using the records of Subiaco (RM), Collepardo (FR) and Capistrello (AQ) station (1992-2012 period) (Tab. 3.3).

Due to the absence of termo-pluviometric stations in the study area, it has been impossible to calculate the Correct Temperature parameter which requires both temperature and precipitation data for each meteorological station. Thus, the temperature parameter used in the present work is the Interannual

Temperature (TMI), obtained from the historical series. Starting from the above-mentioned precipitation and temperature data, available for the 1992-2012 period, both rainfall-elevation and temperature-elevation regression lines have been built (Figs. 3.8 and 3.9).

Table 3.3 Meteorological stations used for the groundwater budget evaluation

Meteorological Stations	Type	Elevation (m a.s.l.)
Vallepietra	Pluviometric	825
Filettino		1062
Subiaco (Santa Scolastica)		511
Carsoli		640
Subiaco	Termometric	458
Capistrello		735
Collepardo		820

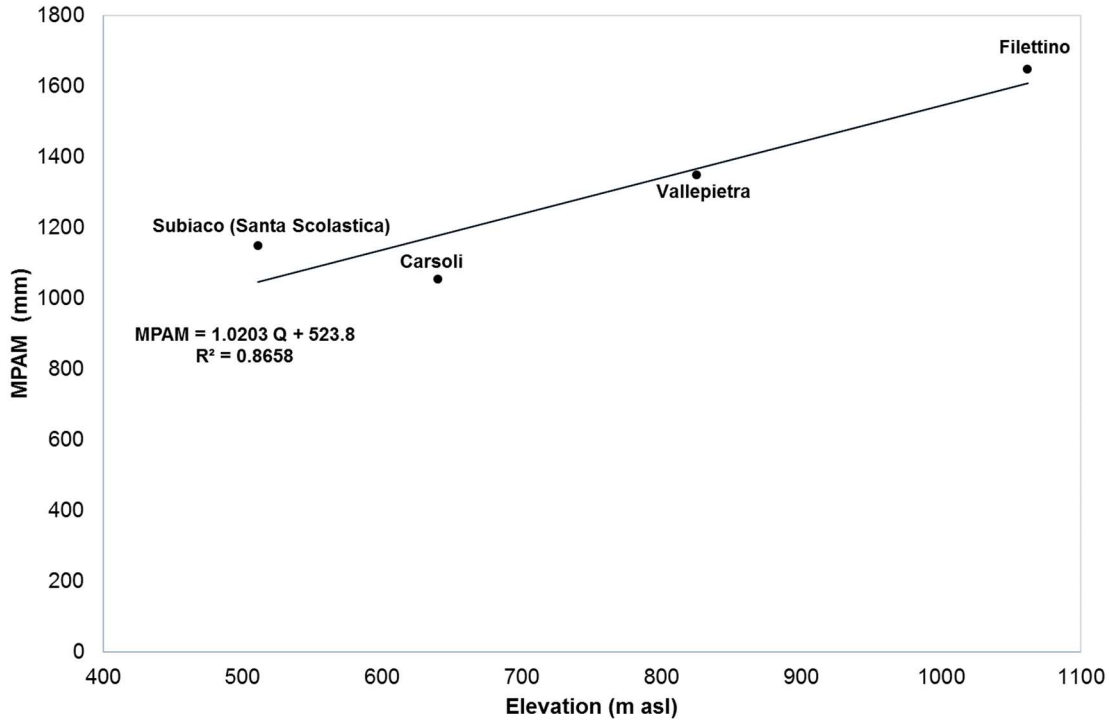

Figure 3.8 Precipitation - Elevation relation

The relationships described above, valid for the whole basin, have been used to compute the water balance within each FSE. For the calculation of specific rainfall (P) and temperature (T) in each FSE, mean elevation of each FSE has been determined by the extraction with QuantumGIS from DEM raster layer.

The distribution of the temperature and rainfall within the hydrogeological basin of the Pertuso Spring (Figs. 3.10 and 3.11) allow to estimate the specific evapotranspiration (ETR) using Turc model [36] through the identification of the potential infiltration coefficients (χ), on the basis of surface lithological properties of rock mass, soil texture and land use (Tab. 3.4).

Using three values of the coefficient of potential infiltration (max, min and mean) as a function of the hydrogeological complexes outcropping in the study area [34], we calculated the inverse hydrogeological water budget to the karst aquifer feeding the Pertuso Spring.

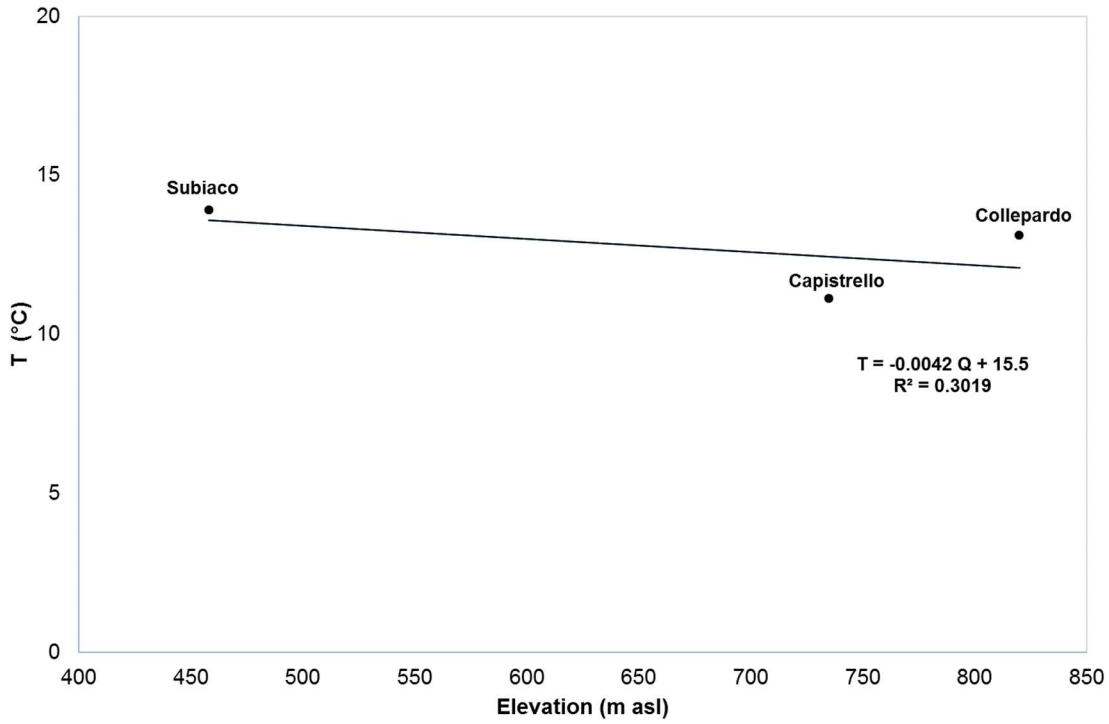

Figure 3.9 Temperature - Elevation relation

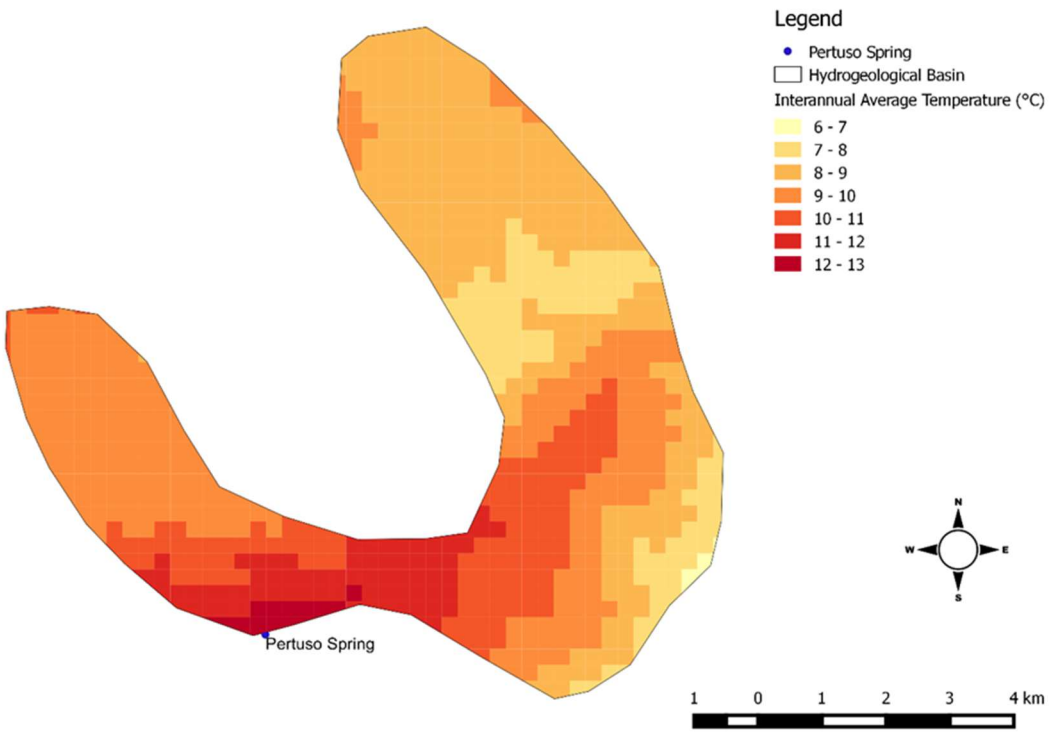

Figure 3.10 Temperature distribution

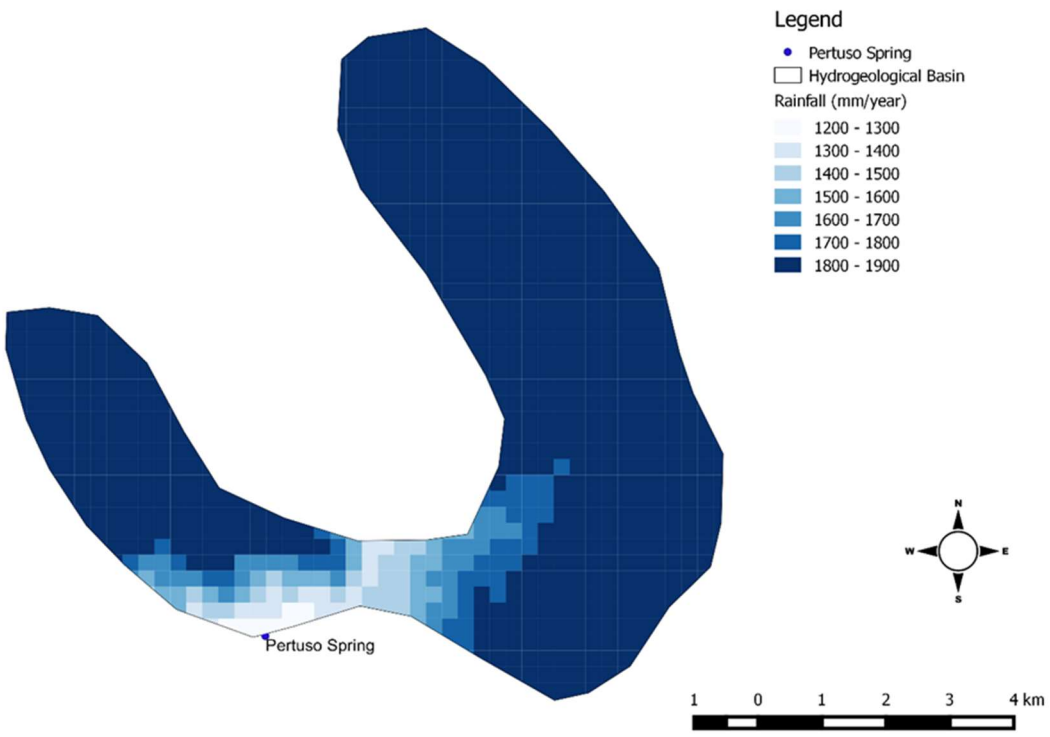

Figure 3.11 Rainfall distribution

Table 3.4 Potential infiltration coefficients as a function of the hydrogeological complexes [34]

Hydrogeological Complexes	Potential Infiltration Coefficient (χ) Range
Debris flow	0.15-0.48
Ancient floods	0.15-0.48
Conglomerates	0.30-0.50
Breccia with calcareous cement	0.65-1.00
Pudding stones	0.30-0.50
White and yellow granular limestone	0.75-1.00
Compact limestone with dolomite	0.50-0.85
Compact limestone, dolomite and dolomitic limestone	0.50-0.85
Gray and white crystal dolomite	0.48-0.65

In the aim of obtaining a prudentially evaluation of the karst aquifer recharge, it has been decided to take into account only the result related to the lower value of the coefficient of potential infiltration. The aquifer feeding the Pertuso Spring is mainly made of highly permeable Cretaceous carbonate rocks, deeply fractured and mostly soluble. For this reason, the given potential infiltration coefficient assumes is very high value (0.875) in most part of the study area, due to the outcropping of karstified limestone and lacking in pedological coverage. Standing on these results, the specific effective rainfall ($P_E = P\text{-}Er$) for each grid cell and the specific active recharge ($I = P_E * \chi$) has been calculated.

The results of the inverse hydrogeological water budget applied to the karst aquifer feeding the Pertuso Spring (Figs. 3.12 and 3.13) show that the total amount of groundwater active recharge is about 54 m^3/year, averaged in 20 years of observations (1992-2012).

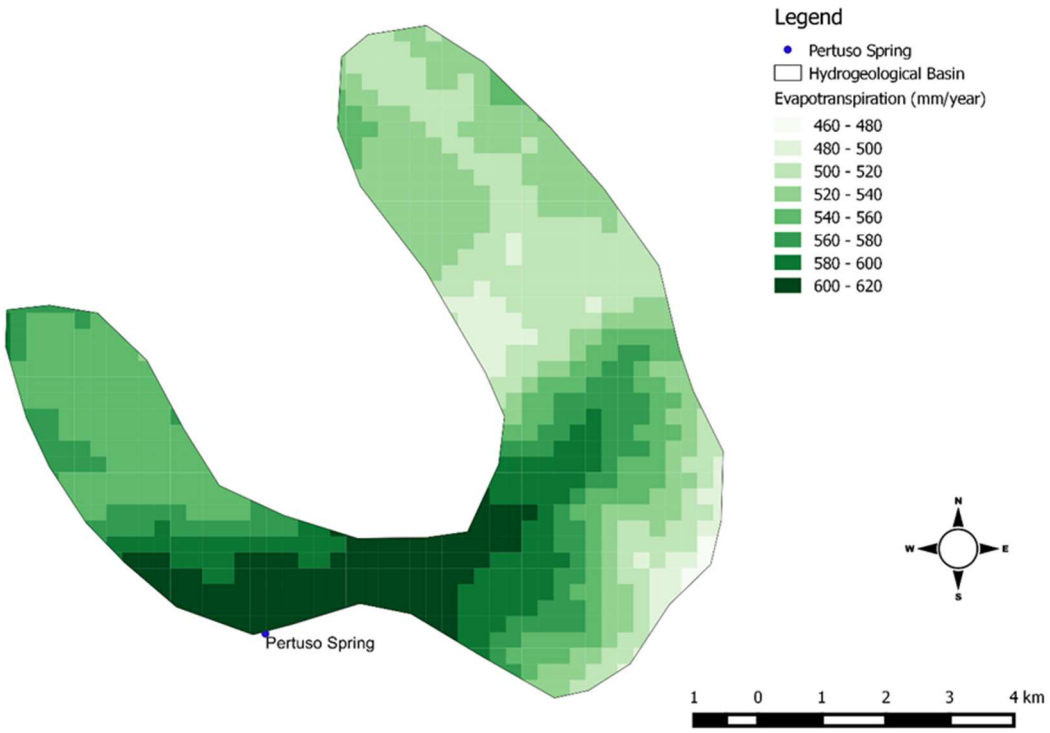

Figure 3.12 Evapotranspiration distribution

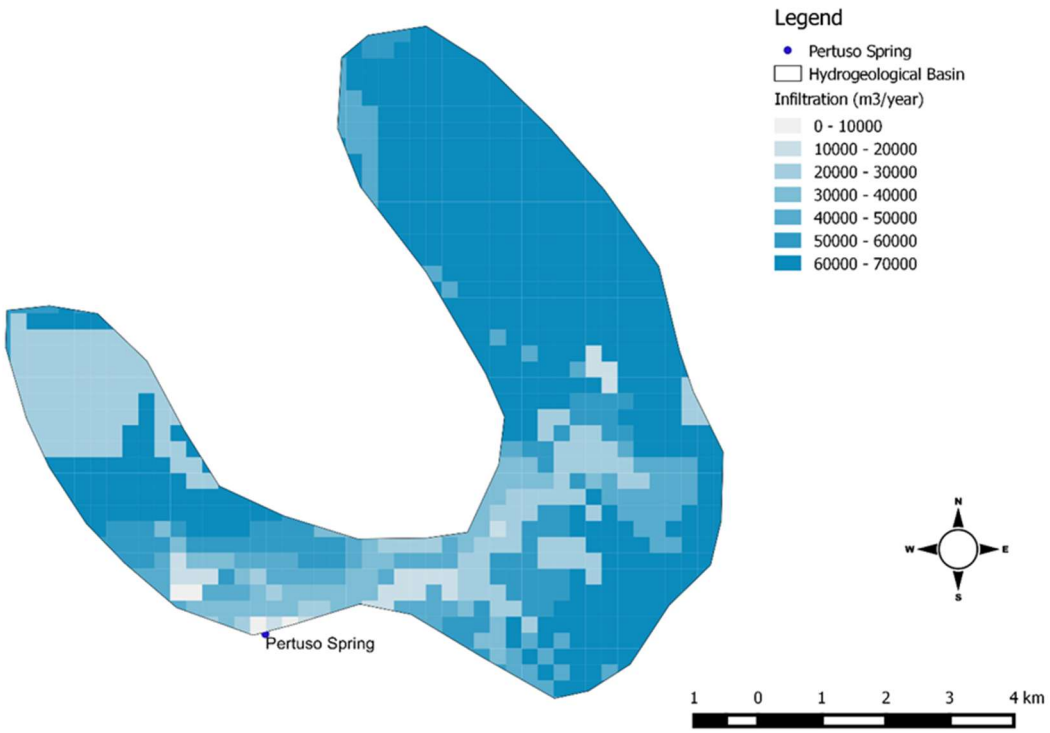

Figure 3.13 Infiltration distribution

Recharge map (Fig. 3.13), according to the presented methodology, shows in dark blue the main recharge areas, where geological units are more permeable [35].

CHAPTER 4

VULNERABILITY ASSESSMENT OF THE KARST AQUIFER FEEDING THE PERTUSO SPRING

4.1 The concept of groundwater vulnerability

4.1.1 The concept of groundwater vulnerability

The concept of vulnerability of groundwater to contamination was first introduced in the sixties of the last century in France by Margat [36] and can be defined as "*the possibility of percolation and diffusion of contaminants from the ground surface into the groundwater system that can reduce the groundwater quality"* [37].

Vulnerability is the degree to which the physical properties of the groundwater system offer a certain rate of protection to groundwater with respect to human influence and inflow of contaminations into the subsurface. For this reason, vulnerability is usually considered as an intrinsic property of a groundwater system, only depending on its hydrogeological setting and its natural protection to groundwater against human impacts, especially with regard to contaminants entering the subsurface environment [38].

Vulnerability is a relative, unquantifiable, and non-dimensional property that may be either intrinsic (natural) or specific [38]. The former should only depend on the natural properties of an area, while the latter should, additionally, take into account the properties of the contaminants [39].

The intrinsic vulnerability of groundwater to contaminants takes into account the geological, hydrological and hydrogeological characteristics of the area, but is independent of both the pollutant nature and the mode of contamination [12,40]. On the contrary, the specific vulnerability takes into account the properties of a particular contaminant or group of contaminants in addition to the intrinsic vulnerability of the area [12].

The vulnerability assessment provides an important tool for identifying protection zones for water supply and highlighting areas where the aquifer is more susceptible to pollution, introduced from the ground surface [41]. Groundwater vulnerability assessments often result in maps, where the resource is vulnerable to contamination coming from surface activities. A map showing areas of different colour representing different degrees of vulnerability (or natural protection, respectively) is easily to interpret and can be used as a practical tool for land-use planning, protection zoning and risk assessment [12]. With the development of Geographic Information System technology (GIS), there has been developed many approaches in the evaluation of groundwater vulnerability to pollution [42,43].

Traditional approaches have strong limitations in vulnerability assessment of karst aquifers, due to the fact that in these aquifers, the contaminants transport occurs mostly along preferential pathways (karst features), which makes modeling of karst systems challenging. Thus, in this study has been developed a karst aquifer vulnerability technique, which emphasizes the karst formations outcropping in the study area. Two different methods for assessing intrinsic aquifer vulnerability were tested in the chosen case study and their results have been compared.

4.1.2 The source-pathway-target model

The concept of groundwater vulnerability is based on a source-pathway-target model for environmental management (Fig. 4.1).

The source of contamination is the assumed place of release of a contaminant. For vulnerability mapping, it is assumed that the contamination takes place at the land surface. The pathway is the flowpath of a potential contaminant from its point of release (source), through the system, to the point that has to be protected (target). For water resource protection, the pathway is the mostly vertical passage, within the protective cover, while for source protection it also includes horizontal flow in the aquifer. The target is groundwater, which has to be protected. For resource protection the target is the groundwater table in the relevant aquifer under consideration, for source to be protected it is the water in the well or spring [12].

For water resource protection, the groundwater surface in the aquifer is the target. In case of confined and/or artesian conditions, the target is to the top of the saturated zone of the aquifer under consideration and not to the potentiometric surface. The pathway, consequently, consists of the mostly vertical passage, through the layers above the groundwater surface or surface of the aquifer respectively. These overlying layers are mostly unsaturated, but may be temporally and locally saturated [12].

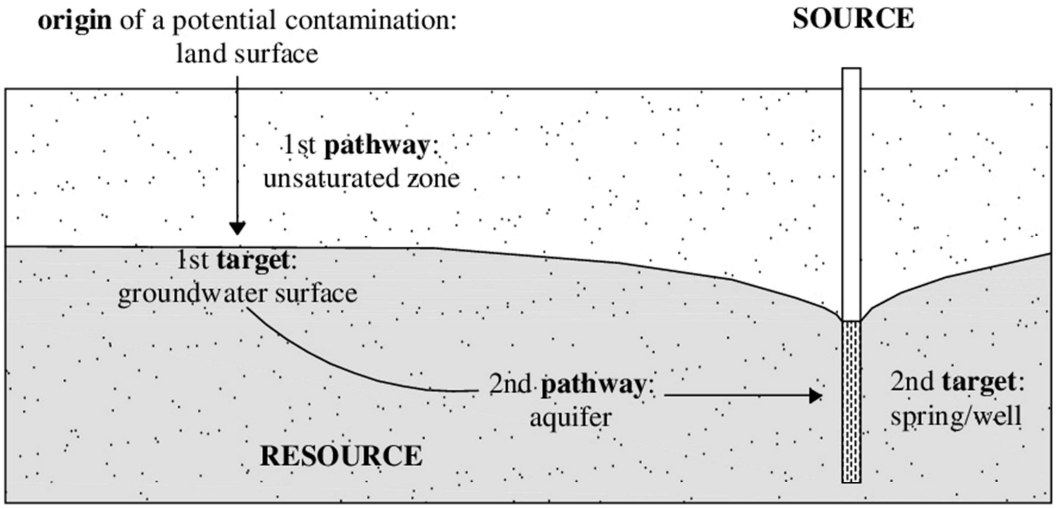

Figure 4.1 The origin-pathway-target conceptual model of the European Approach (modified from [12])

4.2 Karst groundwater vulnerability assessment

4.2.1 Karst groundwater vulnerability

Karst aquifers, including coastal ones, represent the most important fresh-water resources for human life and economic activities in Europe [6]. Carbonate rocks occupy 35 % of the EU land-surface and a significant portion of the drinking water is coming from karst aquifers. In some European countries,

karst water gives 50 % of the total drinking water supply and, in many regions, it is the only available source of fresh water [39].

The concept of groundwater vulnerability is applicable to any type of aquifers, granular, fractured and karst. However, due to the special properties of karst, karst groundwater resources are often highly vulnerable to contamination from human activity more than other ones. As a result, appropriate protection measures must be put in place, a point recognised in the Water Framework Directive [12].

Karst aquifers are well known for their complex hydrogeological characteristics, related to the high heterogeneity of hydraulic properties that make them different from other aquifers [10]. Their heterogeneous distribution of permeability is due to conduits and voids developed by the dissolution of carbonate rocks (karst conduits, rutted fields, sinkholes, cave systems and ponors), frequently embedded in a less permeable fractured rock matrix [11,24]. Their special properties result in contaminants easily reaching groundwater, where they are transported rapidly in karstic conduits over large distances. Flow velocities into a well-developed karst system are extremely high and contaminants can reach quickly the saturated zone. As the residence time of contaminants in the system is often short and their interaction with the aquifer limited, many processes of contaminant attenuation like filtration and adsorption, as well as chemical and microbiological decay, often do not work effectively in karst systems [12]. Thus, karst aquifers are very vulnerable to contamination mainly due to the concentration of flow in the epikarst and vadose zone that allows the contaminants to reach easily and rapidly groundwater.

4.2.2 Karst system characteristics relevant with respect to groundwater vulnerability

The most relevant characteristics of karst systems with respect to groundwater vulnerability that should be taken into account in the vulnerability assessment are [12]:

- Each karst system has its peculiar characteristics; consequently, a detailed hydrogeological study is required for vulnerability assessment;
- Due to the high heterogeneity and anisotropy of karst aquifers, the interpolation and extrapolation of field data is more problematic than for other aquifers.
- Karst groundwater is recharged both by diffuse infiltration through the soil and by concentrated point recharge like dolines and swallow holes.
- The layers above the groundwater surface provide some protection. However, lateral surface or subsurface flow has to be expected in areas covered by low permeable layers. These lateral flow components may be tributary to a stream sinking into the karst aquifer via a swallow hole and bypass the protective function of the overlying layers.
- Karst aquifer may be characterized by the presence of an epikarst zone, located at the top of the vadose zone. The functions of the epikarst are water storage and concentration of flow. The first process increases the natural protection of the system, while the second one increases vulnerability. The structure and function of the epikarst zone are difficult to assess because of a large portion of it is not visible at the land surface.
- Karstic aquifers are characterized by a dual hydraulic conductivity, due to fractures and conduits, and very often by a triple porosity, due to the additional presence of intergranular pores (matrix). Groundwater storage takes place in the pores and fractures, while conduits act as drains. As there are both extremely fast and slow flow components within a karst system, contaminants can be transported very fast or stored for a very long time.

- Karst systems are characterized by a fast and strong hydraulic reaction to hydrologic events. The temporal variations of groundwater table often reach several tens of metres. In many karst systems, the groundwater table is discontinuous and difficult to determine.
- Karst catchments are often extremely large and hydraulically connected over long distances. Watersheds are often difficult to determine and variable in time, dependent on the respective hydrologic conditions. The catchments of karst springs often overlap and the flow paths proved by tracer tests often cross each other.

With respect to the specific vulnerability, the mobility and persistence of contaminants into the karst aquifer is related to the combination of hydraulic and mineralogical-geochemical properties of the system [12].

The hydraulic properties play a significant role in contaminants migration. In particular, these properties are related to the existence of three layers with difference hydraulic behaviours. The epikarst is a high conductivity layer. It collects infiltration and gathers it to the vertical conduits of the unsaturated zone. This layer contributes to the quick transit of the low-persistent contaminants to the water table. Transit can be very fast in conduits, slow in fissured blocks. Consequently, conduits can quickly convey non-persistent pollutants, whilst blocks preserve conservative contaminants, enabling self-purification or reduction of the other pollutants. Furthermore, these voids control the flux of contaminants. Several types of contaminants (hydrocarbons) or particles (pathogens) require a minimum opening to transit through. Thus, the percentage of diffuse flow will be a significant parameter in the retardation and attenuation processes acting in the specific vulnerability.

Mineralogical and geochemical properties are also important because the presence of different minerals makes specific retention conditions [12]:

- The carbonate medium restricts mobility of reactive contaminants such as phosphate, which precipitates as apatite, and heavy metals that can precipitates as carbonate species. The H^+ proton, which can come from acid rains and pedogenetic processes, is quickly buffered by the carbonate medium, enabling the production of Ca^{2+} and HCO_3^-. Generally, this carbonate medium is absent from the covering soils, which are residual formations, and this role is played by the subsoil and the epikarst. The pH value, despite its low variability in karst environments, due to the buffer effect of the carbonate medium, can play together with Eh a role in the solubility of inorganic metals.
- Clays play a double mineralogical and geochemical role: their specific surface enables adsorption of non-ionic substances (organics, bacteria) and their Cationic Exchange Capacity (CEC) enables retention of cations, especially heavy metals. These clays exist in covering soils (residual clays), non-karstic covering formations (geological clays), and detrital sediments, which are present in the karstic network, both in the unsaturated and saturated zones.
- Organic matter, which is abundant in topsoil, and in the soil infillings of karren, plays two roles: adsorption of organic contaminants and formation of ligands with metals.
- *Eh* is generally high in the epikarst, which is widely open to the atmospheric reservoir. In this case, dissolved heavy metals can precipitate (oxides, hydroxides), organic matter and nitrogen species oxidise. Nevertheless, reducing conditions can exist in a carbonate environment, in different layers: in the soil, which can be hydromorphic and anoxic, and in the saturated zone, which can be confined, when it is covered by impervious layers. In both cases, redox potential becomes low and mobilisation of metallic oxides and hydroxides is possible. Nitrogen can also be reduced, in the

best case as gaseous N_2, in the worst as NO_2^- or NH_4^+. Oxidizing or reducing conditions can select aerobial and anaerobial bacteria, which role can improve or worsen water quality.

– Temperature sometimes plays an active role: several degradation processes are more active at higher temperatures, so seasonal variations may modulate the attenuation.

4.2.3 The European Approach

The European approach to intrinsic groundwater vulnerability mapping and assessment suggested by COST 620 aims at mapping and assessing those properties that influence the travel time of a potential contaminant from the source to the target, as well as the concentration level and the duration of a potential contamination [12]. The conceptual model of this approach takes into account four factors, as described in Fig. 4.2: Overlying layers (O), Concentration of flow (C), Precipitation regime (P) and Karstic network development (K).

Figure 4.2 The European Approach to groundwater vulnerability mapping (modified from [12])

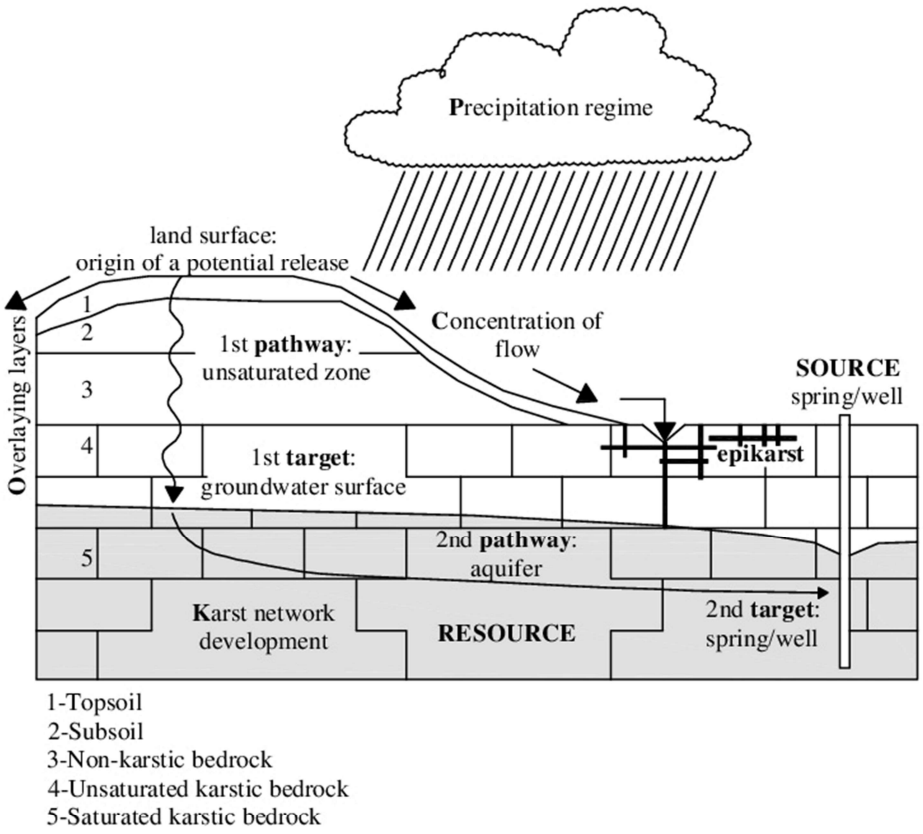

The factors O, C and K represent the internal characteristics of the system, while the P factor is an external stress applied to the system. For resource vulnerability mapping, the factors O, C and P should be taken into consideration, while the factor K should be additionally taken into account for source vulnerability mapping [12].

4.2.3.1 Overlying layers (O factor)

The overlying layers (O factor) are layers, located between the land surface and the groundwater surface: topsoil, subsoil, non-karst rock and unsaturated karst rock. Some of these layers may be separated into several sub-layers and each layer is not always present [12]. Many karst areas only consist of karst rock unsaturated layers and topsoil; the latter is absent in the zone of bare karst. Granular

aquifers only comprise the layers topsoil and subsoil, while fractured aquifers are often protected only by the topsoil and the unsaturated non-karst rock [12].

The O factor characterizes the natural protection provided to the groundwater by the layers above the saturated zone [12,44].

- The topsoil (layer 1) is the biologically active zone of weathering of the earth crust and is composed of minerals, organic substance, water, air and living matter. This layer is the most important for specific contaminant attenuation processes, but less relevant for intrinsic vulnerability assessment. The most important characteristics of the topsoil, which can be used as a mean to evaluate its protective function are thickness, porosity and permeability, in particular the two latter are mainly controlled by the grain size distribution. Macropores play an important role as they enable the topsoil to be bypassed. The effective field capacity (eFC) can be used as a mean to assess the protective function of the topsoil: a high eFC means a high capacity to store water and, consequently, to delay and attenuate contaminants. Indirect means are the soil type, vegetation and drainage density [12].
- The subsoil (layer 2) is the granular, non-lithified material below the topsoil. The most relevant factors for the subsoil are thickness, porosity and permeability. Preferential flowpaths (macropores) are usually far less likely to occur than in the topsoil. The degree of saturation and the vertical hydraulic gradient in saturated, low permeability parts of the subsoil may be relevant for site-specific situations. The lateral continuity of each layer should also be considered because low permeability layers can be bypassed if they are not laterally extensive, but occur in the form of lenses. The grain size distribution can be used as a means to evaluate its protective function. In many cases, the subsoil type as given on the geological map will be the only available source of information.
- The non karst rock (layer 3) consists of lithified, non karstified rocks. The most relevant factors for the non karst rock are thickness, permeability, type and degree of porosity. Three situations can be distinguished: fissured permeability (the least protective), intergranular porosity (the most protective) and the combination of both, which provides intermediate protection. The most important means to assess these characteristics are geological information, particularly lithology and tectonics. The density, width, continuity, spatial distribution, roughness and infilling of fissures control the hydraulic function and protection provided by the bedrock.
- The unsaturated karst rock (layer 4) is the vadose zone of the karst aquifer. The epikarst, if present, plays an important role in infiltration and percolation from the surface to the groundwater and consequently influences the protective function of the unsaturated zone. Two extreme situations can be defined: if the epikarst allows for diffuse infiltration, significant water storage and diffuse percolation, some protective function can be assigned to the unsaturated karst rock. In this case, it may be practicable to define a separate epikarst sub-layer. On the other hand, if flow concentration is the dominant process in the epikarst zone, it must not be treated as a protective sub-layer as it may enable the unsaturated zone of the karstic bedrock to be partially or totally bypassed. This situation is present for karren fields, with or without soil cover, drained by visible or hidden vertical shafts. The characteristics controlling the protective function of this layer are thickness, permeability, degree and spatial distribution of karstification. The presence of a fissured and/or intergranular porosity increases the protective function of the layer. In the case of strong flow concentration in the epikarst zone, the thickness of the unsaturated zone loses its relevance and the

protective function of the whole layer might be insignificant. Indirect means of determining these characteristics are the analyses of surface and underground karst features, the lithology, tectonics, landscape history, analyses of surface waters, springs and swallow holes, the soil development and the vegetation [12].

Several existing methods provide possible assessment schemes for the O factor, for example the EPIK [45], the PI [46] and the SINTACS methods [33,47].

4.2.3.2 Concentration of flow (C factor)

The O factor represents the natural protection of groundwater to contamination, if all precipitation infiltrates diffusely into the soil and percolates through the unsaturated zone towards the groundwater. However, this is often not the case in karst systems, particularly in areas where the karst aquifer is confined by formations of low permeability. These areas often produce surface runoff, which may sink into the karst aquifer at another place (e.g. via a swallow hole), bypassing the protective function provided by the overlying layers.

On the other hand, surface runoff, which does not sink underground, but flows out of the karst systems, provides good protection to contamination. Therefore, the C factor represents the degree to which precipitation is concentrated towards places where fast infiltration can occur. If infiltration occurs diffusely without significant concentration of flow, the C factor is not an issue, as the overlying layers are not bypassed. Precipitations can be concentrated, and the overlying layers can be completely bypassed by a swallow hole through which surface water and contaminants directly enter the karst aquifer. In such a case, the C factor is a significant issue in the vulnerability assessment. The degree of flow concentration depends on parameters, which control the origin of surface runoff and/or subsurface flow, like slope gradient, surface properties (e.g. thickness, permeability and infiltration capacity of the soils) and vegetation, and on the presence of features which allow concentrated infiltration (swallow holes, areas with higher infiltration capacity) [12]. The C factor of the European Approach is as adapted parameter coming from the I factor (infiltration conditions) of the EPIK [45] and PI methods [46].

4.2.3.3 Karst network development (K factor)

The K factor represents the degree of karst network development in the aquifer. It is based on a general description of the bedrock, giving a range of possibilities from non-karstified carbonate rocks with only intergranular porosity to karst aquifers with fast active conduit systems. This factor should be used together with a criterion of distance and/or travel time in the karst aquifer. The means of assessing the karst network factor are the following:

- geology and geomorphology
- cave and karst maps
- groundwater-tracing results
- pumping-tests results
- spring hydrograph and chemograph analyses
- remote sensing and geophysical prospecting
- borehole data and geophysical-logging results
- bedrock sampling and laboratory experiments
- calibrated modelling results

Indicators, which may provide information on the underground characteristics, are drainage density, soil and vegetation [12].

4.2.3.4 Precipitation regime (P factor)

The P factor represents the climatic conditions and takes in account not only the total quantity of annual precipitation, but also the frequency, duration, and intensity of extreme events, which can have a major influence on the infiltration and, consequently, on the vulnerability. A large amount of rainfall, together with favourable infiltration conditions and limited evapotranspiration, causes a high recharge rate, a fast percolation through the unsaturated zone and, consequently, a fast contaminant transport. However, a larger quantity of recharge also means greater dilution and a shorter duration of pollution. Extreme precipitation events lead to significant surface runoff and lateral subsurface flow (interflow), which may sink into the karst aquifer via a swallow hole. Extreme events also allow fast contaminant transport in the karst network. The P factor is consequently an external stress, which influences the O, C and K factor. In many cases, there is not a large variation of the precipitation regime within one catchment, but there may be large differences between different test sites in different climatic zones. Thus, the precipitation factor may not be an issue on the catchment scale, but it is relevant on a national or European scale [12].

4.2.4 The COP method

The European Approach [12,40] is a general conceptual framework for groundwater vulnerability mapping. The O, C and P factors of the European Approach have been quantified and categorised and their combination and weighting determined. The definition of vulnerability ranges has been established in order to develop the COP method, which can be used for intrinsic vulnerability mapping [48].

The COP method was tested on two carbonate aquifers in Southern Spain, a conduit flow system and a diffuse flow system, and the results were compared with three methods widely applied in different aquifers around the world (AVI, GOD and DRASTIC) [48].

The COP method is based on three factors (flow Concentration, Overlying layers and Precipitation), as is the European Approach for assessing the intrinsic vulnerability of groundwater resources [12,40]. To assess the vulnerability of the source an additional factor (K=Karst network) of the European Approach must be considered. COP is an acronym derived from the initials of the vulnerability factors. Two conditions are necessary to assess intrinsic vulnerability by the COP method: firstly, that the contaminant depends on the characteristics of the water to move through the aquifer, and secondly, that the contaminant infiltrates from the surface by means of rainfall. The O factor refers to the protection of the unsaturated zone of the aquifer, against a contaminant event. It indicates the capability of the unsaturated zone, by means of various processes, to filter out or attenuate contamination and thus reduce its adverse effects. The C and P factors are used as modifiers that correct the degree of protection provided by the overlying layers (O factor). The C factor takes into account the surface conditions that control water flowing towards zones of rapid infiltration. These zones have less capacity to attenuate contamination because of the shorter transit time of contaminants to reach the saturated part of the aquifer. The C factor varies between 0 and 1. Thus, the protection capacity of groundwater, as described by O factor, may be zero when C factor is 0 and may be the same as that given by O factor when C factor is 1. The O and C factors refer to the layers in which transport takes place. The P factor considers the characteristics of the agent (water) that transports the contaminants through the unsaturated zone. The influence of precipitation on vulnerability is not as great as that of the flow concentration, and so the value of the P factor ranges from 0.4 to 1. Thus, the aquifer protection capacity (O factor) will fall by half when P factor is 0.4, and will remain unchanged when it is equal to 1. The main significance of

the P factor is that it is a parameter that was developed to differentiate zones with widely varying rates of rainfall, such as ones occurring in the continent of Europe [12].

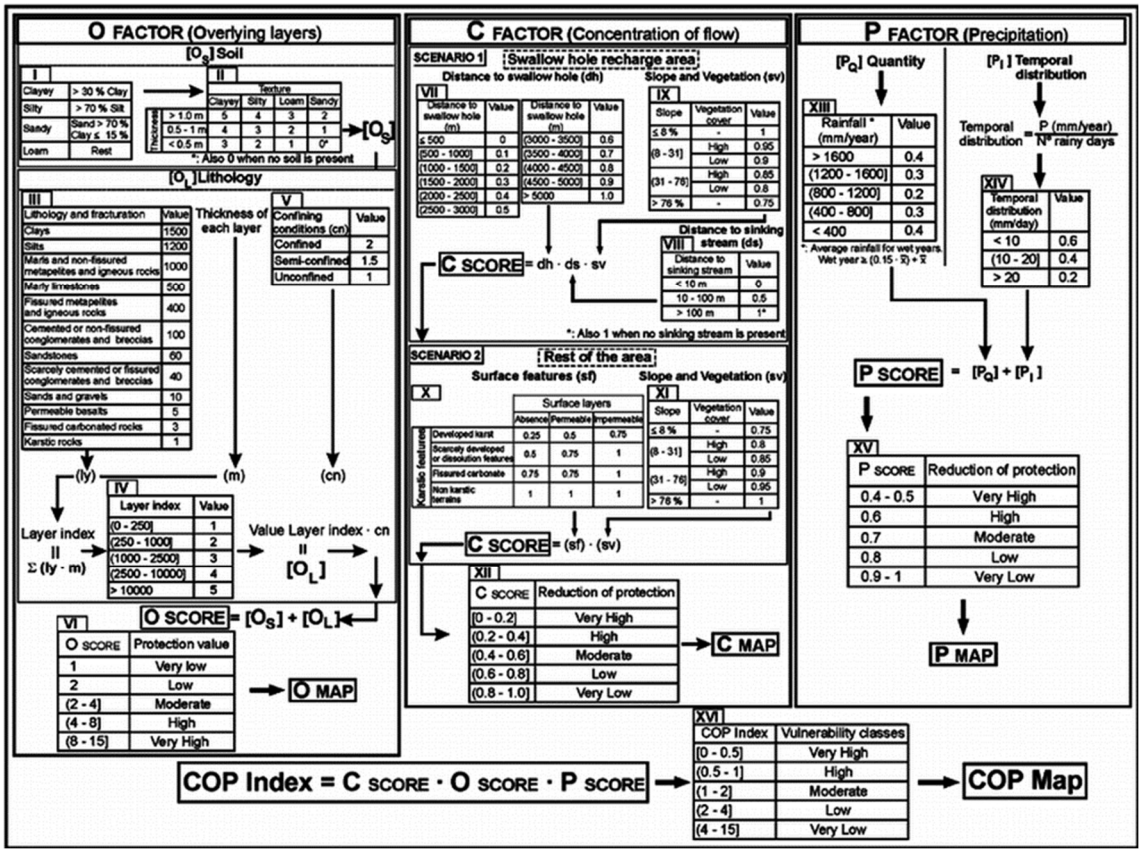

Figure 4.3 The COP method [12]

Both factors P and O can be used to evaluate the vulnerability to contamination for any type of aquifer, while the C factor is specific to karst aquifers. Figure 4.3 summaries the COP method, showing the different values assigned to the variables evaluated for each factor, the procedure used to calculate the C, O and P factors, and the final vulnerability index.

Five ranges have been established to evaluate these three factors, to distinguish relative degrees of groundwater protection (Fig. 4.3, Tab. XVI). The final vulnerability index is obtained by multiplying the three factors and from the resulting index; five classes of vulnerability are obtained, ranging from Very Low to Very High.

4.2.4.1 Estimation of the O factor

Following the European Approach [12,40], the O factor takes into account the protective function of the unsaturated zone and the properties of its layers to attenuate potential contamination. In the COP method, only two layers are used in order to evaluate the O factor, each related to layers in the unsaturated zone with a different hydrogeological behaviour:

- soil (O_S)
- lithology of the unsaturated zone (O_L)

The soil subfactor (O_S) deals with the biologically active part of the unsaturated zone and consequently its self-cleaning process [12]. Two parameters enable an evaluation of this sub-factor soil (O_S): texture and thickness. In order to facilitate the application of the method, four texture classes,

depending mainly on grain size distribution, and three-soil thickness classes were adopted (Fig. 4.3, Tab. I).

The soil subfactor (O_S) is evaluated using the textural class and the thickness of the soil profile (Fig. 4.3, Tab. I). The lithology subfactor (O_L) reflects the attenuation capacity of each layer of the unsaturated zone. For its quantification, three parameters were adopted:

- Lithology and fracturation (*ly*)
- Thickness of each layer (*m*)
- Degree to which an aquifer is confined (*cn*)

The assessment criteria for the evaluation of *ly* are the type of rock (which represents its hydrogeological characteristics, mainly effective porosity and hydraulic conductivity) and the degree of fracturation (Fig. 4.3, Tab. III).

Successive addition of the product of the thickness of each layer (*m*) and the lithology characteristics (*ly*) enables the calculation of the protection index (*layer index*). This value rises with number of layers increase in the unsaturated zone and with their thickness increasing.

The *layers index* ranges between a minimum value of 0 and a maximum value that varies depending on the number and thickness of layers in the aquifer. The *layers index* has been divided into 5 ranges (Fig. 4.3, Tab. IV), and a protection value has been assigned to limit the maximum value of this parameter.

The *cn* parameter is referred to the confinement degree of an aquifer and is a weighting coefficient for the classes of the *layers index*. The values assigned to the *cn* parameter (Fig. 4.3, Tab. V) show a confined aquifer as more highly protected, whereas an unconfined aquifer is not affected by this parameter (*cn*=1). The final value of the (O_L) subfactor is obtained from the product of the value of the *layers index* by the *cn* parameter.

The subfactor (O_L) ranges from a value of 1, equivalent to a minimum degree of protection, to a maximum value of 10. The protection factor O is obtained by combining the subfactors soil (O_S) and lithology (O_L). The value of the O factor ranges between 1 (the lowest degree of protection) and 15 (the highest degree of protection) (Fig. 4.3, Tab. VI). As the attenuation capacity constantly increases with the sum of the protective layers, the values of the protective factor have been grouped into five classes, following an almost geometric 2-order progression (Fig. 4.3, Tab. VI). The Very Low and Low values correspond to areas where carbonate materials outcrop and where the soil is poorly developed or absent. Values described as Moderate and High refer to areas where the degree of protection is high, both because of the presence of soil and because of low-permeability lithology. Very High values characterize the sectors of the aquifer that are confined (the O factor is higher than 10 for a confined aquifer) [12].

4.2.4.2 Estimation of the C factor

According to Daly et al. (2002), the C factor is taken as a corrector coefficient of the O factor (Overlying layers). The C factor represents the concentration rate of water flow towards karstic features that are directly connected with the saturated zone. It also represents how the protection capacity is reduced in such areas. Two scenarios can be differentiated [12]:

1) *Scenario 1*: the catchment area of a stream sinking through a swallow hole
2) *Scenario 2*: the rest of the area

In the first case, all the water circulating through the catchment area is considered to flow towards the swallow hole. The values of the C factor depend on the distance to the swallow hole and to the sinking stream, as well as on the topographic characteristics (slope and vegetation). In the second case,

runoff or infiltration can exist, depending on the slope, the vegetation and, especially, on the characteristics of the surface (karst features and permeability). In both scenarios, slope and vegetation are considered, but in different ways. Thus, in Scenario 1, the shallower the slope and the greater the development of vegetation, the smaller is the modification of the value by the O factor and, therefore, the greater the protection. In Scenario 2, however, the shallower the slope and the greater the development of vegetation, the less is the protection, as infiltration exceeds runoff.

Scenario 1 describes the situation within the catchment area of a swallow hole. The recharge area of a swallow hole is characterized as being covered by a layer of low permeability. Thus, all the water that flows on the surface flows towards the swallow hole. Under such conditions, evaluation of the C factor requires several variables to be taken into account:

- distance to swallow hole (*dh*)
- distance to sinking stream (*ds*)
- slope (*s*)
- vegetation (*v*)

It is assumed that *dh* is 0 in zones located less than 500 m far from the swallow hole and that the protection capacity of the aquifer increases as a linear function of the distance. The value of *dh* follows a 0.1-difference arithmetic progression and the distance follows a 500-difference arithmetic progression (Fig. 4.3, Tab. VII). The *dh* parameter establishes the distance from a swallow hole when a Hortonian flow predominates. If this flow type does not occur, the value of *dh* is 1. The distance to the sinking stream (*ds*) is taken into account, as shown in Fig. 4.3, Tab. VIII. Zones less than 10 m far from the stream are classified as zero protection areas; in those up to 100 m away, protection is reduced to half, and at greater distances the protection is unchanged [46]. The vegetation parameter (*v*) takes into account the presence or absence of permanent vegetation and its density, which could affect the infiltration-runoff regime. On the contrary respect to vegetation, the slope parameter (*s*) is positively correlated with the generation of runoff and negatively so with infiltration. In the COP method, four ranges of slope (as a percentage) have been selected and the combination of these with the vegetation provides the value for the slope/vegetation parameter (*sv*) (Fig. 4.3, Tab. IX). The values of *sv* show that the greater the slope and the less the vegetation, the lower the protection, and so $sv<1$. Water flows more easily to the swallow hole and transit time to the water table is less. The value of the C factor under these recharge conditions is obtained by multiplying the values of the parameter for slope and vegetation (*sv*) by those for the distances from the swallow hole *(dh*) and from the sinking stream (*ds*).

Scenario 2 represents areas where the aquifer is not recharged by a swallow hole. In this case, the C factor is evaluated by the combination of three variables:

- surface features (*sf*)
- slope (*s*)
- vegetation (*v*)

The surface features parameter (*sf*) indicates the geomorphological aspects of carbonate rocks and the presence or absence of a layer (permeable or impermeable) above these materials that addresses the importance of runoff and/or infiltration processes (Fig. 4.3, Tab. X). In this scenario, evaluation of the vegetation and of the slope is carried out in the opposite way to that performed inside the catchment area of a swallow hole. Thus, when the slope is steeper and vegetation is absent (Fig. 4.3, Tab. XI), runoff is more favorable respect to infiltration, and so the protection offered by the O factor is not reduced. To obtain the value of C factor in Scenario 2, the slope-vegetation (*sv*) parameter is weighted by the surface

features (*sf*) parameter. In Scenario 1, the C factor ranges between 0 and 1 whilst in Scenario 2, the C factor ranges between 0.2 and 1. This is because the possibility of a potential contaminant reaching the saturated zone of a karst aquifer is higher in the first case. A value of C factor equal to 0 means that its natural protection in terms of Overlaying layers (O factor) is zero because of the presence of a swallow hole. A value of C factor equal to 1 characterizes an aquifer in which the protection, calculated from the O factor, is not modified. After obtaining the C values, five classes of protection were established (Fig. 4.3, Tab. XII). The Very High class corresponds to zones where protection is low, because of the presence of one or more swallow holes. The High class refers to zones near a swallow hole or sinking stream or to zones that present highly developed karst forms where runoff is nil. The Moderate and Low classes are referred to zones, where karst forms are influenced by surface runoff. The Very Low class is used for sectors of the aquifer, where only runoff processes are present, or where the distance from a swallow hole or sinking stream is very considerable [12].

4.2.4.3 Estimation of the P factor

According to Daly et al. (2002) this factor reflects the total quantity of precipitation and includes the frequency, duration and intensity of extreme rainfall events, which can have a big influence on the quantity and rate of infiltration. Thus, the P factor comprises all aspects of precipitation that determines the way contaminants follow, it means the pathway from the surface to the groundwater. The O and C factors provide the ground properties affecting the transport of contaminants, whereas the P factor refers to the availability of water to transport contaminants. The P factor modifies the protection capacity of the aquifer depending on the quantity and intensity of the rainfall. Thus, a greater capacity of the transport agent (water) to carry contaminants towards the aquifer implies a higher vulnerability. The P factor is evaluated by two subfactors:

- quantity of precipitation (P_Q)
- intensity of precipitation (P_I)

The quantity of rain sub-factor (P_Q) represents the effect of rainfall and the resulting annual net recharge on groundwater vulnerability. There are two aspects, which have to be considered: transit time and dilution. In fact increasing, precipitation height results in decreasing transit time and increasing dilution. However, decreasing transit time means increasing vulnerability, while increasing dilution means decreasing vulnerability. Mean annual precipitation values are ranged into five intervals (Fig. 4.3, Tab. XIII), each with a value that depends on the transit time of the potential contaminant and the dilution capacity. These data are average values of a historical series of wet years, the latter defined as precipitation values that are 15% above the average. Such years, therefore, are unfavourable from the point of view of aquifer protection. Based on experience, theoretical reflections and taking into account the SINTACS [47] and the PI [46] methods, the COP method, consequently, assumes that the protection given by O factor is poorly modified if precipitation values are below 400 mm/year. An increasing in precipitation, up to 1200 mm, decreases protection, because the transport process (transit time) is more important than the dilution process. When precipitation exceeds 1200 mm/year the dilution of potential contaminant is more important than transit time and, consequently the protection given by O factor is scarcely modified. The intensity subfactor (P_I) concerns the temporal distribution of precipitation in a certain period of time. To estimate this subfactor, two variables were considered (Fig. 4.3, Tab. XVI):

- average annual precipitation for the wet years
- average number of rainy days (in a wet year)

This subfactor enables a comparison among different zones within the continent of Europe, where rainfall and intensity conditions are very different. The value assigned to the (P_I) subfactor follows the criterion that higher intensity drives to a higher recharge and thus the protection of the resource is reduced. The intensity of rainfall in karst media makes easier the development of a high and, mainly, fast infiltration volume, through fissures or karst conduits. More intense rainfall yields more runoff to those conduits that favour concentrated infiltration. If rainfall intensity is low, more diffuse and slower infiltration occurs, and the probability of other processes, such as evapotranspiration, is higher. This, eventually, produces a lower recharge volume. All the above information are included in the proposed value for the intensity subfactor (P_I), in which an increase of the (P_I) value is associated to a decrease in protection (Fig. 4.3, Tab. XVI). The final value of the P factor was obtained by adding the values of the two subfactors (P_Q) and (P_I). The variation in P values as a function of (P_Q) follows an arithmetic progression with two units of difference and the values of the P factor reflect the greater importance of (P_I) than of (P_Q). Five classes were established for the values of the P factor (Fig. 4.3, Tab. XV). These values range between 0.4 (minimum protection) and 1 (highest protection). Values closer to 1 indicate that precipitation has little influence on the protection calculated from the O factor. Values closer to 0.4 indicate that precipitation, as a function of quantity and intensity, decreases the protection of the aquifer and increases its vulnerability. The extreme class intervals have a greater range due to the lower probability of such values occurring [12].

4.3 Vulnerability assessment of the karst aquifer feeding the Pertuso Spring using COP method

4.3.1 Discretization of the study area

The vulnerability of karst aquifer feeding the Pertuso Spring has been evaluated applying COP method, which focuses on the key role of karst features, responsible of the aquifer natural protection and of its pollution decreasing. Numerous techniques have been used to perform to display the various components of the vulnerability assessment, normally following advances in the allied fields of computer, graphic, and statistical sciences. The traditional vulnerability assessment approaches use, generally, grid-cell based systems and Geographic Information System (GIS).

In the study area, where the well-developed karst features are responsible of the fast rainfall infiltration in the saturated zone and, consequently, of the high discharge rate of Pertuso Spring, the location and the spatial distribution of karst features are very useful data which can influence the vulnerability assessment.

For this reason, every concentrated recharge zone has been identified with the main karst features detectable from satellite images (Fig. 4.4) and about 50 different karst features in the hydrogeological basin have been plotted in GIS using polygons.

With the aim of carrying on a comparative evaluation of vulnerability assessment, in this study COP method has been applied starting from two different discretization approaches of the hydrogeological basin: Finite Square Elements (FSE) of 250 m per side and polygonal layers. The polygonal layers are the result of an overlapping of two layers (Fig. 4.5): the direct recharge area related to the karst features, where a possible contaminant may, directly, reach the aquifer with reasonable certainty (50 polygons), and the outcropping geology (22 polygons).

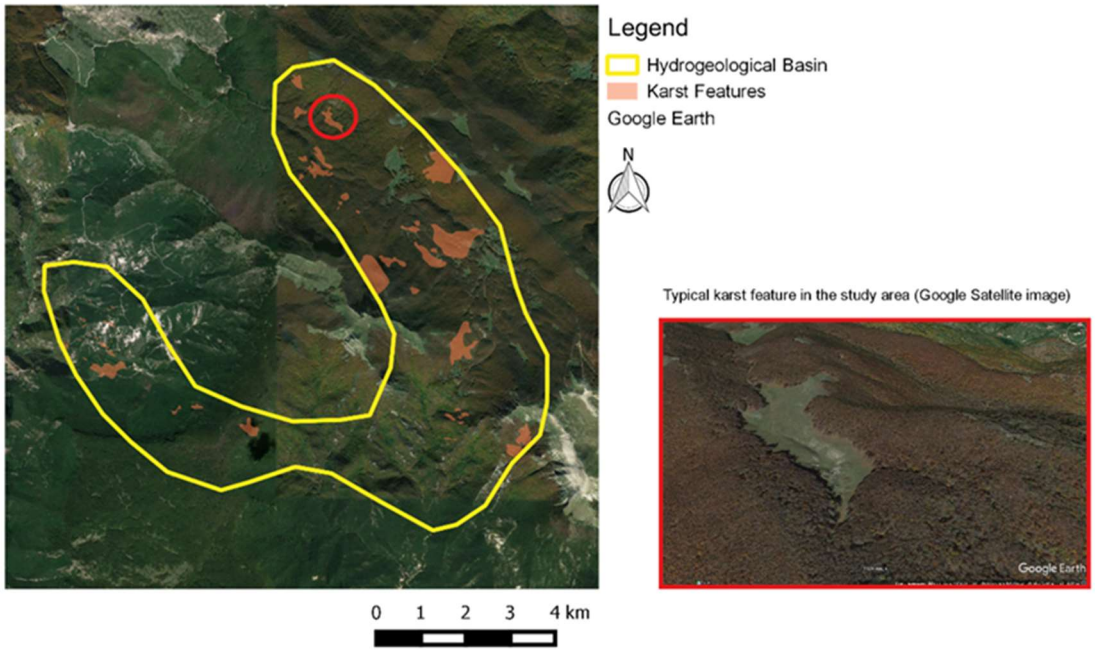

Figure 4.4 Karst features detection in the study area

Figure 4.5 Polygonal layers discretization of the study area

4.3.2 Required data

The vulnerability assessment is based on the background data coming from previous studies [49,50] and the compilation of the information collected from various technical reports about the catchment area of the Pertuso Spring [29] (Tab. 4.1). Data analyses and model implementation were processed with QuantumGIS software.

Table 4.1 Data (type, reference and format) used for the vulnerability assessment

Data	Reference	Type
Precipitation	Rome Hydrographic Office Abruzzo Region and Rome Hydrographic Office	Table
Temperature	Abruzzo Region Hydrographic Office	Table
Geology	Italian Geological Survey and drilling profiles	Map/Digital
Topography (slope)	Digital Elevation Model (DEM) Sapienza University of Rome	Digital
Land use and land cover	Lazio and Abruzzo Region ISPRA (http://www.sinanet.isprambiente.it)	Digital
Karst features	Identified from aerial photographs and satellite images	Digital

Regarding to the evaluation of C factor, in this study, Scenario 1 has been applied in the higher permeability areas (karst features) and Scenario 2 in the lower permeability ones (aquifer lithology). The slope and vegetation (*sv*) came out from the Digital Elevation Model (DEM) elaborated by QGIS, divided into 4 classes of percentage (≤8%, 8% ÷ 31%, 31%÷75% and >75%), to which scores have been assigned, respectively from 0.75 to 1. Based on the land cover maps provided, land use has been divided into two main types, mainly "no vegetation" and "vegetation". In this study the distance to swallow holes (*dh*), consisting of a series of buffer zones whose thickness has been defined, was not considered because the whole area, located around each karst feature was assumed to be characterized by high vulnerability. According to the absence of sinking streams, it has been given the value 1 to the parameter (*ds*) referred to the distance to fast communication to groundwater. Ratings from 0.5 to 1 have been assigned to the surface features parameter (*sf*) according to the existing surface geology. The O_S and O_L factors have been obtained using geological map and drilling profiles of the study area [29].

Precipitation data of four meteorological stations located nearby the study area, from 1992 to 2012, were used to calculate the average annual rainfall (MPAM) for each station (Tab. 4.2). At last, a linear relation between the elevation and the average annual rainfall module was obtained in order to assign to each FSE a precipitation value (as explained in Section 3.3).

Table 4.2 Rainfall data about four different meteorological stations in the study area

Meteorological station	MPAM (mm/year)	Elevation (m a.s.l.)	Rainy days
Vallepietra	1346.78	825	91
Filettino	1647.00	1062	107
Carsoli	1053.25	640	100
Subiaco (Santa Scolastica)	1147.88	511	100

4.3.3 Application of the COP method

4.3.3.1 C factor

The two C factor maps generated using FSE and polygon discretization are shown in Figs. 4.6 and 4.7. The C factor presents score values ranging between very high to very low, with values ranging between 0 and 0.9. It is very low (≤ 0.2) in the higher permeability area (karst features), whereas it is very high (0.9) in non-karstic terrains, such as pudding stone, conglomerate, alluvial soil. As a matter of fact, the mapping results clearly show a sound difference in vulnerability values between FSE discretization and the polygonal layer one. The first one (Fig. 4.6) generally assigns a high vulnerability to the most part of the study area, whereas the second one assigns a moderate vulnerability value to the same part (Fig. 4.7).

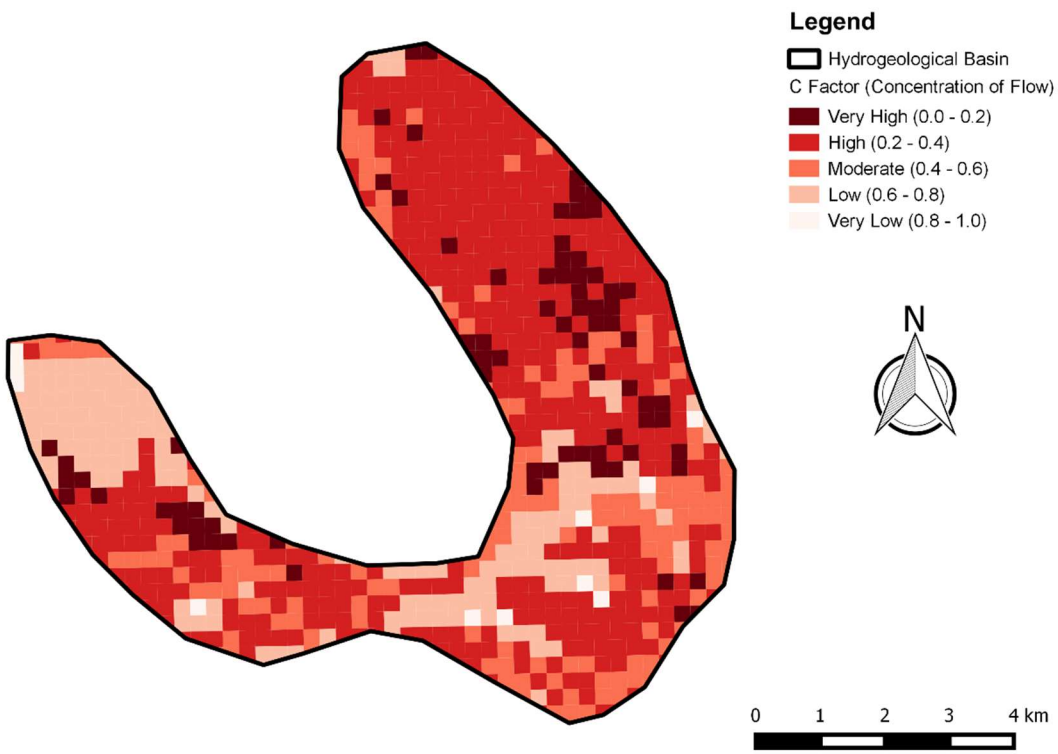

Figure 4.6 Map of the C Factor (FSE)

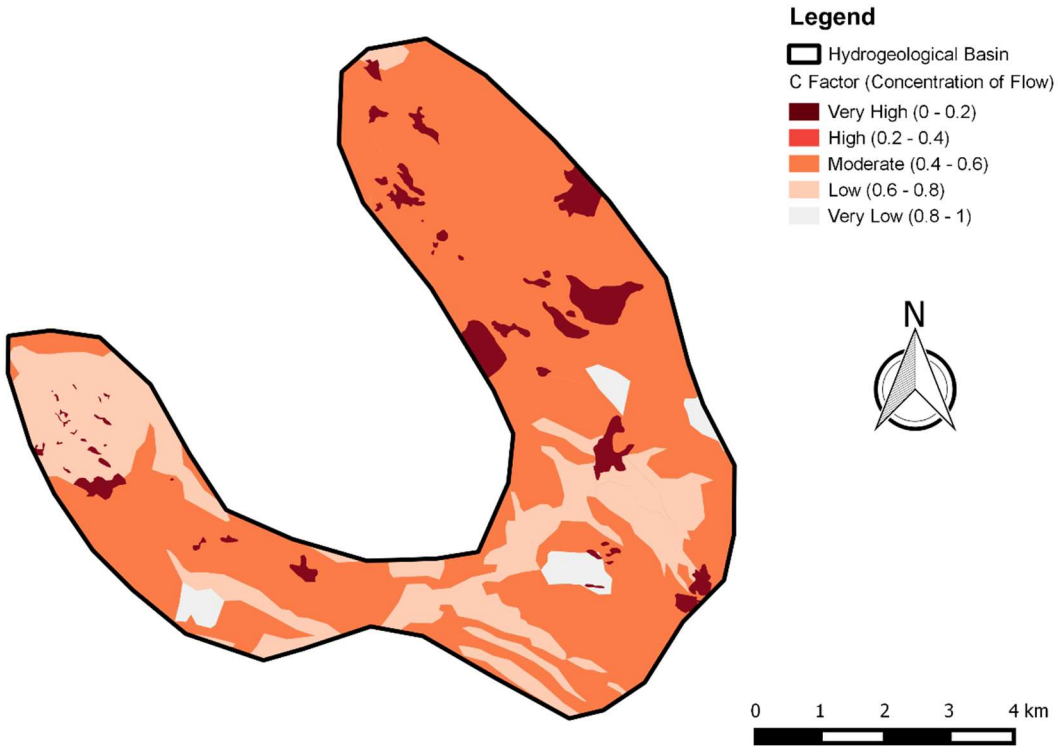

Figure 4.7 Map of the C Factor (polygonal layer)

This difference is related to the computation of the slope parameter (s). The terrain slope is a very important factor in vulnerability assessment because it defines the surface runoff as a part of precipitation, and thus determines the areas in which there is a greater possibility for contaminants to infiltrate from the surface into the aquifer. The polygon discretization, averaging slope values on very

wide areas, lead to the evaluation of lower values of the slope parameter than the FSE ones, which allows a better precision, but does not allow a clear identification of fast recharge areas due to karst features.

4.3.3.2 O factor

The O factor maps generated using FSE and polygon discretization are shown in Figs. 4.8 and 4.9.

Figure 4.8 Map of the O Factor (FSE)

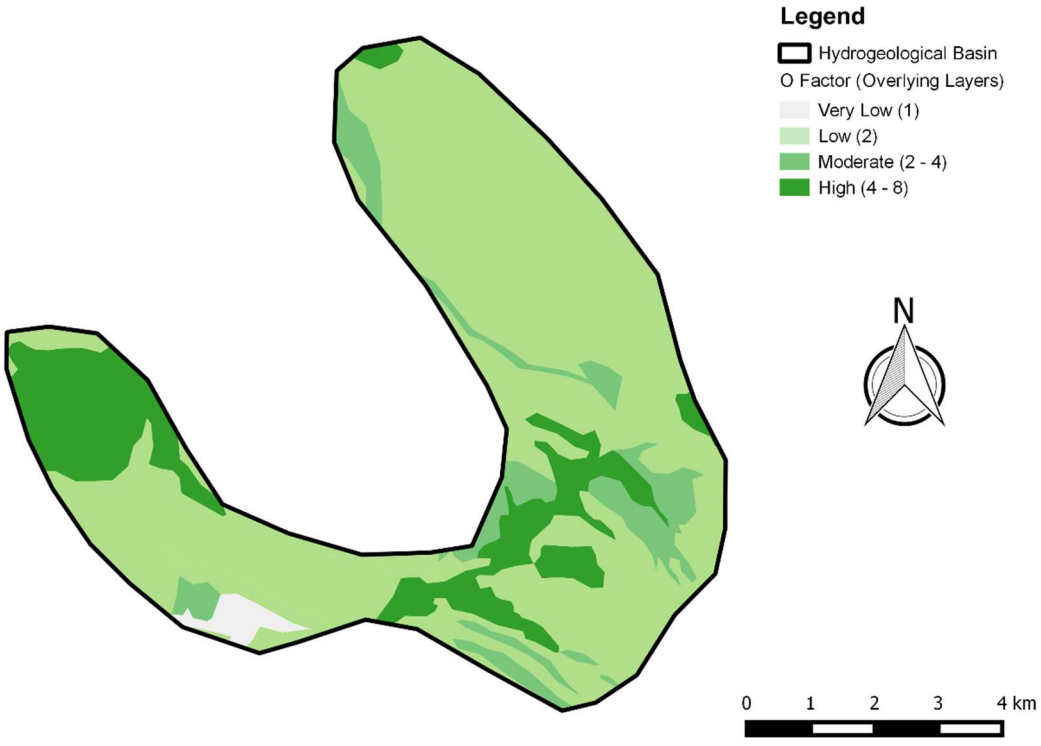

Figure 4.9 Map of the O Factor (polygonal layer)

The higher protection areas are related to the presence of conglomerates and pudding stones, which have a weaker state of fracturing. On the contrary, the lower ones are due to the presence of carbonate rocks, which are the dominant geological formations, in the study area, and present the highest fracturation. Hence, the O factor is low in most of the study area.

As it is shown in Fig. 4.8 and Fig. 4.9, there are no remarkable differences between the two-discretization approaches, but the FSE discretization method seems to give a more gradated output referring to this parameter. On the other hand, karst features have no impact on the O factor and, consequently, most part of the area presents the same protection values in both maps.

4.3.3.3 P factor

P factor has been obtained using a linear relation, between elevation and average annual rainfall as explained in Section 3.3. The number of rainy days in the study area ranges from a minimum of 91 to a maximum of 107 days per year, based on the analysis of precipitation data over a time series that goes from 1992 to 2012 (Tab. 4.2). The average value is 100 rainy days per year.

P factor ranges between 0.6 and 0.8. Most part of the study area present a high value (dark blue) in both maps (Figs. 4.10 and 4.11). In particular, the polygonal layer discretization approach leads to obtain an enhanced coverage of high value. The reduction of protection is generally high (0.6) in mountain areas, because even if the precipitation quantity P_Q is higher there due to elevation values, the much wider temporal distribution is a key factor for contaminant transport and implies a decreasing protection.

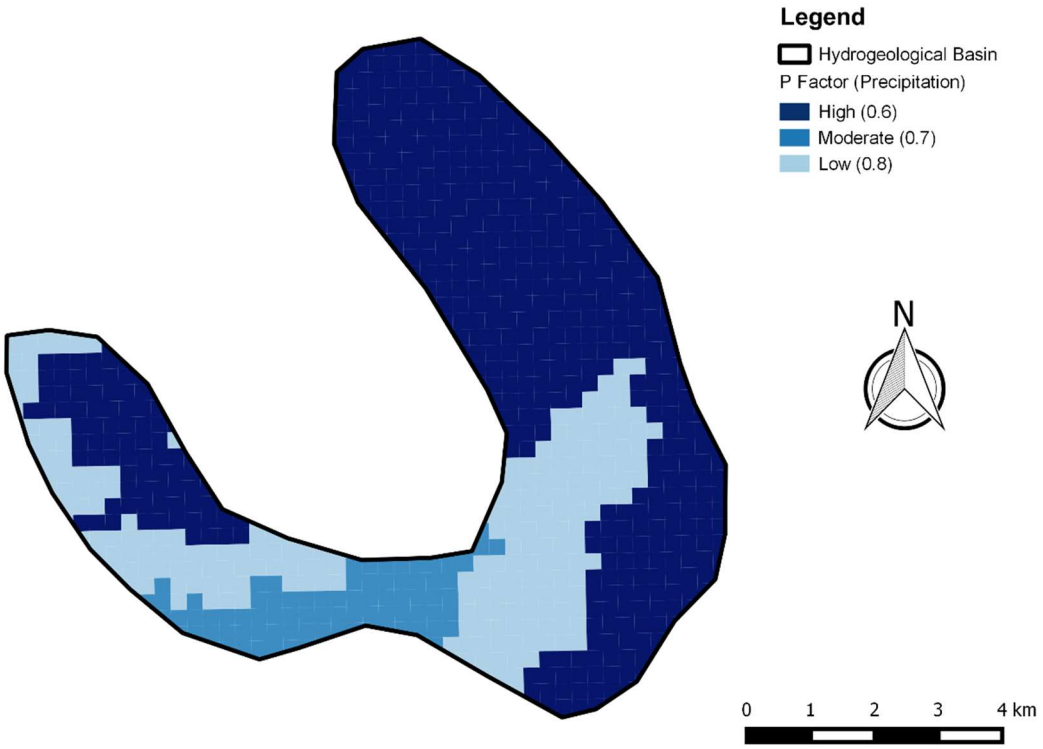

Figure 4.10 Map of the P Factor (FSE)

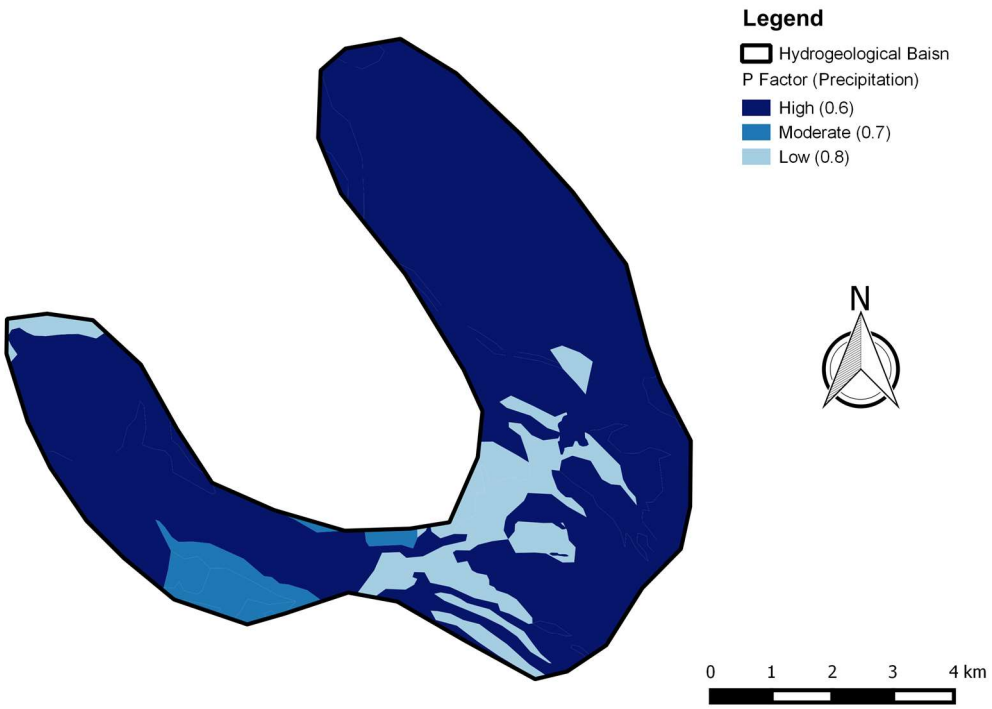

Figure 4.11 Map of the P Factor (polygonal layer)

4.3.3.4 COP Index

Finally, the COP maps were obtained by overlaying the O, C and P maps and from the product of their scores. Figures 4.12 and 4.13 show the results of COP method in the hydrogeological basin of the Pertuso Spring, respectively for FSE and polygonal discretization.

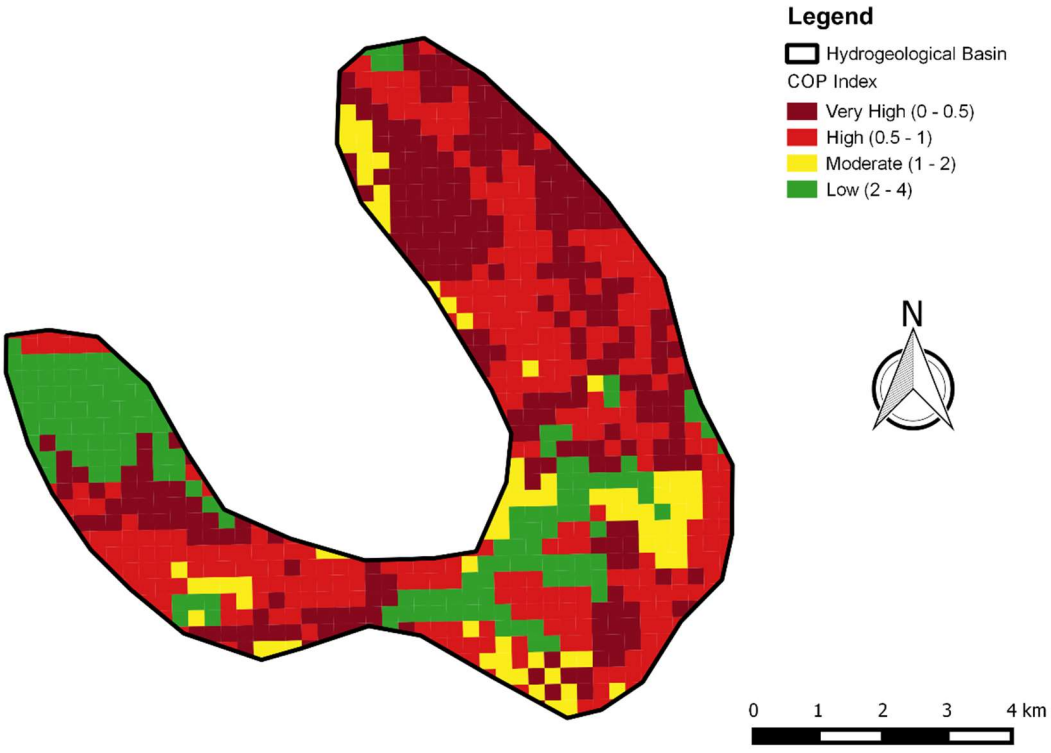

Figure 4.12 Map of the COP index (FSE)

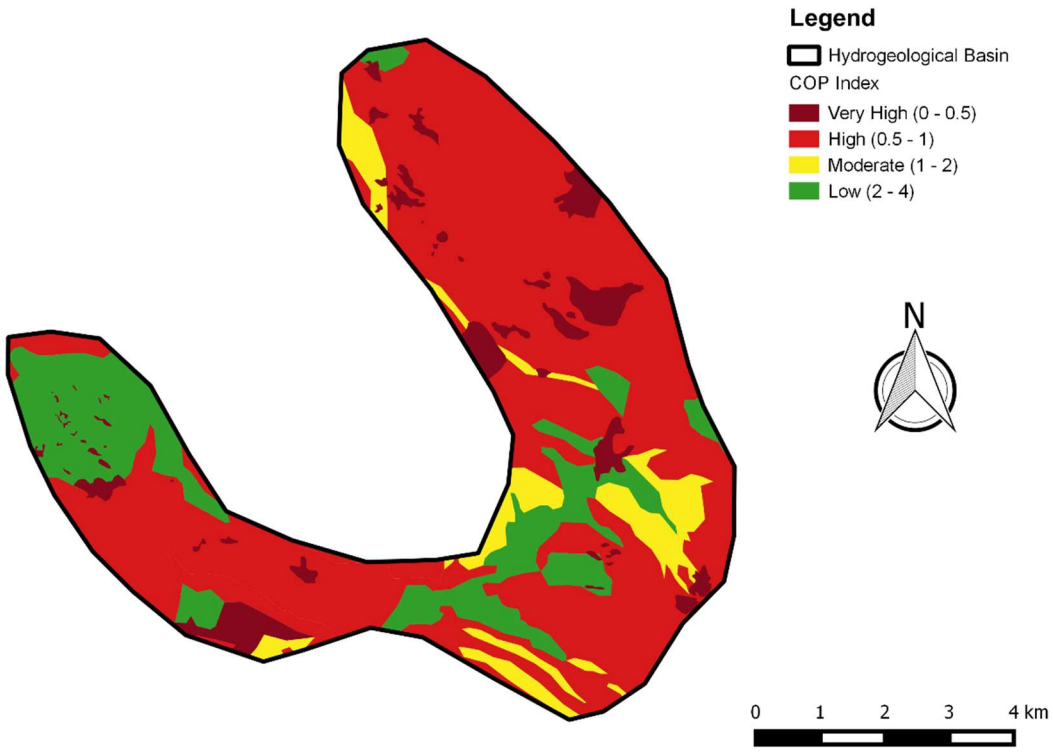

Figure 4.13 Map of the COP index (polygonal layer)

The results obtained by COP vulnerability method, applied to Finite Square Elements and polygonal layer, show different vulnerability degrees for several areas within the hydrogeological basin. As expected, the COP vulnerability maps show generally the dominance of high vulnerability classes (shades of red) in the northern part of the basin, while the south-east and western part are characterized by low vulnerability class (shades of green) and moderate class (shades of yellow). There is no very low vulnerability class. Details in percentages of area for each vulnerability class are given in Fig. 4.14.

The karst features, present in the study area, have been classified with the very high vulnerability degree (Very High: 0-0.5), due to the presence of swallow holes and dolines, that decreases the residence time of water in the unsaturated zone, reducing the potential attenuation capacity of the aquifer. This highest class of vulnerability index is due to the absence of an impermeable covering layer, which allowed rapid infiltration towards the saturated zone (C factor).

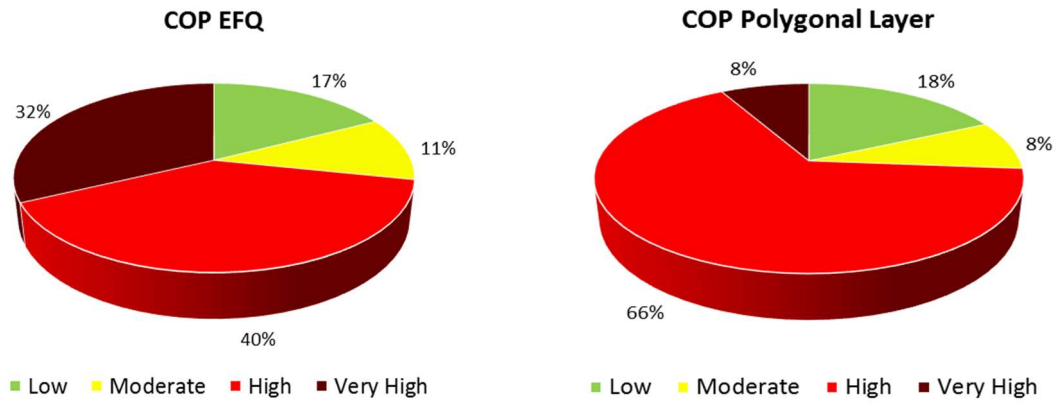

(a) (b)

Figure 4.14 COP indexes percentage distribution: FSE (a) and polygonal layer (b)

The low vulnerability class (Low: 2-4) covers similar percentages of the study area (17% and 18%) (Fig. 4.14), mainly in the outcropping pudding stone, conglomerate and alluvial soil. In these areas, the low permeability of cover layers and the slope gradient are responsible of an increase of C and O factors and, consequently, of a vulnerability reduction.

The moderate vulnerability class (Moderate: 1-2) covers not more than 8 and 11% of the Pertuso Spring hydrogeological basin, respectively for polygonal layer and FSE discretization approaches (Fig. 4.14). In these areas dolomitic limestone, compact limestone with dolomite and crystal dolomite outcrop, decreasing the protective capacity assigned to the unsaturated zone by the O factor.

The COP method assigns the high vulnerability degree (High: 0.5-1) to most part of the study area. This result is due to the presence of the karstified Cretaceous limestone outcropping. Vulnerability maps obtained for both discretization approaches, result to be different just in the high and very high vulnerability degree assignment. The FSE discretization approach leads to a 32% of very high and 40% of high vulnerability rates, whereas in the polygonal layer discretization approach there is a lower presence of areas with the very high degree (8%) and a higher presence of areas with the high one (66%). This difference depends on the choice of using a polygonal layer, that allows to identify more precisely karst features and fast recharge area, giving the potential contamination risk only to these areas and not to the rest. In this discretization hypothesis, karst features have a key-role for the C factor evaluation and their presence is predominant to each other consideration about vulnerability assessment. The FSE discretization approach, on the contrary, generally assigns COP index rates taking into account the lithology, the karst setting and the elevation, at the same level. As a consequence of it, in this case, a wider area of the whole basin has been considered very high vulnerable and the potential contamination risk result to be spread all over the study area, even out of karst features.

A comparison between the FSE discretization approach and the polygonal layer one is necessary for better understanding which one is more suitable to the specific case study.

As to be expected, in a karst setting like the Pertuso Spring hydrogeological basin area, the presence of highly fractured rocks and most of all the specific permeability conditions, due to the local karst processes development, cause a spread high vulnerability degree to contaminants.

Even if the FSE discretization approach leads to a more precautionary vulnerability assessment in the study area, the polygonal layer shows a greater accuracy, identifying the areas actually interested by karst processes at local scale and giving the higher vulnerability rate only to these ones. This choice allows to better highlighting protection areas, in order to protect groundwater quality. At the same time, the polygonal layer discretization approach needs a very detailed work, based on the detection and the outline representation of any karst features. The visual detection and the graphic reconstruction of the areas, where karst features outcrop, is today easier to carry out, thanks to the remote sensing and the geographic information system (GIS) software. This process is strongly recommended for small basins as the Pertuso Spring one, but it may result to be not always suitable, above all in case of very wide areas [51,52].

CHAPTER 5

THE ENVIRONMENTAL MONITORING PLAN OF THE PERTUSO SPRING

5.1 Introduction

This paper outlines the results of the first three years of the Environmental Monitoring Plan, applied to the catchment project of the Pertuso Spring, which is going to be exploited to supply an important civil water network in the South part of Roma district, in Central Italy.

Groundwater coming from the Pertuso Spring is currently used for hydroelectric purposes by ENEL Green Power S.p.A. as part of the hydroelectric system of the Upper Valley of the Aniene River. In particular, spring groundwater and Aniene River surface water are carry out to the Comunacqua power plant through a hydroelectric tunnel of about 6 km in length.

On 28 June 2002, a Legislative Decree of the President of the Council of Ministers has established the drought emergency state of the municipalities in the south part of Roma district. For this reason, the Pertuso Spring, since 2002, also supplies, by a provisional work, the Simbrivio Aqueduct, for a maximum of 360 l/s, in addition to the volumes not available from Simbrivio historical springs. The aim of this catchment project is to deal with the water emergency through the construction of the works for catching groundwater coming from Pertuso Spring, in order to integrate the water resource available for network powered by the New Aqueduct Simbrivio-Castelli (NASC). The water shortage of the Simbrivio aqueduct system is due to the reduction of water resources, related with a decrease in rainfall trend of recent years and, on the other hand, to an increase in water demand.

In 2002 summer, the huge water shortage has been reduced using the existing hydroelectric tunnel of about 4.4 km to move Pertuso Spring groundwater (360 l/s) to a tunnel access window, from which a DN600 steel pipe is delivered to the Ceraso booster system with a length of about 2 km.

This solution provides the exclusive use of the hydroelectric tunnel for drinking supply, losing the energy production related with both the Pertuso Spring groundwater and Aniene River surface water.

In order to reduce costs and make this spring independent from the plant owned by ENEL group, in the program of actions to resolve the state of drought emergency was included a catchment work project of the Pertuso Spring allowing an increasing groundwater transfer from 360 to 690 l/s.

The target of this Environmental Monitoring Plan is to set up the background framework on the hydromorphological, physico-chemical and biological properties of water resources in the water basin, influenced aim by any potential environmental impact due to the construction activities. The aim of the

Environmental Monitoring is to ensure hydrogeological data about (i) temporal and spatial variations in groundwater and surface water levels, (ii) temporal and spatial variations in groundwater and surface water quantity and quality and (iii) impacts due to the drainage of groundwater through the Druni Hill tunnel and the interaction with surface water linked with groundwater.

Thus, according to the Legislative Decree 152/2006, as modified by D.M. 260/2010, the Environmental Monitoring Plan suggested to characterize the most important environmental components (i.e. surface water and groundwater) of the Upper Valley of the Aniene River for the evaluation of the environmental parameters during survey, excavation and post-excavation phase of the project. For this reason a long-term water quantity and quality monitoring has been established in the study area [30].

5.2 The catchment project of the Pertuso Spring

The definitive design of the catchment work includes the construction of an aqueduct, long about 6.1 km, inside the Upper Aniene River Valley, form the Pertuso Spring to the Ceraso booster plant.

These works are, moreover, part of a wider design, aimed to move groundwater coming from the Pertuso Spring up to the Altipiani di Arcinazzo from which the resource will feed the municipalities powered by the Simbrivio Aqueduct. In particular, the project provides:

- a pipeline (DN1000mm) to transfer the Pertuso Spring groundwater to the Ceraso plant
- a booster system adjacent to the Ceraso plant to move groundwater towards the Altipiani di Arcinazzo
- a pipeline (DN600mm) for the connection between the booster and the New Aqueduct Simbrivio-Castelli (NASC)
- a reservoir at the Altipiani di Arcinazzo.

The catchment project of the Pertuso Spring is shown in Fig. 5.1.

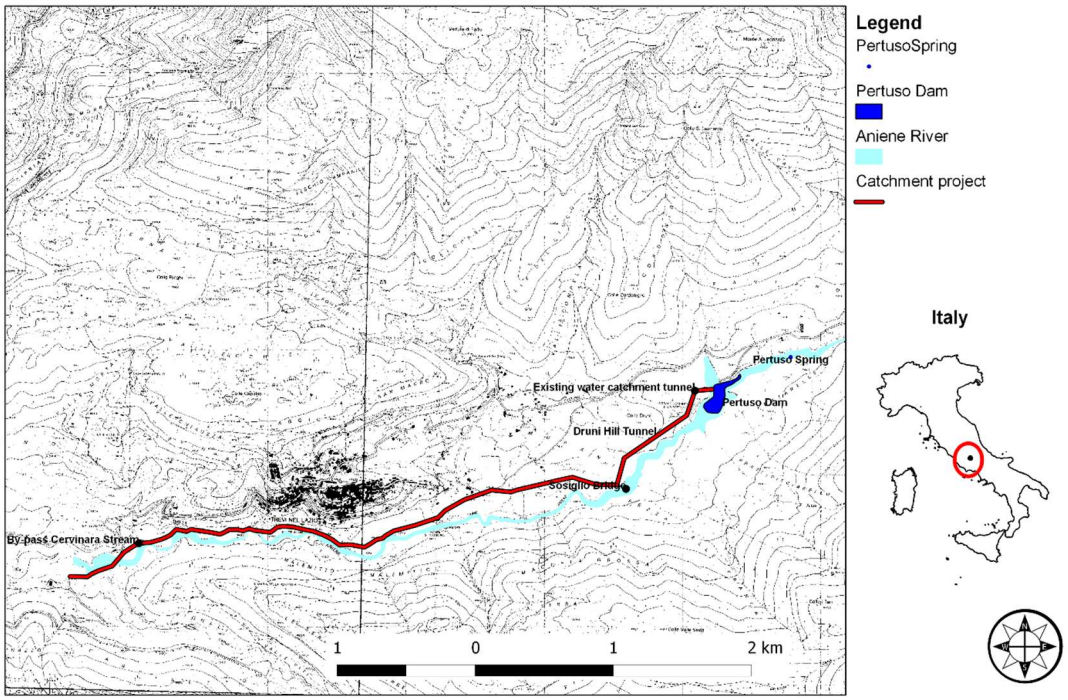

Figure 5.1 Catchment project of the Pertuso Spring

The catchment design includes:

- a first section from Pertuso Dam to Sosiglio Bridge, characterized by the excavation with TBM of a tunnel in Druni Hill (Construction site 1)
- second one, from Sosiglio Bridge to Cervinara Stream, in open excavation, until the intersection with the existing conduct which leads to the Ceraso hydroelectric power plant (Construction site 2).

5.3 Monitoring network design

The design of groundwater and surface water monitoring network must consider the targets of the monitoring program and it is set up to meet rule requirements and to collect data to build the conceptual model of the hydrogeological system.

For this reason, in the study area, a monitoring network has been set up to assess the karst aquifer - Aniene River hydrodynamics properties (Fig. 5.2).

The recommendation for monitoring in karst aquifer is to focus on the sensitive connections between surface water and groundwater. Thus, the representative monitoring points are chosen as representative of the hydrogeological conceptual model, with regard to groundwater flow and its interaction with surface water [30]. In particular, the monitoring stations, selected for the enhancing of the Environmental Monitoring Plan of the karst aquifer, feeding the Pertuso Spring were chosen according to:

- Lithologic characteristics: texture, structure, mineralogy, stratification and thickness.
- Hydrogeological characteristics: hydraulic conductivity, porosity and hydraulic gradient.
- Aquifer characteristics: boundaries, type of aquifer, saturated/unsaturated conditions, and occurrence and distribution of multiple aquifers.
- Presence of surface water bodies on, or adjacent to, the study area (Aniene River).

This monitoring network are been designed with the aim to (i) minimize the number of monitoring stations and (ii) maximize the probability of detecting any potential environmental impact due to the construction activities.

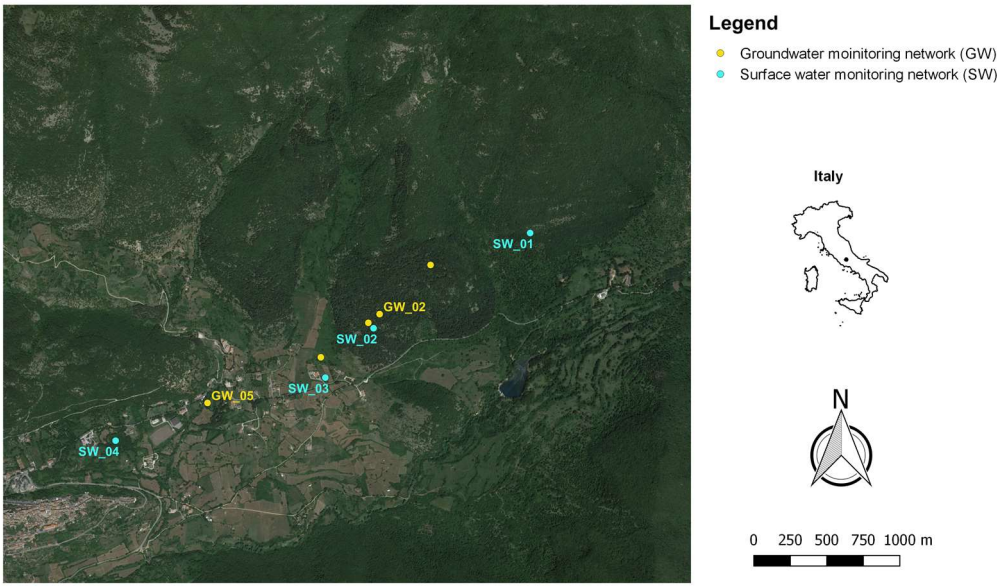

Figure 5.2 Location of groundwater and surface water monitoring stations

The monitoring network has been used to provide baseline hydrogeological conditions and temporal changes in groundwater and surface water conditions prior to project development. This network has been monitored in the long term (before construction activities) to provide ongoing measurement of quality and quantity, including temporal and seasonal changes. Long-term water monitoring has been carried on several monitoring stations, chosen according to the importance and the significance of the each environmental component (groundwater and surface water), depending on the conditions for accessibility. For this reason, the groundwater monitoring network includes four existing piezometers (GW_02, GW_03, GW_04 and GW_05) [29]. The Aniene River basin is characterized by a complex network of catching and reservoirs, which does not allow a direct evaluation of the average annual recharge of this system [53]. Thus, to assess quantitative and quality alterations of the karst aquifer feeding the Pertuso Spring, an additional groundwater monitoring station (GW_01) has been installed in the spring to evaluate the undisturbed conditions upstream the karst aquifer. GW_02 (Fig. 5.3a) and GW_03 (Fig. 5.3b) monitoring stations were chosen as representative of aquifer conditions downstream the construction of Druni Hill tunnel, while GW_04 (Fig. 5.4a) and GW_05 (Fig. 5.4b) are site respectively upstream and downstream the second construction site, in order to monitor groundwater quantity and quality (Tab. 5.1) [30].

(a) (b)

Figure 5.3 Groundwater monitoring points downstream the first construction site GW_02 (a) and GW_03 (b)

(a) (b)

Figure 5.4 Groundwater monitoring points upstream GW_04 (a) and downstream GW_05 (b) the second construction site

The surface water monitoring network includes four specific river sections along the Aniene River, referred, each one, to the two construction sites. These sections has been chosen followed these criteria as possible:

- cross section lies within a straight reach, and streamlines are parallel to each other
- velocities are greater than 0.15 m/s and depths are greater than 0.15 m
- streambed is relatively uniform and free of numerous boulders and heavy aquatic growth
- flow is relatively uniform and free of eddies, slack water, and excessive turbulence

SW_01 (Fig. 5.5a) and SW_03 (Fig. 5.5b) are designed to control environmental conditions upstream each construction site, while SW_02 (Fig. 5.5c) and SW_04 (Fig. 5.5d) are designed to control the same conditions downstream each of them, along the Aniene River stream (Tab. 5.1) [30].

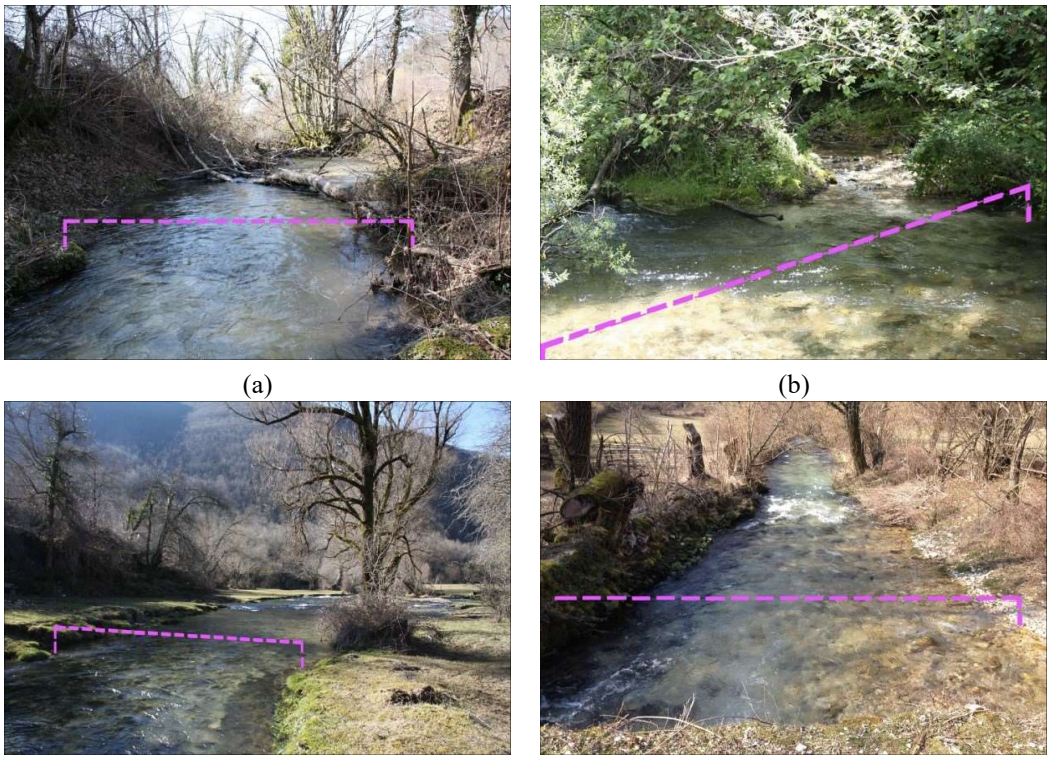

(a) (b) (c) (d)

Figure 5.5 Surface water monitoring points SW_01 (a), SW_02 (b), SW_03 (c) and SW_04 (d)

Table 5.1 Main characteristics of the monitoring stations

Monitoring Station		Latitude N	Longitude E	Type & Location
Groundwater	GW_01	41°52'14.94"	13°16'54.42"	spring (upstream 1° construction site)
	GW_02	41°52'4.08"	13°16'39.30"	piezometer (downstream 1° construction site)
	GW 03	41°52'2.16"	13°16'39.30"	piezometer (downstream 1° construction site)
	GW_04	41°51'54.54"	13°16'21.84"	piezometer (upstream 2° construction site)
	GW_05	41°51'44.46"	13°15'48.48"	piezometer (downstream 2° construction site)
Surface water (Aniene River)	SW_01	41°52'22"	13°17'24"	upstream 1° construction site
	SW_02	41°52'0.96"	13°16'37.50"	downstream 1° construction site
	SW_03	41°51'51"	13°16'26"	upstream 2° construction site
	SW_04	41°51'36.12"	13°15'20.88"	downstream 2° construction site

5.4 Methodology

5.4.1 Water samples collection

Because of the interconnection of matrix, fractures, and conduits network, karst aquifers are extremely heterogeneous and have peculiar hydraulic and chemical properties, which are highly scale dependent and temporally variable [54]. For this reason, the Environmental Monitoring Plan involves collecting samples of surface water and groundwater for quantitative and quality characterization of the karst aquifer feeding the Pertuso Spring.

The Environmental Monitoring target is to set up the environmental state and quantitative and quality analysis of temporal water trends for the evaluation of potential interactions between project design and karst aquifer. The aim of this monitoring plan is to build a background framework on the hydromorphological, physico-chemical and biological properties of groundwater and surface water resources in the aim to prevent and evaluate any potential environmental effect coming from the construction activities.

Surface water and groundwater samples for major dissolved species and trace elements analysis concentration (Tab. 5.2) were collected applying standard techniques [55,56].

Table 5.2 Water quality monitoring parameters

Typology	Parameter	Unit	Surface water	Groundwater
In Situ Parameters	Water Temperature	°C	x	x
	Dissolved Oxygen	mg/l	x	x
	Conductivity	µS/cm	x	x
	pH	-	x	x
	Flow	m^3/s	x	x
Laboratory Parameters	Turbidity (residue at 105°C and 550°C)	mg/l		x
	Total Suspended Solids	mg/l	x	
	Total Hardness	mg/l $CaCO_3$	x	x
	Bicarbonates (Temporary Hardness)	mg/l		x
	Bicarbonate Alkalinity	mg/l		x
	Carbonate Alkalinity	mg/l		x
	Bicarbonate Ion	mg/l		x
	Total Nitrogen	N µg/l	x	
	Ammonia Nitrogen	N µg/l	x	x
	Nitrate Nitrogen	N µg/l	x	x
	Nitrous Oxide	µg/		x
	BOD5	O_2 mg/l	x	
	COD	O_2 mg/l	x	
	Orthophosphate	P µg/l	x	
	Total Phosphorus	P µg/l	x	x
	Chloride	Cl^- µg/l	x	x
	Non-ionic Surfactants	µg/l		x
	Anionic Surfactants	µg/l		x
	Colour	µg/l		x
	Odour	µg/l		x
	Sodium	µg/l		x
	Calcium	µg/l		x
	Potassium	µg/l		x
	Magnesium	µg/l		x
	Sulphates	SO_4^{2-} µg/l	x	x
	Boron	µg/l		x
	Free Cyanide	µg/l		x
	Fluorides	µg/l		x
Metals	Cadmium	µg/l	x	x
	Total Chromium	µg/l	x	x

Typology	Parameter	Unit	Surface water	Groundwater
Metals	Chromium Vi	µg/l		x
	Mercury	µg/l	x	x
	Nickel	µg/l	x	x
	Lead	µg/l	x	x
	Copper	µg/l	x	x
	Zinc	µg/l	x	x
	Aluminium	µg/l		x
	Antimony	µg/l		x
	Silver	µg/l		x
	Arsenic	µg/l		x
	Beryllium	µg/l		x
	Cobalt	µg/l		x
	Iron	µg/l		x
	Selenium	µg/l		x
	Manganese	µg/l		x
Organic Compounds	Aldrin	µg/l	x	
	Dieldrin	µg/l	x	
	Endrin	µg/l	x	
	Isodrin	µg/l	x	
	DDT	µg/l	x	
	Benzene	µg/l		x
	Ethylbenzene	µg/l		x
	Styrene	µg/l		x
	Toluene	µg/l		x
	Para-Xylene	µg/l		x
	Hexachlorobenzene	µg/l	x	
	Hexachlorocyclohexane	µg/l	x	
	Hexachlorobutadiene	µg/l	x	
	1,2-Dichloroethane	µg/l	x	
	Trichloroethylene	µg/l	x	
	Trichlorobenzene	µg/l	x	
	Chloroform	µg/l	x	
	Carbon Tetrachloride	µg/l	x	
	Perchloroethylene	µg/l	x	
	Pentachlorophenol	µg/l	x	
	Hydrocarbons C> 12	µg/l		x
	Hydrocarbons C <12	µg/l		x
	Total Hydrocarbons	µg/l		x
	BTEX Hydrocarbons	µg/l		x
	Methyl Tert-Butyl Ether MTBE	µg/l		x
	Total Polycyclic Aromatic	µg/l		x
Microbiological Parameters	Escherichia Coli	UFC/100 ml	x	x

Water samples were stored at 4°C until analysis in the Elabori S.p.A. Laboratory of Rome. Laboratory analysis were carried on by a certified water testing procedure for chemical-physical, organic, inorganic, and microbiological parameters, following D.L. 152/2006 prescriptions.

Properties such as temperature (T), electrical conductivity (EC), pH, dissolved-oxygen (DO), static water level and stream flow were measured directly in the field before the water sample collection.

All field instruments were calibrated according to manufacturer's recommendations prior to being taken into the field. Calibration standards were selected based on historic data for best instrument accuracy.

The environmental monitoring instruments used for field investigations are shown in Tab. 5.3.

Table 5.3 Monitoring instruments used for water quality filed investigations

Date	Instruments	Parameters
July 2014	PC 650 Eutech Instruments KLL-Q Seba Hydrometrie	T, pH, EC DO
November 2014	HI 9813-6 Hanna Instruments LDO 10101 HACH	T, pH, EC DO
January 2015 May 2015 December 2015 May 2016 November 2016	HI 9813-6 Hanna Instruments LDO 10101 HACH	T, pH, EC DO

5.4.2 Sampling frequency

The water sampling survey was carried on during the first three years of the Environmental Monitoring Plan, from July 2014 to November 2016. The sampling frequency depends on the monitoring purposes, established by the Environmental Monitoring Plan (D.M. 260/2010). However, a more detailed sampling frequency is required for supervisory and operating monitoring, while a low sampling frequency (1/year) could be enough for survey monitoring, if any trouble would have come out during previous monitoring phases. The frequency sampling is related to the aim of set up the hydrogeological conceptual model of the karst aquifer. As a consequence of it, groundwater and surface water have been monitored seasonally (4/year) for the first year of monitoring and twice a year the other ones (Tab. 5.4), to assess seasonal and natural fluctuations.

Table 5.4 Sampling frequency for groundwater and surface water

Monitoring Stations	Date	Samples (n°)
Groundwater	July 2014	4
	November 2014	5
	January 2015	3
	May 2015	3
	December 2015	3
	May 2016	3
	November 2016	3
Surface water	July 2014	4
	November 2014	4
	January 2015	4
	May 2015	4
	December 2015	4
	May 2016	4
	November 2016	4

5.4.3 Groundwater monitoring

The target of groundwater sampling is to take some quantity of water that represents groundwater chemical and physical properties in the study area, referred to any season, in any monitoring period. To obtain a representative sample it is necessary to remove the stagnant water from the well, immediately prior to sampling, causing its replacement by groundwater from the adjacent formation that is representative of actual aquifer conditions. Prior to initiating the purge, the amount of water standing in the water column (water inside the well riser and screen) was determined using the diameter of the well, the water level and total depth of the well [57]. With respect to volume calculated, before collecting groundwater samples, the boreholes were purged removing five well volumes of water were purged (Fig. 5.6).

The static water level in well was determined by a water level sounder (OTR 100m).

(a) (b)

Figure 5.6 Well purging procedures for obtaining valid water samples from monitoring wells: before (a) and after (b) three well volumes removing (GW_02, May 2016)

5.4.4 Stream discharge measurements

Stream discharge and water quality parameters such as turbidity, dissolved oxygen, water temperature and electric conductivity monitoring is important to have a referring trend, along the year, of these values range and to be ready to evaluate potential modifications due to construction activities.

Discharge is an important parameter that influences many aspects of stream function, such as habitat diversity and rates of nutrient export. The measurement of stream flow rate is also a direct measure of the amount of water available to meet instream and extractive water uses and is usually required for river management purposes including water resources planning and protection of flood prevention.

Stream flow measurement technology has evolved rapidly over recent decades. The most common approach to discharge measurement is the velocity-area method, which involves measuring water depth and velocity at some points across a stream section with a current meter. According to the U.S. Geological Survey (USGS) procedure, river discharge can be usually calculated by the velocity area method, as the product of average stream flow velocity at a cross section, perpendicular to the main stream flow, and the cross sectional area. In this method, the river section is divided into sectors and the discharge through each sector is calculated by multiplying the average velocity in each sector by its area. A current meter is usually used to measure the stream velocity at each selected sector. The sum of the products of velocity for each sector area gives the total stream discharge [58].

The conventional velocity area method has some limitations in mountains stream where the irregular cross section and the strong turbulence decrease the accuracy with which water depth and flow velocity can be measured. In addition, flow depths and velocities during low flow conditions may be too small for reliable measurements [59]. This method is also both expensive and difficult, especially during floods or unsteady flow conditions, due to the instability of measuring instrument. The unsteady flow may be caused by turbulent conditions, irregular bed stream geometry and the growth of weeds. Thus, the current meter method requires a definitive relationship between velocity measurement and area of the cross section, which is difficult to establish in mountain river, where the hydraulic pattern changes seasonally (Fig. 5.7). This method is generally used because is the most friendly and quick for stream flow measurements, except where the river is very shallow or in turbulent condition. Thus, under such

conditions, the alternative method of salt dilution may be more suitable [60].

Salt dilution method can be effective, where current metering would not be accurate, and vice versa, so the techniques are complementary. In this method, a tracer solution is injected into the river to be diluted by the stream discharge. Downstream of the injection point, when vertical and lateral dispersion throughout the flow is complete, the discharge may be calculated by the measurement of the electrical conductivity as a function of time. Common eatable salt (sodium chloride, NaCl) is generally used for salt dilution measurements, because it is cheap, easily available and non-toxic for the concentrations and exposure times, typically associated with discharge measurements.

The salt dilution method is generally used for discharge measurements in mountain streams, where swallow depths, turbulent conditions and the irregular geometry of the stream can make difficult to establish the hydraulic profile, and even difficult to measure stream flow velocity with the traditional current meter [61]. A limit of this methodology is the amount of tracer to be added to increase the electrical conductivity in the stream flow, which is related to the stream background level of the conductivity. Moreover, only a runoff less than $4 m^3 s^{-1}$ can be made easily, because the amount of salt to be dissolved is difficult to handle (about 20 kg of salt for 4 $m^3 s^{-1}$ runoff) [62].

For this reason, stream discharge, in the study area, has been carried out performing slug injections of a conservative tracer (NaCl) and recording electrical conductivity evolution in the monitoring station located along the Anine River, while at the same time, conventional current meter measurements have been taken the same gauging station to validate the experimental tests.

(a) (b)

Figure 5.7 SW_01 gauging station seasonally changes: July 2014 (a) and February 2015 (b)

5.4.4.1 Tracer dilution method

In the tracer dilution method for measuring discharge, a tracer solution is injected into the stream to be diluted by the discharge of the stream. The basic principle of salt dilution methods is to inject a conservative solute at some point along the stream, and to measure the tracer concentration in stream water at a downstream point, where the tracer has become uniformly mixed with the stream water. For a given volume or rate of injection, greater stream discharges will result in greater tracer dilution and lower concentrations measured at the downstream site. The computation of the stream discharge is obtained used equations based on the mass balance principle [63,64].

There are two variations on dilution gauging, depending on whether the tracer is injected into the stream at a constant rate or as an instantaneous slug. The first method, the constant-rate- injection method, requires that the tracer solution be injected into the stream at a constant flow rate for a period

long enough to achieve a constant concentration of the tracer in the streamflow at the downstream sampling cross section. The second method, the sudden- injection method, requires the instantaneous injection of a slug of tracer solution and an accounting of the total mass of tracer at the sampling cross section.

The most important hypothesis of the method are [65,66]:

- constant discharge (steady flow),
- no lateral inflows or outflows within the investigated reach;
- suspended load only (negligible bed load);
- minimal pools or backwater areas in general;
- complete vertical mixing and complete lateral spreading, which indeed occurs only after a certain distance called the complete mixing length

The basic principle of salt dilution method is to add instantaneously a known quantity of a NaCl solution into the stream and observe the variations in electrical conductivity at a point where it is fully mixed with the flow.

According to IS0 9555-1:1994(E) requirements [67] the salt dilution method involves the injection of a volume of a NaCl solution at a cross section in which the discharge remains constant for the duration of the gauging. At a second cross section placed downstream the injection point, at a distance sufficient for the injected solution to be uniformly diluted, the stream electrical conductivity is determined over a period of time sufficiently long to ensure that the NaCl solution has passed through the second cross section.

Electrical conductivity values (EC) must be therefore measured at very close intervals (a few seconds) in order to build the so called “breakthrough curve” representing the conductivity path over time. The choice of sodium chloride as a tracer comes from many factors: it is not expensive and easily available, its effects can be rather accurately and almost continuously measured using an electrical conductivity meter and it is nontoxic for the concentrations and residence times, usually detected, within the range of applicability of the method [68]. The procedure aimed to obtain a discharge estimation starts imposing the continuity of mass between the injection and the measuring section [69], according to equation (5.1):

$$M = \int Q \cdot C(t) dt \tag{5.1}$$

where M is the mass of tracer injected, Q the unknown flow and $C(t)$ the tracer concentration over time; hence, the discharge can be expressed by (5.2):

$$Q = \frac{M}{\int C(t) dt} = \frac{M}{A} \tag{5.2}$$

where A is the area under the graph of concentration over time [63] (Fig. 5.8).

During the salt dilution measurement, the background chloride concentrations in the stream were generally low and rises rapidly due to injection of the tracer solution, and then fell rapidly after the tracer pumping stopped (Fig. 5.8).

Since no direct measurement of tracer concentration is provided, it is anyway proved that an almost linear relation exists between conductivity and concentration value. The concentration can be then calculated by the equation (5.3):

$$C(t) = \left(\chi(t) - \chi_0(t)\right) \cdot \alpha \tag{5.3}$$

where $\chi(t)$ is the conductivity value, $\chi_0(t)$ is the baseline conductivity and α is the coefficient in the almost linear relation between conductivity and concentration, obtained in laboratory in standard conditions during the calibration of the instrument.

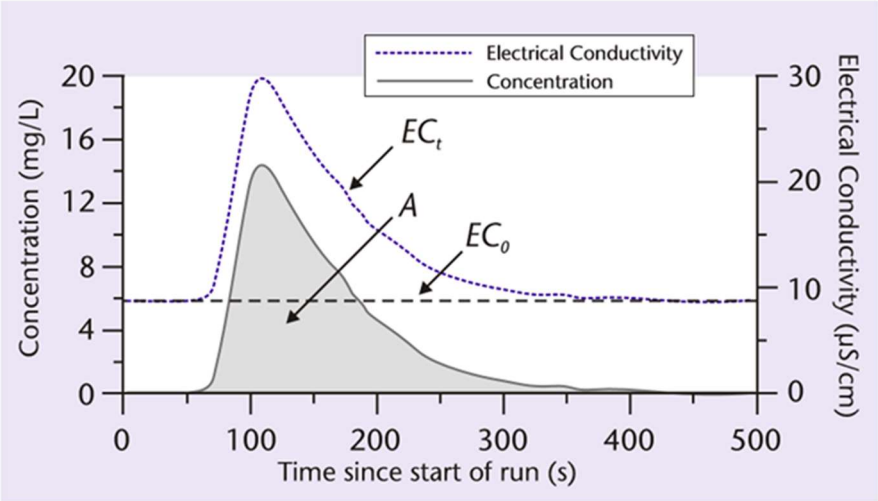

Figure 5.8 Typical concentration curve with sudden tracer injection [62]

Under suitable conditions, discharge measurements made by slug injection can reach up ±5% accuracy [65]. Different sources of error may occur [67] such as the incomplete dissolving of tracer; the inaccuracy in measuring the mass of tracer injected; the uncertainty in the determination of the relation between conductivity and concentration; the unknown potential amount of tracer lost by adsorption or entrapped in a dead zone. The slug injection method may also become unreliable when too low velocities are detected which means poor lateral mixing and excessive long salt wave durations.

The salt dilution method by slug injection was tested from September to October 2014, in the study area, because of the difficulty of handling the large quantities of salt solution required by the constant rate injection.

San Teodoro Bridge (SW_04) (Fig. 5.9) has been chosen as gauging section, allowing easy set up and management of the current meter, but also satisfying the salt dilution method requirements.

San Teodoro Bridge gauging station is relatively straight to ensure streamlines parallel to each other and reduce errors in velocity measurements. The bed stream relatively uniform and free of heavy aquatic growth allows keeping the current meter perpendicular to the flow while measuring velocity, to ensure a stable relation between stage and discharge. SW_04 gauging station is also suited for measuring stream flow by salt dilution method. As a matter of fact, in the section there are no backwater areas and local inflows between the injection and measurement points, where the salt can be delayed and separated from the main flow. The bridge makes easy the slug injection of the tracer solution and allows rapid dissolution and complete mixing into the flow.

At SW_04 gauging station the Aniene River surface width ranges from 4.5 to 5 meters and its depth from 0.2 to 1 meter, according to the limits imposed by the type of current meter used [60]. SW_04 gauging station is an ideal injection site, because it has the basic characteristics for accurate streamflow measurements by salt dilution method. In fact, the turbulent condition allows completely dissolution and fully mixing with the flow at the point, where electrical conductivity is measured. SW_04 has been used to dump the salt, directly into the injection point: the turbulence created below the bridge allows the dissolution of the salt and the mixing into the stream [60].

Figure 5.9 San Teodoro Bridge gauging section (SW_04)

It has been used a saturated NaCl-solution made by dissolving about 2 kg of salt in 10 litres of stream water, depending on the temperature and the background conductivity of the stream. A PC650 probe (Eutech Instruments) was used to register the electrical conductivity measured data. The instrument is auto-ranging between 0 and 500 mS/cm, with an accuracy of ± 0.05%. The dissolution of NaCl in water is proportional to water temperature and inversely proportional to the existing concentration of salt. After injection, the salt mixes into the stream by longitudinal dispersion, a process in which the salt dissolved in the plume moves where its concentration gradient decreases until it becomes constant [65].

5.4.4.2 Current meter method

Streamflow discharge is defined as the volume of water flowing across a fixed point in one unit of time. The current meter method involves measuring the area and the velocities of a stream at a cross section which is perpendicular to the main flow of the river. Usually, river discharge (Q) is calculated as the product of the cross section area (A) of flow by the average stream flow velocity (v) in that cross section (5.4):

$$Q = v \cdot A \tag{5.4}$$

The current U.S. Geological Survey (USGS) procedure for rivers discharge is to measure stage and then to calculate discharge from an empirically generated stage discharge relation (rating curve) [58,59]. In natural river systems, a common approach is to build the stage–discharge relationship with the help of several sectors only valid for a given range of stages. For this reason, flow measurements have been collected at a number of equally spaced verticals (N), inside the river cross section, at multiple depths at each monitored vertical. The rating-curve will be regarded as a relation fitted to N points (h_i, Q_i), i=1,2,…,N, the measured stage h_i and corresponding measured discharge Q_i recorded on N steps.

Thus, the river cross section is divided into a number vertical sub-sections (n), in each one the area is obtained by measuring the width (l_i) and depth (h_i) of the sub-section and the stream flow velocity is determined using a current meter. The total discharge is then computed by summing the discharge of each sub-section (5.5) [70]:

$$Q \sum_{i=1}^{n} l_i \cdot h_i \cdot \overline{v_i} \tag{5.5}$$

The discharge measurements were carried out along the Aniene River by the application of traditional current meter [70,71].

A current meter is an instrument that measures the velocity of flowing water. Traditional mechanical current meters are based on the principle that the velocity of water is proportional to the angular velocity of the meter's rotating propeller. A relationship exists therefore between stream velocity and the number of spins during a certain lapse of time.

The main equipment needed to measure the stream flow velocity is a SEBA horizontal axis current meter F1 (Fig. 5.10a), having a propeller diameter of 80 mm which, combined with SEBA Z6 pulse counter (Fig. 5.10b), allows to measure velocity between 0,025 m/s and 10 m/s.

(a) (b)

Figure 5.10 Universal Wing SEBA F1 (a) and counting device SEBA Z6 (b)

The SEBA current meter has been used as rod equipment with tail plane for best positioning to the flow direction. For each measurement point, flow velocity is determined counting the number of spins of the meter rotor during a fixed interval of time. Thus, in order to assess any fluctuations due to the turbulence condition and, also, to avoid accidental measurement errors, velocity has been measured for at least 60 seconds, according to EN ISO 748:2007 requirements [71].

The operating principle is based on the proportionality between the flow velocity and the resulting angular velocity of the rotor. For each measurement point, flow velocity is determined counting the number of spins of the meter rotor during a fixed interval of time. The current meter responds instantly to any changes in water velocity but in unsteady flow conditions is difficult obtain accurate measurements due to the difficult of keeping the current meter attached to the measuring line. Thus, in order to assess any fluctuations due to the turbulence condition and, also, to avoid accidental measurement errors, velocity has been measured for at least 60 seconds, according to EN ISO 748:2007 requirements.

This current meter method gives the local water velocity in each vertical following the application of a calibration equation between stream velocity (cm/sec) and the number of spins (sec^{-1}) according to equations (5.6) and (5.7).

$$v = 0.82 + 33.32 \cdot n' \qquad n' = \frac{n}{60} > 1 \tag{5.6}$$

$$v = 2.8 + 31.34 \cdot n' \qquad n' = \frac{n}{60} < 1 \tag{5.7}$$

CHAPTER 6

QUALITATIVE AND QUANTITATIVE ASSESSMENT OF WATER RESOURCES IN THE STUDY AREA

6.1 Groundwater and surface water quality assessment

6.1.1 Physico-chemical parameters

The following physico-chemical parameters of groundwater and surface water were measured on field:

- *Water temperature (T)*: temperature is an important water quality parameter, as it affects the degradation rate of the biodegradable pollutants. Temperature also influences the rate of dissolved oxygen in water and the treatment efficiency of both water and wastewater. Sharp increases or decreases of temperature cause high adverse impacts on the ecological system. Temperature plays a very important role in wetland dynamism affecting the various parameters such as alkalinity, salinity, dissolved oxygen, electrical conductivity, etc. In an aquatic system, these parameters affect the chemical and biological reactions such as solubility of oxygen, carbon-di-oxide-carbonate-bicarbonate equilibrium, increase in metabolic rate and physiological reactions of organisms, etc.
- *Electrical conductivity (EC): electrical* conductivity is the numerical expression of the water's ability to conduct electricity. Electrolytes in water solutions disassociate into positive (cations) and negative (anions) ions and give them *electrical* conductivity. In general, the higher the concentration of dissolved salts in the water, the easier it is for electricity to pass through water. Conductivity is reported in micromhos (μmhos) or microSiemens (μS) per centimeter (cm) and depends on the total concentration, mobility, valence and the temperature of the solution of ions. The concentration of total dissolved solids (TDS) is related to electrical conductivity: the conductivity increases as the TDS concentration increases. Because they are temperature dependant, electrical conductivity measurements are usually corrected and reported as if they were taken at 25°C.
- *pH:* it is one of the most important parameter in water chemistry and is defined as -log $[H^+]$, and measured as intensity of acidity or alkalinity on a log-scale ranging from 0-14. If free H^+ are more, water it is considered acidic (pH<7), while if more are OH^- ions, water is defined as alkaline (pH>7). In natural waters, pH is governed by the equilibrium between carbon dioxide/bicarbonate/carbonate ions and ranges between 4.5 and 8.5, although mostly basic. pH tends to increase during day, mostly due to the photosynthetic activity (consumption of carbon-di-

oxide) and decreases during night due to respiratory activity. Wastewater and polluted natural waters have pH values lower or higher than 7 based on the nature of the pollutant.

- *Dissolved oxygen (DO)*: dissolved oxygen is an indicator of the physical, chemical and biological activities of water bodies. The two main sources of dissolved oxygen are diffusion of oxygen from the air and photosynthetic activity. Diffusion of oxygen from the air into water depends on the solubility of oxygen, and is influenced by many other factors like water movement, temperature, salinity, etc. Photosynthesis, a biological phenomenon carried out by the autotrophs, depends on the plankton population, light condition, gases, etc.. Oxygen is considered as the main influencing factor in water bodies with organic materials. In the progress of summer, dissolved oxygen decreases due to temperature increase and due to microbial activity increasing [72]. The high DO in summer is due to increase in temperature and duration of bright sunlight has influence on the % of soluble gases (O^2 & CO^2). During summer, the day length and intense sunlight seem to accelerate photosynthesis by phytoplankton, utilizing CO_2 and giving off oxygen. Dissolved Oxygen is a particularly useful parameter and indicator of water quality. Its presence in surface water plays a key role in the self-purification and maintenance of aquatic life. However, its presence in urban water is seen as troublesome due to the possibility of corrosion of metal distributors [73].

Tables 6.1 and 6.2 contain the results of physical-chemical parameters of groundwater samples.

The average water temperature distribution during the 7 sampling campaigns (July 2014 – November 2106) is consistent with the expected seasonal variations for temperate regions (Figs. 6.1 and 6.2). The deviations were calculated by considering all of the seven results, obtained for each sampling point (if available). Surface water temperature among the study area range from 5.8°C – 11.3°C. Pertuso Spring shows the lower value of temperature (7.8°C) for groundwater and the little variation in comparison to other monitoring points.

Table 6.1 Physico-chemical parameters of groundwater samples

ID	Date	T (°C)	EC (µS/cm)	pH	D.O. (mg/l)
GW_01	July 2014	8.0	321.6	7.4	11.7
	November 2014	8.0	300.0	7.2	10.6
	January 2015	9.5	410.0	6.9	10.3
	May 2015	8.5	300.0	10.8	10.8
	December 2015	8.0	350.0	7.3	10.7
	May 2016	7.8	209.6	7.7	11.6
	November 2016	8.0	289.0	8.0	11.1
GW_02	July 2014	14.6	395.5	7.6	7.9
	November 2014	9.9	350.0	7.3	10.0
	January 2015	8.3	320.0	6.8	10.3
	May 2015	12.4	360.0	7.2	9.3
	December 2015	10.7	380.0	7.0	9.9
	May 2016	15.6	339.5	7.6	9.8
	November 2016	9.8	364.0	7.9	7.6
GW_03	July 2014	13.9	456.0	7.1	8.0
	November 2014	10.1	430.0	7.3	9.4
	January 2015	10.0	400.0	6.3	9.9
	May 2015	12.6	370.0	8.9	7.6
	December 2015	10.8	480.0	6.7	9.4
	May 2016	15.6	388.4	7.2	9.3
	November 2016	11.8	441.0	7.6	9.7
GW_04	November 2014	11.0	430.0	7.2	9.3
GW_05	July 2014	14.2	448.4	7.3	8.1
	November 2014	12.2	290.0	7.4	8.4

Table 6.2 Physico-chemical parameters of surface water samples

ID	Date	T (°C)	EC (µS/cm)	pH	D.O. (mg/l)
SW_01	July 2014	11.3	422.5	8.3	9.7
	November 2014	7.7	360.0	8.3	10.7
	January 2015	5.8	340.0	7.3	11.3
	May 2015	10.7	390.0	9.6	9.8
	December 2015	6.1	410.0	7.4	11.4
	May 2016	9.3	295.3	8.2	11.2
	November 2016	5.9	378.0	8.3	11.0
SW_02	July 2014	9.9	351.6	7.8	11.0
	November 2014	7.3	320.0	7.6	10.6
	January 2015	7.2	270.0	6.9	10.9
	May 2015	8.9	280.0	8.1	10.4
	December 2015	6.7	320.0	7.4	10.9
	May 2016	8.7	245.7	8.1	11.4
	November 2016	8.7	311.0	8.0	10.8
SW_03	July 2014	9.3	350.4	7.9	10.9
	November 2014	8.3	300.0	7.9	10.4
	January 2015	7.2	380.0	7.2	11.3
	May 2015	12.3	260.0	11.0	9.4
	December 2015	7.2	340.0	7.1	11.0
	May 2016	9.4	248.4	8.0	11.3
	November 2016	8.3	313.0	8.1	10.2
SW_04	July 2014	10.0	341.4	8.0	10.6
	November 2014	8.2	310.0	7.8	11.1
	January 2015	6.7	580.0	7.4	11.5
	May 2015	10.0	280.0	10.1	10.2
	December 2015	7.1	340.0	7.6	11.2
	May 2016	10.0	253.3	8.2	11.3
	November 2016	8.4	313.0	8.3	10.4

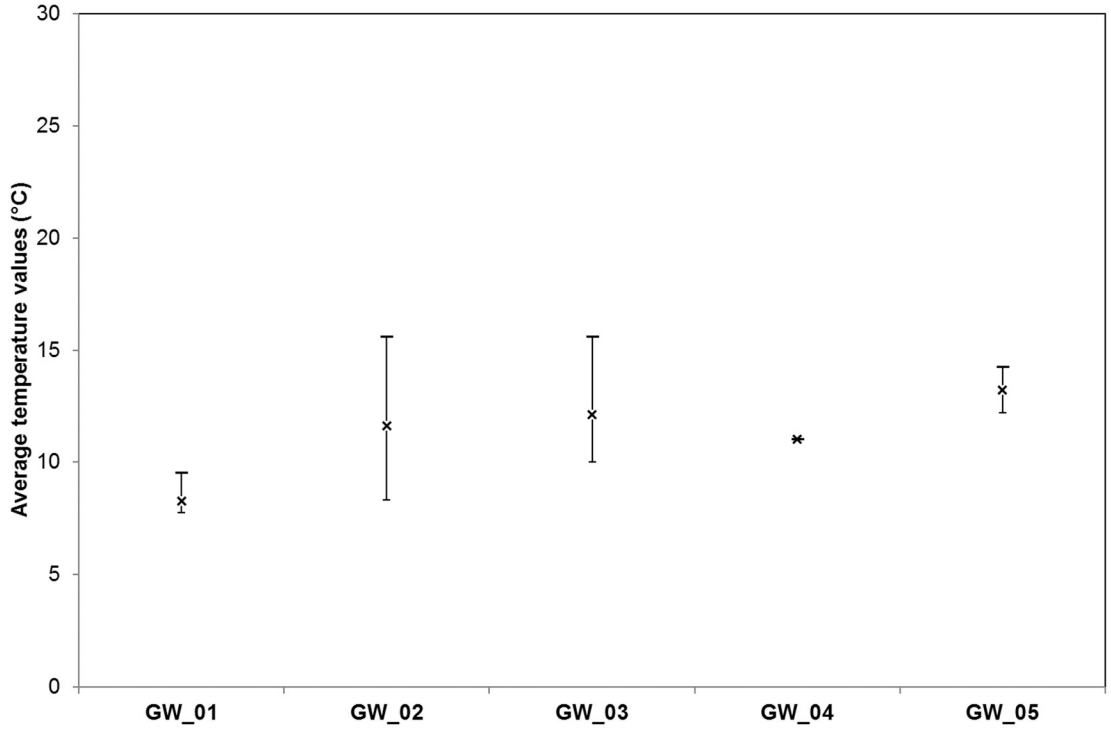

Figure 6.1 Average water temperature for groundwater samples

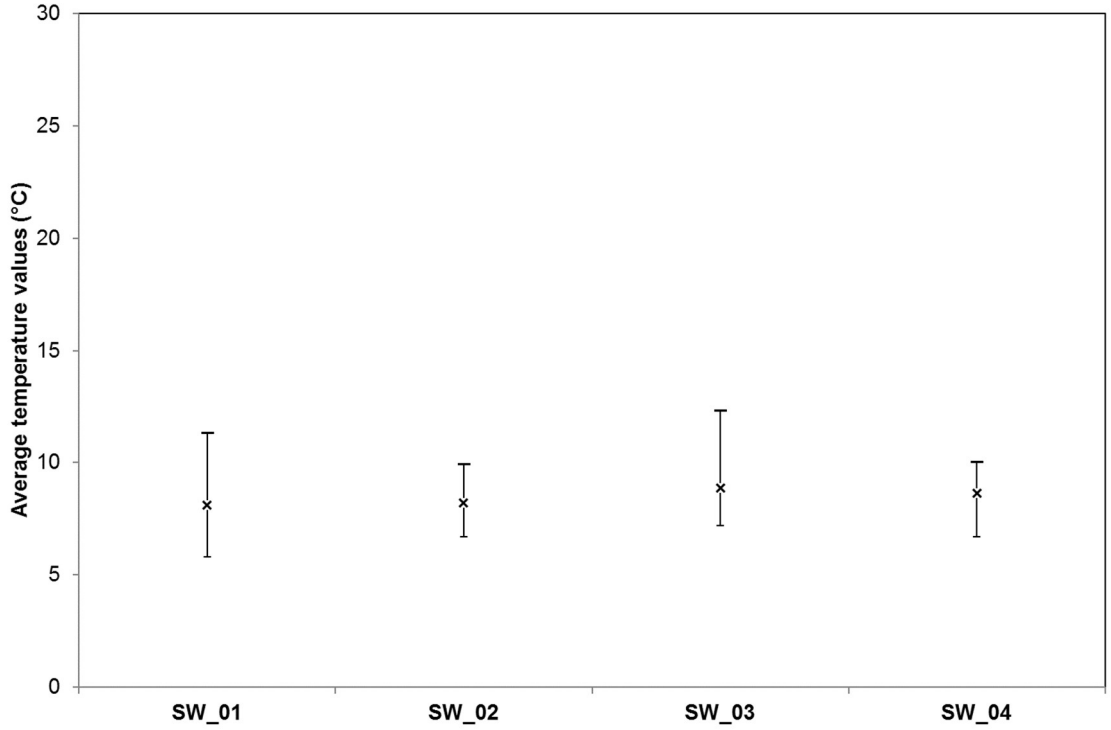

Figure 6.2 Average water temperature for surface water samples

The pH is almost similar in both the groundwater (Fig. 6.3) and surface water (Fig. 6.4).

pH of all water samples collected show a large range of variation, from 6.3 to 11.0 indicating slightly acidic to slightly alkaline nature.

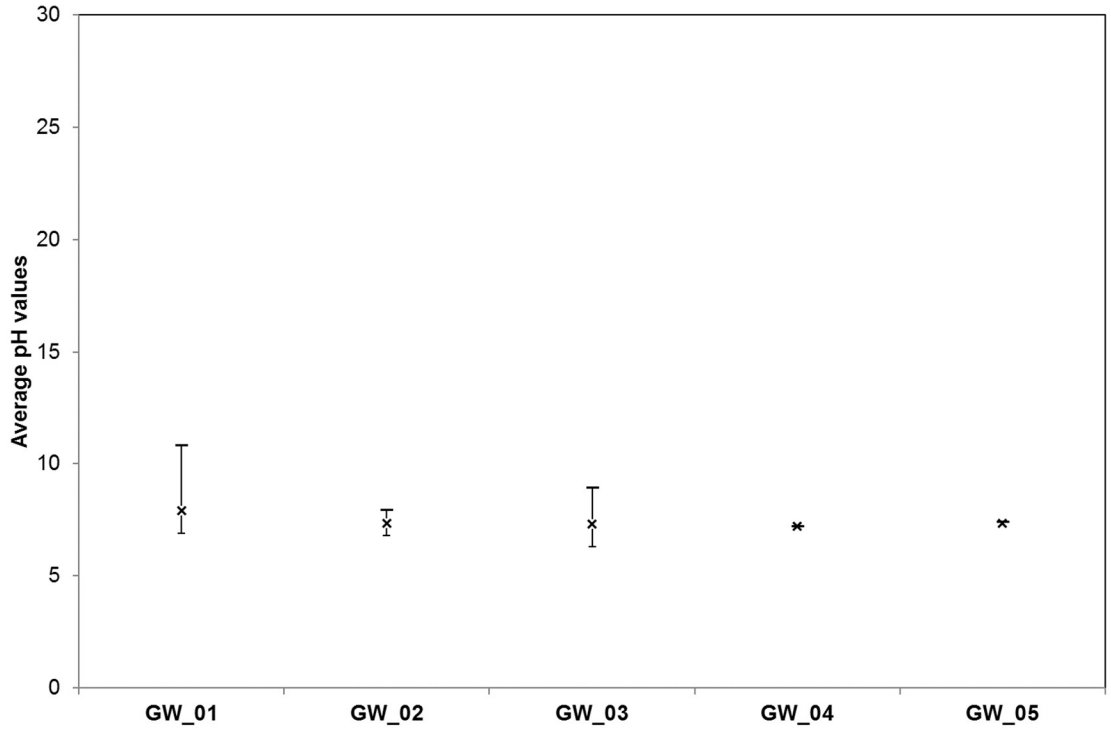

Figure 6.3 Average pH for groundwater samples

The pH values in water samples were generally alkaline during the dry season in every sampling point and generally slightly acidic during rainy. This can come out as a result of precipitation contribution to water budget in this aquifer. The regular pH values shows the absence of sensitive sources of acidic or alkaline compounds in the evaluated area, or immediately upstream thereof.

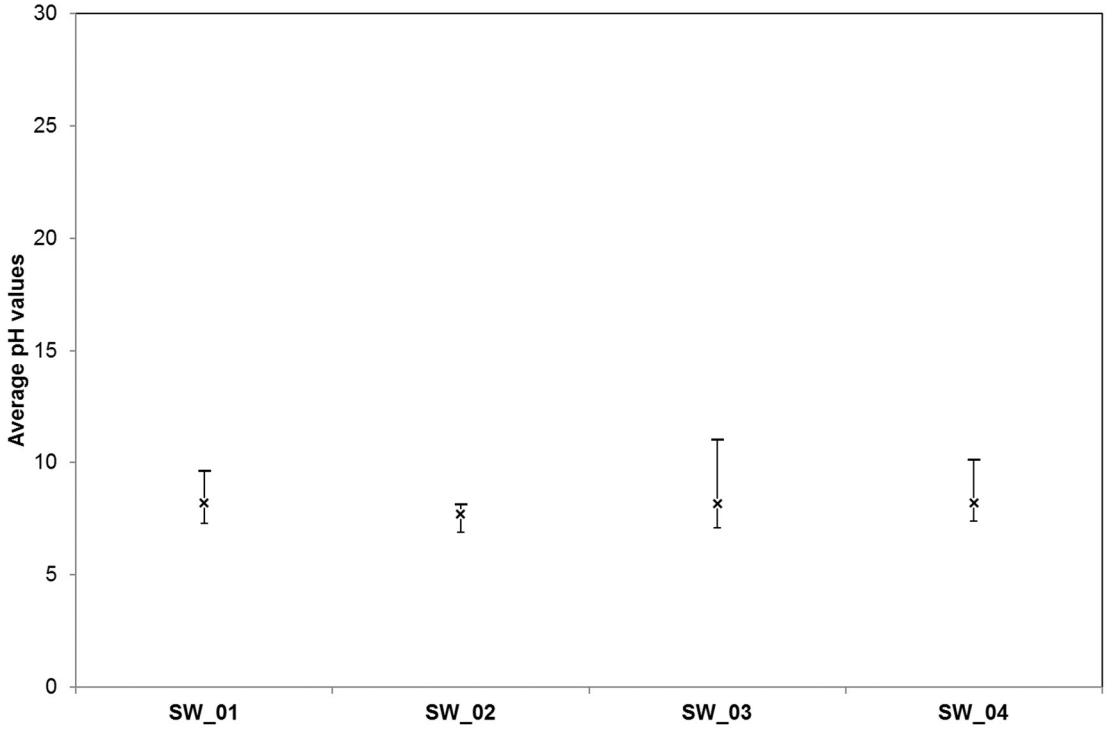

Figure 6.4 Average pH for surface water samples

The electrical conductivity in groundwater was found variable, from 210 to 480 μS/cm (Fig. 6.5) while in stream water range from 246 to 580 μS/cm (Fig. 6.6). There is a sharp increase in conductivity observed in January 2015 in SW_04, the farthermost gauging station from the Pertuso Spring. Higher values obtained in electrical conductivity in the dry season compared with rainy season may be due to concentration increasing of electrolytes and other elements in the surface water as a result of rainfall decrease contribution (Fig. 6.6). Moreover, significant differences between the conductivity of surface and deep samples were not identified.

The average levels of dissolved oxygen during the sampling campaigns and at different monitoring points are presented in Figures 6.7 and 6.8. The solubility of oxygen or its ability to dissolve in water increases as the water temperature and salinity decreases [74]. Higher dissolved oxygen (DO) concentrations were found in stream water of the Aniene River (Fig. 6.8). These values of DO increased sharply from October to November and became gradually lower until May. This trend can explained by the large rainfall contribution to the waterbody in the aquifer recharge period and, on the contrary by tiered lowering of it during the period of not recharge. [75].

The lowest values of dissolved oxygen were found downstream the Pertuso Spring (SW_02), where it is found the large variation in comparison to other monitoring points (Fig. 6.8). Pertuso Spring groundwater, near to upstream, have relatively high dissolved oxygen levels, due to stream flow influence (Fig. 6.7).

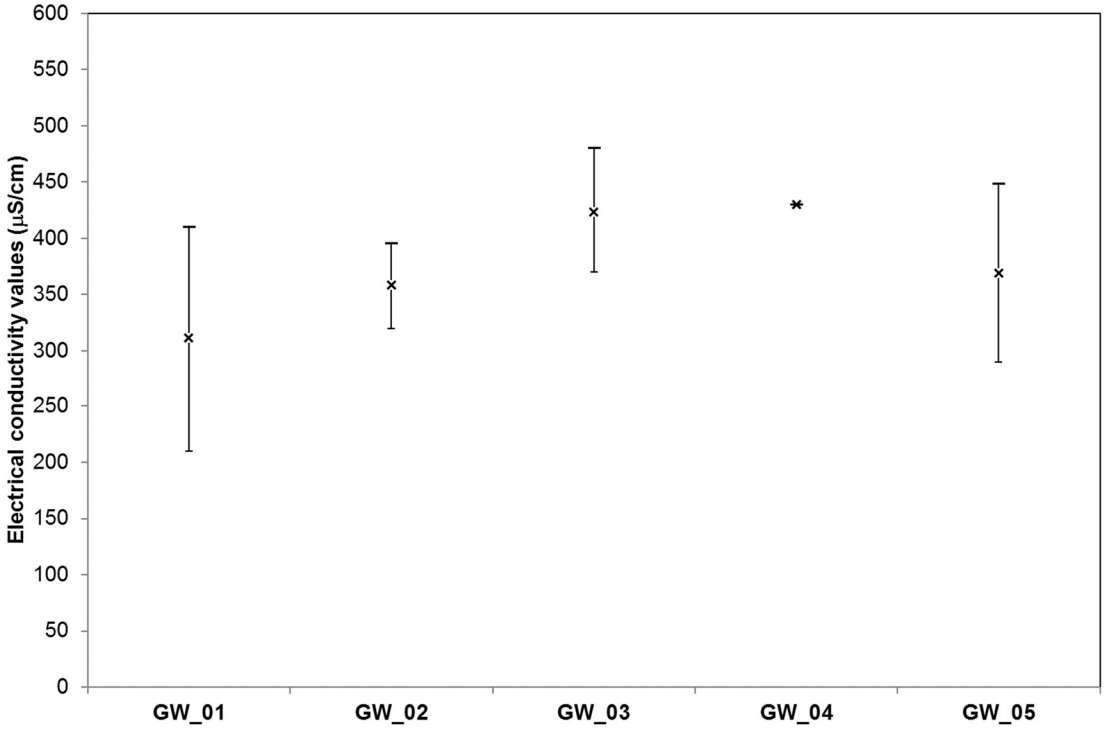

Figure 6.5 Average electrical conductivity for groundwater samples

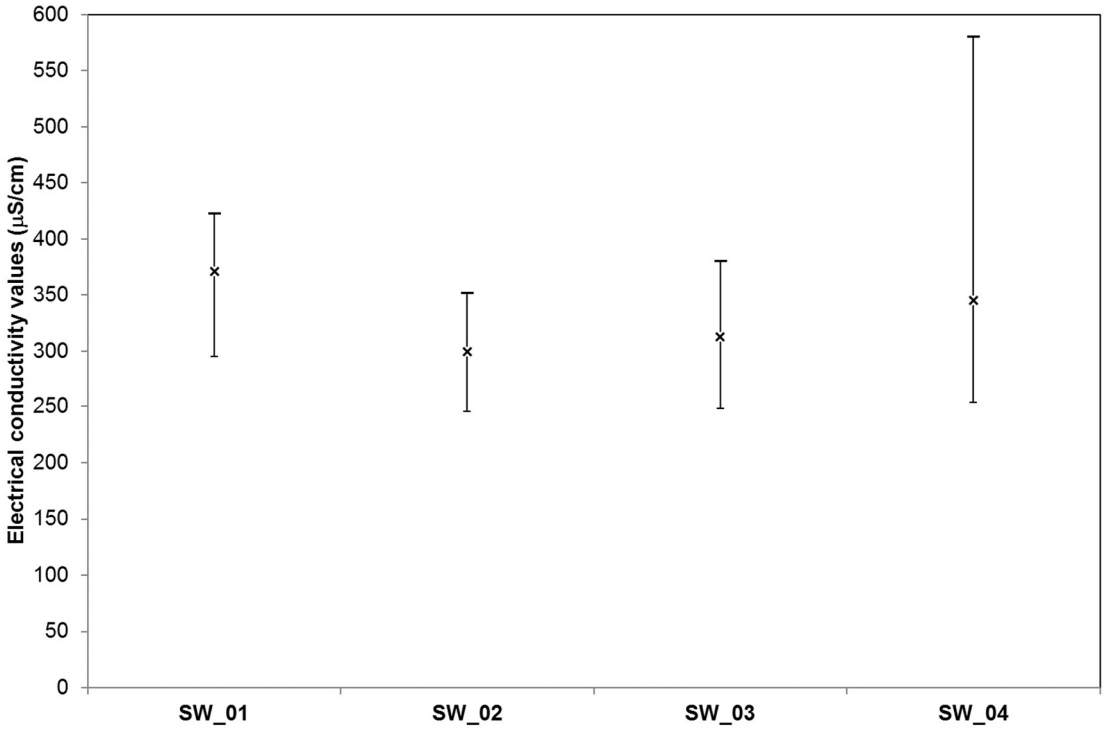

Figure 6.6 Average electrical conductivity for surface water samples

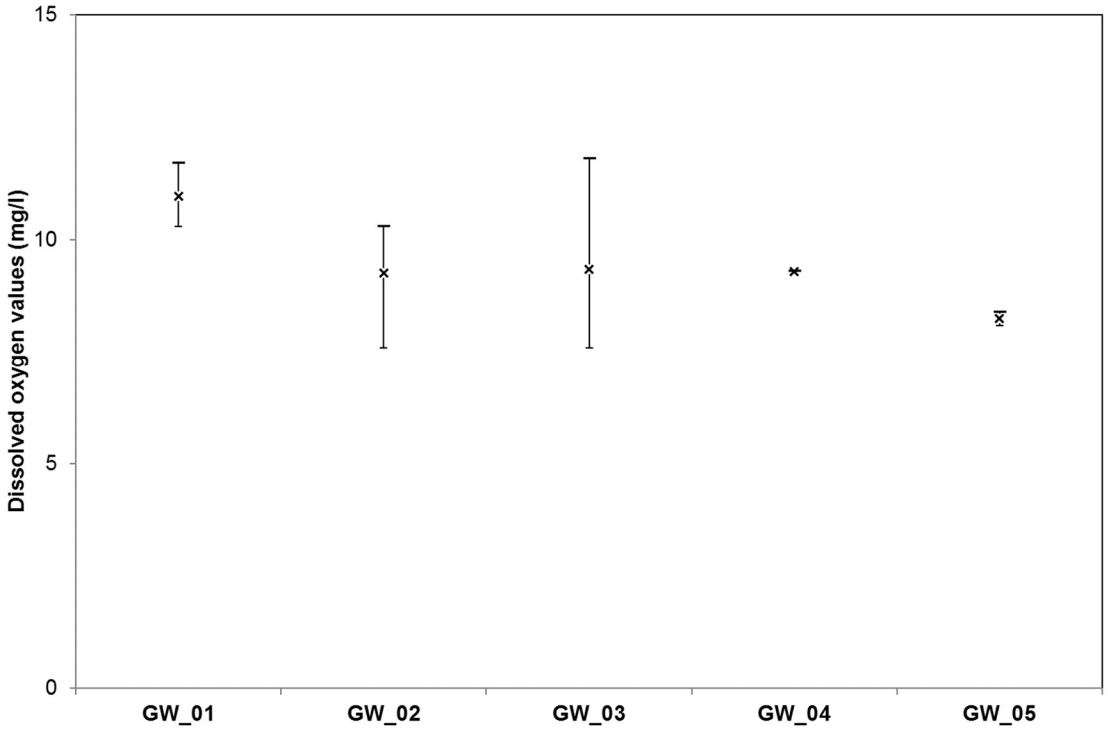

Figure 6.7 Average dissolved oxygen for groundwater samples

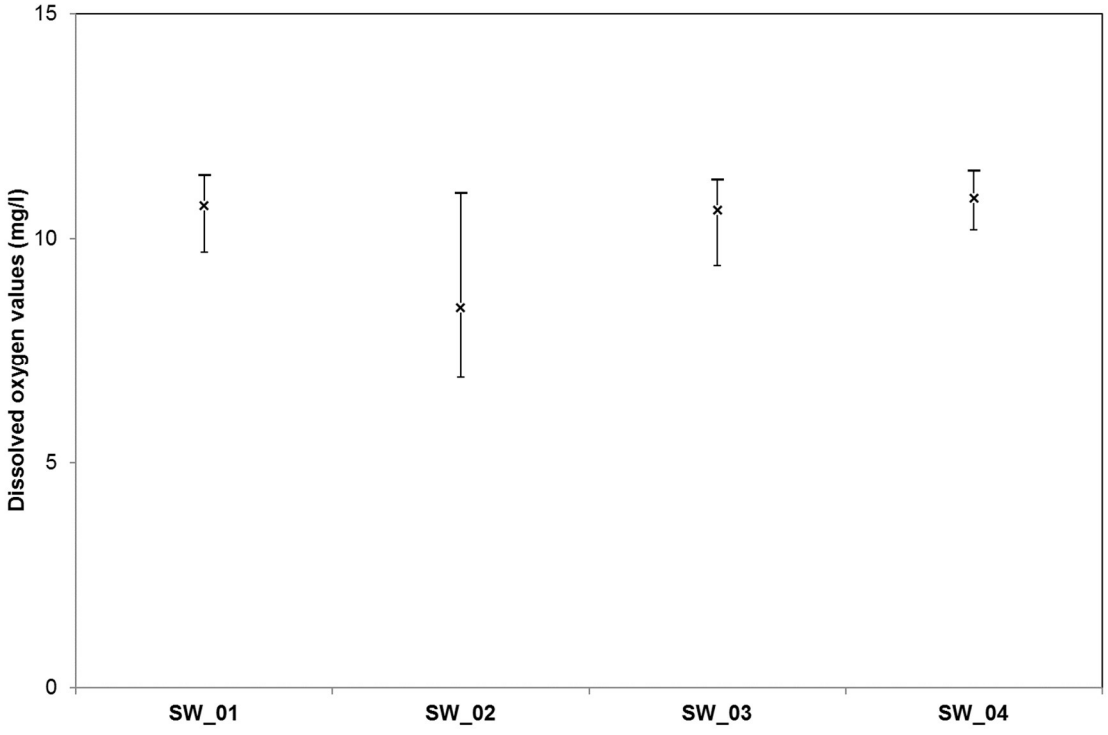

Figure 6.8 Average dissolved oxygen for surface water samples

6.1.2 Groundwater and surface water chemistry

Major ions concentrations of the analysed groundwater and surface water samples are presented in Tables 6.3 and 6.4.

Table 6.3 Major ions concentrations of groundwater samples

ID	Date	Ca^{2+} (mg/l)	Mg^{2+} (mg/l)	$Na^{+}+K^{+}$ (mg/l)	Cl^{-} (mg/l)	SO_4^{2-} (mg/l)	HCO_3^{-} (mg/l)
GW_01	July 2014	48.9	9.8	2.4	3.5	2.4	210
	November 2014	51.0	8.3	2.2	3.5	2.4	216
	January 2015	53.3	9.9	2.5	3.7	2.5	206
	May 2015	49.0	9.3	2. 2	3.4	2.3	224
	December 2015	51.6	10.4	2.3	3.3	2.4	238
	May 2016	53.2	9.5	2.5	3.2	2.4	237
	November 2016	52.2	9.8	2.3	3.2	2.6	224
GW_02	July 2014	58.5	14	3.2	4.3	3.0	372
	November 2014	59.3	13.7	4.0	5.5	2.9	267
	January 2015	63.4	14.6	4.8	5.9	3.2	305
	May 2015	59.1	13.9	3.2	4.4	2.8	270
	December 2015	62.2	15.2	3.4	4.5	2.8	298
	May 2016	63.7	14.7	3.5	4.8	2.8	301
	November 2016	62.3	14.1	3.8	4.2	3.1	277
GW_03	July 2014	90.3	1.9	2.8	3.1	2.7	336
	November 2014	93.9	2.4	3.0	3.9	2.0	321
	January 2015	97.3	2.3	3.5	4.2	2.1	331
	May 2015	88.4	1.6	3.5	4.4	2.2	301
	December 2015	102.0	1.9	3.2	4.0	2.2	346
	May 2016	94.9	4.9	2.7	4.3	2.2	338
	November 2016	97.3	2.0	5.9	8.24	2.3	328
GW_04	July 2014	-	-	-	-	-	-
	November 2014	94.8	1.4	3.8	3.4	2.1	322
	January 2015	-	-	-	-	-	-
	May 2015	-	-	-	-	-	-
	December 2015	-	-	-	-	-	-
	May 2016	-	-	-	-	-	-
	November 2016	-	-	-	-	-	-
GW_05	July 2014	81.2	3.5	3.8	3.5	5.4	322
	November 2014	61.8	2.5	3.1	2.6	3.2	210
	January 2015	-	-	-	-	-	-
	May 2015	-	-	-	-	-	-
	December 2015	-	-	-	-	-	-
	May 2016	-	-	-	-	-	-
	November 2016	-	-	-	-	-	-

Table 6.4 Major ions concentrations of surface water samples

ID	Date	Ca^{2+} (mg/l)	Mg^{2+} (mg/l)	$Na^{+}+K^{+}$ (mg/l)	Cl^{-} (mg/l)	SO_4^{2-} (mg/l)	HCO_3^{-} (mg/l)
SW_01	July 2014	53.4	23.6	2.7	4.2	2.9	282
	November 2014	54.0	23.6	2.8	4.3	3.0	283
	January 2015	57.8	25.2	3.1	4.5	3.2	303
	May 2015	53.9	24.6	2.8	4.1	2.9	288
	December 2015	56.0	25.2	2.8	3.8	3.0	298
	May 2016	56.6	25.2	2.8	4.1	3.0	299
	November 2016	57.2	23.8	2.8	3.9	3.0	294
SW_02	July 2014	51.3	12.8	2.3	3.7	2.5	221
	November 2014	52.4	12.0	2.6	3.7	2.6	220
	January 2015	55.6	13.0	2.9	4.2	2.7	234
	May 2015	51.4	12.2	2.3	3.5	2.5	218
	December 2015	52.9	14.7	2.7	3.3	2.6	235
	May 2016	54.6	12.5	2.5	3.7	2.5	229
	November 2016	54.4	13.5	2.5	3.4	2.6	233
SW_03	July 2014	51.2	12.8	2.3	3.7	2.5	221
	November 2014	52.5	11.8	2.7	3.8	2.6	220
	January 2015	56.0	12.8	3.1	3.9	2.8	235
	May 2015	51.3	12.1	2.4	3.5	2.5	217
	December 2015	53.5	14.5	3.1	3.4	2.6	235
	May 2016	55.4	12.8	2.6	3.6	2.5	233
	November 2016	54.8	13.4	2.5	3.4	2.6	234
SW_04	July 2014	51.4	12.8	2.3	3.6	2.5	221
	November 2014	53.1	11.8	2.4	4.3	2.6	221
	January 2015	56.3	12.8	2.6	3.8	2.7	235
	May 2015	51.2	12.1	2.5	3.6	2.5	217
	December 2015	53.3	14.4	3.2	3.4	2.6	234
	May 2016	55.1	12.3	2.4	3.6	2.5	229
	November 2016	55.2	13.4	2.5	3.4	2.7	235

Ca, Mg and HCO_3 represent over 90% of the dissolved solids in groundwater and surface water (Figs. 6.9 and 6.10). Calcium is the most abundant cation in every water sample; it varies from 48.9 to 102 mg/l with an average of 70.4 mg/l in groundwater and ranges from 51.2 to 57.6 with an average of 54 mg/l in surface water. Magnesium varies in concentration ranging from 1.3 to 15.2 mg/l, with average of 8 mg/l in groundwater, and from 11.8 to 25.2 mg/l with an average of 15.8 mg/l in surface water (Figs. 6.11 and 6.12). The sources of these ions in the groundwater and surface water are from the dissolution of carbonate minerals forming limestone, which is the most dominant formations in the study area. Aniene River samples show TDS average value lower than groundwater highlighting different weathering processes. The highest calcium (58 mg/l) and magnesium (25 mg/l) was observed in water samples from SW_01, upstream the Pertuso Spring. The highest calcium (102 mg/l) was observed in groundwater samples from GW_03, while the maximum magnesium concentration (15 mg/l) were observed in water samples from GW_02.

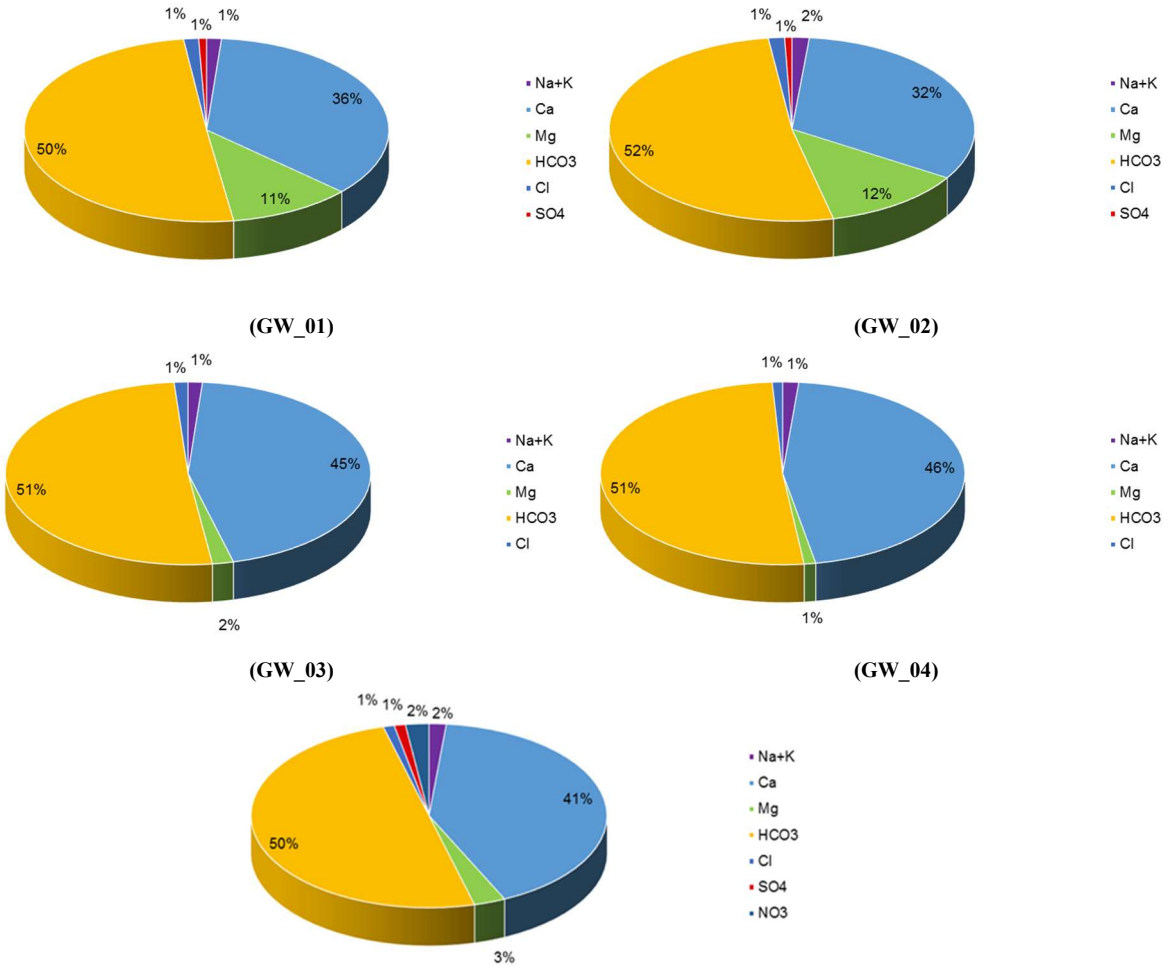

Figure 6.9 Average ionic composition of groundwater samples

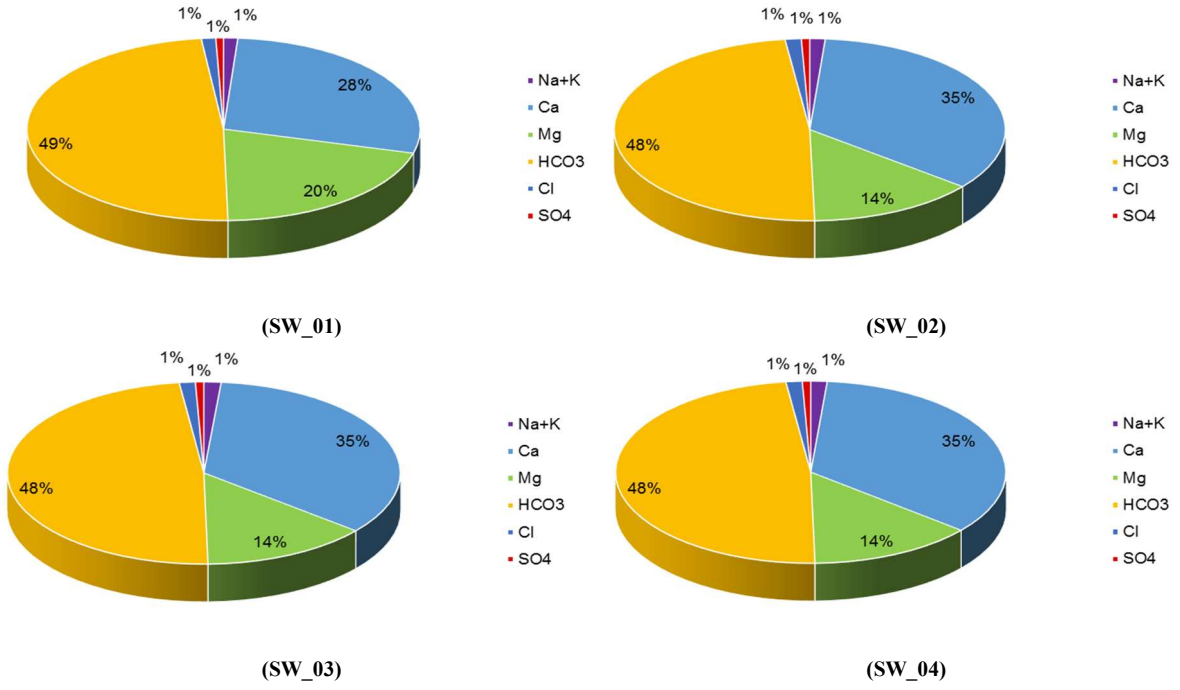

Figure 6.10 Average ionic composition of surface water samples

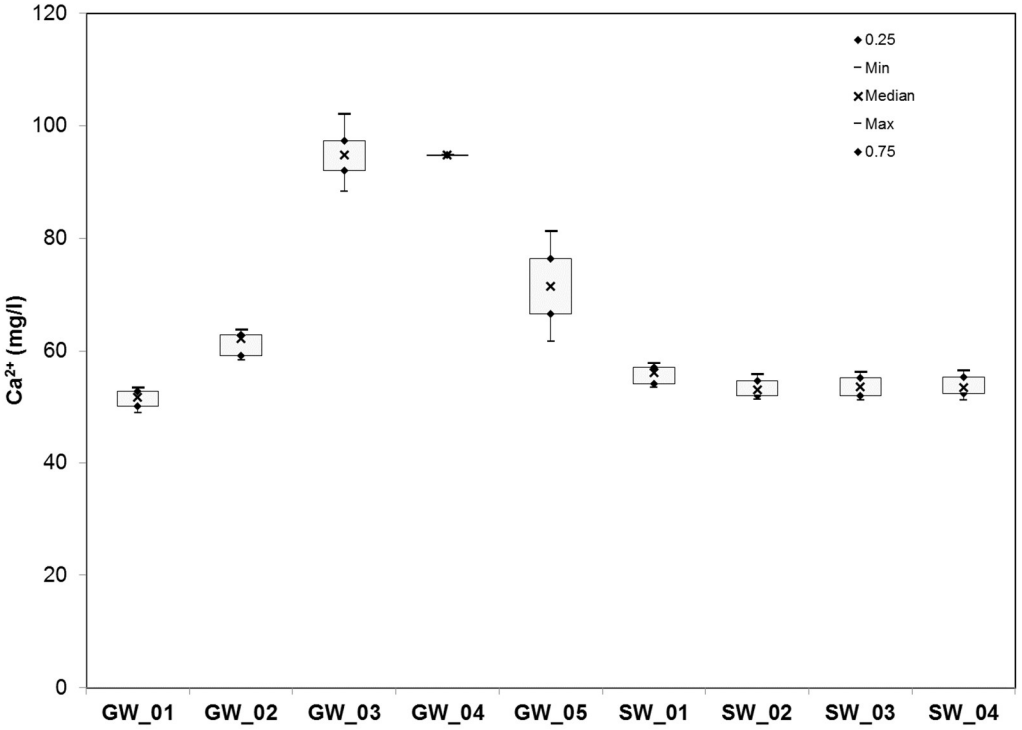

Figure 6.11 Box plot of calcium distribution for water samples

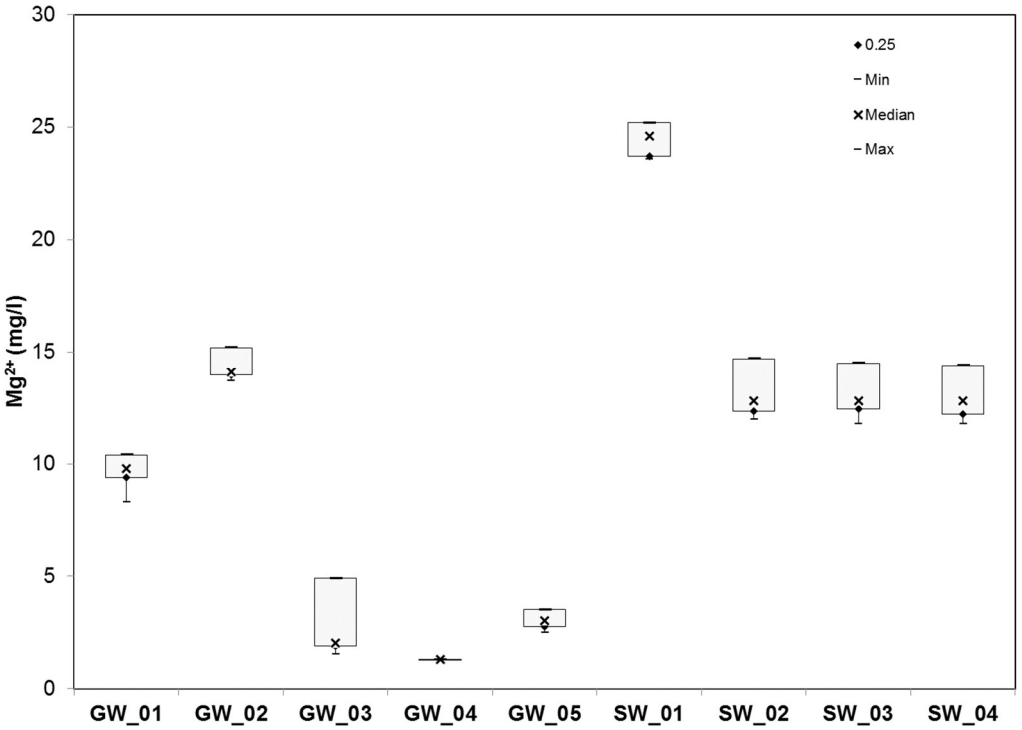

Figure 6.12 Box plot of magnesium distribution for water samples

As a natural consequence of lithological assessment, sodium and potassium concentrations are generally lower in groundwater and surface water, with an average of 2.4 and 0.8 mg/l for groundwater and an average of 2.2 and 0.5 mg/l for surface water, respectively.

Bicarbonate is the dominant anion, found in all water samples, varying from 206 to 372 mg/l in groundwater and from 217 mg/l to 303 mg/l in surface water.

Weathering of carbonate and/or alumino-silicate rocks, with a secondary contribution from dissolution of CO_2 gases are the primary source of HCO_3^- in groundwater and surface water. The unsaturated zone in the shallow subsurface environment, contains high CO_2 pressure (produced as result of anoxic biodegradation of organic matter and root respiration), which in turn combines with rainwater to form bicarbonate. The higher concentration of HCO_3 in comparison with other anions indicates weathering of primary silicate minerals, dominated by alkaline earths [76]. Chloride and sulphate ions show an average of 4.1 and 2.7 mg/l for groundwater and an average of 3.8 and 2.7 mg/l for surface water, respectively. Nitrate ion ranges from 0.2 to 15.7 mg/l with an average of 1.9 mg/l in groundwater and from 0.8 to 5.7 mg/l with an average of 1.2 mg/l in surface water. Concentrations of NO_3 are the result of different pollution processes involving municipal wastewaters, fertilizers and the application of agricultural pesticides, among others.

The highest NO_3 concentration levels were found in areas where large amounts of N fertilizers (commonly urea, nitrate or ammonium compounds) are used due to intensive agricultural practices (GW_05) [77].

The abundance of the major cations and anions in groundwater follows this order:

Ca>Mg>Na>K

and

HCO_3>Cl >SO_4>NO_3

respectively.

6.1.3 Hydrochemical classification and facies

The classification of groundwater was studied by plotting the concentrations of major cations and anions in the Piper trilinear diagram [78] to identify hydrogeochemical processes controlling groundwater chemistry (Figs. 6.13 and 6.14).

Major ion concentrations, given in meq/l, for each groundwater (24) and Aniene River surface water (28) samples are reported as percentages of the total anion and cation content. The occurrence of these water types in the aquifers may be due to the interactions of groundwater with rocks, having different mineralogical compositions along the flow paths.

The diamond diagram shows that nearly all groundwater samples seem to be of alkali type as soil member are more present than the alkali elements (Ca+Mg > Na+K). Weak acidic roots are bigger than the strong acidic roots (HCO_3 > Cl+SO_4). The plot clearly represents that some groundwater samples are closer to the Ca vertex, as Ca enrichment comes from the interaction with carbonate rocks making most part of the aquifer. As is to be expected in waters that circulate in karst aquifer, the Ca-HCO_3 water type is the main hydrochemical facies of groundwater samples. According to Piper diagram, the distribution of hydrochemical facies of waters that occur in the study area can be classified into three groups:(a) Facies Ca-HCO_3; (b) Facies Ca-Mg-HCO_3 with Mg/Ca = 0.5; (c) Facies Ca-Mg-HCO_3 with Mg/Ca = 0.25. The dominance of Ca-Mg-HCO_3 and Ca-HCO_3 type water suggest water-rock interactions involving the dissolution of carbonate minerals by the recharging groundwater. The Ca-Mg-HCO_3 facies is dominant in the Aniene River samples as a result of limestone and dolomite rocks dissolution, which are abundant within the Triassic and Cretaceous formations which underlie much of the basin. Ca-Mg-HCO_3 water type with higher magnesium concentration predominates in SW_01

reflecting the weathering of Mg-rich Triassic dolomites in Filettino area, where dolomite rocks are more present, compared to the limestone (Fig. 6.14). Groundwater coming from GW_03, GW_04 and GW_05 belong to Ca-HCO_3 water type reflecting the main rock types, outcropping in that part of the study area, where limestone and dolomitic limestone are the most dominant formations. On the contrary, groundwater coming from Pertuso Spring and GW_02 show a tendency to the group of Ca-Mg-HCO_3 water type with lower magnesium concentration, highlighting groundwater - surface water interactions (Fig. 6.13).

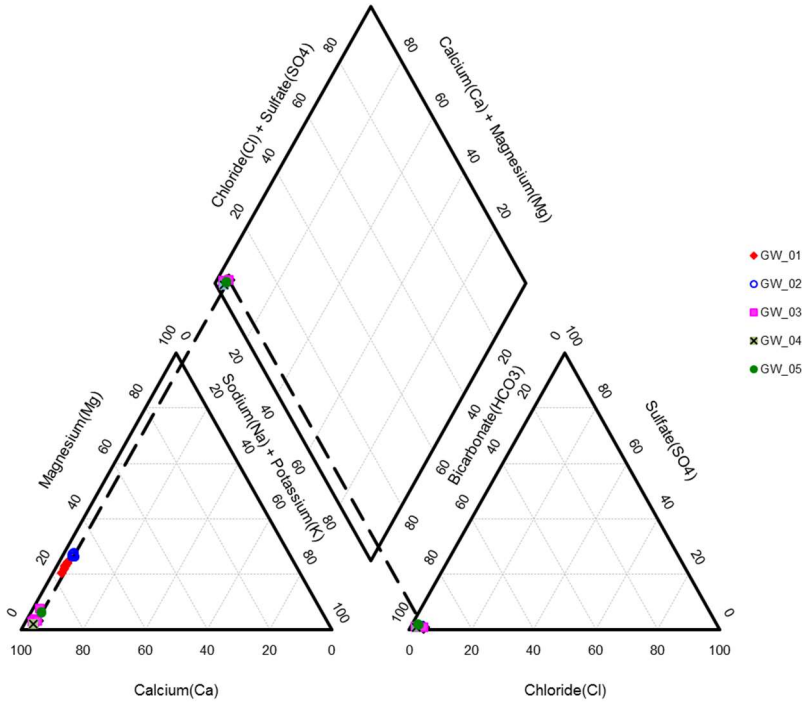

Figure 6.13 Piper ternary diagram for hydrochemical facies evolution and water classification for groundwater

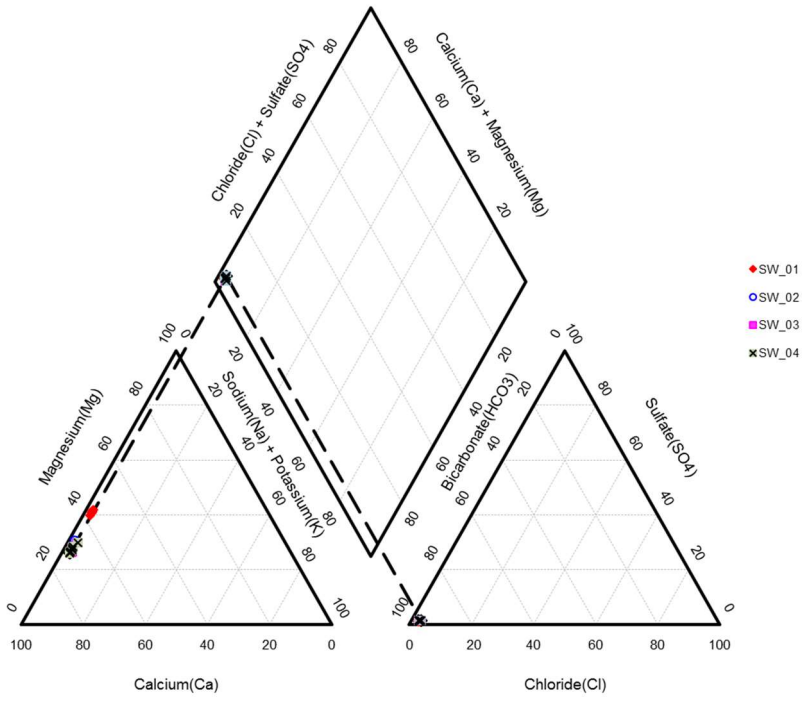

Figure 6.14 Piper ternary diagram for hydrochemical facies evolution and water classification for surface water

6.1.4 Water-rock interaction

Ca and Mg are the dominant cations and HCO_3 is the most present anion in study area. The abundance of Ca and Mg in groundwater and surface water could be related to the presence of carbonate rock in the basin, while weathering of carbonate and silicates may contribute Ca and Mg in the water. In particular, calcium and magnesium ions presence in groundwater is particularly derived from leaching of limestone, dolomites, gypsum and anhydrites, whereas the Ca ions is also derived from cation exchange process [79]. The concentration of Mg ion in this groundwater samples is relatively high when compared to calcium ion concentration and the magnesium concentration is mostly due to weathering of magnesium minerals and leaching of dolomites.

The interaction with carbonate rocks can be explained by means of the absorbed carbon dioxide coming from the soil, during recharge, which reacts with the carbonate rocks of the aquifer, dissolving calcite and dolomite minerals according to the following main reactions (eqs. 6.1 and 6.2):

$$CaCO_3 + CO_2 + H_2O = Ca^{2+} + HCO_3^- \quad (6.1)$$

$$CaMg(CO_3)_2 + 2CO_2 + H_2O = Ca^{2+} + Mg^{2+} + 4HCO_3^- \quad (6.2)$$

The results from the water analysis were used as a tool to identify the process affecting the chemistry of groundwater from the study area. Gibbs [80] suggested TDS versus Na/Na+Ca for cations and TDS versus Cl/(Cl+HCO) for anions to illustrate the natural process controlling groundwater chemistry, including the rainfall dominance, rock weathering dominance, and evaporation and participation dominance [81].

All water samples from both groundwater and surface water fall in rock dominance field of the Gibbs diagram (Fig. 6.15) suggesting the interaction between rock chemistry and the chemistry of the percolation waters under the subsurface.

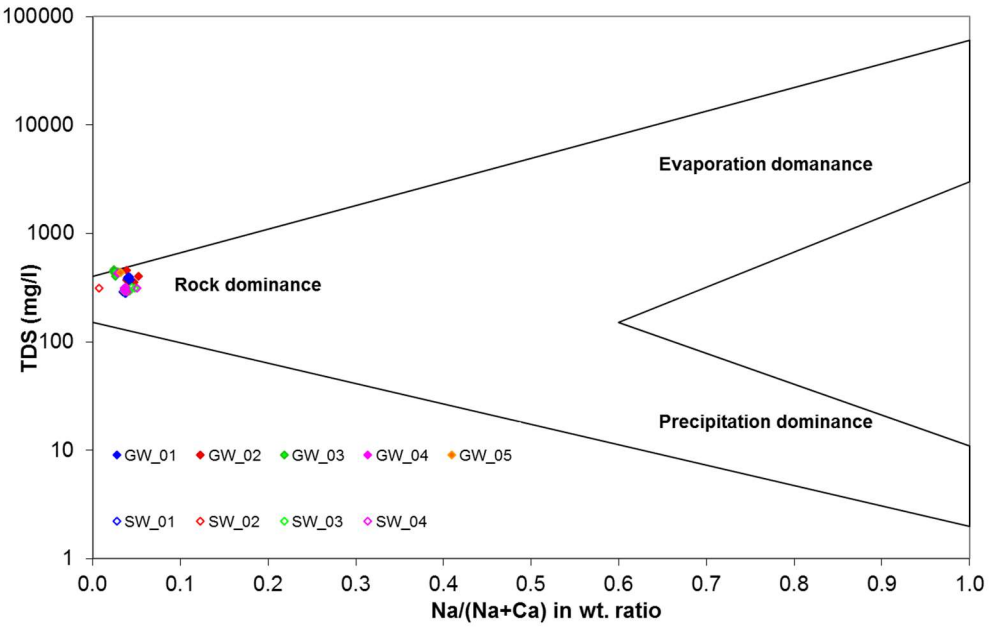

Figure 6.15 Gibbs's diagram representing the ratio of Na/(Na+Ca) as a function of TDS

Weathering of carbonate, silicate and sulphide minerals and dissolution of evaporites are the major lithogenic source of the dissolved ions in the water. The plot of (Ca+Mg) versus (HCO_3+SO_4) will be close to 1:1 line if the dissolution of calcite, dolomite and gypsum are the dominant reactions in a system [82,83,84]. When ion exchange takes place the points shift right due to excess (Ca+Mg) over (SO_4+HCO_3). If reverse ion exchange is the process, it will shift the points to the left due to a large excess of (Ca+Mg) over (SO_4+HCO_3).

The plot for (Ca+Mg) versus (HCO_3+SO_4) is a major indicator to identify ion exchange process activated in the study area. If ion exchange is the process, the points shift to right side of the plot due to excess (SO_4+HCO_3). If reverse ions exchange is the process, points shift left due to excess (Ca+Mg). The plotted points of the majority of the surface water on Figure 6.16 are falling along the equiline suggesting that these ions come from weathering of carbonates. However, groundwater samples are clustered below the 1:1 line, indicating that the weathering of silicate is the dominant process for supply of the calcium ions to the groundwater.

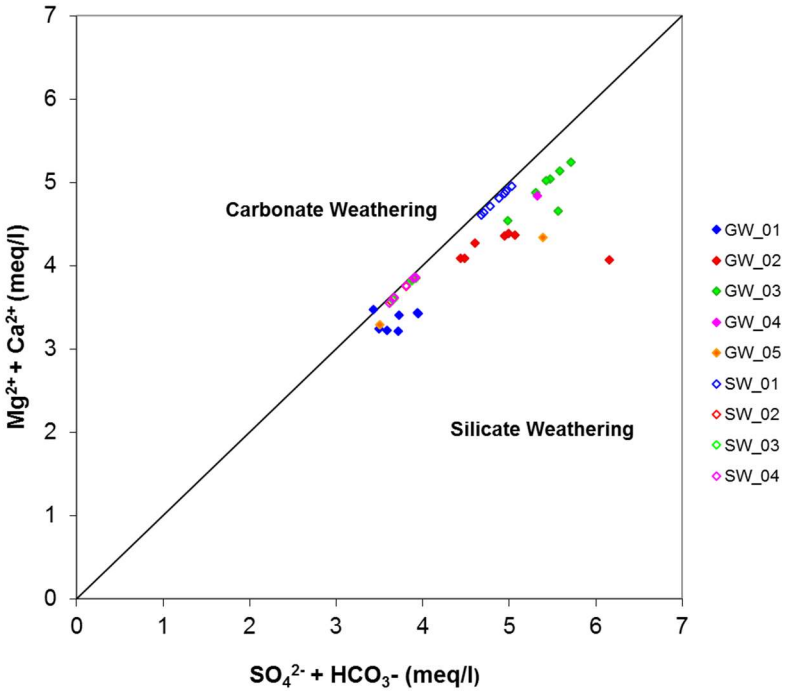

Figure 6.16 Scatter plot of (Ca+Mg) vs. (HCO_3+SO_4)

The excess of (HCO_3+SO_4) over (Ca+Mg) in groundwater samples (GW_02, GW_03, GW_04 and GW_05) suggests significant contribution from non-carbonate source and demanding the required portion of the (HCO_3+SO_4) to be balanced by the alkalies (Na+K). In addition to the weathering of silicate, the carbonate weathering process is also a Ca ions increasing factor in these groundwater. The plot (Ca+Mg) versus HCO_3 (Fig. 6.17) shows that data cluster around 1:1 equiline. Evaluation of the slopes of Ca and Mg with HCO_3 gives valuable information about the stoichiometry of the process.

The dissolution of carbonate minerals is the major source of Ca and Mg in groundwater, whereas HCO_3 is produced by weathering of silicate and carbonate minerals [85]. The most common weathering reaction in the case of carbonate is simple dissolution, giving a 1:2 ratio of Ca:HCO_3 or a (Ca+Mg):HCO_3 equivalence ratio of 1:1. The plot of (Ca+Mg) versus HCO_3 shows a lack of (Ca+Mg) referred to HCO_3 in most of groundwater samples and suggests that excess negative charge of bicarbonate alkalinity should be balanced by the alkali ions (Na+K), provided by silicate weathering.

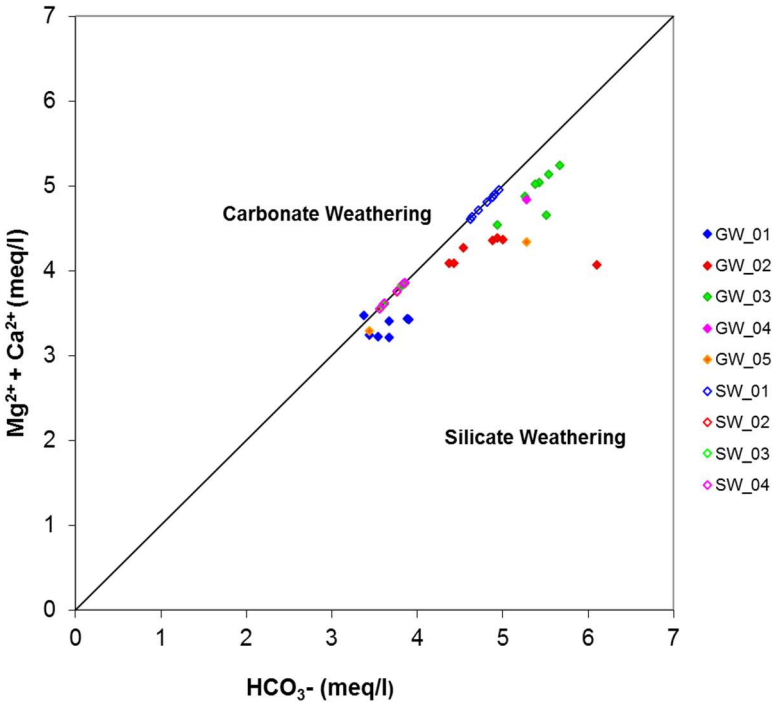

Figure 6.17 Scatter plot of (Ca + Mg) vs. HCO_3

The compositional changes in Mg and Ca concentrations mainly depend on the residence times of water in karstic systems and they are controlled by the distance from the recharge area and the dissolution and/or precipitation reaction of calcite and dolomite [24,86,87]. For this reason the Mg/Ca ratio is commonly used in carbonate aquifers as an indicator of the residence time of circulating groundwater [88,89].

The analysis of the ionic ratio Mg/Ca (Fig. 6.18) show that water rock interaction mechanisms and dissolution of carbonate and silicate minerals have influenced the groundwater chemistry in the study area. Groundwater from GW_03, GW_04 and GW_05 show the lowest Mg/Ca ratios (~0.02). Pertuso Spring (GW_01), GW_02, SW_02, SW_03, SW_04 show Mg/Ca ratio < 0.5, while the gouging station upstream the study area (SW_01) shows higher Mg/Ca ratios (up to 0.5) (Tabs. 6.5 and 6.6).

Nevertheless, the increase in magnesium concentrations, and hence Mg/Ca ratio not only depends on the dissolution/precipitation reaction of calcite and dolomite, but also on an increase in water temperature which makes faster the kinetics of the dissolution of dolomite [90,91].

The highest Mg/Ca ratios (~0.7) were found in SW_01 gauging station, located upstream the Pertuso Spring, highlighting long residence time and enhanced weathering along the groundwater flow paths. These waters are saturated with respect to calcite and dolomite; however, they are much more saturated with respect to dolomite than calcite. The high Mg/Ca ratio may be due to the weathering of Mg-rich dolomite, where dolomitic limestone and dolomite are the most dominant formations in this area. Gypsum and halite may participate in water-rock interactions, probably as natural salts, which are more soluble than calcite and dolomite and will further affect the amount and type of dissolved solids in groundwater.

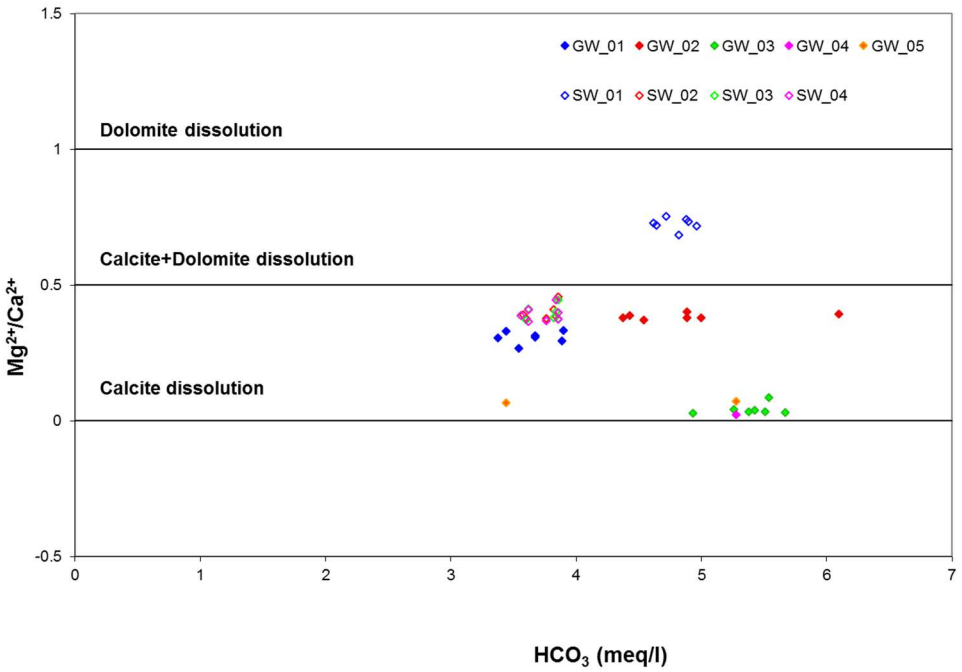

Figure 6.18 Mg/Ca vs. HCO_3

Figures from 6.19 to 6.22 show the stratigraphic reports referred to the groundwater monitoring points GW_02, GW_03, GW_04 and GW_05, respectively. As it can be seen from mentioned figures, the wells are mainly drilled in carbonate rocks. As a consequence of it groundwater flowing through an aquifer composed dominantly of carbonate rocks and the weathered products coming from them are characterized by elevated concentration on these elements.

These reports don't seem to correspond to what comes out from hydrochemical characterization of samples, taken at GW_02 and GW_03 wells, which are close, one to the other less than 100 meters. As a matter of fact, water level values and the short distance let suppose that these groundwater samples belong the same aquifer, but chemical data clearly deny this hypothesis. The significant difference in Mg and Ca concentrations between GW_02 and the rest of wells downstream highlights the presence of an aquifer boundary in the small area between GW_02 and GW_03 (Figs. 6.19 and 6.20).

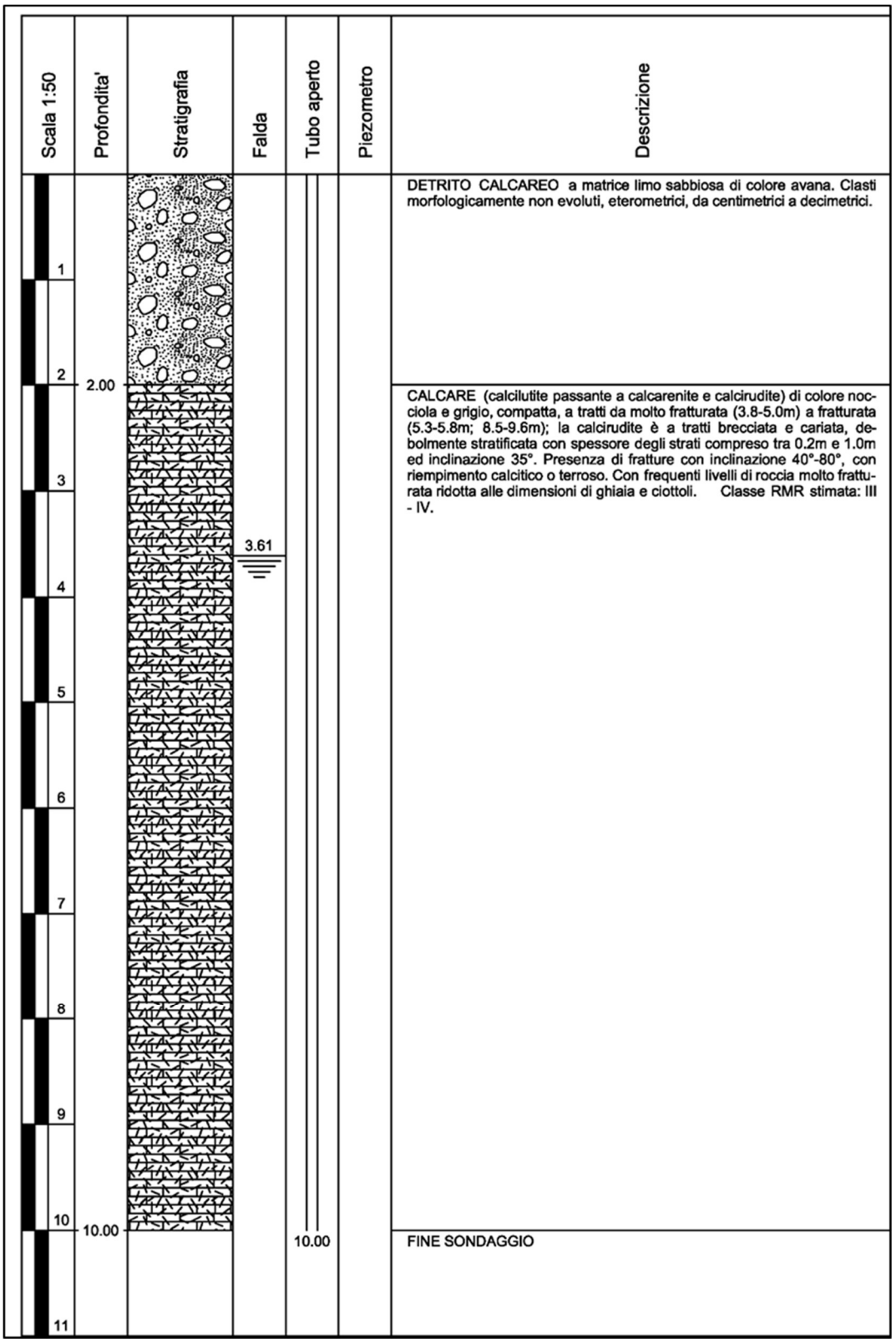

Figure 6.19 Stratigraphic units of GW_02

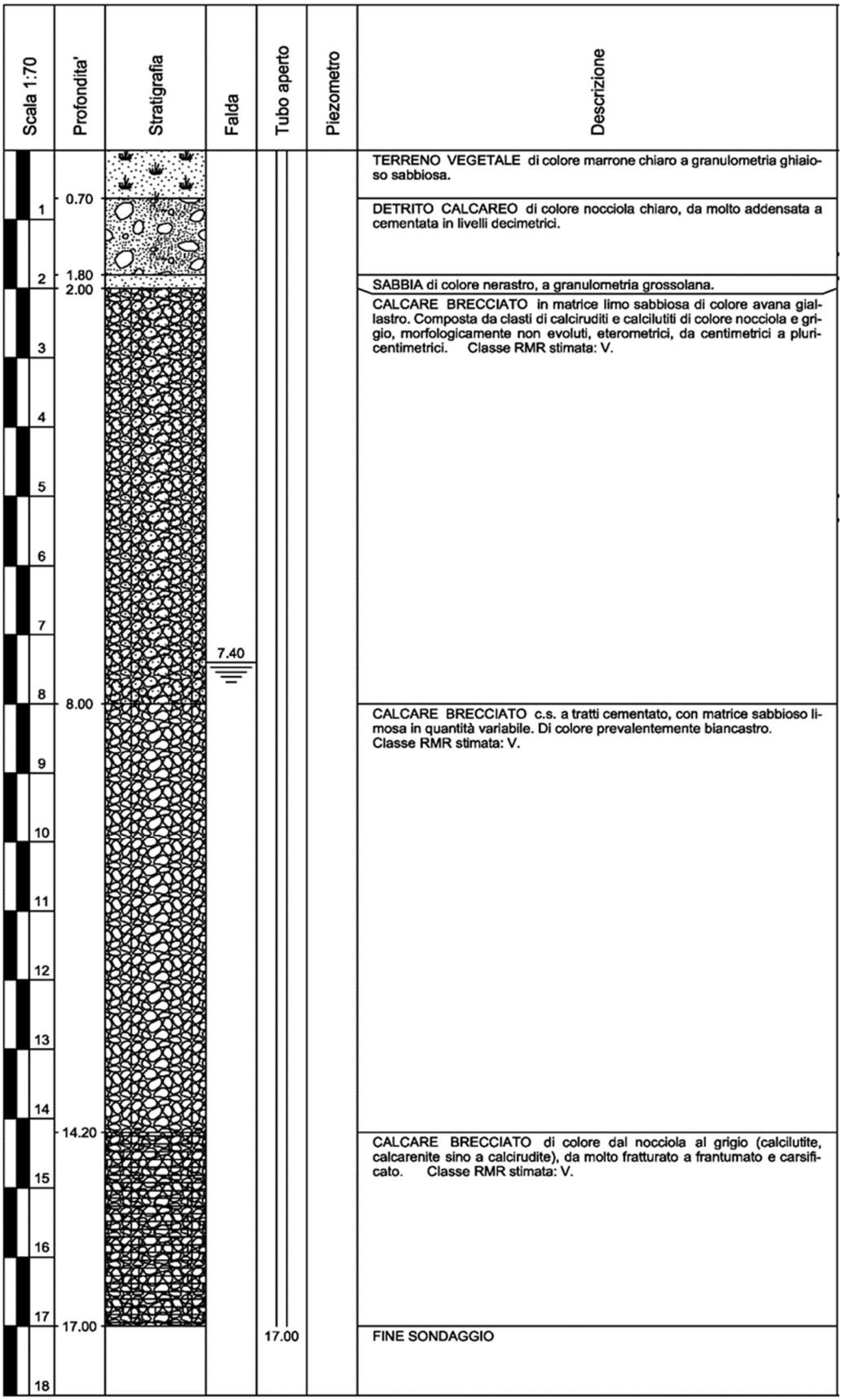

Figure 6.20 Stratigraphic units of GW_03

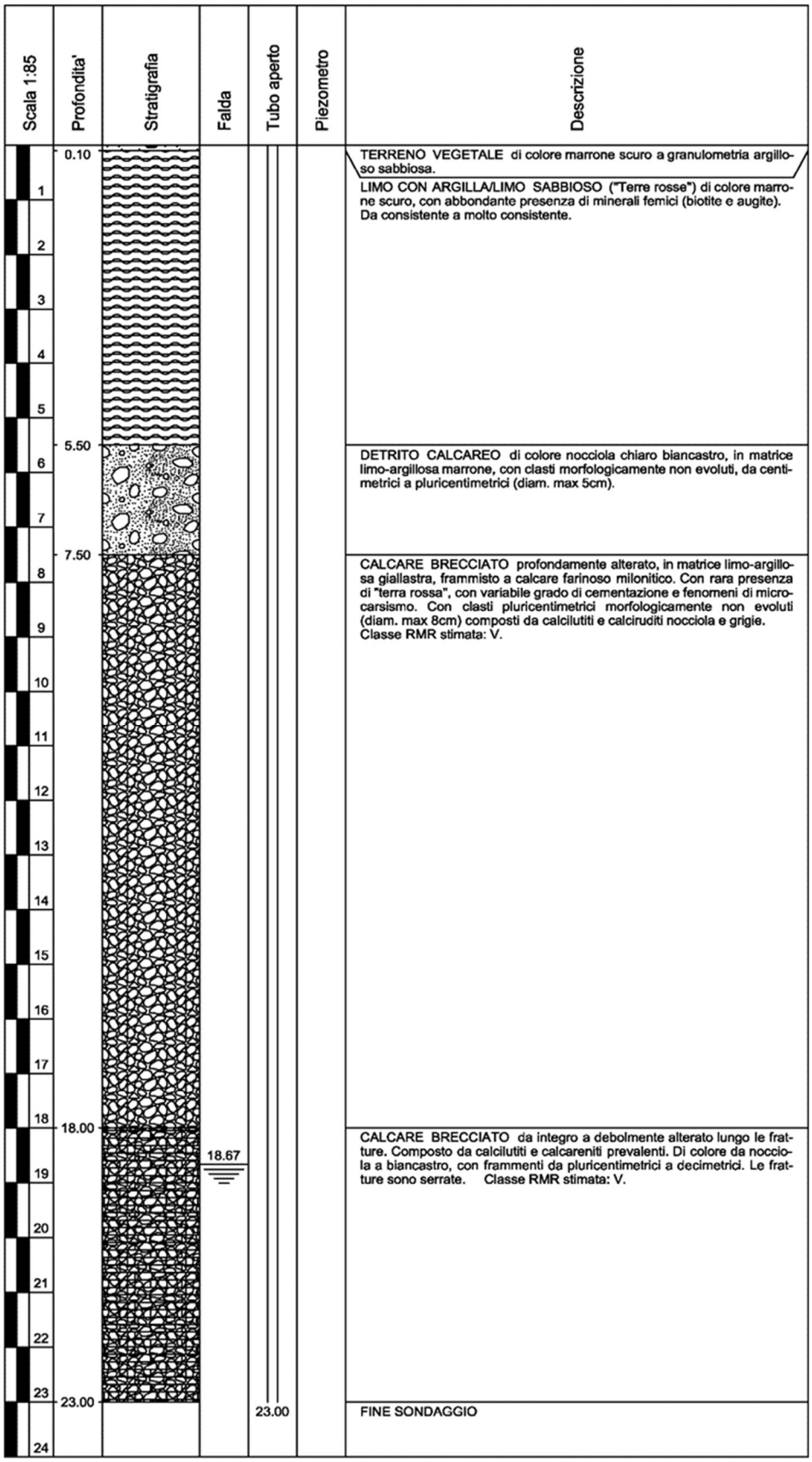

Figure 6.21 Stratigraphic units of GW_04

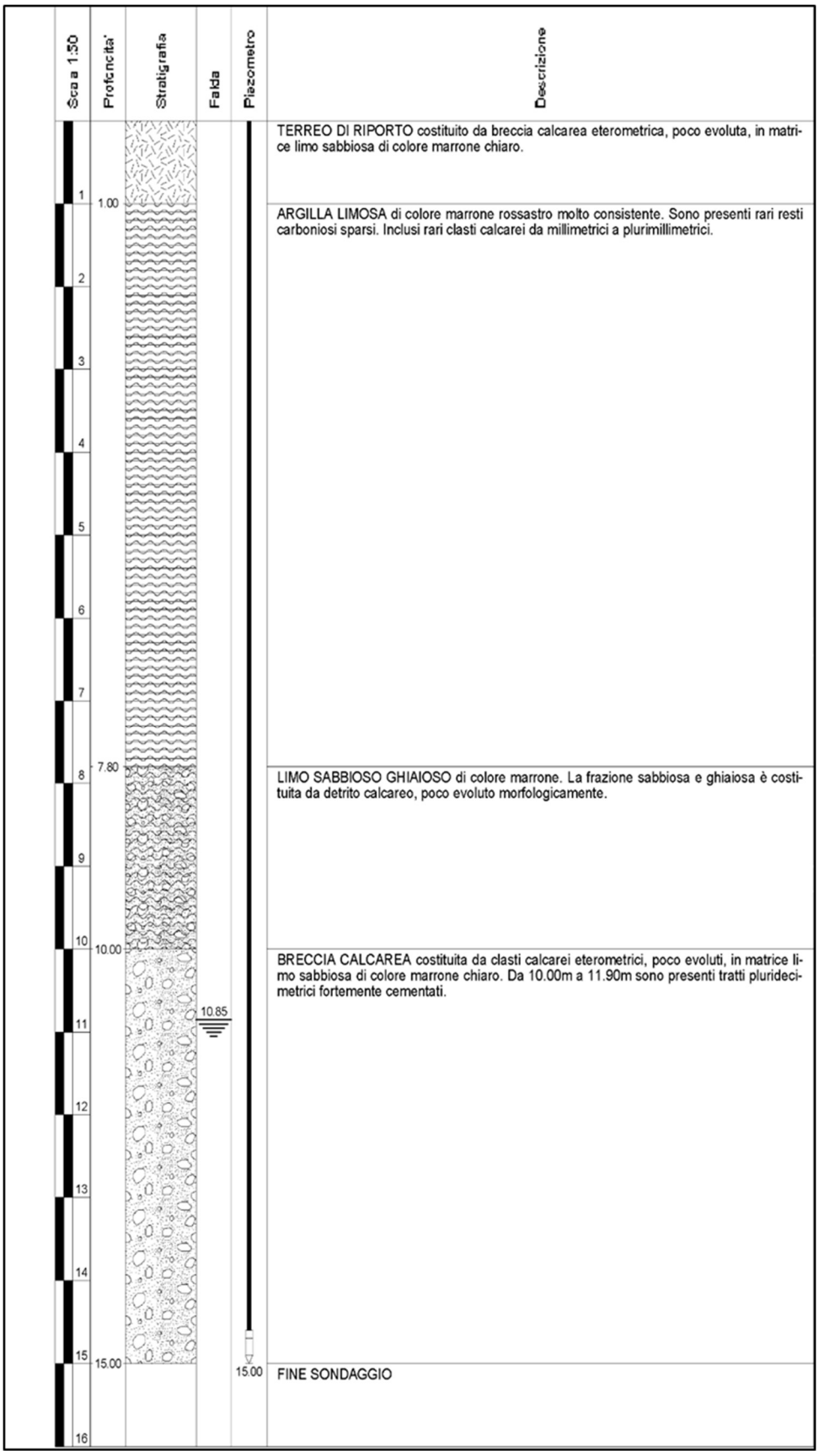

Figure 6.22 Stratigraphic units of GW_05

6.1.5 Saturation indices

The equilibrium state of the water with respect to a mineral phase can be determined by calculating a saturation index using analytical data [92]. By using the saturation index approach, it is possible to predict the reactive mineralogy of the subsurface from groundwater data, without collecting the samples of the solid phase and analysing mineralogy.

Table 6.5 Mg/Ca ratio, saturation index of calcite, aragonite, dolomite and gypsum for groundwater samples

ID	Date	Mg/Ca (meq/l)	$SI_{calcite}$	$SI_{aragonite}$	$SI_{dolomite}$	SI_{gypsum}
GW_01	July 2014	0.33	0.33	0.17	0.01	-3.33
	November 2014	0.27	-0.63	-0.79	-1.98	-3.30
	January 2015	0.31	0.37	0.22	0.08	-3.30
	May 2015	0.31	-0.63	-0.79	-1.92	-3.32
	December 2015	0.33	-0.59	-0.75	-1.81	-3.31
	May 2016	0.29	0.40	0.24	0.09	-3.30
	November 2016	0.31	0.38	0.23	0.09	-3.30
GW_02	July 2014	0.39	-0.28	-0.43	-0.98	-3.14
	November 2014	0.38	-0.48	-0.63	-1.51	-3.28
	January 2015	0.38	0.57	0.42	0.58	-3.09
	May 2015	0.39	-0.43	-0.58	-1.35	-3.29
	December 2015	0.40	-0.40	-0.56	-1.30	-3.28
	May 2016	0.38	0.67	0.52	0.90	-3.29
	November 2016	0.37	-0.44	-0.60	-1.43	-3.09
GW_03	July 2014	0.03	-0.15	-0.30	-2.08	-3.14
	November 2014	0.04	-0.20	-0.35	-1.95	-3.42
	January 2015	0.04	-0.17	-0.33	-1.91	-3.11
	May 2015	0.03	-0.22	-0.37	-2.22	-3.14
	December 2015	0.03	-0.13	-0.29	-2.16	-3.09
	May 2016	0.09	-0.10	-0.25	-1.37	-3.14
	November 2016	0.03	-0.16	-0.32	-1.87	-3.11
GW_04	July 2014	-	-	-	-	-
	November 2014	0.02	-0.18	-0.33	-2.19	-3.12
	January 2015	-	-	-	-	-
	May 2015	-	-	-	-	-
	December 2015	-	-	-	-	-
	May 2016	-	-	-	-	-
	November 2016	-	-	-	-	-
GW_05	July 2014	0.07	-0.20	-0.35	-1.63	-2.78
	November 2014	0.07	-0.50	-0.66	-2.33	-3.06
	January 2015	-	-	-	-	-
	May 2015	-	-	-	-	-
	December 2015	-	-	-	-	-
	May 2016	-	-	-	-	-
	November 2016	-	-	-	-	-

Table 6.6 Mg/Ca ratio, saturation index of calcite, aragonite, dolomite and gypsum for surface water samples

ID	Date	Mg/Ca (meq/l)	$SI_{calcite}$	$SI_{aragonite}$	$SI_{dolomite}$	SI_{gypsum}
SW_01	July 2014	0.73	0.51	0.36	0.80	-3.35
	November 2014	0.72	0.46	0.30	0.61	-3.16
	January 2015	0.72	0.47	0.31	0.61	-3.14
	May 2015	0.75	0.50	0.35	0.78	-3.35
	December 2015	0.74	0.47	0.32	0.64	-3.15
	May 2016	0.73	0.52	0.37	0.80	-3.33
	November 2016	0.69	0.46	0.30	0.55	-3.13
SW_02	July 2014	0.41	0.38	0.22	0.23	-3.32
	November 2014	0.38	0.35	0.20	0.13	-3.31
	January 2015	0.39	0.40	0.24	0.24	-3.29
	May 2015	0.39	0.36	0.20	0.18	-3.32
	December 2015	0.46	0.36	0.21	0.20	-3.31
	May 2016	0.38	0.40	0.25	0.23	-3.30
	November 2016	0.41	0.41	0.25	0.28	-3.30
SW_03	July 2014	0.41	0.38	0.22	0.23	-3.32
	November 2014	0.37	0.37	0.21	0.15	-3.31
	January 2015	0.38	0.41	0.25	0.22	-3.28
	May 2015	0.39	0.42	0.27	0.37	-3.33
	December 2015	0.45	0.39	0.23	0.26	-3.31
	May 2016	0.38	0.43	0.28	0.31	-3.30
	November 2016	0.40	0.41	0.25	0.28	-3.30
SW_04	July 2014	0.41	0.40	0.24	0.28	-3.32
	November 2014	0.37	0.38	0.22	0.16	-3.30
	January 2015	0.37	0.40	0.24	0.17	-3.28
	May 2015	0.39	0.39	0.23	0.27	-3.32
	December 2015	0.45	0.39	0.23	0.26	-3.31
	May 2016	0.37	0.43	0.27	0.29	-3.30
	November 2016	0.40	0.42	0.26	0.29	-3.30

Saturation index (*SI*) of a given mineral is defined as the logarithm of the ratio of ion activity product (*IAP*) to the mineral equilibrium constant at a given temperature (*Ksp*) and express as (6.3) [93]:

$$SI = \log_{10}\left(IAP / Ksp\right) \tag{6.3}$$

The saturation index represents the degree of chemical equilibrium between water and minerals and the trend to water-rock interaction. If undersaturated (SI<0), the solid phase could be dissolved by the groundwater and, thus, could be a potential source of constituents. Similarly, if oversaturated (SI>0), that phase feasibly could precipitate. The positive and negative values of the saturation index represent the thermodynamic potential for precipitation and dissolution, respectively. Positive values of SI indicate that the water is oversaturated with respect to the particular mineral phase and therefore incapable of dissolving more of the mineral and under suitable physico-chemical condition, the mineral

phase in equilibrium may precipitate. A negative index indicates undersaturation condition and dissolution of mineral phase, while neutral SI is in equilibrium state with the mineral phase. Saturation indices for calcite, aragonite, dolomite, and gypsum of groundwater and surface water samples were calculated using PHREEQC program version 3.0 [94] to study mixing of groundwater and surface water to understand spatial and temporal patterns of mixing during base flow conditions (Tabs. 6.5 and 6.6).

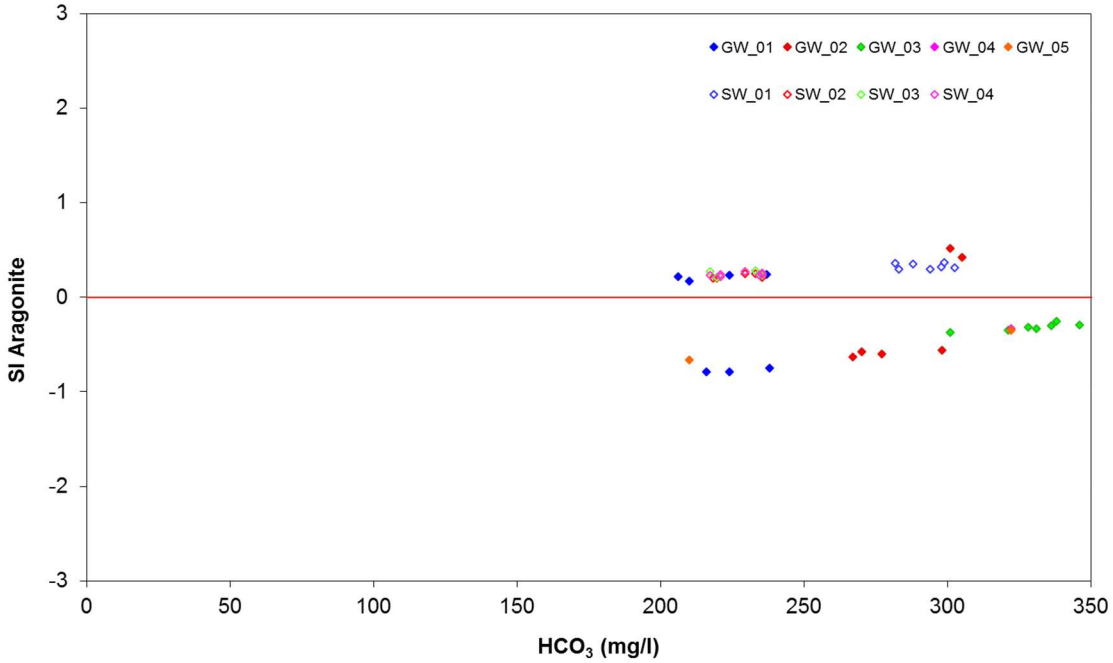

Figure 6.23 Saturation index of calcite minerals and its relation to HCO_3 in groundwater and surface water

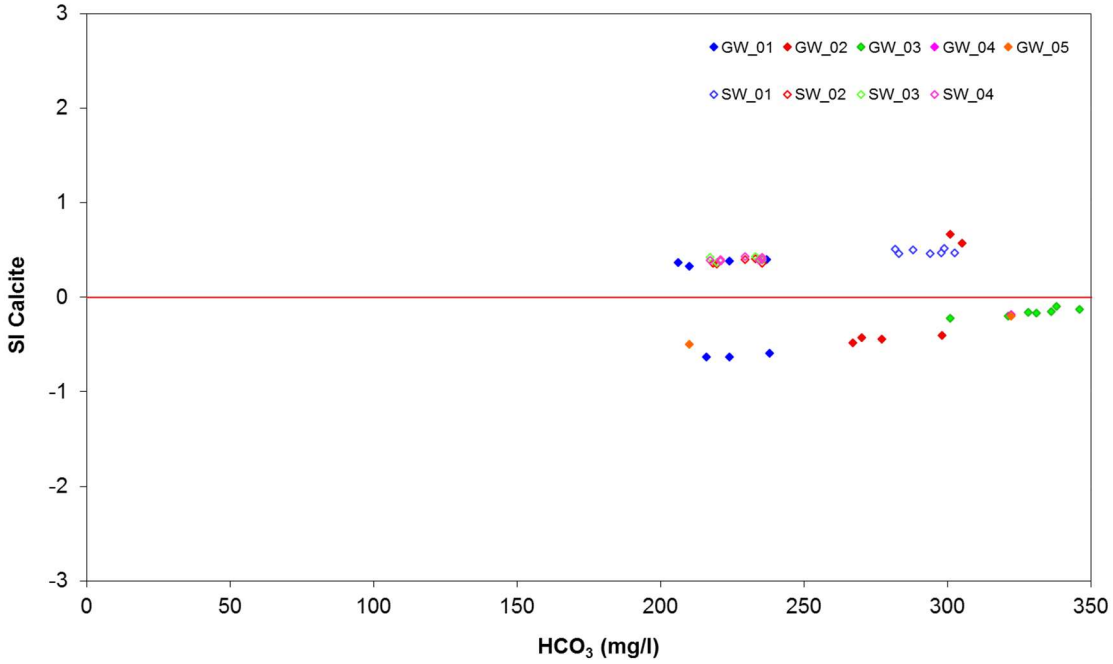

Figure 6.24 Saturation index of aragonite minerals and its relation to HCO_3 in groundwater and surface water

The results of geochemical modeling suggest that all surface water samples are saturated with respect to calcite, aragonite and dolomite, which implies a great dissolution and strong mineralization along groundwater flow paths. The high dissolution rate for carbonate rocks allows for waters close to saturation with respect to calcite and dolomite to remain undersaturated, resulting in continued dissolution along flow paths. All surface water samples are at or close to saturation with respect to calcite, aragonite and dolomite (Figs. 6.23, 6.24 and 6.25) and undersaturated with respect to gypsum (Fig. 6.26). More than half of groundwater samples are undersaturated with respect to all mineral phases (Figs. 6.23, 6.24, 6.25 and 6.26).

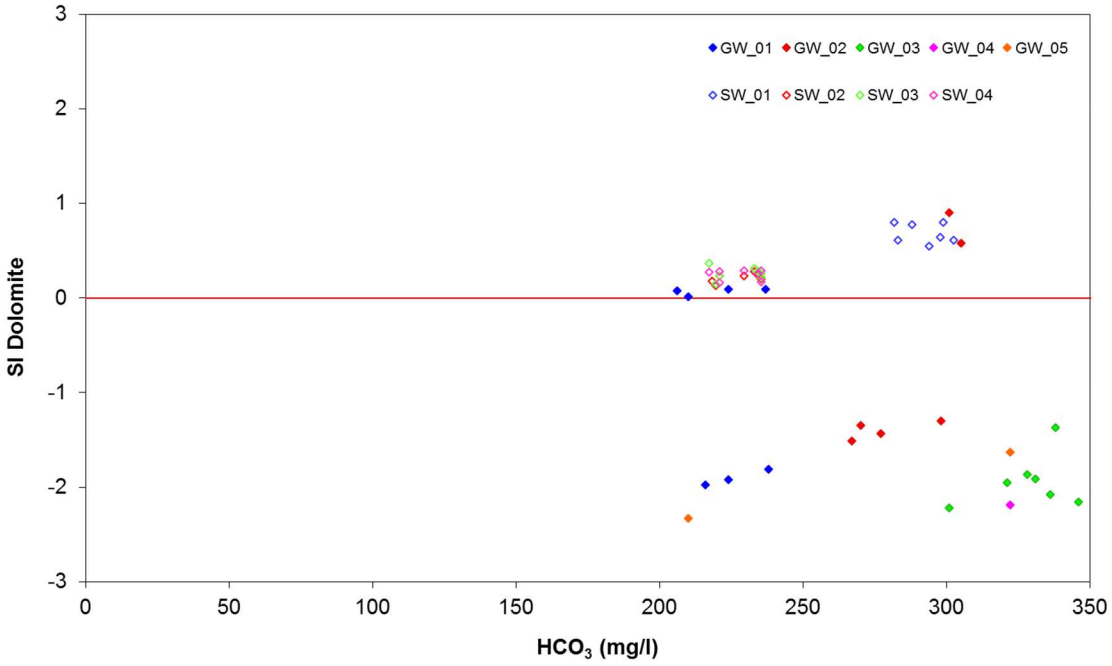

Figure 6.25 Saturation index of dolomite minerals and its relation to HCO_3 in groundwater and surface water

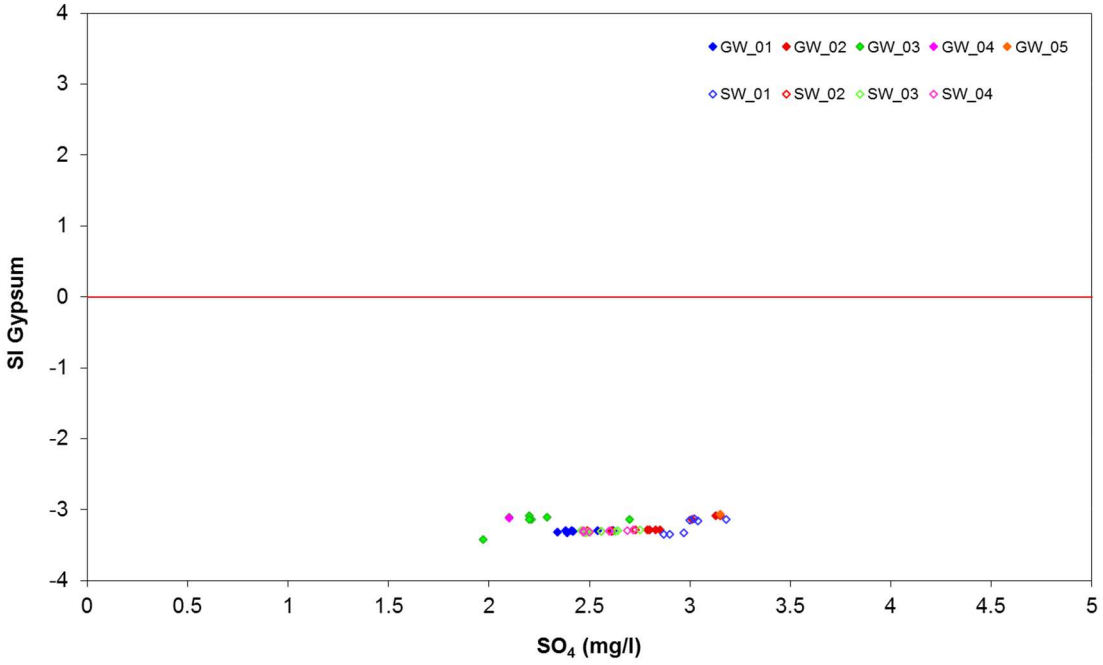

Figure 6.26 Saturation index of gypsum minerals and its relation to SO_4 in groundwater and surface water

The plot of SI of calcite versus dolomite (Fig. 6.27) demonstrates that the waters coming from the Pertuso Spring and GW_02 are saturated with respect to dolomite and calcite and the dolomite SI values are higher than the calcite SI values. This plot highlights an interaction between surface water and groundwater responsible of the high magnesium concentration in Pertuso Spring and GW_02 water samples.

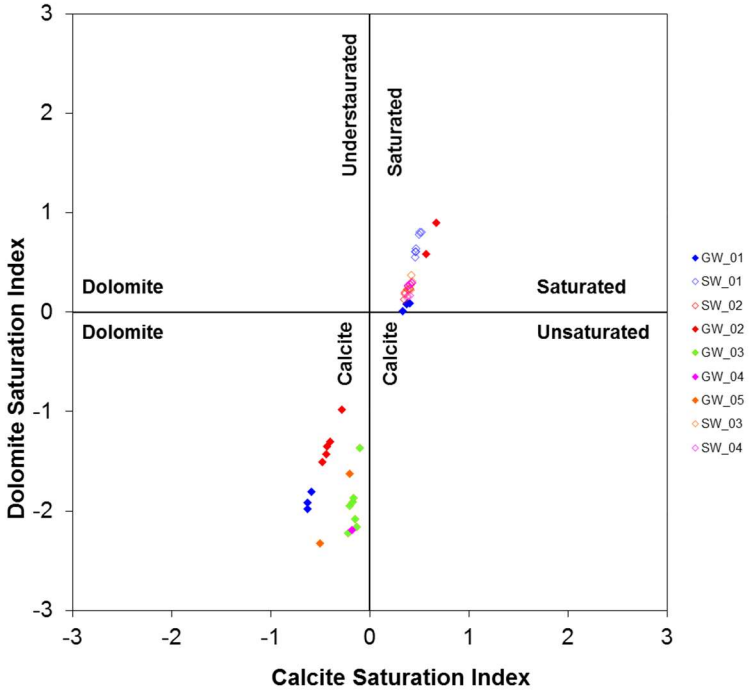

Figure 6.27 Saturation index of calcite versus dolomite

6.1.6 Trace elements

Heavy metals and trace elements in groundwater and soils come from natural and anthropogenic sources. The weathering of minerals is one of the most important natural sources. Anthropogenic sources include fertilizers, industrial effluent and leakage from wastewater networks. Many researchers on contaminated waters carried out trace element studies in order to identify the origin of the pollution [95,96]. Understanding the distribution of trace elements in groundwater is essential to understand contamination processes and to the develop suitable remediation technologies, identifying high-risk areas [97,98,99,100].

A series heavy metals, including Al, Ag, Be, Co, Cr, As, Cu, Fe, Pb, Mn, Hg, Ni, Cd, Se, Sb, and Zn were determined in under study groundwater. Results of the analysis of the heavy metals in groundwater samples are reported in Table 6.7. Groundwater samples collected in the study area are assumed free from any anthropogenic contaminations and thus trace elements sources can be explained by the weathering of minerals. The concentration of Cd, Hg and Be and Co in groundwater samples is lower than 1 µg/l. Se, As, Cr_{tot}, Ni and Cu content in the study area range not exceed 5 µg/l. The Fe and Zn content range from 5.0 to 135.8 µg/l and from 0.8 to 77.1 µg/l respectively. The Mn content in groundwater exceeds the drinking water limit of 50 µg/l (D.L. 152/2006). Fe and Mn are common metallic elements that occurs naturally, together, especially in deeper wells with little or no oxygen presence. The extent to which Fe and Mn dissolves in groundwater depends on the amount of oxygen in water and, to a lesser extent, upon its degree of acidity (pH).

Table 6.7 Heavy metals concentrations in groundwater samples

ID	Date (dd/mm/yyyy)	Se µg/l	Zn µg/l	Fe µg/l	As µg/l	Cr µg/l	Ni µg/l	Cu µg/l	Pb µg/l	Cd µg/l	Mn µg/l	Hg µg/l	Al µg/l	Sb µg/l	Ag µg/l	Be µg/l	Co µg/l
GW_01	22/07/2014	1.5	2.5	<5.0	<1.0	<5.0	<2.0	1.5	<0.2	<0.2	2	<0.2	2.1	<1.0	9.2	<0.2	<0.2
	20/11/2014	<1.0	29.1	<5.0	<5.0	<5.0	<2.0	<1	<0.2	<0.2	<0.2	<0.2	4.4	<1.0	<0.2	<0.2	<0.2
	28/01/2015	<1.0	1.7	<5.0	<1.0	<5.0	<2.0	<1	<0.2	<0.2	<0.2	<0.2	3.1	<1.0	<0.2	<0.2	<0.2
	12/05/2015	<1.0	1.1	<5.0	<1.0	<5.0	<2.0	0.3	<0.2	<0.2	<0.2	<0.2	1.5	<1.0	<0.2	<0.2	<0.2
	03/12/2015	<1.0	1.4	<5.0	<1.0	<5.0	<5.0	<1	<0.2	<0.2	<0.2	<0.2	<1.0	<1.0	<0.2	<0.2	<0.2
	25/05/2016	<1.0	<1.0	<5.0	<1.0	<5.0	<2.0	<1	<0.2	<0.2	<0.2	<0.2	2	<1.0	<0.2	<0.2	<0.2
	24/11/2016	<1.0	2.9	<5.0	<1.0	<5.0	<2.0	<1	<0.2	<0.2	<0.2	<0.2	2	<1.0	<0.2	<0.2	<0.2
GW_02	22/07/2014	<1.0	0.8	16	<1.0	<5.0	<2.0	1.1	1.5	<0.2	20.1	<0.2	48.3	0.8	1.1	<0.2	0.2
	20/11/2014	<1.0	77.1	39.6	<1.0	<5.0	3	4.4	3.8	<0.2	5.6	<0.2	40.1	<1.0	<0.2	<0.2	<0.2
	28/01/2015	<1.0	25.1	30.8	<1.0	<5.0	<2.0	1.8	0.8	<0.2	5.1	<0.2	67.6	<1.0	<0.2	<0.2	0.2
	12/05/2015	<1.0	10.5	7.8	<1.0	<5.0	<2.0	0.9	1.7	<0.2	<0.2	<0.2	21.5	1.4	<0.2	<0.2	<0.2
	03/12/2015	<1.0	11	<5.0	<1.0	<5.0	<5.0	<1	1.1	<0.2	<0.2	<0.2	7.6	<1.0	<0.2	<0.2	<0.2
	25/05/2016	<1.0	12.8	10.9	<1.0	<5.0	<2.0	1.51	1.2	<0.2	0.3	<0.2	35.2	1.8	<0.2	<0.2	<0.2
	24/11/2016	<1.0	40.1	<5.0	<1.0	<5.0	<2.0	2.7	45.4	<0.2	8.6	<0.2	2.8	6.4	<0.2	<0.2	<0.2
GW_03	22/07/2014	1	16.4	7.9	<1.0	<5.0	<2.0	0.8	1.6	<0.2	0.9	<0.2	12.6	0.7	26.1	<0.2	0.2
	20/11/2014	<1.0	64.5	12.3	<1.0	<5.0	<2.0	<1	6.1	<0.2	1.5	<0.2	80.7	<1.0	<0.2	<0.2	<0.2
	28/01/2015	<1.0	35.4	44.5	<1.0	<5.0	<2.0	3.3	12.7	<0.2	2.7	<0.2	118.3	1.1	<0.2	<0.2	0.4
	12/05/2015	<1.0	7.9	<5.0	<1.0	<5.0	<2.0	0.3	4	<0.2	<0.2	<0.2	4.4	<1.0	<0.2	<0.2	<0.2
	03/12/2015	<1.0	7.8	<5.0	<1.0	<5.0	<5.0	<1	1.9	<0.2	<0.2	<0.2	1.2	<1.0	<0.2	<0.2	<0.2
	25/05/2016	<1.0	15.1	<5.0	<1.0	<5.0	<2.0	<1	9.1	<0.2	0.2	<0.2	2.1	<1.0	<0.2	<0.2	<0.2
	24/11/2016	<1.0	2.5	<5.0	<1.0	<5.0	<2.0	<1	0.6	<0.2	0.3	<0.2	42.1	<1.0	<0.2	<0.2	<0.2
GW_04	20/11/2014	<1.0	45.7	97.5	<1.0	<5.0	<5.0	<1	16.9	<0.2	17.1	<0.2	130	<1.0	<0.2	<0.2	0.4
GW_05	22/07/2014	<1.0	11.6	14.1	1.2	<5.0	2.2	0.8	2.5	<0.2	176	<0.2	46.6	0.9	<0.2	<0.2	0.6
	20/11/2014	<1.0	29.7	135.8	<1.0	<5.0	<2.0	1.3	3.3	<0.2	5.2	<0.2	264.3	<1.0	<0.2	<0.2	<0.2

Natural sources of Fe and Mn may include weathering of iron and manganese bearing minerals like amphibole, iron sulfide and iron rich clay minerals. In areas, where groundwater flow through an organic rich soil, Fe and Mn will also dissolve in groundwater. Fe and Mn can also have anthropogenic sources including industrial effluents, landfill leakages and acid mine drainage [101]. In natural conditions, water percolates through the organic soil, where dissolved oxygen is consumed by the decomposition of organic matter and microbes in the soil. The decomposition process reduces the pH due to the microbial action. In combination with the lack of oxygen, the Fe and Mn atoms are also reduced from Fe^{3+} and Mn^{4+} to Fe^{2+} and Mn^{2+}. The most dominant form of dissolved iron is the soluble Fe^{2+} under the pH range of 5 to 8. When groundwater is pumped up to the surface it gets into contact with air (O_2), which incomes the solutions and starts the oxidation process that releases carbon dioxide (CO_2) from the groundwater to the atmosphere. When this process happens, the pH values increase and hence the Fe^{2+} and Mn^{2+} are changed into the insoluble Fe^{3+} and Mn^{4+} minerals. The highest concentrations of Mn and Fe were detected in groundwater sample collected in GW_05 in November 2014 and are related to low dissolved oxygen content (8.4 mg/l) and pH slightly more acidic (7.4). These conditions make easier, iron and manganese dissolution. Dissolved oxygen content is typically low in deep aquifers; particularly in GW_05 where the piezometric level measured is the lowest in the study area (666.3 m

a.s.l.). Aluminium ion exceeds permissible concentration of 200 µg/l in GW_05 with value of 264.3 µg/l. Aluminium is a lithophile element and is the most abundant metal in the lithosphere, forming several of its own minerals, including sillimanite (Al_2SiO_5), corundum (Al_2O_3) and kaolinite ($Al_2Si_2O_5(OH)_4$). Aluminium has a low mobility under most environmental conditions, although below pH 5.5 its solubility increases as it is released from silicate rocks [102]. It is a major constituent in many rock-forming minerals, such as feldspar, mica, amphibole, pyroxene and garnet. The weathered products of primary Al minerals include secondary clay minerals, e.g., kaolinite and dioctahedral smectite, and Al-hydroxides, such as gibbsite, nordstrandite and bayerite, which may control the equilibrium concentration of Al in soil solution, groundwater and stream water [11]. The aluminium concentrations observed in GW_05 waters have been explained by the presence of clay minerals due to the weathering of primary silicates (Fig. 6.22). Polluting elements Pb, Sb and Ag (the concentration of which in grounds exceeds permissible values for groundwater) appear rarely to be present in the groundwater in GW_02 (November 2016), GW_03 (July 2014 and January 2015) and GW_04 (November 2014).

6.2 Groundwater and surface water quantity assessment

6.2.1 Groundwater table levels

Groundwater recharge is typically a small part of annual rainfall also in fractured bedrock aquifers [103,104,105]. Recharge in fractured rocks depends on many factors such as overburden thickness and cover, the topography of the bedrock surface, fracture connectivity and aperture, fracture spacing, and the nature of the interface between the soil overburden and the fractures [106,107]. Within a watershed these factors can vary in a wide range resulting in groundwater recharge that is highly spatially variable [108,109]. Depth to water table measurements are the most common form of hydrological monitoring because of they reflects the entire water balance. In temperate coastal regions, the highest water table occurs in winter, during periods of heavy rainfall, and the lowest in summer when there is little precipitation. Water table variations in relation to the rainfall distribution as shown in Fig. 6.28.

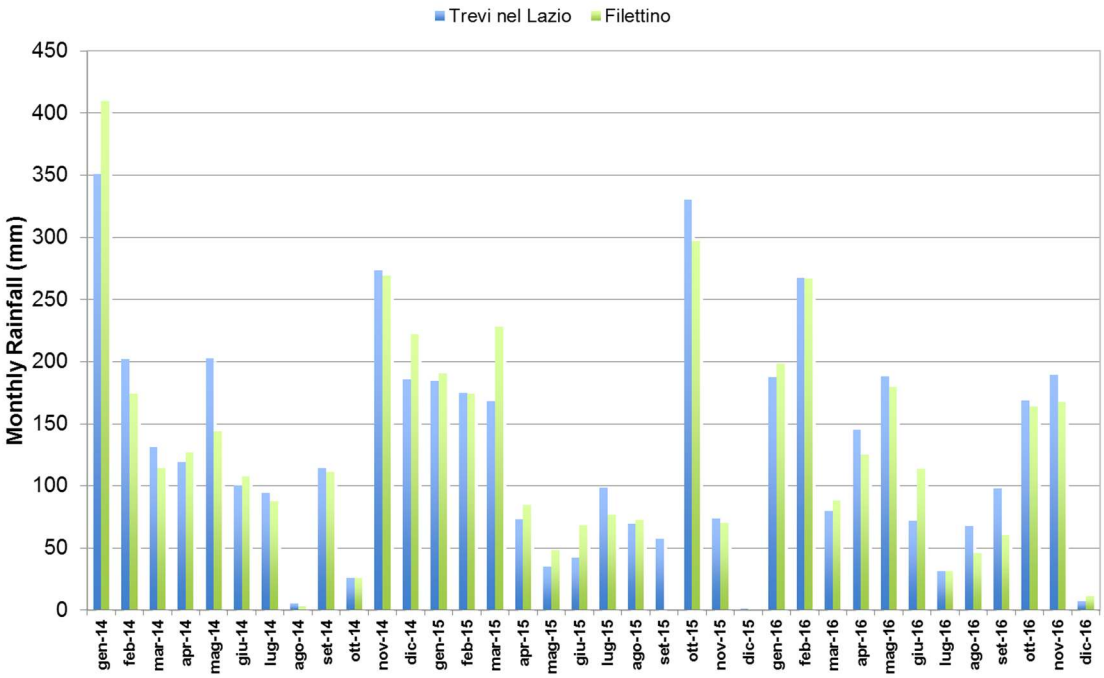

Figure 6.28 Monthly rainfall data for Filettino and Trevi nel Lazio meteorological station from 2014 to 2016

Water table fluctuations were determined by making depth-to-water monthly measurements in monitoring wells from July 2014 to November 2016 (Tab. 6.8). Sometimes, monthly measurement could not be obtained due to difficulties in accessing the site (GW_04 and GW_05).

Rainfall data have been collected from 2014 through 2016 in two meteorological stations located upstream (Filettino) and downstream (Trevi nel Lazio) the monitoring wells. The changes in water table in all the wells follow the same trend. In general, the water table is at its highest level between November and March, and decrease from April onwards in response to precipitation going less and evapotranspiration increases. It reaches a lower point in May and increases slightly to the high winter water level in response to rainfall in November or December. All the four monitoring well show their lower value during the year of lesser precipitation (2015). The depth of the low point of the water table is variable between years and dependent on the extent of the summer drought period.

Table 6.8 Water table measurements in monitoring wells

ID	Date (dd/mm/yyyy)	Ground Level (m a.s.l.)	Well depth (m)	Static Water Level (m)	Water Table (m asl)
GW_02	22/07/2014	688.1	10	2.9	685.2
	20/11/2014			3.0	685.1
	28/01/2015			3.0	685.2
	12/05/2015			3.0	685.2
	03/12/2015			2.8	685.3
	25/05/2016			4.1	684.0
	24/11/2016			3.6	684.5
GW_03	22/07/2014	692.3	17	8.3	684.1
	20/11/2014			6.0	686.3
	28/01/2015			7.0	685.3
	12/05/2015			9.0	683.3
	03/12/2015			9.0	683.3
	25/05/2016			7.8	684.6
	24/11/2016			8.5	683.8
GW_04	22/07/2014	701.3	23	-	-
	20/11/2014			18.0	683.4
	28/01/2015			20.9	680.4
	12/05/2015			20.9	680.4
	03/12/2015			20.8	680.5
	25/05/2016			-	-
	24/11/2016			20.8	680.5
GW_05	22/07/2014	681	15	12.2	668.8
	20/11/2014			10.2	670.8
	28/01/2015			14.5	666.5
	12/05/2015			14.4	666.6
	03/12/2015			14.7	666.3
	25/05/2016			-	-
	24/11/2016			-	-

The water table in GW_02 monitoring point does not show any substantial variations during the monitoring campaigns carried out (Fig. 6.29).

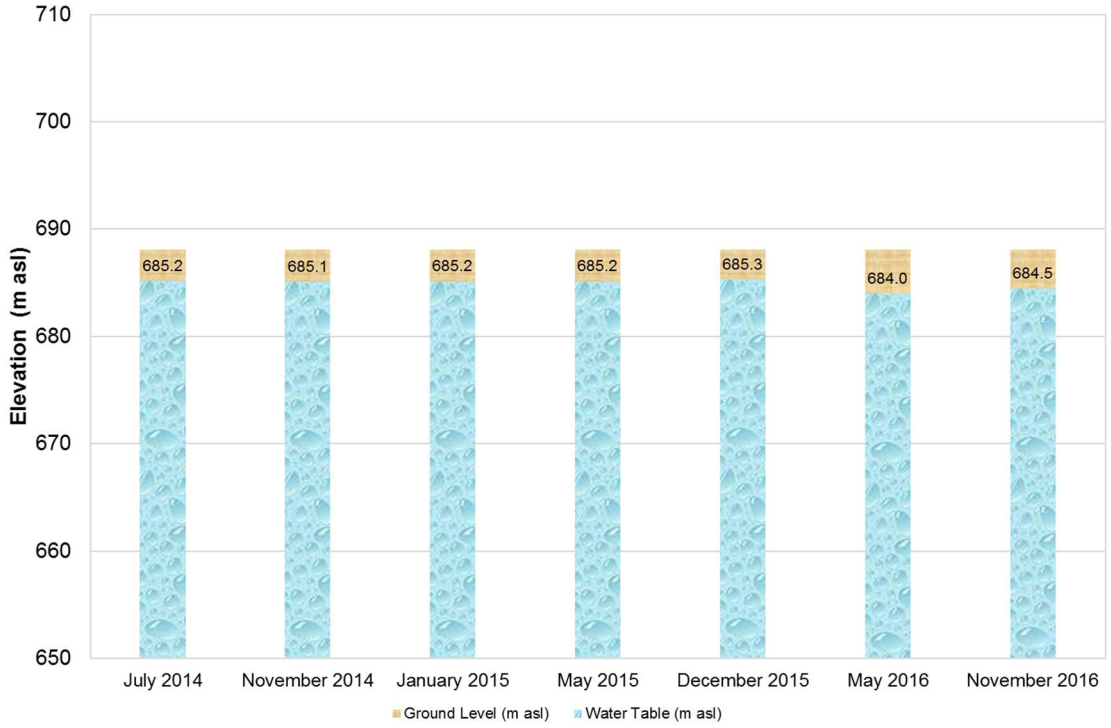

Figure 6.29 Water table fluctuations in m a.s.l. in monitored piezometer GW_02

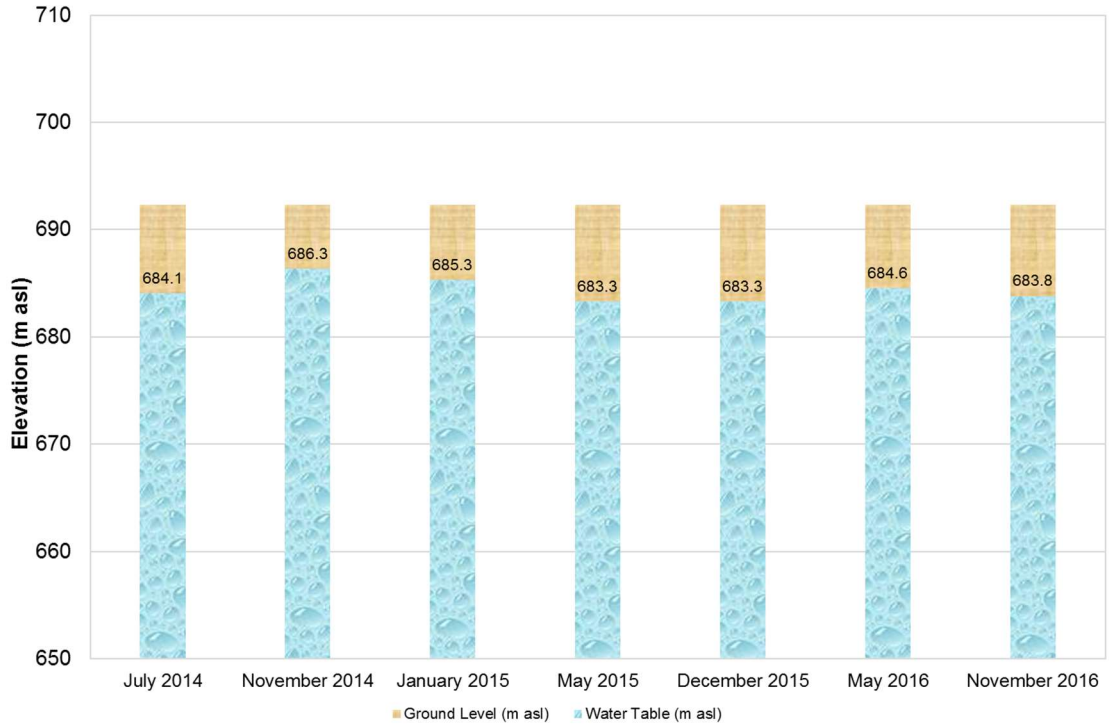

Figure 6.30 Water table fluctuations in m a.s.l. in monitored piezometer GW_03

Seasonal variations of water table have been observed in GW_03, GW_04 and GW_05, which show a fast reaction to rainfall, with a highest value measured during the November 2014 campaign and at least until May 2015 and confirmed in December 2015 (Fig. 6.30, 6.31 and 6.32).

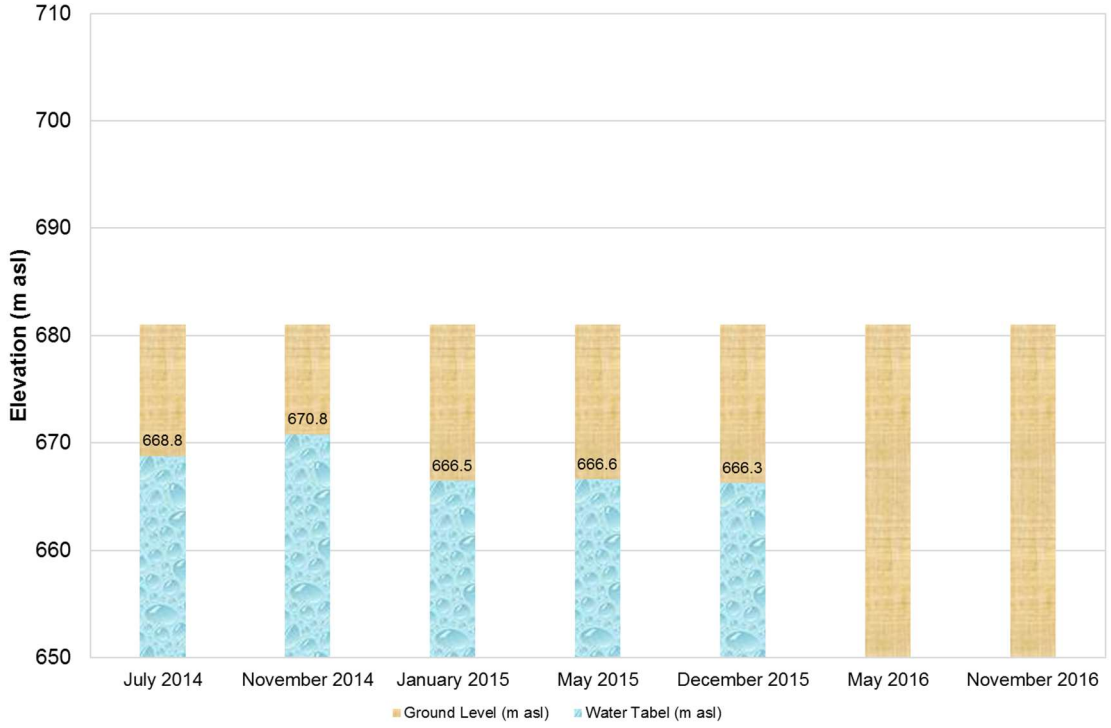

Figure 6.31 Water table fluctuations in m a.s.l. in monitored piezometer GW_04

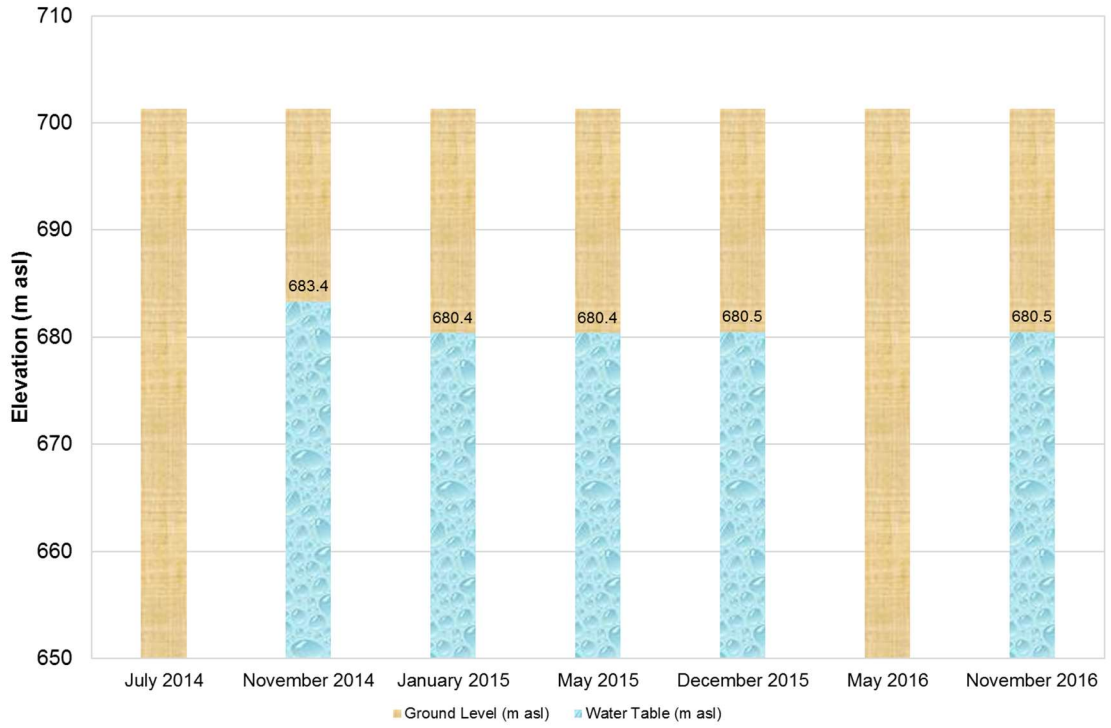

Figure 6.32 Water table fluctuations in m a.s.l. in monitored piezometer GW_05

The behaviour of GW_02, however, is not to be considered unusual for a karstic aquifer often characterized in the superficial part by insoluble rests of the karst dissolution process, consisting of fine sediments, predominantly clay matrix.

6.2.2 Discharge measurements

6.2.2.1 Current meter method

6.2.2.1.1 Measurement of width and depth

First of all, in a stream flow measurement it is necessary to survey the horizontal cross section. Width needs to be measured using the proper equipment and procedures that apply to the type of measurement being made (that is, wading, bridge, cableway, boat, or ice) [110].

The horizontal distance to any vertical in a cross section was measured by stringing a measuring tape from bank to bank at right angles to the direction of flow (Fig. 6.33).

Figure 6.33 Measuring channel width (SW_01)

The second measurement made at a vertical was the stream depth. The water depth of a stream at a selected vertical can be measured in several ways, depending on the type of measurement being made, the total depth of the stream, and the velocity of the stream. In this study, stream depth was measured by use of a rigid meter ruler (Fig. 6.34). The meter ruler was held in a vertical position with the meter parallel to the direction of flow while the velocity has being observed.

This measuring tape is used to define the hydraulic profile of the cross section and the location of each velocity measurements. Determining the cross sectional area of a stream involves measuring water depths at a series of points across the stream and multiplying by the width of the stream within each sector represented by the depth measurement [111].

In mountain stream, where the hydraulic pattern changes from time to time, more than a single measurement is needed to characterize, accurately, the hydraulic profile of the cross section. For this reason, it has been necessary determine the hydraulic profiles for any discharge measurements campaigns driven from July 2014 to November 2016.

At SW_01 gauging stations, the Aniene River surface width ranges from 10 cm (November 2016) to 60 cm (May 2015) and the depth ranges from 310 cm (November 2014) to 560 cm (November 2016) (Fig. 6.35).

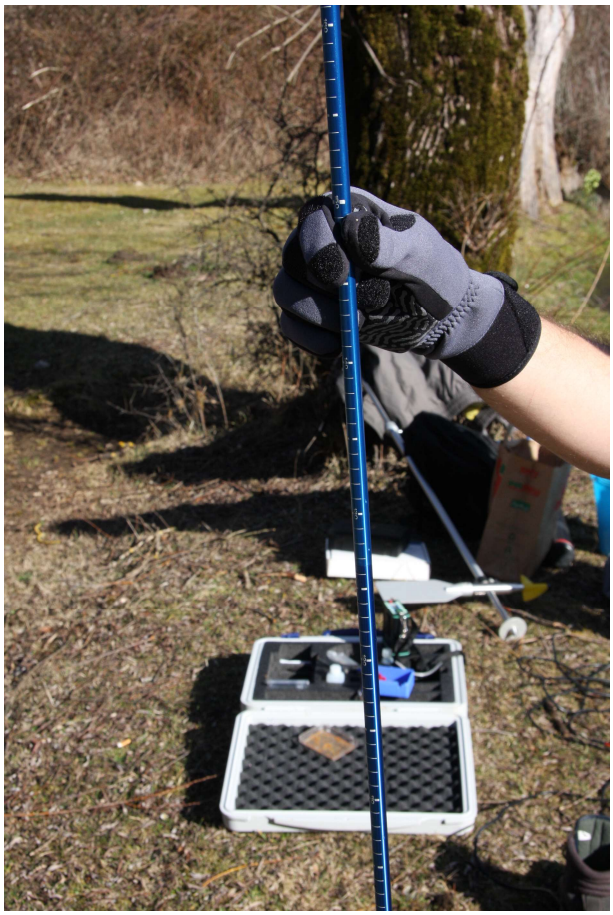

Figure 6.34 Meter ruler used for measuring channel depth

At SW_02, the stream surface width ranges from 30 cm (November 2014) to 60 cm (May 2015) and the depth ranges from 520 cm (November 2014 and December 2015) to 850 cm (May 2015) (Fig. 6.36).

The free surface width at SW_03 ranges from 55 cm (November 2016) to 75 cm (January 2015) and its depth from 545 cm (November 2016) to 600 cm (July 2014) (Fig. 6.37).

At SW_04, the stream surface width ranges from 35 cm (December 2015) to 70 cm (July 2014) and the depth ranges from 310 cm (November 2014) to 670 cm (May 2015) (Fig. 6.38).

The tendency of the stream is to increase width and depth downstream, and generally the smaller cross section of the Aniene River results in November, at the beginning of the rainy period, while is bigger at May, in spring season. The seasonal changes in width and depth in the stream section are related to the climate of the study area. In winter, rain and snow are responsible of more water draining into the Aniene River, while in the summer there is more water in the stream compared to the winter.

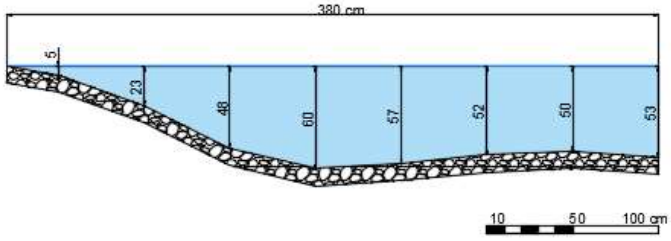

July 2014

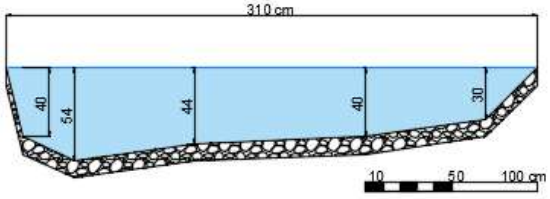

November 2014

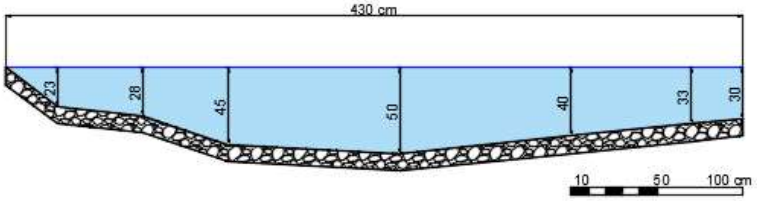

January 2015

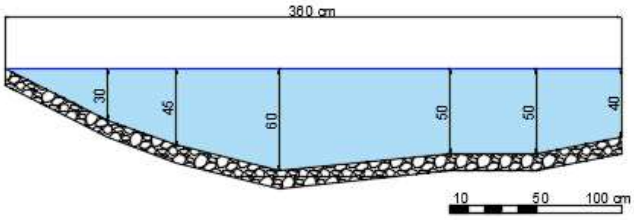

May 2015

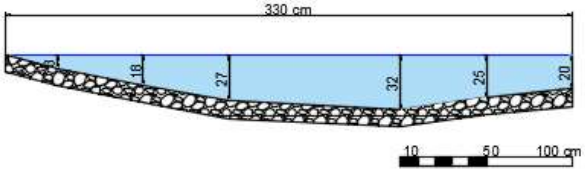

December 2015

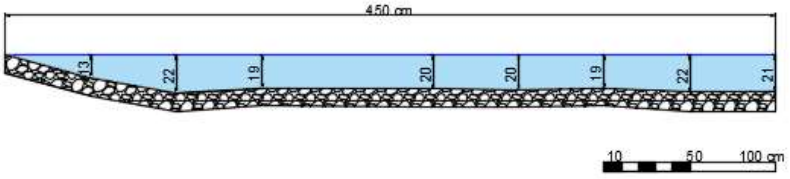

May 2016

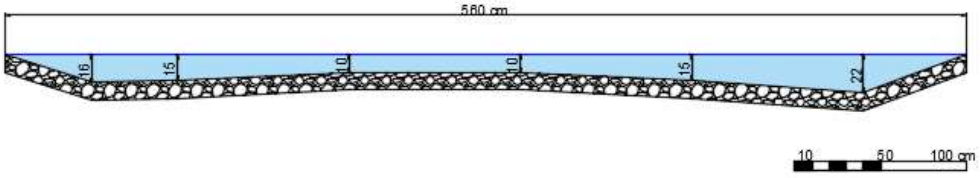

November 2016

Figure 6.35 Cross section SW_01 set up from July 2014 to November 2016

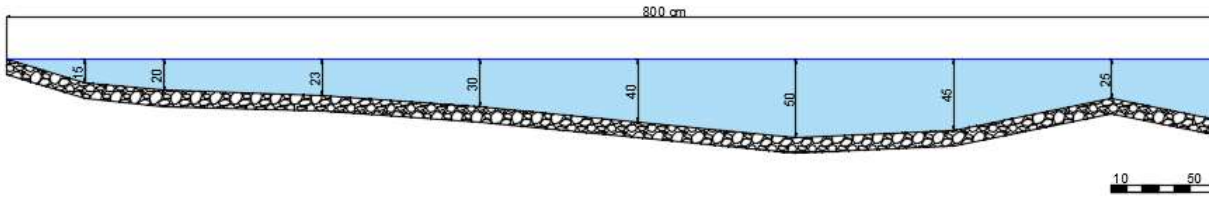

July 2014

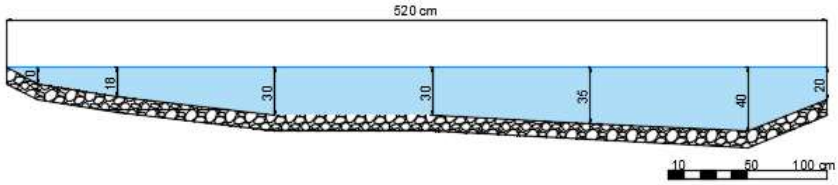

November 2014

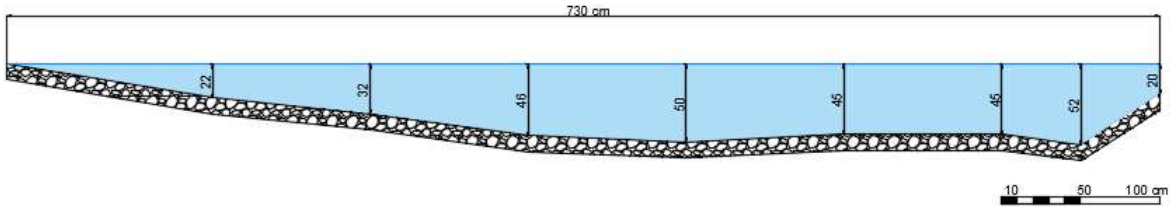

January 2015

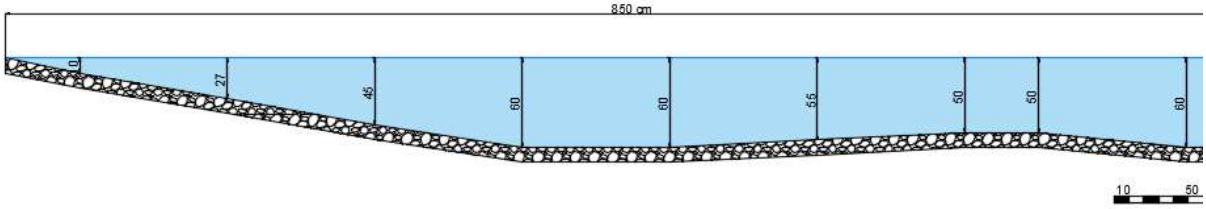

May 2015

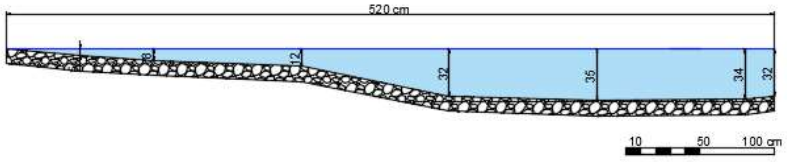

December 2015

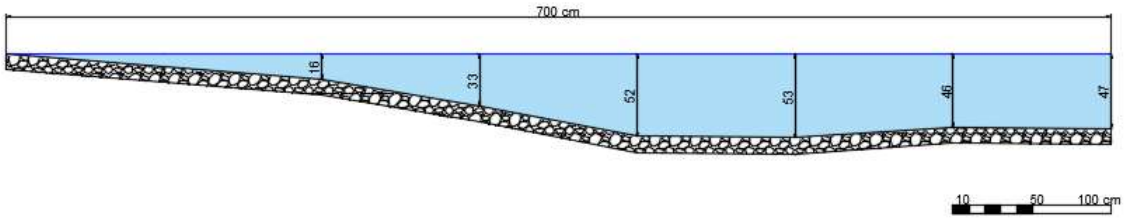

May 2016

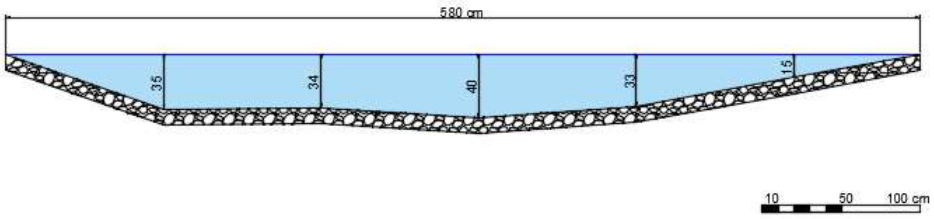

November 2016

Figure 6.36 Cross section SW_02 set up from July 2014 to November 2016

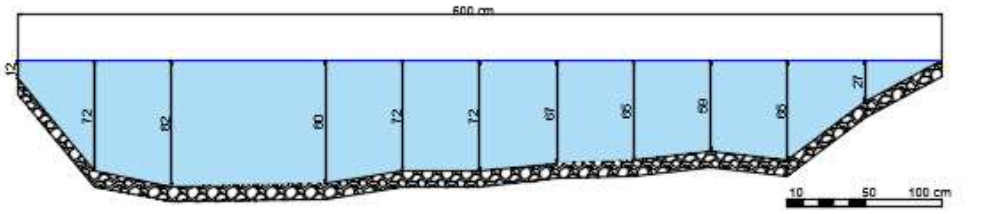

July 2014

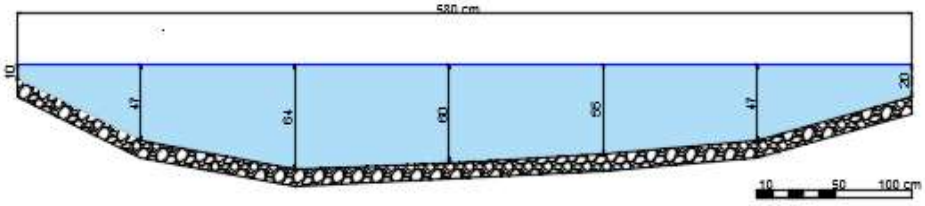

November 2014

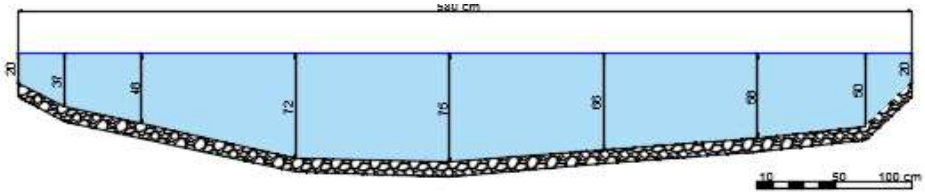

January 2015

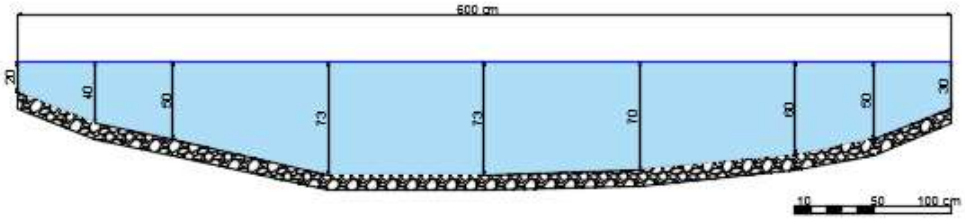

May 2015

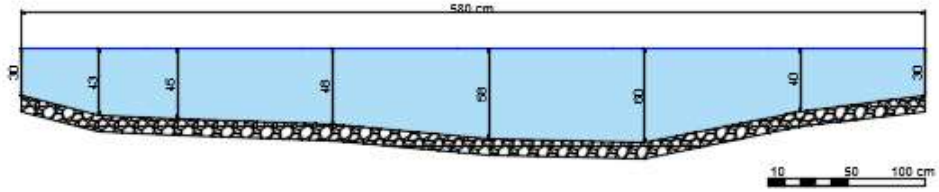

December 2015

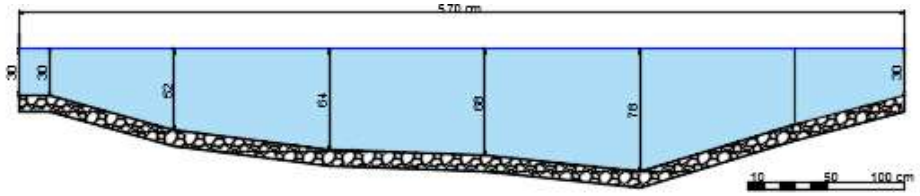

May 2016

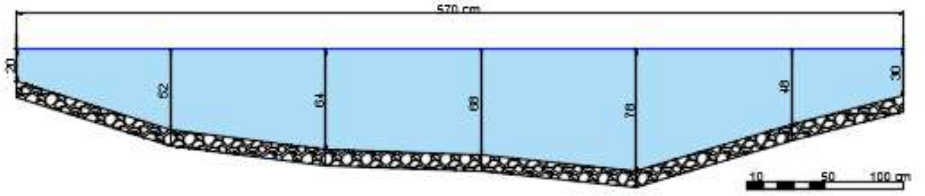

November 2016

Figure 6.37 Cross section SW_03 set up from July 2014 to November 2016

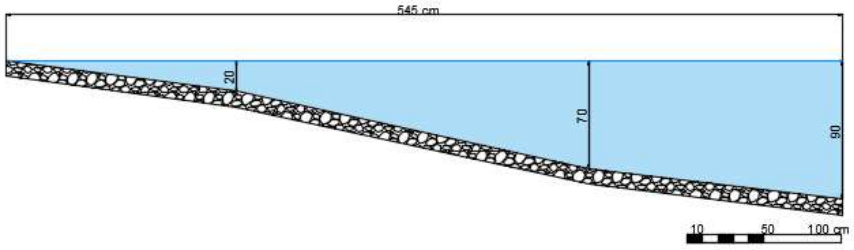

July 2014

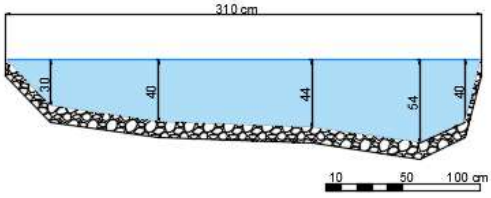

November 2014

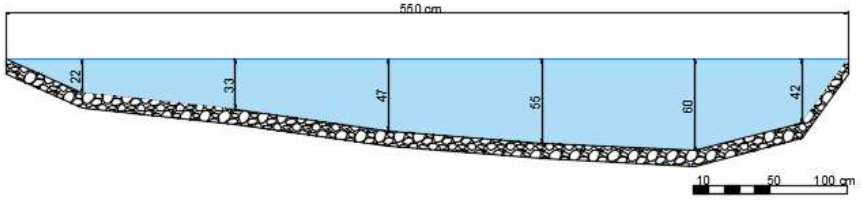

January 2015

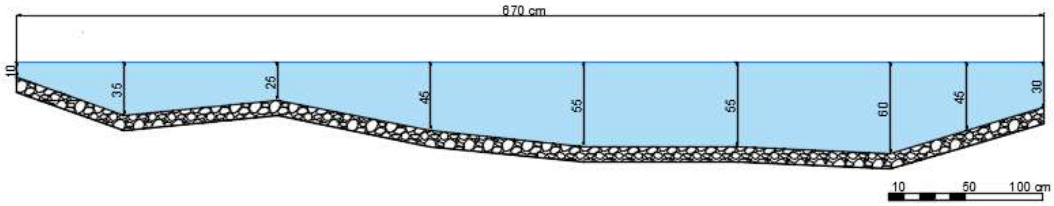

May 2015

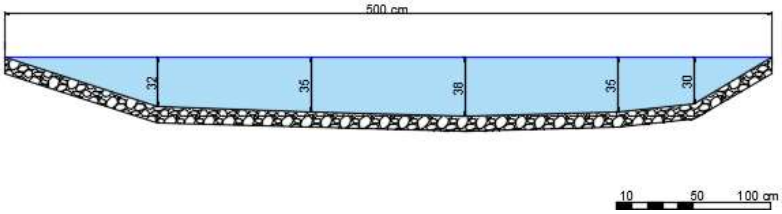

December 2015

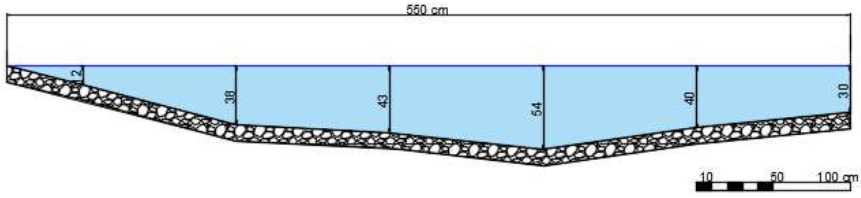

May 2016

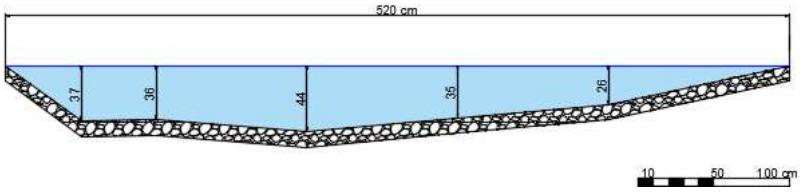

November 2016

Figure 6.38 Cross section SW_04set up from July 2014 to November 2016

6.2.2.1.2 Measurement of velocity

The first step in measuring stream velocity has been the preparation of the measurement note sheets for recording observations for each discharge measurement:

- name of stream
- location
- date
- type instrument
- bank of stream that was the starting point
- gauge heights and corresponding times
- number of spins of the meter rotor
- any other interesting information regarding the accuracy of the discharge measurement

After recording on the note sheet the station (distance from initial point) of the edge of water, the current meter was checked and the measurement was ready to be started. In this study was used current-meter measurements by wading (Fig. 6.39).

After the meter is placed at the proper depth and pointed into the current (Fig. 6.39), the number of revolutions made by the rotor was counted for a period of 60 seconds. The stopwatch was started simultaneously with the first signal or click, which is counted as zero, and not one.

The stopwatch was stopped on a convenient number coinciding with one of those given in the column headings of the meter-rating table and is read to the nearest second. The number of seconds and the number of revolutions were then recorded.

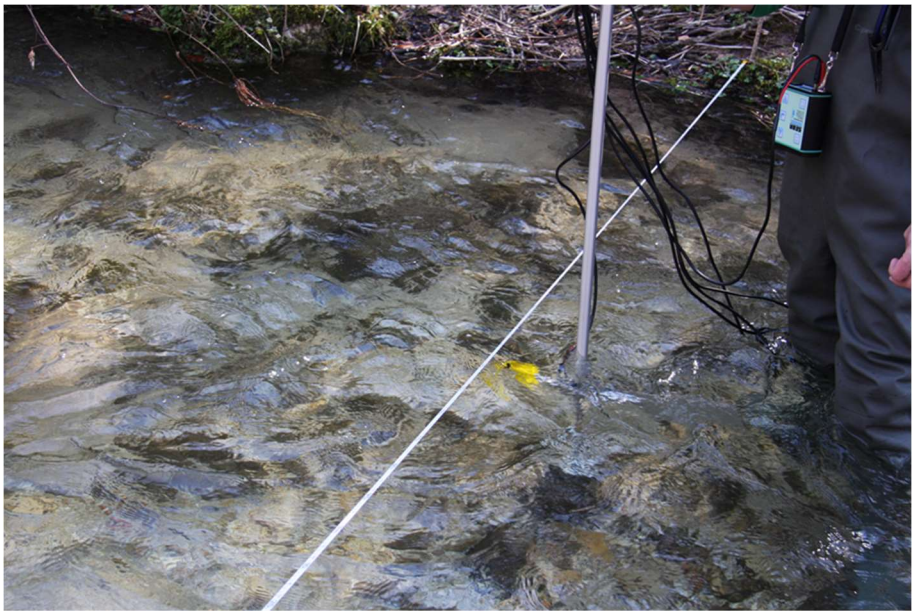

Figure 6.39 Current meter measurements by wading

With the aim to obtain a mean velocity, after the cross sections has been selected and the width of the stream was determined, the next step was determined the spacing of the verticals to provide numerous subsections, almost equally spaced by 1.00 m. To obtain a mean velocity in a vertical, velocity distribution observations can be made at a number of points along each vertical.

Along each one of these investigated verticals, up to 3 measuring points have been defined at different depths (0.1, 0.2, 0.3 and 0.5 m from bed stream) as given in Table 6.9.

For each of those points 3 readings have been recorded, in order to assess velocity fluctuations due to turbulence and also to avoid accidental bad measures, allowing about 60 seconds for each reading to stabilise.

Twenty-eight discharge measurements were carried out along the Aniene River in SW_01, SW_02, SW_03 and SW_04 by the application of traditional current-meter, from July 2014 to November 2016.

Table 6.9 Number of subsection and number of observations points along each vertical

ID	Date	Number of subsections	Number of observations along each vertical	Depth (cm)
	July 2014	3	2	20-30
	November 2104	4	2	20-30
	January 2015	4	2	20-30
SW_01	May 2015	4	2	20-30
	December 2015	4	2	10-20
	May 2016	5	1	10
	November 2016	6	1	10
	July 2014	6	3	10-20-30
	November 2104	4	1	20
	January 2015	5	2	20-30
SW_02	May 2015	8	2	20-30
	December 2015	5	2	20-30
	May 2016	6	2	20-30
	November 2016	5	3	10-20-30
	July 2014	5	2	20-30
	November 2104	5	2	20-30
	January 2015	5	2	20-30
SW_03	May 2015	5	2	20-30
	December 2015	6	2	20-30
	May 2016	6	3	20-30-50
	November 2016	5	3	20-30-50
	July 2014	4	2	20-30
	November 2104	5	2	20-30
	January 2015	5	2	20-30
SW_04	May 2015	7	2	20-30
	December 2015	5	2	20-30
	May 2016	5	2	20-30
	November 2016	4	2	20-30

6.2.2.1.3 Application of velocity-area method – Calculation of discharge

The velocity-area method of measuring the discharge of a stream is made by dividing a stream cross section into sectors, and by measuring the depth and velocity along a vertical within each sector. The

total discharge is the addition of the products between the partial areas of the stream cross section and the velocity averaged over the vertical at each section.

Discharge is measured by integrating the area and velocity of each point across the stream; that is, the stream is divided into sections based on where velocity and stage height measurements were taken in the cross-section of the stream. By multiplying the cross-sectional area (width of section x stage height) by the velocity, one can calculate the discharge for that section of stream. Considering the total area to be divided into *N*-1 segments, the total discharge is calculated as follows (6.4):

$$Q = \sum_{i=1}^{n-1} Q_i \tag{6.4}$$

Q_i is the discharge in the i^{th} stream vertical and is obtained multiplying the area of the i^{th} stream cross section (A_i) and the average velocity (v_m) between two adjacent sectors, according to equation (6.5).

$$Q_i = A_i \cdot v_m \tag{6.5}$$

where:

$$Ai = \frac{(h_i + h_{i-1}) \cdot d_m}{2} \tag{6.6}$$

$$d_m = (d_i - d_{i-1}) \tag{6.7}$$

$$v_m = \frac{(v_i + v_{i-1})}{2} \tag{6.8}$$

and

- d_i: distance of the i^{th} vertical from initial point
- h_i: free surface depth measured at the i^{th} vertical
- v_i: average velocity at the i^{th} vertical

In the following tables (Tabs. from 6.10 to 6.16) are reported the data used for the application of the velocity-area method of measuring the discharge in SW_03 for each monitoring campaign, where:

- n_x: number of spins recorded at a depth of x cm
- $n'_x = n_x/60$
- v_x: velocity at a depth of x cm, calculated by eq. 5.6 and 5.7
- Q_i: discharge in the i th stream cross section

Figures from 6.40 to 6.46 show the application of the velocity-area method for the evaluation of SW_03 discharge, for each monitoring campaign, from July 2014 to November 2016.

Table 6.10 Discharge measurement at the Aniene River gauging station SW_03 (July 2014)

d_i (m)	h_i (m)	n_{20}	n_{30}	n'_{20} (s^{-1})	n'_{30} (s^{-1})	v_{20} (m/s)	v_{30} (m/s)	v_i (m/s)	v_m (m/s)	A_i (m^2)	Q_i (m^3/s)
0	0.12	-	-	-	-	-	-	-	-	-	-
1	0.82	93	58	1.550	0.967	0.525	0.331	0.428	0.214	0.470	0.101
2	0.80	203	195	3.383	3.250	1.136	1.091	1.113	0.771	0.810	0.624
3	0.72	172	201	2.867	3.350	0.963	1.124	1.044	1.079	0.760	0.820
4	0.65	229	189	3.817	3.150	1.280	1.058	1.169	1.106	0.685	0.758
5	0.65	152	89	2.533	1.483	0.852	0.502	0.677	0.923	0.650	0.600
6	0	-	-	-	-	-	-	-	0.339	0.325	0.110

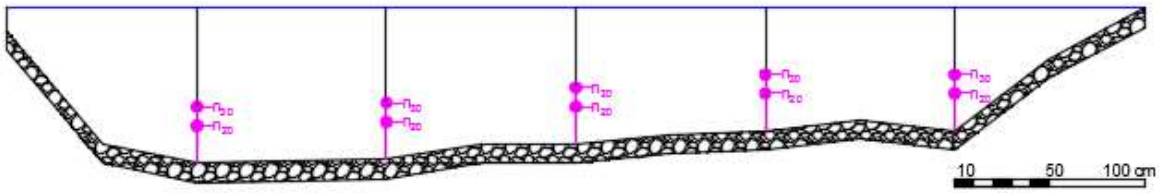

Figure 6.40 Application of the velocity-area method for the evaluation of SW_03 discharge (July 2014)

Table 6.11 Discharge measurement at the Aniene River gauging station SW_03 (November 2014)

d_i (m)	h_i (m)	n_{20}	n_{30}	n'_{20} (s^{-1})	n'_{30} (s^{-1})	v_{20} (m/s)	v_{30} (m/s)	v_i (m/s)	v_m (m/s)	A_i (m^2)	Q_i (m^3/s)
0	0.10	-	-	-	-	-	-	-	-	-	-
1	0.47	34	38	0.567	0.633	0.206	0.226	0.216	0.108	0.285	0.031
2	0.64	94	102	1.567	1.700	0.530	0.575	0.552	0.384	0.555	0.213
3	0.60	107	127	1.783	2.117	0.602	0.713	0.658	0.605	0.620	0.375
4	0.55	99	106	1.650	1.767	0.558	0.597	0.577	0.618	0.575	0.355
5	0.47	44	13	0.733	0.217	0.258	0.096	0.177	0.377	0.510	0.192
6	0.20	-	-	-	-	-	-	-	0.088	0.335	0.030

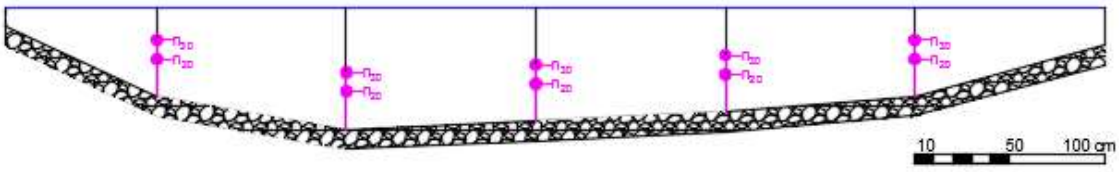

Figure 6.41 Application of the velocity-area method for the evaluation of SW_03 discharge (November 2014)

Table 6.12 Discharge measurement at the Aniene River gauging station SW_03 (January 2015)

d_i (m)	h_i (m)	n_{20}	n_{30}	n'_{20} (s^{-1})	n'_{30} (s^{-1})	v_{20} (m/s)	v_{30} (m/s)	v_i (m/s)	v_m (m/s)	A_i (m^2)	Q_i (m^3/s)
0	0.20	-	-	-	-	-	-	-	-	-	-
1	0.48	64	70	1.067	1.167	0.364	0.397	0.380	0.190	0.340	0.065
2	0.72	129	159	2.150	2.650	0.725	0.891	0.808	0.594	0.600	0.356
3	0.75	139	181	2.317	3.017	0.780	1.013	0.897	0.852	0.735	0.626
4	0.66	127	138	2.117	2.300	0.713	0.775	0.744	0.820	0.705	0.578
5	0.58	49	16	0.817	0.267	0.284	0.112	0.198	0.471	0.620	0.292
5.8	0.20	-	-	-	-	-	-	-	0.099	0.312	0.031

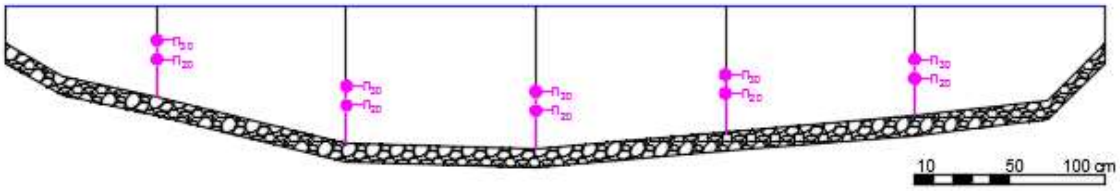

Figure 6.42 Application of the velocity-area method for the evaluation of SW_03 discharge (January 2015)

Table 6.13 Discharge measurement at the Aniene River gauging station SW_03 (May 2015)

d_i (m)	h_i (m)	n_{20}	n_{30}	n'_{20} (s^{-1})	n'_{30} (s^{-1})	v_{20} (m/s)	v_{30} (m/s)	v_i (m/s)	v_m (m/s)	A_i (m^2)	Q_i (m^3/s)
0	020	-	-	-	-	-	-	-	-	-	-
0.5	0.40	102	106	1.700	1.767	0.575	0.597	0.586	0.293	0.150	0.044
1	0.50	65	117	1.083	1.950	0.369	0.658	0.514	0.550	0.225	0.124
2	0.73	163	169	2.717	2.817	0.913	0.947	0.930	0.722	0.615	0.444
3	0.73	160	198	2.667	3.300	0.897	1.108	1.002	0.966	0.730	0.705
4	0.70	185	218	3.083	3.633	1.036	1.219	1.127	1.065	0.715	0.761
5	0.60	51	36	0.850	0.600	0.294	0.216	0.255	0.691	0.650	0.449
5.5	050	-	-	-	-	-	-	-	0.128	0.275	0.035

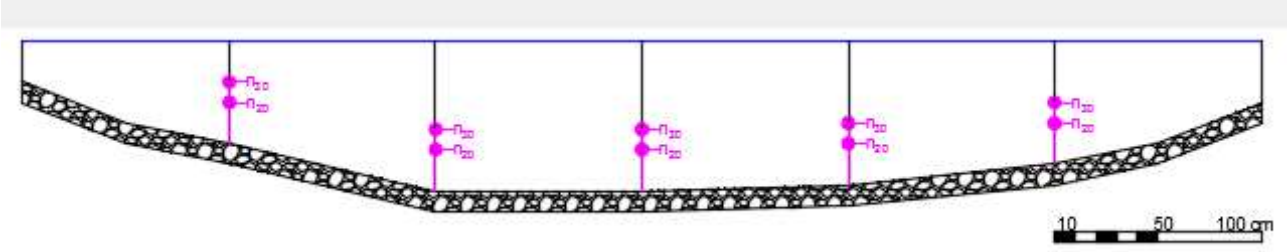

Figure 6.43 Application of the velocity-area method for the evaluation of SW_03 discharge (May 2015)

Table 6.14 Discharge measurement at the Aniene River gauging station SW_03 (December 2015)

d_i (m)	h_i (m)	n_{20}	n_{30}	n'_{20} (s^{-1})	n'_{30} (s^{-1})	v_{20} (m/s)	v_{30} (m/s)	v_i (m/s)	v_m (m/s)	A_i (m^2)	Q_i (m^3/s)
0	0.30	-	-	-	-	-	-	-	-	-	-
0.5	0.43	10	-	0.167	-	0.080	-	0.080	0.040	0.183	0.007
1	0.45	42	42	0.700	0.700	0.247	0.247	0.247	0.164	0.220	0.036
2	0.48	82	95	1.367	1.583	0.464	0.536	0.500	0.374	0.465	0.174
3	0.58	102	108	1.700	1.800	0.575	0.608	0.591	0.545	0.530	0.289
4	0.60	83	88	1.383	1.467	0.469	0.497	0.483	0.537	0.590	0.317
5	0.40	38	9	0.633	0.150	0.226	0.075	0.151	0.317	0.500	0.158
5.8	0.30	-	-	-	-		-	-	0.075	0.280	0.021

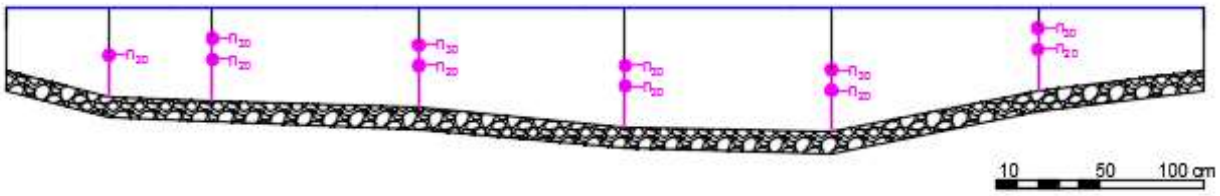

Figure 6.44 Application of the velocity-area method for the evaluation of SW_03 discharge (December 2015)

Table 6.15 Discharge measurement for the Aniene River gauging station SW_03 (May 2016)

d_i (m)	h_i (m)	n_{20}	n_{30}	n_{50}	n'_{20} (s^{-1})	n'_{30} (s^{-1})	n'_{50} (s^{-1})	v_{20} (m/s)	v_{30} (m/s)	v_{50} (m/s)	v_i (m/s)	v_m (m/s)	A_i (m^2)	Q_i (m^3/s)
0	0.30	-	-	-	-	-	-	-	-	-	-	-	-	-
0.2	0.30	114	-	-	1.900	-	-	0.641	-	-	0.641	0.321	0.060	0.019
1	0.52	60	75	96	1.000	1.250	1.600	0.341	0.425	0.541	0.436	0.539	0.328	0.177
2	0.64	152	161	176	2.533	2.683	2.933	0.852	0.902	0.986	0.913	0.675	0.580	0.391
3	0.68	168	189	196	2.800	3.150	3.267	0.941	1.058	1.097	1.032	0.973	0.660	0.642
4	0.78	150	159	189	2.500	2.650	3.150	0.841	0.891	1.058	0.930	0.981	0.730	0.716
5	0.48	149	163	-	2.483	2.717	-	0.836	0.913	-	0.875	0.902	0.630	0.568
5.7	0.30	-	-	-	-	-	-	-	-	-	-	0.437	0.273	0.119

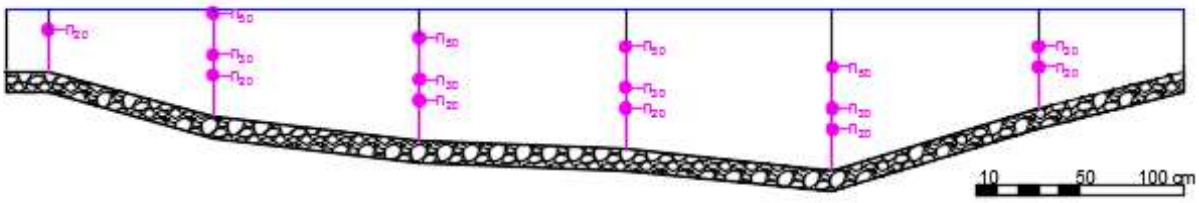

Figure 6.45 Application of the velocity-area method for the evaluation of SW_03 discharge (May 2016)

Table 6.16 Discharge measurement for the Aniene River gauging station SW_03 (November 2016)

d_i (m)	h_i (m)	n_{20}	n_{30}	n_{50}	n'_{20} (s^{-1})	n'_{30} (s^{-1})	n'_{50} (s^{-1})	v_{20} (m/s)	v_{30} (m/s)	v_{50} (m/s)	v_i (m/s)	v_m (m/s)	A_i (m^2)	Q_i (m^3/s)
0	0.20	-	-	-	-	-	-	-	-	-	-	-	-	-
1	0.52	29	48	-	0.483	0.800	-	0.179	0.279	-	0.229	0.115	0.360	0.041
2	0.64	117	126	118	1.950	2.100	1.967	0.658	0.708	0.663	0.676	0.453	0.580	0.263
3	0.68	72	74	79	1.200	1.233	1.317	0.408	0.419	0.447	0.425	0.551	0.660	0.363
4	0.78	111	97	89	1.850	1.617	1.483	0.625	0.547	0.502	0.558	0.491	0.730	0.359
5	0.48	36	-	-	0.600	-	-	0.216	-	-	0.216	0.387	0.630	0.244
5.7	0.30	-	-	-	-	-	-	-	-	-	-	0.108	0.273	0.029

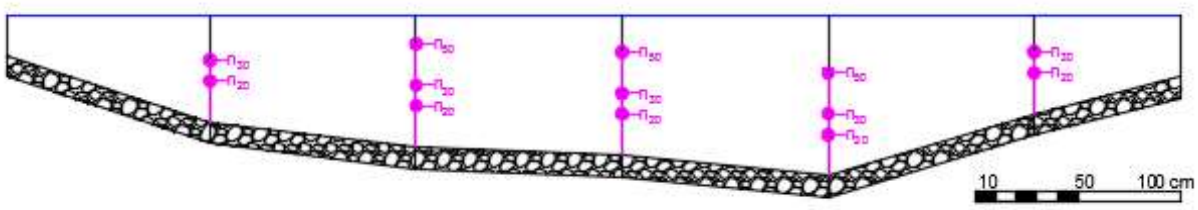

Figure 6.46 Application of the velocity-area method for the evaluation of SW_01 discharge (November 2016)

Fig. 6.47 and Table 6.17 show discharge values recorded in SW_01, SW_02, SW_03 and SW_04 gauging stations all over the first three years of the Environmental Monitoring Plan of the Pertsuo Spring.

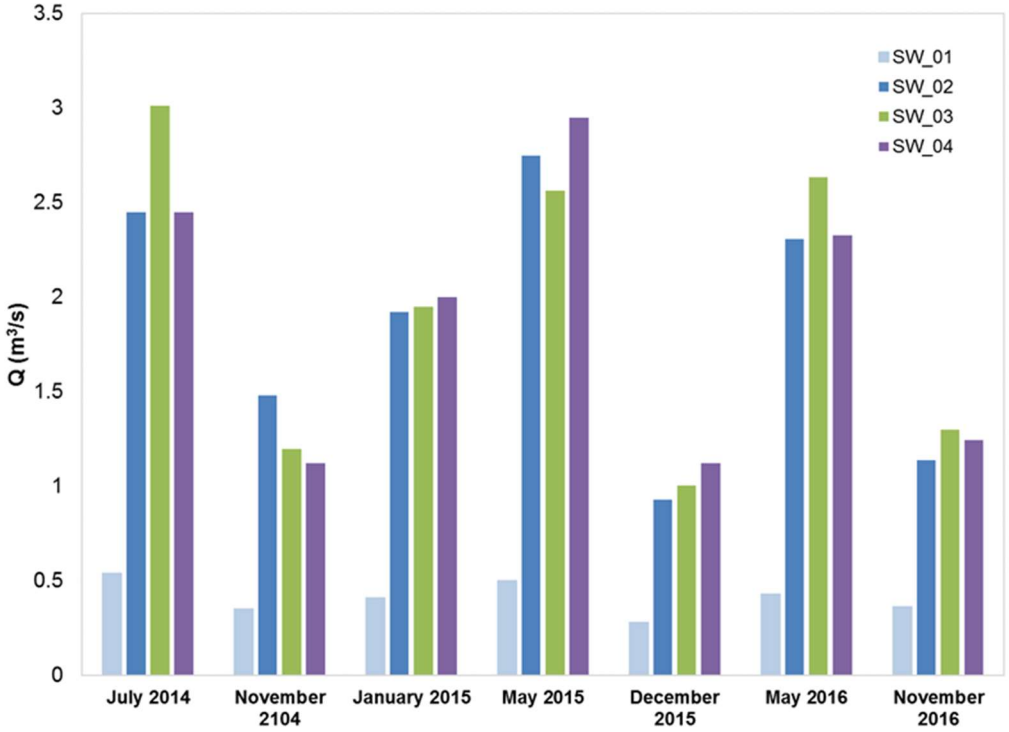

Figure 6.47 Discharge trend at four monitoring stations located along the Aniene River (July 2014 - November 2016)

Table 6.17 Mean discharge values obtained by current-meter method

Q (m^3/s)	SW_01	SW_02	SW_03	SW_04
July 2014	0.540	2.450	3.012	2.450
November 2104	0.350	1.480	1.196	1.120
January 2015	0.410	1.920	1.949	2.000
May 2015	0.501	2.747	2.562	2.947
December 2015	0.278	0.931	1.003	1.122
May 2016	0.430	2.305	2.633	2.327
November 2016	0.363	1.137	1.299	1.244

6.2.2.2 Validation of salt dilution method for discharge measurements

In this study, it has been tested the salt dilution method for the evaluation of discharge in mountain streams, where turbulent flows and flow depths make difficult apply the conventional current meter method.

In the following they are presented the preliminary results of stream discharge measurements, coming from three different campaigns driven from September to October 2014, executed SW_04. The comparison of these elaborations, carried on by the application of both methods, is useful to define the reliability and accuracy of discharge measurements carried out by salt dilution method.

San Teodoro Bridge gauging station (SW_04) has been chosen as experimental site for the application of the salt dilution method because has the basic characteristics for accurate streamflow measurements. In fact, the turbulent condition allows completely dissolution and fully mixing with the flow at the point where electrical conductivity is measured. San Teodoro Bridge has been used to dump the salt directly into the injection point: the turbulence created below the bridge allows the dissolution of the salt and the mixing into the stream. According to IS0 9555-1:1994(E) requirements [112] the salt dilution method involves the injection of a volume of a NaCl solution at a cross section in which the discharge remains constant for the duration of the gauging. At a second cross section placed downstream the injection point, at a distance sufficient for the injected solution to be uniformly diluted, the stream electrical conductivity is determined over a period of time sufficiently long to ensure that the NaCl solution has passed through the second cross section [113].

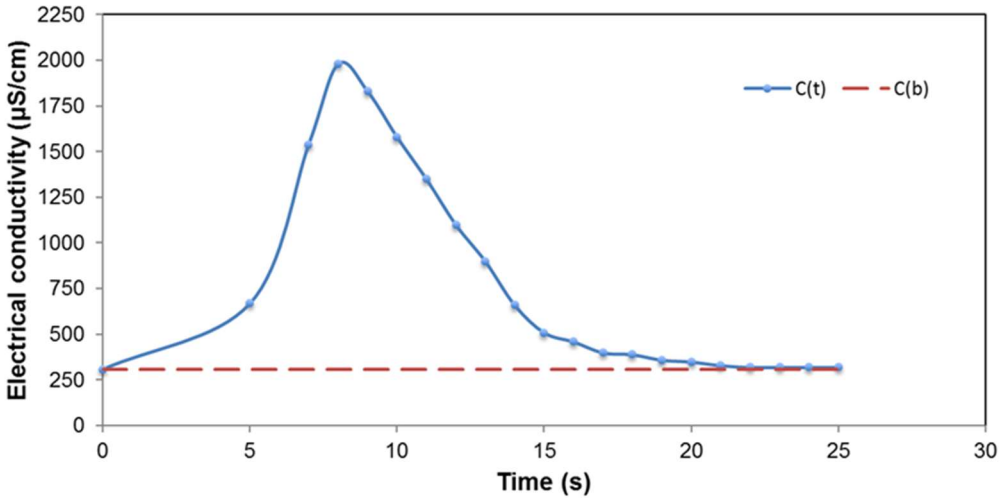

Figure 6.48 An example of a salt dilution measurement done at SW_04 in September 2014

It has been used a saturated NaCl-solution made by dissolving about 2 kg of salt in 10 liters of stream water, depending on the temperature and the background conductivity of the stream. The dissolution of NaCl in water is proportional to water temperature and inversely proportional to the existing concentration of salt. After injection, the salt mixes into the stream by longitudinal dispersion, a process in which dissolved salt in the plume moves along its concentration gradient until a uniform concentration exists [65]. The instantaneously injection of NaCl solution into the stream produces downstream a wave of electrical conductivity increase, as shown in Fig. 6.48. Table 6.18 lists discharge measurements obtained by the application of the salt dilution method carried out from September to October 2014. In Tab. 6.19, they are presented the results, coming from the application of the two methods, and the percentage differences, between each campaign result.

Table 6.18 Mean discharge values obtained by salt dilution method

Date (dd/mm/yyyy)	Gauge Height (m)	Q (m^3/s)
10/09/2014	0.60	1.30
29/09/2014	0.50	0.99
17/10/2014	0.70	1.71

Table 6.19 Mean discharge values obtained by current meter method (1) and salt dilution method (2)

Date (dd/mm/yyyy)	Q^1 (m^3/s)	Q^2 (m^3/s)	Δ (%)
10/09/2014	1.38	1.30	8
29/09/2014	0.98	0.99	1
17/10/2014	1.77	1.71	6

These preliminary results seem to give good indications for the validation of salt dilution method for discharge measurements. For example, at San Teodoro Bridge, both methods provide discharge measurements very close to the other so that both methods could be performed for comparative purposes (Fig. 6.49).

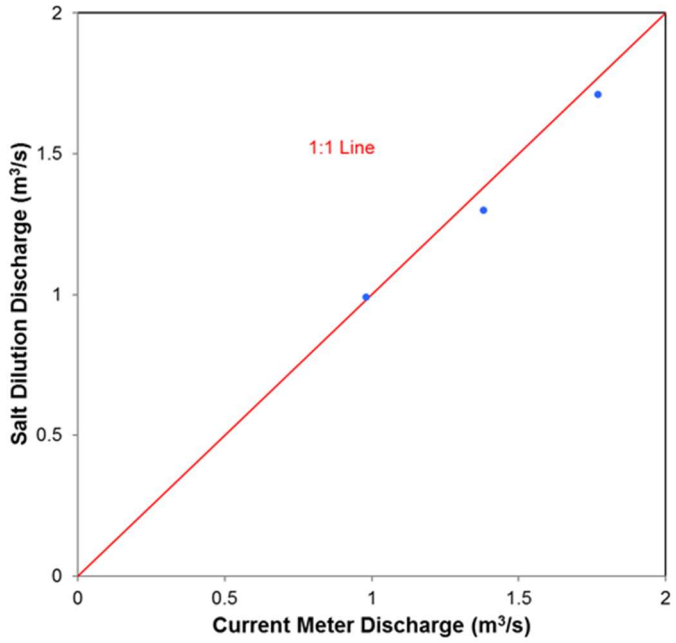

Figure 6.49 Comparison of current-meter and tracer dilution discharge measurements at SW_04

The rating curves for SW_04 gauging station show the changes in the stream flow depending on gauge height from September to October 2014.

Rating curve based on current meter and salt dilution measurements, fitted by an exponential function, are very similar, with comparable discharge values coming from the application of both methods (Fig. 6.50).

The measurements collected by salt dilution method fell close to the rating curve based on current meter method, with percentage differences of less 8%.

The salt dilution method compares favorably in accuracy with current metering as a method of measuring streamflow in mountain river, and appears to be more accurate where the turbulence flow might interfere with current meter measuring.

Furthermore, the salt dilution method is easier to apply and more economical in terms of equipment cost. Current meter method is well suited where flow conditions are close to laminar, whereas the salt dilution method are better fitting to river with unsteady flow conditions and the irregular stream bad geometry. However, in the traditional current meter method, excess sediment and seasonal growths of weeds can change the hydraulic profile of the cross section, requiring new rating curves at any measurements campaign.

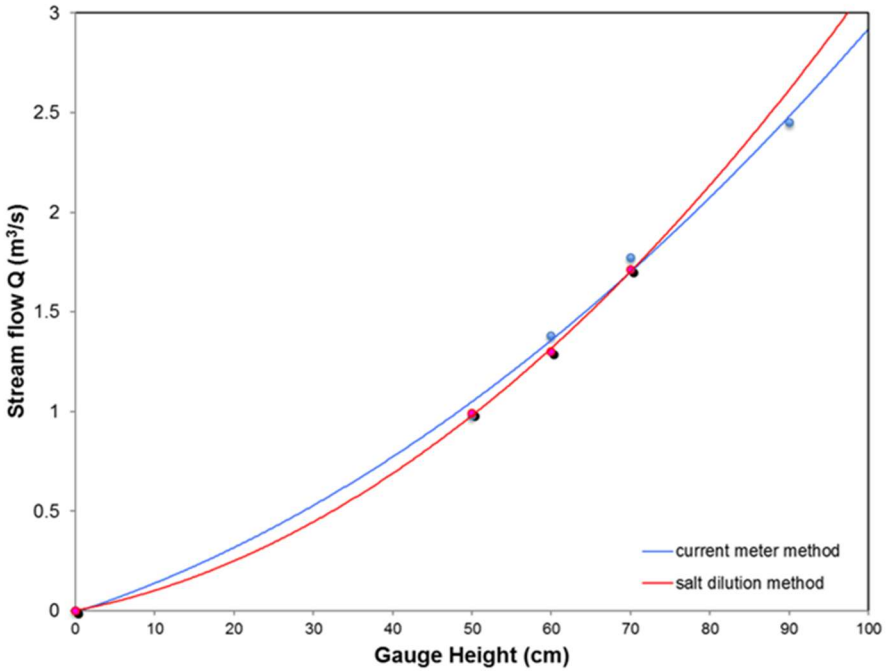

Figure 6.50 Comparison of stream flow discharge as a function of time for current meter and salt dilution method

Both methods seem to be complementary: in fact, while current metering requires laminar flow and is unsuited under turbulent conditions, the reverse is true of salt dilution gauging.

Even if the comparison with discharge measurements carried on by the application of both methods shows comparable values, several factors can affect the accuracy the discharge measurements obtained by salt dilution method. The loss of tracer between the injection point and the downstream cross section makes not applicable the equation for the conservation of mass and consequently the computation of stream discharge. Other factors that may have caused inaccuracies between current meter and salt dilution stream flow measurements are the tracer probe accuracy limits and the incomplete mixing throughout the stream cross section before the downstream gauging section is reached.

This fact let us pointing out the real importance of the determination of the degree to which an added tracer is diluted by the flowing water. The success of the slug injection methods requires the complete mixing of the added tracer diluted by the flowing water in as short a distance as possible [111].

CHAPTER 7

Mg^{2+} BASED METHOD FOR PERTUSO SPRING DISCHARGE EVALUATION

7.1 Groundwater environmental tracers

Groundwater represents a vital resource for the society, and for the ecosystems. The interest of researchers for better understanding the groundwater origin, the subsurface processes, and the factors controlling the residence time has gradually increased, and the investigation techniques evolved continuously [13], in the aim of better protect these resources.

In recent years, surface water and groundwater tracing techniques have been used in a variety of complex hydrogeological settings to aid in characterizing groundwater flow systems [114,115,116,117,118, 119]. Tracer methods are particularly suitable to assess transit times and flow properties in karst aquifers, partly because the necessary equipment is manageable [120].

Environmental tracers are natural and anthropogenic chemical and isotopic substances that can be measured in groundwater and used to understand hydrologic properties of aquifers [121]. Groundwater tracers include any substance that can become dissolved or suspended in water, or attached to the water molecule, and recovered or measured from a water sample that can be used to trace the source of groundwater in terms of its specific or relative location and time of recharge. Groundwater tracers can include both artificially introduced and naturally occurring substances [122,123].

Environmental tracers are more and more used in hydrological studies, in order to have a complete view about the water cycle, the groundwater recharge, water-rock interactions, and geochemical processes [13] and to understand potential groundwater contamination processes [48].

In particular, these tracers provide information about the flow and mixing processes of water coming from different sources [124]. They are also useful to point out directions of groundwater flow and to determine origin and residence times of karst groundwater [125,126].

In karst aquifers, where flow may be concentrated in subsurface conduits, a Darcy law approach is usually not suitable, for this reason groundwater tracing techniques application can be an effective approach to better understand the hydrology of these systems [114].

Typical natural tracers are major ions, trace elements, dissolved organic carbon and water isotopes [127,128]. An important class of tracers are the ionic tracers, as they are not subject to decay or gas exchange. Moreover, biogeochemical reactions can modify concentrations of most ions [129].

The number of ion types which might be used is very large. However, because of low cost, ease of detection and low sorption, chloride (Cl) and bromide (Br) are most popular [130]. But other ions can be used from time to time for special purposes such as Li, NH_4, NO_3, Mg, K, I.

Groundwater circulating in karst aquifer generally has great concentrations of calcium and magnesium as the result of bedrock weathering processes. Variations of Ca and Mg in groundwater are used very successfully as natural tracers in studies aiming to evaluate groundwater residence time within the karst aquifers [125]. The changes in Ca and Mg concentration values mainly depend on the residence time of groundwater in karst systems, which are controlled by the volume and mechanism of recharge, the distance from the recharge area and the dissolution of carbonate minerals [24,86]. The dissolution kinetics of magnesium is longer than that of calcium, so the increasing Mg/Ca ratio implies the saturation of water with calcite, highlighting long residence time and enhanced weathering along the groundwater flow paths [24,131]. The Mg content in groundwater also depends on other parameters such as chemical and mineralogical purity of limestone and presence of dolomite within the rock masses they flow across [132].

Nevertheless, the increase in Mg concentration values, and hence Mg/Ca ratio not only depend on the dissolution/precipitation reaction of calcite and dolomite, but also an increase in water temperature accelerates the kinetics of the dissolution of dolomite [90,91]. However, it has been noticed that even in karst aquifers mainly made of limestone, the presence of slight impurities of Mg in calcite can be responsible of significant changes in Mg/Ca ratio due to a high residence time of flowing waters [133,134]. Thus, environmental tracers and hydrochemical investigation techniques provide much information for the identification of groundwater flow systems and the main hydrogeochemical processes affecting the composition of water within the karst aquifers [134].

Calcium and magnesium offer special promise as seepage tracers for basins set in thick calcareous glacial drift, or doline basins set in carbonate-rich areas. Magnesium is also an obvious tracer in areas of ultramafic rock. In humid regions with abundant dolomite, Mg offers advantages over Ca as a tracer because, once in solution, it does not re-form a carbonate unless $Mg/Ca > 2$ [135].

In the past, the magnesium was used as a tracer to evaluate the steady-state influx to seepage lakes by using a solute mass balance. For lakes set in the dolomitic glacial drift of Wisconsin, Mg was an ideal groundwater tracer, both because it has the highest ratio of groundwater concentration to concentration in precipitation and because it behaves nearly conservatively in lakes set in semi humid climates [134].

Bencala et al. (1987) [136] and Schemel et al. (2006) [137] made comparisons of natural tracers at the confluence of two streams in Colorado and studied, through tracer's mass balance, the behaviour of naturally occurring calcium, magnesium, silica, sulphate, fluoride, and manganese; concluding that magnesium exhibited conservative or nearly conservative behaviour.

It is quite important to underline that a conservative behaviour may depend on site-specific environmental condition. Generally, for conservative solute tracers it has to be expected a simple physical attenuation mechanism due to dilution, whereas any chemical attenuating mechanism would remove no-conservative solute in varying amounts [136].

Most recently, it was showed that variations in chlorofluorocarbon (CFC), ^{222}Rn, and Mg concentrations within streams can be used to quantify rates of groundwater inflow. It has been proposed a mass balance that takes in account changes in solute load within a stream receiving groundwater inflow [129].

Thus, in several studies Mg presented the right qualities to be used as a conservative or nearly conservative tracer [135,136,137]. Particularly, Mg has proved to be a useful tracer for chemical mass balance techniques, which are necessary in order to assess surface water or groundwater flow in karst hydrology settings where conventional measurements are more difficult.

7.2 Karst spring discharge evaluation

The determination of groundwater discharge is a direct measure of the amount of water available for drinking, industrial, and agricultural purposes. Karst springs react to rainfall events by sinkhole drainage and discharge from conduits in bedrock, responsible for the subsurface outflow [10]. Assessing water balance in a karst aquifer can be very difficult, due to the complex interactions and exchanges between groundwater and surface water. The estimation of karst spring discharge is affected by methodological difficulties, data deficiencies, and resultant uncertainties due to spatial variability of permeability in carbonate rocks [138], and also because the pathway of groundwater outcoming is not always the same along the year. The traditional quantitative approach for the evaluation of groundwater discharge is the application of water balance, which requires the estimation of water storage and flow. Water balance calculation requires the estimation of two main parameters: recharge (precipitation, agriculture water, surface runoff, etc.) and discharge (underground outflow) which are affected by the highly heterogeneous distribution of permeability due to conduits and voids developed by the dissolution of carbonate rocks [139,140].

Thus, in these complex hydrogeological scenarios, such as karst aquifers, understanding the behaviour of the groundwater system and the recharge-discharge relation is required to formulate a reliable water balance [32]. In karst aquifer the presence of underground stream flows, that are not accurately measurable, makes very difficult to develop a reliable methodology that includes physical assessments of the input-output relation [24,141].

Therefore, measurements of streamflow and spring discharges are useful to assess karst aquifers available budget. Because no continuous discharge measurements of the Pertuso Spring were available, in this study, different methods (velocity-area using current meter and geochemical assessment) were applied to evaluate the discharge of the spring and the stream flow during the monitoring period from July 2014 to November 2016. In this paper, an indirect groundwater model has been set up in the aim of evaluating karst spring discharge. The aim of this study is to present the preliminary results of an indirect method for the estimation of the Pertuso Spring discharge, based on magnesium concentration changes in groundwater and surface water.

7.2.1 Pertuso Spring discharge aspects

Groundwater coming from the Pertuso Spring are collected by a well-known volume of carbonate rocks that make up the aquifer. The conduit network draining the groundwater flow coming from the surrounding aquifer matrix is able to discharge large quantities of water very fastly through this karst aquifer (up to 3 m^3/s) [139].

Karst springs are generally characterized by high and very variable discharge rate and represent the headwaters of important surface streams. These springs typically come out at the boundary of the hydrogeological basin, at a location of the minimum hydraulic head of the aquifer and sometimes next to the elevation of the base-level surface stream [24].

Groundwater basin boundaries are not strictly fixed, they may shift depending seasonally on the rates of recharge [25]. Many groundwater flow paths may route into adjacent groundwater basins causing difficulties to identify a single closing section. In addition, karst springs discharge is not easily measurable by standard techniques or conventional instruments. Sometimes channels are unsuitable for metering the flow, being shallow, choked with vegetation and with ill-defined banks [61]. In karst aquifers, the drainage network typically develops in a system of conduits that flows into a single trunk that discharges through the spring [11]. However, some karst aquifers may have a spread flow pattern, related to the enlargement of fractures and smaller conduits, located near the stream discharge boundary, or to the collapse of an existing trunk conduit [142].

Underflow springs are often hidden, for example by rising in the bed of the surface stream [25]. Thus, even if in this study we have identified a prevailing outlet section of the groundwater coming from the Pertuso Spring, there is no chance to be sure that the whole spring contribution to the Aniene River may always flow through that cross section. Consequently, the difficulty in measuring the Pertuso Spring discharge makes the use of the traditional current meter method, which provides information on stream discharge in each cross section, limited and less reliable [140]. Moreover, cross section morphology and flow regime are influenced by seasonal variations and anthropic operations, as reported in Figure 7.1, related to the monitoring campaign of July 2014 (Fig. 7.1a) to December 2015 (Fig. 7.1b).

(a) (b)

Figure 7.1 Pertuso Spring cross section in July 2014 (a) and in December 2015 (b)

Karst system dynamics are rapid, renewing most of the storage within a hydrologic year or less, which makes the effects of seasonal variations rapidly observable in the spring flow regime [10].

It has been noticed in dry season, at the Pertuso Spring outlet section, a reverse water inflow from the Aniene River that makes unreliable the current meter measurement in that specific case. Hence, to be sure to evaluate a reliable quantification of the Pertuso Spring discharge contribution to the Aniene River we have decided to assess it as the difference of measured values along the river, upstream and downstream the spring [139].

In spite of being the spring, certainly, the only place where one can obtain information on the functioning of the whole system and consequently the organization of conduits and storage [10]. In this case, data coming directly from the Pertuso Spring have been elaborated to set up an indirect model aimed to evaluate the spring discharge.

Karst hydrology requires a mix of surface water concepts and ground water concepts [24]. For this reason, to better understand the behaviour of this complex system and to validate discharge values calculated, it has been included a quali-quantitative characterization based on the Mg contents of groundwater and surface water samples. In this study, the Mg ion concentration has been used as conservative water tracer, allowing us to obtain an alternative discharge calculation model based on mixing and dilution process due to the Pertuso Spring and to compare the results of this model with those of traditional current meter method [53, 139,140].

7.3 Mg^{2+} based method for discharge evaluation

7.3.1 Background of the method

The karst aquifer system has been studied in order to evaluate factors, which modify the Aniene River flow, due to groundwater-surface water interactions. This hydrochemical characterization leads to a groundwater flow pattern in which two main recharge areas have been identified: the first one in the Cretaceous limestone, feeding the Pertuso Spring groundwater; the second one in the Triassic dolomite, feeding the surface water upstream the spring.

In this model, it has been considered a control volume around the Pertuso Spring. In this control volume, the incoming flows are the discharge Q_1, recorded upstream the spring (SW_01) and the Pertuso Spring discharge Q_P, characterized by the relative Mg concentration values C_1 e C_P. The outgoing flow is the Aniene River discharge Q_2, characterized by the Mg concentrations C_2, recorded at the SW_02 gauging station located downstream the Pertuso Spring.

The study area belongs to a special protected area in the Natural Park of Simbruini Mountains. As a matter of fact, the control volume can be considered free from any anthropic activities and only characterized by a surface water – groundwater interaction in the hypothesis of well mixing. Thus, the SW_02 gauging station discharge values, comes from the contribution of the Pertuso Spring discharge (Q_P) to the original SW_01 discharge value, can be represented by (7.1):

$$Q_2 = Q_1 + Q_P \tag{7.1}$$

and applying to this closed system the conservation of mass equation, it means (7.2):

$$Q_1 C_1 + Q_P C_P = Q_2 C_2 \tag{7.2}$$

The parameter n is defined as the percentage of the Pertuso Spring groundwater contribution to total discharge measured (7.3).

$$n = \frac{Q_P}{Q_2} = \frac{(C_2 - C_1)}{(C_P - C_1)} \tag{7.3}$$

Combining the equation (7.2) and the equation (7.3), we have obtained the discharge of the Pertuso Spring (7.4).

$$Q_P = Q_1 \cdot \frac{n}{1-n} \tag{7.4}$$

From the equation (7.4) it comes out that the discharge rate of the Pertuso Spring depends on the discharge values measured in the gauging station located along the river upstream the spring (Q_1) and the Mg concentration values recorded in groundwater and surface water samples (C_1, C_2, C_P).
Thus, thanks to the proposed conceptual model, starting from the Mg concentrations and the upstream discharge, it has been possible to evaluate the Pertuso Spring discharge.

7.3.2 Application of the method and results

A combined approach based on discharge measurements and hydrogeochemical data analysis was used to study flow paths and the groundwater-surface water interaction in the study area. Ca, Mg and HCO_3 represent more than 80% of the dissolved solids in water samples. These high concentrations are mostly due to the dissolution of carbonate minerals, forming limestone, which are the most dominant formations outcropping in the study area. The hydrochemical facies of groundwater and surface water was studied by plotting the concentrations of major cations and anions in the Piper trilinear diagram (Fig. 7.2) [78].

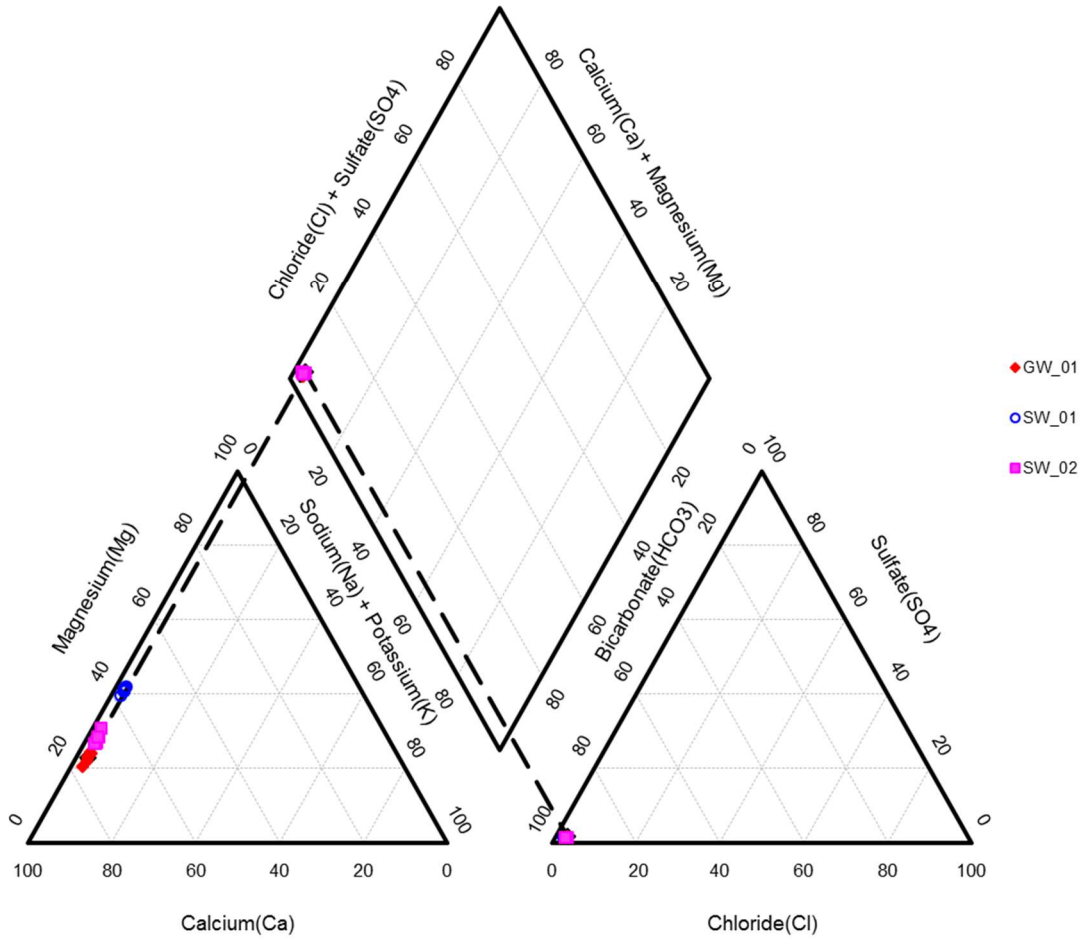

Figure 7.2 Piper plot for hydrochemical facies classification of Pertuso Spring groundwater (GW_01) and Aniene River surface water upstream (SW_01) and downstream (SW_02) the spring

Based on the dominance of major cationic and anionic species two hydrochemical facies have been identified: (1) Ca-Mg-HCO_3 and (2) Ca-HCO_3. These results are due to the presence of limestone, dolomitic limestones and dolomites outcropping in the study area. Water samples coming from SW_01 gauging station present higher values of concentration in Mg, while those coming from Pertuso Spring are definitely poorer in it, and show a clear composition of Ca-HCO_3 water type (Fig. 7.2). The different hydrochemical facies between groundwater and surface water reflects on the high concentration of Mg in the Aniene River. These hydrochemical facies highlight that carbonate weathering processes (e.g. calcite and dolomite) are the most important factors of the observed water type. To study the difference in Mg content between groundwater and surface water, a ternary diagram of cations (Ca, Mg and Na+K) [131] was used to highlight how the weathering type processes influence the enrichment in Magnesium (Fig. 7.3). As shown in Figure 7.3 all samples are placed along the Ca-Mg side of the diagram, these groundwater samples are very poor in Na and K. The higher Mg concentrations in SW_01 water samples suggest an increased residence time, depending on the dissolution/precipitation reactions of calcite and dolomite, which occur in the aquifer part, where groundwater cross dolomitic sandstones.

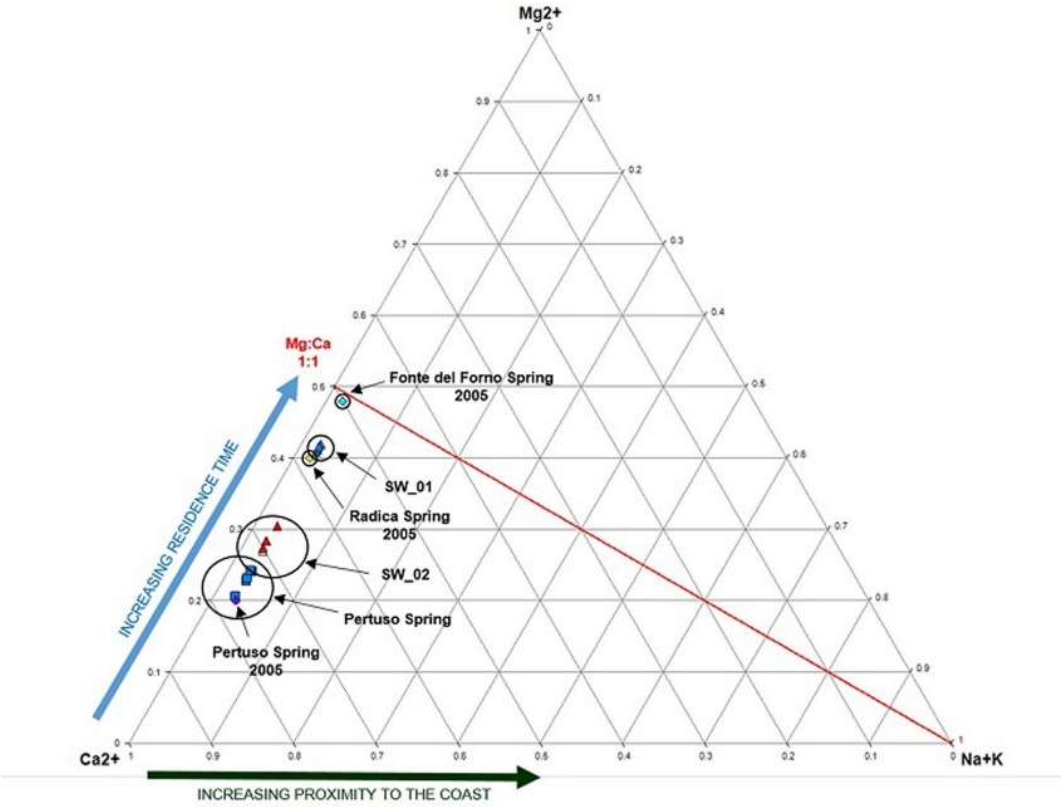

Figure 7.3 Ternary diagram of cations Ca, Mg and (Na+K). Relative concentrations of dissolved major cations compared with the composition of local groundwater [29]

As a matter of fact, according to previous studies of the area [29], similar results have been obtained for other springs located in the upper part of Aniene River coming out in the Triassic dolomite outcropping close to the Pertuso Spring basin (Fig. 7.4).

This hydrochemical characterization leads to a groundwater flow pattern in which two main recharge areas are defined: the first one in the Cretaceous limestone, feeding the Pertuso Spring groundwater; the second one in the Triassic dolomite, feeding the surface water upstream the spring.

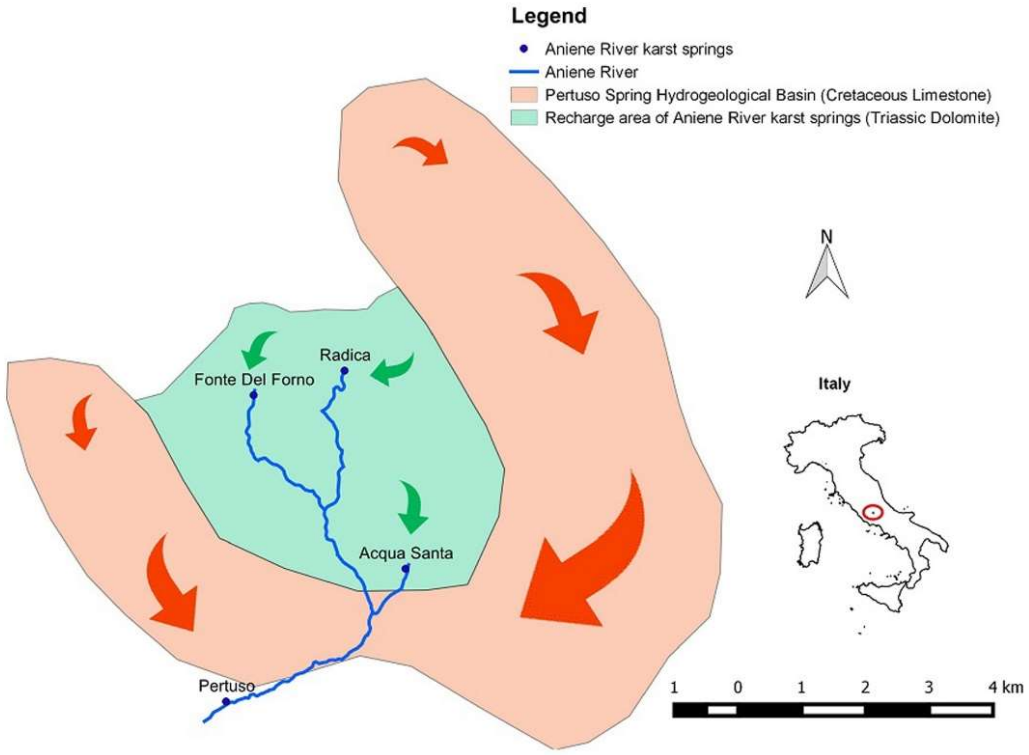

Figure 7.4 Recharge areas of the main karst springs in the Upper Valley of Aniene River [142]

The scatter plots diagram in Figure 7.5 shows that the high content of Mg in SW_01, upstream the Pertuso Spring, and consequently the high Mg/Ca ratio may be due to the weathering of Mg-rich Triassic dolomites, where dolomitic limestones and dolomites are the most outcropping formations in this area.

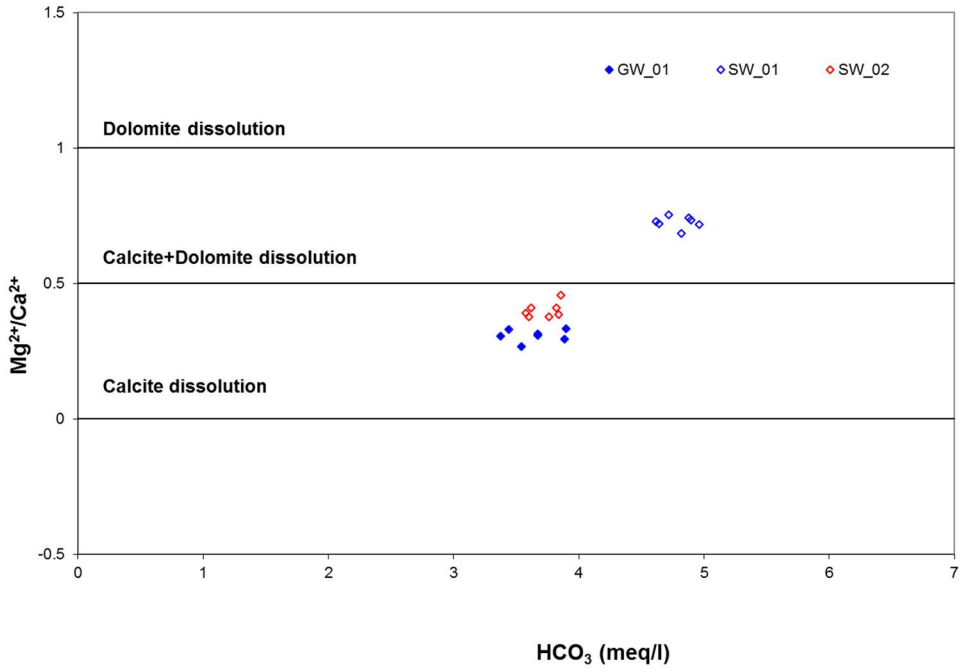

Figure 7.5 Mg/Ca ratio versus HCO_3 6in groundwater and surface water

As regards the Pertuso Spring groundwater, the Mg/Ca ratios values (~0.3) mainly depend on the residence of water in the karst system, highlighting weathering along the groundwater flowpaths of low-Mg calcite. As a consequence of these properties water samples collected downstream the Pertuso Spring (SW_02) present chemical composition typical of mixing of these two different kinds of waters (Fig. 7.5).

As a matter of fact, the highest Mg/Ca ratio has been recorded in water samples coming from dolomite rock masses (SW_01 ~ 0.7), with intermediate values at SW_02 gauging station (~ 0.4). On the other hand, the lowest value of this ratio in groundwater has been observed in Cretaceous limestone area (~ 0.3).

To investigate the mixing of groundwater and surface water, in this study it has been used PHREEQC software to perform a series of geochemical simulations, with the aim to investigate the speciation of an aqueous solution made of the mixing of water coming from Pertuso Spring (GW_01) and SW_01 gauging station.

The simulation in this paper is divided into 3 procedures:

1) Define the water quality in GW_01 based on the data of major ion contents.
2) Define the water quality in SW_01 based on the data of major ion contents.
3) Mixing the two solutions together in the proportions 78% groundwater and 22% surface water and then calculating the of major ions content of the solution.

The mixing ratio has been chosen according to the proportional contribution of groundwater fraction and surface water in SW_02 gauging station discharge [140].

Table 7.1 shows the simulation results compared with to laboratory values.

Table 7.1 Magnesium concentration of SW_02 and the virtual solution made by mixing water coming from Pertuso Spring and SW_01

Date	Mg^{2+} (mg/l)			Ca^{2+} (mg/l)		
	Phreeqc Mixing Concentration	Measured Concentration	Percent difference (%)	Phreeqc Mixing Concentration	Measured Concentration	Percent difference (%)
July 2014	12.7	12.8	0	49.60	51.3	3
November 2014	11.7	12.0	3	51.56	52.4	2
January 2015	13.3	13.0	2	54.20	55.6	3
May 2015	127	12.2	4	50.00	51.4	3
December 2016	13.7	14.7	7	52.48	52.9	1
May 2016	13.0	12.5	4	53.84	54.6	1

Figure 7.6 shows the composition of the mixed water determined from the Batch reaction compared to measured concentrations obtained by laboratory analyses, highlighting that the calculated values fit quite well the experimental values reported in Table 7.1.

The results obtained by PHREEQC fall close to the equiline of 1:1, and this fact confirms that SW_02 surface water comes from the mixing of groundwater outflowing from Pertuso Spring with surface water of the Aniene River (SW_01).

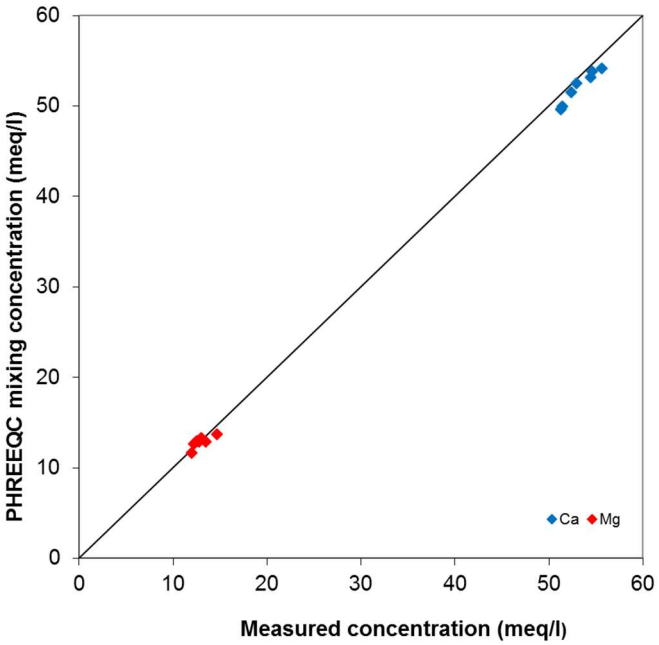

Figure 7.6 Comparison between the ionic compositions of SW_02 and the virtual solution made by mixing water coming from Pertuso Spring and SW_01

Aniene River discharge was measured during the period July 2014 –November 2016, in order to cover the range of seasonal conditions characteristics of this complex hydrogeological system. Measurements by current meter have been carried out in two gauging stations located upstream (SW_01) and downstream (SW_02) Pertuso Spring (Tab. 7.2).

Table 7.2 Mean discharge values obtained by current meter method, upstream (SW_01) and downstream (SW_02) Pertuso Spring

Q (m^3/s)	SW_01	SW_02
July 2014	0.540	2.450
November 2014	0.350	1.480
January 2015	0.410	1.920
May 2015	0.501	2.747
December 2015	0.278	0.931
May 2016	0.430	2.305
November 2016	0.363	1.137

Table 7.3 shows discharge values recorded in SW_01 and SW_02 gauging stations all over the hydrological year. The source of Mg concentration values in the Aniene River upstream the Pertuso Spring (SW_01) is the dissolution of Magnesium rich minerals in Triassic dolomites, sited in north-east part of the Pertuso Spring basin. Along the Aniene River, this decrease in Mg concentration values is related to an increase in stream flow discharge. SW_02 surface water is the product of the confluence of groundwater coming from the Pertuso Spring into the Aniene River (SW_01). As a matter of fact, the Aniene River, which is characterized by water with higher Magnesium concentration values, is affected in its chemical composition by the Pertuso Spring groundwater inflowing, and this influence can be measured by Mg concentration values variability along the river downstream. The karst aquifer system

has been studied in order to evaluate factors which modify the Aniene River flow due to groundwater-surface water interactions.

The *n* parameter, i.e. the percentage of the Pertuso Spring groundwater contribution to total discharge measured at the SW_02, has been calculated according to (7.3) and reported in Table 7.2.

Table 7.3 *n* values as percentage contribution of the Pertuso Spring groundwater to total discharge measured at the SW_02 gauging station

Date	n	n (%)
July 2014	0.780	78.0
November 2014	0.752	75.2
January 2015	0.794	79.4
May 2015	0.812	81.2
December 2015	0.709	70.9
May 2016	0.810	81.0
November 2016	0.736	73.6

Since December 2015, due to the riverbed and banks arrangement, it was possible to carry out the discharge measurements using the current-meter method on a representative section of the spring flowing into the Aniene River. Table 7.4 summaries the values of discharges evaluated. In particular, this table presents values of the Pertuso Spring discharge obtained by Magnesium tracer method. These values have been compared to those ones obtained, from July 2014 to May 2015, as the difference between the values measured with the current meter in SW_01 and SW_02, and from December 2015 as direct measurements in a cross section.

It is easy to see how discharge values obtained with both methods are very similar.

Table 7.4 Magnesium content and discharge values obtained by current-meter and Magnesium tracer method (Q*: discharge values obtained by current meter method; Q**: discharge values obtained by the difference between the values measured with the current meter in SW_01 and SW_02)

Date	SW_01		Pertuso Spring			SW_02		
	Q* (m^3/s)	Mg^{2+} (mg/l))	Q** (m^3/s)	Q_{Mg} (m^3/s)	Mg^{2+} (mg/l)	Q* (m^3/s)	Q_{Mg} (m^3/s)	Mg^{2+} (mg/l)
July 2014	0.540	23.6	1.91	1.92	9.8	2.450	2.46	12.8
November 2014	0.350	23.6	1.13	1.06	8.3	1.480	1.41	12.0
January 2015	0.410	25.2	1.51	1.58	9.9	1.920	1.99	13.0
May 2015	0.501	24.6	2.25	2.16	9.3	2.747	2.66	12.2
December 2015	0.278	25.2	0.67	0.68	10.4	0.931	0.96	14.7
May 2016	0.430	25.2	1.87	1.84	9.5	2.305	2.29	12.5
November 2016	0.363	23.8	0.77	0.78	9.8	1.137	1.060	13.5

The results of hydrogeochemical analysis and current discharge measurements confirm the groundwater-surface water mixing due to the presence of the Pertuso Spring, highlighting the key role of Mg content to identify different recharge areas and water flow paths within this karst setting.

Several previous studies used different conservative solute tracer to evaluate quantification of discharge in stream confluences starting from chemical mass balance techniques [117,118].

In this work, assessing the conservative behaviour of Mg for this specific system, it was possible to propose an inverse model for Pertuso Spring discharge evaluation based only on Mg concentration data.

The dilution mechanism, due to the groundwater and surface water interaction at Pertuso confluence point, is the only mechanism responsible of the Mg concentration change along the Aniene River (Fig. 7.7).

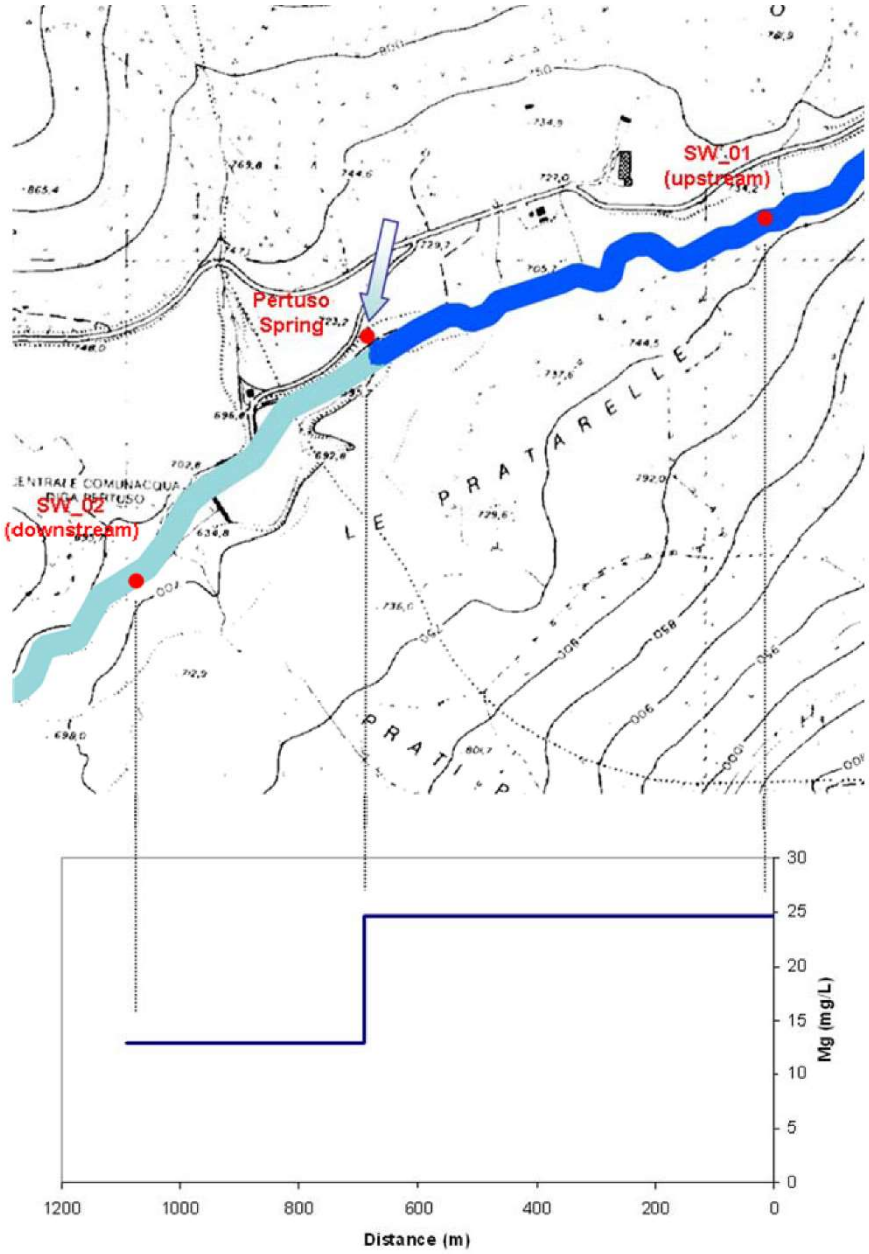

Figure 7.7 Schematic dilution mechanism in Mg concentration along the Aniene River

The box plot graphically highlights the main characteristics of Mg content (Fig. 7.8) for the utilization in the chemical mass balance technique, whereas Ca does not show the same adaptability (Fig. 7.9). The two main characteristics are:

– the concentration difference between the two inflows must be significant;

– the concentration difference between the two inflows also must be greater than the uncertainty in the concentration data.

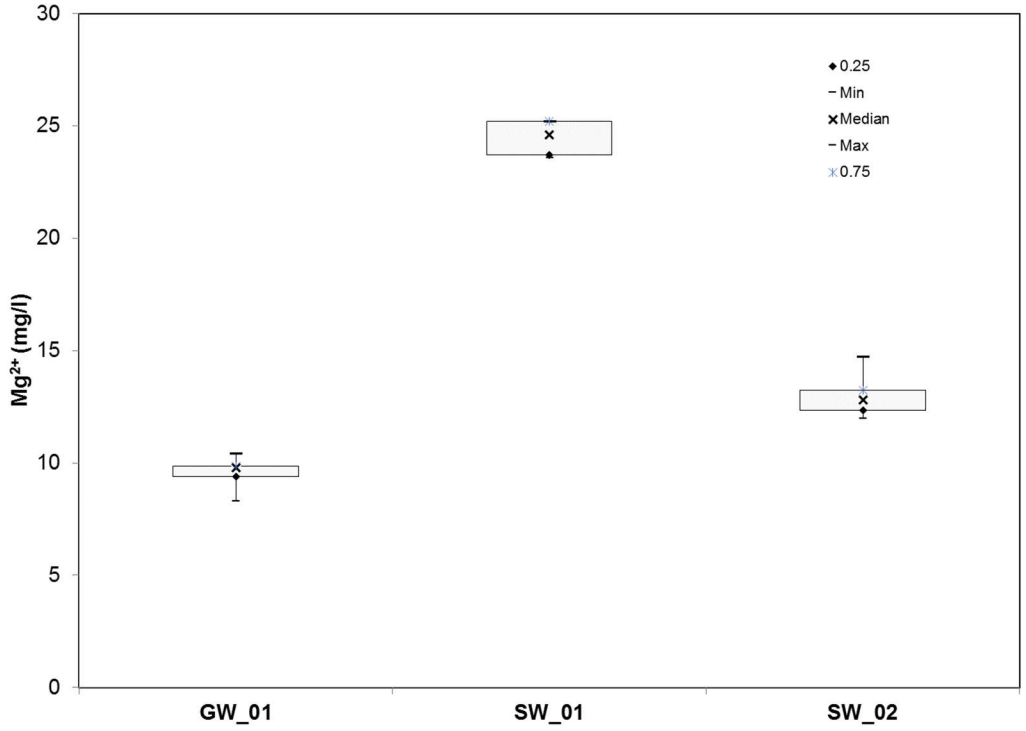

Figure 7.8 Box plot of mean, median, maximum and minimum values of Magnesium distribution

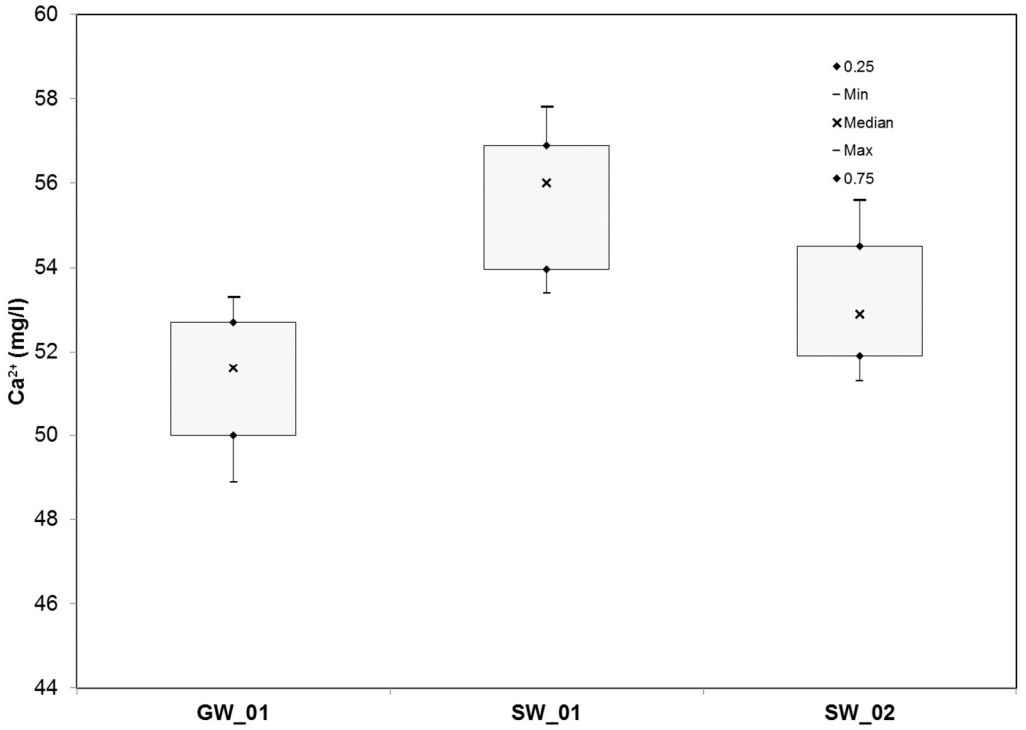

Figure 7.9 Box plot of mean, median, maximum and minimum values of Calcium distribution

As a matter of fact, differently from Ca, Mg concentration data shows a very low variability in each sampling point and a high difference between the Pertuso Spring and SW_01, due to the water transit in different geological formations (calcareous and dolomitic rocks).

These properties lead to the correct evaluation of the *n* parameter in the mass balance and, consequently, to valid discharge results for the Pertuso Spring confirmed by the comparison with conventional current meter discharge values (Fig. 7.10). As a matter of fact, differently from Ca, Mg concentration data shows a very low variability in each sampling point and a high difference between the Pertuso Spring and SW_01, due to the water transit in different geological formations (calcareous and dolomitic rocks).

These properties lead to the correct evaluation of the *n* parameter in the mass balance and, consequently, to valid discharge results for the Pertuso Spring confirmed by the comparison with conventional current meter discharge values (Fig. 7.10).

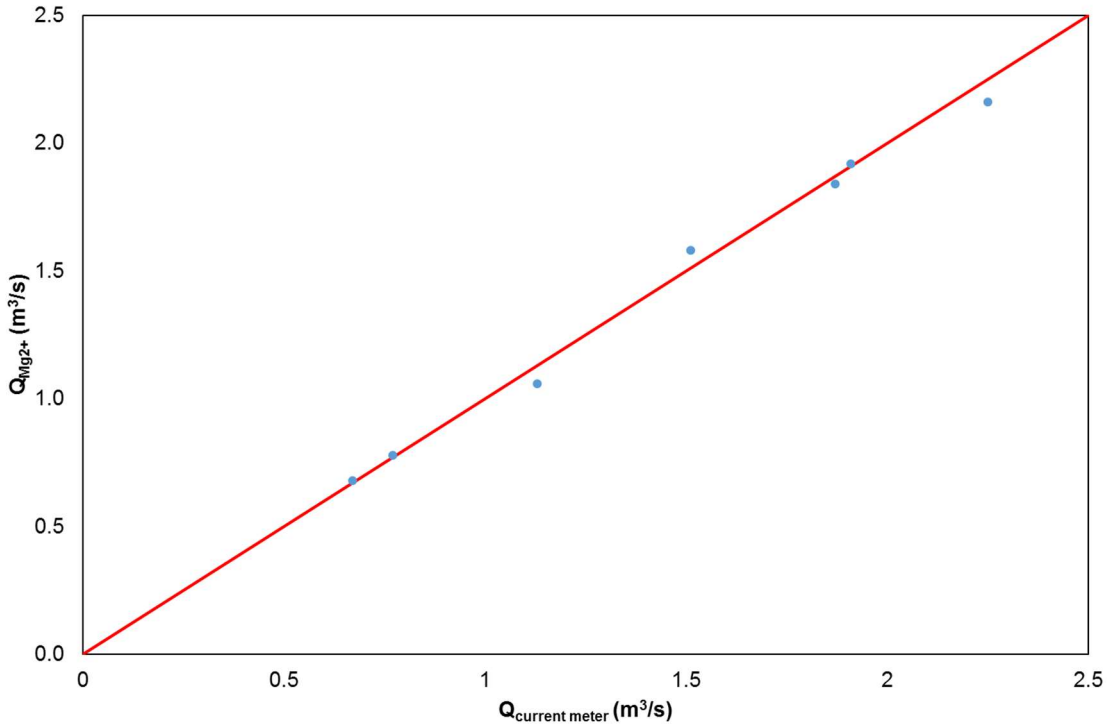

Figure 7.10 Relationship between Pertuso Spring discharge values obtain with the combined Magnesium tracer approach and the traditional current method

The low variability of Mg concentration in water samples is due to the slower process of dissolution for dolomitic rocks within the karst aquifer, resulting in a best discharge evaluation factor in base-flow conditions. On the contrary, during a storm, rainwater inflow and transit in karst conduits is too much rapid and do not allow the same dissolution process. Hence, in this karst setting, Mg is to be considered as a suitable conservative tracer only for main storage groundwater which, however, is the most important for spring exploitation projecting and planning. As a consequence, the Mg vs Q scatter plot diagram (Fig. 7.11) shows that all plotted points, except for November 2014 and November 2016 data, follow a linear trend, highlighting that the increasing base-flow contribution of Pertuso Spring discharge

rate is responsible of the decreasing in Mg concentration values. This is possible because data referred to November 2014 and 2016 monitoring campaign have to be considered as an outlier (Fig. 7.11).

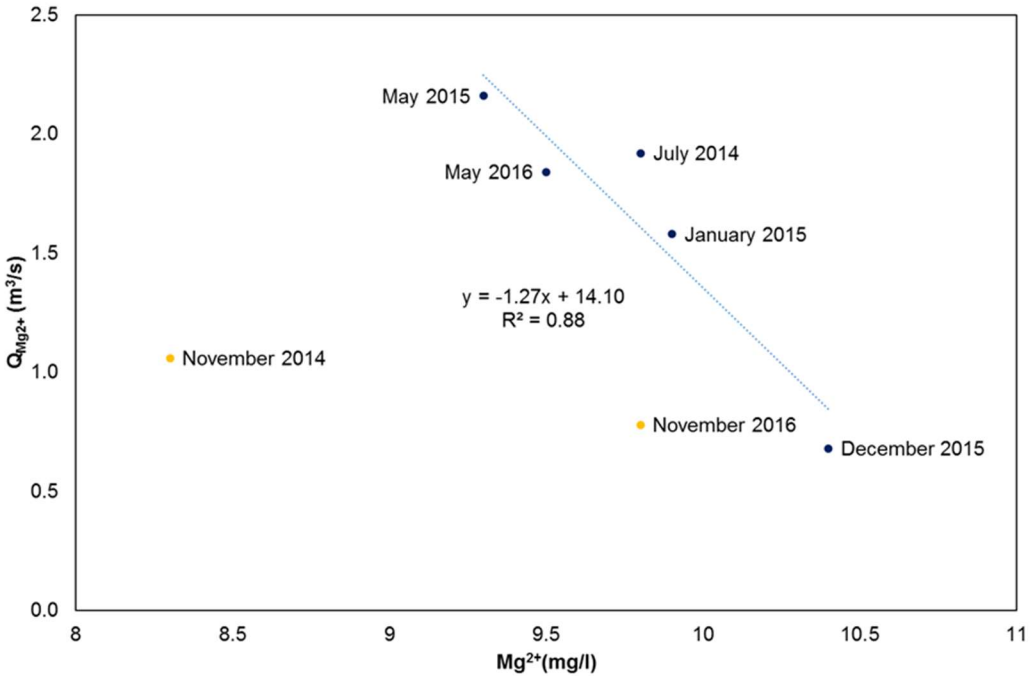

Figure 7.11 Relationship between the Mg^{2+} concentration and Pertuso Spring discharge values obtain with the combined Magnesium-discharge tracer approach

In fact, the lower Mg concentration measured at November 2014 can be related to a high precipitation rate, recorded at Trevi nel Lazio meteorological station, before the sampling date (Fig. 7.12). As previously said the consequent aquifer rapid response probably influenced, by dilution, the Mg concentration in groundwater that was no more significant for the conceptual model.

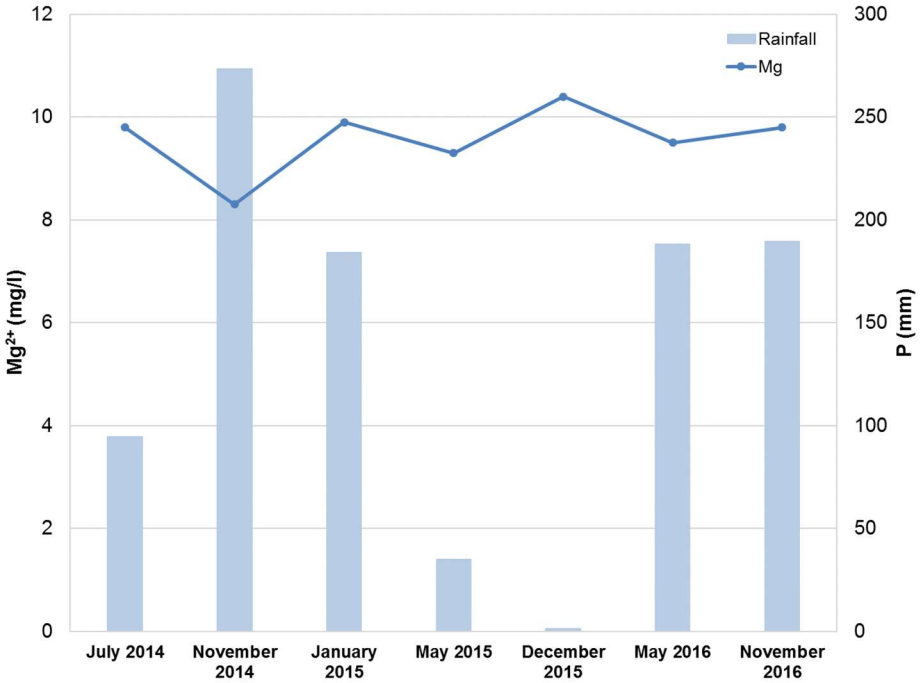

Figure 7.12 Relationship between the Mg^{2+} concentration in Pertuso Spring groundwater and rainfall (Trevi nel Lazio meteorological station)

CHAPTER 8

REMOTE MONITORING OF THE KARST WATER RESOURCES

8.1 Introduction

Groundwater monitoring systems can be an important part of many construction projects, where water resources are involved. Electronic data collection systems allow monitoring information to be shared rapidly via mobile communication networks and internet. Secure data access can be provided to remote users. who are part of the project team, such as contractors, consultants, regulator and other stakeholders. Regular monitoring of the operations can allow long-term trends in system performance to be identified, and to allow preventive maintenance to be planned. Real time monitoring of systems can allow alarm signals to be triggered to warn operators of power supply interruption or other problems.

In this study, a remote groundwater monitoring system has been developed and tested to monitor and manages groundwater coming from the Pertuso Spring, in the Upper Valley of Aniene River (Central Italy). According to the Environmental Monitoring Plan purposes, as well as the already existing monitoring of groundwater and surface water, an additionally monitoring station has been installed in the Pertuso Spring. This monitoring system can provide considerable insight into changes that occur during those intervals when data from the official monitoring network are unavailable. This monitoring system was implemented to continuously acquire, transmit and process groundwater quality data, in the aim of improving knowledge of the local aquifer and to make local water resources managers to take timely decisions regarding sustainable management of water resources. For this reason, in January 2015, a multiparametric probe has been installed at the outlet of the Pertuso Spring and equipped with automatic monitoring equipment.

8.2 The remote monitoring system

8.2.1 The multiparametric probe

The Pertuso Spring remote monitoring system consists of a multiparametric probe (Nesa WMP6) which measures up to six parameters simultaneously: pH, water level, Temperature, Electrical Conductivity, Redox, and Dissolved Oxygen (Tab. 8.1). The WMP6 probe has been developed for monitoring of water-bearing stratums, rivers, basins, rubbish dumps, seas or however clear or semi-clear waters.

Thanks to reduced dimensions (70 mm of diameter), the WMP6 probe is perfectly adapted in piezometric tubes of small diameter (Fig. 8.1).

Table 8.1 Technical data of the Nesa WMP6 multiparametric probe

Parameters	Range
pH	0÷14
Level	0÷20 mt / 0÷50 mt
Temperature	-5 ÷ +60 °C
Electrical conductivity	0÷6.000 µS Autorange
Dissolved oxygen	0÷200% optical
Redox	±1100 mV

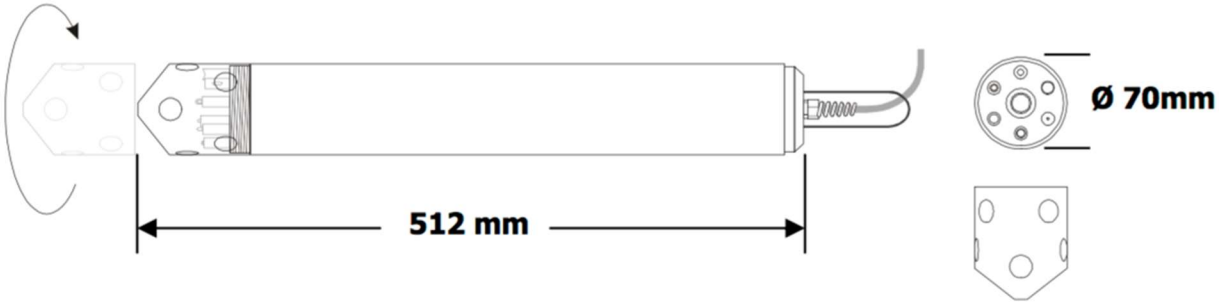

Figure 8.1 Dimensions of the Nesa WMP6 multiparametric probe

The probe WMP6 was used for continuous measurement of groundwater coming from the Pertuso Spring from a fixed location just upstream the confluence with the Aniene River (Fig. 8.2).

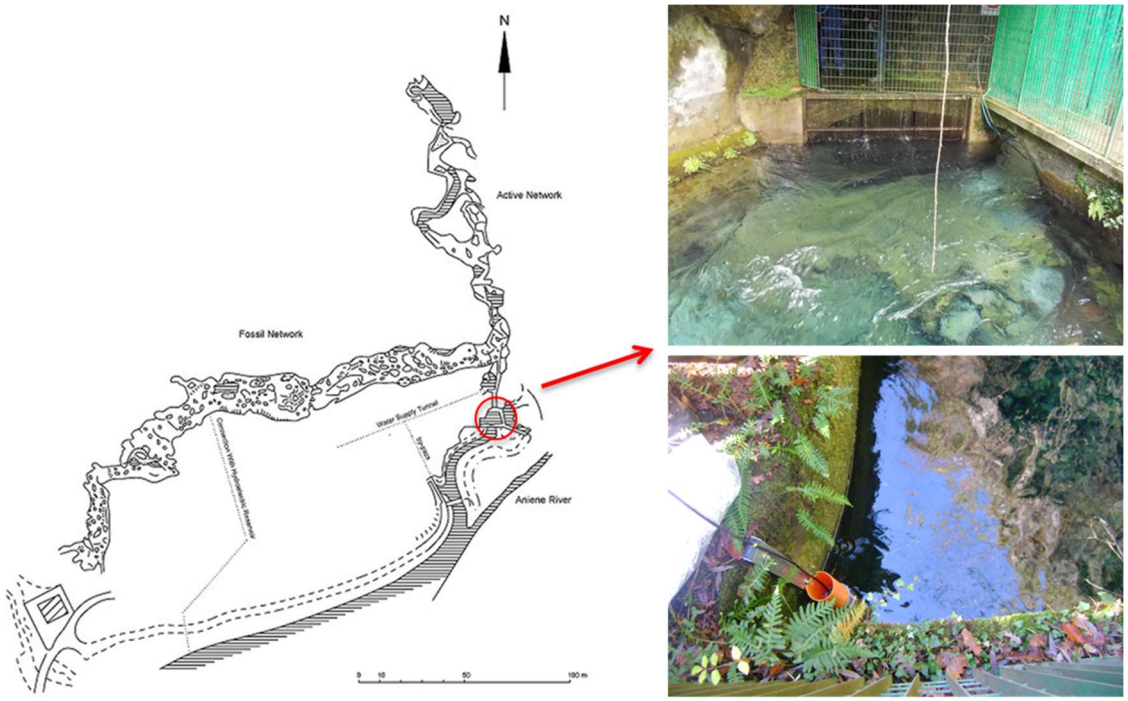

Figure 8.2 Location of the monitoring system

This probe is easy to use in continuous mode, thanks to an USB interface and to a web program that permits to transform the PC in a data logger. The probe permits to analyse several parameters concurrently and compare data in real time (with interface USB) and data transfer them by GPRS using an external data logger. With this probe it is possible to manage the data acquisition in continuous, or at any specific programmable range. In this way, the probe has been connected to a data logger Nesa series TMF100, managed in a completely automatic way and supplied from it (Fig. 8.3).

(a) (b)

Figure 8.3 Nesa WMP6 multiparametric probe (a) and data logger Nesa TMF100 (b)

The datalogger, via RS485, periodically calls each sensor and processes the data by storing them locally, and by a line of remote communication GPRS, it transfers all acquired data to an internet area using the FTP protocol (File Transfer Protocol) (Fig. 8.4).

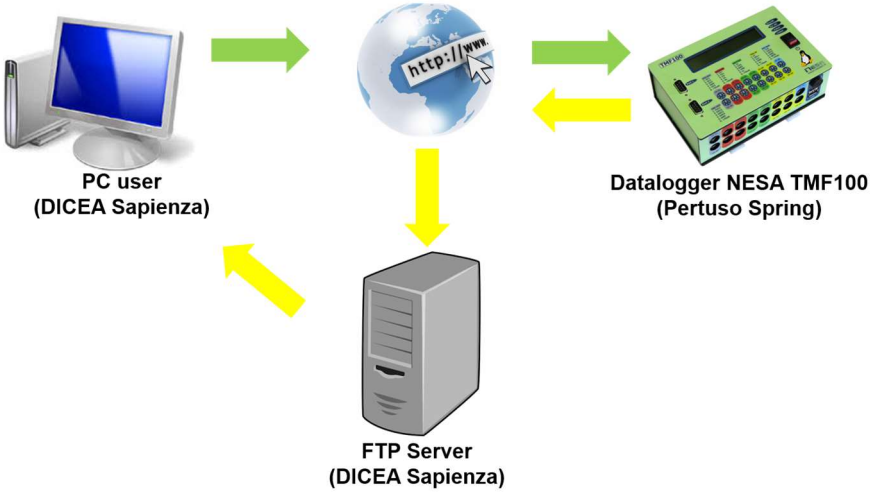

Figure 8.4 System diagram

The probe WMP6 through six independent electrodes, each one calibrated separately, managed by a specific electronic, allows seeing in real time the values of the main physic-chemical parameters of water. The connection of the probe was realized via USB interface by IS485/USB module that, thanks to an effective web software, allows viewing data, recording them on the PC, as if it were a data logger, obtaining a file directly in Excel compatible format.

8.2.2 "Pertuso Data Viewer 1.0" Software

Pertuso Data Viewer version 1.0 is a software for the visualization, interpretation, download and web access to real time groundwater monitoring data, coming from the Environmental Monitoring Plan of Pertuso Spring.

This software has been developed in the programming language Matlab® by Sapienza University of Rome for the analysis of time-series data measured by a multiparametric probe developed for the monitoring of water-bearing stratums. This probe directly interfaces with a data logger for real-time visualization of instantaneous data in graphical and numerical modes and storages data in a FTP server.

Pertuso Data Viewer is supported for Windows XP®, Vista®, Windows 7®, 8 e 10 and the corresponding version of Microsoft Office® (64 bit operating systems) and allows a real-time access of groundwater monitoring data and the automatic generation of data report and data chart at user specified time intervals for each parameter for a rapid interpretation of long time series data sets.

Pertuso Data Viewer version 1.0 allows the visualization of concentration plots of each parameter measured (Fig. 8.5a) which can be expanded in separate windows and saved to a variety of different formats including "jpeg ", "tiff", "pdf", "metafile".

Moreover, this software exports data, starting from the raw file in ASCII format, in Excel-compatible format (Fig. 8.5b).

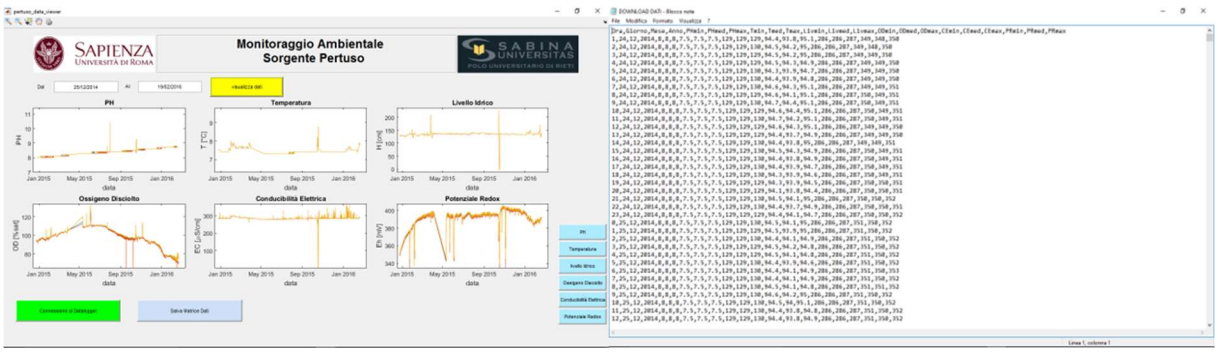

(a) (b)

Figure 8.5 Visualization of concentration plots of each parameter measured (a) and raw file in ASCII format (b)

Pertuso Data Viewer allows to change the datalogger configuration (type of sensors, acquisition time, and memorization time) and to set up thresholds on measures in manual mode or automatic.

The probe WMP6 can be configured to report to the FTP Server on a daily, hourly, or interval schedule; alarm condition, or on user demand. In this study, this groundwater multiparametric probe simultaneously collects hourly time series data.

8.3 Real time data analysis

The real-time water quality monitoring system of Pertuso Spring has been operational since January 2015. Live data will be collected every hour from the spring.

The use of water quality sensors for in situ investigations has a narrow limit of use at this time, because of problems associated with sensor accuracy. In fact, unlike water level sensors, the performance of the water quality sensors over periods greater than a year is reduced either because of

the naturally occurring constituents in the water that interfere with the sensors or because of loss of sensors calibration.

In March 2016, it has been observed a loss of the dissolved oxygen sensor calibration. For this reason, the instrument had to be repaired, resulting in the interruption of the recording for about 9 months, until December 2016.

The results coming from the Pertuso Spring real time monitoring data have been analyzed in order to study the groundwater circulation in the feeding aquifer. This karst aquifer is characterized by a high permeability and consequently by very rapid flows, suggesting the presence of large conduits that could quickly transport a possible contaminant. The experience of more than a year of function has shown that electrical conductivity is one of the most useful parameters, monitored for quality status classification. In particular, water temperature, electrical conductivity and rainfall data coming from meteorological stations (Filettino and Trevi nel Lazio), sited nearby the spring, have been studied to identify the groundwater circulation in the aquifer feeding the Pertuso Spring. The study of the lag time between peak rainfall and peak of T and EC allow highlighting the aquifer seasonal vulnerability.

In a karst system, the spring is, very often, the only point, where one can obtain information about the whole aquifer system. Different variations of T and EC allow distinguishing different kind of water circulating in the karst system, principally rainwater and base-flow groundwater.

The variations of Pertuso Spring discharge are very marked, strictly conditioned by the local weather trend. If infiltrators are absent, the water flow is reduced, while in the case of abundant precipitation, monthly the flow has remarkable increases, with pronounced peaks, not of a longer duration.

In presence of significant infiltration events, even after a prolonged period of drought, in parallel with the increase in recharge, a sudden decreasing values of mineralization (Fig. 8.6) and generally also of the temperature (Fig. 8.7).

Results from monitoring generally show decreasing water EC values with increasing Pertuso Spring flows, due to storm events. The decrease is proportional to the rainfall values (Fig 8.7), suggesting a fast recharge system with a small saturated zone and large karst conduits, where storm water flows rapidly mixing with groundwater and reaching the spring in a very short time [143].

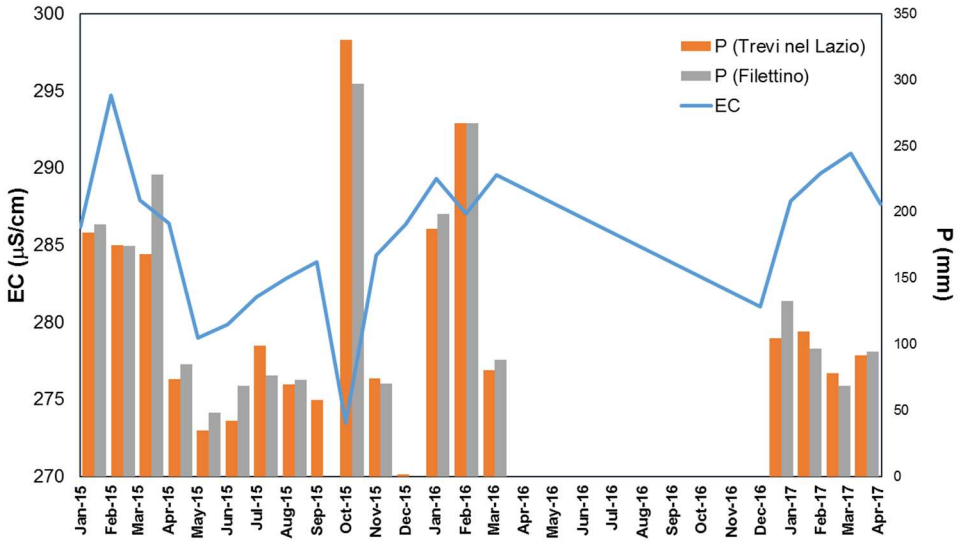

Figure 8.6 Pertuso Spring electric conductivity response to rainfall events (January 2015 - April 2017)

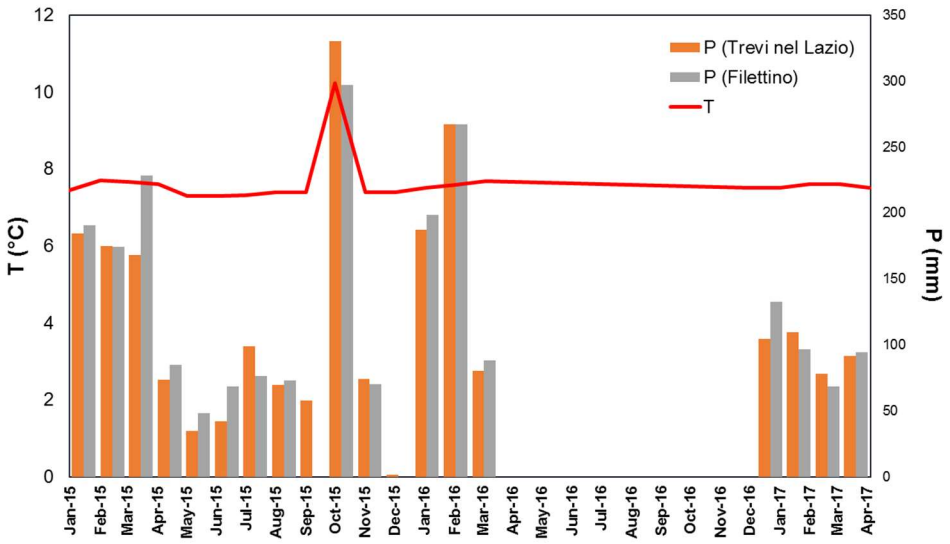

Figure 8.7 Pertuso Spring temperature response to rainfall events (January 2015 - April 2017)

Also water temperature, showing small increases, changes according to the rainfall events, confirming this circulation model in the aquifer feeding the Pertuso Spring. During these periods, it may be possible to experience a significant increase in the battery charge or the turbidity content of the water, which is due to the intense drainage of the organic matter present in the absorbent areas [143]. When the infiltrative phenomenon is finished, as evidenced by the decrease in the flow rate, the groundwater physical-chemical parameters increase very slowly. This is due to the decrease of flow velocities, which lead to long water-rock interaction and long time of residence in the aquifer.

Until now, there is not enough data to validate the underlying considerations about the aquifer circulation.

Real-time monitoring provides a very useful option through data processing that could not otherwise be implemented by conventional monitoring programs of any frequency. Collected groundwater data can be used to create 3D numerical models to observe groundwater flow patterns and over time capture seasonal variations. Real time groundwater monitoring improves data availability and reduces the need for regular access to difficult mountain sites to download groundwater data. This results in significant labour and travel costs.

CONCLUSIONS

This study presents the results of the first three years of the Environmental Monitoring Plan related to the catchment project of the Pertuso Spring, the main perennial outlet of the karst aquifer in the Upper Valley of the Aniene River, which is an important source for drinking water supply in the southeast part of Latium Region, in Central Italy.
The purpose of this work is to outline the key monitoring requirements to control the environmental performance of the catchment project of the Pertuso Spring. The Environmental Monitoring Plan is a formal and approved document for project execution management. The plan set up the monitoring methodology and the actions needed to evaluate the potential environmental impacts, due to the catchment works. The Environmental Monitoring Plan, combined with the implementation of measures designed to reduce the potential adverse effects of the proposed project on the karst aquifer feeding the Pertuso spring, is crucial to evaluate the environmental sustainability of the catchment project. The monitoring plan provides that, in the event of environmental impact, construction activities will stop and remediation measures will restore the environment status of the hydrogeological system.

In the first part of this study, a comparative evaluation of vulnerability assessment of the karst aquifer feeding the Pertuso Spring was carried out, applying the COP method. Thus, with the aim of highlighting the karst features key-role in the unsaturated zone, COP method has been applied starting from two different discretization approaches of the hydrogeological basin: using a polygonal layer and the Finite Square Elements (FSE). The combined use of two vulnerability assessment approaches allows a better understanding of pollution vulnerability mechanisms in the study area.
The results of this study highlight that the vulnerability of the karst aquifer feeding the Pertuso Spring mainly ranges from low to very high in each approach. Vulnerability maps show a high variability according to the geological and hydrogeological settings of the study area. The highest contribution to vulnerability is due to karst features such as karren, sinkhole, groove and swallow holes. The highly developed epikarst, the high recharge and high hydraulic conductivity minimizes the protective function of the unsaturated zone.
As to be expected, COP method comes out to be a very suitable methodology for the vulnerability assessment in karst settings. As a matter of fact, the use of a polygonal layer as the basis for subsequent

evaluations of the vulnerability is an effective option, because it allows to highlight the nature of outcropping lithology and the presence, shape and extent of karst features, responsible of fast infiltration and leakage. On the other hand, the FSE discretization comes out to be more sensitive to precipitation rates variations as well as to elevation and slopes, which are related to the water runoff. For these reasons, it is possible to say that the polygonal layer discretization is more recommended for small study areas such as the Pertuso Spring hydrogeological basin, whereas the FSE discretization is to be preferred for wide areas, where the higher range of precipitations and slope factors variations may play a key role in vulnerability assessment.

The second part of this work outlines the results of a hydrogeological study based on the results of the Environmental Monitoring.
In order to identify the hydrogeochemical processes governing the evolution of groundwater and surface water and their circulation patterns, water samples from different parts of the study area were collected in seven different monitoring campaigns, carried out between July 2014 and November 2016.
The analysis of the hydrogeochemical processes due to groundwater-surface water interactions let us to highlight the source of their mineralization and the influence of rock masses they flow across in the aim to address groundwater protection policy. As is to be expected in waters that circulate in karst aquifer, the Ca-Mg-HCO_3 facies is dominant in water samples and result from dissolution of limestone and dolomite rocks which are abundant within the Triassic and Cretaceous formations which underlie much of the basin. Results from geochemical interpretation of water chemistry using PHREEQC of surface water sampled indicate that all samples were saturated with respect to calcite and dolomite.
Most of groundwater samples are undersaturated with respect to calcite and dolomite. However, some samples are saturated with respect to calcite and dolomite, which implies a great dissolution and strong mineralization along groundwater flow paths (GW_01 and GW_02).
In the aim to quantitatively assess surface water resources, discharge surveys were carried out in four monitoring stations located along the Aniene River, upstream and downstream the Pertuso Spring, from July 2014 and November 2016. These results have been compared to the discharge measurements using the salt dilution method, in the aim if defining a reliable methodology for the evaluation of discharge in mountain streams, where turbulent flows make difficult apply the conventional current meter method. Even if the comparison with discharge measurements carried on by the application of both methods shows comparable values, several factors can affect the accuracy the discharge measurements obtained by salt dilution method. The loss of tracer between the injection point and the downstream cross section makes not applicable the equation for the conservation of mass and consequently the computation of stream discharge. Other factors that may have caused inaccuracies between current meter and salt dilution stream flow measurements are the tracer probe accuracy limits and the incomplete mixing throughout the stream cross section before the downstream gauging section is reached. This fact let us pointing out the real importance of the determination of the degree to which an added tracer is diluted by the flowing water. The success of the slug injection methods requires the complete mixing of the added tracer diluted by the flowing water in as short a distance as possible.

The third part of this work deals with the assessment of the groundwater - surface water interactions on the basis of Aniene River discharge measurements and water geochemical tracers data in the aim to set up an inversed model, which allows to estimate groundwater flow coming out from the Pertuso Spring, starting from discharge measurements and geochemical characterization. In this study, we presented the

first results of the application of an indirect method, based on Magnesium as a tracer, with its concentration changes in groundwater and surface water, for the evaluation of karst spring discharge. The measurements of Magnesium concentration, along the Aniene River and groundwater coming from the Pertuso Spring, have confirmed potential for using Magnesium, as a suitable aqueous tracer, to assess karst spring discharge. These preliminary results show that the dilution of naturally dissolved Magnesium ion in groundwater and surface water can give a reliable estimate of dolomite dissolution where tradition methodologies are not easily applied. This value depends on the Pertuso Spring water, which is undersaturated with respect to dolomite until it joins the main stream of Aniene River, where the magnesium content is much higher due to the saturation whit respect to dolomite. Thus, the decreasing of Magnesium concentrations downstream the Pertuso Spring is due to this mixing with spring waters. Although it is subject to some uncertainties, the Mg^{2+} concentration, as an environmental tracer, provides a mean to predict discharge evaluation of the Pertuso Spring, due to the mixing of surface water and groundwater and, provides information on changes in water quantity and quality. This method applied in the Upper Valley of the Aniene River showed its reliability and indicates that such measurements can be useful to better understand groundwater movement in this karst system. In fact, the use of Magnesium, as an aqueous tracer, is well suited because it occurs naturally in the environment and it is easy to monitor and its measurements inexpensive to be performed.

LIST OF REFERENCES

1. UN-WWAP (United Nations World Water Assessment Programme). The United Nations World Water Development Report 2017. Wastewater: The Untapped Resource. UNESCO Pub., Paris, 2017, p. 198.
2. UN-WWAP (United Nations World Water Assessment Programme). Water for People, Water for Life: A Joint Report by the Twenty Three UN Agencies Concerned with Freshwater. UNESCO Pub., New York, 2003, p. 36.
3. Sappa, G.; **Ferranti**, **F**.; Ergul, S.; Ioanni, G. Evaluation of the groundwater active recharge trend in the coastal plain of Dar Es Salaam (Tanzania). Journal of Chemical and Pharmaceutical Research, 5(12), 2013, pp. 548-552 (*Appendix A*).
4. FAO (Food and Agriculture Organization of the United Nations). Coping with water scarcity - An action framework for agriculture and food security. FAO Water Reports n. 38, Rome, 2012, p. 100.
5. Sappa, G.; Luciani, G. Groundwater Management in Dar Es Salam Coastal Aquifer (Tanzania) under a Difficult Sustainable Development. WSEAS Transactions on Environment and Development, 10, 2014, pp. 465-477.
6. Foster, S.; Hirata, R.; Andreo, B. The aquifer pollution vulnerability concept: Aid or impediment in promoting groundwater protection? Hydrogeology Journal, 2013, 21, pp. 1389-1392.
7. Ford, D.C.; Williams, P.W. Karst Geomorphology and Hydrology. John Wiley & Sons, Chichester, England, 2007.
8. Boni, C.; Bono, P.; Capelli, G.; Lombardi, S.; Zuppi, G.M. Contributo all'Idrogeologia dell'Italia Centrale: Analisi Critica dei Metodi di Ricerca. Memorie Società, Geologica Italiana, vol.35, 1986, pp. 947-956.
9. Guo, Q.; Wang, Y.; Ma, T.; Li, L. Variation of karst springs discharge in recent five decades as an indicator of global climate change: a case study at Shanxi, northern China. Science in China Series D: Earth Science, 48(11), 2005, pp. 2001-2010.

10. Bakalowicz, M. Karst groundwater: A challenge for new resources. Hydrogeology Journal, 2005, 13, pp. 148-160.

11. White, W.B. Conceptual models for carbonate aquifers. Ground Water, 1969, 7, pp.15-22.

12. Zwahlen, F. Vulnerability and risk mapping for the protection of carbonate aquifers, final report, COST Action 620, Final Report; European Commission, Directorate- General XII Science, Research and Development, Brussels, Report EUR 20912, COST Action 620, Luxembourg, Belgium, 2004, p. 297.

13. Cozma, A.I.; Baciu, C.; Moldovan, M.; Pop, I.C. Using natural tracers to track the groundwater flow in a mining area. Procedia Environmental Sciences, 2016, 32, pp. 211-220.

14. Montanari, A.; Staniscia, B. An overview of territorial resources and their users in the Rome and Chieti-Pescara areas. In Sustainability in the coastal urban environment: thematic profiles of resources and their users, Khan A.Z, et al., Sapienza Università Editrice, 2012.

15. Cipollari, F.; Cosentino, D.; Parrotto, M. Modello cinematico-strutturale dell'Italia centrale. Studi Geol. Camerti, 1995, 2, pp. 135-143.

16. Devoto, G. Note geologiche sul settore centrale dei Monti Simbruini ed Ernici (Lazio nord-orientale). Bollettino della Società dei naturalisti in Napoli, 1967, 76, pp. 1-112.

17. Devoto, G. Sguardo geologico dei Monti Simbruini (Lazio nord-orientale). Geologia Romana, 1970, 9, pp. 127-136.

18. Devoto, G.; Parotto, M. Note geologiche sui rilievi tra Monte Crepacuore e Monte Ortara (Monti Ernici-Lazio nord-orientale). Geologia Romana, 1967, 6, pp. 145-163.

19. Accordi, G.; Carbone, F. Sequenze carbonatiche meso-cenozoiche. Note illustrative alla Carta delle Litofacies del Lazio-Abruzzo ed aree limitrofe. Quad Ric. Scient., 1988, 114(5), pp. 11-92.

20. Damiani, A.V. Studi sulla piattaforma laziale-abruzzese. Nota I. Considerazioni e problematiche sull'assetto tettonico e sulla paleogeologia dei Monti Simbruini. Memorie. Descrittive Carta Geologica D'Italia, 1990, 38, pp. 145-176.

21. Bono, P.; Percopo, C. Flow dynamics and erosion rate of a representative karst basin (Upper Aniene River, Central Italy). Environmental Geology, 1996, 27, pp. 210-218.

22. Ventriglia, U. Idrogeologia della Provincia di Roma, IV, Regione Orientale. Amministrazione provinciale di Roma, LL.PP., Viabilità e Trasporti, 1990.

23. De Felice, A.M.; Dragoni, W.; Giglio G. Methods of hydrological basin comparison. Roorkee India: Report No. 120. Institute of Hydrology, 1992.

24. White, W.B. Geomorphology and hydrology of karst terrains. Oxford University Press, New York, 1988.

25. White, W.B. Karst hydrology: recent developments and open questions. Engineering Geology, 2002, 65, pp. 85-105.

26. Amoruso, A.; Crescentini, L.; Petitta, M.; Tallini, M. Parsimonious recharge/discharge modeling in carbonate fractured aquifers: The groundwater flow in the Gran Sasso aquifer (Central Italy). Journal of Hydrology, 2013, 476(7), pp. 136-146.

27. Goldscheider, N.; Drew, D. Methods in karst hydrogeology. IAH: International Contributions to Hydrogeology, CRC Press, 2007.

28. Williams, P.W. The role of the epikarst in karst and cave hydrogeology: a review. International Journal of Speleology, 2008, 37(1), pp. 1-10.

29. ACEA ATO2. Studio idrogeologico - Proposta di aree di salvaguardia della Sorgente Pertuso. Unpublished, 2005.

30. Sappa, G.; **Ferranti**, **F**. An integrated approach to the Environmental Monitoring Plan of the Pertuso Spring (Upper Valley of Aniene River). Italian Journal of Groundwater, 2014, 136, pp. 47-55 (*Appendix A*).

31. Palmer, A.N. Patterns of dissolution porosity in carbonate rocks. In Karst modelling, Palmer, A.N.; Palmer, M.V.; Sasowsky, I.D.; Leesburg, Va. Karst Waters Institute Special Publication, 1999, 5.

32. Cherubini, C.; Pastore, N.; Francani, V. Different approaches for the characterization of a fractured karst aquifer. WSEAS Transactions on fluid mechanics, 2008, 3, pp. 29-35.

33. Civita, M.; De Maio, M.; Vigna B. Una metodologia GIS per la valutazione della Ricarica Attiva degli Acquiferi. Atti del 3° convegno nazionale sulla protezione delle acque sotterranee per il III millennio. Roma 13-15 ottobre 1999.

34. Sappa, G.; **Ferranti**, **F**.; De Filippi, F.M. Hydrogeological water budget of the karst aquifer feeding Pertuso Spring (Central Italy). Proceeding of the 16th International Multidisciplinary Scientific GeoConference Surveying Geology and Mining Ecology Management (SGEM), 2016, 1, pp. 847-854.

35. Turc, L. Estimation of irrigation water requirements, potential evapotranspiration: a simple climatic formula evolved up to date. Annals of Agronomy, 1961, 12, pp. 13-49.

36. Margat, J. Vulnérabilité des nappes d'eau souterraine à la pollution. BRGM Pubblication 68 GSL 198 HYD, Orléans, France, 1968.

37. Albinet, M.; Margat, J. Chartographie de la vulnerabilité la pollution des nappes d'eau souterraine. Bull. BRGM 2nd Ser., 1970, 3(4), pp. 13-22.

38. Vrba, J.; Zoporotec, A. Guidebook on Mapping Groundwater Vulnerability. International Contributions to Hydrogeology (IAH), 1994, 16, p. 131.

39. COST 65. Hydrogeological aspects of groundwater protection in karstic areas, Final report (COST action 65). – European Comission, Directorat-General XII Science, Research and Development, Report EUR 16547 EN: p. 446, Brüssel, Luxemburg, 1995.

40. Daly, D.; Dassargues, A.; Drew, D.; Dunne, S.; Goldscheider, N.; Neale, S.; Popescu, I.C.; Zwahlen, F. Main concepts of the European Approach for (karst) groundwater vulnerability assessment and mapping. Hydrogeology Journal, 2002, 10(2), pp. 340-345.

41. Marin, A.I.; Andreo, B.; Mudarra, A. Vulnerability mapping and protection zoning of karst springs. Validation by multitracer tests. Science of the Total Environment, 2015, 532, pp. 435-446.

42. Doerfliger, N.; Jeannin, P.Y.; Zwahlen, F. Water vulnerability assessment in karst environments: a new method of defining protection areas using multi-attribute approach and GIS tools (EPIK method). Environmental Geology, 1999, 39(2), pp. 165-176.

43. Hadzic, E.; Lazovic, N.; Mulaomerovic-Seta, A. The importance of groundwater vulnerability maps in the protection of groundwater sources. Key study: Sarajevsko Polje. Procedia Environmantal Science. 7th Groundwater Symposium of the International Association for Hydro-Environment Engineering and Research (IAHR), 2015, 25, pp. 104-111.

44. Vıas, J.M.; Andreo, B.; Perles, M.J.; Carrasco, F.; Vadillo, I.; Jimenez, P. Proposed method for groundwater vulnerability mapping in carbonate (karstic) aquifers: the COP method, application in two pilot sites in Southern Spain. Hydrogeology Journal, 2006, 14, pp. 1-14.

45. Doerfliger, N.; Zwahlen, F. Practical guide, groundwater vulnerability mapping in karstic regions (EPIK). Swiss Agency for the Environment, Forest and Landscape (SAEFL), 1998, p. 56.

46. Goldscheider, N.; Klute, M.; Sturm, S.; Hötzl, H. The PI method - a GIS based approach to mapping groundwater vulnerability with special consideration of karst aquifers. Zeitschrift fur Angewandte Geologie, 2000, 46(3), pp. 157-166.

47. Civita, M.; De Maio, M. Valutazione e cartografia automatica della vulnerabilità degli acquiferi all'inquinamento con sistema parametrico SINTACS R5. Pitagora Editrice, 2000, p. 248.

48. Vıas, J.M.; Andreo, B.; Perles, M.J.; Carrasco, F. A comparative study of four schemes for groundwater vulnerability mapping in a diffuse flow carbonate aquifer under Mediterranean climatic conditions. Environmental Geology, 2005, 47, pp. 586–595.

49. Sappa, G.; Ergul, S.; **Ferranti, F**. Vulnerability Assessment of Mazzoccolo Spring Aquifer (Central Italy), combined with Geo-chemical and Isotope Modelling. IAEG XII Congress, Torino 15-19 Settembre 2014, in Engineering Geology for Society and Territory – Volume 5 Urban Geology, Sustainable Planning and Landscape Exploitation, 2014, pp. 1387-1392 (*Appendix A*).

50. Sappa, G.; Ergul S.; **Ferranti, F**. Preliminary results of vulnerability assessment of the karst aquifer feeding Pertuso Spring, In Central Italy. Proceeding of the 14th International Multidisciplinary Scientific Geoconference and Expo, SGEM2014, 2014, 1(3), pp. 539-546 (*Appendix A*).

51. Sappa, G.; **Ferranti**, **F**.; Luciani, L. Vulnerability assessment of karst aquifer feeding Pertuso Spring (Central Italy): comparison between different applications of COP method. Geophysical Research Abstracts EGU 2016, 2016, 18 (*Appendix A*).

52. Sappa, G.; **Ferranti**, **F**.; De Filippi, F.M. Vulnerability assessment of the karst aquifer feeding the Pertuso Spring (Central Italy): comparison between different applications of COP method. International Journal of Engineering Sciences & Research Technology (IJESRT), 6(6), 2017, pp. 483-492 (*Appendix A*).

53. Sappa, G.; **Ferranti**, F. Water resources exploitation in the Upper Valley of Aniene River. L'Acqua, 2013, 2, pp. 59-68 (*Appendix A*).

54. Toran, L.; Herman, E.K.; White, W.B. Comparison of flow paths to a well and spring in a karst aquifer. Ground Water, 2007, 45, pp. 281-287.

55. Brown, E.; Skougstad, M.W.; Fishman, M.J. Methods for collection and analysis of water samples for dissolved minerals and gases, laboratory analysis. U.S. Geological Survey Techniques of Water Resources Investigation, 1970, Book 5, Chap. C1.

56. Wood, W.W. Guidelines for collection and field analysis of groundwater samples for selected unstable constituents. U.S. Geological Survey Techniques of Water Resources Investigation, Book 1, Chap. D2, 1976.

57. US EPA Region 4. Operating Procedure for Groundwater Level and Well Depth measurement (SESDPROC-301-R3) Groundwater Sampling, 2013.

58. Chow, V.T. Handbook of Applied Hydrology. New York, McGraw-Hill, 1964.

59. Rants, S.E. Measurement and computation of streamflow. US Geological Survey Water Supply paper 2175, 1982.

60. Sappa, G.; **Ferranti**, **F**.; Pecchia, G.M. Validation of salt dilution method for discharge measurements in the Upper Valley of Aniene River (Central Italy). WSEAS Recent Advances in Environmental, Ecosystem and Development, 2015 *(Appendix A*).

61. Pitty, A.F. The estimation of discharge from a karst rising by natural salt dilution. Journal of Hydrology, 1966, 4, pp. 63-69.

62. Gees, A. Flow measurement under difficult measuring conditions: filed experience with the salt dilution method. Hydrology in mountainous regions I. Hydrological measurements. The water cycle. Lang H, e Musy A., IAHS Publ., 1990.

63. Hudson, R.; Fraser, J. The Mass Balance (or Dry Injection) Method. Streamline Watershed management Bulletin, 2005, 9(1), pp. 6-12.

64. Moore, R.D. Introduction to salt dilution gauging for streamflow measurement: Part 1. Streamline Watershed Management Bulletin, 2004, 7(4), pp. 20-23.

65. Day, T.J. Observed mixing lengths in mountain streams. Journal of Hydrology, 1977, 35, pp. 125-136.

66. Fischer, H.B.; List, J.; Koh, C.; Imberger, J.; Brooks, N. Mixing in inland and coastal waters. Academic Press, 2013.

67. ISO 9555-1/1994. Measurements of liquid flow in open channel - Tracer dilution methods for the measurement of steady flow - Part 1, 1994.

68. Wood, P.J.; Dykes, A.P. The use of salt dilution gauging techniques: ecological consideration and insights, Water Research, 2002, 36, pp. 3054-3062.

69. Elder, K.; Kattelmann, R.; Ferguson, R. Refinements in dilution gauging for mountain streams. Proceedings of two Lausanne Symposia, August 1990, IAHS Publication No. 193, 1990, pp. 247-254.

70. US EPA Region 6 Standard operating procedure for stream flow measurement, 2003.

71. BS EN ISO 748:2007. Hydrometry Measurement of liquid flow in open channels using current meters or floats, 2007.

72. Morrissette, D.G.; Mavinic, D.S. BOD Test Variables. Journal of Environment: Engg. Division. EP. 6, 1978, pp. 1213-1222.

73. MC Bride, G.B.; Rutherford, J.C. Handbook on estimating dissolved oxygen depletion in polluted rivers. Water and Soil Misc Publ., Wellington, 1983, 51, pp. 1-69.

74. Saravanakumar, A.; Rajkumar, M.; Sesh Serebiah, J.; Thivakaran, G.A. Seasonal variation in physicochemical characteristics of water, sediment and soil texture in arid zone mangroves of Kachchh-Gujarat. Journal of Environmental Biology, 2008, 29(5), pp. 725-732.

75. Das, J.; Das, S.N.; Sahoo, R.K. Semidiurnal variation of some physicochemical parameters in the Mahanadi estuary, east coast of India. Indian Journal of Marine Science, 1997, 26, pp. 323-326.

76. Rose, S. Comparative major ion geochemistry of piedmont streams in the Atlanta. Georgia region: possible effects of urbanization. Environmental Geology, 2002, 42, pp.102-113.

77. Srinivasamoorthy, K.; Nanthakumar, C.; Vasanthavigar, M.; Vijayaraghavan, K.; Rajivgandhi, R.; Chidambaram, S.; Anandhan, P.; Manivannan, R.; Vasudevan, S. Groundwater quality assessment from a hard rock terrain. Salem district of Tamilnadu. India. Arabian Journal of Geosciences, 2009.

78. Piper, M. A Graphic Procedure in the Geochemical Interpretation of Water-Analyses. Transactions of the American Geophysical Union, 1944, 25, pp. 914- 923.

79. Garrels, R.M.; Mackenzie, F.T. Gregor's denudation of the continents. Nature, 1971, 231, pp. 382-383.

80. Gibbs, R.J. Mechanisms controlling world water chemistry. Science, 1970, 17, pp.1088-1090

81. Sappa, G.; Ergul, S.; **Ferranti**, **F**. Water Quality Assessment Of Carbonate Aquifers In Southern Latium Region, Central Italy: A Case Study For Irrigation And Drinking Purposes. Applied Water Science, 2013 (*Appendix A*).

82. Cerling, T.E.; Pederson, B.L.; Damm, K.L.V. Sodium-calcium ion exchange in the weathering of shales: implication for global weathering budgets. Geology, 1989, 17, pp. 552-554.

83. Fisher, R.S.; Mullican, W.F. Hydrochemical evolution of sodium sulphate and sodium chloride groundwater beneath the Northern Chihuahuan desert. Trans-Pecos. Texas. USA. Hydrogeology Journal, 1997, 5, pp. 4-16.

84. McLean, W.; Jankowski, J.; Lavitt, N. Groundwater quality and sustainability in an alluvial aquifer. Australia. In: Sililo O. et al (eds) Groundwater, past achievements and future challenges. A Balkema. Rotterdam, 2000, pp. 567-573.

85. Srinivasamoorthy, K.; Vasanthavigar, M.; Vijayaraghavan, K.; Sarathidasan, R.; Gopinath, S. Hydrochemistry of groundwater in a coastal region of Cuddalore district. Tamilnadu, India: implication for quality assessment. Arabian Journal of Geosciences, 2011.

86. Langmuir, D. Geochemistry of Some Carbonate Ground Waters in Central Pennsylvania. Geochimica et Cosmo-chimica Acta, 1971, 35(10), pp. 1023-1045.

87. Fairchild, J.; Borsato, A.; Tooth, A.F.; Frisia, S.; Hawkesworth, C.J.; Huang, Y.M.; McDermott, F.; Spiro, B. Controls on Trace Element (Sr-Mg) Compositions of Carbonate Cave Waters: Implications for Speleothem Climatic Records. Chemical Geology, 2000, 166, pp. 255-269.

88. Sappa, G.; Ergul, S.; **Ferranti**, **F**. Distribution of Ca and Mg in groundwater flow systems in carbonate aquifers from Southern Latium Region (Italy): its implications on drinking water quality. IAH - Selected Papers on Hydrogeology: Calcium and Magnesium in Groundwater: Occurrence and Significance for Human Health, Editor(s): Lidia Razowska-Jaworek, IAH - Selected Papers on Hydrogeology, 2014 (*Appendix A*).

89. Sappa, G.; **Ferranti**, **F**.; Luciani, G. Groundwater geochemical characterization in the karst aquifer feeding the Pertuso spring (Italy), Proceeding of the World Multidisciplinary Earth Sciences Symposium (WMESS 2015), Prague, Czech Republic, September 7-11, 2015 (*Appendix A*).

90. Palmer, C.D.; Cherry, J.A. Geochemical Evolution of Groundwater in Sequences of Sedimentary Rocks. Journal of Hydrology, 1984, 75(2), pp. 27-65.

91. Herman, J.S.; White, W.B. Dissolution Kinetics of Dolomite: Effects of Lithology and Fluid Flow Velocity. Geochimica et Cosmochimica Acta, 1985, 49, pp. 2017-2026.

92. Stumm, W.; Morgan, J.J. Aquatic chemistry. Wiley Interscience. New York, 1981.

93. Lloyd, J.W.; Heathcote, J.A. Natural inorganic hydrochemistry in relation to groundwater, an introduction. Clarendon Press. Oxford, 1985.

94. Parkhurst, D.L.; Appello, C.A.J. User's Guide to PHREEQC (Version 2)-A Computer Program for Speciation. Batch-Reaction. One-Dimensional Transport and Inverse Geochemical Calculations." US Geological Survey Water-Resources Investigations. Report 99-4259. 1999.

95. Langmuir, D. Aqueous Environmental Geochemistry Prentice Hall Publishers. Upper Saddle River. New Jersey, 1996.

96. Appelo, C.A.J.; Postma, D. Geochemistry. Groundwater and Pollution. Balkema. Rotterdam, 1993.

97. Aiuppa, A.; Federico, C.; Allard, P.; Gurrieri, S.; Valenza, M. Trace metal modelling of groundwater–gas–rock interactions in a volcanic aquifer: Mount Vesuvius. Southern Italy. Chemical Geology, 2005, 2163(4), pp. 289-311.

98. Buschmann, J.; Berg, M.; Stengel, C.; Sampson, M.L. Arsenic and manganese contamination of drinking water resources in Cambodia: coincidence of risk areas with low relief topography. Environmental Science & Technology, 2007, 41(7), pp. 2146-2152.

99. Giammanco, S.; Ottaviani, M.; Valenza, M.; Veschetti, E.; Principio, E.; Giammanco, G.; Pignato, S. Major and trace elements geochemistry in the groundwaters of a volcanic area: Mount Etna (Sicily. Italy). Water Research, 1998, 32, pp. 19-30

100. Parisi, S.; Paternoster, M.; Perri, F.; Mongelli, G. Source and mobility of minor and trace elements in a volcanic aquifer system: Mt. Vulture (Southern Italy). Journal of Geochemical Exploration, 2011, 110(3), pp. 233-244.

101. Hasan, S.; Ashraf Ali, M. Occurrence of manganese in groundwater of Bangladesh and its implications on safe water supply. Journal of Civil Engineering (IEB), 2010, 38(2), pp. 121-128.

102. Shiller, A.M.; Frilot, D.M. The geochemistry of gallium relative to aluminium in Californian streams. Geochimica et Cosmochimica Acta, 1996, 60(8), pp. 1323-1328.

103. Rodhe, A; Bockgård, N. Groundwater recharge in a hard rock aquifer: a conceptual model including surface-loading effects, Journal of Hydrology, 2006, 330, pp. 389-401.

104. Gleeson, T.; Novakowski, K.; Kyser, T.K. Extremely rapid and localized recharge to a fractured rock aquifer, Journal of Hydrology, 2009, 376, pp. 496-509.

105. Chesnaux, R. Regional recharge assessment in the crystalline bedrock aquifer of the Kenogami Uplands. Canada, Hydrological Sciences Journal, 2013, 58, pp. 421-436.

106. Croteau, A.M.; Nastev, R. Lefebvre Groundwater recharge assessment in the Chateauguay River watershed, Canadian Water Resources Journal, 2010, 35(4), pp. 451-468.

107. Fetter, C.W. Applied Hydrogeology Prentice Hall. New Jersey, 2001.

108. Lee, J.; Lee, K. Use of hydrologic time series data for identification of recharge mechanism in a fractured bedrock aquifer system, Journal of Hydrology, 2000, 229, pp. 190-201.

109. Risser, D.W.; Gburek, W.J.; Folmar, G.J. Comparison of recharge estimates at a small watershed in east-central Pennsylvania. USA Hydrogeology Journal, 2009, 17, pp. 287-298.

110. USGS Discharge measurements at gaging stations. Techniques of Water-Resources Investigations 3A-8, 1969.

111. Sappa, G.; **Ferranti**, **F**.; De Filippi, F.M. Environmental tracer approach to discharge evaluation of Pertuso Spring (Italy). WSEAS Recent Advances on Energy and Environment, Proceeding of the 10th International Conference on Energy & Environment (EE'15), Budapest, Hungary, December 12-14, 2015, Editor Aida Bulucea (*Appendix A*).

112. ISO 9555-1/1994. Measurements of liquid flow in open channel - Tracer dilution methods for the measurement of steady flow - Part 1, 1994

113. Moore, R.D. Slug injection using salt in solution, Streaml. Watershed Manage. Bull., 2005.

114. Tallini, M.; Parisse, B.; Petitta, M.; Spizzico, M. Long-term spatio-temporal hydrochemical and ^{222}Rn tracing to investigate groundwater flow and water–rock interaction in the Gran Sasso (central Italy) carbonate aquifer, Hydrogeology Journal, 2013, 21(7), pp 1447-1467.

115. Nigro, A.; Sappa, G.; Barbieri, M. Application of boron and tritium isotopes for tracing landfill contamination in groundwater. Journal of Geochemical Exploration, 2017, 172, pp. 101-108.

116. Petitta, M.; Fracchiolla, D.; Aravena, R.; Barbieri, M. Application of isotopic and geochemical tools for the evaluation of nitrogen cycling in an agricultural basin, the Fucino Plain, Central Italy. Journal of Hydrology, 2009, 372(1-4), pp. 124-135.

117. Alvarado, J.A.C.; Purtschert, R.; Barbecot, F.; Chabault, C.; Ruedi, J.; Schneider, V.; Aeschbach-Hertig, W.; Kipfer, R.; Loosli, H.H. Constraining the age distribution of highly mixed groundwater using ^{39}Ar: A multiple environmental tracer (^{3}H/^{3}He, ^{85}Kr, ^{39}Ar, and ^{14}C) study in the semiconfined Fontainebleau Sands Aquifer (France). Water Resources Research, 2007, 430(3), pp. 1-16.

118. Troldborg, L.; Jensen, K.H.; Engesgaard, P.; Refsgaard, J.C.; Hinsby, K. Using environmental tracers in modeling flow in a complex shallow aquifer system. Journal of Hydrology, 2008, 13, pp. 1037-1084.

119. Caschetto, M.; Colombani, N.; Mastrocicco, M.; Petitta, M.; Aravena, R. Nitrogen and sulphur cycling in the saline coastal aquifer of Ferrara, Italy. A multi-isotope approach. Applied Geochemistry, 2017, 76, pp. 88-98.

120. Lauber, U.; Goldscheider, N. Use of artificial and natural tracers to assess groundwater transit-time distribution and flow systems in a high-alpine karst system (Wetterstein Mountains, Germany). Hydrogeology Journal, 2014, 22, pp. 1807-1824.

121. Cook, P.G.; Herczeg, A. Environmental Tracers in Subsurface Hydrology. Kluwer Acad., Boston, 1999.

122. Aquilanti, L.; Clementi, F.; Nanni, T.; Palpacelli, S.; Tazioli, A.; Vivalda, P. DNA and fluorescein tracer tests to study the recharge, groundwater flowpath and hydraulic contact of aquifers in the Umbria-Marche limestone ridge (Central Apennines, Italy). Environmental Earth Sciences, 2016, 75:626.

123. Cervi, F.; Corsini, A.; Doveri, M.; Mussi, M.; Ronchetti, F.; Tazioli, A. Characterizing the recharge of fractured aquifers: A case study in a flysch rock mass of the northern Apennines (Italy). In Engineering Geology for Society and Territory, Lollino, G., Arattano, M., Rinaldi, M., Giustolisi, O., Marechal, J.C., Grant, G.E., Eds., Springer Cham, Switzerland, 2014, 3, pp. 563-567.

124. Guida, M.; Guida, D.; Guadagnuolo, D.; Cuomo, A.; Siervo, V. Using Radon-222 as a naturally occurring tracer to investigate the streamflow-groundwater interactions in a typical Mediterranean fluvial-karst landscape: the interdisciplinary case study of the Bussento River (Campania region, Southern Italy). WSEAS Transactions on System, 2013, 12(2), pp. 85-104.

125. Batiot, C.; Emblanch, C.; Blavoux, B. Total Organic Carbon (TOC) and magnesium (Mg^{2+}): two complementary tracers of residence time in karstic systems. Comptes Rendus Geoscience, 2003, 35, pp. 205-214.

126. Sappa, G.; **Ferranti**, **F**.; De Filippi, F.M. Preliminary validation of an indirect method for discharge evaluation of Pertuso Spring (Central Italy). WSEAS Transactions on Environment and Development, 2016, 12, pp. 214-225 (*Appendix A*).

127. Hunkeler, D.; Mudry, J. Hydrochemical tracers, in methods in karst hydrogeology. Taylor and Francis, London, UK, 2007.

128. Leibundgut, C.; Maloszewski, P.; Kulls, C. Tracers in hydrology. 1st ed. Wiley-Blackwell, Chichester, UK, 2009.

129. Cook, P.G.; Favreau, G.; Dighton, J.C.; Tickell, S. Determining natural groundwater influx to a tropical river using radon, chlorofluorocarbons and ionic environmental tracers. Journal of Hydrology, 2003, 277, pp. 74-88.

130. Davis, S.D.; Thompson, G.M.; Bentley, H.W.; Stiles, G. Ground-Water Tracers - A Short Review. Groundwater, 1980, 18, pp. 14-23.

131. Edmunds, W.M.; Cook, J.M.; Darling, W.G.; Kinniburgh, D.G.; Miles, D.L.; Bath, A.H.; Morgan-Jones, M.; Andrews, J.N. Baseline geochemical conditions in the Chalk aquifer, Berkshire, UK: a basis for groundwater quality management. Applied Geochemistry, 1987, 2, pp. 251-274.

132. Mudarra, M.; Andreo, B. Relative importance of the saturated and the unsaturated zones in the hydrogeological functioning of karst aquifers: the case of Alta Cadena (Southern Spain). Journal of Hydrology, 2011, 397(3-4), pp. 263-280.

133. Celle-Jeanton, H.; Emblanch, C.; Mudry, J.; Charmoille, A. Contribution of time tracers (Mg^{2+}, TOC, δ^{13}CTDIC, NO_3^-) to understand the role of the unsaturated zone: A case study-Karst aquifers in the Doubs valley, eastern France, Geophysical Research Letters, 2003, 30(6).

134. Tooth, A.F.; Fairchild, I.J. Soil and karst aquifer hydrological controls on the geochemical evolution of speleothem-forming drip waters, Crag Cave, southwest Ireland Journal of Hydrology, 2003, 273, pp. 51-68.

135. Stauffer, R.E. Use of solute tracers released by weathering to estimate groundwater inflow to seepage lakes. Environmental Science Technology, 1985, 19, pp. 405-411.

136. Bencala, K.E.; McKnight, D.M.; Zellweger G.W. Evaluation of Natural Tracers in an Acidic and Metal-Rich Stream. Water Resources Research, 1987, 23(5), pp. 827-836.

137. Schemel, L.E.; Cox, M.H.; Runkel, R.L.; Kimball, B.A. Multiple injected and natural conservative tracers quantify mixing in a stream confluence affected by acid mine drainage near Silverton, Colorado. Hydrological Processes, 2006, 20, pp. 2727–2743.

138. Scanlon, B.R.; Healy, R.W.; Cook P.G. Choosing appropriate techniques for quantifying groundwater recharge. Hydrogeology Journal, 2002, 10, Springer, pp. 18-39.

139. Sappa, G.; **Ferranti**, **F**.; De Filippi, F.M. A proposal of conceptual model for Pertuso Spring discharge evaluation in the Upper Valley of Aniene River. Italian Journal of Groundwater, 2016, 5(3) (*Appendix A*).

140. Sappa, G.; **Ferranti**, **F**. Pertuso Spring discharge assessment in the Upper Valley of Aniene River (Central Italy). International Journal of Energy and Environment, 2016, 10, pp. 30-40 (*Appendix A*).

141. Hess, J.W.; White, W.B. Storm response of the karstic carbonate aquifer of south central Kentucky. Hydrogeology Journal, Springer, 1988, 99, pp. 235-252.

142. Quinlan, J.F.; Ewers, R.O. Subsurface drainage in the Mammoth Cave area, in White W.B. and White E.L., eds., Karst hydrology concepts from the Mammoth Cave area: New York, Van Nostrand Reinhold, 1989, pp. 65-104.

143. Sappa, G.; **Ferranti**, **F**.; De Filippi, F.M.; Cardillo, G. Mg^{2+} based method for Pertuso Spring discharge evaluation. Water (Switzerland), 2017, 9(1), p. 16 (*Appendix A*).

144. Vigna, B. Acquisition and interpretation of the springs monitoring data. Geoingegneria Ambientale e Mineraria, 2014, 143(3), pp. 43-58.

APPENDIX - SCIENTIFIC CONTRIBUTIONS

Available online www.jocpr.com

Journal of Chemical and Pharmaceutical Research, 2013, 5(12):548-552

Research Article

ISSN : 0975-7384
CODEN(USA) : JCPRC5

Evaluation of the groundwater active recharge trend in the coastal plain of Dar es Salaam (Tanzania)

Giuseppe Sappa*, Flavia Ferranti, Sibel Ergul and Giancarlo Ioanni

Department of Civil, Building and Environmental Engineering, Sapienza - University of Rome, Via Eudossiana, Rome, Italy

---

ABSTRACT

This paper deals with a part of the preliminary results of three years investigation activity, carried in Dar es Salaam coastal plain (Tanzania), ACC-DAR project, supported by the European Union, in cooperation with Sapienza University of Rome and Ardhi University of Dar es Salaam. Here, they are presented the effects of rainfall data evolution in the last 50 years on the groundwater active recharge, due to land cover evolution. As a matter of fact, in the last fifteen years the Dar es Salaam coastal plan has been involved in a hard increasing of groundwater exploitation, due to increased population. On the on the hand, the groundwater active recharge has been decreased, due to the evolution of land cover. In the framework of the project, the rainfall data have been collected referred to 50 years of observations in the three urban stations of Dar es Salaam. Starting from the data collection of the continuous historical rainfall series, it has been evaluated the groundwater active recharge for different land cover scenarios from remote sensing data. The results have been compared to water demand evolution values, referred to the same temporal range, and it has been outlined that in the last few years the water demand, in this area, has overpassed the groundwater active recharge.

Keywords: Tanzania, groundwater recharge, climate changes, water demand

---

INTRODUCTION

The present study is related to the application of the reverse water balance technique (P = ET + R + I) [1] in order to determine the active average recharge (I) of the aquifer in the coastal plain of Dar es Salaam (Tanzania). The management of the large available quantity of figures asked the application of a Geographical Information System (ESRI ArcGIS10), to set up a distributed parameters mathematical model.

The United Republic of Tanzania is a country in Sub-Saharan Africa and Eastern Europe. It borders the Kenya to the North and the Uganda, Rwanda, Burundi and the Democratic Republic of the Congo to the West while the Zambia, Malawi and Mozambique to the South. The area under study covers all the urban and the periurban zones of Dar es Salaam and it is selected starting from the natural hydrogeological boundaries. The geological setting of the study area comprises unconsolidated sediments, which are classified by their geological age into two major periods: Quaternary and Neogene deposits [2]. The Quaternary deposits consist of three geological layers: alluvial, coastal plain and coral reef limestone deposits (Fig. 1).

The alluvial deposits and coastal plain deposits are of Pleistocene to Recent age and are found mainly moving from the coast towards the mainland within the river valleys [4]. The main part of the study area corresponds to such a valley. These deposits consist of sand, clay, gravels and pebbles. Fine to coarse-grained sands occur widely within valleys creeks, deltas and mangrove sites of the Mzinga, Kizinga and Msimbazi Rivers. Msindai (1988) reported on limestones, which are mainly coralliferous and are found along the coastal strip. They are generally weathered and normally covered on the surface by white buff sands or reddish brown soil. The present study deals with the

elaboration of the rainfall data (from 1960 – 2010) in order to assess the active recharge of the aquifer system in coastal plain of Dar es Salaam (Tanzania).

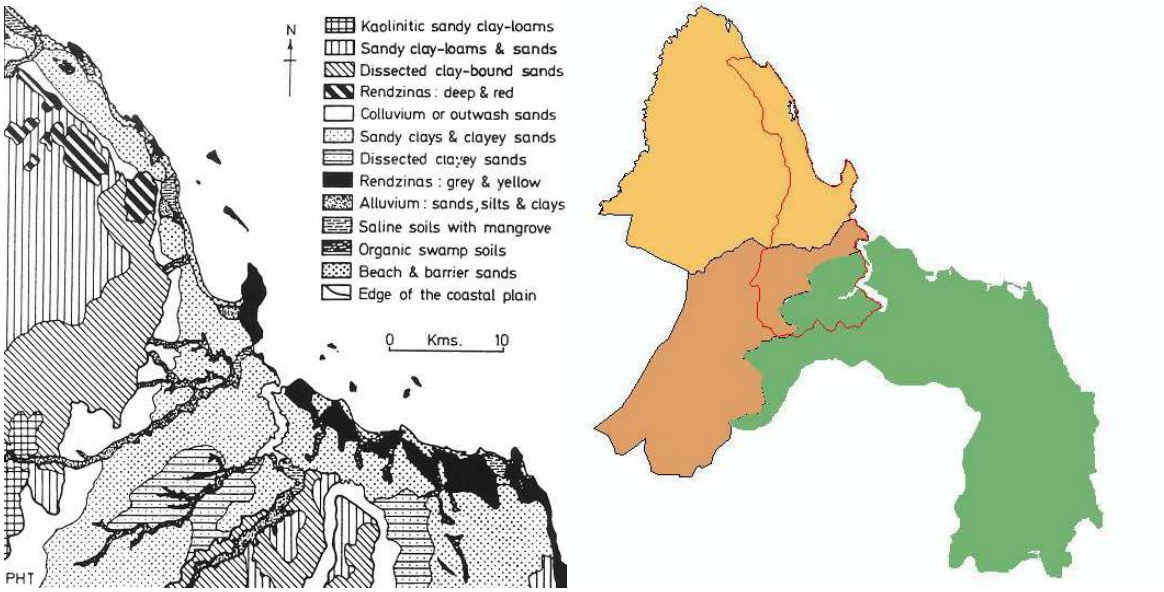

Fig. 1: The study area ([3] modified)

EXPERIMENTAL SECTION

They were available 50 years of rainfall observation (1960 - 2010), related to three different stations (Jnia, Wazohill, Ocean Road), and so all these data have been adapted to certain probability distributions (Fig. 2).

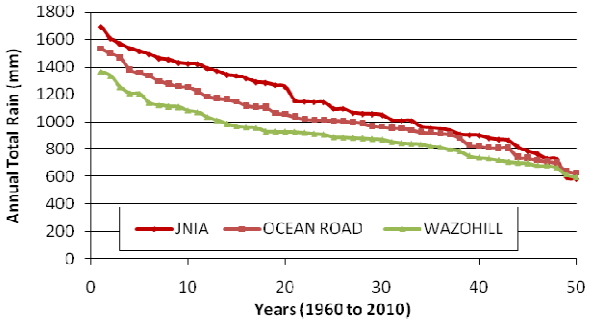

Fig. 2: Rainfall data for the three different urban stations of Dar es Salaam

Since some of these rainfall observations were not a complete data series, it has been applied a well known statistic elaboration process in order to create the lacking data. To fill these data three different methods have been used: (i) Between-station method based on the average between the previous and the following data; (ii) Within-station method based on the average between the data registered in different stations; (iii) Regression based on a important result, the difference or ratio between values of a given element observed in a different stations can be established from corresponding sums or mean values. The adjustment was obtained with the method of moments, calculating firstly the parameters of the distributions (Gauss, Galton, Gumbel, Frechet), equating theoretical moments with one of the distributions (it is assumed that the statistical parameters coincide with those of the sample). In order to determine the setting more representative of the statistical distribution, two different statistic tests have been verified: Pearson and Kolgomorov Smirnof Test. Only the Gaussian distribution has passed both tests (Fig. 3).

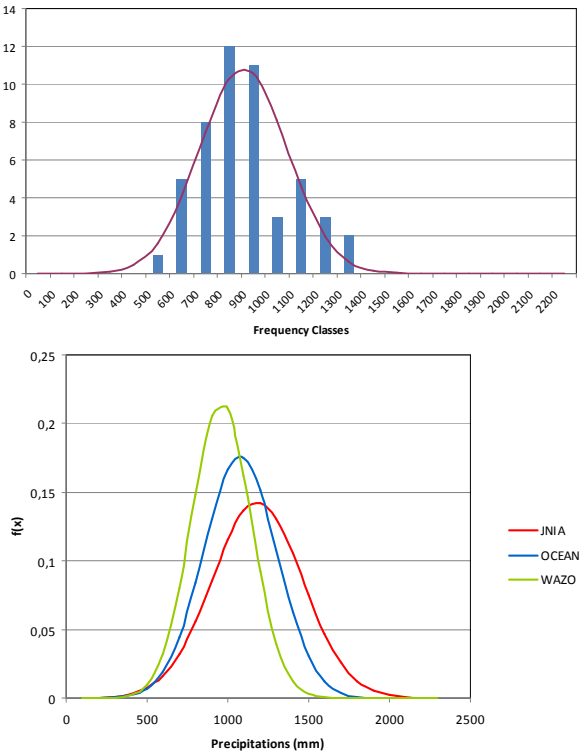

Fig. 3: Gaussian distribution

Consequently, they have been chosen the rain values, referring to one with 70% of probability of happening (Tab. 1).

Tab. 1: 70% probable annual rainfall data

Jnia	μ+σ	1410,6 mm
	μ–σ	854,2 mm
Ocean Road	μ+σ	1249,9 mm
	μ–σ	801,2 mm
Wazohill	μ+σ	1091,9 mm
	μ–σ	727,8 mm

The Inverse Distance Weighting (IDW) method, which is a deterministic one for multivariate interpolation, starts from a known scattered set of point data, in order to spread them on an area (Fig. 4). In this aim the area under study has been divided in meshes of 500 mt of dimension.

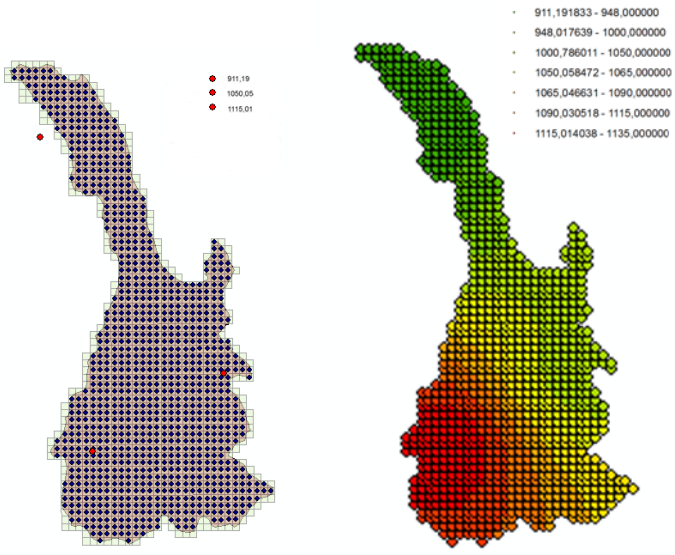

Fig. 4: Application of the Inverse Distance Weighting method to the study area

RESULTS AND DISCUSSION

Over the last ten years, the changes of the area have seen a significant growth of discontinuous and continuous urban land [5]. In the course of time, the consequences of this transformation have influenced the recharge areas extension, and groundwater active recharge have been decreased (Fig. 5).

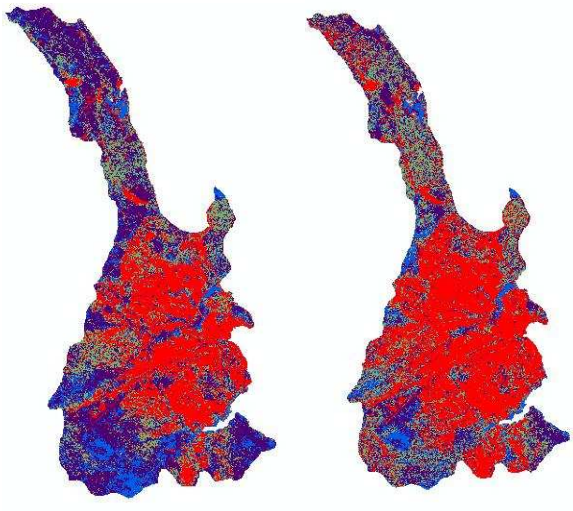

2002 **2011**

Fig. 5: Land cover distribution in 2002 and 2011

The graph shows (Fig. 6) the changes concerning the land cover between the 2002 and the 2011. It is important to underline that the percentage of continuous urban soil doubled over less than ten years.

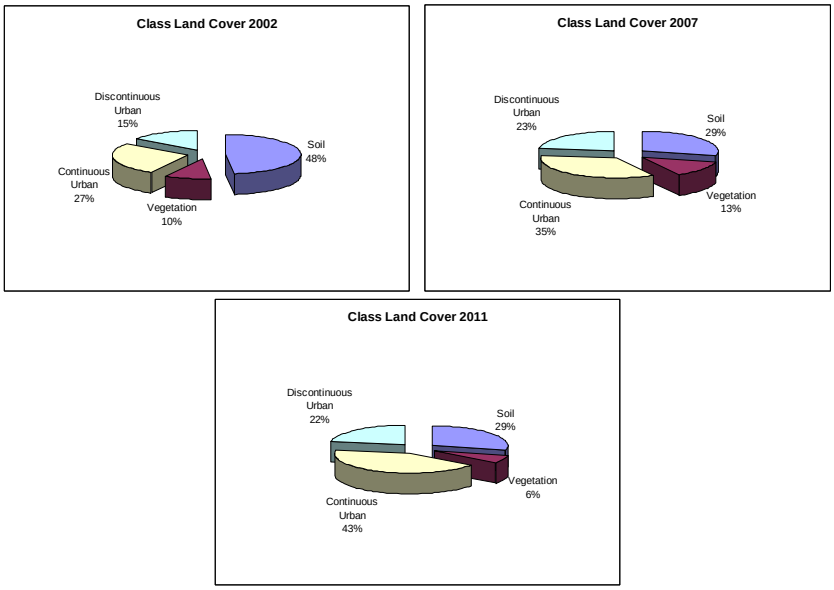

Fig. 6: Land cover distribution from 2002 to 2011

The assignment of the potential infiltration factor χ_s let us to separate the infiltration from rainfall, taking in account runoff and evapotranspiration, which do not contribute to the active recharge (Tab. 2).

Tab. 2: Potential Infiltration Factor referred to the different land cover class

Land Cover Class	Potential Infiltration Factor (χ_s)
Continuous Urban	0,1
Discontinuous Urban	0,2
Vegetative	0,3
Soil	0,4

By this way for each mesh it has been calculated the volume of recharge, through the multiplication of the rainfall (mm) by the factor χ_s (-) and the area (m^2). Adding up all the mesh values, the resulting volume has been compared with the annual water demand (Fig. 7).

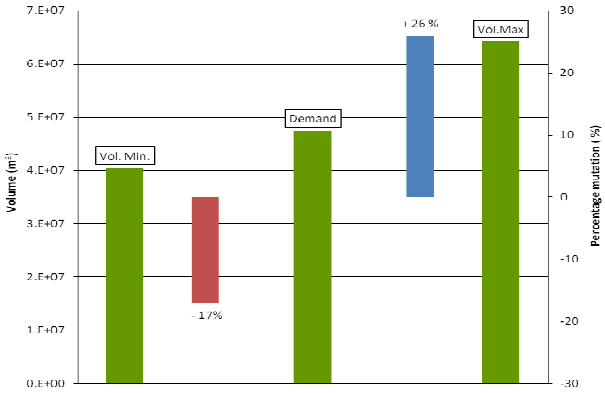

Fig. 7: Annual recharge compared with water demand

According to land cover changing the volume of water is decreased from 2002 to 2011. The bar graph (Fig. 8) shows that the volume of groundwater active recharge in Dar Es Salam coastal plan has decreased by almost 5% for each year.

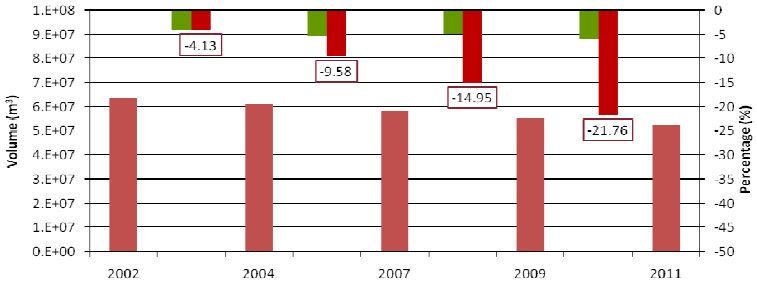

Fig. 8: Volume trend from 2002 to 2011

It true, on the other hand that part of groundwater active recharge in the coastal plan comes form Pugu Hills, but it will be necessary, all the same, to stop the groundwater exploitation, due to new building construction, to reverse the nowadays trend of budget between demand and recharge.

REFERENCES

[1] M Civita; M De Maio. Average ground water recharge in carbonatic aquifers: a GIS processed numerical model, 7th Conf. on Limestone Hydrology and Fissured Media, Besançon, 20-23 sept.2001, **2001**, 93-100
[2] IC Mjemah. Hydrogeological and Hydrogeochemical Investigation of a Coastal Aquifer in Dar es Salaam, Tanzania. Ph.D. Thesis, Ghent University, Ghent, **2007**.
[3] P Temple. Aspects of the geomorphology of the Dar es Salaam area. *Tanzania Notes and Records* 71, **1970**, 21-54.
[4] K Msindai. Engineering geological aspects of soils and rocks in the Dar es Salaam region, Tanzania. Publications of the University of Turku, Academic Press, Helsinki, **1988**.
[5] G Sappa; A Trotta; S Vitale. Climate change impact on groundwater active recharge in coastal plain of Dar es Salam (Tanzania). IAEG XII Congress, Torino, September 15-19, **2014**, in press.

DOI 10.7343/AS-073-14-0099

DOI 10.7343/AS-073-14-0099

An integrated approach to the Environmental Monitoring Plan of the Pertuso spring (Upper Valley of Aniene River)

Un approccio integrato al Piano di Monitoraggio Ambientale della sorgente Pertuso (Alta Valle del Fiume Aniene)

Giuseppe Sappa, Flavia Ferranti

Riassunto: La caratterizzazione idrogeologica delle acque sotterranee e superficiali è uno strumento di fondamentale importanza per una corretta gestione e salvaguardia ambientale delle risorse idriche. Il presente lavoro illustra la pianificazione del programma di monitoraggio multi-disciplinare relativo al progetto di consolidamento della derivazione della sorgente Pertuso, nell'Alta Valle del Fiume Aniene, per il superamento delle emergenze idriche nei Comuni a sud di Roma. Alla luce di quanto prescritto dal D.Lgs. 152/2006, così come modificato dal D.M. 260/2010, la realizzazione di opere di ingegneria, interessanti il sottosuolo, non può prescindere dalla predisposizione di un Programma di Monitoraggio Ambientale, dal quale ricavare il patrimonio informativo sull'assetto idrogeologico dell'area di studio. La caratterizzazione idrogeologica, realizzata attraverso il Programma di Monitoraggio Ambientale, costituisce uno strumento utile per valutare i potenziali impatti ambientali correlabili al progetto di derivazione. Per la valutazione e la conseguente gestione sostenibile delle risorse idriche, un requisito fondamentale è la quantificazione della ricarica della falda acquifera. Per tale motivo è stata inclusa nel piano di monitoraggio una dettagliata caratterizzazione quantitativa delle acque sotterranee erogate dalla sorgente Pertuso, al fine di garantire che i lavori di derivazione non alternino il naturale equilibrio idrogeologico della falda acquifera. A questo scopo è stato redatto un Programma di Monitoraggio Ambientale delle acque sotterranee e superficiali dell'Alta Valle del Fiume Aniene, di cui il presente studio illustra nel dettaglio gli obiettivi e l'articolazione.

Parole chiave: sorgente Pertuso, fiume Aniene, acquifero carsico, Piano di Monitoraggio Ambientale.

Keywords: *Pertuso spring, Aniene River, karst aquifer, Environmental Monitoring Plan.*

Abstract: *Quantitative assessment of groundwater and surface water is an important tool for sustainable management and protection of these important resources. This paper deals with the design of a multi-disciplinary monitoring plan related to the catchment project of the Pertuso spring, in the Upper Valley of Aniene River, which is going to be exploited to supply an important water network in the South part of Roma district. According to the Legislative Decree 152/2006, as modified by DM 260/2010, any infrastructure design should take in consideration an Environmental Monitoring Plan for the hydrogeological settings of the study area. Thus, the hydrogeological characterization combined with an Environmental Monitoring Plan provides to evaluate the potential adverse environmental impacts due catchment works. For water resources assessment and management, the quantification of groundwater recharge is a preliminary step. As a matter of fact, it has been included the quantitative characterization of the Pertuso spring, in the aim of to protect catchment area, which is directly affect by the natural hydrogeological balance of this aquifer. Thus, a multi-disciplinary monitoring plan has been set up, including quantitative and hydrogeochemical measurements, both for groundwater and surface water of the Upper Valley of Aniene River. The target of this Environmental Monitoring Plan is to set up the background framework on the hydromorphological, physico-chemical and biological properties of water resources in the water basin influenced aim by any potential environmental impact due to the construction activities. The Environmental Monitoring Plan and main features of the monitoring network will be presented in this study.*

Giuseppe SAPPA
Flavia FERRANTI
Dipartimento di Ingegneria Civile, Edile e Ambientale,
Sapienza - Università di Roma,
Via Eudossiana 18, 00186, Roma.
Tel: +39-0644585010 Fax: +39-0644585016
giuseppe.sappa@uniroma1.it
flavia.ferranti@uniroma1.it

Ricevuto: 15 maggio 2014 / Accettato: 30 giugno 2014
Pubblicato online: 31 luglio 2014

DOI 10.7343/AS-073-14-0099

Introduction

Karst aquifers constitute more than 30 % of the EU land mass (Foster et al., 2013) and these groundwater resources are the most important source of water supply for worldwide (Sappa et al., 2013). The hydraulic behaviour of karst aquifers is controlled by a network of highly permeable flow features (i.e. karst conduits, rutted fields, sinkholes, cave systems and ponors) embedded in a less permeable fractured rock matrix. Depending on their sizes (hydraulic capacity) and interconnection, conduit networks are responsible of discharging large volumes of water rapidly through a karst aquifer (White, 1993). Flow velocities into well-developed karst networks range on the order of hundreds to thousands of feet per day are not uncommon (White, 1988). The hydrogeologic characteristics of these aquifers are largely controlled by the structure and development of the conduit network, which generally produces short-circuit surface drainage providing alternative subsurface flow paths that have lower hydraulic gradients and resistance (White, 1999). The heterogeneous distribution of permeability within the karst aquifer and the limited attenuation processes make them more vulnerable to pollution than porous aquifer. Due to their vulnerability, the exploitation of groundwater from karst aquifers requires special strategies for protection and management (Bakalowicz, 2005).

The Pertuso karst spring is located in the Upper Valley of Aniene River (Central Italy) westward of Filettino (FR), at an elevation of about 700 m a.s.l.. Until now, it has been one of the largest fresh water springs in Latium Region. The study area is located in the upper part of Aniene River basin, between the town of Filettino and Trevi nel Lazio (FR) and outcrops from an important karst aquifer, mainly made of dolomitic limestones and dolomites of Cretaceous age. The northern part of this basin, belonging to the Regional Park of Simbruini Mountains, the largest protected area of Latium Region, has a remarkable environmental value and belongs to Nature 2000 network as Special Protection Areas (SPAs) (Habitats Directive 92/43/CEE). The proposed environmental monitoring plan will provide water quantity and quality data useful for monitoring activities and impacts associated with the catchment project of the Pertuso spring, and will contribute useful information to (i) monitor water quantity and quality; (ii) set up monitoring methodology and identify monitoring parameters; (iii) identify any adverse environmental impact, and (iv) design the performance and effectiveness of mitigation measures proposed.

This paper presents an overview of the Environmental Monitoring Plan that will be used for the hydrogeologic investigation and characterization of the karst aquifer feeding the Pertuso spring.

Geological and hydrogeological setting

The study area is located along the SW boundary of the Simbruini Mountains, characterized by the confluence of the Fiumata Valley and the Granara Valley from which starts the Valley of Aniene River (Cipollari et al., 1995). The Pertuso spring is sited about 1 km down from the confluence of these valleys. An important carbonate karst aquifer mainly made of dolomitic limestone and dolomites of Cretaceous age outcrops in this area (Fig. 1). On the top, there are Quaternary fluvial and alluvial deposits, downward pudding and Miocene clay and shale, while the bottom of the series consists of Upper Cretaceous carbonates, made from alternating layers of granular limestone and dolomites (Ventriglia, 1990).

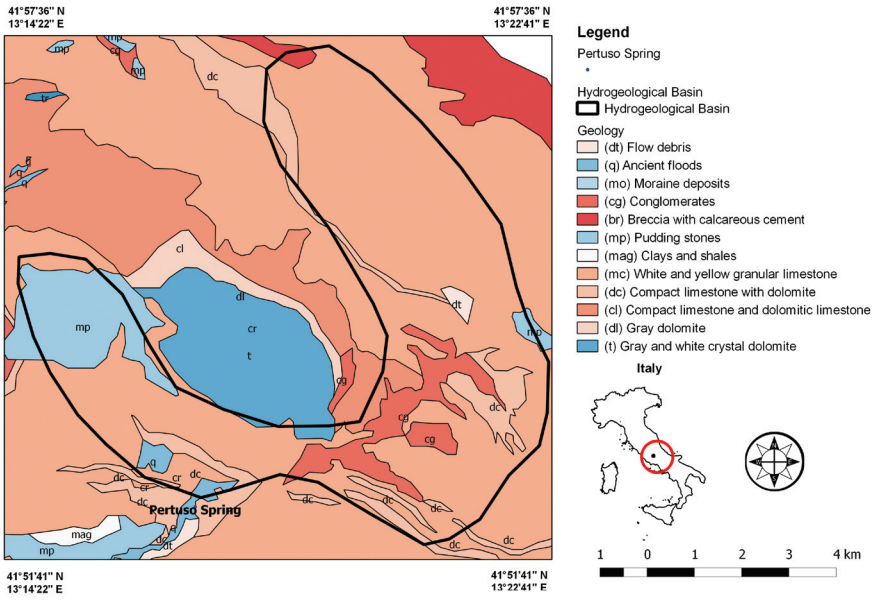

Fig. 1 - Simplified geological map of the study area.

Fig. 1 - Carta geologica semplificata dell'area di studio.

DOI 10.7343/AS-073-14-0099

This area is mostly made of highly permeable Cretaceous carbonate rocks, deeply fractured and mostly soluble. Due to weathering, distinctive surface and underground karst formations are developed in this area at small and large scales. The most important karst landforms are rutted fields, karren, sinkholes and swallow holes. The karst surface is very permeable and enables the rapid infiltration of rainfall into the underground system, where the carbonate dissolution makes cavities (Accordi and Carbone, 1988; Bosellini, 1989; Damiani, 1990). Dissolution conduits strongly influence groundwater flow and evolve into complex networks, often crossing several kilometres throughout the limestone matrix.

The Pertuso spring is located in the dolomite outcrop upstream the town of Trevi nel Lazio and flows into the Aniene River, close to the boundary of the carbonate hydrogeological system (Ventriglia, 1990).

The Pertuso karst spring is the natural outcrop of groundwater discharging from these conduits and it comes out when this aquifer made of this high enhanced karst network, matches topographic surface (Fig. 2).

The Pertuso spring discharges groundwater coming from an about 50 km^2 karstified Cretaceous calcareous rock area. In the Upper Valley of Aniene River the total average annual discharge amounted to about 3800 l/s of which up to 1400 l/s are referred to the Pertuso spring (Acea ATO 2 S.p.A., 2005). The discharge at this karst spring is usually rapid and displays pronounced peaks following recharge events. Unfortunately they are not available data referred to groundwater discharge more than ones represented in Fig. 3.

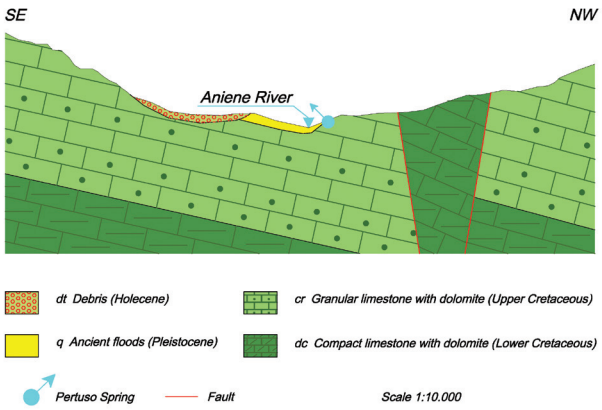

Fig. 2 - Geological cross section of the Pertuso spring.

Fig. 2 - Sezione geologica della sorgente Pertuso.

The catchment project of the Pertuso spring

On 28 June 2002, a Legislative Decree of the President of the Council of Ministers has established the drought emergency state of the municipalities in the south part of Roma district. For this reason, the Pertuso spring, currently feeding the Comunacqua hydroelectric power plant, owned by ENEL group, since 2002 also supplies the Simbrivio water supply network, for a maximum of 360 l/s, in addition to the volumes not available from Simbrivio historical springs. In order to reduce costs and make this spring independent from the plant owned by ENEL group, in the program of actions to resolve the state of drought emergency was included a catchment work project of the Pertuso spring for a maximum of

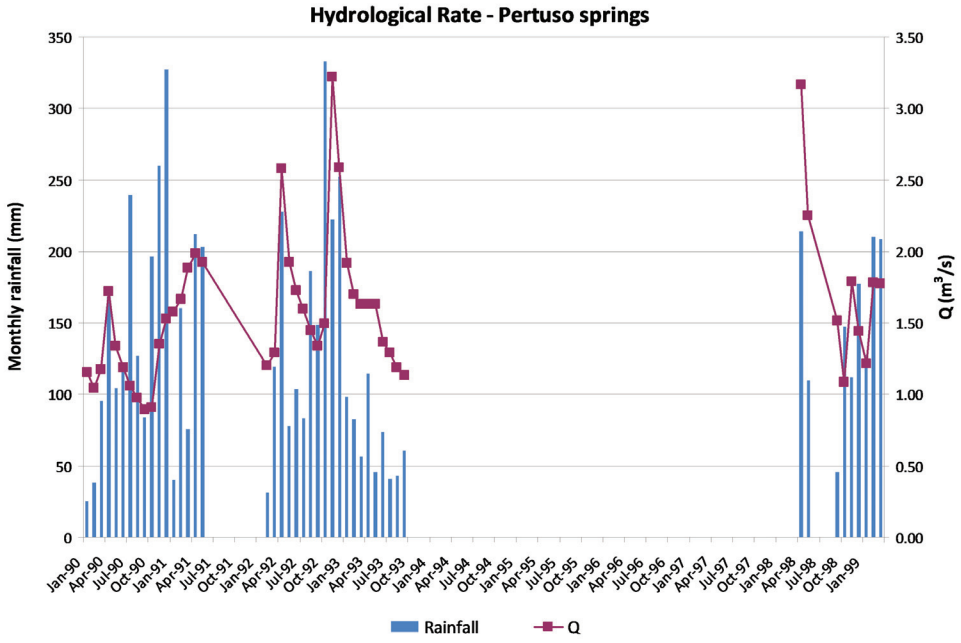

Fig. 3 - Hydrological rate of Pertuso spring in the 1990 - 1999 period (Filettino meteorological station).

Fig. 3 - Regime idrologico della sorgente Pertuso relativo al periodo 1990 – 1999 (stazione meteorologica di Filettino).

DOI 10.7343/AS-073-14-0099

360 l/s. The design of the exploitation project includes a first section from Pertuso Dam to Sosiglio Bridge, characterized by the excavation with TBM of a tunnel across Druni Hill (Construction site 1), and a second one, from Sosiglio Bridge to Cervinara Stream (Fig. 4), in open excavation, till the intersection with the existing water pipe which leads to the Ceraso hydroelectric power plant (Construction site 2). The primary aim of the Environmental Monitoring Plan is to ensure hydrogeological data about (i) temporal and spatial variations in groundwater and surface water levels, (ii) temporal and spatial variations in groundwater and surface water quantity and quality and (iii) impacts due to the drainage of groundwater through the Druni Hill tunnel and the interaction with surface water linked with groundwater. Thus, according to the Legislative Decree 152/2006, as modified by DM 260/2010, the Environmental Monitoring Plan suggested to characterize the major environmental components (i.e. surface water and groundwater) of the Upper Valley of Aniene River for the evaluation of the environmental parameters during survey, excavation and post-excavation phase of the project. For this reason a long-term water quantity and quality monitoring has been established in the study area.

Environmental Monitoring Regulatory Requirements

The European Union, by Water Framework Directive 2000/60/EC, identified the need to create a legal framework for sustainability and protection of all waters (surface water, groundwater, inland waters, transitional waters and coastal waters) and sets out specific objectives that must be achieved by specified dates. The Water Framework Directive aims to prevent further deterioration, protect and enhance all water resources and sustain the natural ecosystems that depend on them. The main purpose is the achievement of good status for all water bodies by 2015; and if this is not possible, aim to achieve good status by 2021 or 2027. Good status means good ecological status for surface waters up to one nautical mile from the coast; good chemical status for all territorial waters, good chemical and good quantitative status for groundwater and good ecological potential for heavily modified water bodies. Italian law system (i.e. D.M. 260/2010), in agreement with Water Framework Directive, establishes an Environmental Monitoring Plan both for protection and sustainability purposes of water resources. The Ministerial Decree D.M. 260/2010 identifies three categories of monitoring in the following: (i) Supervisory monitoring, to define the hydrogeological conceptual model of the aquifer; (ii) Operating monitoring, to measure the potential impact that could result from project operations; (iii) Survey monitoring, to assess the effectiveness of remedial measures. Through supervisory activities will be carried on the environment characterization of the study area, including the definition of spatial and temporal trends in measured parameters. This monitoring is useful to establish the baseline values for environmental quality and quantity indicators so that long-term changes can be evaluated. The operating monitoring allows the existing physical and chemical characterization, the evaluation of the environmental parameters and the examination of the potential contamination sources due to the catchment project. The monitoring plan aims to assess the status of water bodies, to check whether the environmental targets are being effectively

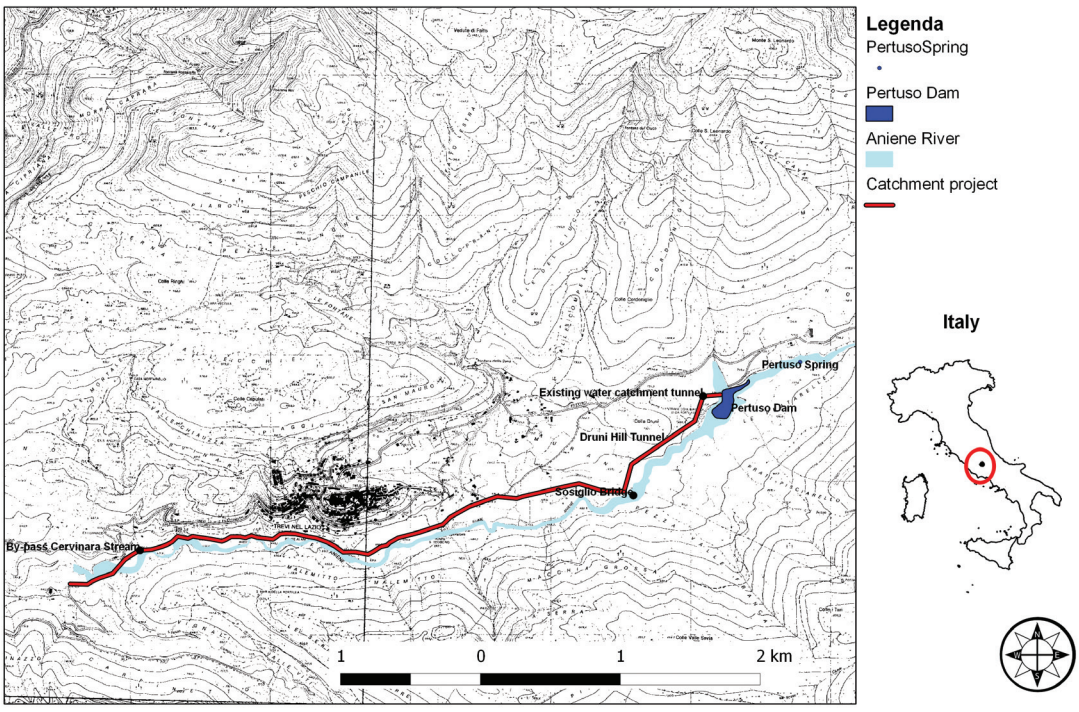

Fig. 4 - Design of the exploitation project of Pertuso spring.
Fig. 4 - Progetto di consolidamento della sorgente Pertuso.

DOI 10.7343/AS-073-14-0099

achieved. This approach was needed to identify the environmental status of groundwater and surface water and to localize where management action is required to achieve the purposes of the Water Framework Directive. The Environmental Monitoring Plan integrates water policy bringing together, within its framework, the actions that are required by all EU and national water legislation.

Water monitoring network design

In the study area a monitoring network has been set up to assess the karst aquifer – Aniene River hydrodynamics properties. The recommendation for monitoring in karst aquifer is to focus on the sensitive connections between surface water and groundwater. The monitoring points should be representative of the hydrogeological conceptual model, with regard to groundwater flow and its interaction with surface water.

The monitoring network will be used to provide baseline hydrogeological conditions and temporal changes in groundwater and surface water conditions prior to project development. The network will also be monitored in the long term (i.e. before, during and after construction activities) to provide ongoing measurement of quality and quantity, including temporal and seasonal changes. In addition, to providing baseline information, the results from the monitoring plan will provide a reference to measure any environmental impacts that could occur. Long-term water monitoring will be conducted at several monitoring stations, chosen according to the importance and the significance of the each environmental component, subjecting to identify the conditions for accessibility.

For the purpose of this study, the monitoring network is based on in situ gauge stations shown in Fig. 5, located along the proposed catchment project.

Four stations are located along a 2 km long Aniene River main stream (SW_01, SW_02, SW_03 and SW_04), referred each one to the two construction sites, as SW_01 and SW_03 are the monitoring stations, designed to control environmental conditions upstream each construction site, while SW_02 and SW_04 are designed to control the same conditions downstream each of them, along the Aniene River main stream.

The groundwater monitoring network includes three existing piezometers (GW_02, GW_03 and GW_04). The Aniene River basin is characterized by a complex network of catching and reservoirs, which doesn't allow a good evaluation of the average annual recharge of this system (Sappa and Ferranti, 2013). Thus, to assess quantitative and quality alterations of the karst aquifer feeding the Pertuso spring, an additional groundwater monitoring station (GW_01) will be installed in the spring to evaluate the undisturbed conditions upstream the karst aquifer. GW_02 monitoring stations were chosen as representative of aquifer conditions downstream the construction of Druni Hill tunnel, while GW_03 and GW_04 are site respectively upstream and downstream the second construction site, in order to monitor groundwater quantity and quality.

Each of the monitoring stations will be identified with a set of Global Positioning System (GPS) coordinates (Table 1).

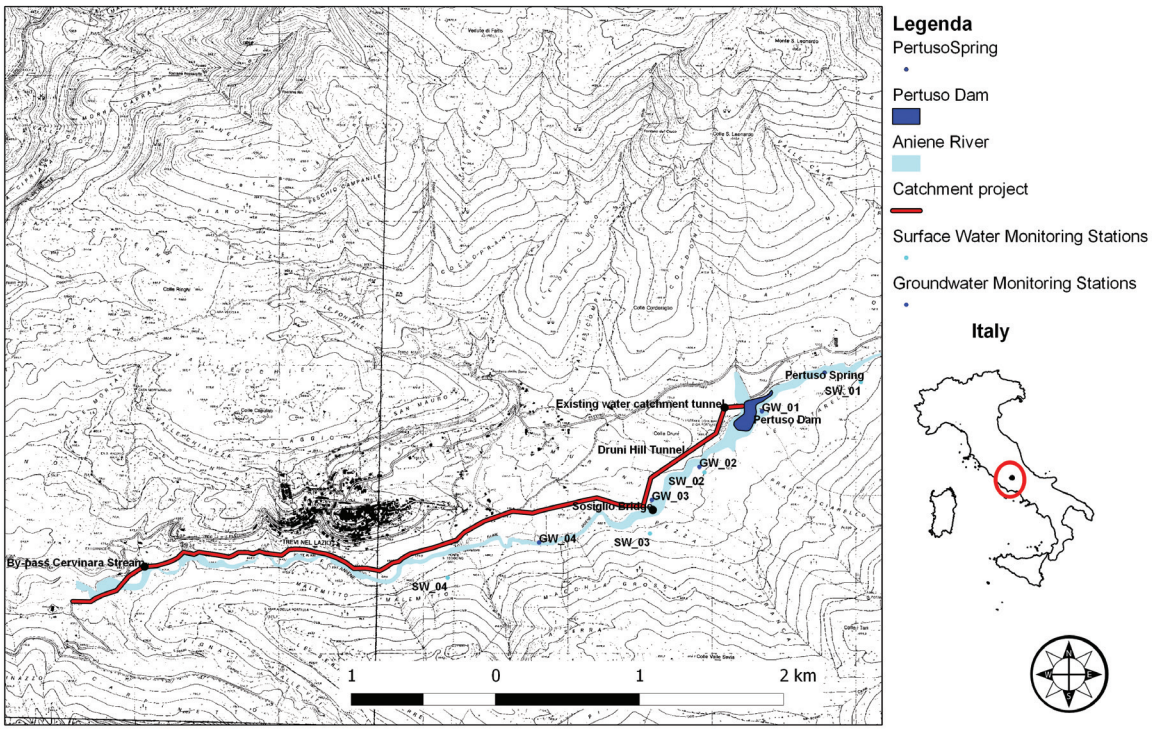

Fig. 5 - Location of monitoring stations (SW: surface water; GW: groundwater).

Fig. 5 - Localizzazione delle stazioni di monitoraggio (SW: acque superficiali; GW: acque sotterranee).

DOI 10.7343/AS-073-14-0099

Tab. 1 - Main characteristic of the monitoring stations.

Tab. 1 - Caratteristiche principali delle stazioni di monitoraggio.

	Monitoring Station	N (m)	E (m)	Location
Groundwater	Pertuso spring	4637128.87	357846.31	Spring (Upstream 1° construction site)
	GW_01	4636860.56	357411.6	Piezometer (Upstream 1° construction site)
	GW 02	4636474.9	356977.6	Piezometer (Downstream 1° construction site)
	GW_03	4636246.5	356647.9	Piezometer (Upstream 2° construction site)
	GW_04	4635951.2	355865.5	Piezometer (Downstream 2° construction site)
Surface water (Aniene River)	SW_01	4637064.68	358097.8	Upstream 1° construction site
	SW_02	4636437.2	357012.9	Downstream 1° construction site
	SW_04	4636013.5	356634.9	Upstream 2° construction site
	SW_03	4635706.8	355230.9	Downstream 2° construction site

Methodology

Because of the interconnection between matrix, fractures, and conduits network, karst aquifers are extremely heterogeneous and have hydraulic and chemical properties that are highly scale dependent and temporally variable (Toran et al., 2007). For this reason, the Environmental Monitoring Plan involves collecting samples of surface water and groundwater for quantitative and quality characterization of the karst aquifer feeding the Pertuso spring.

The Environmental Monitoring target is to set up the environmental state and quantitative and quality analysis of temporal water trends for the evaluation of potential interactions between project design and karst aquifer. The aim of this monitoring plan is to build a background framework on the hydromorphological, physico-chemical and biological properties of groundwater and surface water resources in the aim to prevent and evaluate any potential environmental effect coming from the construction activities.

Samples of surface water and groundwater for major dissolved species and trace elements will be collected using standard techniques (Brown et al., 1970; Wood, 1976) that include field filtration using a 0.45 µm membrane filter for major ions and trace elements. Laboratory analysis will be carried on by a certified water testing laboratory for chemical-physical, organic, inorganic, and microbiological parameters, following DLgs. 152/06 prescriptions (Tab. 2). Properties such as temperature, electrical conductivity, pH, dissolved-oxygen, oxidation-reduction potential, static water level and stream flow can be measured directly in the field before the water sample collection. The choice of measures equipment depends on several factors including the accuracy of measurement required and the type and accessibility of well (monitoring or water supply).

All field instruments will be calibrated according to manufacturer's recommendations prior, to be taken into the field. Calibration standards will be selected based on historic data for best instrument accuracy.

Surface Water Monitoring

Stream discharge and water quality parameters such as turbidity, dissolved oxygen, water temperature and electric conductivity monitoring is important to have a referring trend, along the year, of these values range and to be ready to evaluate potential modifications due to construction activities.

Stream discharge will be indirectly estimated by the calculation of discharge from the in situ measured data set. Seasonal measurements of Aniene River water stream, along with periodical measurements of cross-sectional area, water surface width, flow velocity, bed channel depth will be started on August 2014. These measurements will be made with conventional measurements methods such as reels current meter method for discharge. Thus, the Aniene River flow will be measured using a current-meter (SEBA F1 - Seba Hydrometrie) which, combined with SEBA Z6 pulse counter, allows to measure velocity between 0,025 m/s and 10 m/s.

The current U.S. Geological Survey (USGS) procedure for gagging discharge in rivers is to measure stage and then to calculate discharge from an empirically generated stage discharge relation (rating curve) (Chow, 1964 and Rantz, 1982). In natural river systems a common approach is to build the stage–discharge relationship with the help of several segments only valid for a given range of stages. For this reason, flow measurements will be collected at a number of equally spaced verticals (N), inside the river cross section, at multiple depths at each monitored vertical. The rating-curve will be regarded as a relation fitted to N points (h_i, Q_i), i=1,2,…,N, the measured stage hi and corresponding measured discharge Q_i recorded on N occasions.

Groundwater Monitoring

The groundwater monitoring network is made on the first by the GW_01 station (Pertuso spring), where will be placed a multiparameter probe, connected to a data logger to collect daily time series of temperature, electrical conductivity, pH, dissolved-oxygen, oxidation-reduction potential and water

DOI 10.7343/AS-073-14-0099

Tab. 2 - Water Quality Monitoring Parameters.
Tab. 2 - Parametri oggetto del monitoraggio.

Tipology	Parameter	Unit	Surface water	Groundwater
In Situ Parameters	Water Temperature	°C	x	x
	Dissolved Oxygen	mg/l	x	x
	Conductivity	µS/cm	x	x
	pH	-	x	x
	Flow	m^3/s	x	x
Laboratory Parameters	Turbidity (Residue At 105 ° C And 550 ° C)	(mg/l)		x
	Total Suspended Solids	mg/l	x	
	Total Hardness	mg/l $CaCO_3$	x	x
	Bicarbonates (Temporary Hardness)	(mg/l)		x
	Bicarbonate Alkalinity	(mg/l)		x
	Carbonate Alkalinity	(mg/l)		x
	Bicarbonate Ion	(mg/l)		x
	Total Nitrogen	N µg/l	x	
	Ammonia Nitrogen	N µg/l	x	x
	Nitrate Nitrogen	N µg/l	x	x
	Nitrous Oxide	µg/		x
	BOD5	O_2 mg/l	x	
	COD	O_2 mg/l	x	
	Orthophosphate	P µg/l	x	
	Total Phosphorus	P µg/l	x	x
	Chloride	Cl^- µg/l	x	x
	Nonionic Surfactants	µg/l		x
	Anionic Surfactants	µg/l		x
	Color	µg/l		x
	Odor	µg/l		x
	Sodium	µg/l		x
	Calcium	µg/l		x
	Potassium	µg/l		x
	Magnesium	µg/l		x
	Sulphates	SO_4^{2-} µg/l	x	x
	Boron	µg/l		x
	Free Cyanide (	µg/l		x
	Fluorides	µg/l		x
Metals	Cadmium	µg/l	x	x
	Total Chromium	µg/l	x	x
	Chromium Vi	µg/l		x
	Mercury	µg/l	x	x
	Nickel	µg/l	x	x
	Lead	µg/l	x	x
	Copper	µg/l	x	x
	Zinc	µg/l	x	x
	Aluminum	µg/l		x
	Antimony	µg/l		x
	Silver	µg/l		x
	Arsenic	µg/l		x
	Beryllium	µg/l		x
	Cobalt	µg/l		x
	Iron	µg/l		x
	Selenium	µg/l		x
	Manganese	µg/l		x

DOI 10.7343/AS-073-14-0099

belows Tab. 2 - Water Quality Monitoring Parameters.
segue Tab. 2 - Parametri oggetto del monitoraggio.

Tipology	Parameter	Unit	Surface water	Groundwater
Organic Compounds	Aldrin	µg/l	x	
	Dieldrin	µg/l	x	
	Endrin	µg/l	x	
	Isodrin	µg/l	x	
	DDT	µg/l	x	
	Benzene	µg/l		x
	Ethylbenzene	µg/l		x
	Styrene	µg/l		x
	Toluene	µg/l		x
	Para-Xylene	µg/l		x
	Hexachlorobenzene	µg/l	x	
	Hexachlorocyclohexane	µg/l	x	
	Hexachlorobutadiene	µg/l	x	
	1,2-Dichloroethane	µg/l	x	
	Trichloroethylene	µg/l	x	
	Trichlorobenzene	µg/l	x	
	Chloroform	µg/l	x	
	Carbon Tetrachloride	µg/l	x	
	Perchloroethylene	µg/l	x	
	Pentachlorophenol	µg/l	x	
	Hydrocarbons C> 12	µg/l		x
	Hydrocarbons C <12	µg/l		x
	Total Hydrocarbons	µg/l		x
	BTEX Hydrocarbons	µg/l		x
	Methyl Tert-Butyl Ether MTBE	µg/l		x
	Total Polycyclic Aromatic Hydrocarbons	µg/l		x
Microbiological Parameters	Escherichia Coli	UFC/100 ml	x	x

level, starting from September 2014, till one year after construction activities end. All these data will be sent daily to a PC station, to control every day groundwater spring properties, and they will be display on a website.

Spring discharge will be indirectly evaluated, at the Aniene River cross – section shown in Figure 6, by the calculation of discharge from the in situ water level data set, in order to evaluate the contribution of the Pertuso spring to Aniene River flow.

Seasonal sampling will be carried out on August 2014 and groundwater samples will be taken directly from each monitoring stations (boreholes and spring). Boreholes are GW_02, GW_03 and GW_04, placed, respectively, downstream of the first construction area, GW_02, upstream and downstream of the second construction area, GW_03 and GW_04.

The target of groundwater sampling is to have a water sample that represents the groundwater properties, in the area under study, in any season, as a reference database to relate the results of analysis carried on during construction activities. To obtain a representative sample it is necessary to remove the stagnant water from the well before a sample is taken. Before collecting a groundwater sample, the boreholes will be purged to remove any stagnant water in it and to ensure that the water sample is representative of the aquifer being sampled: so, a minimum of three to five well volumes of water will be purged.

Purging must continue until temperature, electric conductivity, and pH level readings stabilize. The readings will be taken and logged every few minutes and recorded in a field log book together with the pumping method and the volume of water pumped.

The water level will be measured using a probe attached to a permanently marked polyethylene tape, fitted on a reel. The probe detects the presence of a conductive liquid between its two electrodes, when contact is made with water; the circuit is closed, sending a sound back to the reel. The water level is then determined by taking a reading directly from the tape, at the top of the well. Some physico-chemical parameters cannot be reliably measured in the laboratory as their characteristics change over a very short time scale. Parameters that will be measured in the field include pH, electrical conductivity, temperature, dissolved oxygen and redox potential. The field parameters will be reliably measured using a multiparameter probe—usually with an electrode for each parameter.

Sampling frequency

The sampling frequency depends on the monitoring purposes, established by the Environmental Monitoring Plan (DM 260/2010). However, for surface water a more detailed sampling frequency is required for supervisory and operating monitoring, while a low sampling frequency (1/year) could be enough for survey monitoring, if any trouble would have

DOI 10.7343/AS-073-14-0099

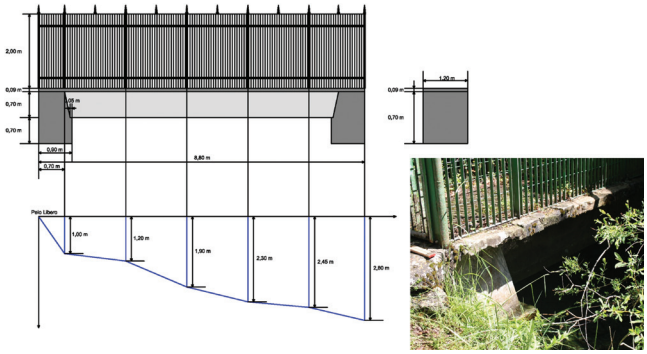

Fig. 6 - Detail of the Pertuso spring monitoring station (GW_01).

Fig. 6 - Particolare della stazione di monitoraggio in corrispondenza della sorgente Pertuso (GW_01).

come out during previous monitoring phases. The groundwater frequency sampling is related to the aim of set up the hydrogeological conceptual model of the karst aquifer. Thus, groundwater will be monitored monthly (12/year), in the whole monitoring network, for supervisory and operating monitoring, to assess seasonal and natural groundwater fluctuations, while annual sampling (1/year) will be carried out for survey monitoring. Water measurements at the Pertuso long-term monitoring station (GW_01) will be collected one time daily.

The Environmental Monitoring Plan will be reviewed annually, according to the monitoring results and ongoing of the catchment project of the Pertuso spring. The review of the monitoring plan will upgrade the potential environmental impacts and will adapt the monitoring to the updated risk rating. It will evaluate the effectiveness of each monitoring station, to assess where new locations and modifications to the monitoring network may be needed, and evaluate any impacts that may be occurring. An additional monitoring plan will be considered in case of a sensitive environmental accident. The annual review of the monitoring plan, including analysis of results, will be submitted to the authorities for review.

Conclusions

This study presented the Environmental Monitoring Plan of groundwater and surface water in the Upper Valley of Aniene River, in southern part of Latium Region. The purpose of this work is to outline the key monitoring requirements to control the environmental performance of the catchment project of the Pertuso spring. The Environmental Monitoring Plan is a formal and approved document for project execution management. The plan set up the monitoring methodology and the actions needed to evaluate the potential environmental impacts, due to the catchment works. The Environmental Monitoring Plan will be updated elaborated by updates, throughout the project ongoing with the purpose to support the implementation of environmental remediation works as part of the project.

The Environmental Monitoring Plan, combined with the implementation of measures designed to reduce the potential adverse effects of the proposed project on the karst aquifer feeding the Pertuso spring, is crucial to evaluate the environmental sustainability of the catchment project. The monitoring plan provides that, in the event of environmental impact, construction activities will stop and remediation measures will restore the environment status of the hydrogeological system.

References

Accordi G., Carbone F. (1988). Carta delle litofacies del Lazio-Abruzzo ed aree limitrofe "Map of the lithofacies of Lazio-Abruzzo region and neighboring areas". Quaderni de "La ricerca scientifica" n. 114 vol. 5, CNR Edizioni, Roma.

Acea ATO 2 S.p.A. (2005). Studio idrogeologico – Proposta di aree di salvaguardia della sorgente del Pertuso "Hydrogeological study - Proposal for protection areas of the Pertuso spring"

Bakalowicz, M. (2005). Karst groundwater: a challenge for new resources. Hydrogeology Journal 13: 148–160.

Brown E., Skougstad M.W., Fishman M.J. (1970). Methods for collection and analysis of water samples for dissolved minerals and gases, laboratory analysis. U.S. Geological Survey Techniques of Water Resources Investigations, Book 5, Chap. C1.

Bosellini A. (1989). Dynamics of Tethyan carbonate platforms. In Controls on Carbonate platform and basin development (eds Crevello P. D., Wilson J. L., Sarg J. F. & Read J. F.), SEPM (Society for Sedimentary Geology), Special Publication 44, 3-13.

Chow V.T. (1964). Handbook of Applied Hydrology. McGraw-Hill, New York, NY, 1964.

Cipollari F., Cosentino D., Parotto M. (1995). Modello cinematico-strutturale dell'Italia centrale "Structural-kinematic model of Central Italy". Studi Geol. Camerti, 2: 135-143

Damiani A. V. (1990). Studi sulla piattaforma carbonatica laziale-abruzzese. Nota I. Considerazioni e problematiche sull'assetto tettonico e sulla paleogeologia dei Monti Simbruini, Roma "Studies on the carbonate platform of Lazio-Abruzzo region. Note I. Considerations and problems on the tectonic and paleontology of Simbruini Mountains, Rome" In: Memorie descrittive Carta Geologica d'Italia vol. 38: 177-206.

Foster S., Hirata R., Andreo B. (2013). The aquifer pollution vulnerability concept: aid or impediment in promoting groundwater protection? Hydrogeology Journal, Springer, 21(7): 1389-1392.

Rantz S.E., et al. (1982). Measurement and computation of streamflow. Volume 1: Measurement of stage and discharge. Volume 2: Computation of discharge. U.S. Geological Survey Water Supply Paper 2175.

Sappa G., Ferranti F., 2013. Water resources exploitation in the Upper Valley of Aniene River. L'Acqua, 2:59-68.

Sappa G., Ergul S., Ferranti F. 2013. Water Quality Assessment Of Carbonate Aquifers In Southern Latium Region, Central Italy: A Case Study For Irrigation And Drinking Purposes. Applied Water Science, Springer, 14.

Toran L., Herman E.K., White W.B. (2007). Comparison of flow paths to a well and spring in a karst aquifer. Ground Water 45, 281-287

Ventriglia U. (1990). Idrogeologia della Provincia di Roma, IV, Regione orientale "Hydrogeology of the Province of Rome, IV, Eastern Region". Amministrazione Provinciale di Roma, Assessorato LL.PP, Viabilità e trasporti, Roma.

White W.B. (1988). Geomorphology and hydrology of karst terrains: New York, Oxford University Press, 464p.

White W.B. (1993). Analysis of karst aquifers, in Alley W.M., ed. Regional ground-water quality: New York, Van Nostrand Reinhold, p. 471–489.

White W.B. (1999). Conceptual models for karstic aquifers,in Palmer A.N., Palmer M.V., and Sasowsky I.D., eds. Karst modeling: Leesburg, Va., Karst Waters Institute Special Publication 5, 11–16.

Wood W.W. (1976). Guidelines for collection and field analysis of groundwater samples for selected unstable constituents. U.S. Geological Survey Techniques of Water Resources Investigations, Book 1, Chap. D2.

Vulnerability Assessment of Mazzoccolo Spring Aquifer (Central Italy), Combined with Geo-Chemical and Isotope Modeling

Giuseppe Sappa, Sibel Ergul, and Flavia Ferranti

Abstract

The present study deals with the characterization of Mazzoccolo karst spring which feeds the most important water supply network in southern part of Latium region, in Central Italy. During sample collections from 2006 to 2008, a series of in situ measurements were conducted for pH, electrical conductivity (EC), total dissolved solids (TDS) and temperature. The environmental isotopic and hydrochemical measurements were carried out for the vulnerability assessment and geochemical modeling with the aim of achieving (i) proper management and protection of this important resource, (ii) hydrochemical processes controlling the evolution of groundwater and (iii) identification of recharge areas. All sampled spring waters are characterized as Ca-HCO_3 type waters reflecting the main rock types in the area investigated, where limestones and Pliocene conglomerates are the most dominant formations. The electrical conductivity (EC) and TDS values of water samples from springs varies from with a maximum value of 341 μS/cm and 268 mg/l and minimum value of 28 μS/cm and 104 mg/l, respectively. The pH values of spring samples range from 7.4 to 9 indicating alkaline nature. The anion composition is quite stable showing $HCO_3^->Cl^->SO_4^{2-}$ (in mg/l), while calcium is the dominant cation, followed by magnesium, sodium and potassium. The comparison of $\delta^{18}O$ and δ^2H values of spring water samples with meteoric water lines shows that most of the samples fall to the Local Meteoric Water Line suggesting input to local rain-fall derives from the Mediterranean Sea. The elevation of the recharge areas range between 600 and 800 m a.s.l confirming the Aurunci karst aquifer is feeding Mazzoccolo spring.

Keywords

Karst aquifer • Vulnerability • Major ions and stable isotopes

265.1 Introduction

Due to increasing population pressure and climate change, groundwater resource need an optimization in their exploitation and management. Hydrochemical analysis and isotope studies are recognized as valuable hydrogeologic tools for determining the evolution of water resources and determination of recharge areas which influences the quality of water and vulnerability of the aquifer systems (Clark and Fritz 1999). The application of isotope-based methods and conventional hydrogeochemical studies has become an integral part of many water quality and environmental studies (Marfia et al. 2003; Long and Putnam 2004). This understanding can contribute to effective management, utilization and protection of these natural resources (Casa et al. 2008). In southern Latium region of Central Italy, spring and groundwater from karst aquifers play an important role for drinking and agricultural uses (Sappa et al. 2012). In this

G. Sappa (✉) · S. Ergul · F. Ferranti
DICEA, Department of Civil, Building and Environmental Engineering—Sapienza, University of Rome, Via Eudossiana 18, 00186, Rome, Italy
e-mail: giuseppe.sappa@uniroma1.it

G. Lollino et al. (eds.), *Engineering Geology for Society and Territory – Volume 5*,
DOI: 10.1007/978-3-319-09048-1_265,

region, Mazzoccolo is the most important fragile karst spring that feeds drinking water supply networks of Formia and other communities with an average withdrawal of 900 l/s. This study examines the relationship between water composition, hydrochemical processes, and water vulnerability assessment of this karst spring.

265.2 Geological and Hydrogeological Setting

Mazzoccolo spring take place on the base of Pliocene conglomerates, which is tectonically in contact with the limestones. This spring is located at an altitude of 11.5 m above sea level where the area fractured due to the intersection of numerous faults. Mazzoccolo spring is captured at an elevation of 7.50 m by a drainage tunnel, where the path is generally parallel to the slope (Fig. 265.1).

The morphological setting of the study area is characterized by conglomeratic limestone on the hills (Mola Mountain), surrounded by clayey-arenaceous and alluvial deposits of debris. The abundance of water is due to the permeability of the limestone (high fractured and deep karst), which stores a significant quantity of rainwater feeding perennial springs. The Pliocene conglomerates are strongly cemented, while the contacts with different formations show highly fractured structures. The karstified limestones stored groundwater, which outcrops mostly at Mazzoccolo spring and also some smaller pools, that occur to the west part. The underground reservoir of Mazzoccolo spring was formed by high permeable limestones to the N-W and N-NW of the spring, while the bottom is composed of impermeable dolomites underlying the West part of the limestones.

265.3 Methodology

The main spring water sampling survey was carried out in Mazzoccolo spring, from 2006 to 2008. Water temperature, electrical conductivity and pH values were determined in the field using PC 300 Waterproof Hand-held meter. Bicarbonate content was measured by titration with 0.1 N HCl. Water samples were filtered through cellulose filters (0.45 µm), and

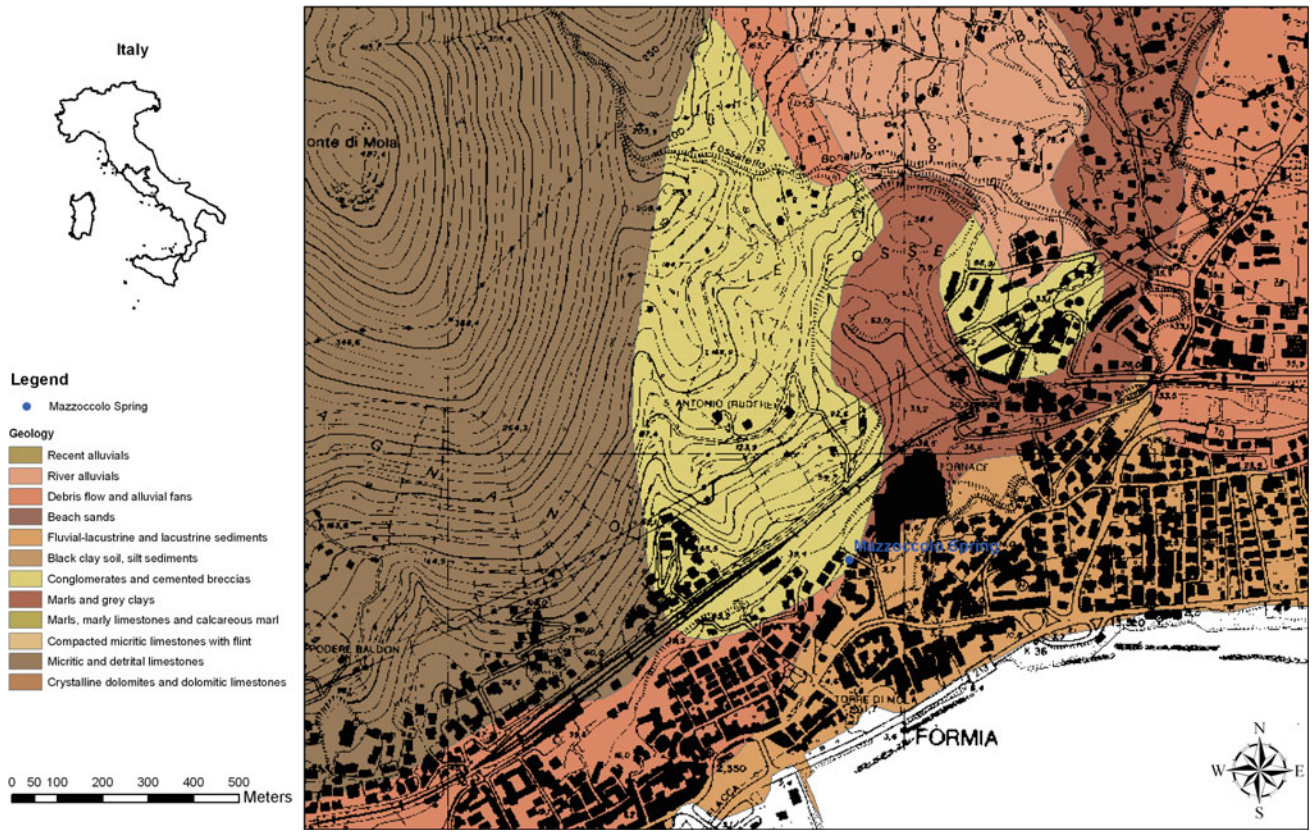

Fig. 265.1 Simplified geological map of the study area

their major and minor constituents were determined by a Metrohm 761 Compact IC ion chromatograph (replicability ± 2 %). Analyses of $^{2}H/H$ isotopes used the method of Kendall and Coplen (1985) (reaction with Zn at 450 C), while $^{18}O/^{16}O$ analyses relied on the CO_2—water equilibration technique (Kendall and Coplen 1985). Mass spectrometry was performed with a Finnigan Delta Plus mass spectrometer and the results are reported in ‰ units (permil deviation of the isotope ratio from the V-SMOW isotopic standard). δ is defined by the relationship:

$$\delta = [(R - R_{SMOW})/R_{SMOW}] \cdot 10^3 \quad (265.1)$$

where R = D/H or $^{18}O/^{16}O$. For the identification of water types, the chemical analysis data of the spring water samples have been plotted on the Piper diagram using Geochemistry Software AqQA. The vulnerability analyses were carried out by SINTACS method.

265.4 Results and Conclusions

Major ion concentrations and physico—chemical characteristics of the analyzed spring and well water samples are presented in Table 265.1. The temperature of springs range from 10 to 15 °C. The pH of these springs ranges from 7.4 to 9 highlighting alkaline nature. The total dissolved solids (TDS) content within the range 104–269 mg/l. Calcium and bicarbonate is the dominant constituents in spring samples, followed by magnesium, chloride, sodium, sulphate and potassium. The electrical conductivity (EC) value varies from 28 to 341 µS/cm.

Based on the dominance of major cationic and anionic species, Ca-HCO_3 water type was identified (Fig. 265.2), suggesting that all groundwater feeding Mazzoccolo spring come from the karst limestone aquifer. The isotopic composition (^{18}O and ^{2}H) and the calculated elevations for recharge areas of springs, recorded in different periods, are presented in Table 265.2.

For the identification of mean recharge elevations, the altitude effect has been employed. The mean isotope gradients for ^{18}O and ^{2}H were calculated using the isotope and elevation values of precipitation, obtained from the four sampling pluviometers near study area The altitude effect is found by the relation between precipitation isotope values and elevation in meters (h) highlighting a depletion of heavy stable isotopes of about –0.22 and –1.55‰ per 100 m elevation for $\delta^{18}O$ and $\delta^{2}H$, respectively. The elevation of the recharge area range between 600 and 800 m a.s.l. (Fig. 265.3).

Table 265.1 Main physico-chemical characteristics and chemical composition of spring samples

Sample codes	Date (dd/mm/yy)	EC (µS/cm)	pH	T (° C)	Ca^{2+} (meq/l)	Mg^{2+} (meq/l)	Na^{+} (meq/l)	K^{+} (meq/l)	Cl^{-} (meq/l)	SO_4^{2-} (meq/l)	HCO_3^{-} (meq/l)
M1	11/05/06	122	8.12	15	23.539	3.230	1.702	0	2.512	1.509	85.428
M2	15/06/06	336	7.84	13	49.252	9.374	4.519	0.44	7.436	3.990	183.06
M3	13/07/06	335	7.78	15	35.221	9.499	4.580	0.445	7.435	3.816	146.448
M4	04/08/06	28	9.03	14	25.440	0.636	0.356	0.007	0.5	0.299	76.275
M5	21/09/06	155	7.91	12	20.848	8.932	4.030	0.209	6.549	2.572	100.683
M6	27/10/06	65	8.1	11	23.673	3.810	1.712	0.210	2.505	1.099	88.479
M7	28/11/06	328	7.75	10	27.492	9.592	4.372	0.474	7.048	3.709	122.04
M8	21/12/06	323	8.04	13	47.725	9.477	4.274	0.463	6.920	3.779	183.06
M9	16/01/07	324	8.08	13	47.477	9.534	4.283	0.468	7.007	3.589	183.06
M10	27/02/07	330	7.57	13	51.866	7.702	4.562	0.41	6.640	4.628	186.111
M11	24/04/07	333	7.65	11	51.522	8.648	4.520	0.414	6.859	4.423	189.162
M12	05/06/07	327	7.62	12	51.325	9.081	4.526	0.402	6.867	4.455	189.162
M13	10/07/07	327	7.42	10	50.370	9.250	4.376	0.471	6.947	4.074	189.162
M14	26/09/07	326	7.65	14	48.54	9.637	4.360	0.442	6.692	4.008	186.7212
M15	25/10/07	341	7.52	15	48.241	9.692	4.259	0.507	6.744	3.855	183.06
M16	27/11/07	328	7.94	13	46.332	9.584	4.156	0.556	7.688	3.666	176.958
M17	19/12/07	332	7.74	11	45.376	9.562	4.066	0.343	7.665	3.528	173.907
M18	31/01/08	326	7.44	10	42.670	8.805	4.012	0.406	7.696	3.68	161.703
M19	26/03/08	334	7.56	14	51.211	7.073	4.323	0.284	7.785	4.428	176.958
M20	22/04/08	325	7.62	12	49.531	7.929	4.655	0.525	7.512	3.838	178.7886

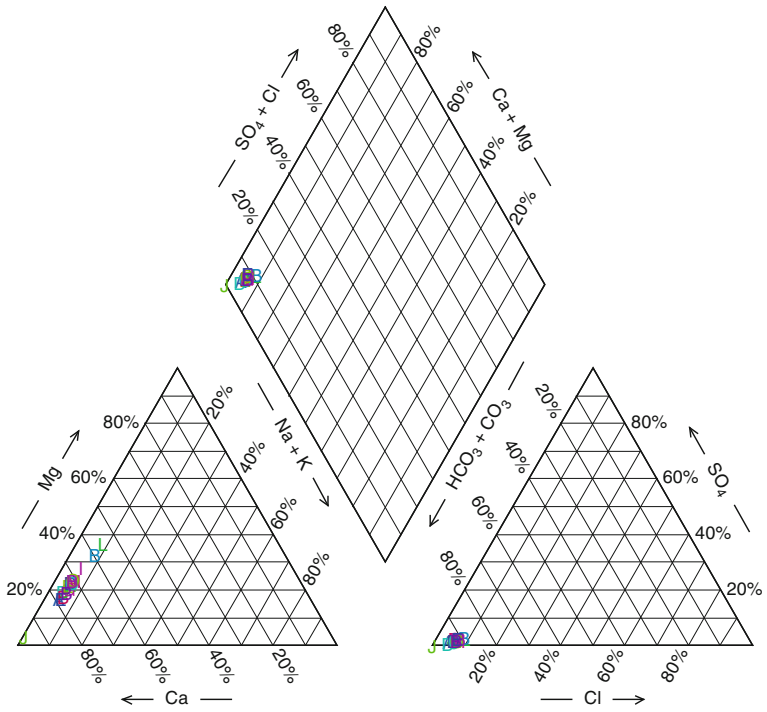

Fig. 265.2 Piper trilinear plot for hydrochemical facies evolution

Table 265.2 Isotope composition and calculated recharge elevations of Mazzoccolo springs

Sample codes	Date (dd/mm/yy)	^{18}O ‰ versus V-SMOW	^{2}H ‰ versus V-SMOW	Discharge elevation (m asl)	Recharge elevation (m asl)
M1	11/05/2006	−6.60	−39.28	7.5	733
M2	15/06/2006	−6.99	−41.11	7.5	880
M3	13/07/2006	−6.98	−41.27	7.5	882
M4	04/08/2006	−6.88	−40.79	7.5	846
M5	21/09/2006	−6.99	−41.86	7.5	902
M6	27/10/2006	−6.95	−41.91	7.5	894
M7	28/11/2006	−7.04	−41.79	7.5	912
M8	21/12/2006	−7.04	−42.14	7.5	922
M9	16/01/2007	−7.07	−42.16	7.5	930

The comparison of $\delta^{18}O$ and $\delta^{2}H$ values of spring water samples with meteoric water lines (Fig. 265.4) shows that most of the samples fall to the local meteoric water line suggesting the input to local rain-fall derives from weather fronts from the Mediterranean Sea.

According to SINTACS method (Civita and De Maio 2004) the karst aquifer feeding the Mazzoccolo spring has a high vulnerability, while presents very low capacity of groundwater protection (Fig. 265.5). The results of applied methods suggest that the identified recharge areas, located in Aurunci Mts., are consistent with the highest vulnerability levels (i.e. obtained by SINTACS method). The geochemical and isotopic characterization of spring water provides us important information for better management of the aquifer systems, which has significant implications for contamination of flow paths, identification of recharge areas and evaluation of aquifer vulnerability.

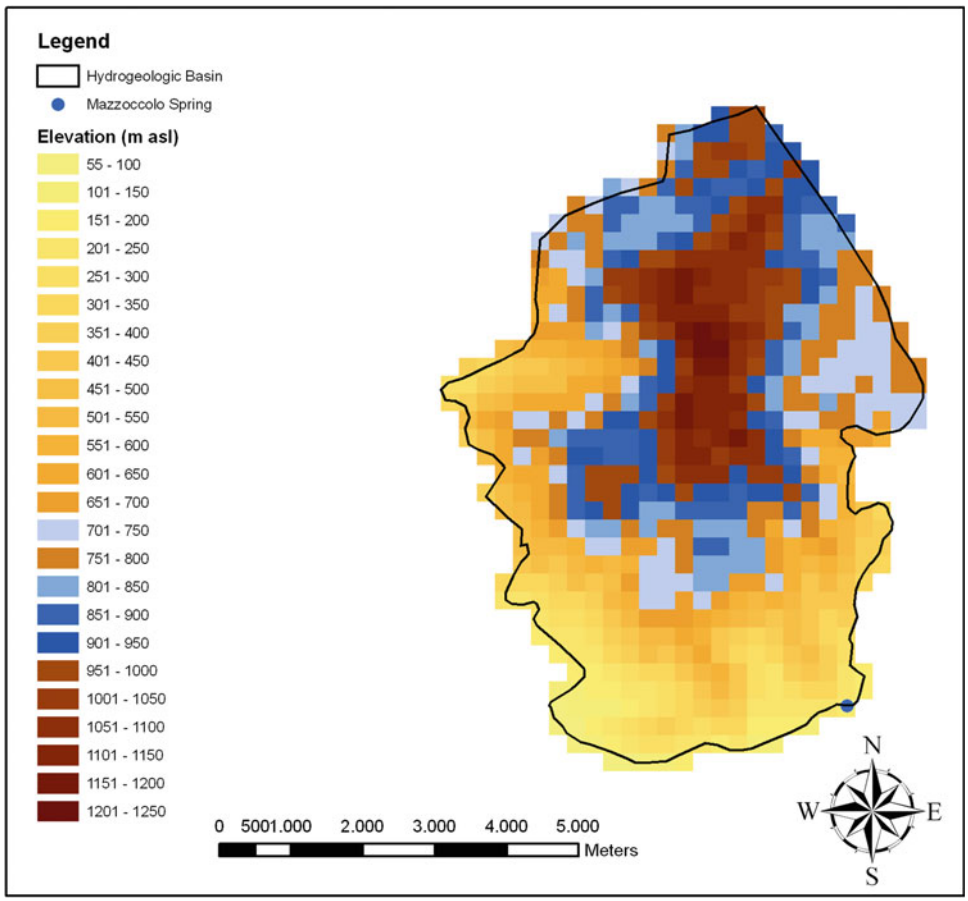

Fig. 265.3 Recharge areas of Mazzoccolo spring

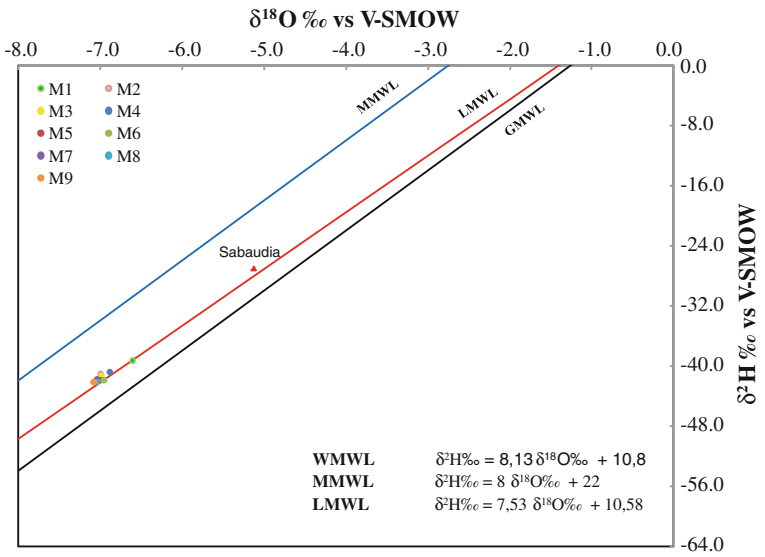

Fig. 265.4 Isotope values (δ^2H and $\delta^{18}O$) of Mazzoccolo spring water samples plotted together with mediterranean meteoric water line (MMWL), the world meteoric water line (WMWL) and the local meteoric water line (LMWL)

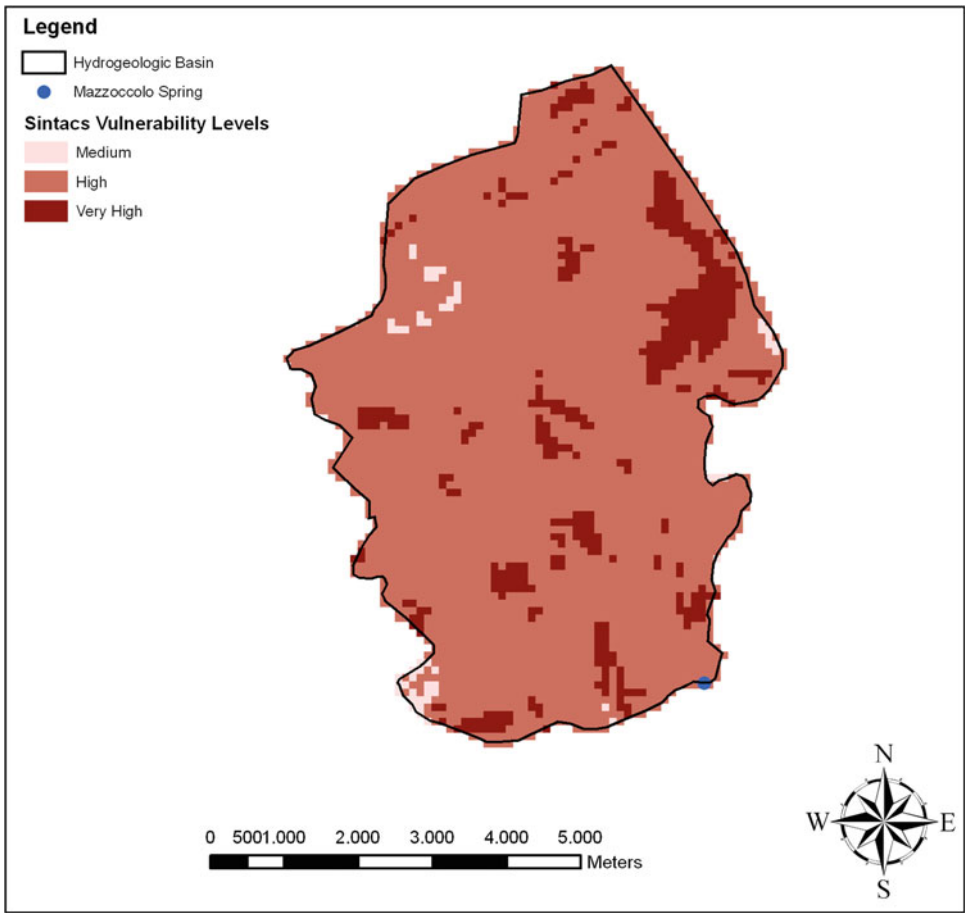

Fig. 265.5 Vulnerability map of the karst aquifer feeding the Mazzoccolo Spring

References

Casa R, Rossi M, Sappa G, Trotta A (2008) Assessing cropwater demand by remote sensing and GIS for the pontina plain, Central Italy. Water Resour Manage 23:1685–1712

Clark I, Fritz P (1999) Environmental isotopes in hydrogeology. Lewis Publishers, New York

Civita M, De Maio M (2004) Assessing and mapping groundwater vulnerability to contamination: the Italian "combined" approach—Geofisica International, vol 43(4). Universidad Nacional Autónoma de México, México pp 513–532

Kendall C, Coplen TB (1985) Multisample conversion of water to hydrogen by zinc for stable isotope determination. Anal Chem 57 (1985):1437–1440. doi:10.1021/ac00284a058

Long AJ, Putnam LD (2004) Linear model describing three components of flow in karst aquifers using ^{18}O data. J Hydrol 296:254–270

Marfia AM, Krishnamurthy RV, Atekwana EA, Panton WF (2003) Isotopic and geochemical evolution of ground and surface waters in a karst dominated geological setting: a case study from Belize, Central America. Appl Geochem 19:937–946

Sappa G, Barbieri M, Ergul S, Ferranti F (2012) Hydrogeological conceptual model of groundwater from carbonate aquifers using environmental isotopes (^{18}O, ^{2}H) and chemical tracers: a case study in Southern Latium Region, Central Italy. J Water Resour Prot 4:695–716. doi:10.4236/jwarp.2012.49080

PRELIMINARY RESULTS OF VULNERABILITY ASSESSMENT OF THE KARST AQUIFER FEEDING PERTUSO SPRING, IN CENTRAL ITALY

Giuseppe Sappa[1]
Sibel Ergul[1]
Flavia Ferranti[1]
[1] DICEA - Dipartimento di Ingegneria Civile Edile ed Ambientale Sapienza - Università di Roma. Via Eudossiana, Rome, **Italy**

ABSTRACT

Vulnerability assessment of the aquifers is an important tool for the groundwater management and protection. This paper aims to assess the intrinsic vulnerability of the karst aquifer feeding Pertuso spring, which is going to be exploited to supply an important water network of the South part of Rome. The study area is located in the Upper Valley of Aniene river and belongs to an important karst aquifer, mainly composed of dolomitic limestones and dolomites of Cretaceous age. The limestones outcropping in the Upper Valley of Aniene river are deeply fractured and karst erosion has occurred on a large scale in this area. The surface karst activity led to the formation of a typical karst landscape. The hydrogeological framework is therefore closely related to the karst nature of carbonate rocks, constituting the reliefs strongly shaped by surface and underground karst activities. The peculiar fragility of this aquifer, feeding Pertuso spring, requires a special attention to protect catchment area, which is directly affected by the natural hydrogeological budget of the aquifer. Therefore, for the evaluation of vulnerability index and maps COP method was applied considering overlying layers (O), concentration of flow (C) and precipitation regime (P) parameters. The vulnerability of the karst aquifer is classified mainly as moderate, high and very high due to the presence of cemented conglomerates, compact dolomitic limestones and granular limestones, respectively. COP method shows that each factor has a different effect on vulnerability index evaluation, however the highest correlation was observed with O factor due to the absence of soil formations. The results obtained by COP method assess the aquifer vulnerability to contamination and are useful for managing the protection of groundwater resources, especially to avoid contamination of karstic aquifers, and land use planning in the area.
Keywords: vulnerability assessment, COP method, karst aquifer, GIS

INTRODUCTION

In central Italy, karst aquifers are the most important drinking water reservoir. However, it is very well known that karst aquifers are particularly vulnerable to contamination due to the presence of thin soils, flow concentration in the epikarst, and point recharge by shallow holes. Thus, the contaminants can easily reach the groundwater, where they may be transported rapidly in karst conduits over large distances [1]. Management of these natural resources has become a worldwide priority and many strategies and methods have been developed to preserve groundwater quality [2-5]. The concept of groundwater vulnerability mapping is an alternative approach for successful protection zoning delineation and land use planning identifying a hydrologic system to

contamination, using different colors to symbolize different degrees of vulnerability. Concerning to different kinds of aquifer systems, different methods on groundwater vulnerability assessment and mapping have been developed including DRASTIC, GOD, AVI, SINTACS, EPIK and PI, however only the last two methods have been developed especially for the vulnerability assessment in karstic areas. The EPIK method takes into consideration four parameters: epikarst (E), protective cover (P), infiltration conditions (I), and karst network development (K) [6]. The E parameter considers the effects in terms of water storage and of the concentration of flow toward vertical conduits. The P parameter describes the protective function of the layers between the ground surface and the groundwater table, mainly soil, subsoil, non-karst rock, and unsaturated karst rock. The I parameter is assessed by distinguishing concentrated infiltration areas and areas in which diffuse infiltration prevails, where the slope and land use are the key sub-factors. K represents the degree of karst network development in the aquifer. The PI method, developed by German Institutions, considers two parameters including I factor, which describes the infiltration conditions and P factor considering protective function of the layers between the ground surface and groundwater [7]. This factor ranges from 1 to 5 and can be calculated using a logical schema based on tabled values of considered local conditions, such as topsoil, recharge, subsoil, lithology, and fracturing [8]. The COST Action 620 proposed a European approach on Vulnerability and Risk Mapping for the Protection of Karst Aquifers [9]. This method considers contaminants infiltration from the surface by means of rainfall and that its transport depends predominantly on the ability of water and contaminants to move through the unsaturated zone. In this study, COP method was applied, considering overlying layers factor (O), the concentration of flow factor (C) and the precipitation regime factor (P), to assess the pollution vulnerability of the karst aquifer feeding Pertuso spring, which is the most important public water supply in the area.

GEOLOGICAL AND HYDROGEOLOGICAL SETTING

The study area is located in the Upper Valley of Aniene River, between the Pertuso spring and the city of Trevi in Lazio (FR) (Fig.1). In this area, it outcrops an important carbonate karst aquifer, mainly composed of dolomitic limestones and dolomites of Cretaceous age. The limestones outcropping in the Upper Valley of Aniene River are very fractured and karst erosion has occurred on a large scale in this area. The surface karst activity led to the formation of a typical karst landscape with rutted fields, sinkholes and flat filled by red soils, while the underground activity has given rise to cavities, sinkholes and cave systems [10-12]. The hydrogeological framework is therefore closely related to the karst nature of carbonate rocks, constituting the reliefs strongly shaped by surface and underground karst activities. The alternation of carbonate formations, limestones and dolomites, together with the epikarst, made of residual of karst activity, and some marly horizons, dating back to the Miocene age, are the main responsible for the hydrogeological system of this area. In this karst aquifer, the major contributions to the Aniene River are provided by the major springs, which lie close the boundary of the carbonate hydrogeological system [13]. Before the town of Trevi nel Lazio (FR), at the altitude of 700 m a.s.l. the Aniene River receives an important contribution on the right side by the Pertuso spring, a karst spring which is the biggest one in this area. The peculiar fragility of this aquifer feeding Pertuso spring, requires a special attention in the planning and implementation of monitoring, as regards the aspects related to surface and groundwater.

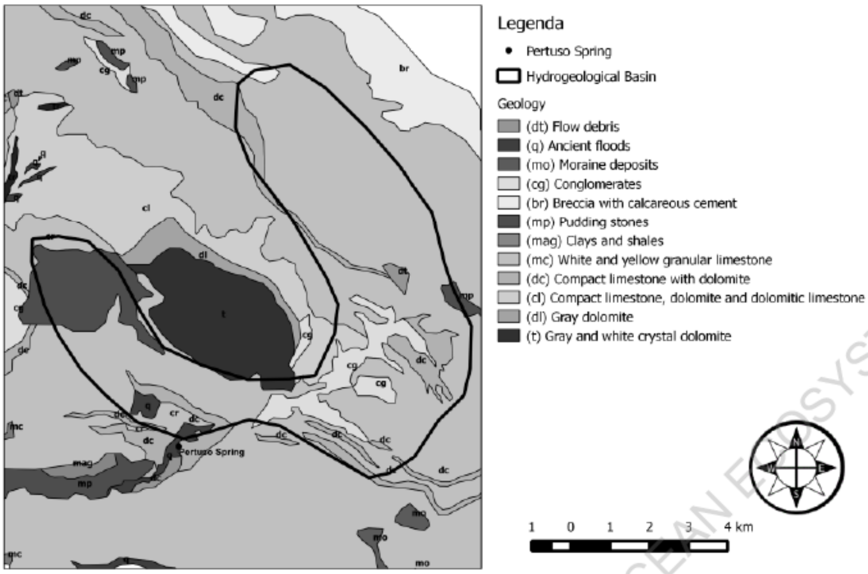

Figure 1. Geology and location of the study area

METHODOLOGY

In the present study, the COP method, proposed by COST Action 620, was applied to one the most important karst aquifer, feeding Pertuso spring, in Lazio region of Central Italy, to secure a sustainable management of this resource and to protect against potential sources of contamination. The vulnerability maps are prepared by a combination of the C, O, and P factors to assess the natural protection of groundwater [14]. The intrinsic vulnerability maps were produced using a GIS approach, which presents vulnerability rate from low to very high. This method suggests that contaminants infiltrated from the surface through rainfall and the transportation depends mainly on the ability of water and contaminants to move through the unsaturated zone.

RESULTS AND CONCLUSIONS

Vulnerability was evaluated by the following factors: (i) Overlying layers (ii) Concentration of flow, and (iii) Precipitation regime. The O factor, determined by properties of overlying soils, provides the protection of unsaturated zone of the aquifer against contamination. In our study, for the evaluation of O factor, two layers were used including soils (O_S) and the lithological layers (O_L) of the unsaturated zone. The soil subfactor concerns the biologically active part of the subsurface, where attenuation processes occur. The lithology subfactor reflects the attenuation capacity of each layer within the unsaturated zone. Different parameters taken into consideration for evaluation of the O factor, however, due to the absence of soil formations, Os factor value was assumed to be zero. The lithology sub-factor is determined by the lithology and fractures (*ly*), thickness of each rock type (*m*) and degree to which an aquifer is confined (*cn*) (Layer index: $\sum$ (Ly * *m*)). In the study area, dolomites, dolomitic limestones and compacted limestones are considered fissured carbonate rocks and they corrispond the value of 3. On the contrary, granular limestones (upper cretaceous age) are attributed to value of 1. The '*cn*' parameter show the highest protection to confined

aquifer, an unconfined aquifer does not affected by this parameter (cn= 1). The karst aquifer investigated, feeding Pertuso spring, is an unconfined aquifer and *cn* value is considered equal to 1. Finally, O score is obtained by adding the subfactors soil [O_S] and lithology [O_L], yielding a corresponding protection value. The resulting O factor predominantly in low protection class. The lowest values of the O factor (higher vulnerability) correspond to areas, where carbonate materials outcrop and where the soil is poorly developed or absent (Figure 2).

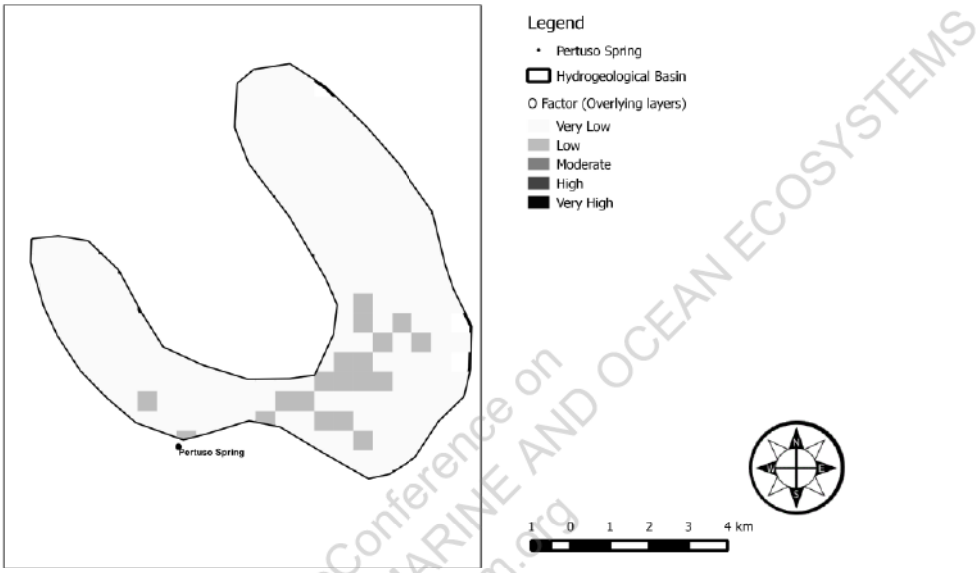

Figure 2. Map of O factor in the Karst aquifer.

The C and P factors are used to correct the degree of protection provided by the overlying layers (O factor). The C factor considers the surface conditions controlling water flowing towards rapid infiltration zones, then represents the degree of concentration of flow towards karstic features. Two scenarios are modelled: Scenario 1 considers the area characterized by sinkholes and surface waters flowing through karst conduits or fractures; Scenario 2 take into consideration the rest of the area without discontinuities, sinkholes or dolines. In the first scenario, four variables can be considered including the distance from the recharge area to the swallow hole (*dh*) and to the sinking stream (*ds*), and the influence of slope (*s*) and vegetation (*v*). On the contrary, the second was evaluated by the combination of only three variables: surface features (*sf*), slope (*s*) and vegetation (*v*). In this case, the calculation of the scores related to the factor O was made by considering only Scenario 2. The C factor calculated based on C: *sf* * *sv*. The areas are only based on the geomorphological features of the karstic rocks and the properties of layers above determining the relative importance of surface runoff and infiltration processes. The evaluation of vegetation and slope parameters were assessed in the opposite way to Scenario 1, because recharge take place directly through sinkholes, whereas zones with high infiltration in the absence of karst structures, the aquifer maintains its natural protection and the values of C

parameter is higher. The surface features parameter considers those geomorphological features specific to carbonate rocks and the presence or absence of any overlying layers (permeable or impermeable) determining the importance of runoff and infiltration. The inverse hydrogeological water budget method was applied to evaluate the average annual active recharge (i.e. the effective infiltration) within a GIS environment. It is applied at each grid cell (EFQ) by which the territory of interest. For the evaluation of *sf* parameter with respect to each EFQ, outcropping lithology was considered. The steepness of the surface topography has been calculated through the reconstruction of the Digital Elevation Model (DEM), while information on the use of soil were extracted from the database of Lazio and Abruzzo regions. For both parameters EFQ includes information about use of soil, slope and geological features of the area. From the combination of the two factors, slope and vegetation, it is possible to attribute to each cell in the score for the parameter *sv*. Figure 3 shows the map of C factor in the area showing elevated vulnerability, where the area characterized by high infiltration. The factor C, which indicates the reduction in the protection of the overlying layers, is given for each cell (in Scenario 2). The lower the value of the parameter C, the higher the reduction in the protection of the overlying layers. In the northeastern part of the basin, the high concentration of granular limestone (*cr)* is attributed to development of karst features, combined with slopes ranging from 8 to 31 % and high values of vegetation.

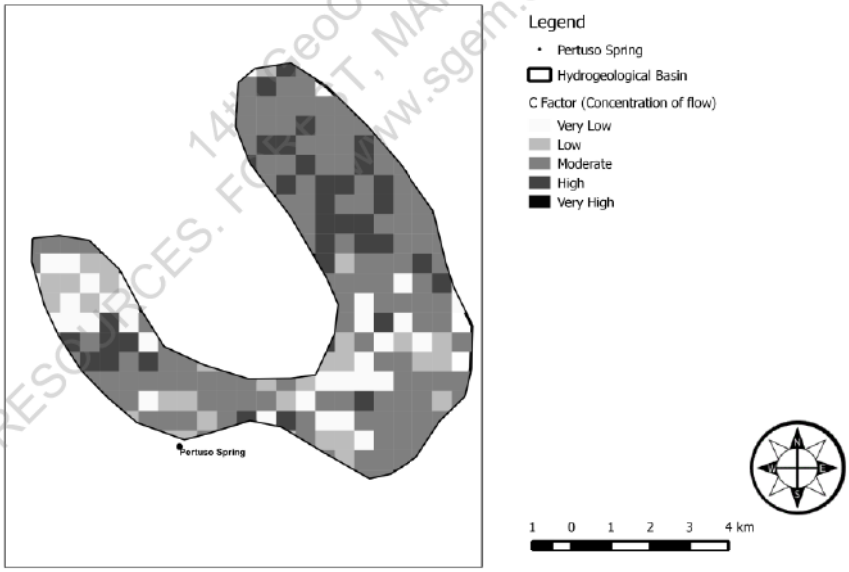

Figure 3. Map of C factor scores in the Karst aquifer.

The P factor considers influence of precipitation, both quantity and intensity, on the transport of contaminants from the surface to the groundwater. The P factor is obtained by two sub-factors including Quantity of precipitation, PQ, and intensity of precipitation, PI, (PI: P = PQ + PI). The calculation of the sub-factor PI is based on the assumption that a higher rainfall intensity results in an increased recharge and thus a

reduced protection of the groundwater resource. The "mean annual intensity" or PI is calculated from mean annual intensity = mean annual precipitation (mm)/mean number of rainy days. The PQ sub-factor describes the effect of rainfall quantity and the annual recharge on groundwater vulnerability. It corresponds to the mean annual rainfall of a historical data series. The higher rates of recharge provide higher dilution and consequently the vulnerability decreases. The PI sub-factor concerns the temporal distribution of precipitation in a certain period of time and thus is indicative of the intensity of precipitation. The higher totals of annual precipitation and lower number of rainy days causes higher PI sub-factor values. Using rainfall data and altitudes it is possible to calculate mean annual intensity for each grid cell. For the evaluation of sub-factor PI two variables were considered: the average annual precipitation and number of rainy days in a year. To assess the number of rainy days in a year, the rainfall data series (from 1997 to 2001 and from 2008 to 2012) from Filettino gouge station was employed. Through the following relationship was, therefore, possible to estimate the sub- factor PI for each grid cell. Figure 4 shows the score map of P factor. The sum of these two sub-factors is referred to higher values of P factor, which decreases groundwater protection with increasing recharge and as a consequence fast infiltration. Thus, O factor is reduced due to rainfall regime. The highest values were observed in the area characterized by granular limestones that facilitates the penetration of groundwater reducing runoff.

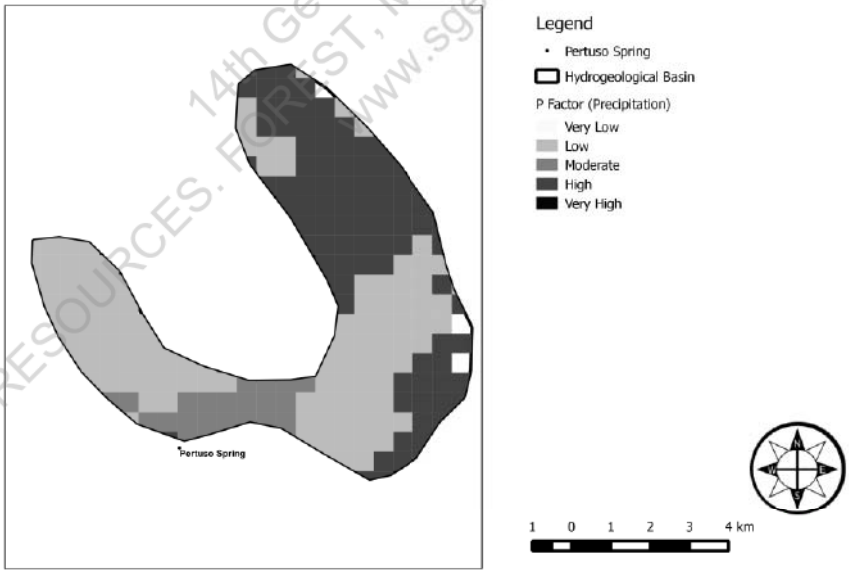

Figure 4. Map of P factor in the Karst aquifer.

Finally, the vulnerability index is obtained by multiplying the three factors: COP – Index = (C score) * (O score) * (P score). Figure 5 presents the vulnerability map, obtained by COP, which identifies three classes of vulnerability, ranging from moderately to very high. The obtained vulnerability index values range between 0 to 2.

The vulnerability of the karst aquifer is classified mainly as moderate, high and very high due to the presence of cemented conglomerates, compact dolomitic limestones and granular limestones, respectively. COP method shows that each factor has a different effect on vulnerability index. The moderate class refers to zones, where potential protection is low to average, in which the C and P factors do not have impacts on vulnerability. However the vulnerability is influenced mainly by O factor due to the absence of soil formations. The O factor determines high vulnerability in the outcrops of granular limestones and compact dolomitic limestones. The selection of the appropriate method for groundwater vulnerability mapping is an important tool to assess aquifer vulnerability to contamination and protection of groundwater resources.

Figure 5. Intrinsic vulnerability map by COP method.

REFERENCES

[1] Goldscheider N. Karst groundwater vulnerability mapping: application of a new method in the Swabian Alb, Hydrogeology Journal, Germany, vol. 13/issue 4, pp 555–564, 2005.

[2] Adams B. & Foster S.S.D. Land-surface zoning for groundwater protection. Journal of the Institute of Water and Environmental Management, vol. 6, pp 312– 20, 1992.

[3] Albinet M. & Margat J. Cartographie de la vulnerabilite a la pollution des nappes dTeau souterraine. Bull Bur Rech Géol Min, vol. 3/issue 4, pp13–22, 1970.

[4] Vrba J. & Zaporozec A. (eds.) Guidebook on mapping groundwater vulnerability, IAH International Contributions to Hydrogeology (Heise Publ.), Hannover/FRG, vol. 16, pp 131, 1994.

[5] Gogu R.C. & Dassargues A. Current trends and future challenges in groundwater vulnerability assessment using overly and index methods. Environ Geol, vol. 39/issue 6, pp 549–559, 2000.

[6] Doerfliger N. & Zwahlen F. Practical Guide, Groundwater Vulnerability Mapping in Karstic Regions (EPIK). Swiss Agency for the Environment, Forests and Landscape (SAEFL). Bern. pp 56, 1998.

[7] Tulipano L. Sappa G. Coviello M.T. Vulnerability mapping of Posta Fibreno (Frosinone - Italy) aquifer, assessed by the SINTACS and PI methods. Proceedings of the 8th IAH Congress, Mar de Plata (Argentina), 21-25 ottobre 2002.

[8] H¨olting B. Haertle T. Hohberger K.H. Nachtigall K.H. Villinger E. Weinzierl W. & Wrobel, J.P. Konzept zur Ermittlung der Schutzfunktion der Grundwasser¨uberdeckung. Hannover. Geol. Jb. vol C63. pp 5–24, 1995.

[9] De Ketelaere D. Hotzl H. Neukum C. Civita M. Sappa G. Hazard analysis and mapping. In: Zwahlen, F. (Ed.), Vulnerability and Risk Mapping for the Protection of Carbonate (karst) Aquifers, EUR 20912. European Commission, Directorate-General XII - Science, Research and Development, Brussels, pp. 86–105, 2004.

[10] Accordi G. & Carbone F. Carta delle litofacies del Lazio-Abruzzo ed aree limitrofe. Quaderni de La ricerca scientifica, Roma, vol. 5/issue 114, 1988.

[11] Bosellini A. Dynamics of Tethyan carbonate platforms. In: Crevello P.D., Wilson J.L., Sarg J.F. & Read J.F (eds.), Controls on Carbonate platform and basin development, SEPM Special Publication, vol. 44, pp 3-13, 1989.

[12] Damiani A.V. Studi sulla piattaforma carbonatica laziale-abruzzese. Nota I. Considerazioni e problematiche sull'assetto tettonico e sulla paleogeologia dei Monti Simbruini, Roma. In: Memorie descrittive Carta Geologica d'Italia, vol. 38, pp 177-206, 1990.

[13] Ventriglia U. Idrogeologia della Provincia di Roma, IV, Regione orientale. Amministrazione Provinciale di Roma, Assessorato LL.PP, Viabilità e trasporti, Roma, pp 547, 1990.

[14] COST 65. Hydrogeological aspects of groundwater protection in karstic areas, EUR 16547. European Commission, Directorate-General XII Science, Research and Development; Brussels, pp 446, 1995.

Geophysical Research Abstracts
Vol. 18, EGU2016-11560, 2016
EGU General Assembly 2016

Vulnerability assessment of karst aquifer feeding Pertuso Spring (Central Italy): comparison between different applications of COP method

Giuseppe Sappa, Flavia Ferranti, and Giulia Luciani

Sapienza, University of Rome, DICEA, Department of Civil, Building and Environmental Engineering, Rome, Italy (giuseppe.sappa@uniroma1.it)

Vulnerability assessment of karst aquifers and vulnerability mapping are important tools for improved sustainable management and protection of karst groundwater resources.
In this paper, to estimate the vulnerability degree of the karst aquifer feeding Pertuso Spring in Central Italy, two different implementations of COP method, supported by an open source GIS, were tested and a comparison of the vulnerability maps is proposed.
The study area is a highly karstified carbonate aquifer located in the Upper Valley of the Aniene River, in the south-east part of Latium Region. The hydrogeological basin covers about 50 km2 and the karst aquifer provides a water supply of about 120.000 m3d-1.
The well-developed karst features in this hydrogeological system is responsible of the fast infiltration of rainfall in the saturated zone and, consequently, of the high discharge rate of Pertuso Spring (up to 3 m3/s). Thus, in the aim of emphasizing the presence of these karst features, due to which, there are limited attenuation processes in the unsaturated zone, in this work COP method has been applied by the implementation of a new discretization methodology of the hydrogeological basin using polygonal layer. Therefore, the hydrogeological catchment basin has been divided into 52 polygonal layer, representative of outcropping lithology and karst features, to which COP method has been applied. The intrinsic vulnerability maps, produced using a GIS approach, has been examinated and compared with the maps obtained using traditional vulnerability assessment method, which provides the discretization of the study area generating a grid map to which associate the Vulnerability Indexes.
The results of this study highlight vulnerability from low to very high. The maximum vulnerability degree is due to karstic features responsible of high recharge and high hydraulic conductivity.
The new proposed discretization of the hydrogeological basin using polygonal layer raise four vulnerability classes, ranging from low to very high, and provide different results for high and very high vulnerability areas whit respect to the traditional grid approach. The traditional implementation of COP method assigns to most of the study area very high vulnerability degree, while the polygon discretization shows the dominance of high vulnerability classes assessing very high vulnerability only to karst features. These results seem to be more realistic because they better consider the role of the highly developed epikarst, which minimizes the protective function of the unsaturated zone.
Comparing the vulnerability maps obtained by both methodologies shows that the traditional discretization approach seems to overestimate the vulnerability of the karst aquifer feeding Pertuso Spring and to provide a low sensitivity to the spatial variation of the hydrogeological parameters.
Between the two different approaches of COP method, the proposed polygon discretization of the hydrogeological basin seems to be more accurate and flexible than the traditional grid mapping.

Giuseppe Sappa, Flavia Ferranti*

UTILIZZAZIONE DELLE RISORSE IDRICHE DELL'ALTA VALLE DELL'ANIENE

WATER RESOURCES EXPLOITATION IN THE UPPER VALLEY OF ANIENE RIVER

Si riferisce sui risultati di uno studio del bilancio idrico del bacino del Fiume Aniene nel tratto fra le sorgenti del Pertuso e la sezione di Subiaco, alla luce di un'analisi dello stato attuale dell'utilizzazione delle risorse idriche sotterranee e superficiali dell'Alta Valle dell'Aniene, per contribuire, per quanto possibile, con la semplice espressione dei numeri, al dibattito sulle migliori modalità di sviluppo sostenibile di questa area. Si tratta, com'è noto di un'area di pregevole valore ambientale, sottoposta in larga parte a vincoli di tutela attraverso l'istituzione di un Parco naturale di interesse regionale.
Gli AA. hanno fatto riferimento alla documentazione ufficiale disponibile in merito alle derivazioni idropotabili ed idroelettriche nell'area; successivamente sono stati elaborati i dati contenuti nei documenti acquisiti; infine, sulla base del bilancio idrico sono state sviluppate alcune considerazioni in merito allo stato attuale dell'utilizzazione idrica dell'Alto Aniene.
Parole chiave: Fiume Aniene, Bilancio idrico, Utilizzazione risorse idriche.

Paper highlights the results of the water balance of Aniene River basin, in the part located between the Pertuso springs and Subiaco. The analysis has been driven on the current state of water resources exploitation in the Upper Valley of Aniene River. This area has a remarkable environmental value, and it is protected by the regional natural park. Paper contributes to a sustainable development of this area.
Therefore, it was taken into consideration the preliminary available official documentation based on the quantitative data of hydroelectric and potable water in the area. Finally, according to the results of water balance, the evolution of current use of water on the Upper Valley of Aniene River has been discussed in the framework of the current laws.
Key words: Aniene River, Water Balance, Exploitation of Water Resources.

1. INTRODUZIONE

Il presente lavoro nasce da alcune analisi quantitative che gli scriventi hanno condotto per valutare l'ecosostenibilità del prelevamento di acqua potabile dalla sorgente del Pertuso, la cui derivazione idropotabile oggi è utilizzata per integrare le portate, progressivamente insufficienti, delle sorgenti che alimentano storicamente l'acquedotto, gestito originariamente dal Consorzio del Simbrivio, ed oggi transitato in ACEA ATO2 S.p.A.. L'esame dei dati disponibili consente alcuni spunti di riflessione sull'interpretazione applicativa della legislazione vigente in materia di utilizzazione delle risorse idriche in questa porzione di territorio.

2. IL TERRITORIO DELL'ALTA VALLE DELL'ANIENE

L'area di studio interessa il bacino del Fiume Aniene nel tratto compreso fra le sorgenti del Pertuso e la sezione di Subiaco, comprensivo del Torrente Simbrivio.
L'Alta Valle dell'Aniene è nell'Appennino Laziale immediatamente ad ovest del confine con l'Abruzzo e ricade nel settore orientale della provincia di Roma ed in piccola parte in quella di Frosinone. Tale bacino, delimitato a nord ed a est dai Monti Sinbruini, a sud dai Monti Ernici ed a ovest dai Monti Affilani, ha un'estensione di circa 222 km^2 ed ha carattere prevalentemente montuoso. La parte nord di tale bacino ricade all'interno del Parco Naturale Regionale dei Monti Simbruini, di notevole valore ambientale di interesse europeo (tra Zona a Protezione Speciale e Sito di Interesse Comunitario) che, su un territorio di circa 30.000 ha, è la più vasta area protetta del Lazio.
Il Parco è compreso tra il Fosso Fioio a nord e la Valle del Sacco a sud, ed è delimitato ad ovest dalla Valle dell'Aniene e ad est dallo spartiacque Monte Virgilio-Monte Crepacuore.

* *Giuseppe Sappa, Professore Associato di Geologia Applicata - Dipartimento di Ingegneria Civile Edile ed Ambientale - Facoltà di Ingegneria - Sapienza Università di Roma; Flavia Ferranti, Ingegnere per l'Ambiente ed il Territorio - Borsista CRITEVAT- Centro Reatino di ricerche di Ingegneria per la Tutela e la Valorizzazione dell'Ambiente e del Territorio - Sapienza Università di Roma.*

Il territorio del Parco ricade in sette comuni situati tra 408 e 1075 m s.l.m.: Camerata Nuova, Cervara di Roma, Jenne, Subiaco e Vallepietra (Roma); Filettino e Trevi nel Lazio (Frosinone).
L'istituzione del Parco, avvenuta con la L.R. n. 8 del 29/01/1983, nasce allo scopo di favorire la conservazione e la valorizzazione delle risorse naturali di un'area storicamente caratterizzata da una ricchezza idrica di valore strategico, inserita però in un territorio carsico molto vulnerabile dal punto di vista ambientale.
L'acqua è sicuramente uno degli elementi più caratterizzanti questo territorio. Infatti, il toponimo "Simbruini", dal latino "*sub imbribus*", "sotto le piogge", testimonia la notevole piovosità che da sempre caratterizza quest'area. Gli abbondanti rovesci e le nevi, insieme all'ambiente carsico reso manifesto da inghiottitoi, doline e profonde grotte, hanno creato, infatti, le condizioni per un sistema di sorgenti pedemontane da cui ancora oggi viene prelevata acqua potabile.
Inoltre per la ricchezza di habitat prioritari e di specie zoologiche e floristiche, minacciate e vulnerabili, che caratterizzano tale territorio, il Parco Naturale Regionale dei Monti Simbruini rientra nella Rete Natura 2000 (Direttiva Habitat 92/43/CEE) come Zona a Protezione Speciale.

3. INQUADRAMENTO GEOLOGICO ED IDROGEOLOGICO

Il bacino imbrifero dell'Alto Aniene, con chiusura a Subiaco, ha una superficie di 222,76 km² (comprese le zone endoreiche periferiche) e una quota media di circa 1140 m s.l.m.. Nel punto di chiusura del bacino, nei pressi di Subiaco, l'Aniene ha già ricevuto gli apporti dei tributari: il Torrente Simbrivio da destra, il Fosso Campo e il Fosso dell'Obaco da sinistra.
L'area è caratterizzata da una successione sedimentaria tipica della *piattaforma carbonatica* di ambiente interno e di rampa, in cui i litotipi affioranti sono quelli tipici della *serie laziale-abruzzese*, una successione marina prevalentemente carbonatica sviluppatasi all'interno di un margine passivo subsidente fra il primo Mesozoico ed il Miocene (*Accordi e Carbone*, 1988; *Bosellini*, 1989-1991; *Damiani*, 1990). Le formazioni rocciose più antiche della serie, affioranti in questa zona, sono le cosiddette Dolomie di Filettino, risalgono a circa 230 milioni di anni fa, e sono anche le più antiche dell'intero Appennino Centrale. In un'epoca più recente nella stessa area si è sviluppata, invece, un'intensa attività carsica: superficiale, con formazione di un caratteristico paesaggio carsico con campi carreggiati, doline e piane colmate dai prodotti dell'alterazione delle rocce carbonatiche (terre rosse); sotterranea, con cavità, inghiottitoi (Camposecco) e sistemi di grotte (Inferniglio). L'alternarsi di formazioni carbonatiche, calcaree e dolomitiche, unitamente alle terre rosse, residuo dell'attività carsica, e ad alcuni orizzonti marnosi, risalenti al Miocene Superiore, sono i temi geologici che condizionano maggiormente l'assetto idrogeologico di quest'area.
Il Torrente Simbrivio si origina a monte di Vallepietra e, dopo avere ricevuto, durante il suo corso, apporti in alveo e puntuali, confluisce nell'Aniene secondo una direzione circa meridiana alla quota di 534 m s.l.m., in corrispondenza del ponte di Comunacque. Il Fosso Campo è invece la prosecuzione a valle della sorgente Foce del Fosso dell'Obaco. Questi torrenti hanno carattere tipicamente carsico con regime effimero e si esauriscono durante i periodi di magra estiva. Il tratto più montano dell'Aniene si origina dalla confluenza dei numerosi fossi disposti a ventaglio in cui confluiscono le acque di ruscellamento e quelle provenienti dallo scioglimento delle nevi.
Queste incisioni convergono in due aste principali: il Fosso di Acqua Corore e il Fosso Vardano che, a circa 2 km a sud-ovest del Comune di Filettino, si uniscono alla quota di circa 817 m s.l.m. per formare il Fiume Aniene.
Il Fosso di Acqua Corore è formato da vari fossi che scendono verso sud dalle pendici meridionali di Monte Tarino e che hanno inizio alla quota di circa 1600 m s.l.m.. Questo in prossimità dell'affioramento delle dolomie triassiche e giurassiche inizia a ricevere contributi lineari e puntuali assumendo un decorso circa meridiano.
Il Fosso Vardano si origina dalle pendici settentrionali di Monte Piano, a circa 1600 m s.l.m., con il nome di Fosso della Moscosa. Tale fosso scende in direzione NE-SW e alla quota di circa 1200 m s.l.m. comincia a ricevere contributi lineari e puntuali in prossimità dell'affioramento delle dolomie poco più a monte di Filettino (*Ventriglia*, 1990).
Le due aste si uniscono a valle di Filettino, alla quota di circa 810 m s.l.m., dando origine all'asta principale del Fiume Aniene che mantiene la direzione NE-SW del Fosso della Moscosa. Questa direzione è mantenuta fino a valle del Ponte delle Tartare, dove l'Aniene si orienta secondo la direzione NW-SE conservando tale allineamento fino a Cineto Romano. In un breve tratto, all'altezza di Subiaco, l'Aniene segue una direzione E-W. Prima di Trevi nel Lazio, alla quota di 700 m s.l.m. circa, il fiume riceve l'importante contributo della sorgente Pertuso che, con una portata media riferita al 2004 di 1,5 m³/s, è la maggiore emergenza dell'area. Proseguendo nel suo corso verso Subiaco, nella stretta valle fluviale che si sviluppa tra le propaggini meridionali dei Monti Simbruini e quelle settentrionali degli Affilani, l'Aniene riceve altri importanti contributi sia in alveo che da sorgenti puntuali (Tartare, Polveriera e Inferniglio).
Nei calcari mesozoici dell'alto bacino, più o meno permeabili per fratturazione, ha sede un'importante falda acquifera di base drenata dal fiume e sono inoltre presenti in essi falde acquifere sospese sostenute dai livelli meno permeabili della serie (livelli più o meno marnosi o compatti, non fratturati, poco o per niente permeabili). Queste falde si manifestano con sorgenti perenni anche di considerevole portata (*Ventriglia*, 1990). Come tutti gli acquiferi carsici anche per l'Alto Aniene i maggiori contributi al corso d'acqua (circa l'80% della portata totale) sono forniti dalle principali sorgenti ubicate nei pressi del reticolo perenne, ai margini dell'idrostruttura carbonatica. Il restante 20% sembra invece dovuto dal drenaggio in alveo che si origina dal reticolo di microfessure che sostiene il flusso di base.
Nel settore orientale del bacino affiorano in prevalenza calcari mesozoici di piattaforma che in prossimità dello spartiacque presentano spesso delle aree endoreiche pianeggianti sub-circolari o ellittiche note come *campi* (Campaegli, Campo dell'Osso, Campo Rotondo, Campo Livata) dove è notevolmente sviluppato il carsismo epigeo. L'area, per via dell'alternarsi nella stratificazione di dolomie, calcari di diversa facies e livelletti argillosi, è sede di numerose piccole sorgenti (soprattutto di trabocco per soglia) che spesso alimentano ruscelli di limitata portata. Il reticolo idrografico, poco sviluppato, è costituito prevalentemente da fossi a regime torrentizio.
Il quadro idrogeologico è perciò strettamente legato alla natura prevalentemente carbonatica e carsica delle rocce costituenti

i rilievi in questione, costituiti dal margine occidentale della piattaforma carbonatica laziale-abruzzese e fortemente modellati da carsismo, superficiale ed ipogeo.
All'interno della struttura idrogeologica dei Monti Simbruini è possibile distinguere abbastanza chiaramente due zone: quella costituita dall'Alto Aniene e dal Simbrivio e quella relativa al margine occidentale della struttura (Gruppo di Agosta). Per effetti tettonici responsabili dell'innalzamento del substrato dolomitico regionale e di un carsismo particolarmente sviluppato, l'Alta Valle dell'Aniene è sede di acquiferi localmente frammentati.
Appare, perciò, evidente come il regime di portata delle numerose sorgenti presenti, con quote distribuite tra i 500 e i 1000 m s.l.m., risulti fortemente influenzato dagli effetti stagionali, con notevoli variazioni tra portate di piena, portate medie e portate di magra. Nel settore occidentale della struttura invece l'acquifero che alimenta le sorgenti del Gruppo di Agosta, distribuite tra i 330 e i 360 m s.l.m., risulta nettamente separato dagli acquiferi che alimentano le sorgenti dell'Alto Aniene, poste a quote più elevate. I limiti che separano questi due settori caratterizzati da un diverso assetto idrogeologico non sono ancora noti (*Boni*, 2006).

4. SISTEMA DELLE CONCESSIONI DELLE ACQUE PUBBLICHE PER USO IDROELETTRICO

Per la redazione del presente lavoro ci si è avvalsi delle informazioni contenute nei seguenti elaborati:
Acea ATO 2 S.p.A. - Misure di portata relative a derivazioni idrico-potabili:
- Sorgenti NASC (Carpinetto, Pantano Bassa, Cornetto) - periodo 2003-2007;
- Sorgenti VAS (Cardellina Alta, Cardellina Media, Cesa degli Angeli) - periodo 2003-2007;
- Sorgente Pertuso - periodo 2003-2007;
- Sorgente Ceraso - periodo 2003-2007;
- Pozzi Ceraso - periodo 2004-2007.

Acea ATO 2 S.p.A. - Rilascio Acque Reflue:
- Comune di Afflile (Dep. Pizziana);
- Comune di Arcinazzo Romano (Dep. Vidiano);
- Comune di Jenne (Dep. Lescuso);
- Comune di Subiaco (Dep. S. Angelo).

Enel - Misure di portata media mensile turbinata e moduli di concessione medi e massimi derivati dalle centrali idroelettriche che operano a valle della Sorgente Pertuso (*Figg. 1-2-3*):
- **Centrale di Comunacqua**: è ubicata in località Contrada Comunacqua (Trevi del Lazio) sulla sponda destra del Fiume Aniene (presso il Ponte delle Tartare). E' la centrale di testa dell'asta ed è alimentata dal bacino Pertuso e dal bacino Simbrivio.
- **Centrale di Scalelle**: è ubicata in località Centrale di Scalelle (Subiaco) sulla riva destra dell'Aniene, di cui utilizza le acque provenienti da un'opera di presa a quota 559 m, in corrispondenza di una traversa. La derivazione, lunga circa 7 km, raccoglie anche gli apporti provenienti dal Torrente Simbrivio e le acque rilasciate dalla centrale di Comunacqua.
- **Centrale di Subiaco**: è ubicata all'estremità del centro abitato di Subiaco. L'impianto utilizza l'acqua di scarico della centrale di Scalelle e gli apporti fluenti captati da un'opera di presa sull'Aniene, in località Ponte delle Scalelle a quota 468 m.

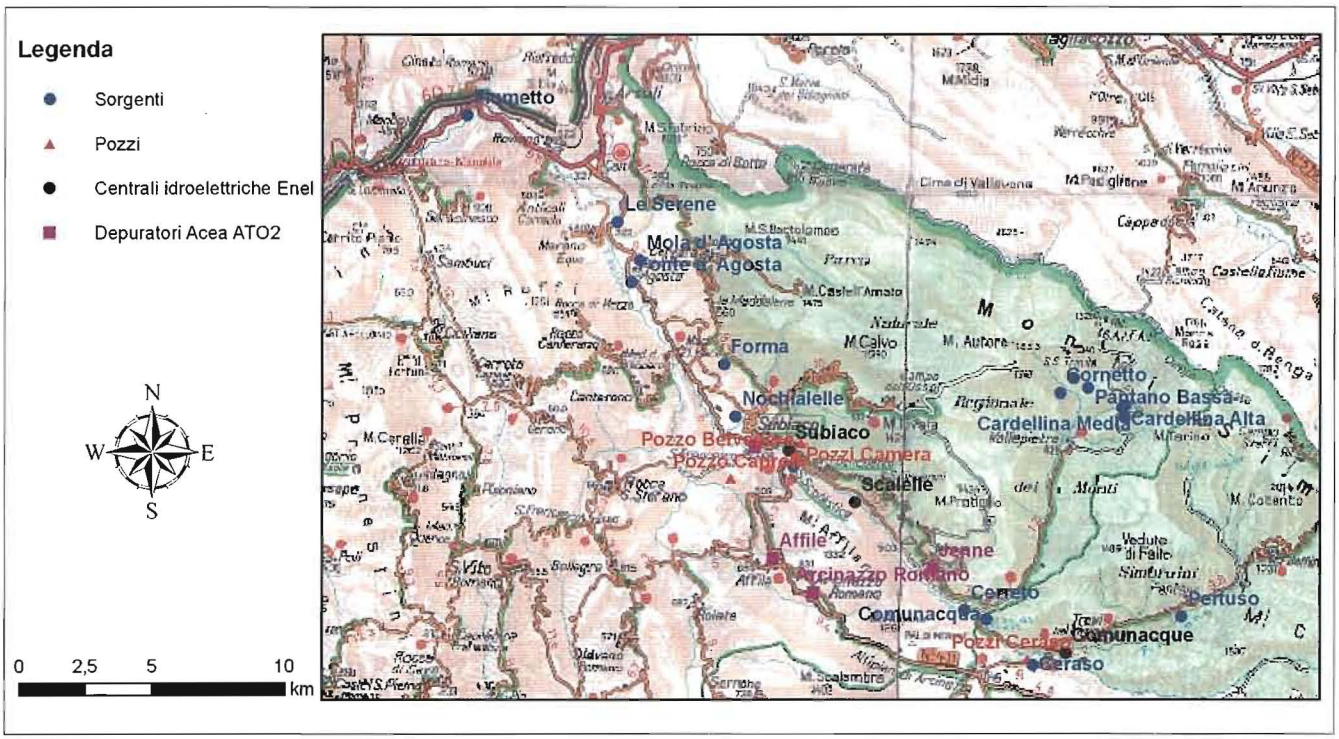

Figura 1 - Shema dei prelievi idropotabili ed idroelettrici e dei rilasci di acque reflue nell'Alta Valle dell'Aniene.

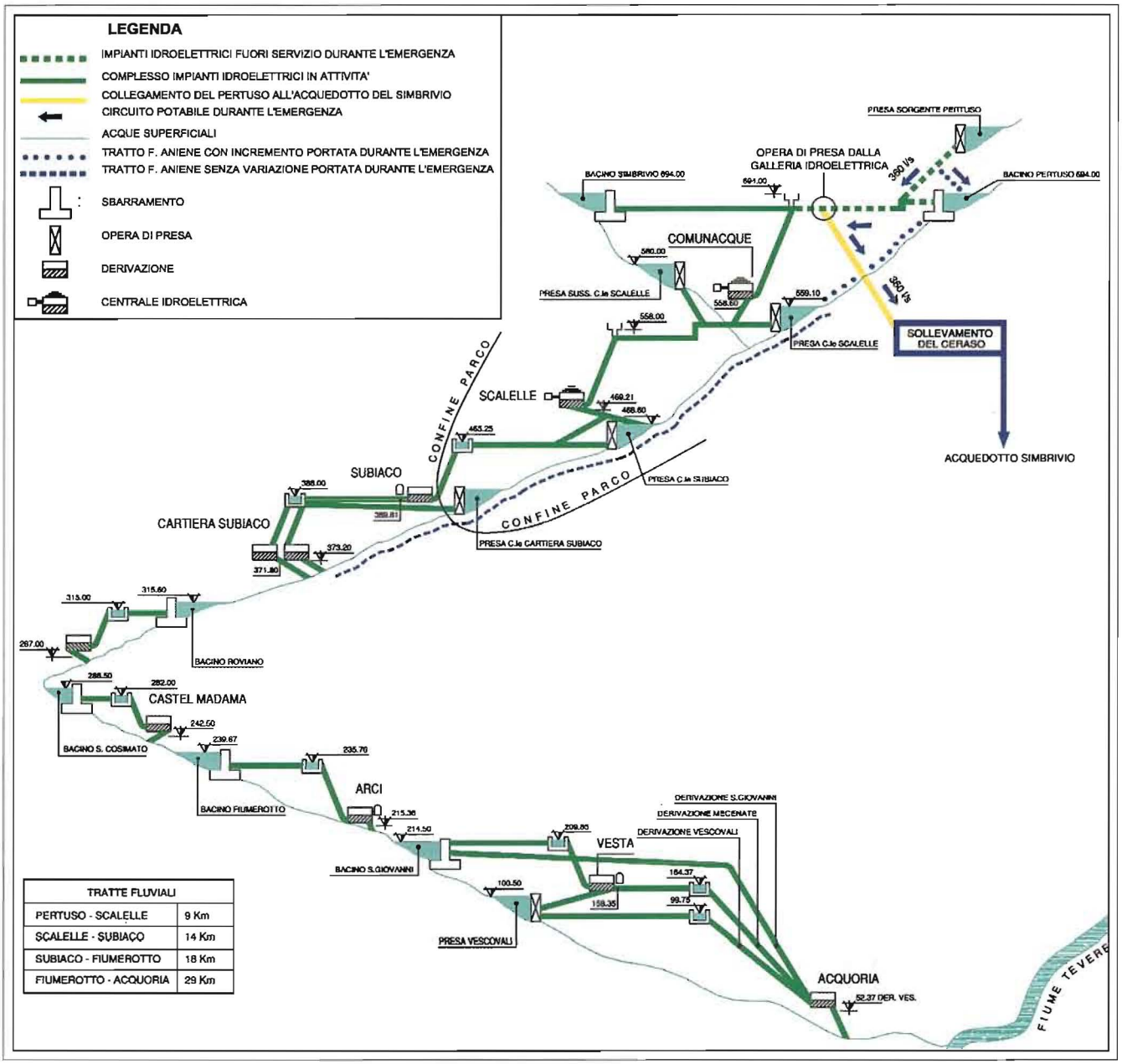

Figura 2 - Schema delle centrali idroelettriche a Valle della Sorgente Pertuso.

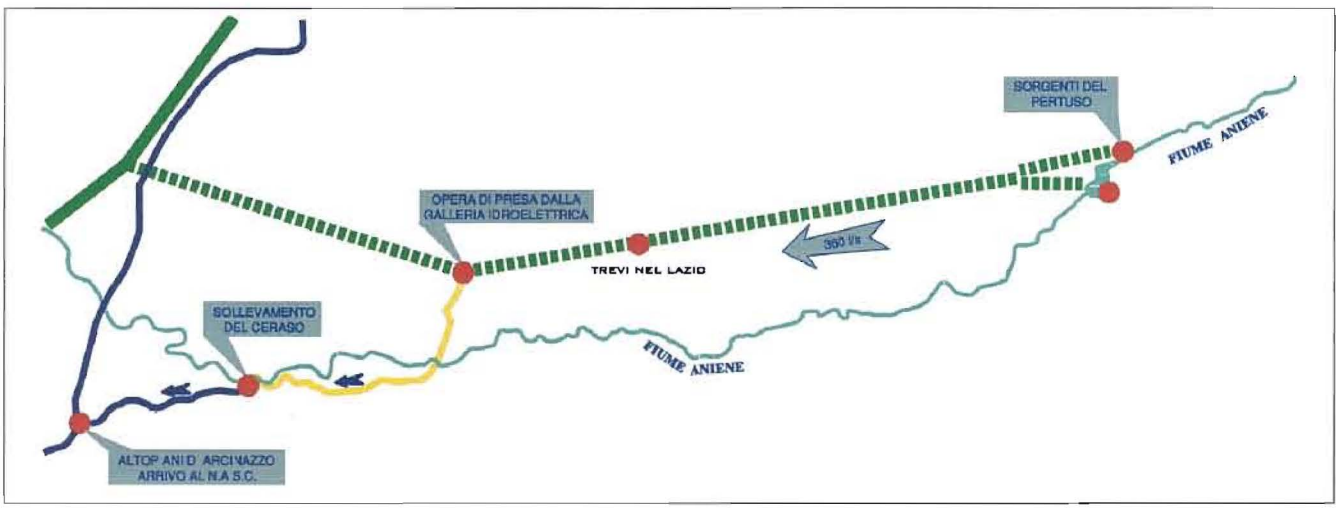

Figura 3- Derivazione potabile di emergenza della Sorgente Pertuso.

I prelievi idroelettrici delle centrali di Comunacqua, Scalelle e Subiaco sono regolamentati dal D.M. Lavori Pubblici del 15/05/1974 e relativo "Disciplinare di obblighi e condizioni cui dovrà essere vincolata la derivazione di acqua dal Fiume Aniene e Simbrivio chiesta dal consorzio idroelettrico Alto Aniene e Simbrivio con istanze 05/08/1938-13/06/1941 e 31/08/1955" (Consiglio Superiore dei Lavori Pubblici - adunanza del 27/09/1990).
Alla data del rilascio di tali concessioni ed all'atto del loro rinnovo, il riferimento legislativo principale in materia era costituito dal R.D. 1773/1933.
Il titolare della concessione di derivazione di acque pubbliche, in questo caso ENEL, ha diritto di derivarle, per la durata della concessione, nei limiti delle quantità stabilite, con le modalità e gli oneri definiti dal provvedimento di concessione e nel rispetto di quanto convenuto con il disciplinare di concessione.
In particolare il concessionario, nel rispetto del provvedimento concessorio, è tenuto a rispettare i seguenti quantitativi d'acqua da derivare (*Tab. I e II*):

TABELLA I - Derivazione acqua dal Fiume Aniene e dal Torrente Simbrivio-Dati disciplinare

Impianto	Corpo Idrico	Punto di derivazione	Luogo e modalità di scarico	Q_{med} derivata (m^3/s)	Q_{max} derivata (m^3/s)
Comunacqua	F. Aniene	Sorgente Pertuso e 600 m a valle della stessa	circa 650 m a monte del Ponticello di Comunacqua e direttamente nel canale derivatore della centrale di Scalelle	2,1	4,5
	T. Simbrivio	località Ponte Renzo		1,93	3,7
Scalelle	F. Aniene	500 m a monte del Ponticello di Comunacqua, immediatamente a valle della confluenza con il Simbrivio	circa 30 m a monte dell'opera di presa della centrale di Subiaco	4,7	7,0
	T. Simbrivio	450 m a monte del Ponticello di Comunacqua		2,8	4,0

TABELLA II - Portate concesse medie e massime (ENEL)

Impianto	Portata media concessa (m^3/s)	Portata massima concessa (m^3/s)
Comunacqua	4,03	8,2
Scalelle	7,5	11,0
Subiaco	6,25	8,1

- *dal Fiume Aniene, in località circa 300 metri a valle della confluenza del Fosso Corore, in Comune di Filettino (Frosinone), la portata media di mod[1]. 9, max 15, per mantenere in servizio la centrale di Filettino;*
- *dal Torrente Simbrivio, in località immediatamente a valle della confluenza del Fosso dei Casali, in Comune di Vallepietra (Roma), la portata media di mod. 19, max 24.5, per mantenere in servizio la centrale di Ponte Renzo;*
- *dal Fiume Aniene, in località Pertuso, immediatamente a valle della sorgente omonima, nel Comune di Trevi nel Lazio (Roma) la portata media di mod. 21, max 45, e dal Torrente Simbrivio, in località Ponte Renzo, in Comune di Vallepietra (Roma), la portata media di mod. 19.3, max 37 (complessivamente moduli medi 40, 30) per mantenere in servizio la centrale di Comunacqua;*
- *dal Fiume Aniene, circa 500 metri a monte del ponticello di Comunacqua, immediatamente a valle della confluenza Aniene-Simbrivio, in Comune di Trevi nel Lazio (Roma), la portata media di mod. 47, max 70 e dal Torrente Simbrivio, circa 400 metri a monte del ponticello di Comunacqua, la portata media di mod. 28, max 40 (complessivamente moduli medi 75) per mantenere in servizio la centrale di Scalelle[2].*

La concessione di derivazione ha una durata stabilita dalla legge che può essere prorogata o rinnovata. L'art. 11 del disciplinare di concessione (Durata della concessione) stabilisce che, salvo i casi di decadenza, revoca o rinuncia la concessione, per gli impianti di Comunacqua e di Scalelle, è accordata per un periodo di anni sessanta (60) successivi e continui decorrenti da 1° ottobre 1940, data dell'autorizzazione provvisoria all'inizio dei lavori.
Al termine della concessione o nel caso di decadenza o rinuncia è previsto che passino in proprietà dello Stato senza compenso tutte le opere di raccolta, regolazione e derivazione, principali ed accessorie, i canoni adduttori dell'acqua, le condotte forzate ed i canali di scarico, il tutto in stato di regolare funzionamento. Allo stato attuale, pur non essendo noto agli scriventi i termini del rinnovo, il fatto che questi impianti siano tutt'ora in esercizio evidenzia che il gestore sia ancora titolare della concessione che, in base alle norme oggi vigenti, è di durata trentennale a partire dall'ottobre 2000.

5. ELABORAZIONE DATI

A partire dai valori medi mensili delle portate turbinate forniti da ENEL, per il periodo 2002-2006, sono stati calcolati i valori medi mensili delle portate derivate dal Fiume Aniene e dal Torrente Simbrivio dalle centrali idroelettriche di Comunacqua, Scalelle e Subiaco (*Tab. III, IV e V*). Si tratta, perciò, di impianti ad acqua fluente che utilizzano le acque di scarico delle centrali a monte integrandole con gli apporti derivati dal fiume (*Fig. 2*).

[1] 1 Modulo=100 l/s
[2] Art.1 (Quantità ed uso dell'acqua da derivare) - D.M. Lavori Pubblici del 15/05/1974 e relativo "Disciplinare di obblighi e condizioni cui dovrà essere vincolata la derivazione di acqua dal fiume Aniene e Simbrivio chiesta dal consorzio idroelettrico Alto Aniene e Simbrivio con istanze 5 Agosto 1938-13 Giugno 1941 e 31 Agosto 1955 (Consiglio Superiore dei Lavori Pubblici-adunanza del 27 settembre 1990).

TABELLA III - Centrale di Comunacque - portate medie mensili derivate dall'Aniene e dal Simbrivio (m^3/s)

Centrale idroelettrica di Comunacqua													
Anno	Gennaio	Febbraio	Marzo	Aprile	Maggio	Giugno	Luglio	Agosto	Settembre	Ottobre	Novembre	Dicembre	Media annuale
2002	0,90	1,29	1,18	0,91	1,50	1,01	0,83	0,58	0,36	0,77	0,92	1,13	0,95
2003	2,10	1,42	0,98	1,24	2,11	1,84	0,66	0,39	0,45	0,74	1,12	1,27	1,19
2004	1,51	1,72	1,97	2,95	5,88	3,53	2,79	1,21	1,14	0,80	0,58	1,16	2,10
2005	0,98	0,51	1,54	2,20	4,03	2,37	1,34	0,91	0,63	0,74	0,51	1,23	1,42
2006	1,26	1,03	1,80	2,05	3,12	2,83	2,01	1,41	0,72	0,63	0,66	0,62	1,51

TABELLA IV - Centrale di Scalelle-portate medie mensili derivate dall'Aniene e dal Simbrivio (m^3/s)

Centrale idroelettrica di Scalelle													
Anno	Gennaio	Febbraio	Marzo	Aprile	Maggio	Giugno	Luglio	Agosto	Settembre	Ottobre	Novembre	Dicembre	Media annuale
2002	0,63	0,78	0,77	0,55	1,16	0,84	0,67	0,44	0,70	1,10	2,15	2,35	1,01
2003	4,13	3,21	3,08	2,52	1,69	0,98	1,12	1,01	0,71	0,99	1,74	3,74	2,08
2004	3,66	4,18	5,45	6,01	3,90	3,78	2,67	2,09	1,30	1,04	1,13	3,46	3,23
2005	3,42	1,96	3,71	6,33	3,53	2,65	1,88	1,24	0,96	1,28	1,36	5,27	2,80
2006	5,74	4,63	5,48	5,72	2,64	2,21	1,11	0,93	0,92	0,60	0,19	0,17	2,53

TABELLA V - Centrale di Subiaco-portate medie mensili derivate dall'Aniene (m^3/s)

Centrale idroelettrica di Subiaco													
Anno	Gennaio	Febbraio	Marzo	Aprile	Maggio	Giugno	Luglio	Agosto	Settembre	Ottobre	Novembre	Dicembre	Media annuale
2002	**-0,36**	1,08	0,53	0,08	0,43	0,49	0,27	**-0,05**	0,54	1,09	0,72	0,73	0,46
2003	1,72	1,76	1,48	0,50	1,24	0,58	0,70	0,58	0,20	0,72	1,60	0,95	1,00
2004	1,17	1,58	0,62	**-1,03**	**-2,08**	0,25	0,95	0,89	0,83	0,42	1,08	0,45	0,42
2005	1,46	0,99	1,90	**-0,81**	**-0,34**	0,59	0,91	0,65	0,53	1,03	0,71	0,35	0,66
2006	0,72	0,77	0,78	0,14	2,25	0,66	0,73	0,34	0,62	0,76	0,02	0,61	0,70

La centrale di Comunacqua è alimentata dal bacino Pertuso, realizzato mediante una diga a gravità in calcestruzzo sul Fiume Aniene, e dal bacino Simbrivio, anch'esso sbarrato con una diga a gravità. In particolare poiché Comunacqua è la centrale di testa dell'asta è lecito, a regime, considerare l'equivalenza tra portate derivate e portate turbinate (*Tab. III*). Dall'andamento delle portate derivate riportato in *Figura 4* è stato possibile notare che in alcuni mesi dell'anno le portate medie derivate dalla centrale di Comunacqua raggiungono valori prossimi alle portate massime concesse. L'analisi di questi dati fa emergere che le massime derivazioni avvengono tra i mesi di Aprile e di Luglio.

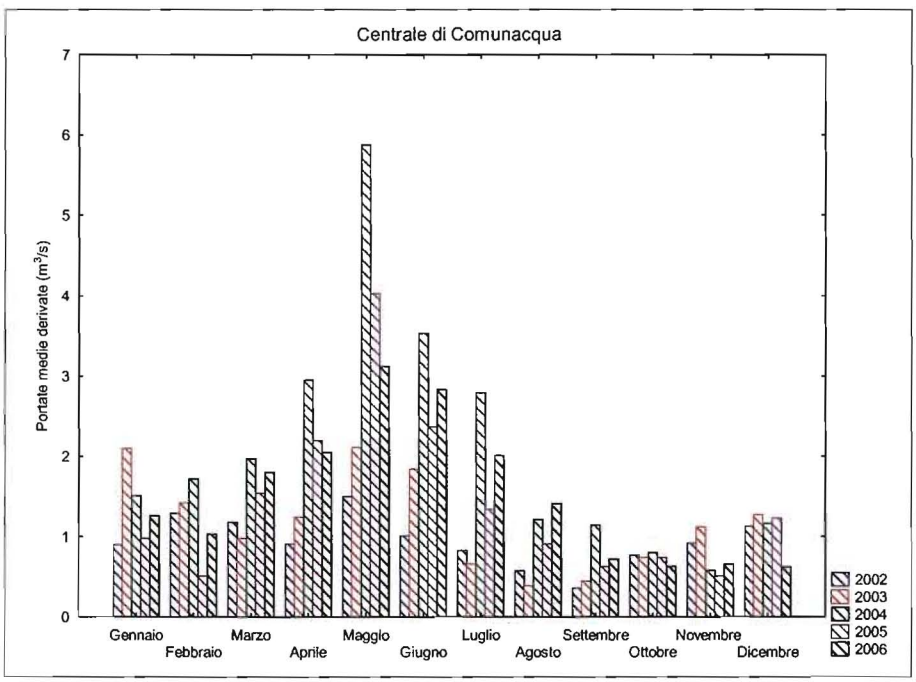

Figura 4 - Portate medie derivate dalla centrale di Comunacqua.

La centrale di Scalelle, a valle di Comunacqua, utilizza invece i rilasci della centrale a monte integrandoli con le acque derivate dall'Aniene e dal Simbrivio.

Tali integrazioni sono state calcolate sottraendo alle portate turbinate dalla centrale di Scalelle le portate in uscita dalla centrale di Comunacqua (*Tab. IV*).

L'analisi dimostra che il funzionamento della centrale di Scalelle si basa in modo preponderante sulle derivazioni dall'Aniene e dal Simbrivio (*Fig. 5*). Inoltre, trattandosi

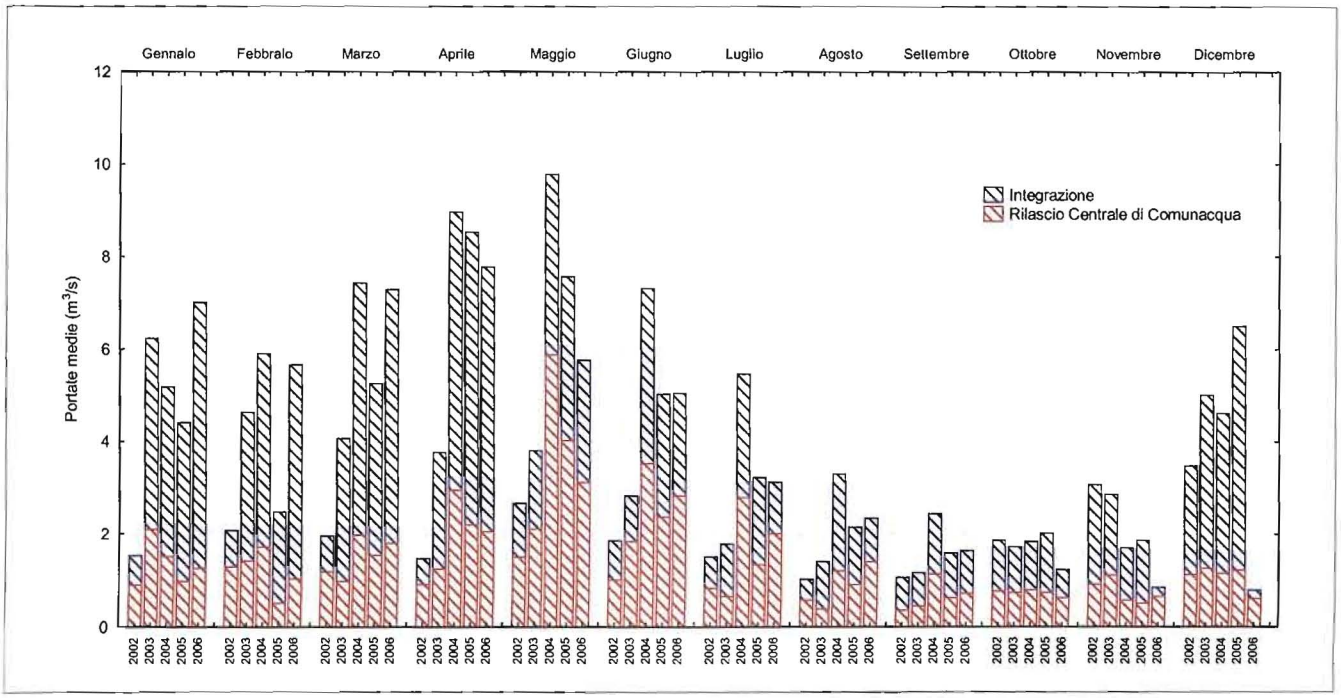

Figura 5 - Portate medie derivate dalla centrale di Scalelle.

di impianti ad acqua fluente, le massime derivazioni registrate nella centrale di Comunacqua tra Aprile e Luglio (*Fig. 4*) si riflettono sull'impianto di Scalelle nello stesso periodo di tempo.
La centrale di Subiaco utilizza invece le acque di scarico di Scalelle e gli apporti da una presa ricavata sul Fiume Aniene, in località Ponte delle Scalelle, in corrispondenza dello scarico della centrale di monte. Anche in questo caso le portate derivate sono state ottenute sottraendo alle portate turbinate dalla centrale di Subiaco le portate in uscita dalla centrale di Scalelle (*Tab. V*).
Per alcuni mesi le elaborazioni di tali misure forniscono valori di portata derivata, che risultano, apparentemente, di valore negativo (*Tab. V*). Questo fenomeno potrebbe essere spiegato da un difetto di funzionamento della centrale di Subiaco che restituisce in alveo l'eccesso di portata proveniente da Scalelle, che non riesce ad essere turbinata. (*Tab. VI*).

TABELLA VI - Centrale di Subiaco-portate medie mensili effettive derivate dall'Aniene (m³/s)

Centrale idroelettrica di Subiaco													
Anno	**Gennaio**	**Febbraio**	**Marzo**	**Aprile**	**Maggio**	**Giugno**	**Luglio**	**Agosto**	**Settembre**	**Ottobre**	**Novembre**	**Dicembre**	**Media annuale**
2002	**0**	1,08	0,53	0,08	0,43	0,49	0,27	**0**	0,54	1,09	0,72	0,73	0,46
2003	1,72	1,76	1,48	0,50	1,24	0,58	0,70	0,58	0,20	0,72	1,60	0,95	1,00
2004	1,17	1,58	0,62	**0**	**0**	0,25	0,95	0,89	0,83	0,42	1,08	0,45	0,42
2005	1,46	0,99	1,90	**0**	**0**	0,59	0,91	0,65	0,53	1,03	0,71	0,35	0,66
2006	0,72	0,77	0,78	0,14	2,25	0,66	0,73	0,34	0,62	0,76	0,02	0,61	0,70

Per la centrale di Subiaco la situazione sembra quindi ribaltarsi: il suo funzionamento si basa quasi esclusivamente sui rilasci delle centrali a monte, con integrazioni di modesta entità dal Fiume Aniene (*Fig. 6*).
Per ogni centrale, inoltre, sono state confrontate rispettivamente le portate medie annuali con i moduli di concessione medi e le portate medie mensili con i moduli di concessione massimi. Si è constatato come in ogni occasione siano stati rispettati i limiti stabiliti dal provvedimento di concessione precedentemente citato (*Tab. II*).
In base ai dati a disposizione si è proceduto quindi alla redazione di un bilancio idrico mensile per il periodo di osservazione 2003-2006.
Nella redazione del presente lavoro si è scelto di considerare separatamente i tre tratti di corsi d'acqua analizzati:
- T1: Fiume Aniene a monte della confluenza con il Torrente Simbrivio;
- T2: Torrente Simbrivio;
- T3: Fiume Aniene a valle della confluenza con il Torrente Simbrivio.

Le portate medie mensili prelevate, per uso idropotabile ed idroelettrico, e i rilasci di acque reflue sono stati i termini considerati per la redazione del bilancio. Partendo dalla sezione di monte (Sorgente Pertuso) e arrivando fino alla sezione di chiusura (Subiaco) sono stati calcolati mensilmente i volumi idropotabili ed idroelettrici derivati e i volumi di acque reflue restituiti.

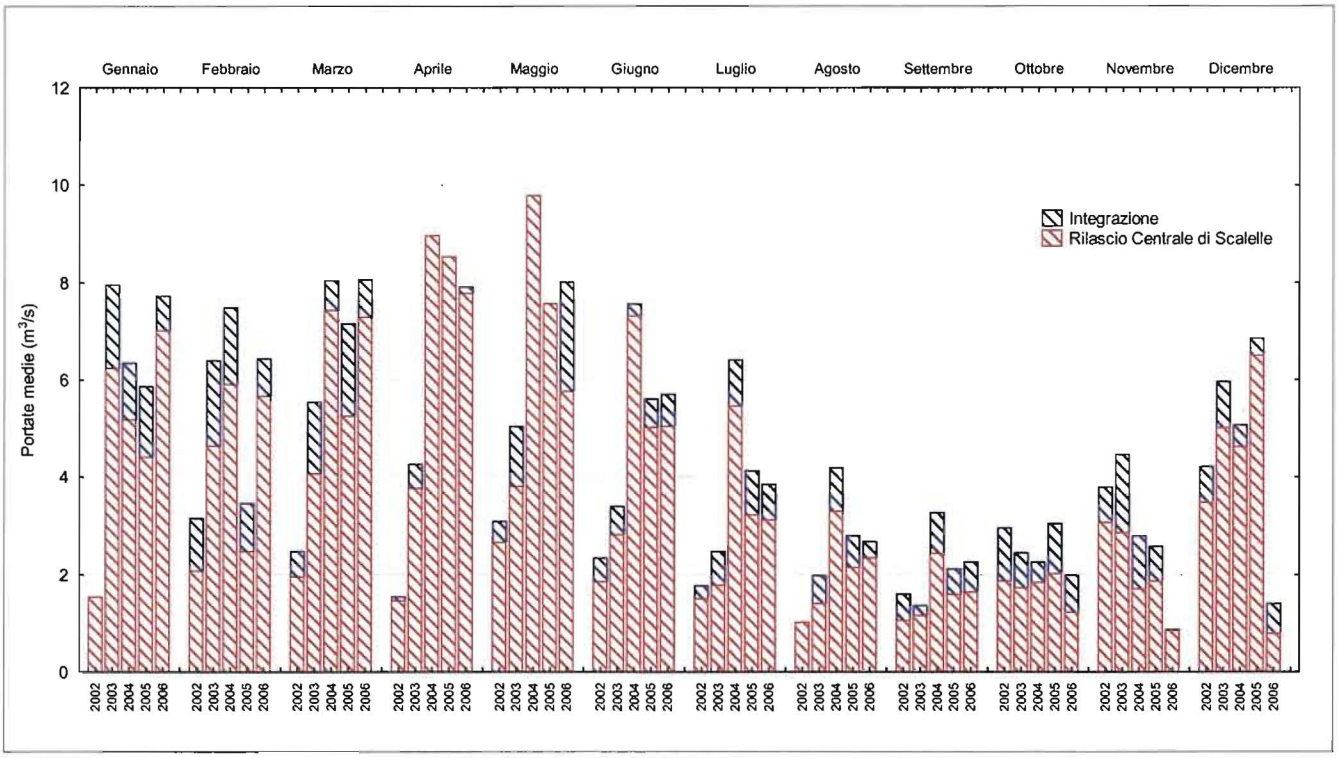

Figura 6 - Portate medie derivate dalla centrale di Subiaco.

Dal bilancio mensile tra derivazioni e restituzioni si è quindi passati al calcolo del volume netto annuale sottratto al Fiume Aniene e al Torrente Simbrivio fino alla sezione di Subiaco (*Tab. VII*).

TABELLA VII - Volumi netti annuali derivati

Anno	Volume Netto Annuale Derivato (m^3)
2003	161.875.989
2004	220.822.562
2005	187.736.200
2006	181.448.440

TABELLA VIII - Volumi netti annuali derivati

Anno	Corpo Idrico	Derivato		
		Idropotabile (m^3)	Idroelettrico (m^3)	Totale (m^3)
2003	T1	13.497.408	52.550.208	66.047.616
	T2	13.489.373	52.550.208	66.039.581
	T3	0[1]	32.221.152	32.221.152
2004	T1	11.255.155	85.588.272	96.843.427
	T2	18.753.206	85.588.272	104.341.478
	T3	0	22.070.016	22.070.016
2005	T1	14.182.646	67.736.736	81.919.382
	T2	16.085.434	67.736.736	83.822.170
	T3	0	24.427.008	24.427.008
2006	T1	14.007.584	64.924.416	79.002.000
	T2	17.455.824	64.924.416	82.380.240
	T3	0	22.498.560	22.498.560

In particolare poichè le centrali di Comunanque e Scalelle sono alimentate sia dall'Aniene che dal Simbrivio, è stata ipotizzata una distribuzione dei prelievi del 50% tra i due alvei. In questo modo, poiché i due corsi d'acqua appartengono al medesimo bacino, non sono stati alterati i termini del bilancio complessivo.

Sono stati quindi considerati i singoli contributi dei tre tratti di corsi d'acqua al volume derivato totale (*Tab. VIII*):

Dalla *Tabella VIII* è possibile notare che i volumi prelevati dalle derivazioni idroelettriche rappresentano di gran lunga la maggior parte dei volumi totali sottratti (80%-100%) rispetto alle derivazioni idropotabili (0%-20%).

Peraltro i maggiori contributi al bilancio, provenienti dai consumi idroelettrici, si riscontrano nei primi due tratti di corsi d'acqua considerati. Infatti, nel tratto a valle della confluenza con il Simbrivio tali volumi diminuiscono notevolmente a causa dell'inversione di tendenza tra prelievi e rilasci registrata nella centrale di Subiaco (*Fig. 6*). Se, infatti, la centrale di Subiaco sembra essere stata dimensionata per turbinare i rilasci di Comunacqua (*Fig. 6*), la centrale di Scalelle appare essere alimentata, quasi esclusivamente, dalle cospicue integrazioni dall'Aniene, di cui ha bisogno per il suo funzionamento (*Fig. 5*). Nel periodo 2003-2006 i prelievi idropotabili si mantengono tra $2x10^6$ e $4x10^6$ m^3 mentre variano sensibilmente quelli idorelettrici che rappresentano il maggior contributo al volume derivato totale (*Fig. 7*).

Nella sostanza, dalle elaborazioni qui presentate, emerge che tali derivazioni non costituiscono un prelievo dissipativo in termini di bilancio complessivo del bacino in esame, tuttavia, se riferiti alla sola Alta Valle dell'Aniene, esse rappresentano il maggior contributo all'utilizzazione idrica locale.

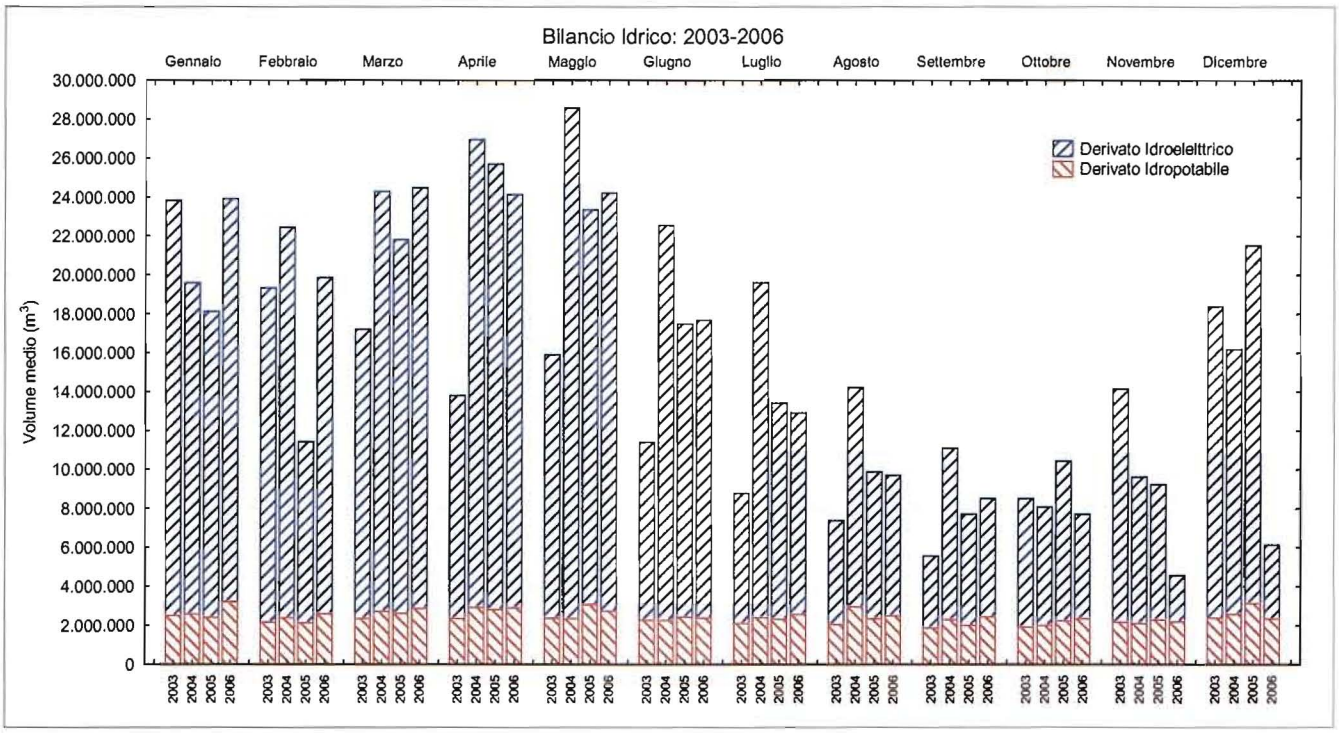

Figura 7 - Volumi derivati nel quadriennio 2003-2006.

6. LA RICARICA DELL'ACQUIFERO

La valutazione della ricarica media annua degli acquiferi carbonatici carsici è, in generale, difficilmente quantificabile con accettabile approssimazione, data la complessità di funzionamento di questi sistemi idrogeologici, nei quali gli scambi con corpi idrici esterni non sono di immediata identificazione. Nel caso particolare il bacino dell'Alto Aniene è caratterizzato dalla presenza di molteplici derivazioni e serbatoi, che, con il loro funzionamento aggiungono fattori significativi di incertezza nella valutazione del bilancio idrico del sistema.

Per tale motivo, probabilmente, non è stato possibile trovare in letteratura un valore consolidato della ricarica media annua relativo al bacino dell'Aniene, e nemmeno alla sua parte alta. Nel presente studio perciò, al fine di definire il quadro di riferimento per la valutazione dello utilizzazione delle risorse idriche nell'area in esame, sono stati elaborati i più recenti dati disponibili, relativi alla portata media in periodo di magra del Fiume Aniene alla sezione di Subiaco (Boni, 2006), giungendo alla stima di un volume medio annuo di ricarica, pari a circa 190.000.000 m³.

Sono stati quindi confrontati i volumi derivati precedentemente calcolati con tale valore della ricarica media annua assunto come riferimento per il Bacino dell'Alto Aniene (*Tab. IX*).

TABELLA IX - Confronto tra volumi derivati e ricarica media annua

Anno	Derivato Idropotabile (m^3)	Derivato Idroelettrico (m^3)
2003	26.986.781	137.321.568
2004	30.008.362	193.246.560
2005	30.268.080	159.900.480
2006	31.533.408	152.347.392

Dalla *Tabella IX* è possibile osservare che i prelievi idropotabili rappresentano circa il 15% della ricarica media annua, mentre quelli idroelettrici costituiscono la parte più rilevante del sistema di derivazione dell'Alto Aniene, arrivando nel 2004 a rappresentare il 100% della ricarica stessa.

7. CONCLUSIONI E CONSIDERAZIONI

La documentazione esaminata, alla luce del quadro geologico, idrogeologico ed ambientale complessivo dell'area di studio, che si riferisce all'Alta Valle del Fiume Aniene, fra la sorgente del Pertuso e Subiaco, evidenzia che la particolare interpretazione della normativa vigente in materia di risorse idriche adottata in questa porzione di territorio sembra condurre ad un uso della risorsa non propriamente economico ed ecosostenibile. In altre parole, com'è noto, la L. 36/94, confluita, senza sensibili modificazioni almeno per quanto di interesse in questa sede, nel D.Lgs. 152/2006 e successivamente nel D.Lgs. 4/2008, sancisce con chiarezza che "L'uso dell'acqua per il consumo umano è prioritario rispetto agli altri usi del medesimo corpo idrico superficiale o sotterraneo. Gli altri usi sono ammessi quando la risorsa è sufficiente e a condizione che non ledano la qualità dell'acqua per il consumo umano."[3] Al tempo stesso è nota e consolidata la giurisprudenza in materia che riconosce agli esercenti di impianti idroelettrici il diritto a beneficiare della titolarità di concessioni pregresse. Ma ciò era vero fino all'anno 2000, in condizioni ordinarie, mentre, successivamente, in seguito all'emanazione della specifica Ordinanza del Presidente del Consiglio dei Ministri, rinnovata annualmente, ed ancora oggi vigente, lo stato di emergenza idrica in cui versano i Comuni originariamente serviti dal Consorzio Acquedottistico del Simbrivio, è tale che qualche valutazione, anche di carattere strategico, sarebbe opportuna; con il presente lavoro si è voluto solo proporre qualche elemento di riflessione.

[3] *Art. 2 - Comma 1 - L. 36/1994 "Disposizioni in material di risorse idriche".*

BIBLIOGRAFIA

Accordi G., **Carbone F.**, *Carta delle litofacies del Lazio-Abruzzo ed aree limitrofe.* Quaderni de "La ricerca scientifica"n. 114, vol. 5, 1988.

Acea ATO 2 S.p.A., *La ristrutturazione dell'approvvigionamento idrico dell'ATO. Documento tecnico preliminare della STO*, Segreteria tecnico operativa. Lazio centrale-Roma, 5 Luglio 2005.

Autorità di Bacino del Fiume Tevere, *Piano Stralcio per la programmazione ed utilizzazione della risorsa idrica*, Giugno 2006.

Boni C., *PS9: Piano Stralcio per la programmazione ed utilizzazione della risorsa idrica. Autorità di Bacino del fiume Tevere*, 2006.

Bosellini A., *Dynamics of Tethyan carbonate platforms. In Controls on Carbonate platform and basin development (eds. Crevello, P.D. et al)*, SEPM (Society for Sedimentary Geology), Special Publication 44, 3–13, 1989.

Bosellini A., *Introduzione allo studio delle rocce carbonatiche,* Bovolenta Ed., Ferrara. 1991.

Cipollari P., **Cosentino D.**, **Parotto M.**, *Modello cinematico-strutturale dell'Italia centrale*. Studi Geologici Camerti, Vol. spec., 1995/2, 135-143, 1997.

Damiani A. V., *Studi sulla piattaforma carbonatica laziale-abruzzese. Nota I considerazioni e problematiche sull'assetto tettonico sulla paleogeologia dei Monti Simbruini*, Roma, Istituto Poligrafico e Zecca dello Stato. (Estr. da: Memorie Descrittive della Carta Geologica d'Italia, vol. 38, 145-175), 1990.

Damiani A. V. et al., *Elementi litostratigrafici per una sintesi delle facies carbonatiche meso-cenozoiche dell'Appennino Centrale; Camerino*, Università degli Studi di Camerino. (Estr. da: Studi Geologici Camerti, Vol. spec., 187-213), 1991.

D.M. Lavori Pubblici del 25 ottobre 1974 e relativo "*Disciplinare di obblighi e condizioni cui dovrà essere vincolate la derivazione di acqua dal fiume Aniene e Simbrivio chiesta dal consorzio idroelettrico Alto Aniene e Simbrivio con istanze 05/08/1938-13/06/1941 e 31/08/1955*" (Consiglio Superiore dei Lavori Pubblici-adunanza del 27/09/1990).

I.G.M., *Carta Geologia D'Italia. Foglio 145, Avezzano.*

Ventriglia U., *Idrogeologia della Provincia di Roma, IV, Regione orientale*, Amministrazione Provinciale di Roma, Assessorato LL.PP, Viabilità e trasporti, 1990.

Validation Of Salt Dilution Method For Discharge Measurements In The Upper Valley Of Aniene River (Central Italy)

GIUSEPPE SAPPA*, FLAVIA FERRANTI, GIAN MARCO PECCHIA
Department of Civil, Building and Environmental Engineering (DICEA)
Sapienza University of Rome
Via Eudossiana 18, 00184, Rome
ITALY
giuseppe.sappa@uniroma1.it

Abstract: - Stream discharge can be measured using several methods, which can be influenced by the natural streaming characteristics of the river. The conventional approach to measuring stream flow is the current meter method, based on determining the mean discharge using the velocity and the cross sectional area. This method allows quick stream flow measurements, but in mountain streams, during turbulent flow conditions, or in case of flow depths, smaller than the recommended performance limits for conventional current meters, can give unreliable measurements. An alternative method of stream flow measurement is the salt dilution method that involves injecting an artificially tracer (usually NaCl) and determining its dilution, following complete mixing into the flow, by means of integration of the electrical conductivity as a function of time. This technique is available for use in mountain streams where the other procedures are more problematic. This paper deals with the preliminary results referred to the validation of the salt dilution method in the Upper Valley of Aniene River (Central Italy), in the aim if defining a reliable methodology for the evaluation of discharge in mountain streams, where turbulent flows make difficult apply the conventional current meter method. In the following they are presented the preliminary results of stream discharge measurements, coming from three different campaigns driven from September to October 2014, executed in one of the sections of Aniene River. The comparison of these elaborations, carried on by the application of both methods, is useful to define the reliability and accuracy of discharge measurements carried out by salt dilution method.

Key-Words: - discharge measurement, salt dilution method, mountain streams, current meter method, slug injection, Aniene River

1 Introduction

Karst aquifers play a key role in human life and economic activity and constitute more than 30 % of the EU land mass [1]. The fast dynamic of karst aquifers discharge is, as a consequence of strong interconnection between groundwater, surface water and precipitation, due to a network of highly permeable flow features, embedded in a less permeable fractured rock matrix [2]. In these complex hydrogeological scenarios, stream discharge can be influenced by changes in meteorological conditions, tributary streams or from groundwater seeping into the river. Variations in stream flow discharge can bee used for characterizing karst systems and investigating the processes that control interactions between groundwater and surface water [3]. Water resources assessment is an important tool to evaluate groundwater dynamics in relation to human impacts and drinking water consumption [4]. Thus, the determination of the amount of stream flow discharge is a direct measure of the amount of water available for drinking, industrial, and agricultural purposes. Stream discharge is also correlated with the habitat biodiversity and the assimilation of nutrients and sediment in runoff, reflecting the integrity of the riparian ecosystem [5]. This paper presents preliminary results of discharge measurements carried out in a gauging section along the Aniene River by the application of traditional current meter and salt dilution method, in framework of the Environmental Monitoring Plan related to the catchment project of the Pertuso spring, in the Upper Valley of Aniene River (Central Italy), which is going to be exploited to supply an important water network in the South part of Roma district [6].

Discharge measurements have been carried out performing a slug injection of a NaCl solution and recording electrical conductivity in a downstream section, while at the same time, current meter measurements have been taken in a section placed

between the injection point and the electrical conductivity measurement section.

The aim of this work is the validation of the salt dilution method as alternative methodology in mountain stream, where the unsteady flow conditions can make difficult and expensive the application of the conventional velocity area method.

2 Problem Formulation

The measurement of stream flow rate is usually required for river management purposes including water resources planning and protection of flood prevention.

Stream flow measurement technology has evolved rapidly over recent decades. According to the U.S. Geological Survey (USGS) procedure, river discharge can be usually calculated by the velocity area method, as the product of average stream flow velocity at a cross section, perpendicular to the main stream flow, and the cross sectional area. In this method, the river is divided into segments and the discharge through each segment is calculated by multiplying the average velocity in each segment by the segment area. A current meter is usually used to measure the stream velocity at each selected segment. The sum of the products of area velocity for each segment gives the total stream discharge [7].

The conventional velocity area method has some limitations in mountains stream where the irregular cross section and the strong turbulence decrease the accuracy with which water depth and flow velocity can be measured. In addition, flow depths and velocities during low flow conditions may be too small for reliable measurements [8]. This method is also both expensive and difficult especially during floods or unsteady flow conditions due to the instability of measuring instrument. The unsteady flow may be caused by turbulent conditions, irregular bed stream geometry and the growth of weeds (Fig. 1). Thus, the current meter method requires a definitive relationship between velocity measurement and area of the cross section, which is difficult to establish in mountain river, where the hydraulic pattern changes seasonally. This method is generally used because is the most practical and quick for stream flow measurements, except where the river is very shallow or in turbulent condition. Thus, under such conditions, the alternative method of salt dilution may be more suitable.

Figure 1 - An example of unsteady flow conditions (Aniene River)

In the salt dilution method, a tracer solution is injected into the river to be diluted by the stream discharge. Downstream of the injection point, when vertical and lateral dispersion throughout the flow is complete, the discharge may be calculated by the measurement of the electrical conductivity as a function of time. Common table salt (sodium chloride, NaCl) is generally used for salt dilution measurements because it is inexpensive, easily available and non-toxic for the concentrations and exposure times typically associated with discharge measurements.

The salt dilution method is generally used for discharge measurements in mountain streams where swallow depths, turbulent conditions and the irregular, bad geometry of the stream can make difficult to establish the hydraulic profile, and even difficult to measure stream flow velocity with the traditional current meter [9].

A limit of this methodology is the amount of tracer to be added to increase the electrical conductivity in the stream flow, which is related to the stream background level of the conductivity. Moreover, only a runoff less than $4m^3s^{-1}$ can be made easily, because the amount of salt to be dissolved is difficult to handle (about 20 kg of salt for $4m^3s^{-1}$ runoff) [10].

2.1 The test site

The study area is located along the SW boundary of the Simbruini Mountains, characterized by the confluence of the Fiumata Valley and the Granara Valley from which starts the Valley of Aniene River [11]. In this area it outcrops an important carbonate karst aquifer, mainly made of highly permeable Cretaceous carbonate rocks, deeply fractured and mostly soluble (Fig. 2).

ISBN: 978-1-61804-301-6

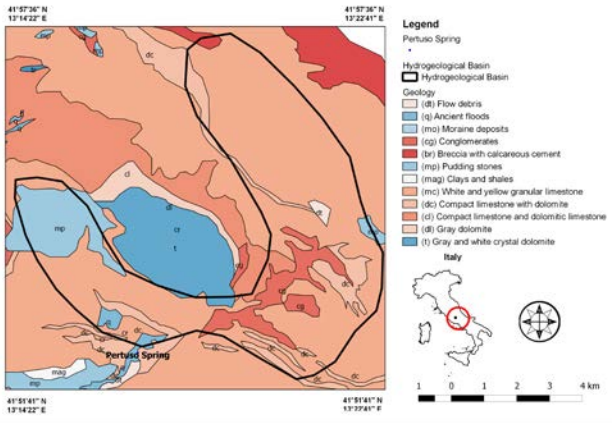

Figure 2 - Simplified geological map of the study area

The discharge measurements were carried out in the Upper Valley of Aniene River, between the town of Filettino and Trevi nel Lazio (FR), in Latium Region, Central Italy (Fig. 3). The Aniene River crosses the Natural Park of Simbruini Mountains, the largest protected area of Latium Region, which belongs to Nature 2000 network as Special Protection Areas (SPAs). The Park is characterized by karst landscape where take origin mountains springs that discharge into the Aniene River, like the Pertuso spring which supplies drinking water to the city of Rome and currently is feeding the Comunacqua hydroelectric power plant, owned by ENEL group.

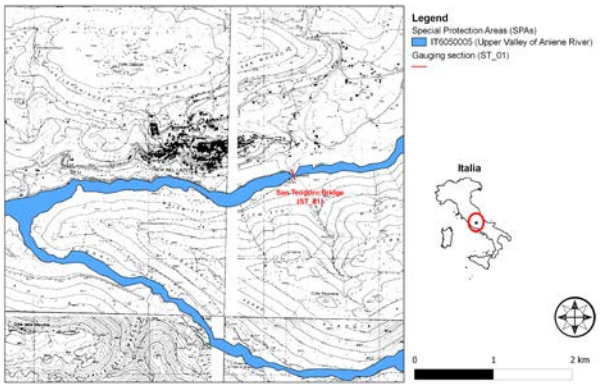

Figure 3 - Study area and location of gauging section

In the framework of this work, the discharge data have been collected referred to three campaigns driven from September to October 2014, using the current meter method and the salt dilution method.
San Teodoro Bridge (Fig. 4) has been chosen as gauging section (ST_01), allowing easy installing and management of the current meter, but also satisfying the salt dilution method requirements.

Figure 4 - San Teodoro Bridge gauging section (ST_01)

San Teodoro Bridge gauging station is relatively straight to ensure streamlines parallel to each other and reduce errors in velocity measurements. The bed stream relatively uniform and free of heavy aquatic growth allows keeping the current meter perpendicular to the flow while measuring velocity, to ensure a stable relation between stage and discharge. ST_01 gauging station is also suited for measuring stream flow by salt dilution method. As a matter of fact, in the section there are no backwater areas and local inflows between the injection and measurement points, where the salt can be delayed and separated from the main flow. The bridge makes easy the slug injection of the tracer solution and allows rapid dissolution and complete mixing into the flow.

At ST_01 gauging station the Aniene River surface width ranges from 4.5 to 5 meters and its depth from 0.2 to 1 meter, according to the limits imposed by the type of current meter used.

2.2 The current meter method

The current meter method involves measuring the area and the velocities of a stream at a cross section which is perpendicular to the main flow of the river. Usually, river discharge (Q) is calculated as the product of the cross section area (A) of flow by the average stream flow velocity (V) in that cross section:

$$Q = V \cdot A \quad (1)$$

Thus, the river cross section is divided into numerous vertical sub-sections (n), in each one the area is obtained by measuring the width (l_i) and depth (h_i) of the sub-section and the stream flow velocity is determined using a current meter. The total discharge is then computed by summing the discharge of each sub-section [12]:

ISBN: 978-1-61804-301-6

$$Q = \sum_{i=1}^{n} l_i \cdot h_i \cdot \overline{v_i} \quad (2)$$

The preliminary step in stream flow measurements is the determination of water widths by stringing a measuring tape from bank to bank at right angles to the direction of flow. In mountain stream, where the hydraulic pattern changes monthly, more than a single measurement is needed to characterize accurately the hydraulic profile of the cross section. For this reason it has been necessary determine the hydraulic profiles of the ST_01 for each discharge measurements campaigns driven in September and October 2014 (Figg. 5 and 6).

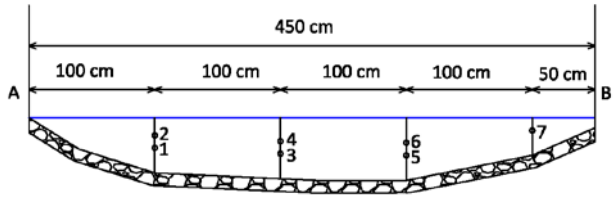

Figure 5 - Stream cross section illustrating sub-sections to determine discharge by current meter method (September 2014)

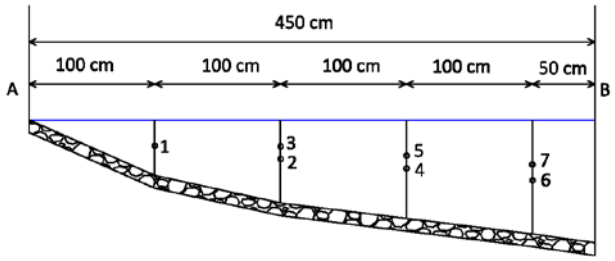

Figure 6 - Stream cross section illustrating sub-section to determine discharge by current meter method (October 2014)

This measuring tape is used to define the hydraulic profile of the cross section and the location of each velocity measurements. Determining the cross sectional area of a stream involves measuring water depths at a series of points across the stream and multiplying by the width of the stream within each segment represented by the depth measurement.

With the aim to obtain a mean velocity, ST_01 section has been divided into 4 vertical parts, almost equally spaced by 1.00 m. Along each one of these investigated verticals, up to 2 measuring points have been defined at different depths (0.2 and 0.3 m from bed stream).

The main equipment needed to measure the stream flow velocity in each verticals is a SEBA horizontal axis current meter F1, having a propeller diameter of 80 mm which, combined with SEBA Z6 pulse counter, allows to measure velocity between 0,025 m/s and 10 m/s. The SEBA current meter has been used as rod equipment with tail plane for best positioning to the flow direction.

The operating principle is based on the proportionality between the flow velocity and the resulting angular velocity of the rotor. For each measurement point, flow velocity is determined counting the number of spins of the meter rotor during a fixed interval of time. The current meter responds instantly to any changes in water velocity but in unsteady flow conditions is difficult obtain accurate measurements due to the difficult of keeping the current meter attached to the measuring line. Thus, in order to assess any fluctuations due to the turbulence condition and, also, to avoid accidental measurement errors, velocity has been measured for at least 60 seconds, according to EN ISO 748:2007 requirements [13].

This current meter method gives the local water velocity in each vertical following the application of a calibration equation between stream velocity (cm/sec) and the number of spins (sec^{-1}) (3).

$$v = 0.82 + 33.32 \cdot n \quad (3)$$

Stream discharge measurements obtained by the velocity area method are summarized in Tab. 1.

Date	Gauge Height (m)	Discharge Q (m^3/s)
10/09/2014	0.60	1.38
29/09/2014	0.50	0.98
17/10/2014	0.70	1.77

Table 1 - Mean discharge values obtained by current meter method

Table 1 shows the discharge values coming out from the three measurements campaigns, referred to the maximum height value, measured in the stream in each campaign. By the chance the average value among the three ones, calculated, is Q = 1.38 m^3/s, which is the same measured in the September 2014 campaign.

2.3 The salt dilution method

There are two variations on dilution gauging, depending on whether the tracer is injected into the stream at a constant rate or as an instantaneous slug. The salt dilution method by slug injection was chosen as the most practical method in the study area, because of the difficulty of handling the large

ISBN: 978-1-61804-301-6

quantities of salt solution required by the constant rate injection.

The basic principle of salt dilution method is to add instantaneously a known quantity of a NaCl solution into the stream and observe the variations in electrical conductivity at a point where it is fully mixed with the flow.

ST_01 gauging station is an ideal injection site because has the basic characteristics for accurate streamflow measurements by salt dilution method. In fact, the turbulent condition allows completely dissolution and fully mixing with the flow at the point where electrical conductivity is measured. San Teodoro Bridge has been used to dump the salt directly into the injection point: the turbulence created below the bridge allows the dissolution of the salt and the mixing into the stream.

According to IS0 9555-1:1994(E) requirements [14], the salt dilution method involves the injection of a volume of a NaCl solution at a cross section in which the discharge remains constant for the duration of the gauging. At a second cross section placed downstream the injection point, at a distance sufficient for the injected solution to be uniformly diluted, the stream electrical conductivity is determined over a period of time sufficiently long to ensure that the NaCl solution has passed through the second cross section [15].

It has been used a saturated NaCl-solution made by dissolving about 2 kg of salt in 10 liters of stream water, depending on the temperature and the background conductivity of the stream. A PC650 probe (Eutech Instruments) was used to collect the electrical conductivity measured data. The instrument is auto-ranging between 0 and 500 mS/cm, with an accuracy of ± 0.05%.

The dissolution of NaCl in water is proportional to water temperature and inversely proportional to the existing concentration of salt. After injection, the salt mixes into the stream by longitudinal dispersion, a process in which dissolved salt in the plume moves along its concentration gradient until a uniform concentration exists [16]. The instantaneously injection of NaCl solution into the stream produces downstream a wave of electrical conductivity increasing, as shown in Fig. 6.

The stream discharge, Q (m^3/s) is calculated by the following formula [17], based on the principle of the conservation of mass:

$$Q = C_s \cdot \frac{V_s}{\int_{t_0}^{t_0+t_p} \left[C(t) - C_b\right] \cdot dt} \qquad (4)$$

where: V_s (m^3) is the volume of injected solution, C_s (µS/cm) is the electrical conductivity of the injected solution, C_b (µS/cm) is the stream baseline electrical conductivity, $C(t)$ (µS/cm) is the stream electrical conductivity at time t, t_0 (s) is the elapsed time, taking as origin the instant at which the injection started and t_p (s) is the time of arrival of the first molecule of tracer at the cross section.

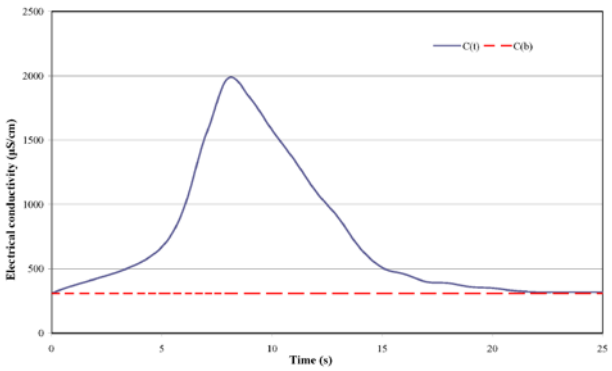

Figure 6 - An example of a salt dilution measurement done at ST_01

Table 2 lists discharge measurements obtain from the application of the salt dilution method carried out from September to October 2014.

Date	Gauge Height (m)	Discharge Q (m^3/s)
10/09/2014	0.60	1.30
29/09/2014	0.50	0.99
17/10/2014	0.70	1.71

Table 2 - Mean discharge values obtained by salt dilution method

The discharge values, measured by the salt dilution method, are definitely comparable with ones obtained by the traditional current meter method and in the following Table 3.

Date	Q (m^3/s)[1]	Q (m^3/s)[2]	Δ%
10/09/2014	1.38	1.30	8
29/09/2014	0.98	0.99	1
17/10/2014	1.77	1.71	6

Table 3 - Mean discharge values obtained by current meter method (1) and salt dilution method (2)

3 Problem Solution

Results of the two methods for determining stream flow discharge at San Teodoro Bridge gauging station (ST_01) were compared. Current meter method is usually the standard by which other stream flow measurement methods are compared.

ISBN: 978-1-61804-301-6

Thus, in Tab. 4, they are presented the results, coming from the application of the two methods, and the percentage differences, between each campaign result, expressed as:

Date	Gauge Height (m)	Q $(m^3/s)^1$	Q $(m^3/s)^2$	Δ %
10/09/2014	0.60	1.38	1.30	8
29/09/2014	0.50	0.98	0.99	1
17/10/2014	0.70	1.77	1.71	6

Table 4 - Mean discharge values obtained by the application of both methods

Preliminary results seem to give good indications for the validation of salt dilution method for discharge measurements. For example, at San Teodoro Bridge, both methods provide discharge measurements very close the to the other so that both methods could be performed for comparative purposes (Fig. 7).

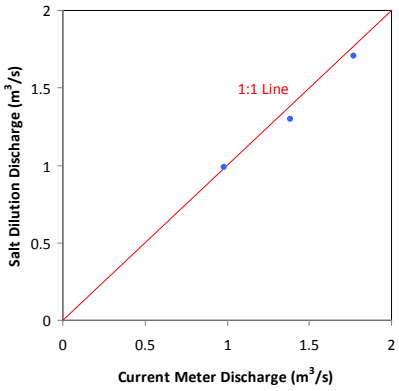

Figure 7 - Comparison of current-meter and tracer-dilution discharge measurements at ST_01

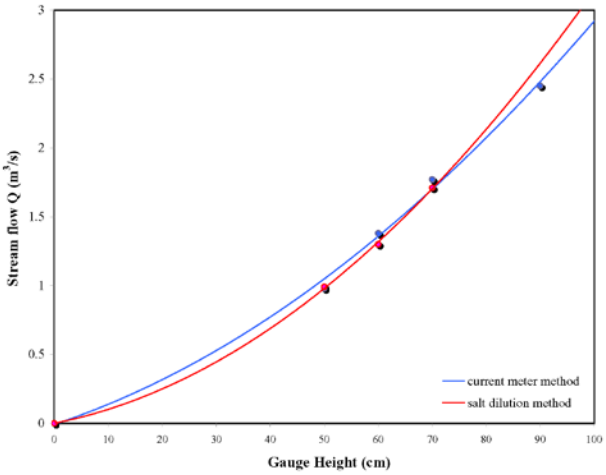

Figure 8 - Comparison of stream flow discharge as a function of time for current meter and salt dilution method

The rating curves for ST_01 gauging station show the changes in the stream flow depending on gauge height from September to October 2014. Rating curve based on current meter and salt dilution measurements, fitted by an exponential function, are very similar, with comparable discharge values coming from the application of both methods (Fig. 8).

The measurements collected by salt dilution method fell close to the rating curve based on current meter method, with a percentage differences of less 8%.

4 Conclusion

The purpose of this paper was to describe the preliminary results of a study to determine the feasibility and accuracy of discharge measurements using the salt dilution method in mountain river.

Data were collected from September to October 2014 at San Teodoro Bridge (ST_01), in the Upper Valley of Aniene River, by the application of conventional current meter and salt dilution method. The salt dilution stream flow has been compared to discharge measurements determined by current meter method. Based on these measurements, two different rating curves were developed to determine streamflow discharge.

The salt dilution method compares favorably in accuracy with current metering as a method of measuring streamflow in mountain river, and appears to be more accurate where the turbulence flow might interfere with current meter measuring. Furthermore, the salt dilution method is easier to apply and more economical in terms of equipment cost. Current meter method is well suited where flow conditions are close to laminar, whereas the salt dilution method are better fitting to river with unsteady flow conditions and the irregular stream bad geometry. However, in the traditional current meter method, excess sediment and seasonal growths of weeds can change the hydraulic profile of the cross section, requiring new rating curves at any measurements campaign.

Both methods seem to be complementary: in fact, while current metering requires laminar flow and is unsuited under turbulent conditions, the reverse is true of salt dilution gauging.

Even if the comparison with discharge measurements carried on by the application of both methods shows comparable values, several factors can affect the accuracy the discharge measurements

ISBN: 978-1-61804-301-6

obtained by salt dilution method. The loss of tracer between the injection point and the downstream cross section makes not applicable the equation for the conservation of mass and consequently the computation of stream discharge. Other factors that may have caused inaccuracies between current meter and salt dilution stream flow measurements are the tracer probe accuracy limits and the incomplete mixing throughout the stream cross section before the downstream gauging section is reached.

This fact let us pointing out the real importance of the determination of the degree to which an added tracer is diluted by the flowing water. The success of the slug injection methods requires the complete mixing of the added tracer diluted by the flowing water in as short a distance as possible.

References:

[1] S. Foster, R. Hirata, B. Andreo, The aquifer pollution vulnerability concept: aid or impediment in promoting groundwater protection?, *Hydrogeology Journal*, Vol.21, Issue 7, Springer, 1999, pp. 1389-1392.

[2] J.W. Hess, W.B. White, Storm response of the karstic carbonate aquifer of south central Kentucky, *Hydrogeology Journal*, Vol.99, Springer, 1988, pp. 235-252.

[3] B. Hagedorn, R.B. Whittier, Solute sources and water mixing in a flashy mountainous stream (Pahsimeroi River, U.S. Rocky Mountains): Implications on chemical weathering rate and groundwater–surface water interaction, *Chemical Geology*, Vol.391, 2015, pp. 123-137.

[4] G. Sappa, M. Barbieri, S. Ergul, F. Ferranti, Hydrogeological Conceptual Model of Groundwater from Carbonate Aquifers Using Environmental Isotopes (^{18}O, ^{2}H) and Chemical Tracers: A Case Study in Southern Latium Region, Central Italy. *Journal of Water Resource and Protection*, pp. 695-716, 2012.

[5] USGS, Sustainability of Groundwater Resources, *U.S. Geological Survey Circular 1186*, 1999.

[6] G. Sappa, F. Ferranti, An integrated approach to the Environmental Monitoring Plan of the Pertuso spring (Upper Valley of Aniene River), *Italian Journal of Groundwater*, 2/136, 2014, pp. 47-55.

[7] V.T. Chow, *Handbook of Applied Hydrology*. McGraw-Hill, NewYork, NY, 1964.

[8] Rantz S.E., et al. (1982). *Measurement and computation of streamflow*. Vol.1: *Measurement of stage and discharge*. Vol.2: Computation of discharge. U.S. Geological Survey Water Supply Paper, 1982.

[9] A.F. Pitty, The estimation of discharge from a karst rising by natural salt dilution, *Journal of Hydrology*, Vol.4, 1966, pp. 63-69.

[10] A. Gees, *Flow measurement under difficult measuring conditions: Field experience with the salt dilution method, in: Hydrology in Mountainous Regions I. Hydrological Measurements; The Water Cycle*, Journal of Hydrology, edited by: Lang, H. and Musy, A., IAHS Publ., 193, 1990, pp. 255-262

[11] F. Cipollari, D. Cosentino, M. Parotto, Modello cinematico-strutturale dell'Italia centrale, *Studi Geol. Camerti*, 1995, pp. 135-143.

[12] US EPA Region 6, Standard operating procedure for stream flow measurement, 2003.

[13] BS EN ISO 748:2007, Hydrometry. Measurement of liquid flow in open channels using current-meters or floats, 2007.

[14] ISO 9555-1/1994, Measurements of liquid flow in open channel - Tracer dilution methods for the measurement of steady flow - Part 1, 1994.

[15] R.D. Moore, Slug injection using salt in solution, *Streaml. Watershed Manage. Bull.*, 2005.

[16] T.J. Day, Field procedures and evaluation of a slug dilution gauging method in mountain streams. *Journal of Hydrology* (New Zealand) 16, pp. 113-133, 1977.

[17] K. Elder, R. Kattelmann, R. Ferguson, *Refinements in dilution gauging for mountain streams*, In Hydrology in Mountainous Regions. I – Hydrological Measurements; the Water Cycle. International Association for Hydrological Science (Proceedings of two Lausanne symposia, August 1990), IAHS Publication No. 193, pp. 247-254, 1990.

Appl Water Sci
DOI 10.1007/s13201-013-0135-9

ORIGINAL ARTICLE

Water quality assessment of carbonate aquifers in southern Latium region, Central Italy: a case study for irrigation and drinking purposes

Giuseppe Sappa · Sibel Ergul · Flavia Ferranti

Received: 27 February 2013 / Accepted: 11 October 2013

Abstract In southern Latium region, Central Italy, groundwater and spring water resources in the carbonate aquifers are the major contributors of drinking and irrigation water supply. The aim of this study was to review hydrochemical processes that control the groundwater chemistry and to determine the suitability of springs and groundwater for irrigation and drinking purposes on the basis of the water quality indices. Physical (pH, electrical conductivity, total dissolved solids) and hydrochemical characteristics (Na^+, K^+, Ca^{2+}, Mg^{2+}, HCO_3^-, Cl^-, and SO_4^-) of springs and groundwater were determined. To assess the water quality, chemical parameters like sodium adsorption ratio (SAR), total hardness, Mg-hazard (MH), sodium percentage (Na %), salinity hazard, permeability index, and Kelly's ratio were calculated based on the analytical results. A Durov diagram plot revealed that the groundwater has been evolved from Ca to HCO_3 recharge water, followed by mixing and reverse ion exchange processes, due to the respective dominance of Na–Cl and Ca–Cl water types. According to Gibbs's diagram plots, chemical weathering of rock forming minerals is the major driving force controlling water chemistry in this area. Groundwater and spring samples were grouped into six categories according to irrigation water quality assessment diagram of US Salinity Laboratory classification and most of the water samples distributed in category C2–S1 and C3–S1 highlighting medium to high salinity hazard and low sodium content class. The results of hydrochemical analyses and the calculated water quality parameters suggest that most of the water samples are suitable for irrigation and drinking purposes, except for the samples influenced by seawater and enhanced water–rock interaction. High values of salinity, Na %, SAR, and MH at certain sites, restrict the suitability for agricultural uses.

Keywords Carbonate aquifers · Geochemical characteristics · Water quality parameters · Salinity · Water–rock interaction

G. Sappa (✉) · S. Ergul
Dipartimento di Ingegneria Civile, Edile e Ambientale, Sapienza Università di Roma, Rome, Italy
e-mail: giuseppe.sappa@uniroma1.it

F. Ferranti
Centro Reatino di ricerche di Ingegneria per la Tutela e la Valorizzazione dell'Ambiente e del Territorio, Sapienza-Università di Roma, Rieti, Italy

Introduction

Groundwater is an important natural resource especially for drinking and irrigation uses. Water quality assessment is essential for human health and the definition of water quality depends on the desired use of water (Hoek et al. 2001; Jain et al. 2009; Kirda 1997). Therefore, different uses require different criteria of water quality as well as standard methods for reporting and comparing results of water analysis (Singh et al. 2004). The natural water analyses for physico-chemical properties are very important for public health studies (Rizwan and Singh 2009). These studies are also a main part of pollution studies in the environment (Palma et al. 2010). The variations of water quality are essentially the combination of both anthropogenic and natural contributions (Chen et al. 2006). Natural variations in groundwater hydrochemistry should be considered when assessing water quality data from groundwater monitoring programmes, as elevated concentrations for certain parameters might be influenced by the aquifer lithology (Kumar et al. 2009). Therefore, to ensure that long-term sustainable groundwater

Published online: 24 October 2013

resources are achieved, groundwater resource management is required through an assessment of anthropogenic pressures and the physical characteristics of the subsurface deposits, i.e. soil, subsoil, and aquifer type. The water quality assessment is mostly based on hydrochemical analysis and many organizations renew and publish the guidelines for drinking water to protect public health.

In Italy, water for different uses (i.e. drinking and agricultural) relies mostly on groundwater resources from carbonate aquifers. Carbonate aquifer systems often respond rapidly to changes in environmental and climatic conditions (Mahler and Massei 2007). Many studies have been conducted on carbonate aquifer systems such as geochemical processes in these systems and their hydrogeological implications. In these systems, chemical composition of groundwater is controlled by many factors, including the composition of the precipitation, variations in flow, seasonal changes in recharge, geological structure, and mineralogy of the aquifers (Chenini and Khmiri 2009). The interaction of all factors leads to various water types. In recent years, hydrochemical investigation techniques provide much information for the identification of main hydrogeochemical processes affecting the composition and the quality of spring and groundwater within the carbonate aquifers (Briz-Kishore and Murali 1992). The hydrochemical properties are generally related to (1) water–rock interactions, (2) natural factors such as mixing between seawater and freshwater, (3) anthropogenic factors, and (4) the type of groundwater circulation (Mercado and Billings 1975; Mayer 1999). On the other hand, the composition of water in carbonate systems is the result of the dissolution of variable quantities of rock forming minerals that controls the water chemistry (White 1988; Ettazarini 2005; Edmunds et al. 1987; Moral et al. 2008).

In the present work, spring waters and groundwater from the carbonate aquifers of the southern Latium region were characterized employing physico-chemical data to determine the water suitability for different uses (i.e. drinking and irrigation). This study was also designed to hydrochemically characterize these aquifer systems, with the aim of achieving proper management and protection of these important resources. The main objectives of this study are (1) evaluation of water geochemistry; (2) determination of water quality parameters; and (3) assessment of water suitability for drinking and irrigation purposes by comparing the identified parameters with the standards and guidelines.

Methodology

The main spring water and groundwater sampling survey was carried out in southern Latium region of Central Italy from 2002 to 2006. Groundwater samples were collected from 20 wells in Pontina Plain and 54 spring water samples were collected from Lepini (12 springs), Ausoni (16 springs), and Aurunci (26 springs) mountains (Fig. 1). All samples were collected in laboratory certified clean bottles and location; date and time of sample collection were recorded. Water temperature, electrical conductivity, and pH values were determined in the field using PC 300 Waterproof Hand-held meter (http://www.eutechinst.com/manuals/english/pc300_r3.pdf). Laboratory analyses included major cations and anions. All samples were maintained in refrigerated conditions before analyses. For chemical analysis, 250 ml of water was collected in polyethylene bottles, filtered and then acidified (http://www.irsa.cnr.it/ShPage.php?lang=en&pag=nma). Water samples were filtered through cellulose filters (0.45 μm), and their major and minor constituents were determined by a Metrohm 761 Compact IC ion chromatograph (replicability ±2 %) (http://www.metrohm.it/Produkte2/IC/index.html). A Metropes C2–100 column was used to determine cations (Na^+, K^+, Mg^{2+}, Ca^{2+}), while a Metropes A Supp 4–250 column was used for anions (Cl^-, SO_4^-, HCO_3^-) (Metrohm 2000) The analytical accuracy of these methods ranged from 2 to 5 %. Bicarbonate content was measured by titration with 0.1 N HCl using colour turning method with methyl orange as indicator. Chemical analyses were performed on the collected water samples at the Geochemical Laboratory of Sapienza, "University of Rome". The characterization of spring and groundwater samples has been evaluated by means of major ions, Ca^{2+}, Mg^{2+}, HCO_3^-, Na^+, K^+, Cl^- and SO_4^-. For the identification of water types, the chemical analysis data of the spring water samples have been plotted on the Piper and Durov diagrams using Geochemistry Software AqQA, version AQC10664 (Rockware AqQA Software 2011). In addition, for the evaluation of water quality parameters magnesium and salinity hazard, sodium adsorption ratio (SAR), sodium percentage (Na %), total hardness (as $CaCO_3$), exchangeable sodium ratio (ESR), Kelly's ratio (KR), permeability index (PI), values of springs and groundwater samples were also determined using AqQA software and some mathematical calculations.

Geology and hydrogeology

Lepini, Ausoni and Aurunci are three different groups of mountains belonging to the pre-Apennines of Latium and they occupy a well-defined geographic area, called "Volscian mountain range" (Fig. 1). The Lepini Mountains are located in the northern part of Pontina Plain and hosts an important karst aquifer. The aquifer in the Lepini massif may be classified as "unconfined with an undefined bottom surface". The Pontina is a coastal plain developed along an extensional marine boundary and positioned between the Lepini–Ausoni mountains of the Central Apennines and the

Tyrrhenian Sea (Fig. 1). In Pontina Plain, much of the groundwater comes out in springs near the boundary between the Pontina Plain and the carbonate massif, all of which join a series of streams and canals that drain to the Tyrrhenian Sea (Memon et al. 2011). Two aquifers are present in Pontina Plain: one is an unconfined aquifer lying under the Quaternary deposits covering the limestones at the south-western margin of the Lepini complex, and the second one is a confined aquifer where the water is discharged from the calcareous aquifer of the Lepini massif and flows to the sea. The Ausoni Mountains rise in southern Latium and extend to the coastline, starting immediately after the middle Amaseno valley (Fig. 1). The Ausoni hydrogeological unit is mainly composed of limestones with interbedded dolomitic limestones. Most of the springs lie along all of its borders but with no sharp separations between their recharge areas. The Aurunci Mountains represent the southeastern part of the Volscian range and are oriented more or less parallel to the Apennine range. The Aurunci Mountains are made of two distinct hydrogeological units: the western Aurunci, belonging to the Ausoni–Aurunci system, and the eastern Aurunci, which is separated from the western ones by a marly-arenaceous flysch complex (Boni 1975). The western Aurunci hydrogeological unit consists of dolomitic limestones and dolomites of Jurassic and Cretaceous age. The springs are supplied by groundwater that is derived from these geological formations. The groundwater is directly discharged into the Liri river through the narrow alluvial belt separating the unit from the river. The unit holds multiple hydrogeological basins, whose boundaries match important tectonic lines that caused the outcropping of the calcareous-dolomitic Jura (Accordi et al. 1976). The eastern Aurunci hydrogeological carbonate structure is surrounded by relatively less-permeable sediments, including the Frosinone flysch, the Roccamonfina volcanites and the Garigliano plain alluvia (Celico 1978).

Results and discussion

Water chemistry

Statistical summary of physical and hydrochemical parameters of sampled waters and guideline values of World Health Organization (WHO), US Environmental Protection Agency (US-EPA) and US Salinity Laboratory (USSL) for comparison are presented in Table 1. The temperature of Lepini springs range from 10 to 15 °C. The pH of these springs ranges from 6.9 to 8.1. Lepini springs show a total dissolved solids (TDS) content within the range 101.5–1,264.3 mg/l. The electrical conductivity (EC) value of the springs varies from 138 to 1,540 µs/cm. The temperature of Ausoni springs ranges from 12 to 15 °C. The pH of the Ausoni springs ranges from 7.1 to 8 indicating alkaline nature of the water. The EC and TDS values of the springs range from 315 to 2,310 µs/cm and 255.3 to 1,318.4 mg/l, respectively. The temperature of Aurunci springs ranges from 3 to 31 °C, with minimum and maximum values, respectively. The TDS content ranges from 245.6 to 1,149.7 mg/l. Aurunci springs show alkaline nature (pH 7.2–8.2) with low to medium electrical conductivity. However, few springs show high total dissolved solids (1,150 mg/l) and electrical conductivity (1,217 µs/cm). This fact is probably related to the more time for water to interact with the host rock. The groundwater of Pontina Plain show alkaline character with pH values ranging from 7.3 to 8.0 corresponding to carbonate system waters. The temperature of groundwater ranges between 12 and 17.6 °C. The electrical conductivity and TDS concentrations of the groundwater samples from Pontina Plain show varieties due to water rock interaction and seawater intrusion near the coastal area. The TDS and EC values of groundwater vary from 336 to 2,790.1 mg/l and 412 to 4,180 µs/cm, respectively (Sappa et al. 2012).

The conventional classification techniques (i.e. Piper and Durov diagrams) were applied to evaluate geochemical processes. The hydrochemical facies of springs and groundwater was studied by plotting the concentrations of major cations and anions in the Piper trilinear diagram (Sappa et al. 2012). The types of water that predominates in the study area are (1) Ca–Mg–HCO_3; (2) mixed facies between Ca–HCO_3 and Na–Cl; (3) Na–Cl; (4) Ca–Cl (Fig. 2). The major cation and anion concentrations of the samples from springs and groundwater in the region are plotted on a Durov diagram in Fig. 3. Durov's diagram helps the interpretation of the evolutionary trends and the hydrochemical processes occurring in the groundwater system and can indicate mixing of different water types, ion exchange and reverse ion exchange processes. In Fig. 3, samples fall in field 3 the zone of low-salinity water (Ca–Mg–HCO_3 recharge water); samples located in fields 5, 6, 7 and 1 of Durov diagram indicate mixing and reverse ion exchange processes, respectively (the dominance of Na–Cl and Ca–Cl water types). Reverse ion exchange consists of exchange Ca^{2+} from the clay fraction in aquifer system. In the higher salinity environment, the process of reverse ion exchange may create $CaCl_2$ waters due to the removal of Na^+ out of solution for bound Ca^{2+}. Alternatively, $CaCl_2$ type waters could also be a result of the mixing process between fresher water with more saline older water (Adams et al. 2001).

The major cations of springs and groundwater dominated by calcium and bicarbonate belong to the group of Ca–HCO_3 water type, followed by magnesium, sodium, sulphate and chloride. However, the composition of spring

Table 1 Descriptive statistics of spring water and groundwater hydrochemistry and guideline values of WHO, US-EPA and USSL

Sampling locations	T (°C)	pH	EC (µs/cm)	Ca (mg/l)	Mg (mg/l)	Na (mg/l)	K (mg/l)	Cl (mg/)	HCO_3^- (mg/l)	SO_4^{-2} (mg/l)	TDS (mg/l)
Lepini springs (12 samples)											
Mean	12.8	7.7	517	64.3	13.7	37.4	2.9	55.4	239.8	16.4	430
Median	12.5	7.7	399.5	67.2	6.5	6.8	1.2	9.6	235.9	4.3	334.4
Min	10	6.9	138	15.4	1.4	2.9	0.1	3.9	67.1	1.7	101.5
Max	15	8.1	1,540	111	44.7	221	15.8	338.4	448	85.4	1,264.3
Ausoni springs (16 samples)											
Mean	12.6	7.7	826.3	65.2	18.2	73.5	3.5	128.4	234.2	27.2	550.2
Median	12	7.8	404	61.6	9.2	8.6	0.8	13.3	232	5.8	324.3
Min	12	7.1	315	41.5	3.8	4.1	0.2	7.5	177	3.8	255.3
Max	15	8	2,310	89.2	47.8	293.1	15.4	524.9	305.1	110.9	1,318.4
Aurunci springs (26 samples)											
Mean	12.1	7.7	545	72.8	25.6	10.6	2.9	12.7	316.5	34.6	475,7
Median	12	7.7	428.5	64.9	9.9	7.6	1.1	9.7	244.1	5.3	337.8
Min	3	7.2	311	44.5	1.5	4.2	0.3	4.5	170.9	2.7	245.6
Max	31	8.2	1,217	197.3	93.4	50.5	21.6	46.7	805.5	195.8	1,149,7
Pontina Plain groundwater (20 samples)											
Mean	14.8	7.8	1,900.7	124	43.1	232.6	17.7	445	297.2	117.2	1,276.8
Median	13.5	7.9	1,448.5	125.6	38.9	58	17.2	397.8	284.5	55.6	970
Min	12	7.3	412	50.2	15.1	10.3	1.1	9.4	92	6.1	336
Max	17.6	8.0	4,180	198.1	76.5	705.6	41.5	1,220	610	348.7	2,790.1
WHO (2006) guideline values	NS	6.5–9.2	1,500	75	30	200	200	250	NS	250	1,000

Na % classification (Wilcox 1955)	Na % classification	<20 % excellent	20–40 % good	40–60 % permissible	60–80 % doubtful
		EC (µs/cm)	Salinity hazard	Salinity hazard class	
US Salinity Laboratory classification diagram (USSL 1954)	US salinity hazard classification	100–250	Low	C1	
		250–750	Medium	C2	
		750–2,250	High	C3	
		>2,250	Very high	C4	
	Sodium hazard classification	SAR	Sodium (alkali) hazard	Sodium hazard class	
		<10	Low	S1	
		10–18	Medium	S2	
		18–26	High	S3	
		>26	Very high	S4	
US-EPA (1986) hardness classification		Hardness as $CaCO_3$ (mg/l)	Water classification		
		0–75	Soft		
		75–150	Moderately hard		
		150–300	Hard		
		>300	Very hard		

NS not stated

samples discharge at lower elevations, issuing from Lepini and Ausoni Mountains, and groundwater from Pontina Plain belong to or show a tendency to the group of Na–Cl dominated by chloride, sodium, sulphate and potassium. The large variations in ion concentrations, TDS and electrical conductivity (EC) were thought to be mainly due to water–rock interaction along the flow paths and seawater intrusion in the coastal area. In the previous studies, this fact was studied by geochemical modeling and saturation index computation of the Lepini, Ausoni and Aurunci springs and Pontina Plain groundwater. The results of geochemical modeling suggest that most of the spring water and groundwater samples are saturated with respect to calcite and dolomite; however, all sampled waters are undersaturated with respect to gypsum and halite (Sappa et al. 2012). The Gibbs plots are employed to understand

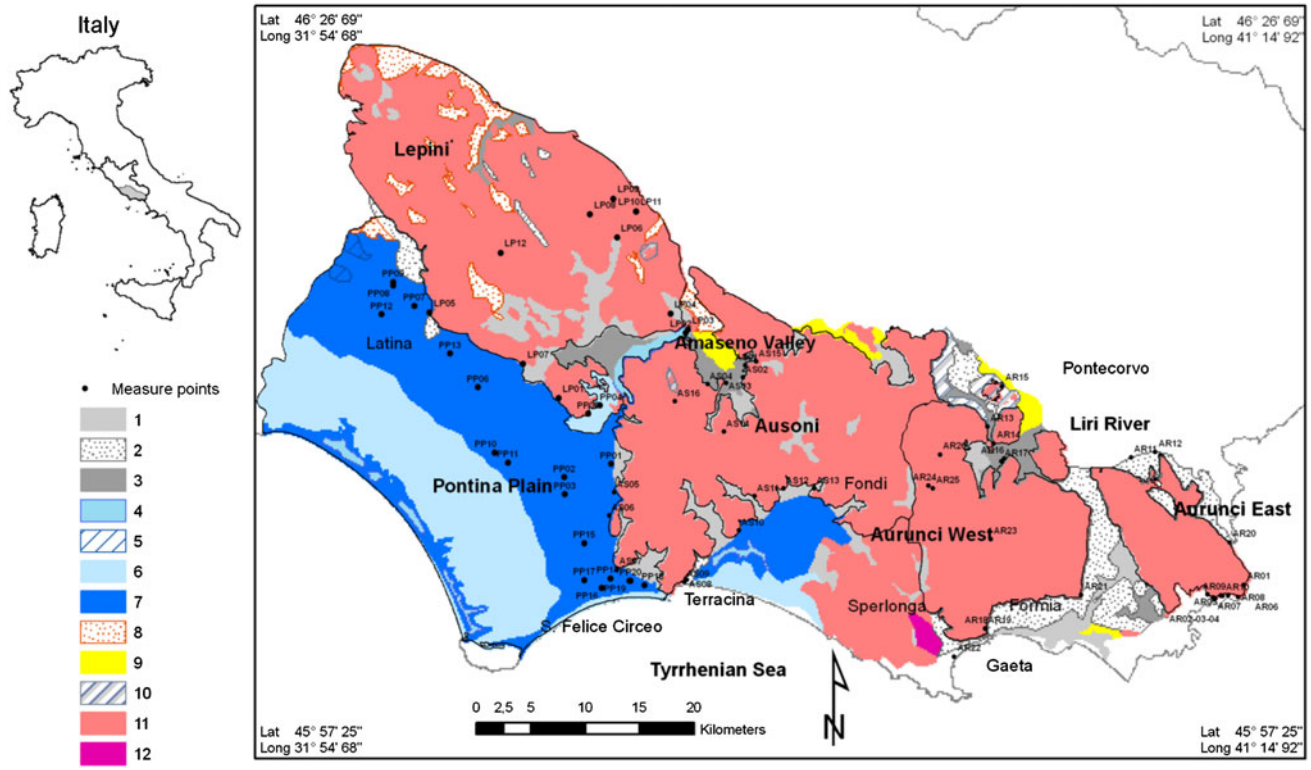

Fig. 1 Simplified hydro-geological map of the study area

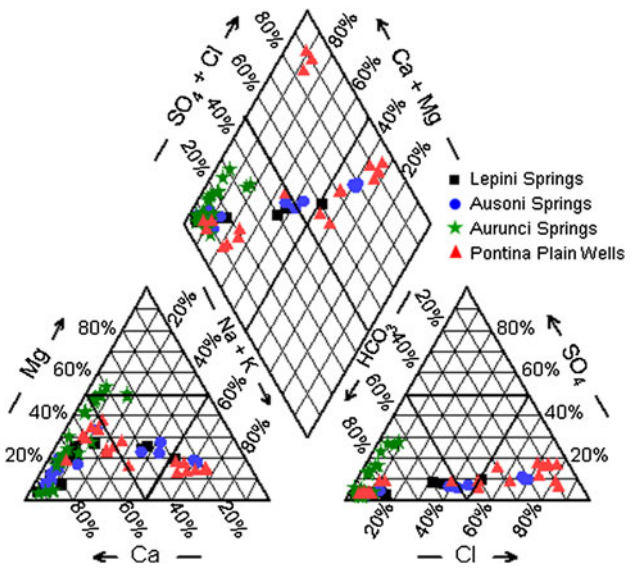

Fig. 2 Piper diagram of springs and groundwater samples

the processes which affect the geochemical parameters of springs and groundwater. These diagrams, representing the plot of log (TDS) versus ratios of $Na^+/(Na^+ + Ca^{2+})$ and $Cl^-/(Cl^- + HCO_3^-)$, are widely used to assess the distinction between waters controlled by water–rock interaction (i.e. leaching and dissolution), evaporation and precipitation (Gibbs 1970). Gibbs's plots (Fig. 4) show that most spring and groundwater samples fall in the rock dominance area. The water–rock interaction (chemical weathering of rock forming minerals) predominates the water chemistry of these springs and groundwater. However, some spring (low discharge Lepini and Ausoni springs) and groundwater samples clustered in the region of evaporation zone. Evaporation increases salinity by increasing Na^+ and Cl^- with relation to increase of TDS. This is also observed by Piper plot, having significant increase of Na^+ and Cl^- in some spring and groundwater samples. This may be attributed to the dissolution of evaporate minerals (such as halite) and seawater intrusion near the coastal area.

Water quality assessment

The chemical parameters play an important role in classifying and assessing water quality. Thus, to evaluate water quality for different uses, water quality indices such as TDS, EC, pH, SAR, Mg-hazard (MH), total hardness, salinity hazard, ESR, permeability index, Kelly's ratio and sodium percentage were calculated from the chemical analyses of 54 spring and 20 groundwater samples. The results of the different indices for irrigation water quality are presented in Table 2. Then, the analytical results of

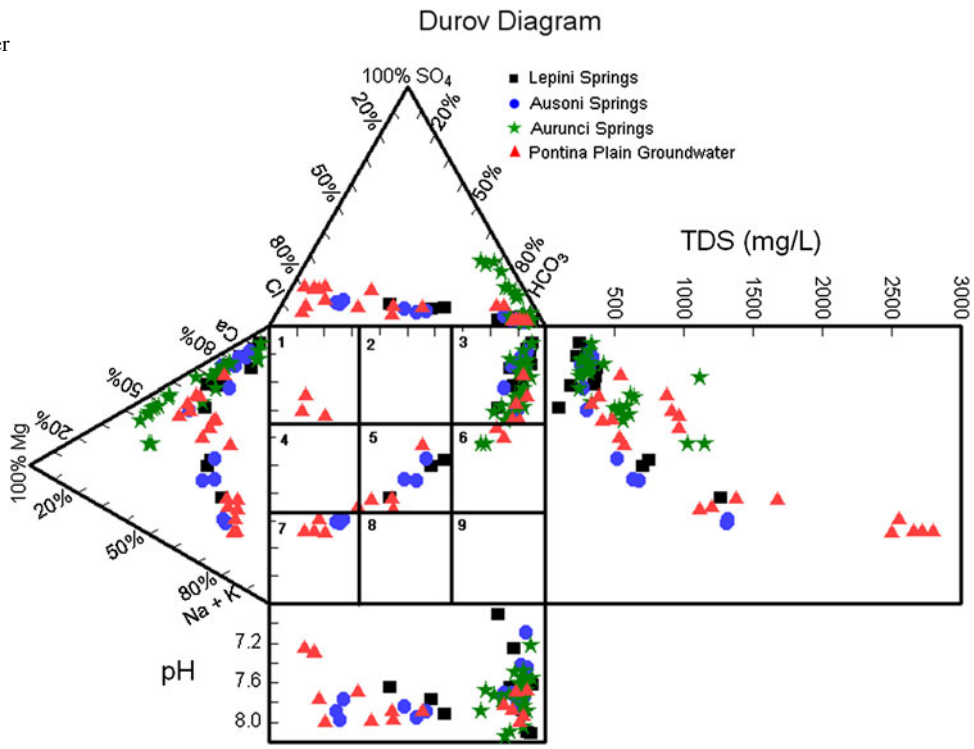

Fig. 3 Durov's diagram of springs and wells for definition of groundwater chemical types

physical and chemical parameters of springs and groundwater were compared with the standard guideline values.

Drinking water quality

Major anions and cations The concentration of various ions in the groundwater and spring samples was compared with WHO standards, which are given in Table 1. The minimum required amounts of magnesium and calcium in drinking water are 10 and 20 mg/l, respectively, and the desired amounts of magnesium and calcium in drinking water are 30–50 and 40–75 mg/l, respectively. The calcium concentrations in water samples range from 15.4 to 198.1 mg/l with minimum and maximum values, respectively. Almost 42 % of the spring and groundwater samples contain Ca concentrations higher than 75 mg/l, while about 3 % of the springs show Ca concentrations less than 40 mg/l. Besides, 55 % of the total samples show Ca concentrations ranging between 40 and 75 mg/l. In the study area, magnesium concentrations range between 1.4 and 93.4 mg/l. Most of the samples (~60 %) show magnesium concentrations <30 mg/l. However, about 17.5 % of 74 samples show magnesium concentrations higher than 50 mg/l. The remaining water samples have magnesium concentrations within the range of 30–50 mg/l. Among the springs, the highest calcium (197.3 mg/l) and magnesium (93.4 mg/l) concentrations were observed in water samples from Aurunci mountains. Besides, groundwater samples from Pontina Plain also show higher Ca (198.1 mg/l) and Mg (76.5 mg/l) concentrations. The sulphate concentration in water samples ranged from 1.7 to 348.7 mg/l. The highest values were observed in Aurunci springs (195.8 mg/l) and Pontina Plain (348.7 mg/l) groundwater; however, most of the samples are within the maximum allowable limits WHO (2006) standards. The high concentration of sulphate is likely due to the dissolution of gypsum minerals which is common in the study area. Nevertheless, high concentrations of sulphate in groundwater of Pontina Plain are attributed to the proximity of the sampling locations to the coast. Bicarbonate values in water samples vary from 67.1 to 805.5 mg/l. The potassium values of the water samples range from 0.1 to 41.5 mg/l and most of the samples in the study area fall within the guideline levels; however, springs and groundwater belonging to Mg–HCO_3 and Na–Cl water types show higher potassium concentrations. The sources of potassium in the water samples are attributed to the dissolution of silicate minerals, seawater intrusion near the coastal area and/or agricultural activities. Sodium and chloride concentrations in the investigated water samples are found in the range of 2.9–705.6 and 3.9–1,220 mg/l with minimum and maximum values, respectively. The highest concentrations were observed in some groundwater samples of Pontina Plain and some low discharge springs from Lepini and Ausoni Mountains. Most of the samples have sodium and chloride levels are not in excess of the permissible limit of 200 and 250 mg/l, respectively (WHO 2006). Based on these results and comparison values, most of the

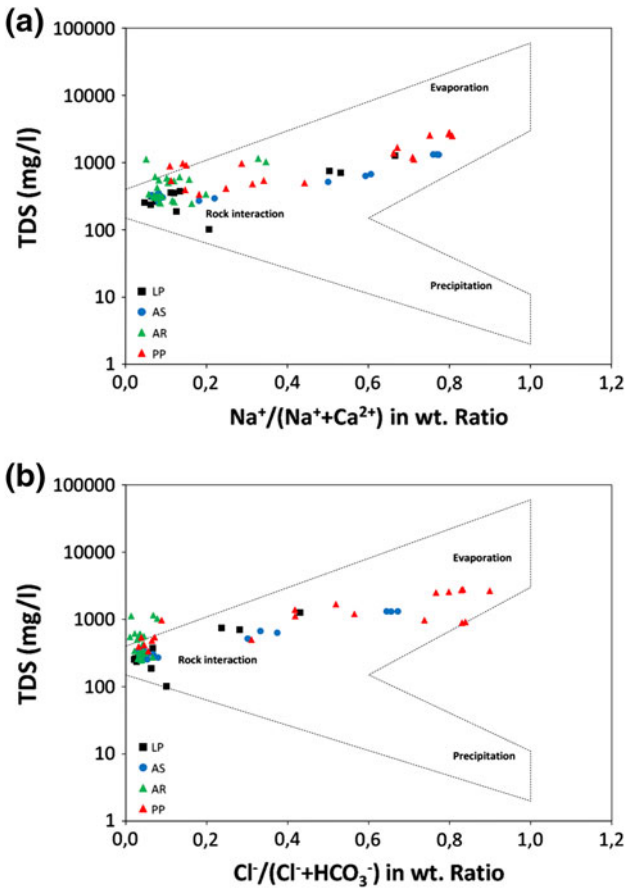

Fig. 4 Gibbs diagrams showing the mechanism controlling water chemistry. **a** Plot of log (TDS) versus $(Na^+)/(Na^+ + Ca^{2+})$ and **b** plot of log TDS versus $Cl^-/(Cl^- + HCO_3^-)$

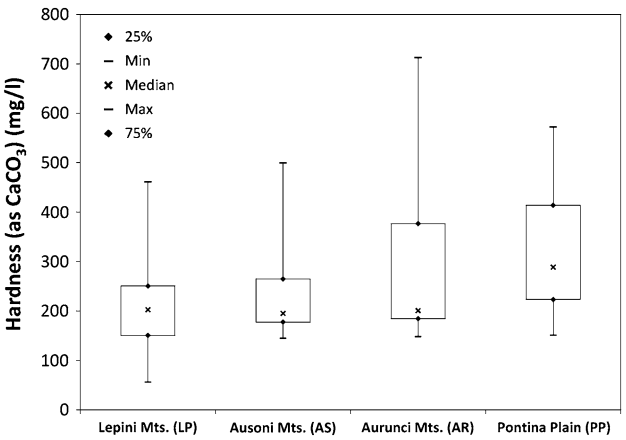

Fig. 5 *Box plots* show mean, median, 25–75 percentile, minimum and maximum values of total hardness

groundwater and spring samples were found to be within the suitable limits.

Total dissolved solids (TDS) High concentration of TDS in drinking water may cause adverse taste effects. A water containing TDS <500 mg/l can be considered as fresh water. Water with a TDS lower than 1,000 mg/l is usually acceptable for consumers (WHO 2006). In the study area, the TDS content of spring water ranges from 101.5 to 1,318.4 mg/l. It was found that 87 % of the spring water samples are classified as fresh water, while the rest of the springs are considered as a brackish water according to the WHO guidelines. Most of the spring samples show TDS values below 1,000 mg/l and suitable for drinking and irrigation purposes. Groundwater samples from Pontina Plain show the highest TDS values ranging from 335.9 to 2,790.1 mg/l. Based on WHO Guidelines for drinking-water quality, 45 % of total groundwater samples fall in brackish water category while, 55 % of total samples classified as fresh water.

Hardness Determination of water hardness is a useful test to measure quality of water for domestic, agricultural and industrial uses. High levels of total hardness does not cause health risk; however, both extreme degrees very soft (<75 mg/l as $CaCO_3$) and very hard (>300 mg/l as $CaCO_3$) are considered as undesirable features in water. Hardness levels between 80 and 100 mg/l (as $CaCO_3$) are generally acceptable in drinking water and are considered tolerable by consumers (Ternan 1972; Bernardi et al. 1995; Memon et al. 2011). The total hardness of water is the sum of calcium and magnesium hardness expressed as mg/l $CaCO_3$. The total hardness (as $CaCO_3$) of water samples can be calculated using the following equation (http://water.usgs.gov/owq/hardness-alkalinity.html#hardness):

$$[CaCO_3] = 2.5[Ca^{2+}] + 4.1[Mg^{2+}]. \quad (1)$$

The US-EPA classified water that contains 0–75 mg/l $CaCO_3$ as soft, 75–150 mg/l $CaCO_3$ as moderately hard, 150–300 mg/l $CaCO_3$ as hard and >300 mg/l $CaCO_3$ as very hard (US-EPA 1986). The total hardness values (mean, median, maximum and minimum) of springs and groundwater were presented in Fig. 5. The total hardness of Lepini spring samples range from 56.2 to 461.2 mg/l (Table 2) and fall between soft and very hard water category. Ausoni spring water samples show total hardness ranging from 144.7 to 499.5 mg/l and classified as moderately hard to very hard water. The highest total hardness values were observed in water samples from Aurunci Mountains ranging from 148.2 to 712.7 mg/l with minimum and maximum values, respectively. Almost all Aurunci spring samples are characterized as very hard water. The classification of water based on total hardness shows that most of the spring water samples fall between hard and very hard water type. The total hardness values of groundwater from Pontina Plain range from 151 to 572.2 mg/l highlighting

Table 2 Water quality parameters for springs and groundwater

Samples	Hardness (as $CaCO_3$) (mg/l)	Indication	Salinity hazard	Mg-hazard	Na-adsorption ratio (SAR)	Exchangeable Na ratio (ESR)	Na %	Kelly's ratio (KR)	Permeability index
LP01	318.6	Very hard	High	40.6	2.09	0.59	37.94	0.6	60.25
LP02	228.2	Very hard	Medium	27.6	0.26	0.09	8.38	0.1	48.47
LP03	221.7	Very hard	Medium	7.8	0.37	0.13	11.72	0.1	51.55
LP04	218.4	Very hard	Medium	22.0	0.25	0.09	8.28	0.1	50.86
LP05	461.2	Soft	High	39.9	4.48	1.04	52.08	1.0	65.44
LP06	157.8	Hard	Medium	17.2	0.15	0.06	5.69	0.1	58.66
LP07	348.4	Very hard	High	37.7	2.05	0.55	36.32	0.5	58.58
LP08	141.0	Hard	Medium	12.0	0.12	0.05	5.09	0.1	61.37
LP09	153.8	Hard	Medium	3.8	0.10	0.04	4.02	0.0	58.06
LP10	112.2	Hard	Medium	23.9	0.20	0.10	10.82	0.1	67.73
LP11	56.2	Soft	Low	31.5	0.23	0.16	15.91	0.2	94.35
LP12	186.4	Very hard	Medium	6.0	0.15	0.06	5.43	0.1	54.21
AS01	191.1	Very hard	Medium	19.6	0.16	0.06	5.92	0.1	53.69
AS02	188.0	Very hard	Medium	20.2	0.13	0.05	4.72	0.0	54.09
AS03	180.8	Very hard	Medium	14.9	0.20	0.08	7.25	0.1	54.43
AS04	144.7	Hard	Medium	19.1	0.38	0.16	13.99	0.2	65.33
AS05	238.4	Very hard	Medium	35.5	1.74	0.56	36.55	0.6	62.89
AS06	259.4	Very hard	High	39.5	2.47	0.77	44.09	0.8	66.05
AS07	419.7	Very hard	Very high	46.9	6.00	1.47	60.19	1.5	69.69
AS08	499.5	Very hard	Very high	46.6	6.35	1.59	61.95	1.6	71.53
AS09	407.9	Very hard	Very high	45.9	6.31	1.56	61.59	1.6	70.81
AS10	280.9	Very hard	High	46.9	2.38	0.71	42.20	0.7	64.85
AS11	157.7	Hard	Medium	16.3	0.16	0.07	6.30	0.1	56.85
AS12	167.1	Hard	Medium	18.8	0.16	0.06	6.02	0.1	56.30
AS13	167.5	Hard	Medium	38.1	0.39	0.15	13.71	0.2	61.04
AS14	199.3	Very hard	Medium	7.8	0.16	0.06	5.39	0.1	51.66
AS15	189.6	Very hard	Medium	12.6	0.15	0.05	5.36	0.1	53.33
AS16	211.7	Very hard	Medium	9.9	0.20	0.07	6.74	0.1	50.73
AR01	639.0	Very hard	High	60.2	0.85	0.17	17.51	0.2	36.17
AR02	332.3	Very hard	Medium	50.2	0.19	0.05	5.74	0.1	41.19
AR03	347.5	Very hard	Medium	52.9	0.21	0.06	6.42	0.1	35.79
AR04	381.4	Very hard	Medium	48.5	0.20	0.05	5.86	0.1	34.92
AR05	413.4	Very hard	High	43.8	0.18	0.04	7.53	0.1	52.89
AR06	326.1	Very hard	Medium	50.9	0.18	0.05	5.61	0.1	39.37
AR07	361.6	Very hard	Medium	57.3	0.26	0.07	7.43	0.1	37.93
AR08	585.4	Very hard	High	59.4	0.91	0.19	18.34	0.2	37.41
AR09	396.6	Very hard	Medium	42.9	0.16	0.04	4.37	0.0	35.43
AR10	388.7	Very hard	Medium	53.7	0.25	0.06	6.81	0.1	36.77
AR11	175.1	Hard	Medium	22.2	0.15	0.06	6.06	0.1	55.99
AR12	183.2	Very hard	Medium	31.6	0.40	0.15	14.04	0.1	60.47
AR13	194.4	Very hard	Medium	19.1	0.17	0.06	6.24	0.1	52.36
AR14	188.6	Very hard	Medium	19.2	0.15	0.05	5.47	0.1	52.87
AR15	252.2	Very hard	Medium	16.8	0.20	0.06	6.10	0.1	47.17
AR16	192.7	Very hard	Medium	19.7	0.15	0.05	5.52	0.1	53.14
AR17	202.5	Very hard	Medium	16.9	0.15	0.05	5.55	0.1	49.61
AR18	149.3	Hard	Medium	25.6	0.15	0.06	6.20	0.1	60.01
AR19	152.0	Hard	Medium	22.8	0.15	0.06	6.11	0.1	59.54

Table 2 continued

Samples	Hardness (as $CaCO_3$) (mg/l)	Indication	Salinity hazard	Mg-hazard	Na-adsorption ratio (SAR)	Exchangeable Na ratio (ESR)	Na %	Kelly's ratio (KR)	Permeability index
AR20	712.7	Very hard	High	30.9	0.17	0.03	3.69	0.0	27.85
AR21	150.9	Hard	Medium	24.5	0.32	0.13	11.84	0.1	60.58
AR22	194.5	Very hard	Medium	22.0	0.19	0.07	6.68	0.1	52.11
AR23	148.2	Hard	Medium	5.0	0.28	0.11	10.37	0.1	62.71
AR24	158.7	Hard	Medium	4.6	0.27	0.11	9.97	0.1	59.05
AR25	188.4	Very hard	Medium	4.0	0.21	0.08	7.26	0.1	54.56
AR26	199.2	Very hard	Medium	3.2	0.15	0.05	5.06	0.1	52.68
PP01	251.8	Hard	Medium	28.5	0.9	0.3	22.85	0.3	58.13
PP02	337.5	Very hard	High	31.7	5.4	1.5	60.04	1.5	75.02
PP03	408.7	Very hard	High	38.7	5.3	1.3	56.91	1.3	68.73
PP04	201.5	Hard	Medium	37.8	0.3	0.1	11.26	0.1	54.26
PP05	312.0	Very hard	Medium	20.0	0.3	0.1	8.50	0.1	45.17
PP06	482.3	Very hard	High	36.9	4.7	1.1	53.57	1.1	66.53
PP07	263.9	Hard	Medium	36.9	9.2	0.3	26.46	0.3	57.31
PP08	213.4	Hard	Medium	29.6	5.9	0.2	22.49	0.2	58.82
PP09	218.6	Hard	Medium	31.8	3.0	0.1	11.12	0.1	54.26
PP10	151.3	Hard	High	37.6	5.0	0.1	14.26	0.1	16.97
PP11	151.0	Hard	High	32.9	3.8	0.1	9.84	0.1	15.03
PP12	428.2	Very hard	High	32.4	1.0	0.2	24.68	0.2	45.96
PP13	251.5	Hard	High	42.9	4.3	0.1	13.62	0.1	18.03
PP14	500.2	Very hard	Very high	43.9	10.5	2.1	67.58	2.0	72.58
PP15	572.2	Very hard	Very high	28.4	6.1	1.3	56.33	1.3	66.53
PP16	450.0	Very hard	Very high	36.3	9.3	1.7	63.06	1.7	67.75
PP17	265.5	Hard	High	23.9	1.7	0.5	35.03	0.5	57.59
PP18	400.0	Very hard	Very high	41.2	11.2	2.0	67.58	2.0	71.50
PP19	225.0	Hard	Very high	42.7	10.8	2.0	67.21	2.0	70.07
PP20	400.0	Very hard	Very high	41.1	11.0	2.0	67.57	2.0	71.52

LP Lepini springs, *AS* Ausoni springs, *AR* Aurunci springs, *PP* Pontina Plain groundwater)

hard to very hard water category. Waters with hardness levels in excess of 200 mg/l are considered poor but have been tolerated by consumers; however, waters with hardness in excess of 500 mg/l are not suitable for most domestic purposes. Few spring and groundwater samples exceed the allowable limit for domestic uses. The observed high total hardness values in water samples are related to the main rock types in the area investigated, where limestone, dolomitic limestones and dolomites are the most dominant formations.

pH values The pH values of spring samples range from 6.91 to 8.15 indicating slightly acidic to alkaline nature. According to the WHO (2004) guidelines, the range of desirable pH values for drinking water is 6.5–9.2. There are no spring and groundwater samples with pH values outside of the desirable ranges.

Suitability of water for irrigation purposes/irrigation water quality parameters

The results of the different irrigation indices sodium percentage, ESR, magnesium hazard, SAR, permeability index and Kelly's ratio for rating irrigation water quality are summarized in Table 2 and some comparison values are presented in Table 1 and discussed in the text.

Magnesium hazard (MH) Magnesium concentration of water plays an important role in determining the quality of water for irrigation purposes and hence, agricultural use. Magnesium hazard can be determined employing the following equation:

$$\mathrm{MH} = \frac{\mathrm{Mg}^{2+}}{\mathrm{Ca}^{2+} + \mathrm{Mg}^{2+}} \times 100. \quad (2)$$

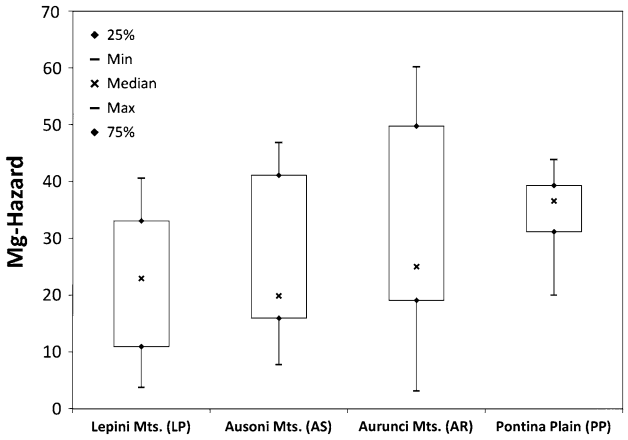

Fig. 6 *Box plots* show mean, median, 25–75 percentile, minimum and maximum values of magnesium hazard (MH)

Generally, magnesium hazard more than 50 is considered harmful and unsuitable for irrigation use (Szabolcs and Darab 1964). The high magnesium content in water will adversely affect crop yields as the soils become more saline (Joshi et al. 2009). Evaluation of mean, median, maximum and minimum values of magnesium hazard are depicted in box plots (Fig. 6). The magnesium hazard values of Lepini spring samples range from 3.8 to 40.6 indicating that they are within the acceptable limit. Similarly, the spring samples from Ausoni Mountains have also magnesium hazard values (7.8–46.9) <50 and can be classified as suitable for irrigation use. The magnesium hazard values of Pontina Plain groundwater are within the range 20–43.9 highlighting their suitability for irrigation. On the contrary, for Aurunci spring samples magnesium hazard values range from 3.2 to 60.2 (Table 2). It is found that 27 % of spring samples from Aurunci Montains have magnesium hazard more than 50 % indicating that they are unsuitable for irrigation.

Sodium adsorption ratio (SAR indicator) The SAR parameter evaluates the sodium hazard in relation to calcium and magnesium concentrations. This parameter is commonly used as an index to evaluate water suitability for irrigation purposes (Ayers and Westcot 1994; Shaki and Adeloye 2006). Thus, the suitability of the spring and groundwater samples was evaluated by determining the SAR. The SAR was calculated by the following equation (Richards 1954):

$$\mathrm{SAR} = \frac{\mathrm{Na}}{\sqrt{(\mathrm{Ca} + \mathrm{Mg})/2}}. \quad (3)$$

If SAR value is <10, the water is safe to irrigate with no structural deterioration. On the other hand, the SAR value is >6–9, the irrigation water will cause permeability problems on shrinking and swelling types of clayey soils (Saleh et al. 1999; FAO 1992). Continued use of water having high SAR leads to breakdown in the physical structure of the soil particles. High salt concentration in water leads to formation of saline soil and high sodium concentration leads to development of an alkaline soil (Singh et al. 2008). The SAR values of springs and groundwater samples are presented in Table 2. The SAR values of Lepini springs range from 0.10 to 4.48. Samples from Ausoni springs show higher SAR values, ranging from 0.13 to 6.35; however, they fall within the recommended limits. The highest SAR values were found in groundwater samples from Pontina Plain ranging from 0.3 to 11.2. SAR values of water samples from Aurunci springs range from 0.15 to 0.91 highlighting their suitability for irrigation purposes. SARs for spring water samples of the study area are <10 indicating excellent quality for irrigation and all the samples fall in excellent (S1) category. However, some groundwater samples from Pontina Plain having SAR value more than 10 are unsuitable for irrigation. To determine how the interaction of the various ions affect the suitability of the water for irrigation, the SAR has been plotted with the conductivity measurement on the classical USSL (1954) classification diagram in Fig. 7. US of salinity diagram uses SAR and EC values for classifying irrigation water quality. In this diagram, waters have been divided into low (C1), medium (C2), high (C3) and very high (C4) types on the basis of salinity hazard. On the basis of sodium hazard waters have been classified low (S1), medium (S2), high (S3) and very high (S4) types (USSL 1954). In the study area, electrical conductivity values show varieties. The electrical conductivity of sampled waters ranges between 138 and 4,180 µs/cm with a minimum and maximum value, respectively. As seen in Fig. 7, most of the water samples fall in C2–S1 class highlighting medium salinity and low sodium content class. Only one sample sample falls in C1–S1 showing low salinity and sodium content class. However, some spring and groundwater samples fall in the field of C3–S1 and C4–S2, which indicates a high to very high salinity hazard and low to medium sodium content. On the contrary, most of the groundwater samples from Pontina Plain fall in the category C3–S1, C3–S2, C4–S3 and C4–S2 with high to very high salinity and low to high sodium hazard. Water that falls in the medium salinity hazard class (C2) can be used in most cases without any special practices for salinity control. Water samples falling in the high salinity hazard class (C3) may have adverse effects on sensitive crops and plants; however, very high salinity water (C4) is not suitable for irrigation. In the study area, spring samples taken near the coast and groundwater samples from Pontina Plain show very high salinity hazard and are unsuitable for irrigation.

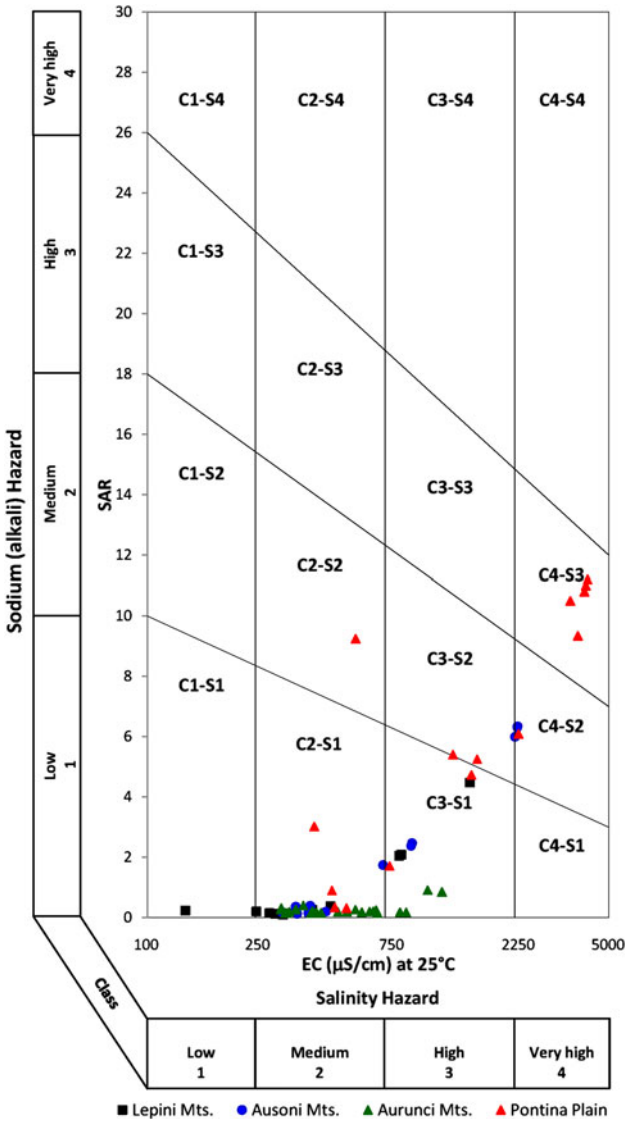

Fig. 7 US salinity classification of springs and groundwater for irrigation (after Richards 1954)

Permeability index (PI) Based on permeability index, Doneen (1964) classified the groundwater as Class I (>75 %), Class II (25–75 %) and Class III (<25 %) to find out suitability of groundwater for irrigation purpose. Accordingly, Class I and Class II are categorized as good for irrigation, while Class III water are unsuitable for irrigation with 25 % of maximum permeability. The permeability index was calculated employing the following equation, where all the ions are expressed in meq/l:

$$\frac{\mathrm{Na}+\sqrt{\mathrm{HCO_3}}}{\mathrm{Ca}+\mathrm{Mg}+\mathrm{Na}}\times 100. \quad (4)$$

The permeability index values range between 15.03 and 94.35 (Fig. 8). Most of the water samples fall in Class II and only two samples fall in Class I indicating good quality

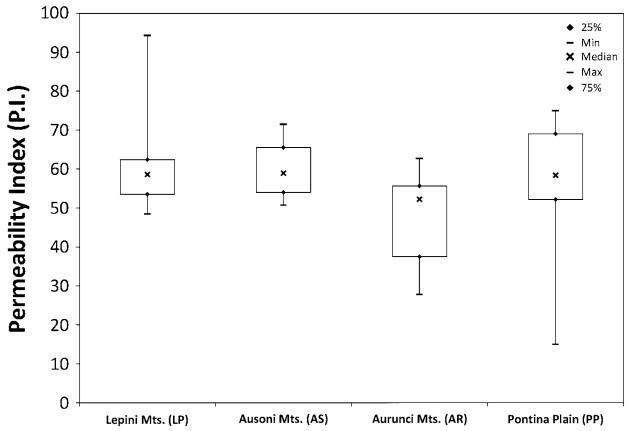

Fig. 8 *Box plot* of mean, median, maximum and minimum values of permeability index (PI)

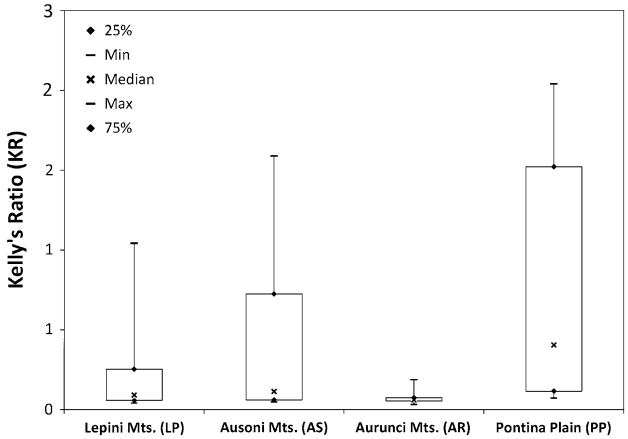

Fig. 9 *Box plot* of mean, median, maximum and minimum values of Kelly's ratio (KR)

for irrigation purposes (Table 2). However, some groundwater samples from Pontina Plain fall in Class III and classified as unsuitable for irrigation purposes.

Kelly's ratio (KR) Kelly's ratio was calculated employing the following equation:

$$\frac{\mathrm{Na^+}}{\mathrm{Ca^{2+}}+\mathrm{Mg^{2+}}}. \quad (5)$$

Groundwater having Kelley's ratio less than one is generally considered suitable for irrigation (Kelley 1940; Paliwal 1967). Kelly's ratio for water samples varies from 0.03 to 2.04 (Table 2). Most of the water samples (~82 %) have KR value <1, highlighting the good quality of groundwater for irrigation purposes (Fig. 9).

Na % Sodium percentage is an important parameter for studying sodium hazard. Na % is calculated using the

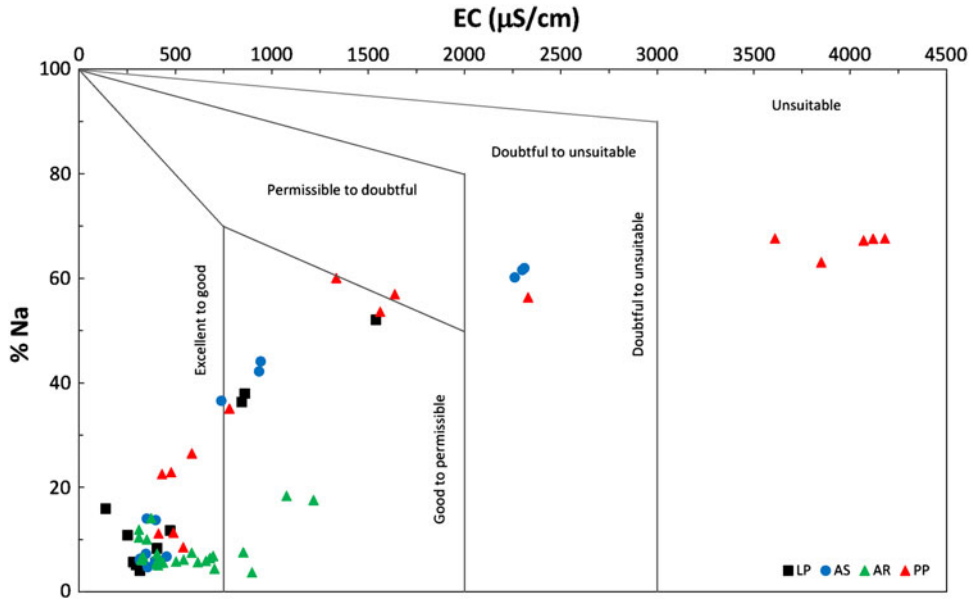

Fig. 10 Plot of per cent sodium versus electrical conductivity (after Wilcox 1955)

following formula (Wilcox 1955) and all concentrations were expressed in meq/l:

$$\frac{\mathrm{Na}+\mathrm{K}}{\mathrm{Ca}+\mathrm{Mg}+\mathrm{Na}+\mathrm{K}}\times 100. \quad (6)$$

High-percentage sodium water for irrigation purpose reduces soil permeability and may prevent the plant growth (Joshi et al. 2009). The classification of groundwater was grouped based sodium as excellent (<20 %), good (20–40 %), permissible (40–60 %), doubtful (60–80 %) and unsuitable (>80 %). The irrigation water classification diagram (Wilcox 1955) was used to assess the water quality (Fig. 10). Water samples were grouped into four categories according to irrigation water assessment with per cent sodium and the results are shown in Table 2. According to Wilcox classification, 69 % of the water samples have excellent irrigation water quality, 12.1 % of the samples have good water quality and 6.8 % of the samples fall in the category of permissible irrigation water. However, 12.1 % of samples which were influenced by seawater were classified as doubtful for irrigation.

Conclusions

Groundwater and spring waters from carbonate aquifers of southern Latium region, Central Italy, were investigated to evaluate the water quality for drinking and irrigation purposes. The results of hydrochemical analysis show that springs and groundwater in the study area are characterized fresh to brackish and slightly acidic to alkaline in nature. The types of water that predominates in the study area are (1) Ca–Mg–HCO_3, (2) mixed facies between Ca–HCO_3 and Na–Cl, (3) Na–Cl and (4) Ca–Cl. The distribution of major anions and cations and occurrence of different hydrochemical facies suggest that the composition of springs and groundwater are influenced by water–rock interaction and seawater intrusion in coastal area to reach a final stage of evolution represented by the Na–Cl water type (i.e. ion exchange interaction). Gibbs diagrams also suggest that water–rock interaction and evaporation are the main mechanisms controlling the water chemistry in the study area. Springs and groundwater samples were classified as hard and very hard water and few samples exceed the allowable limit for domestic uses. According to US-salinity diagram, most of the water samples fall in C2–S1 classes highlighting medium salinity and low sodium content class. However, some spring water (i.e. discharges at lower elevations) and groundwater samples fall in the field of C3–S1 and C4–S2. Most of the groundwater samples from Pontina Plain fall in the category, C3–S2 and C4–S3 showing high to very high salinity and medium to high sodium hazard. Concerning the Na % parameter, about ~70 % of spring and groundwater in the study area is classified as excellent to good for irrigation.

The results of physico-chemical analyses (TDS, pH, EC and major ions) and the calculated water quality parameters (SAR, ESR, Mg-hazard and Na-hazard, total hardness, Kelly's ratio, permeability index, sodium percentage) show that most of the water samples in this area was seen to be good and suitable for drinking and irrigation purposes;

however, some of the groundwater and springs were found to be unsuitable for irrigation in a few places due to sea-water intrusion (i.e. high salinity) and enhanced water–rock interaction (based on magnesium hazard). It was concluded that the most of the calculated indices fall within the recommended limits of US-EPA (1986), WHO and USSL; however, the control of sodium and salinity hazard is required for irrigation.

Acknowledgments The authors would like to thank the Regional Basins Authority of Latium for the financial support of the project.

References

Accordi B, Biasini A, Caputo C, Devoto G, Funiciello R, La Monica GB, Lupia Palmieri E, Matteucci R, Pieruccini U (1976) Geologia e dissesti del territorio montano della Regione Lazio. In: Carta della Montagna, vol 2. Monografia Regionali No. 12 Lazio, Ministero di Agricoltura, Roma, pp 55–101

Adams S, Titus R, Pietersenb K, Tredouxc G, Harris C (2001) Hydrochemical characteristics of aquifers near Sutherland in the Western Karoo. S Afr J Hydrol 241:91–103

Ayers RS, Westcot DW (1994) Water quality for agriculture, irrigation and drainage paper. http://www.fao.org/DOCREP/003/T0234E/T0234E00.htm

Bernardi D, Dini FL, Azzarelli A, Giaconi A, Volterrani C, Lunardi M (1995) Sudden cardiac death rate in an area characterized by high incidence of coronary artery disease and low hardness of drinking water. Angiology 46:145–149

Boni C (1975) The relationship between the geology and hydrology of the Latium–Abruzzi Apennines. In: Parotto M, Praturlon A (eds) Geological summary of the central Apennines, Quaderni de "La ricerca scientifica", vol 90. Structural Model of Italy, pp 301–311

Briz-Kishore BH, Murali G (1992) Factor analysis for revealing hydrochemical characteristics of a watershed. Environ Geol 19:3–9

Celico P (1978) Schema idrogeologico dell'Appennino carbonatico centro-meridionale. Memorie e Note dell'Istituto di Geologia Applicata, Napoli 14:1–97

Chen J, Wang Y, Zhang H (2006) Overview on the studies of nitrate pollution in groundwater. Prog Geogr 25(1):34–44

Chenini I, Khmiri S (2009) Evaluation of ground water quality using multiple linear regression and structural equation modelling. Int J Environ Sci Technol 6(3):509–519

Doneen LD (1964) Water quality for agriculture. Department of Irrigation, University of Calfornia, Davis

Edmunds WM, Cook JM, Darling WG, Kinniburgh DG, Miles DL, Bath AH, Morgan-Jones M, Andrews JN (1987) Baseline geochemical conditions in the Chalk aquifer, Berkshire, UK: a basis for groundwater quality management. Appl Geochem 2:251–274

Ettazarini S (2005) Processes of water–rock interaction in the Turonian aquifer of Oum Er-Rabia Basin, Morocco. Environ Geol 49:293–299. doi:10.1007/s00254-005-0088-x

Food and Agriculture Organization (FAO) (1992) The use of saline waters for crop production. Irrigation and drainage paper 48. FAO, Rome

Gibbs RJ (1970) Mechanisms controlling world water chemistry. Science 170:1088–1090

Jain CK, Bandyopadhyay A, Bhadra A (2009) Assessment of ground water quality for drinking purpose, District Nainital, Uttarakhand, India. Environ Monit Assess Springer 166:663–676. doi:10.1007/s10661-009-1031-5

Joshi DM, Kumar A, Agrawal N (2009) Assessment of the irrigation water quality of River Ganga in Haridwar District India. J Chem 2(2):285–292

Kelley WP (1940) Permissible composition and concentration of irrigation water. Proc Am Soc Civ Eng 66:607–613

Kirda C (1997) Assessment of irrigation water quality. Options Mediterr 31:367–377

Kumar K, Rammohan SV, Dajkumar Sahayam J, Jeevanandam M (2009) Assessment of groundwater quality and hydrogeochemistry of Manimuktha River basin, Tamil Nadu, India. Environ Monit Assess 159:341–351. doi:10.1007/s10661-008-0633-7

US Salinity Laboratory (1954) Diagnosis and improvement of saline and alkali soils, Department of Agriculture, U.S. Handbook 60, Washington DC

Mahler BJ, Massei N (2007) Anthropogenic contaminants as tracers in an urbanizing karst aquifer. J Contam Hydrol 91:81–106

Mayer J (1999) Spatial and Temporal Variation of Groundwater Chemistry in Pettyjohns Cave, Northwest Georgia, USA. J Cave Karst Stud 61(3):131–138

Memon M, Soomro MS, Akhtar MS, Memon KS (2011) Drinking water quality assessment in Southern Sindh (Pakistan). Environ Monit Assess 177:39–50. doi:10.1007/s10661-010-1616-z

Mercado A, Billings GK (1975) The kinetics of mineral dissolution in carbonate aquifers as a tool for hydrological investigations, I. Concentration–time relationships. J Hydrol 24:303–331

Moral F, Cruz-Sanjulián JJ, Olías M (2008) Geochemical evolution of groundwater in the carbonate aquifers of Sierra de Segura (Betic Cordillera, southern Spain). J Hydrol 360:281–296

Paliwal KV (1967) Effect of gypsum application on the quality of irrigation waters. Madras Agric J 59:646–647

Palma P, Alvarenga P, Palma VL, Fernandes RM, Soares AMVM, Barbosa IR (2010) Assessment of anthropogenic sources of water pollution using multivariate statistical techniques: a case study of Alqueva's reservoir, Portugal. Environ Monit Assess 165:539–552

Richards LA (1954) Diagnosis and improvement of saline and alkali soils. Agricultural handbook 60. USDA and IBH Pub. Coy Ltd., New Delhi, pp 98–99

Rizwan R, Singh G (2009) Physico-chemical analysis of groundwater in Angul–Talcher region of Orissa, India. J Am Sci 5(5):53–58

Rockware AqQA Software (2011) Version AQC10664. http://www.rockware.com

Saleh A, Al-Ruwaih F, Shehata M (1999) Hydrogeochemical processes operating within the main aquifers of Kuwait. J Arid Environ 42:195–209

Sappa G, Barbieri M, Ergul S, Ferranti F (2012) Hydrogeological conceptual model of groundwater from carbonate aquifers using environmental isotopes (^{18}O, ^{2}H) and chemical tracers: a case study in southern Latium region, Central Italy. J Water Resour Prot (JWARP) 4(9). doi:10.4236/jwarp.2012.49080

Shaki A, Adeloye A (2006) Evaluation of quantity and quality of irrigation water at Gadowa irrigation project in Murzuq Basin, southwest Libya. Agric Water Manag 84:193–201

Singh K, Malik A, Mohan D, Sinha S (2004) Multivariate statistical techniques for the evaluation of spatial and temporal variations in water quality of Gomti River (India)—a case study. Water Res 38(18):3980–3992

Singh AK, Mondal GC, Kumar S, Singh TB, Tewary BK, Sinha A (2008) Major ion chemistry, weathering processes and water quality assessment in upper catchment of Damodar River basin, India. Environ Geol 54:745–758

Szabolcs I, Darab C (1964) The influence of irrigation water of high sodium carbonate content of soils. In: Proceedings of 8th international congress of ISSS, transmission, vol 2. pp 803–812

Ternan JL (1972) Comments on the use of a calcium hardness variability index in the study of carbonate aquifers: with reference to the central Pennines, England. J Hydrol 16:317–321

US Environmental Protection Agency (1986) Quality criteria for water 1986. EPA 440/5-86-001. Washington, DC 20460

Van der Hoek W, Konradsen F, Ensink JHJ, Mudasser M, Jensen PK (2001) Irrigation water as a source of drinking water: is safe use possible? Trop Med Int Health 6(1):46–54

White WB (1988) Geomorphology and hydrology of karst terrains. Oxford University Press, New York, p 464

WHO (2004) Guidelines for drinking water quality (3rd edn). Recommendations, vol 1. World Health Organization, Geneva

WHO (2006) Guideline for drinking water quality. Vol. recommendations. World Health Organization, Geneva, p 130

Wilcox LV (1955) Classification and use of irrigation waters. USDA Circ. 969, Washington, DC

Chapter 7

Distribution of Ca and Mg in groundwater flow systems in carbonate aquifers in Southern Latium Region (Italy): Implications on drinking water quality

Giueseppe Sappa[1], *Sibel Ergul*[1] & *Flavia Ferranti*[2]
[1]*Dipartimento di Ingegneria Civile, Edile ed Ambientale, Sapienza – Università di Roma, Roma, Italy*
[2]*Centro Reatino di ricerche di Ingegneria per la Tutela e la Valorizzazione dell'Ambiente e del Territorio, Sapienza – Università di Roma, Rieti, Italy*

ABSTRACT

The investigation of hydrochemical properties of springs from the carbonate aquifers of the southern Latium region (Central Italy) aimed to: (i) identify different processes responsible for the hydrochemical evolution of groundwater; (ii) determine the levels of Ca and Mg in the drinking water networks and; (iii) determine the effect of hardness on water quality. Based on the dominance of major cations and anions three hydrochemical facies have been identified: (1) Ca–Mg–HCO_3; (2) Mixed Ca–Na–HCO_3–Cl; (3) Na–Cl. In all cases, Ca–Mg–HCO_3 facies predominates reflecting the main rock types in the area, where limestone, dolomitic limestones and dolomites are common. The Total Dissolved Solids (TDS) and Electrical Conductivity (EC) range from 101 to 1320 mg/l and 138 to 2310 μS/cm, respectively. Most of the springs are supersaturated with respect to carbonate minerals, however all sampled waters were undersaturated with respect to evaporite minerals. The compositional changes in Ca and Mg concentrations are controlled by distance from the recharge area (i.e. groundwater discharging from the lower elevations tends to have the highest concentrations of Mg). The classification of water based on total hardness (as $CaCO_3$) shows that most of the spring water samples fall between hard (150–300 mg/l) and very hard (>300 mg/l) water type.

7.1 INTRODUCTION

As one of the most important water supply sources worldwide, spring water and groundwater from carbonate aquifers have significant importance. Many studies have been carried out on carbonate aquifer systems including investigations of the geochemical processes and their hydrogeological implications. The chemical composition of groundwater is controlled by many factors, including the composition of the precipitation, geological structure and the mineralogy of the aquifers (Chenini & Khmiri, 2009). The interaction of all these factors generates a variety of water types. In recent years, geochemical modelling methods have been employed to obtain information from

hydrochemical datasets in the aquifer systems. These techniques can help to resolve hydrogeological factors such as the hydrochemical components along the groundwater flow paths and geochemical controls on water quality (Briz Kishore & Murali, 1992).

The chemistry of water from carbonate aquifers and the variations in hydrochemical properties are generally related to (i) water-rock interactions (ii) natural factors such as mixing between seawater and freshwater (iii) anthropogenic factors (iv) the type of groundwater circulation. The composition of water in carbonate systems is the result of the dissolution of variable quantities of carbonate (i.e. calcite and dolomite) and evaporite minerals (i.e. gypsum and halite) that control the water chemistry (White, 1988; Ettazarini, 2005). The high dissolution rate and residence time of the circulating water in carbonate rocks and ongoing dissolution allows the water to become more saturated with respect to carbonate minerals along the groundwater flow paths (Plummer, 1977). Consequently, groundwater composition that is controlled by carbonate reactions has a relatively high Ca and HCO_3 concentration, and, if the rock includes some dolomite, could also have quite high Mg concentrations (Shuster & White, 1971). Ca and Mg are the most important elements essential for human health. The presence of Ca and Mg in drinking water has important beneficial effects on human health, however at very high levels they can cause some negative aesthetic effects (undesirable taste and colour). Moreover, water with over 125 mg-Mg/l can cause a laxative effect (Johnson & Scherer, 2012). These elements are the principal natural sources of hardness in water. Many studies have been carried out to emphasise the importance of Ca, Mg and concentrations of hardness in drinking water in relation to human health. These studies suggest that Ca and Mg in drinking water are important protective factors against colon cancer, cardiovascular and cerebrovascular disease and acute myocardial infarction (Ferrandiz *et al.*, 2004; Rubenowitz *et al.*, 1996; Yang & Hung, 1998).

Groundwater resources in the southern part of the Latium region play an important role in providing water for domestic, industrial and agricultural uses. Increased knowledge of geochemical processes that control groundwater chemistry from the aquifer systems can contribute to improved understanding of the processes influencing the composition of water within the carbonate aquifers. The main objectives of this chapter are (i) to identify the source and distribution of calcium and magnesium in water and (ii) its effect on drinking water quality comparing the parameters (i.e. total hardness, TDS, EC, Ph) with the standard guideline values.

7.2 METHODOLOGY

The main spring water sampling survey was carried out in the Lepini, Ausoni and Aurunci Mountains, between 2002 and 2004. On the basis of the hydrogeological setting of the area, 54 spring samples were characterised. Water temperature, electrical conductivity and pH values were determined in the field using a PC 300 Waterproof Hand-held meter. Bicarbonate was measured by titration with 0.1 N HCl. Water samples were filtered through cellulose filters (0.45 μm), and their major and minor constituents were determined by a Metrohm 761 Compact IC ion chromatograph (replicability ±2%). A Metropes C2-100 column was used to determine cations (Na^+, K^+, Mg^{++}, Ca^{++}), while a Metropes A Supp 4-250 column was used for anions (Cl^-, SO_4^{--}, HCO_3^-). Chemical analyses were performed on the water samples at the

Geochemical Laboratory of Sapienza, University of Rome. The analytical accuracy of these methods ranged from 2 to 5%. The geochemical program PHREEQC software, version 2.10.0.0 (Parkhurst & Appello, 1999), with the thermodynamic dataset wateq4f.dat, was employed to evaluate the saturation status of minerals in spring water samples. The SI (Saturation Index) indicates the potential for chemical equilibrium between water and minerals and the tendency for water-rock interaction (Wen, 2008). The characterisation of spring and well water samples has been evaluated by means of major ions, Ca^{++}, Mg^{++}, HCO_3^-, Na^{++}, K^+, Cl^-, SO_4^{--}, as they are the best indicators of chemical evolution along groundwater flow paths. For the identification of water types, the chemical analysis data of the spring water samples have been plotted on a Piper diagram using Geochemistry Software AqQA.

7.3 STUDY AREA

Lepini, Ausoni and Aurunci are three different groups of mountains belonging to the pre-Apennines of Latium and they occupy a well-defined geographical area, called the Volscian Mountain Range. The Lepini Mountains are located in the northern part of the Pontina Plain and host an important karst aquifer. The aquifer in the Lepini massif is unconfined with an undefined depth. The Pontina Plain is a coastal plain developed along an extensional marine boundary. This Plain is positioned between the Lepini-Ausoni mountains of the Central Appenines and the Tyrrhenian Sea. The Ausoni Mountains rise in southern Latium and extend towards the coast, from the middle Amaseno valley. The Ausoni hydrogeological unit is mainly composed of limestones with interbedded dolomitic limestones. Most of the springs lie along the periphery of the aquifer with no sharp distinction from the recharge areas. The Aurunci Mountains represent the south eastern part of the Volscian Range and are oriented parallel to the Apennine Range. The Aurunci Mountains are made of two distinct hydrogeological units: the western Aurunci, belonging to the Ausoni-Aurunci system, and the eastern Aurunci, which is separated from the western part by a marly-arenaceous flysch complex (Boni, 1975). The Western Aurunci hydrogeological unit consists of dolomitic limestones and dolomites of Jurassic and Cretaceous age. The springs are supplied by groundwater derived from these geological formations. The groundwater is directly discharged into the Liri river through the narrow alluvial belt separating the unit from the river. The unit ontains multiple hydrogeological basins and the boundaries match important tectonic lines that caused the outcropping of the calcareous-dolomitic Jura (Accordi *et al.*, 1976). The Eastern Aurunci hydrogeological carbonate structure is surrounded by relatively less-permeable sediments, including the Frosinone flysch, the Roccamonfina volcanites and the Garigliano plain alluvia (Celico, 1978).

7.4 RESULTS & DISCUSSION

7.4.1 Water chemistry and hydrochemical evolution

The summary statistics of major ion concentrations and physico-chemical characteristics of the spring water samples are presented in Table 7.1. The sampled waters in the study area show different characteristics in terms of physico-chemical parameters and elemental concentrations. The temperature of the sampled spring waters range

Table 7.1 Summary statistics of major ion concentrations and physico-chemical parameters of sampled waters.

Sampling locations		*T°C*	*pH*	*EC (µs/cm)*	*Ca (mg/l)*	*Mg (mg/l)*	*Na (mg/l)*	*K (mg/l)*	*Cl (mg/)*	HCO_3^- *(mg/l)*	SO_4^{-2} *(mg/l)*	*TDS (mg/l)*
Lepini	Mean	13.0	7.7	517.0	64.3	13.7	37.4	2.9	55.4	239.8	16.4	430
springs	Median	13.0	7.7	400.0	67.3	6.6	6.8	1.2	9.6	235.9	4.3	334
	Min	10.0	6.9	138.0	15.4	1.4	2.9	0.1	3.9	67.1	1.7	101
	Max	15.0	8.1	1540.0	111.0	44.7	221.0	15.8	338.4	448.0	85.4	1264
Ausoni	Mean	13.0	7.7	826.0	65.2	18.2	73.5	3.5	128.4	234.2	27.2	550
springs	Median	12.0	7.7	404.0	61.6	9.2	8.6	0.8	13.3	232.0	5.8	324
	Min	12.0	6.9	315.0	41.5	3.8	4.1	0.2	7.5	176.9	3.8	255
	Max	15.0	8.1	2310.0	89.2	47.8	293.1	15.4	524.9	305.1	110.9	1320
Aurunci	Mean	12.0	7.7	545.0	70.7	25.6	10.6	2.9	12.7	316.5	34.6	479
springs	Median	12.0	7.8	429.0	63.6	9.9	7.6	1.1	9.8	244.1	5.3	338
	Min	3.0	7.1	311.0	44.5	1.5	4.2	0.3	4.5	170.9	2.7	246
	Max	31.0	8.0	1217.0	197.3	93.4	50.5	21.6	46.7	805.5	195.8	1150

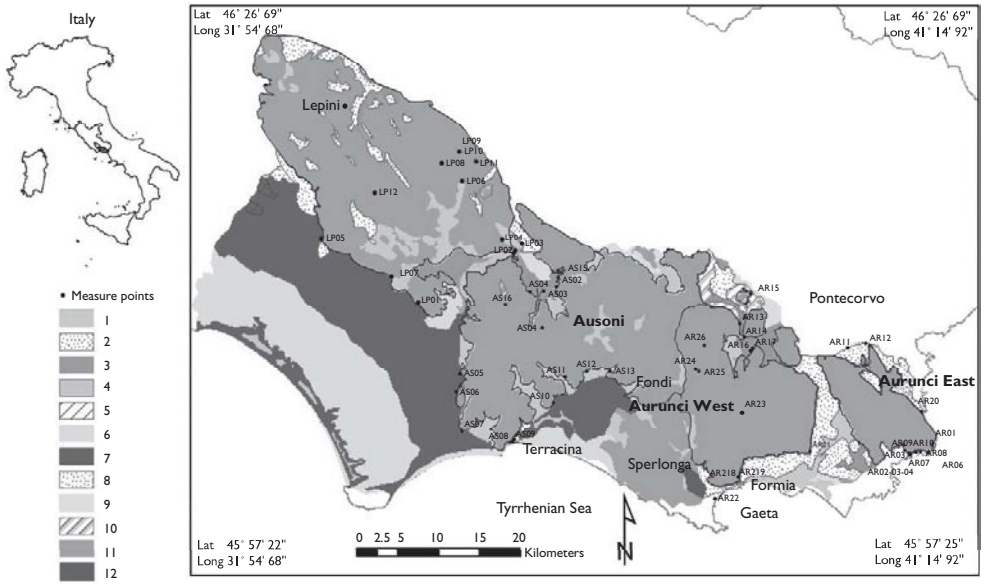

Figure 7.1 Simplified hydro-geological map of the study area. 1. Recent deposits (Holocene); 2. Detritic complex (Pleistocene-Holocene); 3. Alluvial complex (Pleistocene-Holocene); 4. Alluvial deposits from perennial streams (Pleistocene-Holocene); 5. Travertine complex (Pleistocene-Holocene); 6. Sand dunes (Pleistocene-Holocene); 7. Fluvial lacustrine deposits (Holocene); 8. Pyroclastic complex (Pliocene-Pleistocene); 9. Heterogeneous clastic deposits (Pleistocene); 10. Clayey-marly Flysch complex with interbedded lithoids (Cretaceous – Miocene); 11. Carbonate platform complexes (Middle Lias-Upper Cretaceous); 12. Basal dolomite complex (Triassic-lower Lias). Spring and well sampling locations (LP: Lepini springs., AS: Ausoni springs., AR: Aurunci springs).

from 3 to 31°C with the mean value of 13.4°C. The highest temperatures (31°C) were observed in two samples from Aurunci springs. The pH values of the water samples range from 6.91 to 8.12, indicating slightly acidic to slightly alkaline nature. According to the WHO (2004) guidelines, the range of desirable pH values for drinking water is 6.5–9.2. There are no spring water samples with pH values outside of the desirable ranges. The Electrical Conductivity (EC) and Total Dissolved Solids (TDS) values range from 315 to 2310 μS/cm and 255 to 1320 mg/l, respectively. The large variation in Total Dissolved Solids (TDS) is thought to be mainly due to water-rock interaction along the flow paths and proximity of the sampling locations to the coast. Most of the spring samples (~61%) show TDS values below 1000 mg/l and EC values less than the maximum permissible drinking water guideline limit highlighting suitability for drinking and agricultural purposes. The highest calcium (197.3 mg/l) and magnesium (93.4 mg/l) concentrations were observed in water samples from Aurunci springs. Bicarbonate is the dominant anion found in all spring water samples, varying from 67.1 mg/l to 805 mg/l. The highest sodium and chloride concentrations were observed in Ausoni and Lepini springs (i.e. samples taken from low discharge elevations) ranging from 293.1 mg/l to 524.9 mg/l and 221 mg/l to 338 mg/l, respectively.

The hydrochemical facies of the spring waters are illustrated in the Piper trilinear diagram (Figure 7.2). Based on the dominance of major cationic and anionic species,

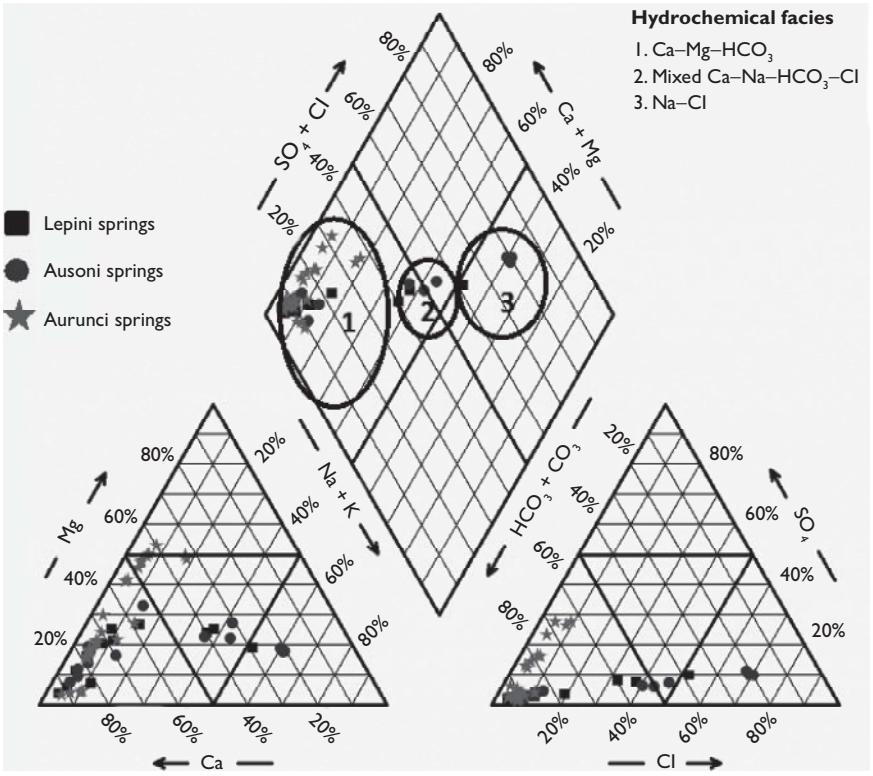

Figure 7.2 Piper trilinear plot for hydrochemical facies evolution and water classification.

three hydrochemical facies have been identified in the study area: (1) Ca–Mg–HCO_3; (2) Mixed Ca–Na–HCO_3–Cl; (3) Na–Cl. The Ca–Mg–HCO_3 water type predominates, reflecting the main rock types in the area, where limestone, dolomitic limestones and dolomites are the most common formations. However, some spring samples discharge at lower elevations, issuing from Lepini and Ausoni Mountains, and belong to or show a tendency towards the Na–Cl type due to the proximity of the sampling locations to the coast. The variations in ion concentrations and the occurrence of different hydrochemical facies can be attributed to water-rock interaction and/or seawater intrusion in the coastal area.

This was confirmed by geochemical modelling and determination of SI for the Lepini, Ausoni and Aurunci springs. The SI indicates the potential for chemical equilibrium between water and minerals and the tendency for water-rock interaction (Jawad *et al.*, 1986). If undersaturated (SI < 0), this phase could be dissolved by the groundwater and, thus, could be a potential source of its constituent chemistry. If supersaturated (SI > 0), that phase, feasibly, could precipitate. Geochemical modelling and saturation index analysis of the Lepini, Ausoni and Aurunci spring samples shows an interaction with carbonate rocks. Calculated saturation indexes with respect to various mineral phases (i.e. calcite, dolomite, gypsum and halite) of the spring water samples are shown in Figure 7.3.

The results of geochemical modelling suggest that most of the spring water samples from the Lepini, Ausoni, and Aurunci Mountains are saturated with respect to

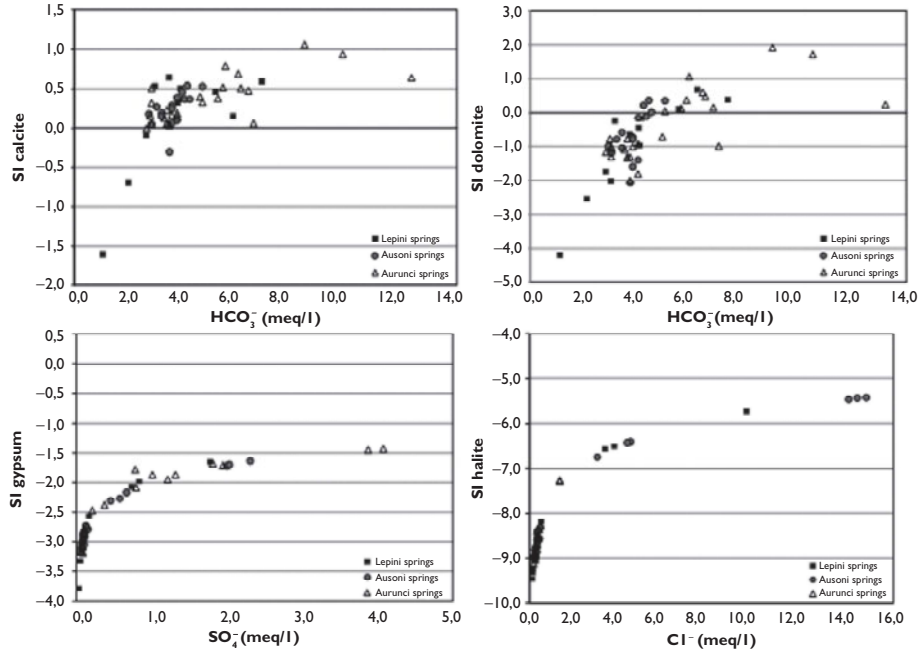

Figure 7.3 Saturation Index (S.I.) values of spring water samples. a) Calcite saturation index versus HCO_3^-; b) Dolomite saturation index versus HCO_3^-; c) Gypsum saturation index versus SO_4^-; d) Halite saturation index versus Cl^-.

calcite. More than half of the samples are undersaturated with respect to dolomite, while all the sampled waters are undersaturated with respect to gypsum and halite. This indicates that the groundwater has capacity to dissolve gypsum and halite along the flow paths so that the concentrations of Ca^{++}, SO_4^{--}, Na^{+} and Cl^{-} in solution could increase down gradient (Stumm & Morgan, 1996). The spring samples that are both saturated with respect to calcite and dolomite imply a greater dissolution and stronger mineralisation down the groundwater flow paths. However, the water samples, undersaturated with respect to dolomite, indicate that dolomite can dissolve in this system adding Ca^{++}, Mg^{++}, and HCO_3^{-} in solution. If Ca and Mg were derived from the dissolution of carbonate (calcite and dolomite) and evaporate (gypsum) minerals the ionic ratios of (Ca + Mg) to (SO_4 + HCO_3) should be a constant value of one (McLean *et al.*, 2000). Thus, binary plots of (Ca + Mg) versus (HCO_3 + SO_4) were prepared to identify the ion ex-change and weathering processes (Figure 7.4). Most of the spring water samples fall along the 1:1 relationship suggesting that these ions have originated from the dissolutions of calcite, dolomite and gypsum. However, spring samples from the Ausoni Mountains are clustered above the 1:1 line indicating ion exchange process. Na:Cl should be a constant value of one, if halite dissolution is responsible for the sodium and chloride (Fisher & Mullican, 1997). The Na:Cl ratios of spring water samples range from 0.08 to 2.25 (Table 7.2). The majority of the samples have a molar ratio greater or equal to one, which indicates Na^{++} may increase due to ion exchange and halite dissolution (Cerling *et al.*, 1989). However, some spring water samples from the Ausoni Mountains have a Na:Cl molar ratio close to and less than the value in seawater (0.86) indicating possible seawater contamination (where groundwater becomes enriched in Cl^{-} the value of the ratio will drop).

The compositional changes in Mg and Ca concentrations mainly depend on the residence of water in carbonate systems and that is controlled by the distance from the recharge area and the dissolution and/or precipitation reaction of calcite and dolomite (Langmuir, 1971). The Mg/Ca ratio is commonly used in carbonate aquifers as an indicator of the residence time of circulating groundwater. The Mg/Ca ratios of

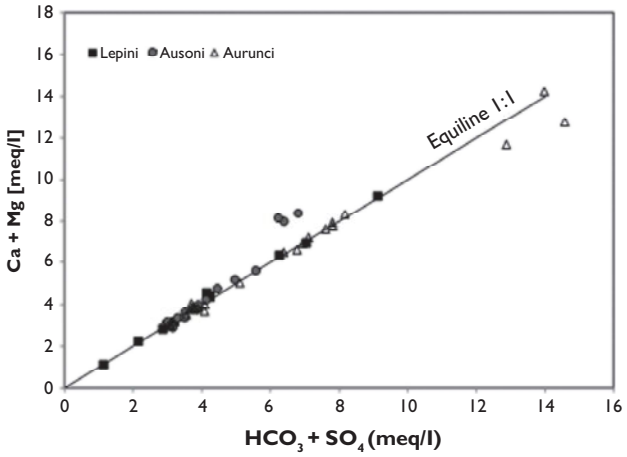

Figure 7.4 Relationship between Ca + Mg vs. HCO_3 + SO_4 in meq/l.

Table 7.2 Some ionic ratios. Total hardness and discharge elevations of springs (LP: Lepini. AS: Ausoni. AR: Aurunci).

Samples	*Discharge elevations (m a.s.l.)*	*Mg/Ca*	*Na/Cl*	*Hardness (as $CaCO_3$) (mg/l)*	*Indication*
LP01	5	0.68	1.00	318.58	Very hard
LP02	42	0.38	1.32	228.16	Hard
LP03	64	0.08	1.11	221.68	Hard
LP04	185	0.28	1.18	218.44	Hard
LP05	12	0.66	1.01	461.24	Very hard
LP06	840	0.21	1.34	157.76	Hard
LP07	5	0.60	1.15	348.35	Very hard
LP08	1110	0.14	1.08	140.98	Moderately hard
LP09	740	0.04	1.15	153.84	Hard
LP10	360	0.31	0.88	112.16	Moderately hard
LP11	360	0.46	0.82	56.16	Soft
LP12	1065	0.06	0.99	186.41	Hard
AS01	92	0.24	0.80	191.14	Hard
AS02	98	0.25	0.70	187.96	Hard
AS03	95	0.18	0.63	180.83	Hard
AS04	95	0.24	1.01	144.70	Moderately hard
AS05	6	0.55	0.90	238.41	Hard
AS06	4	0.65	0.90	259.42	Hard
AS07	2	0.88	0.88	419.73	Very hard
AS08	10	0.87	0.88	499.52	Very hard
AS09	6	0.85	0.86	407.91	Very hard
AS10	4	0.88	0.93	280.88	Very hard
AS11	18	0.20	0.73	157.70	Hard
AS12	20	0.23	0.75	167.12	Hard
AS13	10	0.62	1.57	167.45	Hard
AS14	475	0.08	1.04	199.30	Hard
AS15	100	0.14	0.94	189.55	Hard
AS16	500	0.11	0.93	211.65	Hard
AR01	18	1.51	1.64	639.02	Very hard
AR02	7	1.01	0.99	332.31	Very hard
AR03	13	1.12	1.10	347.49	Very hard
AR04	15	0.94	1.14	381.39	Very hard
AR05	17	0.37	2.85	413.41	Very hard
AR06	12	1.03	1.16	326.06	Very hard
AR07	14	1.34	1.06	361.56	Very hard
AR08	13	1.46	1.68	585.36	Very hard
AR09	8	0.75	1.15	396.60	Very hard
AR10	12	1.16	1.17	388.69	Very hard
AR11	39	0.29	0.79	175.10	Hard
AR12	31	0.46	1.74	183.18	Very hard
AR13	85	0.24	0.88	194.37	Very hard
AR14	77	0.24	0.93	188.56	Very hard

(*Continued*)

Table 7.2 (Continued).

Samples	*Discharge elevations (m a.s.l.)*	*Mg/Ca*	*Na/Cl*	*Hardness (as $CaCO_3$) (mg/l)*	*Indication*
AR15	83	0.20	0.84	252.16	Very hard
AR16	70	0.24	0.91	192.70	Very hard
AR17	74	0.20	0.90	202.48	Very hard
AR18	17	0.34	0.88	149.33	Moderately hard
AR19	17	0.29	0.86	151.95	Hard
AR20	11	0.45	1.50	712.71	Very hard
AR21	65	0.32	2.01	150.86	Hard
AR22	1	0.28	0.82	194.45	Very hard
AR23	1050	0.05	2.12	148.18	Hard
AR24	700	0.05	0.94	158.71	Hard
AR25	870	0.04	1.13	188.38	Very hard
AR26	700	0.03	1.33	199.19	Very hard

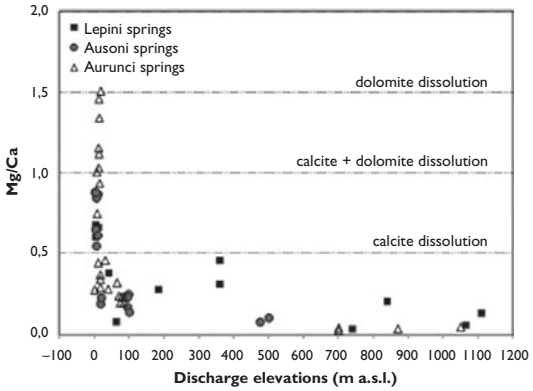

Figure 7.5 Mg/Ca ratio of spring samples vs. discharge elevations (m a.s.l.).

sampled waters are plotted against discharge elevations in Figure 7.5. The relationship between dolomite dissolution and calcite precipitation is thought to increase the Mg/Ca ratios along the flow paths. High elevation springs discharges near the recharge area and have the lowest Mg:/Ca ratios (<0.1), while low-elevation springs farther from the recharge area show higher Mg/Ca ratios (up to 1.5). In general, an increase water temperature can accelerate the kinetics of the dissolution of dolomite, and hence also the Mg/Ca ratio (Herman & White, 1985). The highest Mg/Ca ratios (~1.5) are found in the high temperature Aurunci springs, discharging at lower elevations, highlighting long residence time and enhanced weathering along the groundwater flow paths.

7.4.2 Effects of Ca and Mg on drinking water quality

The presence of low Ca and Mg concentrations in drinking water causes adverse health effects, however, high concentrations may cause domestic and industrial

problems (Yang *et al.*, 2000; Reynolds & Richards, 1996). According to previous studies, the minimum required amounts of Ca and Mg in drinking water are 20 and 10 mg/l respectively, and the desired amounts of M and Ca in drinking water are 30–20 mg/l and 80–40 mg/l, respectively (Kozisek, 2003; Cotruvo, 2009). The maximum and minimum values of Ca and Mg concentrations are present in Table 7.1. The calcium concentrations in water samples range from 15.40 to 197.3 mg/l with minimum and maximum values, respectively. Almost 33.3% of the samples contain Ca concentrations higher than 75 mg/l, while about 66.3% of the springs show Ca concentrations below 75 mg/l. Mg concentrations range between 1.4 to 93.4 mg/l. Most of the samples (~66%) show Mg concentrations <30 mg/l. However, about 9.2% of the 54 samples have a Mg concentration >50 mg/l. The remaining water samples have magnesium concentrations within the range of 30–50 mg/l. The highest calcium (197.3 mg/l) and magnesium (93.4 mg/l) concentrations were observed in water samples from Aurunci springs.

The relationship between Electrical Conductivity (EC) and the Ca–Mg distributions is shown in Figure 7.6. Electrical conductivity values of spring water samples ranges from 138 to 2310 µS/cm indicating fresh (<500 µS/cm), marginal (500–1500 µS/cm) and brackish water types (>1500 µS/cm) in the area. Most of the samples have EC values less than the maximum permissible limit. The greater the conductivity, the greater is its salt content. Ca and Mg contents decreases gradually in groundwater samples, taken near coastal area, with increasing EC. The highest Ca and Mg concentrations were found for water samples with EC of 500–1000 µS/cm representing a typical water from the carbonate aquifer. The decrease in the Ca with increase in EC is possibly due to the proximity of sampling locations to the coast (i.e. samples discharged at lower elevations). The presence of higher concentrations is

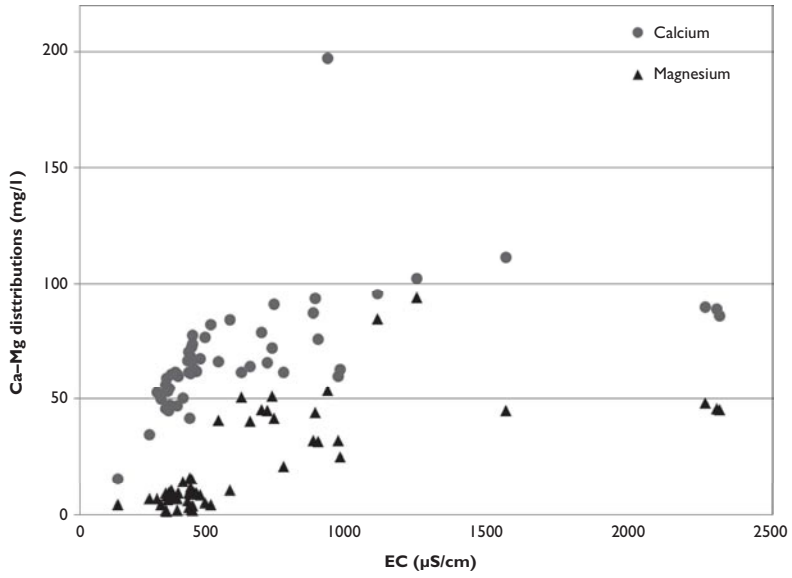

Figure 7.6 Ca–Mg distributions vs. Electrical Conductivity (µS/cm).

attributed to the influence of seawater in the coastal area and weathering of Mg-rich dolomite and calcareous-dolomitic lithologies.

A and Mg are the most important constituents of drinking water, moreover they are major contributors to water hardness. As contributors to hardness, calcium and magnesium ions can affect drinking water quality. High levels of total hardness do not cause a health risk, however, but both the extreme degrees, very soft (<75 mg/l as $CaCO_3$) and very hard (>300 mg/l as $CaCO_3$), are considered as undesirable features in water. Hardness levels between 80 and 100 mg/l (as $CaCO_3$) are generally acceptable in drinking water and are considered tolerable by consumers (Ternan, 1972; USGS, 2012; Bernardi *et al.*, 1995; Memon, 2011). Besides, higher Ca and Mg concentrations affect aesthetic parameters such as taste, smell and colour of water (Lenntech, 1998). Determination of water hardness is a useful test to measure quality of water for drinking, agricultural and industrial uses. The total hardness of water is the sum of calcium and magnesium hardness expressed as mg/l $CaCO_3$. The total hardness (as $CaCO_3$) of water samples can be calculated by the following equation (WHO, 2008):

$$\left[CaCO_3\right] = 2.5\left[Ca^{2+}\right] + 4.1\left[Mg^{2+}\right]$$

The US-EPA classified water that contains 0 to 75 mg/l $CaCO_3$ as soft, 75 to 100 mg/l $CaCO_3$ as moderately hard, 150 to 300 mg/l $CaCO_3$ as hard and >300 mg/l $CaCO_3$ as very hard. The total hardness of Lepini spring samples range from 56 to 461 mg/l (Table 7.2) and fall between soft and very hard water category. For the spring water samples from the Ausoni Mountain total hardness range between 144 to 499 mg/l and is classified as moderately hard to very hard water. The highest total hardness values were observed in water samples from Aurunci Mountains ranging from 148 to 712 mg/l, respectively. Almost all the Aurunci spring samples are characterised as very hard water. The classification of water based on total hardness shows that most of the spring water samples fall between hard and very hard water type. Hardness levels between 80 and 100 mg/l (as $CaCO_3$) are recommended by World Health Organisation (WHO) as the minimum guideline limit for total hardness in drinking water. Waters with hardness levels in excess of 200 mg/l are considered poor but have been tolerated by consumers, however waters with hardness in excess of 500 mg/l are not suitable for most domestic purposes. Almost all sampled spring waters exceed the minimum allowable limit. The observed high total hardness values in spring water samples are related to the main rock types in the area investigated, where limestone, dolomitic limestones and dolomites are the most dominant formations.

7.5 CONCLUSIONS

Hydrochemical data and geochemical modelling techniques were employed to identify the main processes responsible for the evolution of spring waters from the carbonate aquifers of southern Latium region, Central Italy. The variations in major ion concentrations and hydrochemical facies suggest that these water types undergo further geochemical evolution through water-rock interaction along the flow paths with some seawater contamination near the coast. The classification of water based

on total hardness (as $CaCO_3$) shows that most of the spring water samples fall between the hard (150–300 mg/l) and very hard (>300 mg/l) water types. The observed high total hardness in spring water samples are mainly related to the main rock types in the area, where limestone, dolomitic limestones and dolomites are common. The high dissolution rate for carbonate formations and the residence times of the circulating water in carbonate rocks increase the Ca and Mg concentrations and hence also the total hardness. Almost all sampled spring waters exceed the minimum guideline limit for drinking water. Hard water has no adverse effects on human health, however, it may create some problems for domestic and industrial users. The highest Ca and Mg concentrations were found in water samples having EC levels from 500 to 1000 μS/cm representing a typical water from the carbonate aquifer. The results of hydrochemical analyses and the calculated parameters (i.e. total hardness, TDS, pH, EC) suggest that most of the groundwater samples are suitable for drinking purposes. The observed parameters fall within the recommended limits of U.S Environmental Protection Agency (US-EPA), World Health Organisation (WHO).

ACKNOWLEDGEMENTS

The authors would like to thank the Regional Basins Authority of Latium for the financial support of the project.

REFERENCES

Accordi B., Biasini A., Caputo C., Devoto G., Funiciello R., La Monica G.B., Palmieri E.L., Matteucci R. & Pieruccini U. (1976) Geologia e dissesti del territorio montano della Regione Lazio, In: *Carta della Montagna 2, Monografia Regionali No 12 Lazio*, Ministero di Agricoltura, Roma, 55–101.

Bernardi D., Dini F.L., Azzarelli A., Giaconi A., Volterrani C. & Lunardi M. (1995) Sudden cardiac death rate in an area characterised by high incidence of coronary artery disease and low hardness of drinking water. *Angiology* 46, 145–149.

Boni C. (1975) The relationship between the geology and hydrology of the Latium-Abruzzi Apennines. In: M Parotto, A Praturlon, Geological summary of the central Apennines, *Quaderni de La ricerca scientifica* 90, 301–311.

Briz Kishore B.H. & Murali G. (1992) Factor analysis for revealing hydrochemical characteristics of a watershed. *Environmental Geology* 19, 3–9.

Celico P. (1978) Schema idrogeologico dell'Appennino carbonatico centro-meridionale. *Memorie e Note dell'Istituto di Geologia Applicata* 14, 1–97.

Cerling T.E., Pederson B.L. & Damm K.L.V. (1989) Sodium-calcium ion exchange in the weathering of shales: Implications for global weathering budgets. *Geology* 7, 552–554.

Chenini I. & Khmiri S. (2009) Evaluation of ground water quality using multiple linear regression and structural equation modeling. *International Journal of Environmental Science and Technology* 6(3), 509–519.

Cotruvo J. & Bartram J. (2009) *Calcium and magnesium in drinking-water: Public health significance*. Geneva, World Health Organisation, WHO.

Ettazarini S. (2005) Processes of water-rock interaction in the Turonian aquifer of Oum Er-Rabia Basin, Morocco. *Environmental Geology* 49, 293–299.

Ferrandiz J., Abellan J.J., Gomez-Rubio V., López-Quílez A., Sanmartín P., Abellán C., Martínez-Beneito M.A., Inmaculada M., Vanaclocha H., Zurriaga O., Ballester F., Gil J.M., Pérez-Hoyos S. & Ocaña R. (2004) Spatial analysis of the relationship between mortality from cardiovascular and cerebrovascular disease and drinking water hardness. *Environmental Health Perspectives* 112(9), 1037–44.

Fisher R.S. & Mullican W.F. (1997) Hydrochemical evolution of sodium-sulfate and sodium-chloride groundwater beneath the Northern Chihuahua Desert, Trans-Pecos, Texas, USA. *Hydrogeology Journal* 52, 4–16.

Herman J.S. & White W.B. (1985) Dissolution kinetics of dolomite: effects of lithology and fluid flow velocity, *Geochimica et Cosmochimica Acta* 49, 2017–2026.

Jawad S.B. & Hussien K.A. (1986) Contribution to the study of temporal variations in the chemistry of spring water in karstified carbonate rocks. *Hydrological Sciences – Journal – des Sciences Hydrologiques* 31(4), 529–541.

Johnson R. & Scherer T. (2012) Drinking water Quality: Testing and Interpreting Your Results North Dakota State University, WQ-1341.

Kozisek F. (2003) Health significance of drinking water calcium and magnesium National Institute of Public Health Prague; Czech Republic. www.midasspringwater.com/typed%20documents/HealthSignificance.pdf.

Langmuir D. (1971) Geochemistry of some carbonate ground waters in Central Pennsylvania. *Geochimica et Cosmochimica Acta* 35(10), 1023–1045.

Lenntech (1998) www.lenntech.com/ro/water-hardness.

McLean W., Jankowski J. & Lavitt N. (2000) Groundwater quality and sustainability in an alluvial aquifer, Australia. In: Sililo O et al., eds. *Groundwater past achievements and future challenges*, A Balkema, Rotterdam, 567–573.

Memon M., Soomro M.S., Akhtar M.S. & Memon K.S. (2011) Drinking water quality assessment in Southern Sindh, Pakistan. *Environmental Monitoring and Assessment* 177, 39–50.

Parkhurst D.L. & Appello C.A.J. (1999) *User's guide to PHREEQC., version 2. – A computer program for speciation, batch-reaction, one-dimensional transport, and inverse geochemical calculations*. US Geological Survey Water-Resources Investigations Report 99-4259, 312 p.

Plummer L.N. (1977) Defining reactions and mass transfer in part of the Floridan aquifer. *Water Resources Research* 13(5), 801–812.

Reynolds, T.D. & Richards, P.A. (1996) *Unit operations and processes in environmental engineering*. PWS Publishing Company, Boston, MA.

Rubenowitz E., Axelsson G. & Rylander R. (1996) Magnesium in drinking water and death from acute myocardial infarction. *American Journal of Epidemiology* 143(5), 456–62.

Shuster E.T. & White W.B. (1971) Seasonal fluctuations in the chemistry of limestone spring A possible means for characterizing carbonate aquifers. *Journal of Hydrology* 14, 93–128.

Stumm W. & Morgan J.J. (1996) *Chemical equilibria and rates in natural waters, Aquatic Chemistry*. John Wiley and Sons, New York, 1022 p.

Ternan J.L. (1972) Comments on the use of a calcium hardness variability index in the study of carbonate aquifers: with reference to the central Pennines, England. *Journal of Hydrology* 16, 317–321.

US Environmental Protection Agency (1986) *Quality criteria for water 1986*. EPA 440/5-86-001. Washington, DC 20460.

USGS (2012) http://water.usgs.gov/owq/hardness-alkalinity.html#hardness.

Wen X.H., Wu Y.Q. & Wu J. (2008) Hydrochemical characteristics of groundwater in the Zhangye Basin, Northwestern China. *Environmental Geology* 55(8), 1713–1724.

White W.B. (1988) *Geomorphology and Hydrology of Karst Terrains*. Oxford University Press, New York, 464 p.

WHO (2004) *Guidelines for Drinking water Quality*, 3rd edn. *Vol 1 Recommendations*, World Health Organization, Geneva.

WHO (2008) *Guidelines for Drinking-water Quality*, 3rd edn. *Incorporating The First And Second Addenda Volume 1 Recommendations*. World Health Organization, Geneva.

Yang C.Y. & Hung C.F. (1998) Colon cancer mortality and total hardness levels in Taiwan's drinking water. *Archives of Environmental Contamination and Toxicology* 35(1), 148–51.

Yang C.H., Chiu H.F., Cheng M.F., Hsu T.Y., Cheng M.F. & Wu T.N. (2000) Calcium and magnesium in drinking water and the risk of death from breast cancer. *Journal of Toxicology and Environmental Health* 60, 231–241.

Groundwater geochemical characterization in the karst aquifer feeding the Pertuso spring (Italy)

Giuseppe Sappa *, Flavia Ferranti, Giulia Luciani

University of Roma Sapienza, Faculty of Engineering, Department of Civil Engineering, Roma, Italy

ABSTRACT

The present study deals with the geochemical characterization of Pertuso karst spring, the main perennial outlet of the karst aquifer in the Upper Valley of Aniene River, which is an important source for drinking water in the southeast part of Latium Region, in Central Italy. This paper deals with the supervisory monitoring plan related to the catchment project of the Pertuso spring which is going to be exploited to supply an important water network in the south part of Roma district. In order to identify the hydrogeochemical processes governing the evolution of groundwater and its circulation patterns, a multi-tracer approach was used to describe the hydrogeology of this karst system with the aim of achieving proper management and protection of this important resource due catchment works. To investigate the evolution of groundwater compositions, groundwater from different parts of the aquifer was sampled. Groundwater samples were collected from Pertuso karst spring and from four monitoring wells between July 2014 and January 2015 and analysed for major and trace elements. Physico-chemical parameters (e.g., temperature, pH, Eh, EC etc.) were also measured. A detailed analysis provides that all of groundwater samples have the same origin, associated lithologies, and mineral-solution reactions related to hydrodynamic responses. Piper diagram reveals higher bicarbonate and calcium suggests interactions with carbonate rocks, yielding increased Ca concentrations in the groundwater. Groundwater are characterized by low mineralization and low Mg/Ca ratios and represents the flux of rapid infiltration of surface waters through sinkholes and well-developed karst conduits network. Results from geochemical interpretation of groundwater chemistry using PHREEQC and the measured pH and Eh of groundwater sampled indicate that most of the samples were saturated with respect to calcite and aragonite, however all sampled waters were undersaturated with respect to dolomite and gypsum. Geochemical modelling showed that spring water and groundwater are made of surface water, providing quantitative information on the vulnerability of groundwater to potential surface water contamination.

Key words: Karst aquifer; geochemical modelling; Pertuso spring; Upper Valley of Aniene River.

* Corresponding Author

RESEARCHERID
THOMSON REUTERS

[Sappa* *et al.*, 6(6): June, 2017]
IC™ Value: 3.00

ISSN: 2277-9655
Impact Factor: 4.116
CODEN: IJESS7

IJESRT

INTERNATIONAL JOURNAL OF ENGINEERING SCIENCES & RESEARCH TECHNOLOGY

VULNERABILITY ASSESSMENT OF THE KARST AQUIFER FEEDING THE PERTUSO SPRING (CENTRAL ITALY): COMPARISON BETWEEN DIFFERENT APPLICATIONS OF COP METHOD

Giuseppe Sappa[*1], Flavia Ferranti[2] & Francesco Maria De Filippi[3]
[*1,2&3] Department of Civil, Building and Environmental Engineering (DICEA), Sapienza University of Rome, Italy

DOI: 10.5281/zenodo.817855

ABSTRACT

Karst aquifers vulnerability assessment and mapping are important tools for improved sustainable management and protection of karst groundwater resources. In this paper, in order to estimate the vulnerability degree of the karst aquifer feeding the Pertuso Spring in Central Italy, COP method has been applied starting from two different discretization approaches: using a polygonal layer and the Finite Square Elements (FSE). Therefore, the hydrogeological catchment basin has been divided into 72 polygons, related to the outcropping lithology and the karst features. COP method has been applied to a single layer composed by all these polygons. The results of this study highlight vulnerability degrees ranging from low to very high. The maximum vulnerability degree is due to karst features responsible of high recharge and high hydraulic conductivity. Comparing the vulnerability maps obtained by both methodologies it is possible to say that the traditional discretization approach seems to overestimate the vulnerability of the karst aquifer feeding the Pertuso Spring. Between the two different approaches of COP method, the proposed polygonal discretization of the hydrogeological basin seems to be more suitable to small areas, such as the Pertuso Spring hydrogeological basin, than the traditional grid mapping.

KEYWORDS: vulnerability assessment, COP, karst aquifer, Pertuso Spring, karst features.

I. INTRODUCTION

Groundwater vulnerability describes the susceptibility of an aquifer to contaminants that can reduce its quality. Intrinsic vulnerability only depends on the natural properties of the aquifer (soil, lithology, hydraulic properties, recharge, etc.) and is independent of the nature of the contaminant [1,2]. Thus, vulnerability assessment methods may be considered important tools for designing protection zones for water supply and highlighting areas, where the aquifer is more susceptible to pollution introduced at the land surface [3].

Karst groundwater protection is a prior environmental target for water sustainable management in Europe, where more than 30% of the water supply is obtained from these resources [4]. Karst aquifers are characterized by a heterogeneous distribution of permeability due to conduits and voids, developed by the dissolution of carbonate rocks, frequently embedded in a less permeable fractured rock matrix [5,6]. Water flow velocities into a well-developed karst system are extremely fast and contaminants can quickly reach the saturated zone [7]. This system may receive localized inputs from sinking surface streams and as storm runoff through sinkholes, dolines and karst features in general. For this reason, in a karst setting, the identification of these fast recharge areas is an important tool in order to protect groundwater resources [8]. Recently, in order to identify karst landscapes, to describe karst features and to detect geological structures, relevant to karst development, remote sensing and geographic information system (GIS) methods were used for karst research. Because of the computer low cost and processing speed, these applications have come out to be useful tools for karst feature mapping, providing detailed geomorphological info [9,10,11]. At the same time, as Geographic Information System technology (GIS) has improved in the last years, lots of approaches to groundwater vulnerability to pollution evaluation have been developed and worldwide applied [12,13,14]. Traditional approaches have strong limitations in vulnerability assessment of karst aquifer because the contaminants transport mostly occurs along

ISSN: 2277-9655
Impact Factor: 4.116
CODEN: IJESS7

preferential pathways (karst features). Other methods are especially designed for karst environment, taking into account the function of the epikarst and of the karstic network [1]. In this study, a new karst aquifer vulnerability approach has been set up, highlighting the karst features, outcropping in the study area. Two different approaches for the intrinsic aquifer vulnerability assessment have been tested in the case study, comparing their results.

This paper presents the intrinsic vulnerability maps obtained applying the COP method [15] to the karst aquifer, feeding the Pertuso Spring, sited in the Upper Valley of the Aniene River (Central Italy). This method is useful to identify the most vulnerable zones and the main processes controlling the evolution of groundwater in karst settings. The implementation of COP method has been carried out, starting from two different discretization of the study area. The aim of this work is to compare both results of the intrinsic vulnerability mapping, in order to evaluate which is the most suitable for the study area.

II. GEOLOGICAL AND HYDROGEOLOGICAL SETTINGS

The Pertuso Spring is an important karst spring located in the south part of Latium Region, in the Upper Valley of the Aniene River. This spring feeds the Comunacqua hydroelectric power plant, owned by ENEL group [16] and, with a discharge reaching up to 3 m^3/s, is now one of the main water resource for the South part of Rome district [17]. The study area lies in the Upper Valley of the Aniene River, in the Latium Region (Central Italy) and covers an area of about 50 km^2 [18]. The Pertuso Spring hydrogeological basin is located between latitude 41° 51' to 41° 56'N and longitude 13° 13' to 13° 21'E and belongs to the Special Area of Conservation (SAC) of the Aniene River Springs (EC Site Code IT6050029) established under Directive 92/43/EEC. The Aniene basin is made mostly of bare Mesozoic, highly fractured, karstified carbonate rocks of the central Apennine range [19]. The entire area is mostly made of highly permeable Cretaceous carbonate rocks, deeply fractured and mostly soluble (Figure 1). The base of the stratigraphic series is made of Upper Cretaceous carbonates, represented by the alternation of granular limestone and dolomites layers. Above these ones, Quaternary fluvial and alluvial deposits lie, downward pudding and Miocene clay and shale. Karst features in the aquifer feeding the Pertuso Spring are relatively well developed at the surface of the carbonate outcrops, mainly in the Cretaceous limestones, where karren, sinkhole, groove and shallow holes can be observed [20,21]. The lithostratigraphy, detected nearby Subiaco Station, confirms the outcropping of an extensive karst area, especially limestones and dolomites (Latium-Abruzzi succession, Upper Triassic-Upper Miocene) [22]. The karst surface is very permeable and allows the rapid infiltration of rainfall into the underground system, where the carbonate dissolution generates cavities [20,21]. Dissolution conduits strongly influence groundwater flow and evolve into complex networks, often crossing several kilometers, throughout the limestone matrix [23].

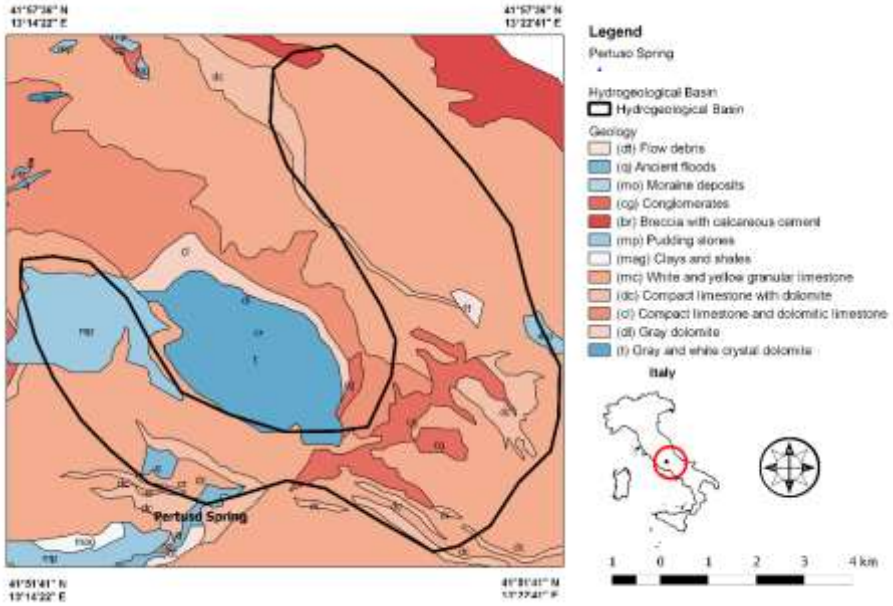

Figure 1. Geological map of the study area

ISSN: 2277-9655
Impact Factor: 4.116
CODEN: IJESS7

Thus, the Pertuso Spring is the natural outcrop of groundwater mostly discharging from these conduits showing an annual recharge of about 45 Mm^3/year [24].

The discharge is usually rapid and shows huge peaks following recharge events due to the receipt of a stormwater component, sourced via rapid preferential flow through karst features and fractures. The Pertuso Spring, located westward of Filettino (Figure 1), in the outcrop of limestone and dolomitic limestone of Upper Cretaceous age, flows into the Aniene River, close to the boundary of the carbonate hydrogeological system [25]. The most distinctive feature of the Pertuso karst spring is the branching network of conduits, whose size increases in the downstream direction. This conduit network is able to discharge very quickly large amounts of water, throughout the karst aquifer (up to 3 m^3/s) [16].

III. MATERIALS AND METHODS

The vulnerability of karst aquifer feeding the Pertuso Spring has been evaluated applying COP methodology, which focuses on the key role of karst features, responsible of the aquifer natural protection decreasing to pollution [15]. The COP method has been set up for the intrinsic vulnerability assessment of carbonate aquifers in the frame of the European COST Action 620 [7]. According to this method, the natural degree of groundwater protection is related to three parameters: the properties of the overlying soils and the unsaturated zone (O factor), the protection due to diffuse or concentrated infiltration processes (C factor) and the variable climatic conditions (P factor). The COP method provides for the C factor two different scenarios.

In Scenario 1, the C factor is calculated based on the following parameters: distance to the swallow hole (*dh*), distance to the sinking stream (*ds*) and the combined effects of slope and vegetation (*sv*) (Equation 1).

$$C = dh \cdot ds \cdot sv \quad (1)$$

Scenario 2 is related to those areas, where the aquifer recharge does not occur through a sinkhole, so the C factor can be calculated on the bases of the parameters surface features (*sf*), slope (*s*) and the combined effects of slope and vegetation (*sv*) (Equation 2).

$$C = sf \cdot sv \quad (2)$$

The COP vulnerability index (ICOP) is obtained by multiplying the three factors (Equation 3).

$$I_{COP} = C \cdot O \cdot P \quad (3)$$

The COP vulnerability index classification defines five classes of vulnerability as shown in Table 1.

Table 1. COP index and corresponding vulnerability class

COP Index (I_{COP})	Vulnerability Class
0-0.5	Very High
0.5-1	High
1-2	Moderate
2-4	Low
4-15	Very Low

The tied relationship between rainfall and discharge rate, in the study area, is due to the preferential flowpaths of groundwater. For this reason, every concentrated recharge zone has been identified with the main karst features detectable from satellite images (Google Earth) (Figure 2) and about 50 different karst features in the hydrogeological basin have been plotted in GIS as polygons.

All these polygons, reported in a single GIS layer only related to the karst features, represent the direct recharge areas, where a possible contaminant may, directly and quickly, reach the aquifer with reasonable certainty. Before the vulnerability rating evaluation, the traditional vulnerability assessment approach would require the partition of the study area into Finite Square Elements (FSE) to which associate the Vulnerability Index calculated. However, in this study, with the aim of highlighting the presence of karst features, COP method has been applied starting from two different discretization approaches of the hydrogeological basin: polygonal layer

ISSN: 2277-9655
Impact Factor: 4.116
CODEN: IJESS7

and Finite Square Elements of 250 m per side (FSE). The polygonal layer is the result of an overlapping of two layers (Figure 3): the first one consists of the direct recharge area, related to the presence of karst features responsible of rainfall fast infiltration in the saturated zone, the second one coincides with the geology of the hydrogeological basin. Thus, the study area, of about 50 km^2, has been divided into 22 polygons, representative of different outcropping lithology and 50 polygons related to karst features. In this paper the aquifer vulnerability results, coming from both discretization application, are laid out, supported by QuantumGIS.

Figure 2. Karst features detection in the study area

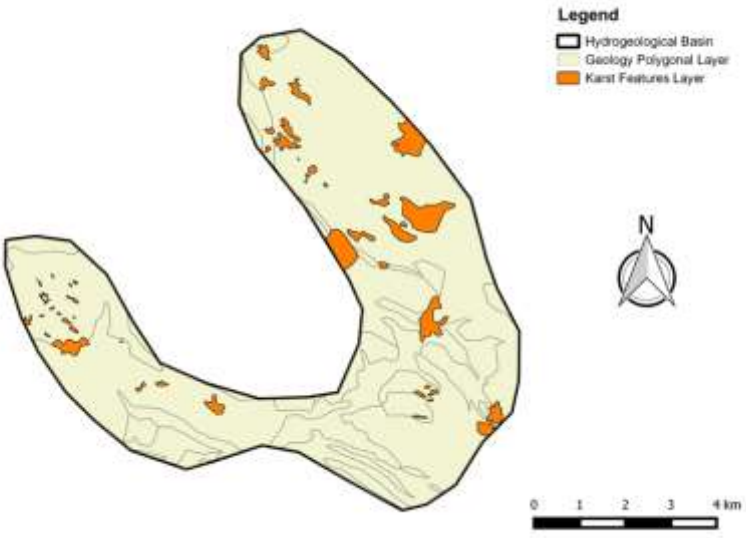

Figure 3. Polygonal layer discretization of the study area

The intrinsic groundwater vulnerability assessment requires data coming from the geological and hydrogeological settings of the aquifer, such as lithology, karst features, land use and land cover, soil, depth to groundwater, topography (slope) and climatic data (precipitation and temperature).

The study is based on the background data coming from previous studies [18,26] and results coming from the Environmental Monitoring Plan, carried out in the karst aquifer of the Upper Valley of the Aniene River, related to the catchment project of the Pertuso Spring. Data was collected from: (i) geological map, (ii) Digital Elevation Model (DEM), (iii) land use and land cover maps (iv) climatic data (precipitation and temperature),

ISSN: 2277-9655
Impact Factor: 4.116
CODEN: IJESS7

(v) airphotographs and satellite images of the study area to identify the position of the main karst features.Regarding to the evaluation of C factor, the COP method considers two scenarios: the first one includes the recharge area of karst features (Scenario 1) and the second one includes the rest of the area, where no surface karst features have been identified (Scenario 2). The C score for Scenario 1 is obtained by multiplying the values of the parameter referred to slope and vegetation (*sv*) by those related to the distances from recharge areas to the swallow hole (*dh*) or the sinking stream (*ds*). The C score for Scenario 2 is evaluated by the multiplication of two main factors: vegetation and slope (*sv*) and surface features (*sf*).

As a matter of fact, in this study, Scenario 1 for the evaluation of C factor has been applied in the higher permeability areas (karst features) and Scenario 2 in the lower permeability areas (aquifer lithology). The slope and vegetation (*sv*) came out by QGIS from the Digital Elevation Model (DEM) in percentage and divided into 4 classes (≤8%, 8% ÷ 31%, 31%÷75% and >75%), to which scores have been assigned, respectively from 0.75 to 1. Based on the land cover maps provided, land use has been divided into two main types, mainly "no vegetation" and "vegetation".In this study the distance to swallow holes (*dh*), consisting of a series of buffer zones with defined thickness, was not considered because the area belonging to each karst feature was assumed to be characterized by high vulnerability. According to the absence of sinking stream, the parameter (*ds*), referred to the distance to sinking stream, was assumed to be equal to 1. The surface features parameter (*sf*) takes into account the specific geomorphological features of carbonate rocks and the presence, or absence, of any overlying layers (permeable or impermeable), which influences the importance of runoff and infiltration processes. Ratings from 0.5 to 1 have been assigned to the surface features parameter (*sf*) according to the existing surface geology.The O factor represents the overlying layers, that is the soil cover (O_S), overlying the bedrock lithology (O_L). The O_S factor is related to the texture and thickness of the soil cover and in the case study, it has been evaluated starting from the soil map information. The O_L factor is representative of the unsaturated zone and it is the product of the layer index and the degree of confinement (*cn*). The layer index is the product of the type of lithology and fracturing (*ly*) and the thickness of the unsaturated zone. The O_S and O_L factors have been obtained using geological map and drilling profiles of the karst aquifer feeding the Pertuso Spring [17].The P Factor represents the climatic conditions in the catchment area and it is given by the sum of two sub-factors (P_Q and P_I) referring to, respectively, the amount and the intensity of yearly precipitation. P_Q represents the amount of precipitation and ranges between 0.2 and 0.4. The precipitation intensity (P_I) represents the ratio of precipitation amount and number of rainy days. Precipitation has been obtained starting from rainfall data, coming from four gauging stations inside the study area: Filettino, Vallepietra, Carsoli and Subiaco (Santa Scolastica). Data time series cover a period of 20 years, from 1992 to 2012 (Table 2) and they were applied to calculate the average annual rainfall module for each station. At last, a linear relation between the elevation and the average annual rainfall module was obtained in order to assign to each FSE a single precipitation value.

Table 2. Rainfall data about four different meteorological stations in the study area

Meteorological Station	MPAM (mm/year)	Elevation (m asl)	Rainy days
Vallepietra	1346.78	825	91
Filettino	1647.00	1062	107
Carsoli	1053.25	640	100
Subiaco (Santa Scolastica)	1147.88	511	100

IV. RESULTS AND DISCUSSION

C Factor

The estimation of the C factor, in the studied area, has been carried out according to Scenario 1 in areas, where the flow is concentrated towards karst features and Scenario 2 in the rest of the basin where the flow is diffuse.
The two C Factor maps generated (Figures 4a and 4b) present C score values ranging between very high to very low, with C Factor values ranging between 0 and 0.9 and it is very low (≤ 0.2) in the higher permeability area (karst features), whereas it is very high (0.9) in non-karstic terrains, such as pudding stone, conglomerate, alluvial soil. As a matter of fact, the mapping results clearly show a sound difference in vulnerability values between FSE version (Figure 4a) and the polygonal layer one (Figure 4b). The first one generally assigns a high vulnerability to the most part of the study area, whereas the second one assigns a moderate vulnerability value to the same part. This difference is related to the intrinsic choice of focusing on the Scenario 1 only for karst

ISSN: 2277-9655
Impact Factor: 4.116
CODEN: IJESS7

feature polygons and not out of these defined areas. On the other hand, FSE discretization allows a better precision on the finite square element elevation and leads to a more "conservative" vulnerability evaluation for the rest of area, but does not allow a clear identification of fast recharge areas due to karst features.

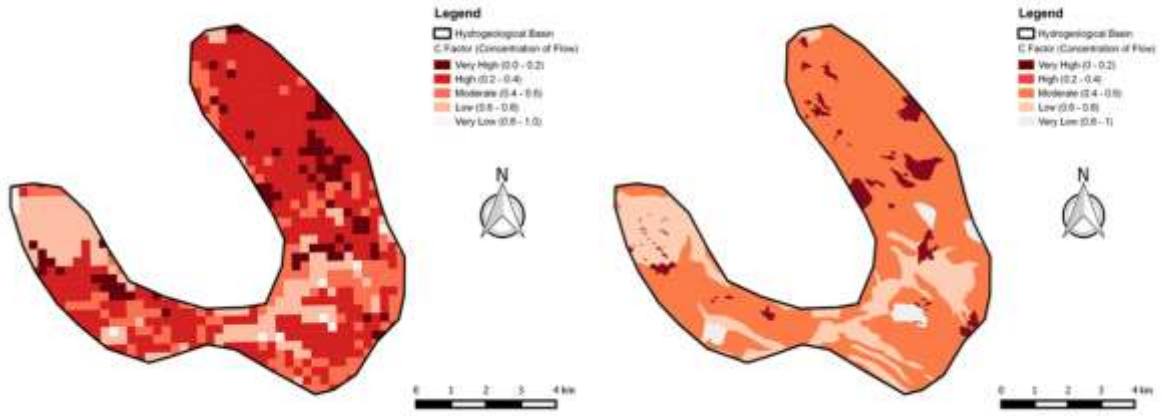

(a) (b)

Figure 4. Map of the C Factor: (a) FSE and (b) polygonal layer

O Factor

The O factor ranges from 1 to 5, according to some properties as thickness of the unsaturated zone, soil type, aquifer confining conditions, lithology and its fracturation.

The higher protection areas (dark green) are related to the presence of conglomerates and pudding stones, which have a weaker state of fracturing. On the contrary, the lower ones are due to the presence of carbonate rocks, which are the dominant geological formations, in the study area, and present the highest fracturation. Hence, the O factor is low in most of the study area.

As it is shown in Figures 5a and 5b, there are no sensitive differences between the two discretization approaches. Karst features have no impact on the O factor and, consequently, most part of the area presents the same protection values in both maps.

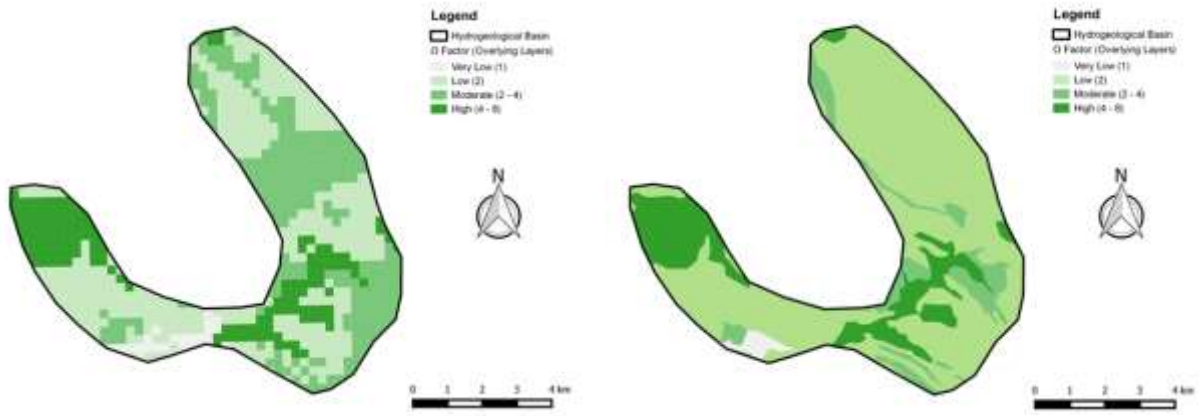

(a) (b)

Figure 5. Map of the O Factor: (a) FSE and (b) polygonal layer

P Factor

P factor has been obtained using a linear relation, between elevation and average annual rainfall starting from data collected in Subiaco (Santa Scolastica), Carsoli, Vallepietra and Filettinometeorological stations, located nearby the study area. The number of rainy days in the study area ranges from a minimum of 91 to a maximum

ISSN: 2277-9655
Impact Factor: 4.116
CODEN: IJESS7

of 107 days per year, based on the analysis of precipitation data over a time series that goes from 1992 to 2012. The average value is 100 rainy days per year.P factor ranges between 0.6 and 0.8. Most part of the study area present a high value (dark blue) in both maps (Figures 6a and 6b). In particular, the polygonal layer discretization approach leads to obtain an enhanced coverage of high value. The reduction of protection is generally high (0.6) in mountain areas, because even if the precipitation quantity P_Q is higher there due to elevation values, the much wider temporal distribution is a key factor for contaminant transport and implies a decreasing protection.

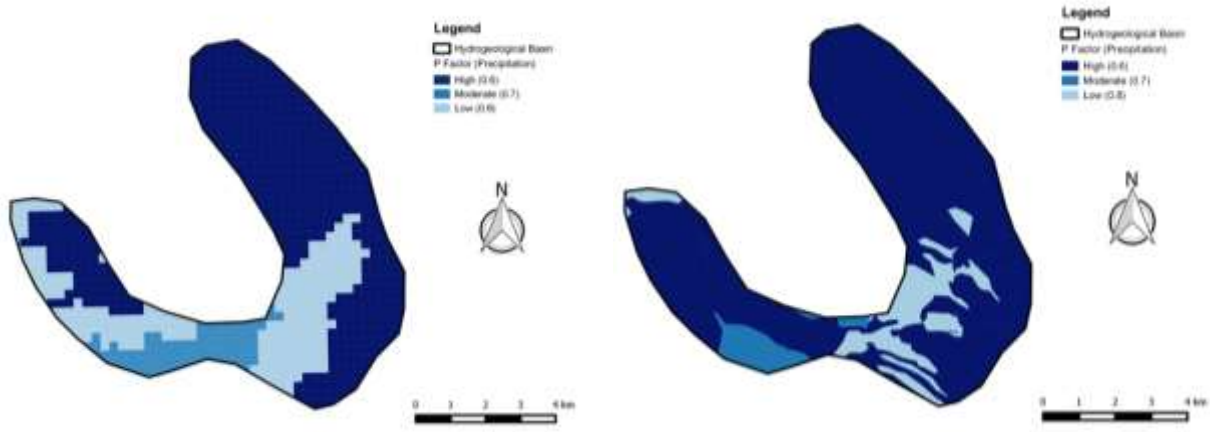

(a) (b)

Figure 6. Map of the P Factor: (a) FSE and (b) polygonal layer

COP Index

Figures 7a and 7b shows the results of COP method in the hydrogeological basin of the Pertuso Spring, respectively for FSE and polygonal discretization.

The results obtained by COP vulnerability method, applied to FSE (Finite Square Elements) and polygonal layer, show different vulnerability degrees for several areas within the hydrogeological basin feeding the Pertuso Spring.

As expected, the COP vulnerability maps show generally the dominance of high vulnerability classes (shades of red) in the northern part of the basin, while the south-east and western part are characterized by low vulnerability class (shades of green) and moderate class (shades of yellow). There is no very low vulnerability class.

Details in percentages of area for each vulnerability class are given in Figure 8.

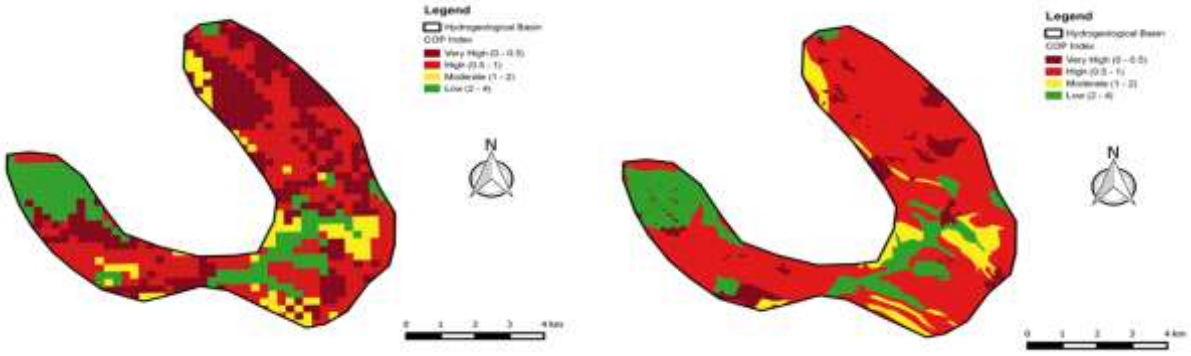

(a) ***(b)***

Figure 7. Map of the COP Index: (a) FSE and (b) polygonal layer

ISSN: 2277-9655
Impact Factor: 4.116
CODEN: IJESS7

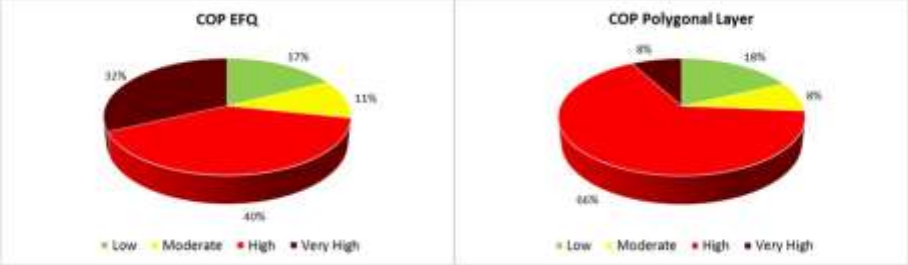

Figure 8. COP vulnerability classes percentage distribution: (a) FSE, (b) polygonal layer

The karst features, present in the study area, have been classified with the very high vulnerability degree (Very High: 0-0.5), due to the presence of swallow holes and dolines, that decreases the residence time of water in the unsaturated zone, reducing the potential attenuation capacity of the aquifer. This highest class of vulnerability index is due to the absence of an impermeable covering layer, which allowed rapid infiltration towards the saturated zone (C factor).

The low vulnerability class (Low: 2-4) covers similar percentages of the study area (17% and 18%) (Figure 13), mainly in the outcropping pudding stone, conglomerate and alluvial soil. In these areas, the low permeability of cover layers and the slope gradient are responsible of an increase of C and O factors and, consequently, of a vulnerability reduction.

The moderate vulnerability class (Moderate: 1-2) covers not more than 8 and 11% of the Pertuso Spring hydrogeological basin, respectively for polygonal layer and FSE discretization approaches (Figure 8). In these areas dolomitic limestone, compact limestone with dolomite and crystal dolomite outcrop, decreasing the protective capacity assigned to the unsaturated zone by the O factor. The COP method assigns the high vulnerability class (High: 0.5-1) to most part of the study area. This result is due to the presence of the karst Cretaceous limestone outcropping. Vulnerability maps obtained for both discretization approaches, result to be different just in the high and very high vulnerability degree assignment. The FSE discretization approach leads to a 32% of very high and 40% of high vulnerability rates, whereas in the polygonal layer discretization approach there is a lower presence of areas with the very high degree (8%) and a higher presence of areas with the high one (66%). This difference depends on the choice of using a polygonal layer, that allows identifying more precisely karst features and fast recharge area, assigning the potential contamination risk only to these areas and not to the rest. In this discretization hypothesis, karst features have a key-role for the C factor evaluation and their presence is predominant to each other consideration about vulnerability assessment. The FSE discretization approach, on the contrary, generally assigns COP index rates taking into account the lithology, the karst setting and the elevation, at the same level. As a consequence of it, in this case, a wider area of the whole basin has been considered very high vulnerable and the potential contamination risk result to be spread all over the study area, even out of karst features.

A comparison between the FSE discretization approach and the polygonal layer one is necessary to better understand which one is more suitable to the specific case study.

As to be expected, in a karst setting like the Pertuso Spring hydrogeological basin area, the presence of highly fractured rocks and most of all the specific permeability conditions, due to the local karst processes development, cause a spread high vulnerability degree to contaminants.

Even if the FSE discretization approach leads to a more cautionary vulnerability assessment in the study area, the polygonal layer shows a greater accuracy, defining all the areas interested by karst processes at local scale and assigning the higher vulnerability rate only to these ones. This choice allows to better highlighting protection areas, in order to protect groundwater quality. At the same time, the polygonal layer discretization approach needs a very detailed work, based on the detection and the outline representation of all the karst features. The visual detection and the graphic reconstruction of the areas, where karst features outcrop, is today easier to carry out, thanks to the remote sensing and the geographic information system (GIS) software. This process is strongly recommended for small basins as the Pertuso Spring one, but it may result to be not always suitable, above all in case of very wide areas.

ISSN: 2277-9655
Impact Factor: 4.116
CODEN: IJESS7

V. CONCLUSION

The aim of this paper was to carry on a comparative evaluation of vulnerability assessment of the karst aquifer feeding the Pertuso Spring, through the COP method application and starting from two discretization approaches: the Finite Square Elements (FSE) of 250×250 m and the polygonal layer, obtained from the overlapping of karst features and geology layers.

Regarding to the second approach, the study area, of about 50 km^2, has been divided into 22 polygons representative of outcropping lithology and 50 polygons related to karst features, which have been identified using satellite images.

The combined use of two vulnerability assessment approaches allows a better understanding of pollution vulnerability mechanisms in the study area.

The results of this study highlight that the vulnerability of the karst aquifer feeding the Pertuso Spring mainly ranges from low to very high in each approach.

Vulnerability maps show a high variability according to the environmental characteristics of the study area (e.g. geological, hydrogeological, morphological, climatic settings). The highest contribution to vulnerability is due to karst features such as karren, sinkhole, groove and swallow holes. The highly developed epikarst, the high recharge and high hydraulic conductivity minimizes the protective function of the unsaturated zone.

As to be expected, COP comes out to be a very suitable method for the vulnerability assessment in karst settings. As a matter of fact, the use of a polygonal layer as the basis for subsequent evaluations of the vulnerability is an effective option, because it allows to highlight the nature of outcropping lithology and the presence, shape and extent of karst features, responsible of fast infiltration and leakage.

On the other hand, the FSE discretization comes out to be more sensible to precipitation rates variations as well as to elevation and slopes, which are related to the water runoff. For these reasons, it is possible to say that the polygonal layer discretization is more recommended for small study areas such as the Pertuso Spring hydrogeological basin, whereas the FSE discretization is to be preferred for wide areas, where the higher range of precipitations and slope factors variations may play a key role in vulnerability assessment.

VI. ACKNOWLEDGEMENTS

The research reported in this paper was supported by the Department of Civil, Building and Environmental Engineering (DICEA) of Sapienza University of Rome. The authors gratefully acknowledge the technical support of ACEA ATO2.

VII. REFERENCES

[1] D. Ducci,"Intrinsic vulnerability of the Alburni karst system (southern Italy)" in Geological Society London Special Publications, vol. 279, pp. 137-151, 2007.
[2] S. Ergul, F. Ferranti, G. Sappa, "Arsenic in the aquifer systems of Viterbo Region, Central Italy: Distribution and geochemistry" in Rendiconti Online SocietàGeologicaItaliana, vol. 24, pp. 116-118, 2013.
[3] A.I. Marin, B. Andreo, A. Mudarra, "Vulnerability mapping and protection zoning of karst springs. Validation by multitracer tests" in Science of The Total Environment, vol. 532, pp. 435-446, 2015.
[4] S. Foster, R. Hirata, B.Andreo, "The aquifer pollution vulnerability concept: aid or impediment in promoting groundwater protection?"in Hydrogeology Journal 2013, vol. 21, no. 7, pp. 1389-1392, 2013.
[5] M. Bakalowicz, "Karst groundwater: a challenge for new resources" in Hydrogeology Journal, vol. 13, pp. 148-160, 2005.
[6] W.B. White, "Conceptual models for carbonate aquifers" in Ground Water, vol. 7, pp. 15-21, 1969.
[7] F. Zwahlen, "Vulnerability and risk mapping for the protection of carbonate aquifers" in COST Action 620Final Report, European Commission, Directorate- General XII Science, Research and Development, Brussels, Report EUR 20912, COST Action 620, Luxembourg, Belgium, p. 297,2004.
[8] G. Sappa, S. Vitale, "Multisystem approach to the identification of main recharge areas of aquifers" inGeoingegneriaAmbientale e Mineraria, vol. 22, pp. 79-92, 2007.

ISSN: 2277-9655
Impact Factor: 4.116
CODEN: IJESS7

[9] B. Theilen-Willige, H.AitMalek, A.Charif, M.Chaibi, "Remote Sensing and GIS Contribution to the Investigation of Karst Landscapes in NW-Morocco" in Geosciences,vol. 4, no. 2, pp. 50-72, 2014.
[10] C. Siart, O.Bubenzer, B.Eitel, "Combining digital elevation data (SRTM/ASTER), high resolution satellite imagery (Quickbird) and GIS for geomorphological mapping: A multi-component case study on Mediterranean karst in Central Crete" in Geomorphology, vol. 112, no. 1-2, pp. 106-121, 2009.
[11] M.P. Kakavas, K.G. Nikolakopoulos, E. Zagana, "Karst features detection and mapping using airphotos, DSMs and GIS techniques" in Proc. of the SPIE - Remote Sensing Conference, Toulouse, France, September 2015.
[12] D. Ducci, "GIS techniques for mapping groundwater contamination risk" in Natural hazards, vol. 20, no. 2, pp. 279-294, 1999.
[13] N. Doerfliger, P.Y.Jeannin, F.Zwahlen, "Water vulnerability assessment in karst environments: a new method of defining protection areas using a multi-attribute approach and GIS tools (EPIK method)" in Environmental Geology,vol. 2, pp. 165-176, 1999.
[14] E. Hadžić, N. Lazović, A.Mulaomerović-Šeta, "The Importance of Groundwater Vulnerability Maps in the Protection of Groundwater Sources. Key Study: SarajevskoPolje" in Procedia Environmental Sciences, vol. 25, pp. 104-111, 2015.
[15] J.M. Vias, B.Andreo, M.Perles, P. Jiménez Gavilán, "Proposed method for groundwater vulnerability mapping in carbonate (karstic) aquifers: the COP method, application in two pilot sites in Southern Spain" in Hydrogeology Journal, vol. 14, no. 6, pp. 915-925, 2006.
[16] Sappa, G.; Ferranti, F.; De Filippi, F.M. Environmental tracer approach to discharge evaluation of Pertuso Spring (Italy). In Recent Advances on Energy and Environment, Proceedings of the 10th International Conference on Energy & Environment, 2015, edited by Aida Bulucea, WSEAS, 54-62.
[17] ACEA ATO 2 S.p.A. "Hydrogeological study - Proposal for protected areas of Pertuso Spring". Unpublished, 2005.
[18] G. Sappa, F. Ferranti, "An integrated approach to the Environmental Monitoring Plan of the Pertuso spring (Upper Valley of Aniene River)" in Italian Journal of Groundwater vol. 3, no. 136, pp. 47-55, 2014.
[19] P. Bono, C.Percopo, "Flow dynamics and erosion rate of a representative karst basin (Upper Aniene River, Central Italy)" in Environmental Geology, vol. 27, pp. 210-218, 1996.
[20] G. Accordi, F. Carbone, "Carta delle litofacies del Lazio-Abruzzo ed aree limitrofe" Consiglio nazionale delle ricerche, 1988.
[21] A.V. Damiani, "Studi sulla piattaforma carbonatica laziale-abruzzese. Nota I. Considerazioni e problematiche sull'assetto tettonico e sulla paleogeologia dei Monti Simbruini, in Memorie descrittive Carta Geologica d'Italia, Publisher: Rome, Italy, vol. 38, pp. 177-206, 1990.
[22] A.M. De Felice, W.Dragoni, G.Giglio, "Report No. 120 Methods of hydrological basin comparison" Institute of Hydrology, 1992.
[23] G. Sappa, F. Ferranti, F.M. De Filippi, G.Cardillo, "Mg^{2+} based method for the Pertuso Spring discharge evaluation" Water (Switzerland),vol. 9, no. 1, p. 16, 2017.
[24] G. Sappa, F. Ferranti, F.M. De Filippi, "Hydrogeological water budget of the karst aquifer feeding Pertuso Spring (Central Italy)" in Proc. 6th International Multidisciplinary Scientific GeoConference: Science and Technologies in Geology, Exploration and Mining, SGEM 2016,Albena, Bulgaria, pp. 847-854, 2016.
[25] U. Ventriglia, "Idrogeologia II Parte" in Idrogeologia della Provincia di Roma, IV, Regione orientale. Amministrazione Provinciale di Roma, Assessorato LL.PP, Viabilità e trasporti, Roma, 1990.
[26] G. Sappa, S.Ergul, F. Ferranti, "Preliminary results of vulnerability assessment of the karst aquifer feeding Pertuso Spring, in Central Italy" in Proc. 4th International Multidisciplinary Scientific Geoconference and EXPO, SGEM 2014,Albena, Bulgaria,pp. 539-546, 2014..

CITE AN ARTICLE

Sappa, G., Ferranti, F., & De Filippi, F. M. (2017). VULNERABILITY ASSESSMENT OF THE KARST AQUIFER FEEDING THE PERTUSO SPRING (CENTRAL ITALY): COMPARISON BETWEEN DIFFERENT APPLICATIONS OF COP METHOD. *INTERNATIONAL JOURNAL OF ENGINEERING SCIENCES & RESEARCH TECHNOLOGY, 6*(6), 483-492. doi:10.5281/zenodo.817855

Environmental tracer approach to discharge evaluation of Pertuso Spring (Italy)

G. SAPPA, F. FERRANTI, F. M. DE FILIPPI
DICEA - Department of Civil, Building and Environmental Engineering
Sapienza University of Rome
Via Eudossiana 18, 00184, Rome
ITALY
giuseppe.sappa@ uniroma1.it http://w3.uniroma1.it/giuseppe.sappa

Abstract: - Discharge evaluation of karst springs used for drinking water supply is a key aspect for sustainable management and protection of the environment status of these water resources. Karst spring discharge is influenced by spatial and temporal variability involved in the transfer of water in hydrological cycle. Thus, quantification of karst spring water budget is essential to determine the groundwater available resources and for better understanding its seasonal changes in the hydrological year.
This paper deals with the results of the first year of the Environmental Monitoring Plan, related to the catchment project of Pertuso Spring, which is going to be exploited to supply an important water network in the South part of Roma district. The aquifer feeding Pertuso Spring is the most important water resource in the southeast part of Latium Region, Central Italy, used for drinking, agriculture and hydroelectric supplies. This complex hydrogeological system is characterized by a strong local hydraulic connectivity between Aniene River and karst aquifer, witch influence the aquifer water budget. Thus, the application of water budget to evaluate Pertuso Spring discharge can be highly uncertain.
The aim of this study is to combine stream discharge measurements and water geochemical properties in order to set up a reliable technique to evaluate karst spring discharge. As a matter of fact, in this paper, it is presented the application of Magnesium as a reliable tracer of discharge evaluation of Pertuso Spring. The concentration values of Magnesium ion have been recorded in some cross sections of the Aniene River, and they have been correlated with discharge values obtained by the traditional current meter, to provide information about groundwater and surface water interactions. The application of Magnesium as an environmental tracer provides a means to evaluate discharge of Pertuso Spring, as it came up to be a marker of the mixing of surface water and groundwater. On the other hand the Magnesium ion concentration provides information on changes in water quantity and quality.

Key-Words: - Aniene River, carbonate aquifer, groundwater, karst spring discharge, Magnesium tracer, Pertuso Spring

1 Introduction

Most of part of groundwater in the southeast part of Latium Region, as in the whole Apennine Mountains chain [1] is stored in karst aquifers.

The increasing of anthropogenic activities and the impacts of climate change are identified to be responsible of karst groundwater depletion [2]-[3]. Thus, groundwater exploitation in karst aquifers requires special management strategies to prevent their quality and quantity depletion and to support decision-making for water resources management [4]-[5].

In karst aquifers, the fast underground outflow in the saturated zone [6]-[7] is due to the heterogeneous distribution of permeability, because there are many conduits and voids developed by the dissolution of carbonate minerals. Therefore, quantification of karst spring discharge and water budget formulation requires defining the karst network geometry, which is not, every time, measurable with reliability [8].

As a matter of fact, the complex hydrological behavior, on one hand, the high heterogeneity of hydraulic properties [9]-[10], on the other one, make data collection about karst networks and groundwater very difficult, and the water budget evaluation is very often too much uncertain. For this reason, environmental tracer are useful tools to provide information about groundwater flow paths and residence times in karst aquifer systems without allowing for the specification of input locations and times [11]-[12].

ISBN: 978-1-61804-356-6

2 Problem Formulation

Environmental tracers are natural and anthropogenic chemical and isotopic substances that can be measured in groundwater and used to understand hydrologic properties of aquifers [13]-[14].

Environmental tracers provide information about the flow and mixing processes of water coming from different sources [15]-[16]. They are also useful to point out directions of groundwater flow and to determine origin and residence times of karst groundwater [17]-[18]. Typical natural tracers are major ions, trace elements, dissolved organic carbon and water isotopes [19]-[20]. Groundwater circulating in karst aquifer generally has great concentrations of Calcium and Magnesium as the result of bedrock weathering processes. Variations of Ca^{2+} and Mg^{2+} in groundwater chemical compositions are used very successfully as natural tracers in studies aiming to evaluate groundwater residence time within the karst aquifers [17]. The changes in Ca^{2+} and Mg^{2+} concentration values mainly depend on the residence time of groundwater in karst systems, which are controlled by the volume and mechanism of recharge, the distance from the recharge area and the dissolution of carbonate minerals [21]-[22]. The dissolution kinetics of Magnesium is longer than that of Calcium, so the increase of the Mg^{2+}/Ca^{2+} ratio implies the saturation of water with calcite, highlighting long residence time and enhanced weathering along the groundwater flow paths [22]-[23]. The Mg^{2+} content in groundwater also depends on others parameters such as chemical and mineralogical purity of limestone and presence of dolomite within the rock masses they flow across [24]. Nevertheless, the increase in Mg^{2+} concentration values, and hence Mg^{2+}/Ca^{2+} ratio not only depend on the dissolution/precipitation reaction of calcite and dolomite, but also an increase in water temperature accelerates the kinetics of the dissolution of dolomite [25]-[26]. However, it has been noticed that even in karst aquifers mainly made of limestone, the presence of slight impurities of Mg^{2+} in calcite can be responsible of significant changes in Mg^{2+}/Ca^{2+} ratio due to a high residence time of flowing waters [27]-[28]. Thus, environmental tracers and hydrochemical investigation techniques provide much information for the identification of groundwater flow systems and the main hydrogeochemical processes affecting the composition of water within the karst aquifers [28]. The analysis of the hydrogeochemical processes due to groundwater-surface water interactions let us to highlight the source of their mineralization and the influence of rock masses forming the aquifer.

2.1 Geological and Hydrogeological Framework

The karst aquifer feeding Pertuso Spring is located in the Upper Valley of the Aniene River (Latium, Central Italy), along the SW boundary of the Simbruini Mountains, in the outcrop of Triassic-Cenozoic carbonate rocks, locally covered by fluvial and alluvial deposits and, at lower altitudes, by Quaternary sediments [29].

The lithological sequence outcropping in the Upper Valley of Aniene River includes the North-West part of the Lower-Middle Miocene Latium-Abruzzi carbonate platform. The stratigraphic succession of dolomite, dolomitic limestone and limestone is distributed homogeneously from North to South and from East to West in the Valley [30]. The base of the stratigraphic series (Triassic) is widely spread among Filettino, Aniene River Springs and Faito Plateau. Dolomite is the dominant lithofacies, characterized by white and gray crystalline dolomite, with some breccia levels. Over this geological formation, limestones and dolomites, of Upper Cretaceous age (Sinemurian) are present, and their immersion is concordant with the Triassic dolomite [30].

Karst springs are numerous along the first part of the Aniene River and form in the Triassic dolomitic formations (Fig. 1). This karst system is characterized by one main outlet, Pertuso Spring, and several springs such as Radica, Valle del Forno and Fonte Santa, which inflow into the Aniene River, at different points (Table 1).

Due to their lower solubility and their lower brittleness, in comparison with limestones, dolomites are less fracturated than these latter ones. As a consequence of it in the Aniene River Basin, almost all groundwater come out where there is a limestone-dolomite contact [29] (Fig. 1) and this latter one is below the former one.

Spring	Annual average rate (l/s)
Radica	250
Valle del Forno	164
Fonte Santa	65
Pertuso	**1400**

Table 1, Main karst springs in the Upper Valley of Aniene River

Pertuso Spring, the largest karst spring in South-East part of Latium Region, is located between Filettino and Trevi nel Lazio (FR) and belongs to the Special Area of Conservation (SAC) of Aniene River Springs (EC Site Code IT6050029) established under Directive 92/43/EEC (Fig.2).

ISBN: 978-1-61804-356-6

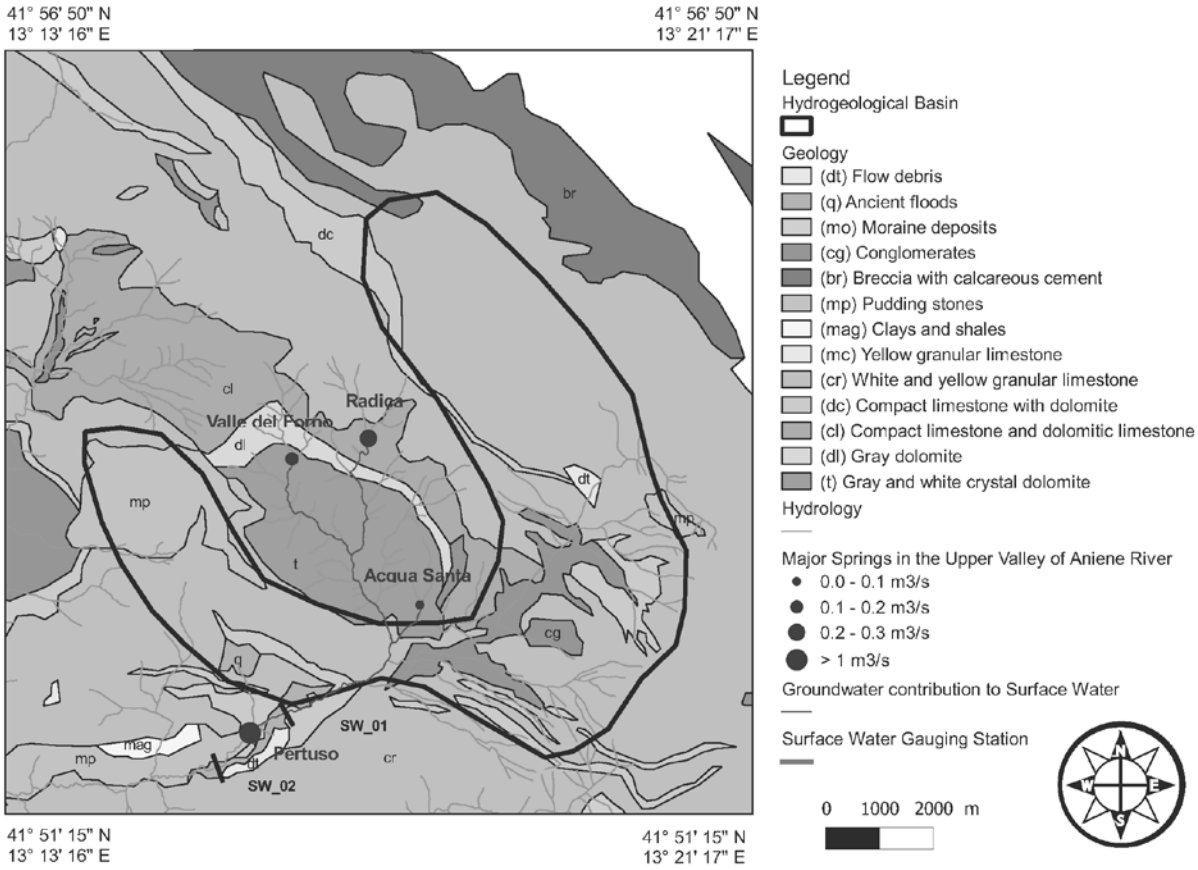

Fig. 1, Simplified geological map of Pertuso Spring hydrogeological basin

Pertuso Spring (elevation of 720 m a.s.l.) is the main outlet of this karst aquifer and comes out about 1 km from the confluence of Fiumata Valley and Granara Valley [31].

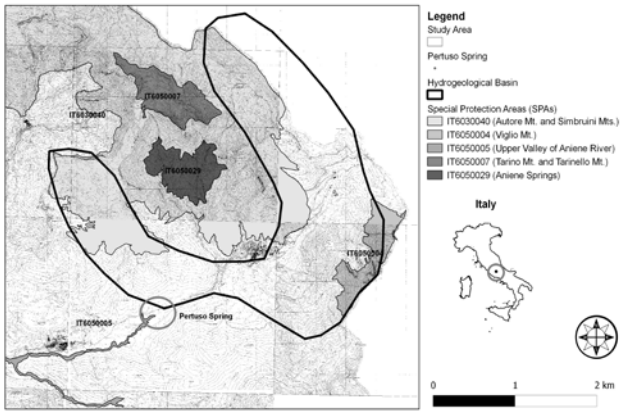

Fig. 2, Map of Special Areas of Conservation (SACs) in the Upper Valley of Aniene River

The outflow of Pertuso Spring is located in alluvial sediments, which cover a very thick layer made of Cretaceous limestone (Fig. 3). Spring water is captured for hydroelectric and drinking supplies, after which it flows into the Aniene River.

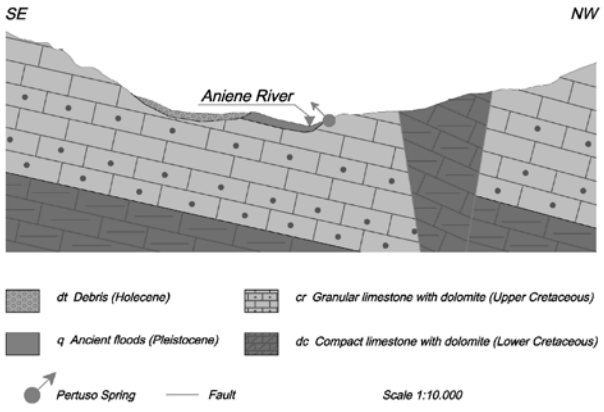

Fig. 3, Geological cross section showing the aquifer in the Cretaceous limestone and the location of the Pertuso Spring

The Pertuso Spring hydrogeological basin is located between latitude 41° 51' to 41° 56'N and longitude 13° 13' to 13° 21'E and collect groundwater coming from a 50 km^2 catchment area [32] bounded by the Triassic dolomite to the NE (Fig. 1).

The aquifer feeding Pertuso Spring is made, for the most part, of Cretaceous karst limestone. The base of the stratigraphic series is constituted by

ISBN: 978-1-61804-356-6

Upper Cretaceous carbonates, made by the alternation of granular limestone and dolomites layers. Above these lie Quaternary fluvial and alluvial deposits, downward pudding and Miocene clay and shale [29] (Fig. 1).

Rainfall is the primary source of recharge to this karst aquifer. Most of the recharge of Pertuso Spring occurs through karst features such as sinkhole, dolines, swallows holes and fractures, which allow fast flow across the recharge zone. Pertuso Spring discharges at an annual average rate of 1400 l/s, based on the record from 1990 to 1999 [33], and responds rapidly to precipitation events, with significant increases in discharge rates which are proportional to the intensity of rainfalls (Fig. 4).

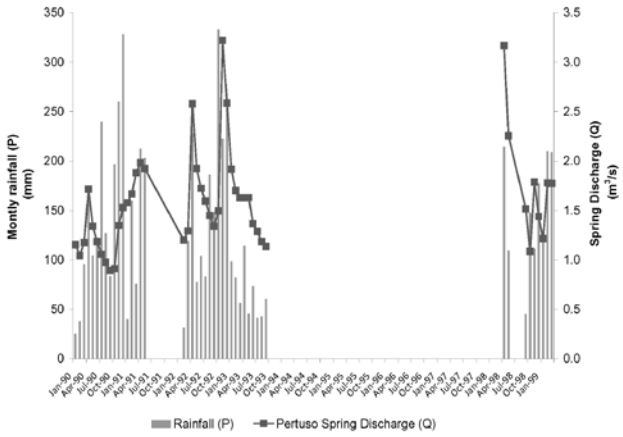

Fig. 4, Monthly rainfall and Pertuso Spring average rate in the 1990 - 1999 period (Filettino meteorological station)

2.2 Materials and Methods

This paper presents the results of the first year of the Environmental Monitoring Plan, related to the catchment project of the Pertuso Spring, which is going to be exploited to supply an important civil water network in the South part of Latium Region, Central Italy.

The experimental data, corresponding to the period July 2014 - May 2015, were obtained from field investigations and from chemical analyses performed in laboratory. Water samples were collected from three sampling points within the study area, i.e. one from Pertuso Spring, two on gauging stations located along the Aniene River, respectively, upstream (SW_01) and downstream (SW_02) the spring (Fig. 1).

Field investigations included in situ measurements of pH, temperature, electric conductivity (HANNA, Model HI9813-6) and redox and dissolved oxygen (HACH, Model LDO10101).

Water samples were filtered by 0.45 μm cellulose filters and stored at 4 °C until analysis in the Geochemical Laboratory of Sapienza University of Rome [34]. Major ions were determined by ion chromatography (IC) by a 761 Professional IC Metrohm (reliability ±2%). A Metrosep C2-150 column was used for determining major cations (Ca^{2+}, Mg^{2+}, Na^{+}, K^{+}), whereas major anions (Cl^{-}, NO_3^{-}, SO_4^{2-}) were determined by Metrosep A sup 4–250 column (accuracy 2-5%). Bicarbonate (HCO_3^{-}) was determined by titration with 0.1 N HCl (reliability ±2%).

The geochemical modeling program PHREEQC v3.0 [35], implemented with the thermodynamic dataset phreeqc.dat, was used to study mixing of groundwater and surface water to understand spatial and temporal patterns of mixing during base flow conditions.

The discharge measurements were carried out along the Aniene River, upstream (SW_01) and downstream (SW_02) Pertuso Spring, by the application of traditional current meter. According to the U.S. Geological Survey (USGS) procedure, stream discharge is calculated as the product of the cross section area by the average stream flow velocity in that cross section obtained using a current meter [36]-[37].

The main equipment needed to measure the stream flow velocity is a SEBA horizontal axis current meter F1, having a propeller diameter of 80 mm which, combined with SEBA Z6 pulse counter, allows to measure velocity between 0,025 m/s and 10 m/s.

The SEBA current meter has been used as rod equipment with tail plane for best positioning to the flow direction. For each measurement point, flow velocity is determined counting the number of spins of the meter rotor during a fixed interval of time. Thus, in order to assess any fluctuations due to the turbulence condition and, also, to avoid accidental measurement errors, velocity has been measured for at least 60 seconds, according to EN ISO 748:2007 requirements [37].

This current meter method gives the local water velocity in each vertical following the application of a calibration equation between stream velocity, v (cm/s) and the number of spins, n (s^{-1}) (1).

$$v = 0.82 + 33.32 \cdot n \quad (1)$$

3 Problem Solution

In order to establish the groundwater discharge pattern, hydrochemical data and discharge measurements were used in the study.

ISBN: 978-1-61804-356-6

Ca^{2+}, Mg^{2+} and HCO_3^- represent more than 80% of the dissolved solids in water samples and are influenced by the dissolution of carbonate minerals, forming limestone, which are the most dominant formations outcropping in the study area.

As a consequence of their flowing in a karst aquifer, all these water samples came out to be rich in Ca-Mg-HCO_3 as it is represented by Schoeller (Fig. 5), but water samples coming from SW_01 gauging station present higher values of concentration in Mg^{2+}, while those coming from Pertuso Spring are definitely poorer in it, and show a clear composition of Ca-HCO_3 water type.

These hydrochemical facies highlight that carbonate weathering processes (e.g. calcite and dolomite) are the most important factors of the observed water type.

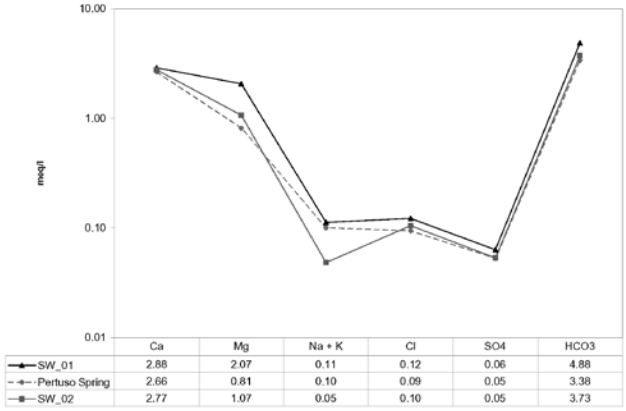

Fig.5, Schoeller plot for hydrochemical facies and water classification (January 2015)

Box plot for Mg^{2+} in groundwater and surface water is presented in Fig. 6. Following differentiation of Magnesium content along the Aniene River, we observed a 47% decrease in Mg^{2+}concentration in surface water downstream Pertuso Spring (SW_02) with respect to Mg^{2+}concentration measured in SW_01 (23.6 mg/l).

The scatter plots diagram for Mg^{2+} vs Ca^{2+} (Fig. 7) shows that all points plotted are located below the equiline 1:1, which is line representing the natural Mg^{2+}/Ca^{2+} ratio in dolomite mineral composition. All samples show an average Ca^{2+} concentration value of about 52 mg/l. Surface water sample coming from SW_01 gauging station, upstream Pertuso Spring, shows the Mg-rich composition coming from dissolution of Triassic dolomites, while groundwater coming from Pertuso Spring is typical of the dissolution of low-Mg calcite. As a consequence of these properties water samples taken in SW_02 gauging station, downstream Pertuso Spring, present chemical composition typical of mixing of these two different kinds of waters (Fig. 7).

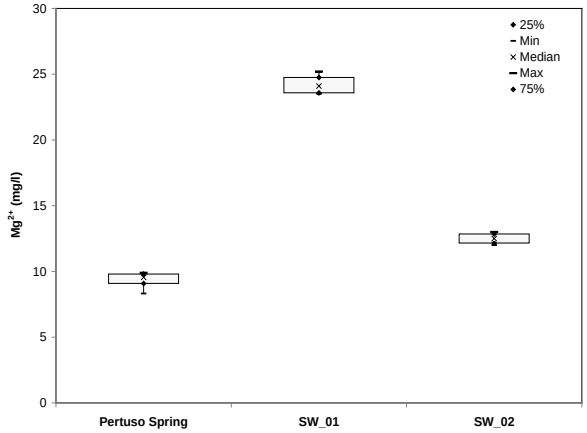

Fig. 6, Box plot of Mg^{2+} concentration in groundwater and surface water

As a matter of fact the highest Mg^{2+}/Ca^{2+} ratio in water sampled has been recorded in dolomite outcropping (SW_01: Mg^{2+}/Ca^{2+} ~ 0.7), with medium value at SW_02 gauging station (Mg^{2+}/Ca^{2+} ~ 0.4). On the other hand the lowest value of this ratio in groundwater has been observed in Cretaceous limestone area (Pertuso Spring: Mg^{2+}/Ca^{2+} ~ 0.3) (Table 2).

Gauging Station	July 2014	November 2014	January 2015	May 2015
Pertuso Spring	0.329	0.269	0.306	0.314
SW_01	0.728	0.717	0.719	0.752
SW_02	0.411	0.377	0.385	0.391

Table 2, Mg^{2+}/Ca^{2+} ratio from Pertuso Spring and Aniene River gauging station

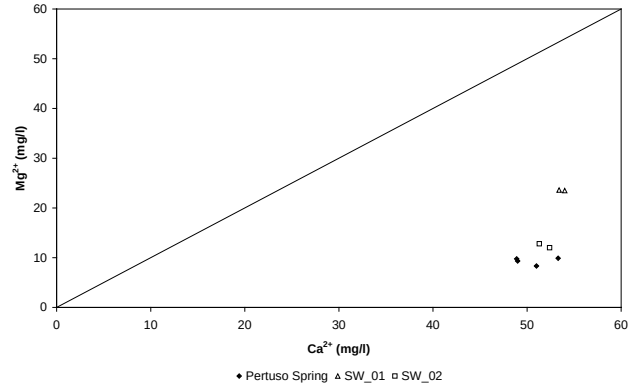

Fig.7, Ca^{2+} versus Mg^{2+} in groundwater and surface water

Aniene River discharge was measured during the hydrological year 2014-2015, in order to cover the range of seasonal conditions characteristics of this

ISBN: 978-1-61804-356-6

complex hydrogeological system. Measurements, e.g. by current meter, were carried on in two gauging stations located upstream (SW_01) and downstream (SW_02) Pertuso Spring (Table 3).

Gauging Station	July 2014	November 2014	January 2015	May 2015
SW_01	0.540	0.350	0.410	0.501
SW_02	2.450	1.480	1.920	2.747

Table 3, Results of mean discharge values obtain by current meter method, upstream (SW_01) and downstream (SW_02) Pertuso Spring

They are represented, in Table 3, discharge values recorded in SW_01 and SW_02 gauging stations all over the hydrological year. It can be noticed that the average discharge value referred to SW_01 gauging station can be well compared with the total average discharge coming from of the most important karst springs outcropping in the Upper Part of Aniene River (Table 1). Thus, the source of Mg^{2+} concentration values in Aniene River water upstream Pertuso Spring (SW_01) is the dissolution of Magnesium rich minerals in Triassic dolomites, sited in north-east part of the Pertuso Spring hydrogeological basin.

Along the Aniene River, this decrease in Mg^{2+} concentration values is related to an increase in stream flow discharge. SW_02 surface water is the product of the confluence of groundwater coming from Pertuso Spring into the Aniene River (SW_01). As a matter of fact, Aniene River water, which is characterized by water with higher Magnesium concentration values, is affected in its chemical composition by Pertuso Spring groundwater inflowing, and this influence can be measured by Mg^{2+} concentration values variability along the river downstream.

Using PHREEQC program it has been calculated the speciation of an aqueous solution of a virtual composed water sample made of the mixing of water coming from Pertuso Spring and SW_01 gauging station. To have the mixed virtual sample composition any source sample, Pertuso Spring and SW_01 gauging station, has been multiplied in its chemical component for their own contribution fraction in SW_02 gauging station discharge.

Figure 8 shows that the calculated values fit quite well the experimental values reported in Table 4.

The results obtained by PHREEQC program fall close to the equiline of 1:1, and this fact confirms that SW_02 surface water comes from the mixing of groundwater outflowing from Pertuso Spring with surface water of Aniene River (SW_01).

Date	Ca^{2+} mg/l		Mg^{2+} mg/l	
	Phreeqc	SW_02	Phreeqc	SW_02
July 2014	48.45	51.20	12.44	12.80
November 2014	48.65	52.50	11.61	11.80
January 2015	52.66	55.60	12.72	13.00
May 2015	48.41	51.40	11.72	12.20

Table 4, Ionic compositions of SW_02 and the virtual solution made by mixing water coming from Pertuso Spring and SW_01

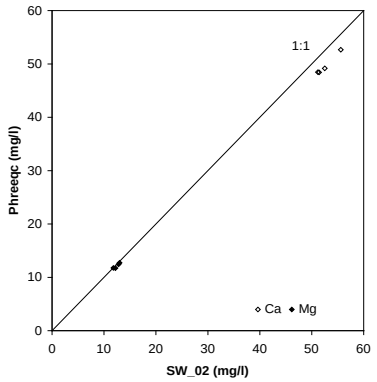

Fig. 8, Comparison between the ionic compositions of SW_02 and the virtual solution made by mixing water coming from Pertuso Spring and SW_01

The karst aquifer/river system has been studied in the aim of evaluating factors, which modify the Aniene River flow due to groundwater-surface water interactions. Three pairs of values, related, each one, to any sampling point, has been considered. The main inputs are the discharge measurements (Q_1) and the Mg^{2+} concentrations (C_1) recorded in the Aniene River upstream Pertuso Spring (SW_01). The secondary inputs are the discharge rate (Q_P) and the Mg^{2+} concentrations (C_P) recorded at Pertuso Spring. The main output are the Aniene River discharge (Q_2) and the Mg^{2+} concentrations (C_2) recorded at the SW_02 gauging station located downstream Pertuso Spring.

Thus, assuming that this is a closed system, the SW_02 gauging station discharge values, comes from the contribution of Pertuso Spring discharge (Q_P) to the original SW_01 gauging station discharge value, and so it can be represented by (2):

$$Q_2 = Q_1 + Q_P \quad (2)$$

ISBN: 978-1-61804-356-6

and applying to this closed system the conservation of mass equation, it means (3):

$$Q_1C_1 + Q_PC_P = Q_2C_2 \quad (3)$$

The n parameter (Table 5), i.e. the percentage contributor of Pertuso Spring groundwater to total discharge measured at the, is defined according to (4).

$$n = \frac{Q_P}{Q_2} = \frac{(C_2 - C_1)}{(C_P - C_1)} \quad (4)$$

Thus, the discharge rate of Pertuso Spring depends on the discharge values measured in the gauging station located along the Aniene River upstream the spring (Q_1) and the Mg^{2+} concentration values recorded in groundwater and surface water samples (C_1, C_2, C_P) (5):

$$Q_P = Q_1 \cdot \frac{n}{1-n} \quad (5)$$

Date	n	n (%)
July 2014	0.780	78.0
November 2014	0.752	75.2
January 2015	0.794	79.4
May 2015	0.812	81.2

Table 5, *n* values as percentage contributor of Pertuso Spring groundwater to total discharge measured at the SW_02 gauging

Pertuso Spring discharge values obtained by this indirect method are showed in Table 6.

Date	SW_01		Pertuso Spring			SW_02		
	Q^* (m^3/s)	Mg^{2+} (meq/l)	Q^{**} (m^3/s)	Q_{Mg} (m^3/s)	Mg^{2+} (meq/l)	Q^* (m^3/s)	Q_{Mg} (m^3/s)	Mg^{2+} (meq/l)
July 2014	0,540	1,94	1,910	1,922	0,800	2,450	2,462	1,050
November 2014	0,350	1,93	1,130	1,061	0,680	1,480	1,411	0,990
January 2015	0,410	2,07	1,510	1,577	0,810	1,920	1,987	1,070
May 2015	0,501	2,02	2,225	2,164	0,767	2,747	2,664	1,003

Table 6, Magnesium content and discharge values obtained by current-meter and Magnesium tracer method (Q^*: discharge values obtained by current meter method; Q^{**}: discharge values obtained by the difference between the values measured with the current meter in SW_01 and SW_02)

The relationship between Mg^{2+} concentration and karst spring discharge values obtained with this combined Magnesium-discharge tracer approach is represented in Fig. 9.

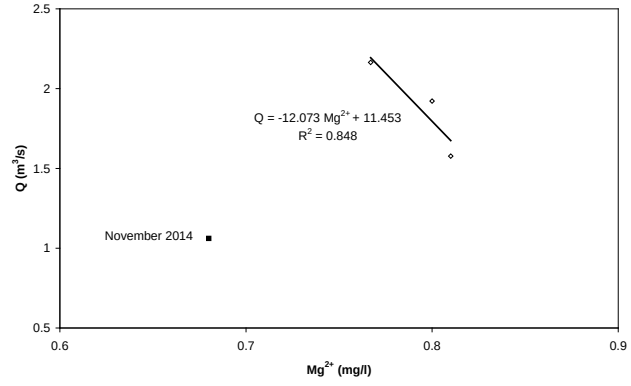

Fig. 9, Relationship between the Mg^{2+}concentration and Pertuso Spring discharge values obtain with the combined Magnesium-discharge tracer approach

The Mg^{2+} vs Q scatter plots diagram shows that all plotted points, except for November 2014 data, follow a linear trend, highlighting that the increasing contribution of Pertuso Spring flow rate is responsible of Mg^{2+} concentration values decreasing. Data, referred to November 2014 monitoring campaign, have to be considered as an outlier (Fig. 9).

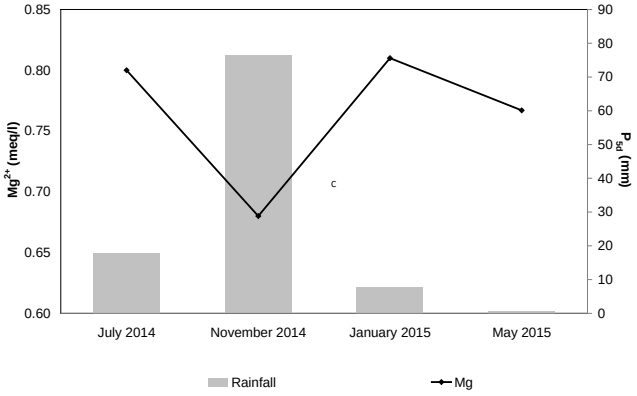

Fig. 10, Relationship between Mg^{2+} concentration and rainfall (Trevi nel Lazio meteorological station)

ISBN: 978-1-61804-356-6

This lower Mg^{2+} concentration measured at November 2014 can be related to a high precipitation rate, recorded at Trevi nel Lazio meteorological station, five days before the sampling date (Fig. 10), which could have influenced, lowering it, especially Mg^{2+} concentration in surface water, flowing in SW_01. As a matter of fact, because of great amounts of precipitation, most part of surface waters flowing in rivers are made by run-off in comparison with ones coming from springs, from which rivers start. And so it could have happened in this case.

4 Conclusion

This paper dealt with the assessment of the interactions between karst aquifer feeding Pertuso Spring and Aniene River surface waters on the basis of stream discharge measurements and water geochemical tracers data in the aim to set up an inversed model, which allows to estimate groundwater flow coming out from Pertuso Spring, starting from surface water discharge measurements and geochemical waters characterization. These preliminary results, carried out in a pilot area, sited in the karst aquifer, outcropping in the Upper Valley of Aniene River, show that, for this karst system, it is possible to have a reliable evaluation of Pertuso spring discharge, by the elaboration of surface water discharge measurements in relationship with Mg^{2+} concentration values, determined as for groundwater, coming from Pertuso Spring, as for surface water sample, taken upstream and downstream of Pertuso Spring, along Aniene River streaming. Although it is subject to some uncertainties, the Mg^{2+} concentration, as an environmental tracer, provides a mean to predict discharge evaluation of Pertuso Spring, due to the mixing of surface water and groundwater and, provides information on changes in water quantity and quality.

References:

[1] C. Boni, P. Bono, G. Capelli, S. Lombardi, G.M. Zuppi, Contributo all'Idrogeologia dell'Italia Centrale: Analisi Critica dei Metodi di Ricerca, *Memorie Società, Geologica Italiana*, Vol.35, 1986, pp. 947-956.

[2] Q. Guo, Y. Wang, T. Ma, L. Li, Variation of karst springs discharge in recent five decades as an indicator of global climate change: a case study at Shanxi, northern China, *Science in China Series D: Earth Science*, Vol.48, No.11, 2005, pp. 2001-2010.

[3] G. Sappa, G. Luciani, Groundwater Management in Dar Es Salam Coastal Aquifer (Tanzania) under a Difficult Sustainable Development, *WSEAS Transactions on Environment and Development*, Vol.10, 2014, pp. 465-477.

[4] G. Sappa, F. Ferranti, S. Ergul, G. Ioanni, Evaluation of the groundwater active recharge trend in the coastal plain of Dar es Salaam (Tanzania), *Journal of Chemical and Pharmaceutical Research*, Vol.5, No.12, 2013, pp. 548-552.

[5] S. Foster, R. Hirata, B. Andreo, The aquifer pollution vulnerability concept: aid or impediment in promoting groundwater protection?, *Hydrogeology Journal*, Vol.21, 2013, pp. 1389-1392.

[6] W.B. White, Conceptual models for carbonate aquifers, *Ground Water*, Vol.7, 1969, pp. 15-22.

[7] W.B. White, Karst hydrology: recent developments and open questions, *Engineering Geology*, Vol.65, 2002, pp. 85-105.

[8] C. Cherubini, N. Pastore, V. Francani, Different approaches for the characterization of a fractured karst aquifer, *WSEAS Transactions on fluid mechanics*, Vol.3, 2008, pp. 29-35.

[9] F. Zwahlen, Vulnerability and risk mapping for the protection of carbonate (karst) aquifers, final report (COST Action 620). *European Commission, Directorate-General XII Science, Research and Development*. Brussels, 2004, pp. 297

[10] M. Bakalowicz, Karst groundwater: a challenge for new resources. *Hydrogeology Journal*, Vol.13, 2005, pp. 148-160.

[11] I.D. Clark, P. Fritz, *Environmental Isotopes in Hydrogeology*, Crc Pr Inc., Boca Raton, Fla., 1997.

[12] E. Mazor, *Chemical and Isotopic Groundwater Hydrology*, Marcel Dekker, New York, 2004.

[13] W.M. Alley (Ed.), *Regional Ground-Water Quality*. Van Nostrand Reinhold, New York, 1993.

[14] P. Cook, A. Herczeg, *Environmental Tracers in Subsurface Hydrology*. Kluwer Acad., Boston, 1999.

[15] M. Guida, D. Guida, D. Guadagnuolo, A. Cuomo, V. Siervo, Using Radon-222 as a Naturally Occurring Tracer to investigate the

streamflow-groundwater interactions in a typical Mediterranean fluvial-karst landscape: the interdisciplinary case study of the Bussento river (Campania region, Southern Italy), *WSEAS Transactions on System*, Vol.12, No.2, 2013, pp. 85-104.

[16] L.N. Plummer, E. Busenberg, J.B. McConnell, S. Drenkard, P. Schlosser, R.L. Michel, Flow of river water into a karstic limestone aquifer: 1. Tracing the young fraction in groundwater mixtures in the Upper Floridan Aquifer near Valdosta, Georgia, *Applied Geochemistry*, Vol.13, No.8, p. 995-1015.

[17] C. Batiot, C. Emblanch, B. Blavoux, Total Organic Carbon (TOC) and magnesium (Mg^{2+}): two complementary tracers of residence time in karstic systems, *Comptes Rendus Geoscience*, No.35, 2003, pp. 205-214.

[18] G. Sappa, F. Ferranti, S. Ergul, Vulnerability assessment of Mazzoccolo Spring aquifer (Central Italy), combined with geo-chemical and isotope modelling, *Engineering Geology for Society and Territory*, Vol.5, Urban Geology, Sustainable Planning and Landscape Exploitation, 2015, pp. 1387-1392.

[19] D. Hunkeler, J. Mudry, Hydrochemical tracers, in Methods in *Karst Hydrogeology*, edited by N. Goldscheider and D. Drew, 2007, pp. 93-121.

[20] C. Leibundgut, P. Maloszewski, C. Kulls, Tracers in *Hydrology*, 1st ed., Wiley-Blackwell, Chichester, U. K., 2009.

[21] D. Langmuir. Geochemistry of Some Carbonate Ground Waters in Central Pennsylvania. *Geochimica et Cosmochimica Acta*, Vol.35, No.10, 1971, pp. 1023–1045.

[22] W.B. White, *Geomorphology and Hydrology of Karst Terrains*. New York, Oxford University Press, 1988.

[23] W.M. Edmunds, J.M. Cook, W.G. Darling, D.G. Kinniburgh, D.L. Miles, Baseline geochemical conditions in the Chalk aquifer, Berkshire, U.K.: a basis for groundwater quality management, *Applied Geochemistry*, Vol.2, No.3, 1987, pp. 251-274.

[24] M. Mudarra, B. Andreo, Relative importance of the saturated and the unsaturated zones in the hydrogeological functioning of karst aquifers: The case of Alta Cadena (Southern Spain), *Journal of Hydrology*, Vol.397, No.3-4, 2011, pp. 263-280.

[25] C.D. Palmer, J.A. Cherry, Geochemical Evolution of Groundwater in Sequences of Sedimentary Rocks, *Journal of Hydrology*, Vol.75, No.2, 1984, pp. 27-65.

[26] J.S. Herman, W.B. White, Dissolution Kinetics of Dolomite: Effects of Lithology and Fluid Flow Velocity, *Geochimica et Cosmochimica Acta*, Vol.49, 1985, pp. 2017-2026.

[27] H. Celle-Jeanton, C. Emblanch, J. Mudry, A. Charmoille, Contribution of time tracers (Mg^{2+}, TOC, $\delta^{13}C_{TDIC}$, NO_3^-) to understand the role of the unsaturated zone: A case study-Karst aquifers in the Doubs valley, eastern France, *Geophysical Research Letters*, Vol.30, No.6, 2003.

[28] A.F. Tooth, I.J. Fairchild, Soil and karst aquifer hydrological controls on the geochemical evolution of speleothem-forming drip waters, Crag Cave, southwest Ireland *Journal of Hydrology*, Vol.273, 2003, pp. 51-68.

[29] U. Ventriglia, Idrogeologia della Provincia di Roma, IV, Regione orientale. *Amministrazione Provinciale di Roma, Assessorato LL.PP, Viabilità e trasporti*, Roma, 1990.

[30] A.V. Damiani, "Studi sulla piattaforma carbonatica laziale-abruzzese. Nota I. Considerazioni e problematiche sull'assetto tettonico e sulla paleogeologia dei Monti Simbruini, Roma", *Memorie descrittive Carta Geologica d'Italia*, Vol.38, 1990, pp.177–206.

[31] F. Cipollari, D. Cosentino, M. Parrotto, Modello cinematico-strutturale dell'Italia centrale. *Studi Geol. Camerti*, Vol.2, 1995.

[32] G. Sappa, F. Ferranti, An integrated approach to the Environmental Monitoring Plan of the Pertuso spring (Upper Valley of Aniene River), *Italian Journal of Groundwater*, Vol. 3, No.136, 2014, pp. 47–55.

[33] Acea ATO 2 S.p.A., *Studio idrogeologico – Proposta di aree di salvaguardia della sorgente del Pertuso*, unpublished.

[34] APHA. *Standard Methods for the Examination of Water and Wastewater*, 20th ed.; American Public Health Association: Washington, DC, USA, 1998.

[35] D. L. Parkhurst, C.A. J. Appello, User's Guide to PHREEQC (Version 2)-A Computer Program for Speciation, Batch-Reaction, One-Dimensional Transport, and Inverse Geochemical Calculations. *US Geological Survey Water-Resources Investigations, Report* 99-4259, 1999.

[36] US EPA Region 6, *Standard operating procedure for stream flow measurement*, 2003.

[37] BS EN ISO 748:2007, *Hydrometry. Measurement of liquid flow in open channels using current-meters or floats*, 2007.

Preliminary validation of an indirect method for discharge evaluation of Pertuso Spring (Central Italy)

G. SAPPA, F. FERRANTI, F. M. DE FILIPPI
DICEA - Department of Civil, Building and Environmental Engineering
Sapienza University of Rome
Via Eudossiana 18, 00184, Rome
ITALY
giuseppe.sappa@ uniroma1.it http://w3.uniroma1.it/giuseppe.sappa

Abstract: - This paper deals with the results of the first year of the Environmental Monitoring Plan, related to the catchment project of Pertuso Spring, which is going to be exploited to supply an important water network in the South part of Roma district. The study area is located in the Upper Valley of the Aniene River (Latium, Central Italy), in the outcrop of Triassic-Cenozoic carbonate rocks, and belong to an important karst aquifer. Pertuso Spring is the main outlet of this karst aquifer and is the one of the most important water resource in the southeast part of Latium Region, used for drinking, agriculture and hydroelectric supplies. Karst aquifer feeding Pertuso Spring is an open hydrogeological system aquifer characterized by complex interactions and exchanges between groundwater and surface water which influence the aquifer water budget. Thus, evaluation of groundwater discharge from this karst spring can be affected by difficulties in performing measurements because of the insufficient knowledge about water transfer processes in the hydrological cycle and geometry of drainage conduits.
The aim of this paper is to assess the interactions between karst aquifer feeding Pertuso Spring and Aniene River based on stream discharge measurements and water geochemical tracer data in order to validate an indirect method for karst spring discharge evaluation. As a matter of fact, in this paper, there are presented the results of the application of Magnesium as a reliable tracer of karst spring discharge. This indirect method is based on the elaboration of surface water discharge measurements in relationship with Mg^{2+} concentration values, determined as for groundwater, coming from Pertuso Spring, as for surface water sample, collected upstream and downstream of Pertuso Spring, along Aniene River streamflow. The application of Magnesium as an environmental tracer provides a means to evaluate discharge of Pertuso Spring, as it came up to be a marker of the mixing of surface water and groundwater. On the other hand, the Magnesium ion concentration provides information for the identification of groundwater flow systems and the main hydrogeochemical processes affecting the composition of water within the karst aquifers.

Key-Words: - Aniene River, carbonate aquifer, groundwater, karst spring discharge, Magnesium tracer, Pertuso Spring

1 Introduction

Most of part of groundwater in the southeast part of Latium Region, as in the whole Apennine Mountains chain [1] is stored in karst aquifers.

The increasing of anthropogenic activities and the impacts of climate change are identified to be responsible of karst groundwater depletion [2]-[3]. Thus, groundwater exploitation in karst aquifers requires special management strategies to prevent their quality and quantity depletion and to support decision-making for water resources management [4]-[5].

In karst aquifers, the fast underground outflow in the saturated zone [6]-[7] is due to the heterogeneous distribution of permeability, because there are many conduits and voids developed by the dissolution of carbonate minerals. Therefore, quantification of karst spring discharge and water budget formulation requires defining the karst network geometry, which is not, every time, measurable with reliability [8].

As a matter of fact, the complex hydrological behavior, on one hand, the high heterogeneity of hydraulic properties [9]-[10], on the other one, make data collection about karst networks and groundwater very difficult, and the water budget evaluation is very often too much uncertain. For this reason, environmental tracer are useful tools to provide information about groundwater flow paths and residence times in karst aquifer systems without allowing for the specification of input locations and times [11]-[12].

2 Problem Formulation

Environmental tracers are natural and anthropogenic chemical and isotopic substances that can be measured in groundwater and used to understand hydrologic properties of aquifers [13]-[14].

Environmental tracers provide information about the flow and mixing processes of water coming from different sources [15]-[16]. They are also useful to point out directions of groundwater flow and to determine origin and residence times of karst groundwater [17]-[18]. Typical natural tracers are major ions, trace elements, dissolved organic carbon and water isotopes [19]-[20]. Groundwater circulating in karst aquifer generally has great concentrations of Calcium and Magnesium as the result of bedrock weathering processes. Variations of Ca^{2+} and Mg^{2+} in groundwater chemical compositions are used very successfully as natural tracers in studies aiming to evaluate groundwater residence time within the karst aquifers [17]. The changes in Ca^{2+} and Mg^{2+} concentration values mainly depend on the residence time of groundwater in karst systems, which are controlled by the volume and mechanism of recharge, the distance from the recharge area and the dissolution of carbonate minerals [21]-[22]. The dissolution kinetics of Magnesium is longer than that of Calcium, so the increase of the Mg^{2+}/Ca^{2+} ratio implies the saturation of water with calcite, highlighting long residence time and enhanced weathering along the groundwater flow paths [22]-[23]. The Mg^{2+} content in groundwater also depends on others parameters such as chemical and mineralogical purity of limestone and presence of dolomite within the rock masses they flow across [24]. Nevertheless, the increase in Mg^{2+} concentration values, and hence Mg^{2+}/Ca^{2+} ratio not only depend on the dissolution/precipitation reaction of calcite and dolomite, but also an increase in water temperature accelerates the kinetics of the dissolution of dolomite [25]-[26]. However, it has been noticed that even in karst aquifers mainly made of limestone, the presence of slight impurities of Mg^{2+} in calcite can be responsible of significant changes in Mg^{2+}/Ca^{2+} ratio due to a high residence time of flowing waters [27]-[28]. Thus, environmental tracers and hydrochemical investigation techniques provide much information for the identification of groundwater flow systems and the main hydrogeochemical processes affecting the composition of water within the karst aquifers [28]. The analysis of the hydrogeochemical processes due to groundwater-surface water interactions let us to highlight the source of their mineralization and the influence of rock masses forming the aquifer.

2.1 Geological and Hydrogeological Framework

The karst aquifer feeding Pertuso Spring is located in the Upper Valley of the Aniene River (Latium, Central Italy), along the SW boundary of the Simbruini Mountains, in the outcrop of Triassic-Cenozoic carbonate rocks, locally covered by fluvial and alluvial deposits and, at lower altitudes, by Quaternary sediments [29]. The lithological sequence outcropping in the Upper Valley of Aniene River includes the North-West part of the Lower-Middle Miocene Latium-Abruzzi carbonate platform. The stratigraphic succession of dolomite, dolomitic limestone and limestone is distributed homogeneously from North to South and from East to West in the Valley [30]. The base of the stratigraphic series (Triassic) is widely spread among Filettino, Aniene River Springs and Faito Plateau. Dolomite is the dominant lithofacies, characterized by white and gray crystalline dolomite, with some breccia levels. Over this geological formation, limestones and dolomites, of Upper Cretaceous age (Sinemurian) are present, and their immersion is concordant with the Triassic dolomite [30]. Karst springs are numerous along the first part of the Aniene River and form in the Triassic dolomitic formations (Fig. 1). This karst system is characterized by one main outlet, Pertuso Spring, and several springs which inflow into the Aniene River, at different points (Table 1).

Spring	Altitude (m a.s.l.)	Average Discharge (l/s)
Acqua Santa	900	65
Acqua Nera	1030	80
Fonte del Forno	950	164
Cesa degli Angeli	940	200
Radica	1110	250
Pertuso	**698**	**1400**

Table 1, Elevation and average annual discharge of the main karst springs of Upper Valley of Aniene River [33]

Due to their lower solubility and their lower brittleness, in comparison with limestones, dolomites are less fracturated than these latter ones. As a consequence of it in the Aniene River Basin, almost all groundwater come out where there is a limestone-dolomite contact [29] (Fig. 1) and this latter one is below the former one. Pertuso Spring, the largest karst spring in South-East part of Latium Region, is located between Filettino and Trevi nel Lazio (FR) and belongs to the Special Area of Conservation (SAC) of Aniene River Springs (EC Site Code IT6050029) established under Directive 92/43/EEC (Fig. 2).

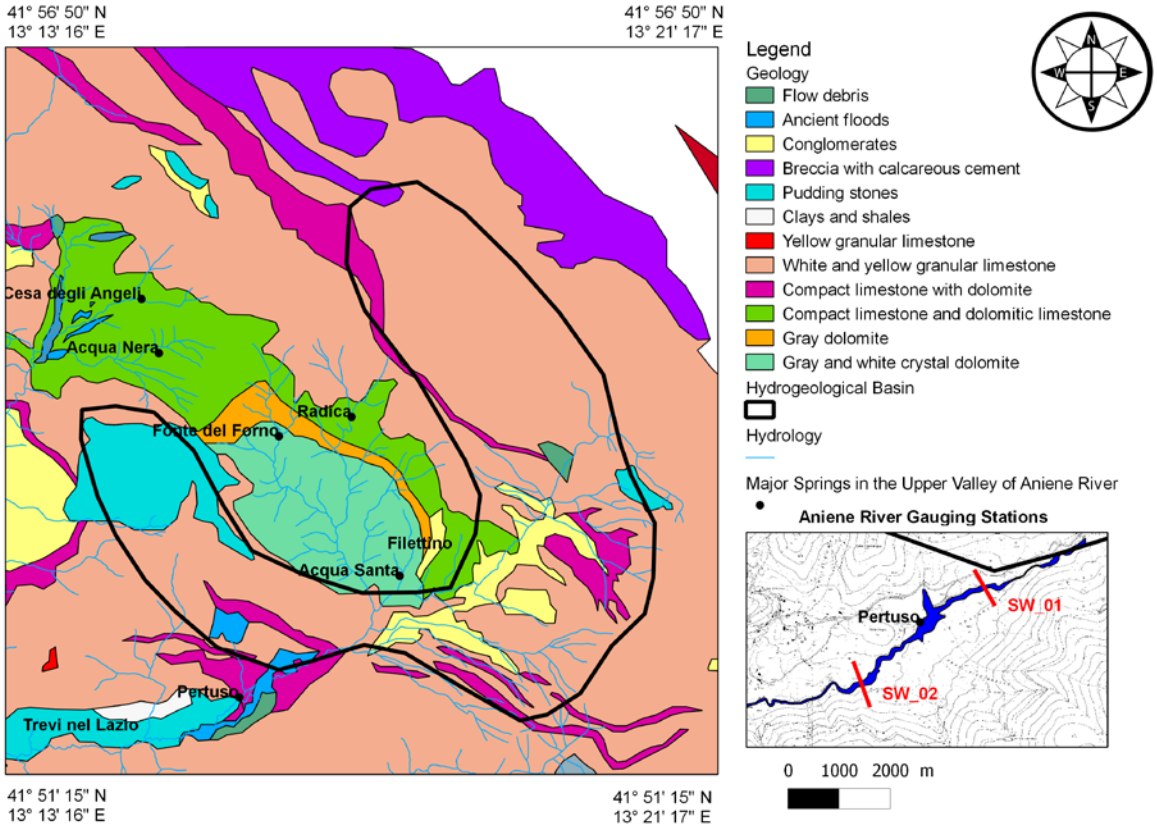

Fig. 1, Simplified geological map of Pertuso Spring hydrogeological basin and location of Aniene River gauging sections

Pertuso Spring (elevation of 720 m a.s.l.) is the main outlet of this karst aquifer and comes out about 1 km from the confluence of Fiumata Valley and Granara Valley [31].

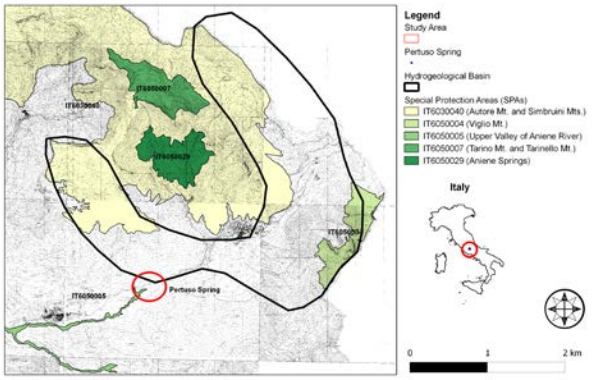

Fig. 2, Map of Special Areas of Conservation (SACs) in the Upper Valley of Aniene River

The outflow of Pertuso Spring is located in alluvial sediments, which cover a very thick layer made of Cretaceous limestone (Fig. 3). Spring water is captured for hydroelectric and drinking supplies, after which it flows into the Aniene River.

The Pertuso Spring hydrogeological basin is located between latitude 41° 51' to 41° 56'N and longitude 13° 13' to 13° 21'E and collect groundwater coming from a 50 km^2 catchment area [32] bounded by the Triassic dolomite to the NE (Fig. 1).

Fig. 3, Geological cross section showing the location of the Pertuso Spring

The aquifer feeding Pertuso Spring is made, for the most part, of Cretaceous karst limestone. The base of the stratigraphic series is constituted by Upper Cretaceous carbonates, made by the alternation of granular limestone and dolomites layers. Above these lie Quaternary fluvial and alluvial deposits, downward pudding and Miocene clay and shale [29] (Fig. 1).

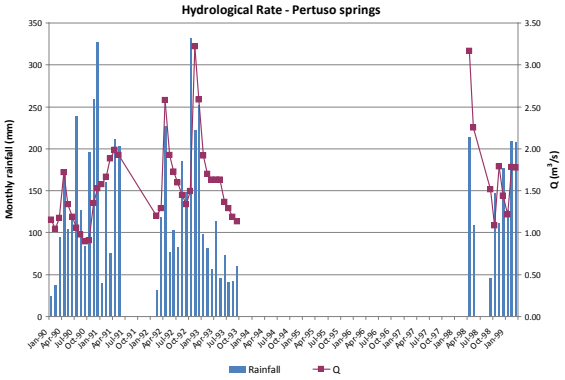

Fig. 4, Monthly rainfall and Pertuso Spring average rate in the 1990 - 1999 period (Filettino meteorological station)

Rainfall is the primary source of recharge to this karst aquifer. Most of the recharge of Pertuso Spring occurs through karst features such as sinkhole, dolines, swallows holes and fractures, which allow fast flow across the recharge zone. Pertuso Spring discharges at an annual average rate of 1400 l/s, based on the record from 1990 to 1999 [33], and responds rapidly to precipitation events, with significant increases in discharge rates which are proportional to the intensity of rainfalls (Fig. 4).

2.2 Pertuso Spring discharge evaluation aspects

Groundwater coming from Pertuso Spring, in the Upper Valley of Aniene River, are collected by a well known volume of carbonate rocks that make up the aquifer. The most distinctive feature of Pertuso karst spring is the branching network of conduits that increase in size in the downstream direction (Fig. 5).

The largest active conduit drains the groundwater flow coming from the surrounding aquifer matrix, the adjoining fractures and the smaller nearby conduits [34]-[35].

This conduit network is able of discharging large quantities of water very fastly through this karst aquifer (up to 3 m^3/s).

Karst springs are generally characterized by high and very variable discharge rate and represent the headwaters of important surface streams. These springs typically come out at the boundary of the hydrogeological basin, at a location of the minimum hydraulic head of the aquifer and sometimes next to the elevation of the base-level surface stream [22].

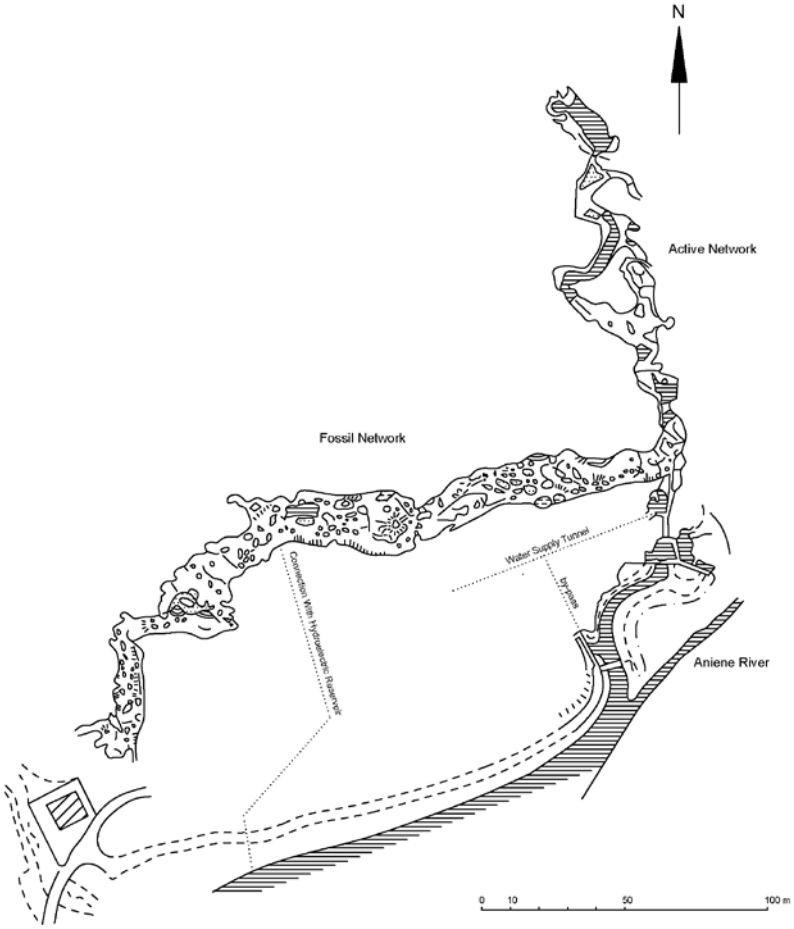

Fig. 5, Pertuso Spring drainage gallery map with plan view of the development of karst drainage network (modified from [33])

Groundwater basin boundaries are not strictly fixed, they may shift depending seasonally on the rates of recharge [7]. Many groundwater flow paths may route into adjacent groundwater basins causing difficulties to identify a single closing section. In addition, karst springs discharge is not easily measurable by standard techniques or conventional instruments. Sometimes channels are unsuitable for metering the flow, being shallow, choked with vegetation and with ill-defined banks [36]. In karst aquifers, the drainage network typically develops in a system of conduits that flows into a single trunk that discharges through the spring [6]. However, some karst aquifers may have a spread flow pattern, related to the enlargement of fractures and smaller conduits, located near the stream discharge boundary, or to the collapse of an existing trunk conduit [37].

Underflow springs are often hidden, for example by rising in the bed of the surface stream [7].

Thus, even if in this study we have identified a prevailing outlet section of the groundwater coming from Pertuso Spring, there is no chance to be sure that the whole spring contribution to Aniene River may always flow through that cross section. Consequently, the difficulty in measuring Pertuso Spring discharge makes the use of the traditional current meter method, which provides information on stream discharge in each cross section, limited and less reliable. Moreover, cross section morphology and flow regime are influenced by seasonal variations and anthropic operations, as reported in Figure 6 and 7, related to the monitoring campaign of July 2014 to December 2015.

Karst system dynamics are rapid, renewing most of the storage within a hydrologic year or less, which makes the effects of seasonal variations rapidly observable in the spring flow regime [10].

It has been noticed in dry season, at the Pertuso Spring outlet section, a reverse water inflow from Aniene River that makes unreliable the current meter measurement in that specific case. Hence, to be sure to evaluate a reliable quantification of Pertuso Spring discharge contribution to Aniene River we have decided to assess it as the difference of measured values along the river, upstream and downstream the spring [38].

In spite of being the spring, certainly, the only place where one can obtain information on the functioning of the whole system and consequently the organization of conduits and storage [10]. In this case, data coming directly from Pertuso Spring have been elaborated to set up an indirect model aimed to evaluate Pertuso Spring discharge.

Fig. 6, Pertuso Spring cross section (July 2014)

Fig. 7, Pertuso Spring cross section (December 2015)

Karst hydrology requires a mix of surface water concepts and ground water concepts [7]. For this reason, to better understand the behavior of this complex system and to validate discharge values calculated, it has been included a quali-quantitative characterization based on the Mg^{2+} contents of groundwater and surface water samples. As a matter of fact, Mg^{2+} content may generally provide information on residence time of ground waters within the aquifer [17] On the other hand, groundwater which have a longer underground flow path usually show the same properties: higher temperatures, higher Mg^{2+} concentrations and as a result a remarkable Mg/Ca ratio. However, the concentration of Mg^{2+} also depends on others

parameters, such as chemical and mineralogical purity of limestone and presence of dolomite within the rock mass [24].
In this study, the Mg^{2+} ion concentration has been used as conservative water tracer, allowing us to obtain an alternative discharge calculation model based on mixing and dilution process due to Pertuso Spring and to compare the results of this model with those of traditional current meter method.

2.3 Materials and Methods

This paper presents the results of the first year of the Environmental Monitoring Plan, related to the catchment project of the Pertuso Spring, which is going to be exploited to supply an important civil water network in the South part of Latium Region, Central Italy. The experimental data, corresponding to the period July 2014 - May 2015, were obtained from field investigations and from chemical analyses performed in laboratory. Water samples were collected from three sampling points within the study area, i.e. one from Pertuso Spring, two on gauging stations located along the Aniene River, respectively, upstream (SW_01) and downstream (SW_02) the spring (Fig. 1).
Field investigations included in situ measurements of pH, temperature, electric conductivity (HANNA, Model HI9813-6) and redox and dissolved oxygen (HACH, Model LDO10101). Water samples were filtered by 0.45 μm cellulose filters and stored at 4 °C until analysis in the Geochemical Laboratory of Sapienza University of Rome [39].

Sample	Date	T (°C)	pH	EC (μS/cm)	OD (mg/l)	Eh (mV)
Pertuso Spring	July 2014	8.0	7.4	322	11.7	112
	November 2014	8.0	7.2	300	10.6	111
	January 2015	9.5	6.9	410	10.3	481
	May 2015	8.5	10.8	300	10.3	243
SW_01	July 2014	11.3	8.3	422	9.7	74
	November 2014	7.7	8.3	360	10.7	89
	January 2015	5.8	7.3	340	11.3	435
	May 2015	10.7	9.6	390	9.8	212
SW_02	July 2014	9.9	7.8	352	10.9	66
	November 2014	7.3	7.6	320	10.6	78
	January 2015	7.2	6.9	270	10.9	449
	May 2015	8.9	8.1	280	10.4	210

Table 2, Summary of T, pH, electric conductivity, dissolved oxygen and redox potential of water samples

Sample	Date	Ca (mg/l)	Mg (mg/l)	Na (mg/l)	K (mg/l)	HCO_3 (mg/l)	Cl (mg/l)	NO_3 (mg/l)	SO_4 (mg/l)
Pertuso Spring	July 2014	48.9	9.77	1.91	0.50	210	3.54	0.92	2.39
	November 2014	51.0	8.32	1.83	0.32	216	3.48	1.15	2.41
	January 2015	53.3	9.89	2.05	0.45	206	3.66	1.11	2.54
	May 2015	49.0	9.33	1.86	0.31	224	3.35	0.94	2.34
SW_01	July 2014	53.4	23.6	2.48	0.35	87	4.16	1.06	2.87
	November 2014	54.0	23.5	2.59	1.61	89	4.34	1.26	3.04
	January 2015	57.8	25.2	n.d.	n.d.	n.d.	4.50	1.23	3.18
	May 2015	53.9	24.6	n.d.	n.d.	n.d.	4.12	0.83	2.90
SW_02	July 2014	51.3	12.8	2.01	0.18	72	3.66	0.96	2.50
	November 2014	52.4	12.0	1.11	0.44	72	3.72	1.14	2.56
	January 2015	55.6	13.0	n.d.	n.d.	n.d.	4.17	1.09	2.73
	May 2015	51.4	12.2	n.d.	n.d.	n.d.	3.53	0.86	2.47

Table 3, Summary of major ions of water samples (n.d.= not determined)

Major ions were determined by ion chromatography (IC) by a 761 Professional IC Metrohm (reliability ±2%). A Metrosep C2-150 column was used for determining major cations (Ca^{2+}, Mg^{2+}, Na^{+}, K^{+}), whereas major anions (Cl^{-}, NO_3^{-}, SO_4^{2-}) were determined by Metrosep A sup 4–250 column (accuracy 2-5%). Bicarbonate (HCO_3^{-}) was determined by titration with 0.1 N HCl (reliability ±2%).

A statistical summary of the major physico-chemical parameters is shown in Table 2 and 3.

The geochemical modeling program PHREEQC v3.0 [40], implemented with the thermodynamic dataset phreeqc.dat, was used to study mixing of groundwater and surface water to understand spatial and temporal patterns of mixing during base flow conditions.

The discharge measurements were carried out along the Aniene River, upstream (SW_01) and downstream (SW_02) Pertuso Spring, by the application of traditional current meter. According to the U.S. Geological Survey (USGS) procedure, stream discharge is calculated as the product of the cross section area by the average stream flow velocity in that cross section obtained using a current meter [41]-[42]. The main equipment needed to measure the stream flow velocity is a SEBA horizontal axis current meter F1, having a propeller diameter of 80 mm which, combined with SEBA Z6 pulse counter, allows to measure velocity between 0,025 m/s and 10 m/s. The SEBA current meter has been used as rod equipment with tail plane for best positioning to the flow direction. For each measurement point, flow velocity is determined counting the number of spins of the meter rotor during a fixed interval of time. Thus, in order to assess any fluctuations due to the turbulence condition and, also, to avoid accidental measurement errors, velocity has been measured for at least 60 seconds, according to EN ISO 748:2007 requirements [42]. This current meter method gives the local water velocity in each vertical following the application of a calibration equation between stream velocity, v (cm/s) and the number of spins, n (s^{-1}) (1).

$$v = 0.82 + 33.32 \cdot n \quad (1)$$

3 Problem Solution

In order to establish the groundwater discharge pattern, hydrochemical data and discharge measurements were used in the study.

Ca^{2+}, Mg^{2+} and HCO_3^{-} represent more than 80% of the dissolved solids in water samples and are influenced by the dissolution of carbonate minerals, forming limestone, which are the most dominant formations outcropping in the study area.

As a consequence of their flowing in a karst aquifer, all these water samples came out to be rich in Ca-Mg-HCO_3 as it is represented by Piper diagram (Fig. 8), but water samples coming from SW_01 gauging station present higher values of concentration in Mg^{2+}, while those coming from Pertuso Spring are definitely poorer in it, and show a clear composition of Ca-HCO_3 water type.

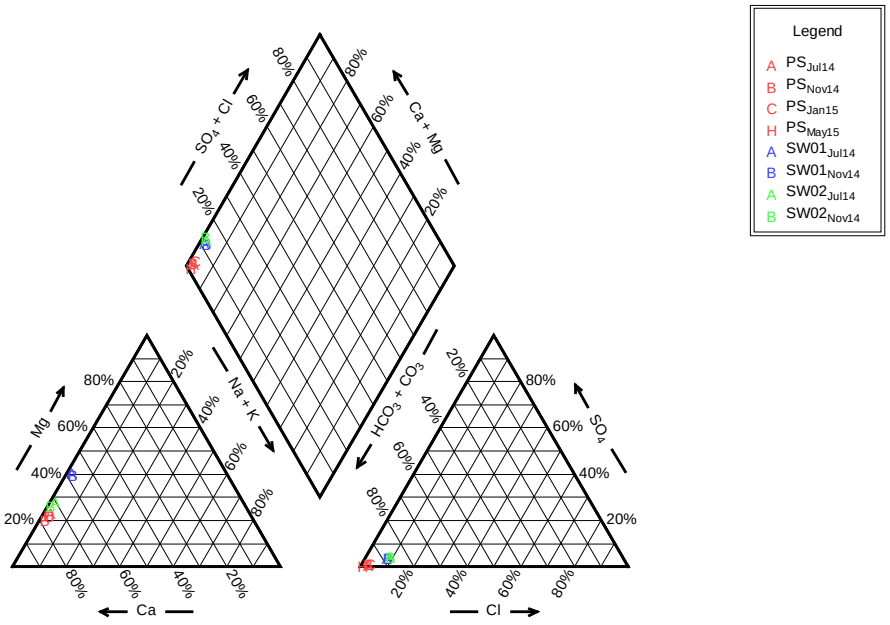

Fig.8, Piper diagram showing the hydrochemical facies of surface and groundwater in the karst aquifer feeding Pertuso Spring

These hydrochemical facies highlight that carbonate weathering processes (e.g. calcite and dolomite) are the most important factors of the observed water type.

Box plot for Mg^{2+} in groundwater and surface water is presented in Fig. 9. Following differentiation of Magnesium content along the Aniene River, we observed a 47% decrease in Mg^{2+}concentration in surface water downstream Pertuso Spring (SW_02) with respect to Mg^{2+}concentration measured in SW_01 (23.6 mg/l).

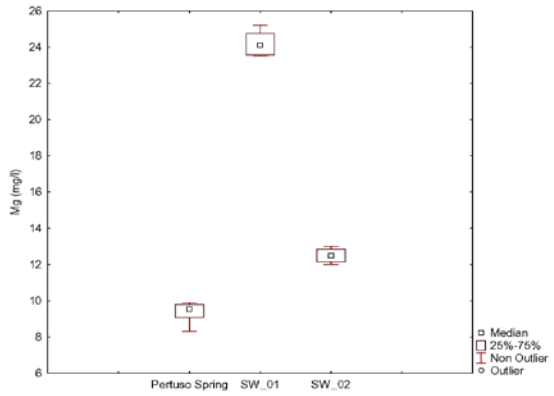

Fig.9, Box plot of Mg^{2+} concentration in groundwater and surface water

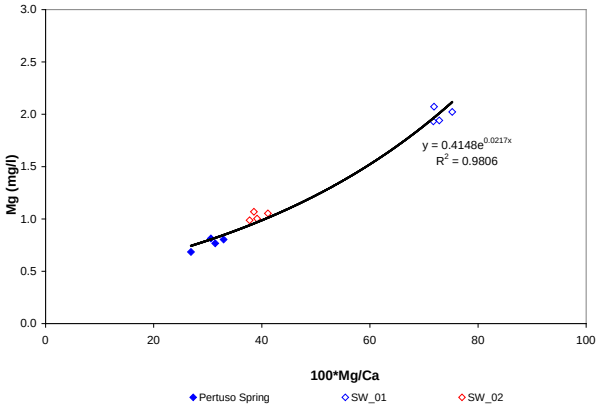

Fig.10, Mg^{2+} versus Mg^{2+}/Ca^{2+} ratio in groundwater and surface water

The scatter plots diagram for Mg^{2+}/Ca^{2+} ratio (Fig. 10) shows that the increase in Mg^{2+} concentrations in surface water, upstream the Pertuso Spring, and hence Mg/Ca ratio may be due to the weathering of Mg-rich Triassic dolomites, where dolomitic limestones and dolomites are the most dominant formations in this area. For Pertuso Spring groundwater, the high Mg/Ca ratios (~0.5) mainly depend on the residence of water in the karst system, highlighting long residence time and enhanced weathering along the groundwater flow paths of low-Mg calcite.

As a consequence of these properties water samples taken in SW_02 gauging station, downstream Pertuso Spring, present chemical composition typical of mixing of these two different kinds of waters (Fig. 11).

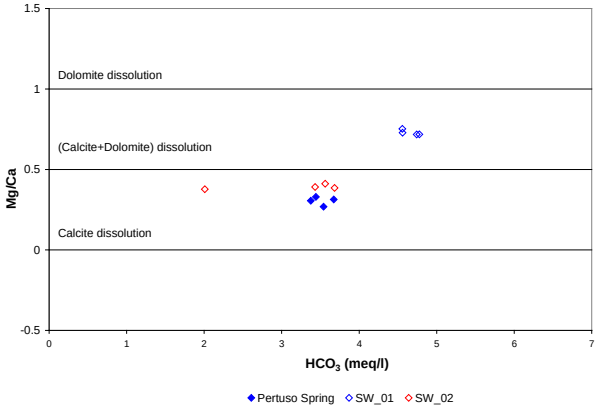

Fig.11, Mg^{2+}/Ca^{2+} ratio versus HCO_3 in groundwater and surface water

As a matter of fact, the highest Mg^{2+}/Ca^{2+} ratio in water sampled has been recorded in dolomite outcropping (SW_01: Mg^{2+}/Ca^{2+} ~ 0.7), with medium value at SW_02 gauging station (Mg^{2+}/Ca^{2+} ~ 0.4). On the other hand, the lowest value of this ratio in groundwater has been observed in Cretaceous limestone area (Pertuso Spring: Mg^{2+}/Ca^{2+} ~ 0.3) (Table 4).

Mg^{2+}/Ca^{2+}	Pertuso Spring	SW_01	SW_02
July 2014	0.329	0.728	0.411
November 2014	0.269	0.717	0.377
January 2015	0.306	0.719	0.385
May 2015	0.314	0.752	0.391

Table 4, Mg^{2+}/Ca^{2+} ratio from Pertuso Spring and Aniene River gauging station

Aniene River discharge was measured during the hydrological year 2014-2015, in order to cover the range of seasonal conditions characteristics of this complex hydrogeological system. Measurements, e.g. by current meter, were carried on in two gauging stations located upstream (SW_01) and downstream (SW_02) Pertuso Spring (Table 5).

They are represented, in Table 5, discharge values recorded in SW_01 and SW_02 gauging stations all over the hydrological year. It can be noticed that the average discharge value referred to SW_01 gauging station can be well compared with the total average discharge coming from of the most important karst springs outcropping in the Upper Part of Aniene River (Table 1). Thus, the source of

Mg^{2+} concentration values in Aniene River water upstream Pertuso Spring (SW_01) is the dissolution of Magnesium rich minerals in Triassic dolomites, sited in north-east part of the Pertuso Spring hydrogeological basin. Along the Aniene River, this decrease in Mg^{2+} concentration values is related to an increase in stream flow discharge. SW_02 surface water is the product of the confluence of groundwater coming from Pertuso Spring into the Aniene River (SW_01). As a matter of fact, Aniene River water, which is characterized by water with higher Magnesium concentration values, is affected in its chemical composition by Pertuso Spring groundwater inflowing, and this influence can be measured by Mg^{2+} concentration values variability along the river downstream.

Q (m^3/s)	SW_01	SW_02
July 2014	0.540	2.450
November 2014	0.350	1.480
January 2015	0.410	1.920
May 2015	0.501	2.747

Table 5, Results of mean discharge values obtain by current meter method, upstream (SW_01) and downstream (SW_02) Pertuso Spring

Using PHREEQC program it has been calculated the speciation of an aqueous solution of a virtual composed water sample made of the mixing of water coming from Pertuso Spring and SW_01 gauging station. To have the mixed virtual sample composition any source sample, Pertuso Spring and SW_01 gauging station, has been multiplied in its chemical component for their own contribution fraction in SW_02 gauging station discharge.

Date	Mg^{2+} (mg/l)		
	Phreeqc	SW_02	Percent difference (%)
July 2014	12.44	12.80	3
November 2014	11.61	11.80	2
January 2015	12.72	13.00	2
May 2015	11.72	12.20	4

Table 6, Magnesium concentration of SW_02 and the virtual solution made by mixing water coming from Pertuso Spring and SW_01

Figure 12 shows that the calculated values fit quite well the experimental values reported in Table 6. The results obtained by PHREEQC program fall close to the equiline of 1:1, and this fact confirms that SW_02 surface water comes from the mixing of groundwater outflowing from Pertuso Spring with surface water of Aniene River (SW_01).

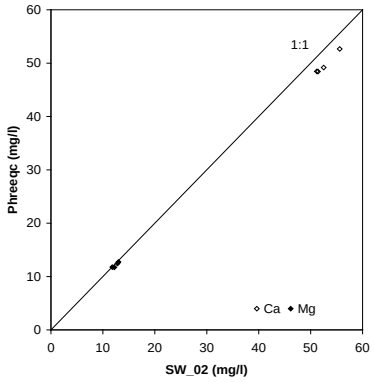

Fig. 12, Comparison between the ionic compositions of SW_02 and the virtual solution made by mixing water coming from Pertuso Spring and SW_01

The karst aquifer/river system has been studied in the aim of evaluating factors, which modify the Aniene River flow due to groundwater-surface water interactions. Three pairs of values, related, each one, to any sampling point, has been considered. The main inputs are the discharge measurements (Q_1) and the Mg^{2+} concentrations (C_1) recorded in the Aniene River upstream Pertuso Spring (SW_01). The secondary inputs are the discharge rate (Q_P) and the Mg^{2+} concentrations (C_P) recorded at Pertuso Spring. The main output is the Aniene River discharge (Q_2) and the Mg^{2+} concentrations (C_2) recorded at the SW_02 gauging station located downstream Pertuso Spring.

Thus, assuming that this is a closed system, the SW_02 gauging station discharge values, comes from the contribution of Pertuso Spring discharge (Q_P) to the original SW_01 gauging station discharge value, and so it can be represented by (2):

$$Q_2 = Q_1 + Q_P \tag{2}$$

and applying to this closed system the conservation of mass equation, it means (3):

$$Q_1 C_1 + Q_P C_P = Q_2 C_2 \tag{3}$$

The n parameter (Table 7), i.e. the percentage contributor of Pertuso Spring groundwater to total discharge measured at the, is defined according to (4).

$$n = \frac{Q_P}{Q_2} = \frac{(C_2 - C_1)}{(C_P - C_1)} \tag{4}$$

Thus, the discharge rate of Pertuso Spring depends on the discharge values measured in the gauging station located along the Aniene River upstream the spring (Q_1) and the Mg^{2+} concentration values recorded in groundwater and surface water samples (C_1, C_2, C_P) (5):

$$Q_P = Q_1 \cdot \frac{n}{1-n} \quad (5)$$

Date	n	n (%)
July 2014	0.780	78.0
November 2014	0.752	75.2
January 2015	0.794	79.4
May 2015	0.812	81.2

Table 7, *n* values as percentage contributor of Pertuso Spring groundwater to total discharge measured at the SW_02 gauging

Pertuso Spring discharge values obtained by this indirect method are showed in Table 8.

The relationship between Mg^{2+} concentration and karst spring discharge values obtained with this combined Magnesium-discharge tracer approach is represented in Fig. 13.

Date	SW_01		Pertuso Spring			SW_02		
	Q^* (m^3/s)	Mg^{2+} (meq/l)	Q^{**} (m^3/s)	Q_{Mg} (m^3/s)	Mg^{2+} (meq/l)	Q^* (m^3/s)	Q_{Mg} (m^3/s)	Mg^{2+} (meq/l)
July 2014	0.540	1.94	1.910	1.922	0.800	2.450	2.462	1.050
November 2014	0.350	1.93	1.130	1.061	0.680	1.480	1.411	0.990
January 2015	0.410	2.07	1.510	1.577	0.810	1.920	1.987	1.070
May 2015	0.501	2.02	2.225	2.164	0.767	2.747	2.664	1.003

Table 8, Magnesium content and discharge values obtained by current-meter and Magnesium tracer method (Q^*: discharge values obtained by current meter method; Q^{**}: discharge values obtained by the difference between the values measured with the current meter in SW_01 and SW_02)

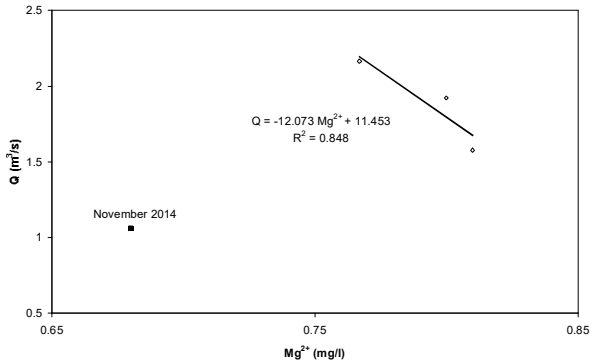

Fig. 13, Relationship between the Mg^{2+}concentration and Pertuso Spring discharge values obtain with the combined Magnesium-discharge tracer approach

The Mg^{2+} vs Q scatter plots diagram shows that all plotted points, except for November 2014 data, follow a linear trend, highlighting that the increasing contribution of Pertuso Spring flow rate is responsible of Mg^{2+} concentration values decreasing. Data, referred to November 2014 monitoring campaign, have to be considered as an outlier (Fig. 14).

This lower Mg^{2+} concentration measured at November 2014 can be related to a high precipitation rate, recorded at Trevi nel Lazio meteorological station, during the five days before the sampling date (Fig. 14), which could have influenced, lowering it, the Mg^{2+} concentration in groundwater.

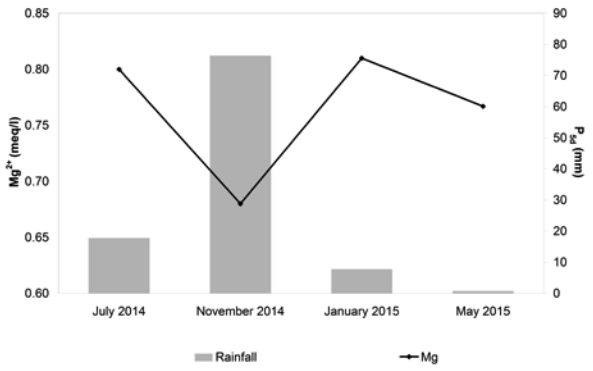

Fig. 14, Relationship between Mg^{2+} concentration in Pertuso Spring groundwater and rainfall (Trevi nel Lazio meteorological station)

4 Conclusion

This paper dealt with the assessment of the interactions between karst aquifer feeding Pertuso Spring and Aniene River surface waters on the basis of stream discharge measurements and water geochemical tracers data in the aim to set up an inversed model, which allows to estimate groundwater flow coming out from Pertuso Spring, starting from surface water discharge measurements and geochemical waters characterization. These preliminary results, carried out in a pilot area, sited in the karst aquifer, outcropping in the Upper Valley of Aniene River, show that, for this karst system, it is possible to

have a reliable evaluation of Pertuso spring discharge, by the elaboration of surface water discharge measurements in relationship with Mg^{2+} concentration values, determined as for groundwater, coming from Pertuso Spring, as for surface water sample, taken upstream and downstream of Pertuso Spring, along Aniene River streaming. Although it is subject to some uncertainties, the Mg^{2+} concentration, as an environmental tracer, provides an indirect method for discharge evaluation of Pertuso Spring, due to the mixing of surface water and groundwater and, provides information on changes in water quantity and quality.

References:

[1] C. Boni, P. Bono, G. Capelli, S. Lombardi, G.M. Zuppi, Contributo all'Idrogeologia dell'Italia Centrale: Analisi Critica dei Metodi di Ricerca, *Memorie Società, Geologica Italiana*, Vol.35, 1986, pp. 947-956.

[2] Q. Guo, Y. Wang, T. Ma, L. Li, Variation of karst springs discharge in recent five decades as an indicator of global climate change: a case study at Shanxi, northern China, *Science in China Series D: Earth Science*, Vol.48, No.11, 2005, pp. 2001-2010.

[3] G. Sappa, G. Luciani, Groundwater Management in Dar Es Salam Coastal Aquifer (Tanzania) under a Difficult Sustainable Development, *WSEAS Transactions on Environment and Development*, Vol.10, 2014, pp. 465-477.

[4] G. Sappa, F. Ferranti, S. Ergul, G. Ioanni, Evaluation of the groundwater active recharge trend in the coastal plain of Dar es Salaam (Tanzania), *Journal of Chemical and Pharmaceutical Research*, Vol.5, No.12, 2013, pp. 548-552.

[5] S. Foster, R. Hirata, B. Andreo, The aquifer pollution vulnerability concept: aid or impediment in promoting groundwater protection?, *Hydrogeology Journal*, Vol.21, 2013, pp. 1389-1392.

[6] W.B. White, Conceptual models for carbonate aquifers, *Ground Water*, Vol.7, 1969, pp. 15-22.

[7] W.B. White, Karst hydrology: recent developments and open questions, *Engineering Geology*, Vol.65, 2002, pp. 85-105.

[8] C. Cherubini, N. Pastore, V. Francani, Different approaches for the characterization of a fractured karst aquifer, *WSEAS Transactions on fluid mechanics*, Vol.3, 2008, pp. 29-35.

[9] F. Zwahlen, Vulnerability and risk mapping for the protection of carbonate (karst) aquifers, final report (COST Action 620). *European Commission, Directorate-General XII Science, Research and Development*. Brussels, 2004, pp. 297

[10] M. Bakalowicz, Karst groundwater: a challenge for new resources. *Hydrogeology Journal*, Vol.13, 2005, pp. 148-160.

[11] I.D. Clark, P. Fritz, *Environmental Isotopes in Hydrogeology*, Crc Pr Inc., Boca Raton, Fla., 1997.

[12] E. Mazor, *Chemical and Isotopic Groundwater Hydrology*, Marcel Dekker, New York, 2004.

[13] W.M. Alley (Ed.), *Regional Ground-Water Quality*. Van Nostrand Reinhold, New York, 1993.

[14] P. Cook, A. Herczeg, *Environmental Tracers in Subsurface Hydrology*. Kluwer Acad., Boston, 1999.

[15] M. Guida, D. Guida, D. Guadagnuolo, A. Cuomo, V. Siervo, Using Radon-222 as a Naturally Occurring Tracer to investigate the streamflow-groundwater interactions in a typical Mediterranean fluvial-karst landscape: the interdisciplinary case study of the Bussento river (Campania region, Southern Italy), *WSEAS Transactions on System*, Vol.12, No.2, 2013, pp. 85-104.

[16] L.N. Plummer, E. Busenberg, J.B. McConnell, S. Drenkard, P. Schlosser, R.L. Michel, Flow of river water into a karstic limestone aquifer: 1. Tracing the young fraction in groundwater mixtures in the Upper Floridan Aquifer near Valdosta, Georgia, *Applied Geochemistry*, Vol.13, No.8, p. 995-1015.

[17] C. Batiot, C. Emblanch, B. Blavoux, Total Organic Carbon (TOC) and magnesium (Mg^{2+}): two complementary tracers of residence time in karstic systems, *Comptes Rendus Geoscience*, No.35, 2003, pp. 205-214.

[18] G. Sappa, F. Ferranti, S. Ergul, Vulnerability assessment of Mazzoccolo Spring aquifer (Central Italy), combined with geo-chemical and isotope modelling, *Engineering Geology for Society and Territory*, Vol.5, Urban Geology, Sustainable Planning and Landscape Exploitation, 2015, pp. 1387-1392.

[19] D. Hunkeler, J. Mudry, Hydrochemical tracers, in Methods in *Karst Hydrogeology*, edited by N. Goldscheider and D. Drew, 2007, pp. 93-121.

[20] C. Leibundgut, P. Maloszewski, C. Kulls, Tracers in *Hydrology*, 1st ed., Wiley-Blackwell, Chichester, U. K., 2009.

[21] D. Langmuir. Geochemistry of Some Carbonate Ground Waters in Central Pennsylvania. *Geochimica et Cosmochimica Acta*, Vol.35, No.10, 1971, pp. 1023–1045.

[22] W.B. White, *Geomorphology and Hydrology of Karst Terrains*. New York, Oxford University Press, 1988, pp. 464.

[23] W.M. Edmunds, J.M. Cook, W.G. Darling, D.G. Kinniburgh, D.L. Miles, Baseline geochemical conditions in the Chalk aquifer, Berkshire, U.K.: a basis for groundwater quality management, *Applied Geochemistry*, Vol.2, No.3, 1987, pp. 251-274.

[24] M. Mudarra, B. Andreo, Relative importance of the saturated and the unsaturated zones in the hydrogeological functioning of karst aquifers: The case of Alta Cadena (Southern Spain), *Journal of Hydrology*, Vol.397, No.3-4, 2011, pp. 263-280.

[25] C.D. Palmer, J.A. Cherry, Geochemical Evolution of Groundwater in Sequences of Sedimentary Rocks, *Journal of Hydrology*, Vol.75, No.2, 1984, pp. 27-65.

[26] J.S. Herman, W.B. White, Dissolution Kinetics of Dolomite: Effects of Lithology and Fluid Flow Velocity, *Geochimica et Cosmochimica Acta*, Vol.49, 1985, pp. 2017-2026.

[27] H. Celle-Jeanton, C. Emblanch, J. Mudry, A. Charmoille, Contribution of time tracers (Mg^{2+}, TOC, $\delta^{13}C_{TDIC}$, NO_3^-) to understand the role of the unsaturated zone: A case study-Karst aquifers in the Doubs valley, eastern France, *Geophysical Research Letters*, Vol.30, No.6, 2003.

[28] A.F. Tooth, I.J. Fairchild, Soil and karst aquifer hydrological controls on the geochemical evolution of speleothem-forming drip waters, Crag Cave, southwest Ireland *Journal of Hydrology*, Vol.273, 2003, pp. 51-68.

[29] U. Ventriglia, Idrogeologia della Provincia di Roma, IV, Regione orientale. *Amministrazione Provinciale di Roma, Assessorato LL.PP, Viabilità e trasporti*, Roma, 1990.

[30] A.V. Damiani, "Studi sulla piattaforma carbonatica laziale-abruzzese. Nota I. Considerazioni e problematiche sull'assetto tettonico e sulla paleogeologia dei Monti Simbruini, Roma", *Memorie descrittive Carta Geologica d'Italia*, Vol.38, 1990, pp.177–206.

[31] F. Cipollari, D. Cosentino, M. Parrotto, Modello cinematico-strutturale dell'Italia centrale. *Studi Geol. Camerti*, Vol.2, 1995.

[32] G. Sappa, F. Ferranti, An integrated approach to the Environmental Monitoring Plan of the Pertuso spring (Upper Valley of Aniene River), *Italian Journal of Groundwater*, Vol. 3, No.136, 2014, pp. 47–55.

[33] Acea ATO 2 S.p.A., *Studio idrogeologico – Proposta di aree di salvaguardia della sorgente del Pertuso*, unpublished.

[34] A.N. Palmer, Patterns of dissolution porosity in carbonate rocks, in A.N. Palmer, M.V. Palmer and I. D. Sasowsky, eds., *Karst modeling*: Leesburg, Va., Karst Waters Institute Special Publication 5, 1999, pp. 71–78.

[35] W.B. White, E.L. White, eds., *Karst hydrology-Concepts from the Mammoth Cave area: New York, Van Nostrand Reinhold*, 1989, pp. 346.

[36] A.F. Pitty, The estimation of discharge from a karst rising by natural salt dilution. *Journal of Hydrology*, 4, 1996, pp. 63-69.

[37] J.F. Quinlan, R.O. Ewers, Subsurface drainage in the Mammoth Cave area, in W.B.White and E.L.White, eds., *Karst hydrology concepts from the Mammoth Cave area: New York, Van Nostrand Reinhold*, 1989, p. 65–104.

[38] G. Sappa, F. Ferranti, F. M. De Filippi, *Environmental tracer approach to discharge evaluation of Pertuso Spring (Italy)*, proceedings of the 10th International Conference on Energy & Environment (EE'15) in Recent Advances on Energy and Environment, edited by Aida Bulucea, WSEAS, 2015, pp. 54-62.

[39] APHA. *Standard Methods for the Examination of Water and Wastewater*, 20th ed.; American Public Health Association: Washington, DC, USA, 1998.

[40] D. L. Parkhurst, C.A. J. Appello, User's Guide to PHREEQC (Version 2)-A Computer Program for Speciation, Batch-Reaction, One-Dimensional Transport, and Inverse Geochemical Calculations. *US Geological Survey Water-Resources Investigations, Report* 99-4259, 1999.

[41] US EPA Region 6, *Standard operating procedure for stream flow measurement*, 2003.

[42] BS EN ISO 748:2007, *Hydrometry. Measurement of liquid flow in open channels using current-meters or floats*, 2007.

DOI: 10.7343/as-2016-224 Special Issue AQUA2015 - Paper Ricerca

A proposal of conceptual model for Pertuso Spring discharge evaluation in the Upper Valley of Aniene River

Proposta di modello concettuale per la stima della portata della sorgente Pertuso nell'Alta Valle del fiume Aniene

Giuseppe Sappa, Flavia Ferranti, Francesco Maria De Filippi

Riassunto: Il bacino idrogeologico della parte alta del Fiume Aniene appartiene ad un grande acquifero carsico, che interagisce con il fiume e rappresenta la più importante risorsa idrica nella parte sud-orientale della Regione Lazio (Italia Centrale) usata per approvvigionamento potabile, agricolo e idroelettrico.
Il presente lavoro fornisce i dati idrogeochimici e alcune loro interpretazioni per una sorgente e 2 sezioni di misura del Fiume Aniene, monitorate da luglio 2014 a dicembre 2015 nell'Alta Valle del Fiume Aniene. Lo scopo principale è stato quello di definire le vie di deflusso delle acque sotterranee e i processi idrogeochimici che governano le interazioni tra acque sotterranee e superficiali in questa zona. Questo articolo è perciò il risultato di attività eseguite per il piano di monitoraggio ambientale nell'ambito del progetto di captazione della Sorgente Pertuso, che sarà sfruttata per rifornire un'importante rete idrica nella zona Sud di Roma. Sono state analizzate le misure di portata e i dati idrogeochimici al fine di sviluppare un modello concettuale di interazione tra fiume e acquifero, con l'obiettivo di raggiungere un corretto grado di gestione e protezione di questo importante sistema idrogeologico. Tutti i campioni d'acqua sono del tipo Ca-HCO_3 (bicarbonato-calcica). La modellazione geochimica e il calcolo dell'indice di saturazione per i campioni di acqua mostrano che la chimica delle acque sotterranee e superficiali nell'area di studio risente dell'interazione con i minerali carbonatici. Tutti i campioni di acqua sotterranea risultano sottosaturi rispetto alla calcite e alla dolomite, tuttavia alcuni campioni del Fiume Aniene sono saturi rispetto alla dolomite. L'analisi dei rapporti Mg^{2+}/Ca^{2+} indica che la dissoluzione dei minerali carbonatici gioca un ruolo significativo nella chimica delle acque sotterranee e superficiali, dipendendo dai processi idrogeologici che controllano il tempo di residenza delle acque sotterranee e gli equilibri chimici nell'acquifero.

Parole chiave: acquifero, carsismo, modellazione idrogeochimica, monitoraggio, tracciante ambientale.

Keywords: *: aquifer, karst, hydrogeochemical modelling, monitoring, environmental tracer.*

Abstract: *The Upper Aniene River basin is part of a large karst aquifer, which interacts with the river, and represents the most important water resource in the southeast part of Latium Region, Central Italy, used for drinking, agriculture and hydroelectric supplies. This work provides hydrogeochemical data and their interpretations for 1 spring and 2 cross section of Aniene River, monitored from July 2014 to December 2015, in the Upper Valley of Aniene River, to identify flow paths and hydrogeochemical processes governing groundwater-surface water interactions in this region. These activities deal with the Environmental Monitoring Plan made for the catchment work project of the Pertuso Spring, in the Upper Valley of Aniene River, which is going to be exploited to supply an important drinking water network in the South part of Rome district. Discharge measurements and hydrogeochemical data were analyzed to develop a conceptual model of aquifer-river interaction, with the aim of achieving proper management and protection of this important hydrogeological system. All groundwater samples are characterized as Ca-HCO_3 type. Geochemical modeling and saturation index computation of the water samples show that groundwater and surface water chemistry in the study area was evolved through the interaction with carbonate minerals. All groundwater samples were undersaturated with respect to calcite and dolomite, however some of the Aniene River samples were saturated with respect to dolomite. The analysis of Mg^{2+}/Ca^{2+} ratios indicates that the dissolution of carbonate minerals is important for groundwater and surface water chemistry, depending on the hydrological processes, which control the groundwater residence time and chemical equilibria in the aquifer.*

Giuseppe SAPPA,
Department of Civil, Building and Environmental Engineering
Sapienza University of Rome
via Eudossiana 18, 00184, Rome, Italy
Tel: +39.06.44585010 - Fax: +39.06.233239345
giuseppe.sappa@uniroma1.it

Flavia FERRANTI, Francesco Maria DE FILIPPI
Department of Civil, Building and Environmental Engineering
Sapienza University of Rome
via Eudossiana 18, 00184, Rome, Italy

Ricevuto: 24 giugno 2016 / Accettato: 14 settembre 2016
Pubblicato online: 3 ottobre 2016

Introduction

Most of groundwater in the southeast part of Latium Region, as in the whole Apennine Mountains chain, is stored in karst aquifers. Karst groundwater depletion is mostly due to the increasing of anthropogenic activities and the impacts of climate change (Guo et al. 2005, Sappa et al. 2013). Thus, groundwater exploitation in karst aquifers requires special management strategies to prevent their quality and quantity depletion and to support decision-making for water resources management (Sappa et al. 2013, Foster et al. 2013). In karst aquifers, the fast underground outflow in the saturated zone (White 1969, White 2002) is due to the heterogeneous distribution of permeability (Zwahlen 2004, Bakalowicz 2005), because there are many conduits and voids developed by the dissolution of carbonate minerals. Therefore, quantification of karst spring discharge and water budget formulation requires defining the karst network geometry, which is not, every time, measurable with reliability (Cherubini et al. 2008).

For this reason, environmental tracers are useful tools to provide information about groundwater flowpaths and residence times in karst aquifers without allowing for the specification of input locations and times (Clark and Fritz 1997, Mazor 2004).

Environmental tracers provide information about the flow and mixing processes of water coming from different sources (Guida et al. 2013). They are also useful to point out directions of groundwater flow and to determine origin and residence times of karst groundwater (Batiot et al. 2003, Sappa et al. 2015a, 2015b). Typical natural tracers are major ions, trace elements, dissolved organic carbon and water isotopes (Hunkeler and Mudry 2007, Leibundgut et al. 2009). Groundwater circulating in karst aquifer generally has great concentrations of Calcium and Magnesium as the result of bedrock weathering processes. Variations of Ca^{2+} and Mg^{2+} in groundwater are used very successfully as natural tracers in studies aiming to evaluate groundwater residence time within the karst aquifers (Batiot et al. 2003). The changes in Ca^{2+} and Mg^{2+} concentration values mainly depend on the residence time of groundwater in karst systems, which are controlled by the volume and mechanism of recharge, the distance from the recharge area and the dissolution of carbonate minerals (Langmuir 1971, White 1988). The dissolution kinetics of Magnesium is longer than that of Calcium, so the increasing Mg2+/Ca2+ ratio implies the saturation of water with calcite, highlighting long residence time and enhanced weathering along the groundwater flow paths (White 1988, Edmunds et al. 1987). The Mg2+ content in groundwater also depends on other parameters such as chemical and mineralogical purity of limestone and presence of dolomite within the rock masses they flow across (Mudarra and Andreo 2011). Nevertheless, the Mg^{2+} concentration values increase and hence Mg^{2+}/Ca^{2+} ratio depend not only on the dissolution/precipitation reaction of calcite and dolomite. In fact, a faster dissolution of dolomite may be due to an increasing in water temperature (Herman and White 1985). Thus, environmental tracers and hydrochemical investigation techniques provide much information about groundwater flow systems and the main hydrogeochemical processes affecting the composition of groundwater within the karst aquifers (Tooth and Fairchild 2003) and their interaction with surface water.

Geological and hydrogeological setting

Karst aquifer feeding Pertuso Spring is located in the Upper Valley of the Aniene River (Latium, Central Italy), along the SW boundary of the Simbruini Mountains, in the outcrop of Triassic-Cenozoic carbonate rocks, locally covered by fluvial and alluvial deposits and Quaternary sediments (Ventriglia 1990). The stratigraphic succession of dolomite, dolomitic limestone and limestone is distributed homogeneously in the Valley (Damiani 1990). Dolomite is the dominant lithofacies, characterized by white and gray crystalline dolomite, with some breccia levels. Over this geological formation, limestones and dolomites of Upper Cretaceous age are present, and their immersion is concordant with the Triassic dolomite (Damiani 1990). Karst springs are numerous along the first part of the

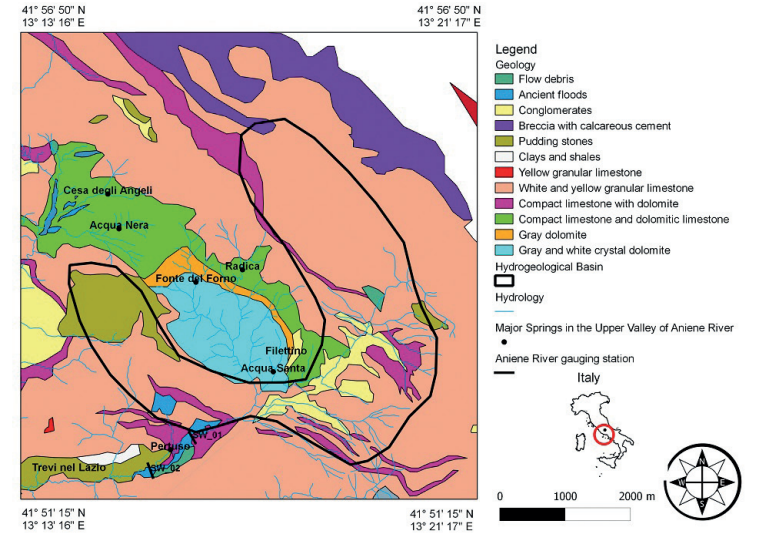

Fig. 1 - Simplified geological map of Pertuso Spring hydrogeological basin and location of Aniene River gauging sections.

Fig. 1 - Carta geologica semplificata del bacino idrogeologico della sorgente Pertuso e posizione delle stazioni di misura lungo il fiume Aniene.

Aniene River and rise in the Triassic dolomitic formations (Fig.1).

This karst system is characterized by one main outlet, Pertuso Spring, and several springs which inflow into the Aniene River, at different points (Tab.1).

Due to their lower solubility and their ductility, dolomites are less fractured than limestone. As a consequence of it in the Aniene River Basin, almost all groundwater come out, where there is a limestone-dolomite contact (Ventriglia 1990) (Fig.1) and this latter one is below the former one.

Pertuso Spring (elevation of 698 m a.s.l.) is located between Filettino and Trevi nel Lazio (FR) and belongs to the Special Area of Conservation (SAC) of Aniene River Springs, established under Directive 92/43/EEC. This spring is the main outlet of this karst aquifer and comes out of alluvial sediments, covering a very thick layer made of Cretaceous limestone (Cipollari et al. 1995). The spring water is partially caught for hydroelectric and drinking supplies, whereas the remaining part directly flows into the Aniene River. The Pertuso Spring hydrogeological basin collects groundwater coming from a 50 km^2 catchment area (Sappa and Ferranti 2014) bounded by the Triassic dolomite to the NE (Fig.1).

This aquifer is made, for the most part, of Cretaceous karst limestone. The base of the stratigraphic series is made of Upper Cretaceous carbonates, represented by the alternation of granular limestone and dolomites layers. Above these ones Quaternary fluvial and alluvial deposits lie, downward pudding and Miocene clay and shale (Ventriglia 1990). Rainfall is the primary source of recharge to this karst aquifer, feeded fastly through karst features such as sinkhole, dolines, swallow holes and fractures (Bono and Percopo 1996).

Pertuso Spring reacts very fastly to precipitation events, with significant increases in discharge rates, which are proportional to the intensity of rainfalls. Groundwater coming from Pertuso Spring is collected within an aquifer mostly made by a well-known volume of carbonate rocks (White 2002). The most distinctive feature of Pertuso karst spring is the branching network of conduits that increases in size in the downstream direction (Fig.2). The largest active conduit drains the groundwater flow coming from the surrounding aquifer matrix, the adjoining fractures and the smaller nearby conduits (White and White 1989). This conduit network is able to rapidly discharge large quantities of water through this karst aquifer (up to 3 m^3/s).

Tab. 1 - Main karst springs of Upper Valley of Aniene River (ACEA ATO 2 S.p.A., unpublished data, 2005).

Tab. 1 - Principali sorgenti carsiche dell'Alta Valle dell'Aniene (ACEA ATO 2 S.p.A., dati non pubblicati, 2005).

Spring	Altitude (m a.s.l.)	Average discharge (L/s)
Acqua Santa	900	65
Acqua Nera	1030	80
Fonte del Forno	950	164
Cesa degli Angeli	940	200
Radica	1110	250
Pertuso	698	1400

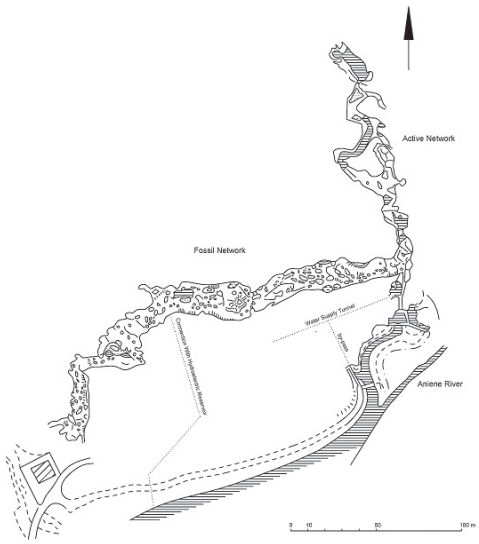

Fig. 2 - Plan view of the development of Pertuso Spring karst drainage network (modified from ACEA ATO 2 S.p.A., unpublished data, 2005).

Fig. 2 - Sviluppo planimetrico della rete carsica della Sorgente Pertuso (modificata da ACEA ATO 2 S.p.A., dati non pubblicati, 2005).

Materials and Methods

This paper presents part of the results of more than one year of monitoring of the Environmental Monitoring Plan, related to the catchment project of the Pertuso Spring. Water samples have been collected from three sampling points within the study area, i.e. one from Pertuso Spring, the others from two gauging stations located along the Aniene River, respectively, upstream (SW_01) and downstream (SW_02) the spring (Fig.1). These gauging stations belong to the monitoring network set up for the Environmental Monitoring Plan in agreement with the Ministerial Decree 260/2010, chosen to focus on the sensitive connections between surface water and groundwater (Sappa and Ferranti 2014). According to the Environmental Monitoring Plan, groundwater and surface water have been monitored seasonally (4/year) with the aim of set up the hydrogeological conceptual model of the karst aquifer (Sappa and Ferranti 2014).

The experimental data, referred to the period July 2014 - December 2015, were obtained from field investigations and from chemical laboratory analyses. Water temperature, electrical conductivity and pH values were determined in field using HANNA HI9813-6 waterproof hand-held meter (Hanna Instruments, Woonsocket, RI, USA). Geochemical analyses were carried out at the Geochemical Laboratory of Sapienza University of Rome. Water samples were filtered through cellulose filters (0.45 µm), and their major and minor constituents were determined by ion chromatography (IC) by a 761 professional IC Metrohm (reliability ±2%) (Metrohm, Herisau, Switzerland). Bicarbonate (HCO_3^-) was determined by titration with 0.1 N HCl (reliability ±2%). A statistical summary of the major physicochemical parameters is shown in Tab.2.

The geochemical modeling program PHREEQC, version 3.0 (Parkhurst and Appello 1999), implemented with the

Tab. 2 - Summary statistics for in situ measurements of physicochemical parameters and chemical concentrations of constituents of water samples (ions in mg/L, electrical conductivity in µS/cm, T in °C, hardness in °F).

Tab. 2 - . Statistica riassuntiva dei parametri fisico-chimici misurati in situ e delle concentrazioni chimiche dei campioni d'acqua (ioni in mg/L, conduttanza elettrica in µS/cm, T in °C, durezza in °F).

Parameters	SW_01			Pertuso spring			SW_02		
	Min	Max	Mean	Min	Max	Mean	Min	Max	Mean
Ca^{2+}	53.4	57.8	55.0	48.9	53.3	50.8	51.3	55.6	52.7
Mg^{2+}	23.6	25.2	24.4	8.3	10.4	9.5	12.0	14.7	12.9
Na^{+}	2.3	2.6	2.4	1.8	2.0	1.9	2.0	2.3	2.1
K^{+}	0.4	0.5	0.4	0.3	0.5	0.4	0.3	0.7	0.43
HCO_3^{-}	281.8	302.6	290.6	206.0	238.0	218.8	218.4	235.5	225.7
SO_4^{2-}	2.9	3.2	3.0	2.3	2.5	2.4	2.5	2.7	2.6
Cl^{-}	3.8	4.5	4.2	3.3	3.7	3.5	3.3	4.2	3.7
NO_3^{-}	0.8	1.3	1.1	0.9	1.2	1.0	0.9	1.1	1.0
T	5.8	11.3	8.56	8.0	9.5	8.5	6.7	10.7	8.3
pH	8.0	8.5	8.4	7.8	8.0	7.9	8.1	8.2	8.2
EC	356.0	395.0	384.4	283.0	291.0	288.0	294.0	317.0	310.2
Hardness	23.1	24.8	23.8	16.1	17.4	16.6	17.9	19.3	18.5

thermodynamic dataset wateq4f.dat, was employed to assess the state of equilibrium among groundwater, surface water and carbonate minerals present in terms of saturation index. The saturation index (SI) indicates the chemical equilibrium potential between water and minerals and the tendency for water-rock interaction (Wen et al. 2008). Negative values of SI highlight that water samples are undersaturated with respect to a particular mineral, indicating the possibility of mineral phase dissolution by groundwater and, thus, a potential source of constituents. Likewise, SI>0 reflects the oversaturated state, showing the possibility of mineral phase precipitation, thus limiting the constituent concentration. SI=0 represents the mineral phase equilibrium state. The discharge measurements were carried out along the Aniene River, upstream (SW_01) and downstream (SW_02) Pertuso Spring, by the application of traditional current meter. According to the U.S. Geological Survey (USGS) procedure, stream discharge has been calculated as the product of the cross section area by the average stream flow velocity in the cross section obtained using a current meter (US EPA Region 6 2003, BS EN ISO 2007). The main equipment needed to measure the stream flow velocity is a SEBA horizontal axis current meter F1 (SEBA Hydrometrie GmbH & Co. KG, Kaufbeuren, Germany), having a propeller diameter of 80 mm which, combined with SEBA Z6 pulse counter, allows to measure velocity between 0.025 m/s and 10 m/s. The SEBA current meter has been used according to EN ISO 748:2007 requirements (BS EN ISO 2007). This current meter method gives the local water velocity in each vertical following the application of a calibration equation between stream velocity, v (cm/s) and the number of spins, n (s-1) (1).

$$v=0.82+33.32n \quad (1)$$

Results and Discussion

In order to establish the groundwater discharge pattern, hydrochemical data and discharge measurements were used in this study. Ca^{2+}, Mg^{2+} and HCO_3^{-} represent more than 80% of the dissolved solids in water samples and these concentrations are influenced by the dissolution of carbonate minerals, forming limestone, which are the most dominant formations outcropping in the study area. The hydrochemical facies of groundwater and surface water were studied by plotting the concentrations of major cations and anions in the Piper trilinear diagram (Fig.3) (Piper 1944).

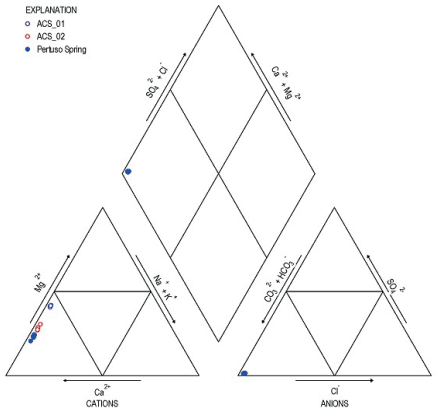

Fig. 3 - Piper plot for hydrochemical facies classification of groundwater and surface water.

Fig. 3 - Diagramma di Piper per la classificazione in facies idrochimiche delle acque sotterranee e superficiali.

Based on the dominance of major cationic and anionic species two hydrochemical facies have been identified: i) Ca-Mg-HCO_3 and ii) Ca-HCO_3. These results are due to the presence of limestone, dolomitic limestones and dolomites outcropping in the study area. Water samples coming from SW_01 gauging station present higher values of concentration in Mg^{2+}, while those coming from Pertuso Spring are definitely poorer in it, and show a clear composition of Ca-HCO3 water type (Fig.3). The different hydrochemical facies between groundwater and surface water are visible in

the high concentration of Mg^{2+} in the Aniene River. These hydrochemical facies highlight that carbonate weathering processes (e.g. calcite and dolomite) are the most important factors of the observed water type.

Thus, the scatter plot of (Ca^{2+}+Mg^{2+}) versus (SO_4^{2-}+HCO_3^-) was prepared to identify the ionic exchange and weathering processes (Fig.4). As shown in Fig.4, all surface water samples are close to the 1:1 equiline suggesting that those ions have resulted from weathering of carbonates. However, water samples from Pertuso Spring are clustered under the 1:1 line indicating ion exchange.

To study the difference in Mg^{2+} content between groundwater and surface water, a ternary diagram of cations (Ca^{2+}, Mg^{2+} and Na^++K^+) (Edmunds et al. 1987) was used to highlight how the weathering type processes influence the enrichment in Magnesium (Fig.5).

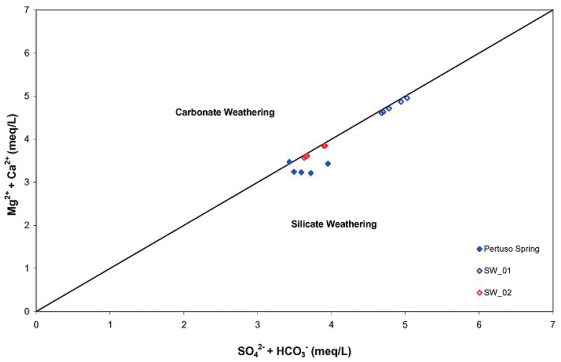

Fig. 4 - Scatter diagram of (Ca^{2+}+Mg^{2+}) versus (SO_4^{2-}+HCO_3^-).

Fig. 4 - Diagramma a dispersione di (Ca^{2+}+Mg^{2+}) versus (SO_4^{2-}+HCO_3^-).

As shown in Fig.5 all samples are placed along the Ca^{2+}-Mg^{2+} side of the diagram, these groundwater samples are very poor in Na^+ and K^+. The higher Mg^{2+} concentrations in SW_01 water samples suggest an increase in residence time and depend on the dissolution/precipitation reactions of calcite and dolomite, which occur in the aquifer.

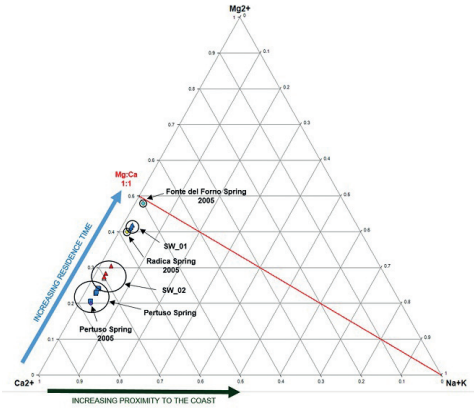

Fig. 5 - Ternary diagram of cations Ca^{2+}, Mg^{2+} and Na^++K^+. Relative concentrations of dissolved major cations compared with the composition of local groundwater.

Fig. 5 - Diagramma ternario dei cationi Ca^{2+}, Mg^{2+} and Na^++K^+. Concentrazioni relative dei principali cationi disciolti in confronto alla composizione delle acque sotterranee locali.

Based on previous studies [ACEA ATO 2 S.p.A., unpublished data (2005)] similar results have been obtained for other springs located in the upper part of Aniene River coming out in the Triassic dolomite outcropping close to the Pertuso Spring basin (Fig.6).

This hydrochemical characterization leads to a groundwater flow pattern in which two main recharge areas are defined: the first one in the Cretaceous limestone, feeding the Pertuso Spring groundwater; the second one in the Triassic dolomite, feeding the surface water upstream the spring. Saturation indexes calculated with respect to calcite and dolomite of Pertuso Spring and surface water are shown in Figs. 7 and 8. All surface water samples are saturated with respect to calcite (Fig. 7) and dolomite (Fig. 8), while all Pertuso Spring samples are saturated with respect to calcite and undersaturated with respect to dolomite. The saturation with respect to calcite and dolomite reflects a great dissolution and strong mineralization along groundwater flowpaths. The scatter plots diagram for Mg^{2+}/Ca^{2+} ratio (Fig. 9) shows that the

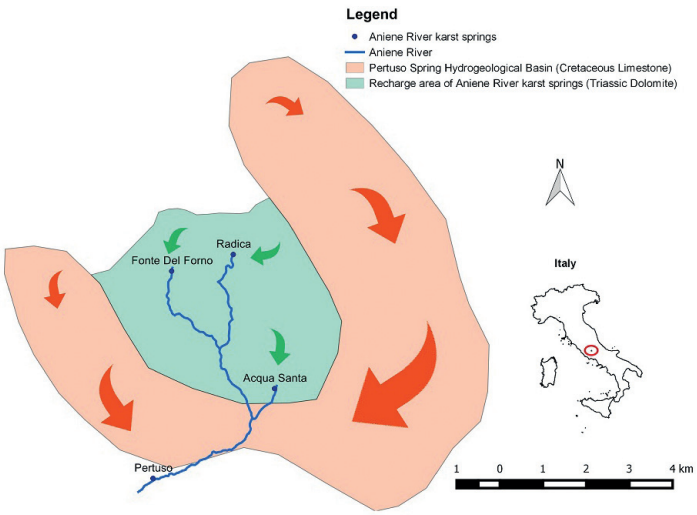

Fig. 6 - Recharge areas of the main karst springs in the Upper Valley of Aniene river.

Fig. 6 - Aree di ricarica delle principali sorgenti carsiche nell'Alta Valle dell'Aniene.

increase in Mg^{2+} concentrations in surface water, upstream the Pertuso Spring, and consequently Mg^{2+}/Ca^{2+} ratio may be due to the weathering of Mg-rich Triassic dolomites, where dolomitic limestones and dolomites are the most outcropping formations in this area.

As regards Pertuso Spring groundwater, the high Mg^{2+}/Ca^{2+} ratios (~0.5) mainly depend on the residence of water in the karst system, highlighting long residence time and enhanced weathering along the groundwater flowpaths of low-Mg calcite. As a consequence of these properties, water samples taken downstream Pertuso Spring (SW_02) present chemical composition typical of mixing of these two different kinds of waters (Fig. 9).

As a matter of fact, the highest Mg^{2+}/Ca^{2+} ratio has been recorded in water samples coming from dolomite rock masses (SW_01~0.7), with medium value at SW_02 gauging station (~0.4). On the other hand, the lowest value of this ratio in groundwater has been observed in Cretaceous limestone area (~0.3) (Tab.3).

Aniene River discharge was measured during the hydrological year 2014-2015, in order to cover the range of seasonal conditions characteristics of this complex hydrogeological system. Measurements by current meter were carried on in two gauging stations located upstream (SW_01) and downstream (SW_02) Pertuso Spring (Tab.4).

Tab.5 shows discharge values recorded in SW_01 and SW_02 gauging stations all over the hydrological year. It can be noticed that the average discharge value referred to SW_01 gauging station can be easily compared with the total average discharge coming from the most important karst springs outcropping in the Upper Part of Aniene River (Tab.1). Thus, the source of Mg^{2+} concentration values in Aniene River upstream Pertuso Spring (SW_01) is the dissolution of Magnesium rich minerals in Triassic dolomites, sited in the north-east part of the Pertuso Spring basin. Along the Aniene River, this decrease in Mg^{2+} concentration values is related to an increase in stream flow discharge. SW_02 surface water is the product of the confluence of groundwater coming from Pertuso Spring into the Aniene River (SW_01). As a matter of fact, Aniene River water, which is characterized by water with higher Magnesium concentration values, is affected in its chemical composition by Pertuso Spring groundwater inflowing, and this influence can be measured by Mg^{2+} concentration values variability along the river downstream. The karst aquifer system has been studied in order to evaluate factors which modify the Aniene River flow due to groundwater-surface water interactions.

The main inputs are the discharge measurements (Q_1) and the Mg^{2+} concentrations (C_1) recorded upstream the spring (SW_01). The secondary inputs are the discharge rate (Q_P) and the Mg^{2+} concentrations (C_P) recorded at Pertuso Spring. The main output is the Aniene River discharge (Q_2) and the Mg^{2+} concentrations (C_2) recorded at the SW_02 gauging station located downstream Pertuso Spring.

The area under study belongs to a special protected area in the Natural Park of Simbruini Mountains, where all the

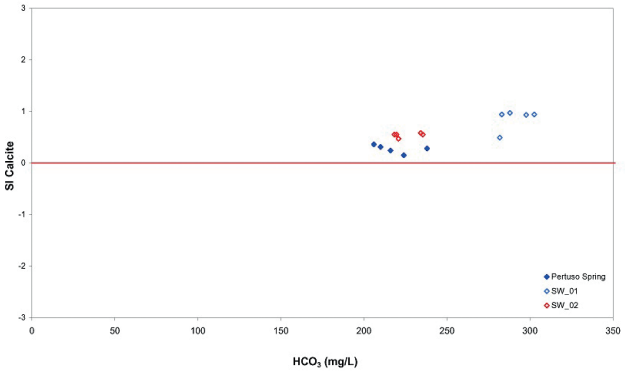

Fig. 7 - Saturation indexes of Calcite of groundwater and surface water.

Fig. 7 - Indice di saturazione in calcite delle acque sotterranee e superficiali.

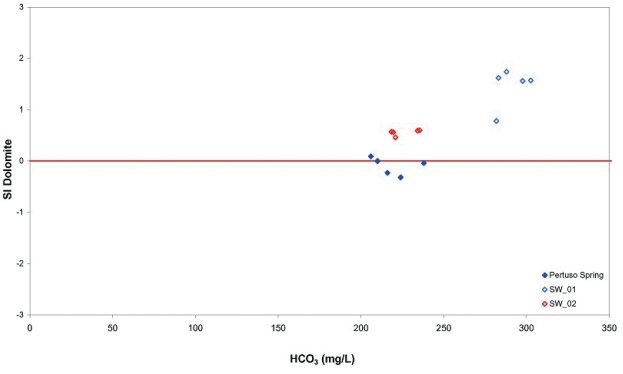

Fig. 8 - Saturation indexes of Dolomite of groundwater and surface water.

Fig. 8 - Indice di saturazione in dolomite delle acque sotterranee e superficiali.

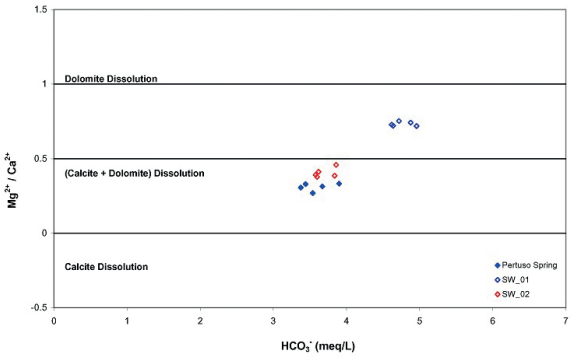

Fig. 9 - Mg^{2+}/Ca^{2+} ratio versus HCO_3^- in groundwater and surface water.

Fig. 9 - Mg^{2+}/Ca^{2+} ratio versus HCO_3^- nelle acque sotterranee e superficiali.

Tab. 3 - Mg^{2+}/Ca^{2+} ratio from Pertuso Spring and Aniene River gauging station.

Tab. 3 - Rapporto Mg^{2+}/Ca^{2+} della sorgente Pertuso e delle sezioni di misura del Fiume Aniene.

Mg^{2+}/Ca^{2+}	Pertuso Spring	SW_01	SW_02
July 2014	0.328	0.728	0.410
November 2014	0.267	0.669	0.357
January 2015	0.305	0.718	0.386
May 2015	0.314	0.752	0.391
December 2015	0.332	0.741	0.458

Tab. 4 - Mean discharge values obtain by current meter method, upstream (SW_01) and downstream (SW_02) Pertuso Spring.

Tab. 4 - Valori della portata media ottenuti con il metodo correntometrico, a monte (SW_01) e a valle (SW_02) della sorgente Pertuso.

Q (m^3/s)	SW_01	SW_02
July 2014	0.540	2.450
November 2014	0.350	1.480
January 2015	0.410	1.920
May 2015	0.501	2.747
December 2015	0.278	0.931

anthropic activities are restricted and controlled. On the basis of this hypothesis we have assumed that this system could be considered closed. Thus, the SW_02 gauging station discharge values, come from the contribution of Pertuso Spring discharge (Q_P) to the original SW_01 discharge value, can be represented by (2):

$$Q_2 = Q_1 + Q_P \qquad (2)$$

Applying the conservation of mass equation to this closed system, it means (3):

$$Q_1 C_1 + Q_P C_P = Q_2 C_2 \qquad (3)$$

The n parameter (Tab.5), i.e. the percentage of Pertuso Spring groundwater contribution to total discharge measured at SW_02 is defined according to (4).

$$n = \frac{Q_P}{Q_2} = \frac{(C_2 - C_1)}{(C_P - C_1)} \qquad (4)$$

Tab. 5 - Values as percentage contribution of Pertuso Spring groundwater to total discharge measured at the SW_02 gauging station.

Tab. 5 - Valori del parametro n come contributo percentuale fornito dalle acque sotterranee della sorgente Pertuso alla portata complessiva misurata nella sezione di misura SW_02.

Date	n	n (%)
July 2014	0.780	78.0
November 2014	0.752	75.2
January 2015	0.794	79.4
May 2015	0.812	81.2
December 2015	0.709	70.9

Thus, the discharge rate of Pertuso Spring depends on the discharge values measured in the gauging station located along the river upstream the spring (Q_1) and the Mg^{2+} concentration values recorded in groundwater and surface water samples (C_1, C_2, C_P) (5):

$$Q_P = Q_1 \cdot \frac{n}{1-n} \qquad (5)$$

The Mg^{2+} versus Q scatter plots diagram (Fig. 10) shows that all plotted points, except for November 2014 data, follow a linear trend, highlighting that the increasing contribution of Pertuso Spring flow rate is responsible of the decreasing values of Mg^{2+} concentration. Data, referred to November 2014 monitoring campaign, have to be considered as an outlier (Fig. 10). This lower Mg^{2+} concentration measured in November 2014 can be related to a high precipitation rate, recorded at Trevi nel Lazio meteorological station, during five days before the sampling date, which could have influenced, by dilution, the Mg^{2+} concentration in groundwater.

Pertuso Spring discharge values obtained by this indirect method are showed in Tab. 6.

The relationship between Mg^{2+} concentration and karst spring discharge values obtained with this combined Magnesium-discharge tracer approach is represented in Fig. 10.

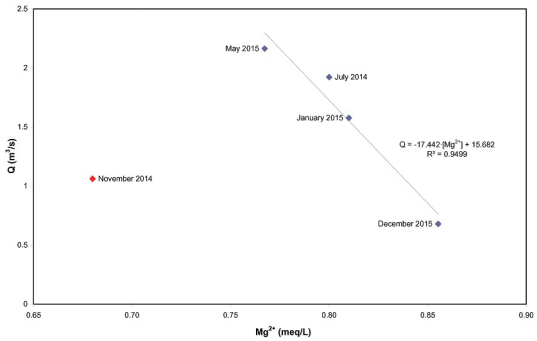

Fig. 10 - Relationship between the Mg^{2+} concentration and Pertuso Spring discharge values obtained with the combined Magnesium-discharge tracer approach.

Fig. 10 - Correlazione tra la concentrazione in Mg^{2+} e i valori di portata della sorgente Pertuso ottenuti con l'approccio combinato magnesio-portata.

Tab. 6 - Magnesium content and discharge values obtained by current-meter and Magnesium tracer method (Q: discharge values obtained by current meter method; Q**: discharge values obtained by the difference between the values measured with the current meter in SW_01 and SW_02).*

Tab. 6 - Tenore di magnesio e valori di portata attenuti con il metodo correntometrico (Q*: valori di portata attenuti con il metodo correntometrico; Q**: valori di portata attenuti come differenza tra I valori misurati con il metodo correntometrico nelle sezioni SW_01 e SW_02).

Date	SW_01		Pertuso Spring			SW_02		
	Q* (m^3/s)	Mg^{2+} (meq/L)	Q** (m^3/s)	Q_{Mg} (m^3/s)	Mg^{2+} (meq/L)	Q* (m^3/s)	Q_{Mg} (m^3/s)	Mg^{2+} (meq/L)
July 2014	0.54	1.94	1.91	1.92	0.80	2.45	2.46	1.05
November 2014	0.35	1.93	1.13	1.06	0.68	1.48	1.41	0.99
January 2015	0.41	2.07	1.51	1.58	0.81	1.92	1.99	1.07
May 2015	0.50	2.02	2.23	2.16	0.77	2.75	2.66	1.00
December 2015	0.28	2.07	0.67	0.68	0.86	0.93	0.96	1.21

Conclusions

This paper dealt with the assessment of the interactions between karst aquifers feeding Pertuso Spring and Aniene River surface waters on the basis of stream discharge measurements and water geochemical tracers data. The aim was to set up an inverse model, which allowed estimating groundwater flow coming out from Pertuso Spring, starting from surface water discharge measurements and geochemical waters characterization. These preliminary results, obtained in area under study, sited in the karst aquifer outcropping in the Upper Valley of Aniene River, show that it is possible to have a reliable evaluation of Pertuso Spring discharge, through the elaboration of surface water discharge measurements and Mg^{2+} concentration values, determined both for groundwater, coming from Pertuso Spring, both for surface water sample, collected upstream and downstream Pertuso Spring, along the Aniene River. Although it is subject to some uncertainties, the Mg^{2+} concentration, as an environmental tracer, provides an indirect method for discharge evaluation of Pertuso Spring due to the mixing of surface water and groundwater, and it provides information o n changes in water quantity and quality.

REFERENCES

Bakalowicz M (2005) Karst groundwater: a challenge for new resources. Hydrogeology Journal 13:148-160.

Batiot C, Emblanch C, Blavoux B (2003) Total Organic Carbon (TOC) and magnesium (Mg2+): two complementary tracers of residence time in karstic systems. Comptes Rendus Geoscience 35:205-214.

Bono P, Percopo C (1996) Flow dynamics and erosion rate of a representative karst basin (Upper Aniene River, Central Italy). Environmental Geology 27(3):210-218.

Cherubini C, Pastore N, Francani V (2008) Different approaches for the characterization of a fractured karst aquifer. WSEAS Transactions on fluid mechanics 3:29-35.

Cipollari F, Cosentino D, Parrotto M (1995) Modello cinematico-strutturale dell'Italia centrale "*Kinematic model-structural of Central Italy*". Studi Geol Camerti 2:135-143.

Clark ID, Fritz P (1997) Environmental isotopes in hydrogeology. CRC Press Inc., Boca Raton, FL, USA.

Damiani AV (1990) Studi sulla piattaforma carbonatica laziale-abruzzese. Nota I. Considerazioni e problematiche sull'assetto tettonico e sulla paleogeologia dei Monti Simbruini, *"Studies on the Lazio-Abruzzi carbonate platform. Note XI. Considerations and problems on tectonic and paleogeologic Simbruini Mts."* Memorie descrittive Carta Geologica d'Italia 38:177-206.

Edmunds WM, Cook JM, Darling WG, Kinniburgh DG, Miles DL, Bath AH, Morgan-Jones M and Andrews JN (1987) Baseline geochemical conditions in the Chalk aquifer, Berkshire, UK: a basis for groundwater quality management. Applied Geochemistry 2:251-274.

EN ISO 748:2007 (2007) Hydrometry. Measurement of liquid flow in open channels using current-meters or floats. react-text: 55 DOI: 10.1007/BF00770434BS

Foster S, Hirata R, Andreo B (2013) The aquifer pollution vulnerability concept: aid or impediment in promoting groundwater protection. Hydrogeology Journal 21:1389-1392.

Guida M, Guida D, Guadagnuolo D, Cuomo A, Siervo V (2013) Using Radon-222 as a naturally occurring tracer to investigate the streamflow-groundwater interactions in a typical Mediterranean fluvial-karst landscape: the interdisciplinary case study of the Bussento river (Campania region, Southern Italy). WSEAS Transactions on System 12(2):85-104.

Guo Q, Wang Y, Ma T, Li L (2005) Variation of karst springs discharge in recent five decades as an indicator of global climate change: a case study at Shanxi, northern China. Science in China Series D: Earth Science 48(11):2001-2010.

Herman JS, White WB (1985) Dissolution kinetics of dolomite: effects of lithology and fluid flow velocity. Geochimica et Cosmochimica Acta 49:2017-2026.

Hunkeler D, Mudry J (2007) Hydrochemical tracers, in methods in karst hydrogeology. Taylor and Francis, London, UK.

Langmuir D (1971) Geochemistry of some carbonate ground waters in Central Pennsylvania. Geochimica et Cosmochimica Acta 35(10):1023–1045.

Leibundgut C, Maloszewski P, Kulls C (2009) Tracers in hydrology. 1st ed. Wiley-Blackwell, Chichester, UK.

Mazor E (2004) Chemical and isotopic groundwater hydrology. Marcel Dekker, New York, NY, USA.

Mudarra M, Andreo B (2011) Relative importance of the saturated and the unsaturated zones in the hydrogeological functioning of karst aquifers: the case of Alta Cadena (Southern Spain). Journal of Hydrology 397(3-4):263-280.

Parkhurst DL, Appello CAJ (1999) User's guide to PHREEQC (Version 2). A computer program for speciation, batch-reaction, one-dimensional transport, and inverse geochemical calculations. US Geological Survey Water-Resources Investigations Report 99-4259.

Piper M (1944) A graphic procedure in the geochemical interpretation of water-analyses. Transactions of the American Geophysical Union 25:914-923.

Sappa G, Ferranti F (2014) An integrated approach to the environmental monitoring plan of the Pertuso spring (Upper Valley of Aniene River). Italian Journal of Groundwater 3(136)47-55.

Sappa G, Ferranti F, De Filippi FM (2015a) Environmental tracer approach to discharge evaluation of Pertuso Spring (Italy), Proceedings of the 10th International Conference on Energy & Environment (EE'15) in Recent Advances on Energy and Environment, edited by Aida Bulucea, WSEAS, pp 54-62.

Sappa G, Ferranti F, Ergul S (2015b) Vulnerability assessment of Mazzoccolo Spring aquifer (Central Italy), combined with geo-chemical and isotope modelling, Engineering Geology for Society and Territory, Vol. 5, Urban Geology, Sustainable Planning and Landscape Exploitation, pp 1387-1392.

Sappa G, Ferranti F, Ergul S, Ioanni G (2013) Evaluation of the groundwater active recharge trend in the coastal plain of Dar es Salaam (Tanzania). Journal of Chemical and Pharmaceutical Research 5(12)548-552.

Tooth AF, Fairchild IJ (2003) Soil and karst aquifer hydrological controls on the geochemical evolution of speleothem-forming drip waters, Crag Cave, southwest Ireland. Journal of Hydrology 273:51-68.

US EPA Region 6 (2003) Standard operating procedure for stream flow measurement.

Ventriglia U (1990) Idrogeologia della Provincia di Roma, IV, Regione orientale "*Hydrogeology of the Province of Rome, IV, Eastern region*". Amministrazione Provinciale di Roma, Assessorato LL.PP, Viabilità e trasporti, Roma.

Wen XH, Wu YQ, Wu J (2008) Hydrochemical characteristics of groundwater in the Zhangye Basin, North-western China. Environmental geology 55(8):1713-1724.

White WB (1969) Conceptual models for carbonate aquifers. Ground Water 7:15-22.

White WB (1988) Geomorphology and hydrology of karst terrains. Oxford University Press, New York, NY, USA.

White WB (2002) Karst hydrology: recent developments and open questions. Engineering Geology 65:85-105.

White WB, White EL (1989) Karst hydrology-concepts from the Mammoth Cave area. Van Nostrand Reinhold, New York, NY, USA.

Zwahlen F (2004) Vulnerability and risk mapping for the protection of carbonate (karst) aquifers, final report (COST Action 620). European Commission, Directorate-General XII Science, Research and Development, Brussels, Belgium.

Pertuso Spring discharge assessment in the Upper Valley of Aniene River (Central Italy)

G. Sappa and F. Ferranti

***Abstract*—**Sustainable management of karst aquifers is an important tool for the protection of these strategic water resources. Assessing water balance in a karst aquifer can be very difficult, due to the complex interactions and exchanges between groundwater and surface water. Therefore, measurements of streamflow and spring discharges are useful to assess karst aquifers available budget. Water balance calculation requires the estimation of two main parameters: recharge (precipitation, agriculture water, surface runoff, etc.) and discharge (underground outflow) which are affected by the highly heterogeneous distribution of permeability due to conduits and voids developed by the dissolution of carbonate rocks. This paper deals with the preliminary results of Pertuso Spring groundwater discharge assessment, in the Upper Valley of Aniene River (Central Italy), where the complex hydrogeological characteristics, related to the high heterogeneity of hydraulic properties, make difficult to set up a reliable methodology of measurement. To achieve this objective, an integrated approach based on the streamflow measurements and geochemical modeling, applied to groundwater and surface water was carried out.

Because no continuous discharge measurements of Pertuso Spring were available, different methods (velocity–area using current meter and geochemical assessment) were applied to evaluate the discharge of the spring and the stream flow during the monitoring period from July 2014 to May 2015. Aniene River streamflow measurements were carried out by using the conventional current-method and the salt dilution method. For the evaluation of the Pertuso Spring discharge, as a support for traditional discharge methodology, various groundwater and surface water monitoring campaigns have been made along the Aniene River, upstream and downstream the Pertuso Spring, for the acquisition of geochemical data. The aim of this study is to present the preliminary results of an indirect method for the estimation of the Pertuso Spring discharge, based on Magnesium concentration changes in groundwater and surface water.

***Keywords* —** Aniene River, current meter method, discharge measurement, environmental tracers, Magnesium concentration, Pertuso Spring.

I. Introduction

KARST aquifers supply more or less the 25% of freshwater worldwide [1]. Water resources assessment is an important tool to evaluate groundwater dynamics in the aim of to maintain high-quality drinking water in the framework of climate change effects [2]. The determination of groundwater discharge is a direct measure of the amount of water available for drinking, industrial, and agricultural purposes. Karst springs react to rainfall events by sinkhole drainage and discharge from conduits in bedrock, responsible for the subsurface outflow [3]-[4]. The estimation of karst spring discharge is affected by methodological difficulties, data deficiencies, and resultant uncertainties due to spatial variability of permeability in carbonate rocks [5], and also because the pathway of groundwater outcoming is not always the same along the year. The traditional quantitative approach for the evaluation of groundwater discharge is the application of water balance, which requires the estimation of water storage and flow. Karst systems are characterized by a highly heterogeneity due to a network of highly permeable flow features, embedded in a less permeable fractured rock matrix [6]. Thus, in these complex hydrogeological scenarios, understanding the behavior of the groundwater system and the recharge–discharge relation is required to formulate a reliable water balance [7]. In karst aquifer the presence of underground stream flows, that are not accurately measurable, makes very difficult to develop a reliable methodology that includes physical assessments of the input–output relation [8]-[9]. In this paper, an indirect groundwater model has been set up in the aim of evaluating karst spring discharge. The model drives to a reliable estimation of groundwater discharge in karst aquifers. The Pertuso Spring, located in the Upper Valley of Aniene River (Central Italy) is used for validate this model. The Aniene River basin is located in the upper part of the shallow karst aquifer, where surface water and groundwater exhibit complex interactions.

This paper presents preliminary results of discharge measurements carried out in two gauging sections along the Aniene River, upstream and downstream the Pertuso Spring, by the application of traditional current meter, in the framework of the Environmental Monitoring Plan related to the catchment project of the Pertuso Spring which is going to be exploited to supply an important water network in the South part of Roma district [10]. In the following they are presented the results obtain with the current method and the comparison with a proposed model based on Magnesium concentration changes in groundwater and surface water. As

G. Sappa is with the Department of Civil, Building and Environmental Engineering (DICEA), Sapienza University of Rome Via Eudossiana 18, 00184, Rome, ITALY (phone: +39-0644585010; fax: +39-0644585016; e-mail: giuseppe.sappa@ uniroma1.it).

F. Ferranti is with the Department of Civil, Building and Environmental Engineering (DICEA), Sapienza University of Rome Via Eudossiana 18, 00184, Rome, ITALY (e-mail: flavia.ferranti@uniroma1.it).

a matter of fact the aim of the present work is to set up an indirect reliable method to estimate spring discharge in karst aquifer where the complex groundwater flows can make difficult the application of traditional quantitative approaches.

II. Geological and Hydrogeological Setting

The study area is located along the SW boundary of the Simbruini Mountains, characterized by the confluence of the Fiumata Valley and the Granara Valley from which starts the Valley of Aniene River [11]. In this area it outcrops an important carbonate karst aquifer, mainly made of highly permeable Cretaceous carbonate rocks, deeply fractured, locally showing distinctive karst features (Fig. 1).

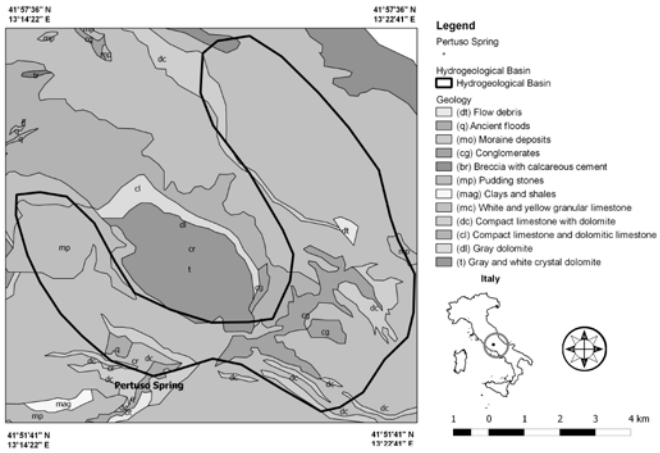

Fig. 1 simplified geological map of the study area

The alternation of carbonate rocks, limestone and dolomite, together with the epikarst, made of residual of karst activity, and some marly horizons, dating back to the Miocene age, are the main responsible for the hydrogeological system of this area [12]. The abundance of water is due to the permeability of the limestone (highly fractured and deep karst), which stores a significant quantity of rainwater feeding perennial springs located in the Upper Valley of Aniene River [13].

Table 1 main springs in the Upper Valley of Aniene River

Spring	Elevation (m a.s.l.)	Mean Annual Discharge (l/s)
Rigoglioso	1110	250
Fonte del forno	950	164
Fonte Santa	900	65
Pertuso	**698**	**1400**
Cesa degli Angeli	940	200
Cardellina bassa	955	10
Cardellina media	970	15
Cardellina alta	990	25
Acqua nera	1030	80
Zompo lo schioppo	900	1200
La Sponga	832	400
Renga	875	40
Capo di Rio	930	30

Groundwater coming out from this karst aquifer discharges from 13 small and large springs located close to the boundary of the carbonate hydrogeological system. Table 1 shows elevation and mean annual discharges of these springs. The mean annual discharge of Pertuso Springs is 1400 l/s, whereas the mean annual discharge of the other springs ranges from 10 to 1200 l/s. The catchment area of Pertuso Spring has been estimated in 50 km^2 [10].

The most important discharge point of this aquifer is the Pertuso Spring, located westward of Filettino (FR) at an elevation of 696 m above sea level. The spring is located in the dolomite outcrop (Fig. 2), upstream the town of Trevi in Lazio and flows into the Aniene River, close to the boundary of the carbonate hydrogeological system [12].

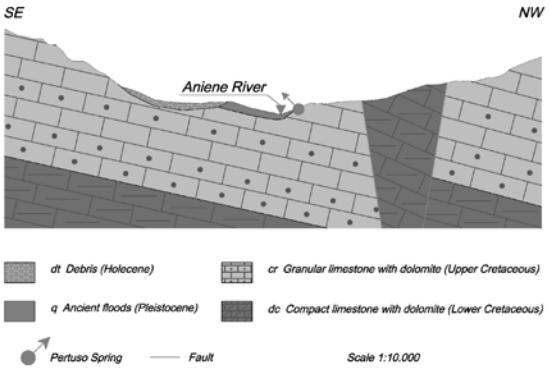

Fig. 2 schematic geological section of the Pertuso Spring

The limestones outcropping in the study area are deeply fractured and mostly soluble; karst erosion has occurred on a large scale on this area, assuming great importance in the modelling of the soil and also of the subsoil. The karst network system, located along the NS boundary, has a total length of about 311 m. This spring, with an average discharge capacity (Q) of 1.4-1.5 m^3/s [13], is one of the most important fresh water springs in the South part of Latium Region and currently is feeding with a rate of 360 l/s the Comunacqua hydroelectric power plant, owned by ENEL group. The Pertuso Spring discharge almost immediately increases after heavy rainfall (from March to May) followed by a retarded decrease in discharge (Fig. 3).

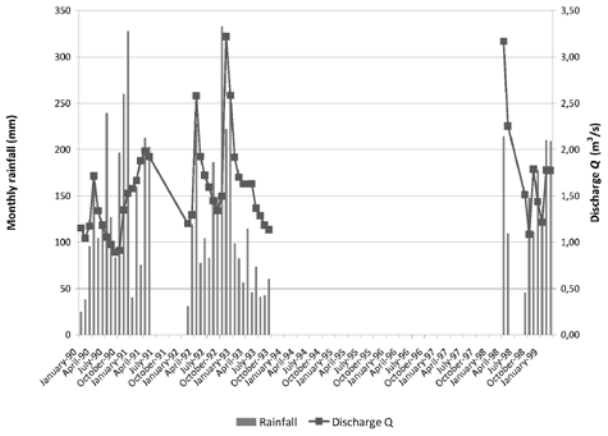

Fig. 3 hydrogeological rate of Pertuso spring in the 1990 – 1999 period (Filettino meteorological station)

This type of reaction is due to the presence of karst features, which receive water from nearby sources in a short period of time. Later, this water stored in the limestone matrix is slowly released back into the karst conduits. Unfortunately they are not available data referred to groundwater discharge more than ones represented in Fig. 3.

III. Materials and Methods

The Pertuso Spring discharge in the karst aquifer of the Upper Valley of Aniene River was studied through the implementation of various methods, tailored to the available set of hydrogeological data. In the framework of this work two main activities were carried out: the execution of four groundwater and surface water monitoring campaigns from July 2014 to May 2015 and six discharge measurements campaigns driven from September 2014 to April 2015, using the current meter method (Fig. 4).

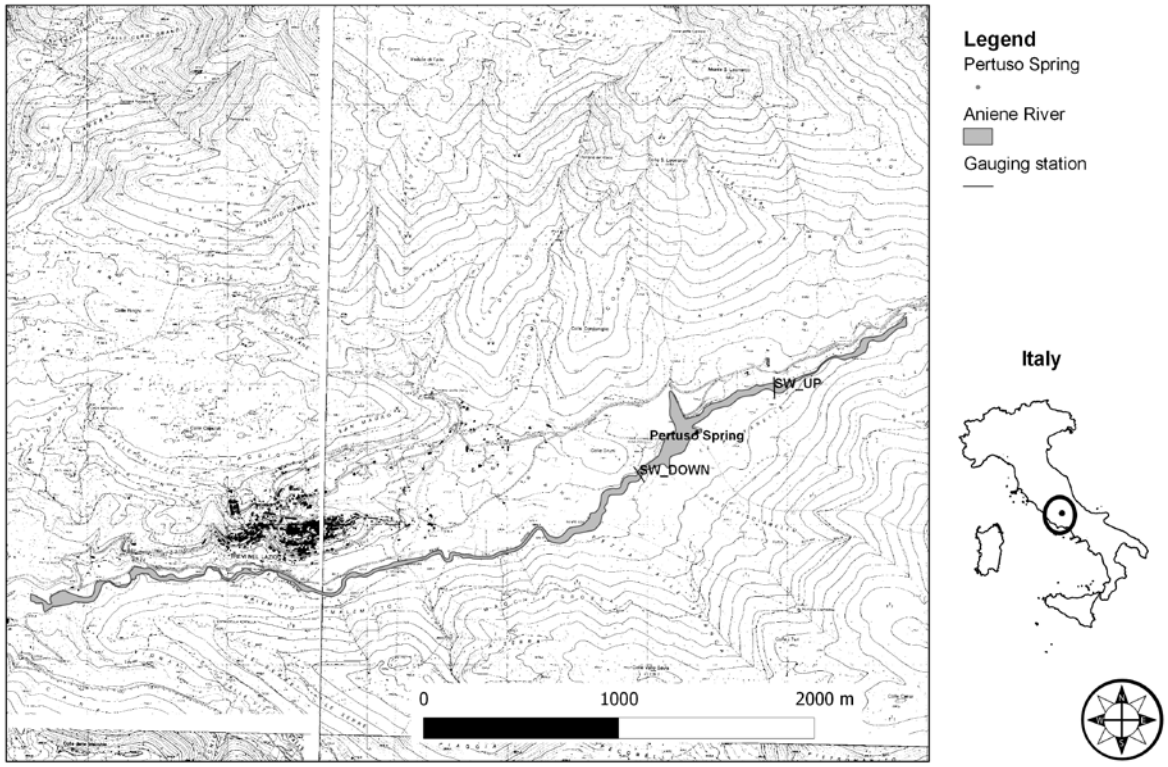

Fig. 4 study area and location of gauging sections

Table 2 main physico-chemical characteristics of water samples (n.d.= not determined)

Sample	Date	T (°C)	EC (µS/cm)	pH	Eh (mV)	Ca (mg/l)	Mg (mg/l)	Na (mg/l)	K (mg/l)	HCO_3 (mg/l)	Cl (mg/l)	SO_4 (mg/l)
Pertuso Spring	July 2014	8.0	322	7.4	112	48.9	9.77	1.91	0.50	210	3.54	2.39
	November 2014	8.0	300	7.2	110	51.0	8.32	1.83	0.32	216	3.48	2.41
	January 2015	9.5	410	6.9	481	53.3	9.89	2.05	0.45	206	3.66	2.54
	May 2015	8.5	300	10.8	243	49.0	9.33	1.86	0.31	224	3.35	2.34
SW_UP	July 2014	11.3	422	8.3	74	53.4	23.6	2.48	0.35	87	4.16	2.87
	November 2014	7.7	360	8.3	89	54.0	23.5	2.59	1.61	89	4.34	3.04
	January 2015	5.8	340	7.3	435	57.8	25.2	2.59	1.61	95	4.50	3.18
	May 2015	10.7	390	9.6	212	53.9	24.6	n.d.	n.d.	86	4.12	2.90
SW_DOWN	July 2014	9.9	352	7.8	66	51.3	12.8	2.01	0.18	72	3.66	2.5
	November 2014	7.3	320	7.6	78	52.4	12.0	1.11	0.44	72	3.72	2.56
	January 2015	7.2	270	6.9	449	55.6	13.0	1.11	0.44	77	4.17	2.73
	May 2015	8.9	280	8.1	210	51.4	12.2	n.d.	n.d.	70	3.53	2.47

Water samples were collected, every three months, from July 2014 to May 2015, from Pertuso Spring and from two cross section located along the Aniene River, upstream and downstream this spring. Field parameters, such as pH, conductivity (EC), water temperature (T), Redox potential (Eh), dissolved oxygen (DO) were measured on-site using a multi-parameter PC650 probe hand-held meter (Eutech Instruments) (Table 2). All samples were filtered by 0.45 µm cellulose filters and stored at 4 °C until analysis in the laboratory. Batches of 12 samples were analyzed in the Geochemical Laboratory of Sapienza University of Rome. Major cations (Ca^{2+}, Mg^{2+}, Na^{+}, K^{+}) were determined by ion chromatography (IC) using an 761 Professional IC Metrohm and Metrosep C2-150 column, whereas major anions (Cl^{-}, SO_4^{2-}) were determined by Metrosep A sup 4–250 column. Alkalinity was determined immediately after sampling by means titration and converted to hydrogen-carbonate (HCO_3^{-}) according to [14]. The saturation index of calcite ($SI_{Calcite}$) and dolomite ($SI_{Dolomite}$) in water samples were calculated by means of PHREEQC [15] with the WATEQ4F database.

The discharge measurements were carried out along the Aniene River, upstream (ST_UP) and downstream (ST_DOWN) the Pertuso Spring, by the application of traditional current meter. These cross sections have been chosen as gauging section because they are relatively straight to ensure streamlines parallel to each other and reduce errors in velocity measurements. The bed stream relatively uniform and free of heavy aquatic growth allows keeping the current meter perpendicular to the flow whereas measuring velocity, to ensure a stable relation between stage and discharge. At ST_UP and ST_DOWN gauging stations, the Aniene River surface width ranges from 3.5 to 4 meters and from 8 to 9 meters, respectively. The depth ranges from 0.3 to 0.8 meter for ST_UP and from 0.4 to 1 meter for ST_DOWN, according to the limits imposed by the type of current meter used.

According to the U.S. Geological Survey (USGS) procedure, the current meter method involves measuring the area and the velocities of a stream at a cross section, which must be perpendicular to the main flow of the river. Usually, river discharge is calculated as the product of the cross section area of flow by the average stream flow velocity in that cross section. Thus, the river cross section is divided into many vertical sub-sections, in each one the area is obtained by measuring the width and depth of the sub-section and the stream flow velocity is determined using a current meter. The sum of the products of area velocity for each segment gives the total stream discharge [16]-[17].

The preliminary step in stream flow measurements is the determination of the section width by stringing a measuring tape from bank to bank at right angles to the direction of flow. In mountain stream, where the hydraulic pattern changes monthly, more than a single measurement is needed to characterize accurately the hydraulic profile of the cross section. For this reason it has been necessary determine the hydraulic profiles of ST_UP and ST_DOWN gauging sections for each discharge measurements campaigns (Figg. 5, 6, 7, and 8). This measuring tape is used to define the hydraulic profile of the cross section and the location of each velocity measurements. Determining the cross sectional area of a stream involves measuring water depths at a series of points across the stream and multiplying by the width of the stream within each segment represented by the depth measurement. With the aim to obtain an average velocity, each section has been divided into vertical parts, spaced by 1.00 m (Figg. 5 and 6). Along each one of these investigated verticals, up to 2 measuring points have been defined at different depths (0.2 and 0.3 m from bed stream).

The main equipment needed to measure the stream flow velocity in each verticals is a SEBA horizontal axis current meter F1, having a propeller diameter of 80 mm which, combined with SEBA Z6 pulse counter, allows to measure velocity between 0,025 m/s and 10 m/s. The SEBA current meter has been used as rod equipment with tail plane for best positioning to the flow direction. For each measurement point, flow velocity is determined counting the number of spins of the meter rotor during a fixed interval of time. Thus, in order to assess any fluctuations due to the turbulence condition and, also, to avoid accidental measurement errors, velocity has been measured for at least 60 seconds, according to EN ISO 748:2007 requirements [18].

This current meter method gives the local water velocity in each vertical following the application of a calibration equation between stream velocity (cm/s) and the number of spins (s-1) (1).

$$v = 0.82 + 33.32 \cdot n \quad (1)$$

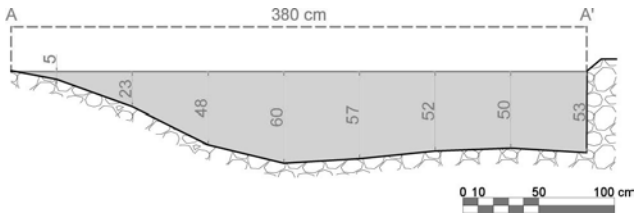

Fig. 5 ST_UP cross section illustrating sub-sections to determine discharge by current meter method (July 2014)

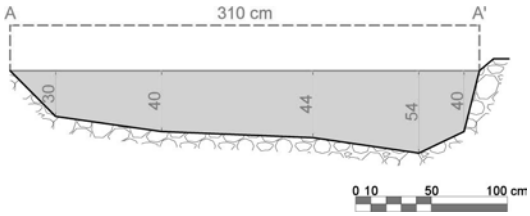

Fig. 6 ST_UP cross section illustrating sub-sections to determine discharge by current meter method (November 2014)

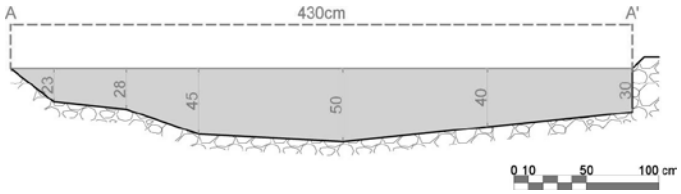

Fig. 7 ST_UP cross section illustrating sub-sections to determine discharge by current meter method (January 2015)

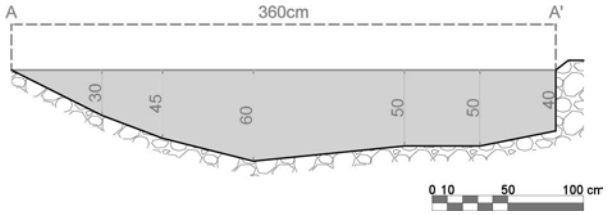

Fig. 8 ST_UP cross section illustrating sub-sections to determine discharge by current meter method (May 2015)

IV. Results and Discussion

Stream discharge measurements obtained by the velocity area method are summarized in Table 3.

Table 3 mean discharge values obtained by current meter method

Date	Discharge Q (m^3/s) ST_UP	Discharge Q (m^3/s) ST_DOWN
July 2014	0.54	2.45
November 2014	0.35	1.48
January 2015	0.41	1.92
May 2015	0.50	2.75

Table 3 shows the discharge values coming out from four measurements campaigns, referred to the maximum height value, measured in the stream in each campaign. The average current meter streamflow for ST_UP and ST_DOWN gauging stations was 0.45 m^3/s and 2.15 m^3/s, respectively.

The temperature of water samples ranges between 5.8 °C and 11.3 °C. The pH of these samples is between 6.9 and 10.8 (average 8) showing neutral to slightly alkaline. The variability in pH of the springs is caused by changes in flow paths, water discharge and residence times within the aquifer [19]. The redox potential of the springs showed partially oxidizing waters (74-449 mV, with an average of 213 mV). Chemistry of groundwater coming from karst aquifer in the unsaturated zone is modified by local flow variations and changes in redox condition [20]. Electrical conductivity ranges between 270 and 422 µS/cm and generally decrees in wet seasons due to the rainfall dilution.

The hydrochemical facies of samples waters was studied by plotting the concentrations of major cations and anions in the Piper diagram (Fig. 9). Based on the dominance of major cationic and anionic species, Ca-HCO_3 water type was identified, suggesting that all groundwater and surface water come from the karst aquifer.

Calculated saturation indexes with respect to calcite, dolomite and gypsum of the spring and surface water samples are shown in Table 4.

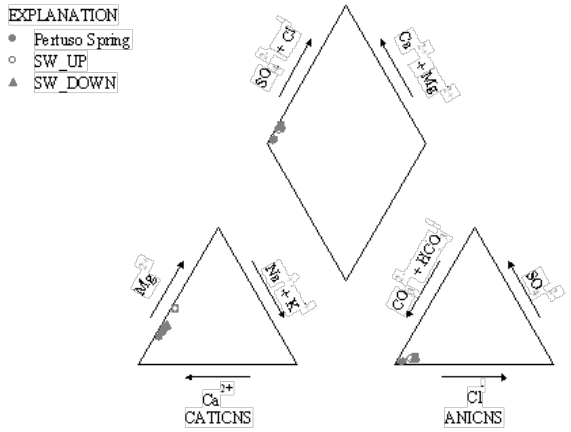

Fig. 9 Piper diagram for hydrochemical facies evolution and water classification

Geochemical modeling shows that water chemistry in the study area is affected by the interaction with carbonate minerals.

Table 4 Saturation Index (SI) values for common carbonate and evaporate minerals of spring and surface water samples

Sample	Date	$SI_{calcite}$	$SI_{dolomite}$
Pertuso Spring	July 2014	-0.25	-1.12
	November 2014	-0.46	-1.54
	January 2015	-0.71	-2.04
ST_UP	July 2014	0.35	0.48
	November 2014	0.29	0.29
	January 2015	-0.68	-1.68
ST_DOWN	July 2014	-0.22	-0.93
	November 2014	-0.49	-1.56
	January 2015	-1.14	-2.85

Figures 10 and 11 show a comparison of calcite and dolomite saturation indexes of all water samples as a function of HCO_3 concentration.

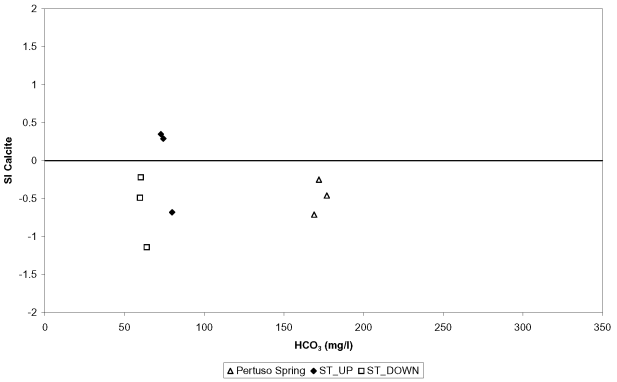

Fig. 10 calcite saturation index versus HCO_3

All samples are undersaturated with respect to calcite and dolomite, expect for water samples collected upstream the

Pertuso Spring in July and November 2014, which implies a huge dissolution and high mineralization along groundwater flow paths. This indicates that the surface water is able to dissolve dolomite along the flow paths and hence, the concentrations of Mg^{2+} in the solution would increase.

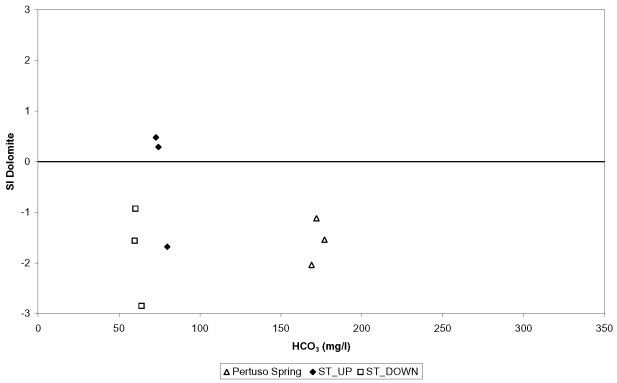

Fig. 11 dolomite saturation index versus HCO_3

The rate of hydrochemical evolution can be determined by the Mg/Ca ratios presented in Fig. 10. The changes in Mg and Ca concentrations in water samples mainly depend on the residence time of groundwater in karst systems which is controlled by the volume and mechanism of recharge, the distance from the recharge area and dissolution of carbonate minerals [21].

The Mg/Ca ratios indicate that the dissolution of carbonate minerals played a significant role in the groundwater and surface water chemistry, depending on the hydrological processes which control the groundwater residence time and chemical equilibrium in the aquifer (Fig. 12). Water samples coming from ST_UP, upstream the Pertuso Spring show the highest Mg/Ca ratios (0.5-1), whereas downstream samples and Pertuso Spring groundwater show lower Mg/Ca ratios (<0.5).

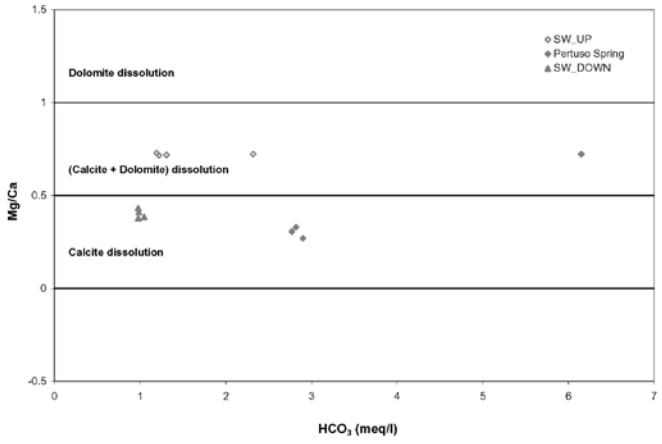

Fig. 12 saturation Index (S.I.) values for common carbonate minerals of water samples

The increase in Mg/Ca ratio, due to a larger concentration of Magnesium upstream the Pertuso Spring (Table 5), is due to the dissolution/precipitation reaction of calcite and dolomite. The ST_UP samples are oversaturated with respect to calcite and dolomite, however, the high Mg/Ca ratio may be due to the weathering of Mg-rich dolomite, where dolomitic limestones and dolomites are the most outcropping formations in this area.

Table 5 comparison of Magnesium concentrations in groundwater and surface water

	Mg^{2+} (mg/l)		
Date	**SW_UP**	**SW_DOWN**	**Pertuso Spring**
July 2014	23.5	12.8	9.8
November 2014	23.5	12.0	8.3
January 2015	25.2	13.0	9.9
May 2015	24.6	12.2	9.3

We observed proportionality between the decreasing of Magnesium concentrations and the increasing of the streamflow discharge (Fig. 13). The higher the flow, the more it dilutes the tracer. For this reason it has been chosen Magnesium concentrations as tracer of dilution processes.

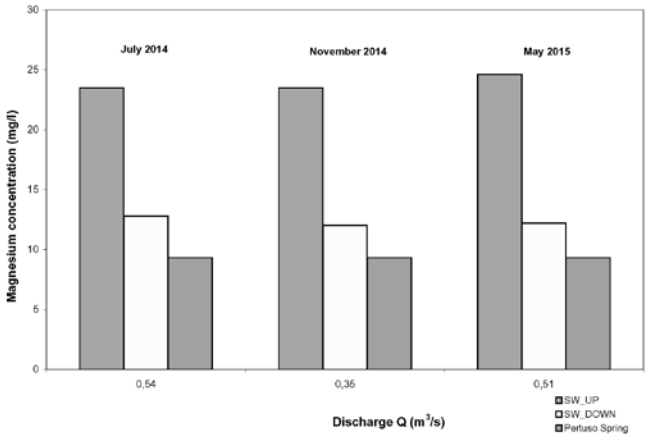

Fig 13 plot of Magnesium concentration vs. discharge in m^3/s

The Pertuso Spring discharge (Q_p) can be computed from the equation for the conservation of mass (2), using the discharge values, Q (l/s) and the Magnesium concentration, C (meq/l) upstream (C_{UP}; Q_{UP}) and downstream (C_{DOWN}; Q_{DOWN}) the spring.

$$Q_{UP}C_{UP} + Q_pC_p = Q_{DOWN}C_{DOWN} \quad (2)$$

Considering *n* the percentage contribution that the Pertuso Spring provides total discharge measured downstream, the Pertuso Spring discharge (Q_p) is defined according to (3).

$$Q_p = Q_{UP} \cdot \frac{n}{1-n} \quad (3)$$

The Pertuso Spring discharge values downstream the Aniene River, obtained by this indirect method, are definitely comparable with ones obtained by the traditional current meter method (Table 6 and Fig. 14).

Table 6 Pertuso spring discharge values obtained by Magnesium tracer method

Date	$Q_{current\_meter}$ (m^3/s)	Q_{Mg} (m^3/s)	Percent difference (%)
July 2014	1.91	1.92	-1
November 2014	1.13	1.06	7
January 2015	1.51	1.58	-7
May 2015	2.25	2.16	9

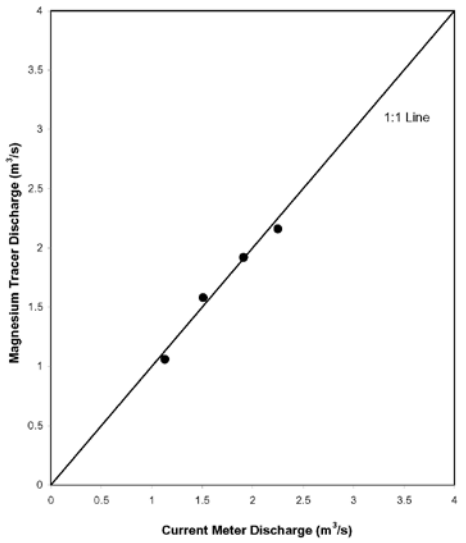

Fig. 14 comparison of current-meter and Magnesium tracer model at the Pertuso Spring

V. Conclusion

A combined geochemical and streamflow discharge techniques were applied to groundwater and surface water from the carbonate aquifer of the Upper Valley of Aniene River, Central Italy, which is the most important groundwater reservoir in this area, in order to set up a reliable methodology for the evaluation of Pertuso Spring discharge.

In framework of the Environmental Monitoring Plan related to the catchment project of the Pertuso Spring, physical-chemical data, in addition and streamflow discharge has been acquired from.July 2014 to May 2015. In this study we presented the first results of the application of an indirect method, based on Magnesium as a tracer, with its concentration changes in groundwater and surface water, for the evaluation of karst spring discharge.

The measurements of Magnesium concentration, along the Aniene River and groundwater coming from the Pertuso Spring , has confirmed potential for using Magnesium, as a suitable aqueous tracer, to assess karst spring discharge. These preliminary results show that the dilution of naturally dissolved Magnesium ion in groundwater and surface water can give a reliable estimate of dolomite dissolution where tradition methodologies are not easily applied. This value depends on the Pertuso Spring water, which is undersaturated with respect to dolomite until it joins the main stream of Aniene River, where the magnesium content is much higher due to the oversaturation whit respect to dolomite (ST_UP). Thus, the decreasing of Magnesium concentrations downstream (ST_DOWN) the Pertuso Spring is due to this mixing with spring waters.

This method applied in the Upper Valley of Aniene River showed its reliability and indicates that such measurements can be useful to better understand groundwater movement in this karst system. In fact, the use of Magnesium, as an aqueous tracer, is well suited because it occurs naturally in the environment and it is easy to monitor and its measurements inexpensive to be performed.

References

[1] D.C. Ford, P.W. Williams, *Karst Geomorphology and Hydrology*, John Wiley & Sons, Chichester, England, 2007.

[2] G. Sappa, G. Luciani, "Groundwater Management in Dar Es Salam Coastal Aquifer (Tanzania) under a Difficult Sustainable Development", WSEAS Transactions on Environment and Development, vol. 10, 2014, pp. 465-477.

[3] M. Bakalowicz, "Karst groundwater: a challenge for new resources", Hydrogeology Journal, vol. 13, Springer, 2005, pp. 148-160.

[4] M. Bakalowicz, "Management for karst groundwater resources", Karst Management, Springer, 2011, pp. 263-284.

[5] B.R.. Scanlon, R.W. Healy, P.G. Cook, "Choosing appropriate techniques for quantifying groundwater recharge", Hydrogeology Journal, vol. 10, Springer, 2002, pp. 18-39.

[6] B. Andreo, J. Vías, J.J. Durán., P. Jiménez, J.A. López-Geta, and F. Carrasco, "Methodology for groundwater recharge assessment in carbonate aquifers: application to pilot sites in southern Spain", Hydrogeology. Journal, 1 vol. 6, Springer, 2008, pp. 911–925.

[7] C. Cherubini, N. Pastore, V. Francani, "Different approaches for the characterization of a fractured karst aquifer", WSEAS Transactions on fluid mechanics, vol. 3, 2008, pp. 29-35

[8] J.W. Hess, W.B. White, "Storm response of the karstic carbonate aquifer of south central Kentucky", Hydrogeology Journal, vol. 99, Springer, 1988, pp. 235-252.

[9] W.B. White, *Geomorphology and Hydrology of Karst Terrains*, Oxford University Press, New York, 1988.

[10] G. Sappa, F. Ferranti, "An integrated approach to the Environmental Monitoring Plan of the Pertuso spring (Upper Valley of Aniene River)", Italian Journal of Groundwater, 2/136, 2014, pp. 47-55.

[11] F. Cipollari, D. Cosentino, M. Parotto, *Modello cinematico-strutturale dell'Italia centrale*, Studi Geol. Camerti, 1995, pp. 135-143.

[12] U. Ventriglia., Idrogeologia della Provincia di Roma, IV, Regione orientale, Assessorato LL.PP, Viabilità e trasporti, Roma. 1990.

[13] Acea ATO 2 S.p.A., *Studio idrogeologico – Proposta di aree di salvaguardia della sorgente del Pertuso*, 2005.

[14] APHA. *Standard Methods for the Examination of Water and Wastewater*, 20th ed.; American Public Health Association: Washington, DC, USA, 1998.

[15] D. L. Parkhurst, C.A. J. Appello, *User's Guide to PHREEQC (Version 2)—A Computer Program for Speciation, Batch-Reaction, One-Dimensional Transport, and Inverse Geochemical Calculations*. US Geological Survey Water-Resources Investigations, Report 99-4259, 1999.

[16] V.T. Chow, Handbook of Applied Hydrology. McGraw-Hill, NewYork, NY, 1964.

[17] US EPA Region 6, *Standard operating procedure for stream flow measurement*, 2003.

[18] BS EN ISO 748:2007, *Hydrometry. Measurement of liquid flow in open channels using current-meters or floats*, 2007.

[19] S. Parisi, M. Paternoster, C. Kohfahl, A. Pekdeger, H. Meyer, H.W. Hubberten, G. Spilotro, G. Mongelli. "Groundwater recharge areas of a volcanic aquifer system inferred from hydraulic, hydrogeochemical and stable isotope data: Mount Vulture, southern Italy". Hydrogeology Journal, 2011, 19, pp. 133–153.

[20] C. Emblanch, G. Zuppi, J. Mudry, B. Blavoux, C. Batiot. “Carbon 13 of TIDC to quantify the role of the unsaturated zone: The example of the Vaucluse karst system (southeastern France)”. Hydrogeology Journal, 2003, 279, pp. 262–274.
[21] D. Langmuir. *Geochemistry of Some Carbonate Ground Waters in Central Pennsylvania*. Geochimica et Cosmo-chimica Acta, Vol. 35, No. 10, 1971, pp. 1023-1045.

water

MDPI

Article

Mg^{2+}-Based Method for the Pertuso Spring Discharge Evaluation

Giuseppe Sappa *, Flavia Ferranti, Francesco Maria De Filippi and Giulia Cardillo

DICEA—Department of Civil, Building and Environmental Engineering, Sapienza University of Rome, Rome 00184, Italy; flavia.ferranti@uniroma1.it (F.F.); f.defilippi89@gmail.com (F.M.D.F.); giuliacardillo@msn.com (G.C.)

* Correspondence: giuseppe.sappa@uniroma1.it; Tel.: +39-064-458-5010 or +39-345-280-8882

Academic Editors: Robert Puls and Robert Powell

Received: 27 October 2016; Accepted: 18 January 2017; Published: 23 January 2017

Abstract: This paper deals with the Environmental Monitoring Plan concerning the catchment work project of the Pertuso karst spring, which is going to be exploited to supply an important drinking water network in the south part of Roma district. The Pertuso Spring, located in the Upper Valley of the Aniene River, is the main outlet of a large karst aquifer, which is one of the most important water resources in the southeast part of Latium Region, Central Italy, used for drinking, agriculture, and hydroelectric supplies. The environmental monitoring activities provided data about one spring and two cross-sections of the Aniene River, from July 2014 to May 2016. A combined approach based on discharge measurements and hydrogeochemical analysis has been used to study flow paths and groundwater–surface water interaction in the study area. Tracer methods are particularly suitable in hydrogeological studies to assess transit times and flow properties in karst aquifers. The analysis of solute contents in the sampling points brought forth the identification of the Mg^{2+} ion as a conservative tracer in this specific system and, consequently, to the development of a conceptual model based on chemical mass balance for the Pertuso Spring discharge evaluation.

Keywords: aquifer; karst spring; discharge; environmental tracer; magnesium

1. Introduction

Groundwater represents a vital resource for the society, and also for the ecosystems. The interest of researchers for better understanding the groundwater origin, the subsurface processes, and the factors controlling the residence time has gradually increased, and the investigation techniques evolved continuously [1], in the aim of better protecting these resources.

The increasing anthropogenic activities and the impacts of climate change are identified as being responsible for karst groundwater depletion [2,3]. Thus, groundwater exploitation in karst aquifers requires special management strategies to prevent their quality and quantity depletion and to support decision-making for water resources management [4,5].

Karst aquifers have complex and original characteristics, which make them very different from other aquifers: high heterogeneity of the rock matrix, large voids, high flow velocities (up to several hundreds of m/h), and high flow rate springs (up to some tens of m^3/s) [6].

In karst aquifers, where flow may be concentrated in subsurface conduits, a Darcy law approach is usually not suitable [7] and karst springs discharge is not easily measurable by standard techniques or conventional instruments. Sometimes, channels are unsuitable for metering the flow, being shallow, choked with vegetation, and with ill-defined banks [8]. In these aquifers, the drainage network typically develops in a system of conduits that flows into a single trunk that discharges through the spring [9]. However, some karst aquifers may have a spread flow pattern, which is related to the

enlargement of fractures and smaller conduits—located near the stream discharge boundary—or to the collapse of an existing trunk conduit [10].

Underflow springs are often hidden, for example, by rising in the bed of the surface stream [11]. Thus, even if it is possible to identify, like in this case, the outlet section of a karst spring, where all of the groundwater discharge comes out, sometimes this is not true and it is not clear where the entire discharge comes out. On the other hand, seasonal changes throughout the year can make difficult or impossible to access cross-sections to carry out traditional measurements. Consequently, the difficulty in measuring karst spring discharge implies that the use of the traditional current-meter method may be limited and less reliable, sometimes leading to erroneous results [12].

In this sense, tracer methods are particularly suitable to assess flow properties in karst aquifers, also because the necessary equipment is manageable [13].

Environmental tracers are used more and more often in hydrological studies, in order to have a complete view about the water cycle, the groundwater recharge, the water–rock interactions, the geochemical processes [1], and, moreover, to understand potential groundwater contamination processes [14].

In recent years, surface water and groundwater tracing techniques have been used in a variety of complex hydrogeological settings to aid in characterizing groundwater flow systems [7,15–18].

Groundwater tracers include any substance that can become dissolved or suspended in water, or attached to the water molecule, and recovered or measured from a water sample that can be used to trace the source of groundwater in terms of its specific or relative location and time of recharge. Groundwater tracers can include both artificially introduced and naturally occurring substances [19–21].

An important class of tracers are the ionic tracers, as they are not subject to decay or gas exchange [22]. Moreover, biogeochemical reactions can modify concentrations of most ions [23].

The number of ion types which might be used is very large. However, because of low cost, ease of detection, and low sorption, chloride (Cl^-) and bromide (Br^-) are most popular [24]. However, other ions can be used from time to time for special purposes, such as Li^+, $NH_4{}^-$, $NO_3{}^-$, Mg^{2+}, K^+, and I^-.

The aim of this work is to apply the potentiality of Mg^{2+} as a natural tracer in the karst system of the Upper Valley of the Aniene River, to support a conceptual model for the Pertuso Spring discharge evaluation [25].

In particular, starting from hydrogeochemical analysis results, the developed model uses a magnesium mass balance to evaluate the spring discharge.

Calcium and magnesium offer special promise as seepage tracers for basins set in thick calcareous glacial drift, or doline basins set in carbonate-rich areas. Magnesium is also an obvious tracer in areas of ultramafic rock. In humid regions with abundant dolomite, Mg^{2+} offers advantages over Ca^{2+} as a tracer because, once in solution, it does not re-form a carbonate unless $Mg^{2+}/Ca^{2+} > 2$ [26].

On the other hand, the increase in Mg^{2+} concentration values, and hence Mg^{2+}/Ca^{2+} ratio, not only depends on the dissolution/precipitation reaction of calcite and dolomite, but also an increase in water temperature, which accelerates the kinetics of the dissolution of dolomite. Moreover, in this process, the lower hydraulic conductivity of dolomites, compared with that of limestones, favors the Mg^{2+} concentration increasing, as the water–rock interaction is longer [12,27]. In the past, magnesium was used as a tracer to evaluate the steady-state influx to seepage lakes by using a solute mass balance. For lakes set in the dolomitic glacial drift of Wisconsin, Mg^{2+} was an ideal groundwater tracer, both because it has the highest ratio of groundwater concentration to concentration in precipitation and because it behaves nearly conservatively in lakes set in semi-humid climates [26].

Bencala et al. (1987) [28] and Schemel et al. (2006) [29] made comparisons of environmental tracers at the confluence of two streams in Colorado and studied, through the tracer's mass balance, the behavior of naturally occurring calcium, magnesium, silica, sulfate, fluoride, and manganese; they concluded that magnesium exhibited conservative or nearly conservative behavior.

It is quite important to underline that a conservative behavior may depend on site-specific environmental conditions. Generally, for conservative solute tracers, it has to be expected that there is a

simple physical attenuation mechanism due to dilution, whereas any chemical attenuating mechanism would remove non-conservative solute in varying amounts [28].

Most recently, it was showed that variations in chlorofluorocarbon (CFC), ^{222}Rn, and Mg^{2+} concentrations within streams can be used to quantify rates of groundwater inflow. A mass balance that takes into account changes in solute load within a stream receiving groundwater inflow has been proposed [23].

Thus, in several studies, Mg^{2+} presented the right qualities to be used as a conservative or nearly conservative tracer [26,28,29]. Particularly, in this study, Mg^{2+} has proved to be a useful tracer for chemical mass balance techniques, which are often necessary in order to assess surface water or groundwater flow in karst hydrology settings, where conventional measurements are more difficult.

2. Geological and Hydrogeological Setting

The Latium Region has several springs, under-lake springs, and shows groundwater with deep water tables. The most important groups of springs are in the Upper Valley of the Aniene River, in the Monti Lucretili area, in the Bracciano lake area, and in Genzano, Cecchignola, Grottarossa, and Castel Giubileo areas [30]. The Pertuso Spring, in the Upper Valley of the Aniene River, supplies drinking water to the city of Rome and feeds the Comunacqua hydroelectric power plant, owned by ENEL group [31].

The Pertuso Spring is sited about 1 km down from the confluence of the Fiumata Valley and the Granara Valley, from where the Valley of the Aniene River starts, close to the boundary of the carbonate hydrogeological system [32]. In fact, the Aniene basin is composed almost entirely of bare Mesozoic, highly fractured, karstified carbonate rocks of the central Apennine range [33].

This area is mostly made of highly permeable Cretaceous carbonate rocks, deeply fractured and mostly soluble (Figure 1).

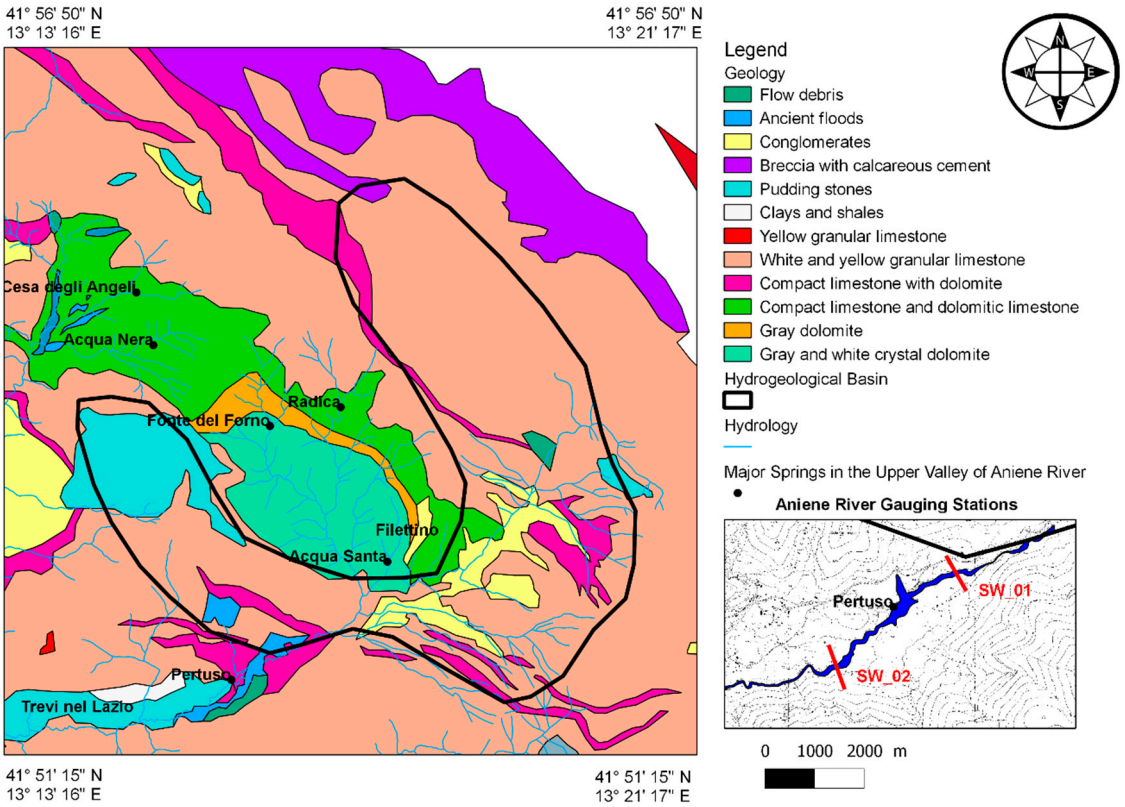

Figure 1. Simplified geological map of the Pertuso Spring hydrogeological basin and location of the Aniene River gauging sections.

The base of the stratigraphic series is made of Upper Cretaceous carbonates, represented by the alternation of granular limestone and dolomites layers. Above these ones lie Quaternary fluvial and alluvial deposits, downward pudding, and Miocene clay and shale [33]. The lithostratigraphy, detected in nearby Subiaco Station, confirms the presence of an extensive karst area, particularly limestones and dolomites (Latium-Abruzzi succession, Upper Triassic-Upper Miocene) [34]. The most important karst landforms are rutted fields, Karren, sinkholes, and swallow holes. The karst surface is very permeable and enables the rapid infiltration of rainfall into the underground system, where the carbonate dissolution generates cavities [35–37]. Dissolution conduits strongly influence groundwater flow and evolve into complex networks, often crossing several kilometres throughout the limestone matrix [38]. Physical and chemical variations that occur during storm events indicate the complex dynamic processes in the karst aquifer and the role undertaken by the epikarst as perched water reservoir, and by the major conduits that develop through the vadose and saturated zones of the karst system [34]. Thus, the Pertuso Spring is the natural outcrop of groundwater discharging from these conduits, coming from an approximately 50 km^2 area (Figure 1) [38], and it comes out when this aquifer, made of this highly enhanced karst network, matches topographic surface (Figure 2). The discharge of this karst spring is usually rapid and displays pronounced peaks following recharge events. These peculiar properties heighten the vulnerability of karstic aquifers and the groundwater emerging from them [39].

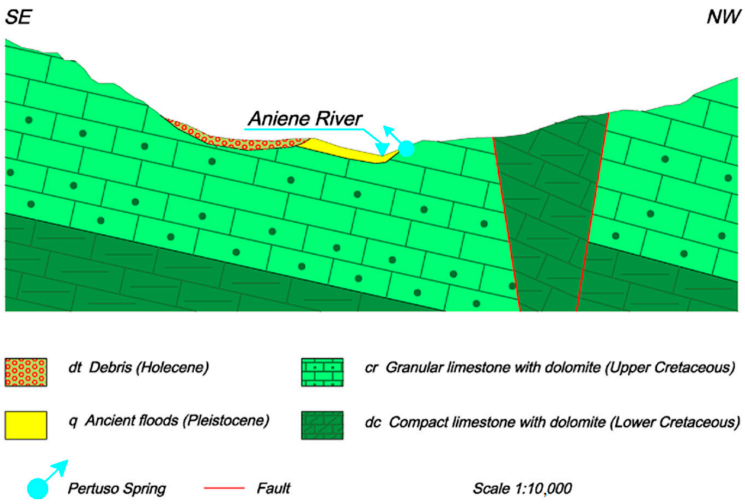

Figure 2. Geological cross-section of the Pertuso Spring.

3. Materials and Methods

The water sampling survey was carried out during the two years of monitoring of the Environmental Monitoring Plan, related to the catchment project of the Pertuso Spring, from July 2014 to May 2016. Eighteen water samples have been collected from three sampling points within the study area: one from the Pertuso Spring, the others from two gauging stations located along the Aniene River, respectively, upstream (SW_01) and downstream (SW_02) the spring (Figure 1). These gauging stations belong to the monitoring network set up for the Environmental Monitoring Plan, in agreement with the Ministerial Decree 260/2010, which focuses on the sensitive connections between surface water and groundwater [38]. According to the Environmental Monitoring Plan, groundwater and surface water have been monitored seasonally (4/year) for the first year of monitoring and twice per year for the second one, with the aim of setting up the hydrogeological conceptual model of the karst aquifer [38], and maintaining control of qualitative and quantitative properties of groundwater, depending on seasonal variations [40].

The experimental data were obtained from field investigations and chemical laboratory analyses and compared to historical data coming from previous studies in the same area [41].

Water temperature, electrical conductivity, and pH values were determined in field using HANNA HI9813-6 waterproof handheld meter. Chemical analyses were carried out at the Geochemical Laboratory of Sapienza University of Rome. Water samples were filtered through cellulose filters (0.45 µm), and their major and minor constituents were determined by ion chromatography (IC) by a 761 Professional IC Metrohm (reliability ±2%). Bicarbonate (HCO_3^-) was determined by titration with 0.1 N HCl (reliability ±2%).

For the identification of water types, the chemical analysis data of the spring water samples have been plotted on the Piper diagram using Geochemistry Software AqQA.

Twelve discharge measurements were carried out along the Aniene River in SW_01 and SW_02 by the application of traditional current-meter. They gave results, referring to the depth, ranging between 0.2 m and 0.7 m as they changed according to the seasonal evolution (Figure 3).

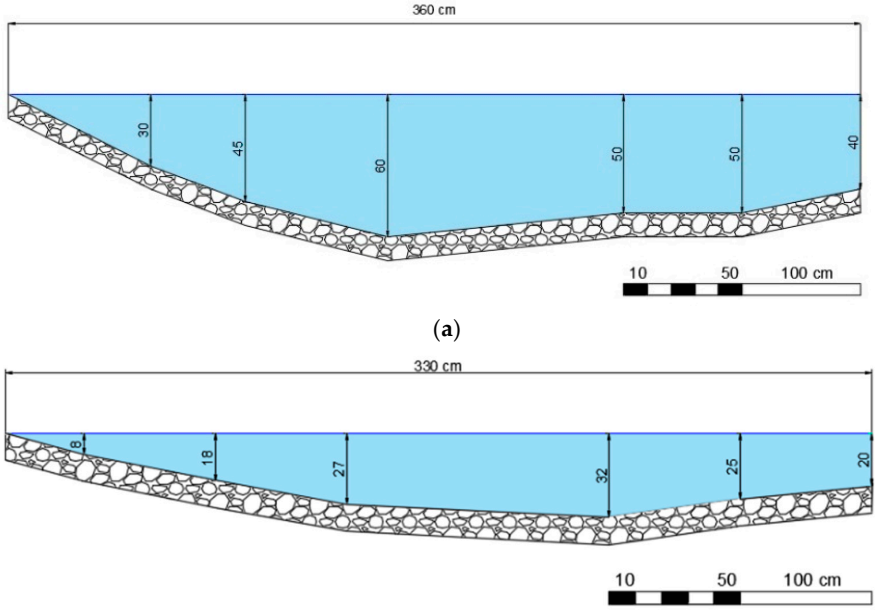

Figure 3. Section SW_01 set up at the May 2015 (**a**) and December 2015 (**b**) measurement campaigns.

According to the U.S. Geological Survey (USGS) procedure, stream discharge has been calculated as the product of the cross-section area by the average stream flow velocity in that cross-section, obtained using a current-meter [42,43]. The main equipment needed to measure the stream flow velocity is a SEBA horizontal axis current-meter F1, having a propeller diameter of 80 mm which, combined with SEBA Z6 pulse counter, allows one to measure velocity between 0.025 m/s and 10 m/s [44]. The SEBA current-meter has been used according to EN ISO 748:2007 requirements [43]. This current-meter method gives the local water velocity in each vertical following the application of a calibration equation between stream velocity, v (cm/s), and the number of spins, n (s − 1).

$$v = 0.82 + 33.32 \cdot n \quad (1)$$

The karst aquifer system has been studied in order to evaluate factors, which modify the Aniene River flow, due to groundwater–surface water interactions. This hydrochemical characterization, due to rock–water interactions, leads to a groundwater flow pattern, which allows referring groundwater flow to two different feeding parts of the basin: the first one in the Cretaceous limestone, feeding the Pertuso Spring groundwater; the second one in the Triassic dolomite, feeding the surface water upstream the spring.

In this model, a control volume around the Pertuso Spring has been considered. In this control volume, the incoming flows are the discharge Q_1, recorded upstream the spring (SW_01), and the discharge Q_P, characterized by the relative Mg^{2+} concentration values C_1 e C_P. The outgoing flow is the Aniene River discharge Q_2, characterized by the Mg^{2+} concentrations C_2, recorded at the SW_02 gauging station located downstream the Pertuso Spring.

The study area belongs to a special protected area in the Natural Park of Simbruini Mountains. As a matter of fact, the control volume can be considered free from any anthropic activities and only characterized by a surface water–groundwater interaction in the hypothesis of good mixing. Thus, the SW_02 gauging station discharge values, which come from the contribution of the Pertuso Spring discharge (Q_P) to the original SW_01 discharge value, can be represented by Equation (2):

$$Q_2 = Q_1 + Q_P \tag{2}$$

Applying the conservation of mass equation to this closed system, therefore, is Equation (3):

$$Q_1C_1 + Q_PC_P = Q_2C_2 \tag{3}$$

The parameter n is defined as the percentage of the Pertuso Spring groundwater contribution to total discharge measured.

$$n = \frac{Q_P}{Q_2} = \frac{(C_2 - C_1)}{(C_P - C_1)}, \tag{4}$$

Combining Equations (3) and (4), we have obtained the discharge of the Pertuso Spring.

$$Q_P = Q_1 \cdot \frac{n}{1-n}, \tag{5}$$

From Equation (5), it is determined that the discharge rate of the Pertuso Spring depends on the discharge values measured in the gauging station located along the river upstream the spring (Q_1) and the Mg^{2+} concentration values recorded in groundwater and surface water samples (C_1, C_2, C_P).

Thus, thanks to the proposed conceptual model, starting from the Mg^{2+} concentrations and the upstream discharge, it has been possible to evaluate the Pertuso Spring discharge.

4. Results

4.1. Hydrogeochemical Results

A statistical summary of the major physicochemical parameters is shown in Table 1.

Table 1. Summary statistics for in situ measurements of physicalochemical parameters and chemical concentrations of constituents of water samples.

Parameters	SW_01			Pertuso Spring			SW_02		
	Min	Max	Mean	Min	Max	Mean	Min	Max	Mean
Ca^{2+} (mg/L)	53.4	57.8	55.3	48.9	53.3	51.2	51.3	55.6	53.0
Mg^{2+} (mg/L)	23.6	25.2	24.6	8.3	10.4	9.5	12.0	14.7	12.9
Na^{+} (mg/L)	2.3	2.6	2.4	1.8	2.1	1.9	0.4	2.2	1.7
K^{+} (mg/L)	0.4	0.5	0.4	0.3	0.5	0.4	0.3	2.3	0.8
HCO_3^{-} (mg/L)	0.4	302.6	292.0	206.0	238.0	221.8	218.4	235.5	226.3
SO_4^{2-} (mg/L)	2.9	3.2	3.0	2.3	2.5	2.4	2.5	2.7	2.6
Cl^{-} (mg/L)	3.8	4.5	4.2	3.2	3.7	3.4	3.3	4.2	3.7
NO_3^{-} (mg/L)	0.8	5.7	1.9	0.9	1.2	1.0	0.9	1.1	1.0
T (°C)	5.8	11.3	8.6	8.0	9.5	8.5	6.7	10.7	8.3
pH	8.0	8.5	8.4	7.8	8.0	7.9	8.1	8.2	8.2
EC (µS/cm)	356.0	399.0	386.8	283.0	291.0	287.7	294.0	317.0	311.2
Hardness (°F)	23.1	24.8	23.9	16.1	17.4	16.7	17.9	19.3	18.6

A combined approach based on discharge measurements and hydrogeochemical data analysis was used to study flow paths and the groundwater–surface water interaction in the study area. Ca^{2+}, Mg^{2+}, and HCO_3^- represent more than 80% of the dissolved solids in water samples. These high concentrations are mostly due to the dissolution of carbonate minerals, forming limestone, which are the most dominant formations outcropping in the study area. The hydrochemical facies of groundwater and surface water were studied by plotting the concentrations of major cations and anions in the Piper trilinear diagram (Figure 4) [45].

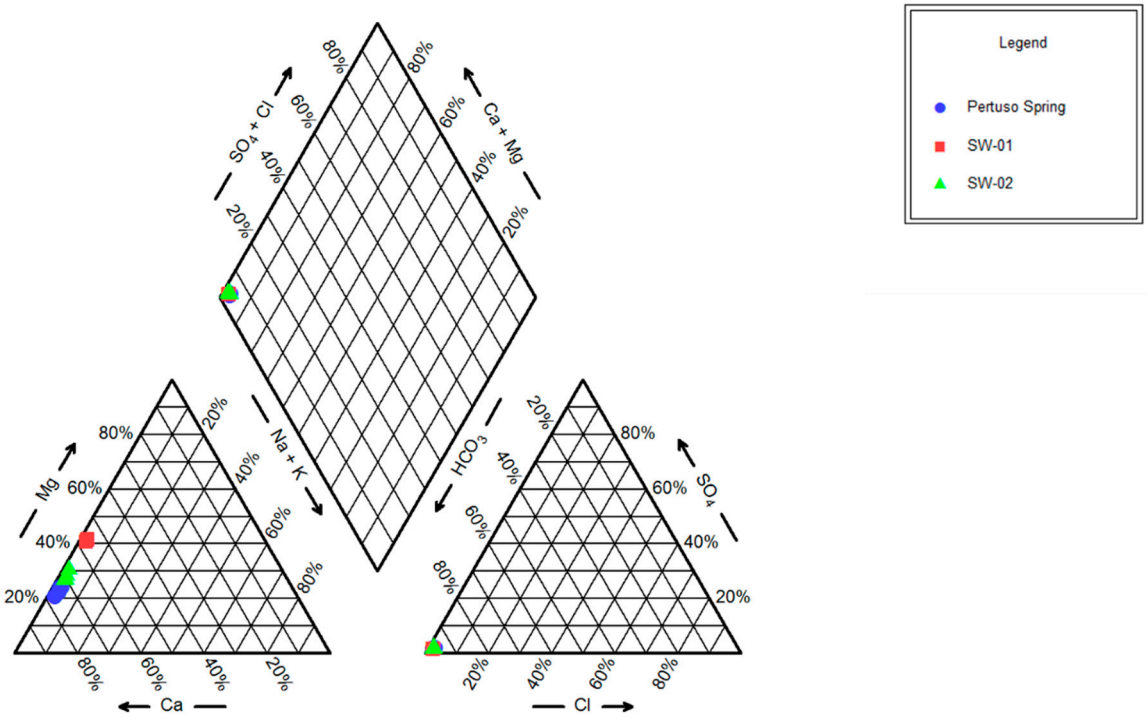

Figure 4. Piper plot for hydrochemical facies classification of groundwater and surface water.

Based on the dominance of major cationic and anionic species, two hydrochemical facies have been identified: (1) Ca-Mg-HCO_3 and (2) Ca-HCO_3. These results are due to the presence of limestone, dolomitic limestones, and dolomites outcropping in the study area. Water samples coming from SW_01 gauging station present higher values of Mg^{2+} concentration, while those coming from the Pertuso Spring are definitely poorer in it, and show a clear composition of Ca-HCO_3 water type (Figure 3). The different hydrochemical facies between groundwater and surface water reflects on the high concentration of Mg^{2+} in the Aniene River. These hydrochemical facies highlight that carbonate weathering processes (e.g., calcite and dolomite) are the most important factors of the observed water type.

To study the difference in Mg^{2+} content between groundwater and surface water, a ternary diagram of cations (Ca^{2+}, Mg^{2+}, and $Na^+ + K^+$) [46] was used to highlight how the weathering type processes influence the enrichment in magnesium (Figure 5).

As shown in Figure 5, all samples are placed along the Ca^{2+}-Mg^{2+} side of the diagram; these groundwater samples are very poor in Na^+ and K^+. The higher Mg^{2+} concentrations in SW_01 water samples suggests an increased residence time, depending on the dissolution/precipitation reactions of calcite and dolomite, which occur in the aquifer part, where groundwater crosses dolomitic sandstones.

As a matter of fact, according to previous studies of the area [41], similar results have been obtained for other springs located in the upper part of the Aniene River coming out in the Triassic dolomite outcropping close to the Pertuso Spring basin (Figures 5 and 6).

This hydrochemical characterization leads to a groundwater flow pattern in which two main feeding areas are defined: the first one in the Cretaceous limestone, feeding the Pertuso Spring groundwater; the second one in the Triassic dolomite, feeding the surface water upstream the spring.

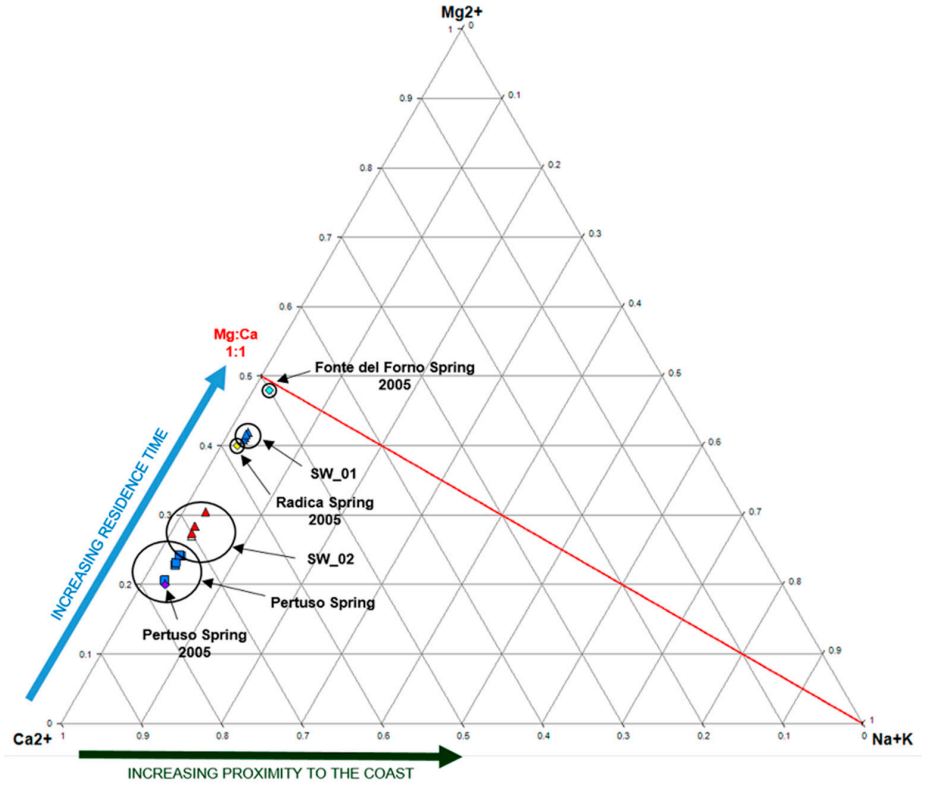

Figure 5. Ternary diagram of cations Ca^{2+}, Mg^{2+}, and Na^{+} + K^{+}. Relative concentrations of dissolved major cations compared with the composition of local groundwater [41].

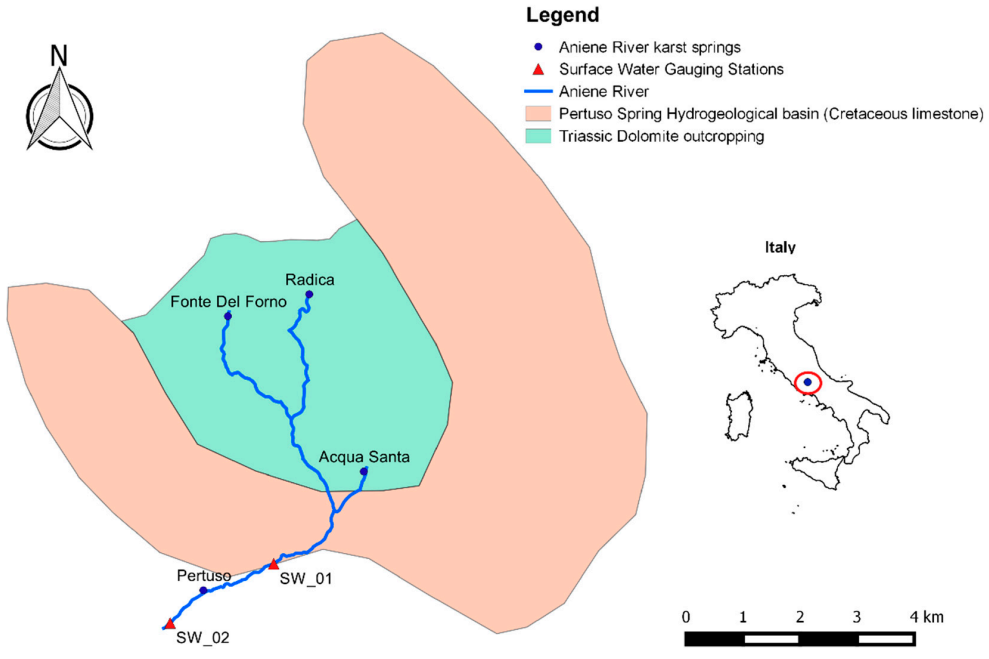

Figure 6. Feeding areas of the main karst springs in the Upper Valley of the Aniene River.

The scatterplot diagram in Figure 7 shows that the high content of Mg^{2+} in SW_01, upstream the Pertuso Spring, and consequently the high Mg^{2+}/Ca^{2+} ratio, may be due to the weathering of Mg-rich Triassic dolomites, where dolomitic limestones and dolomites are the most outcropping formations in this area.

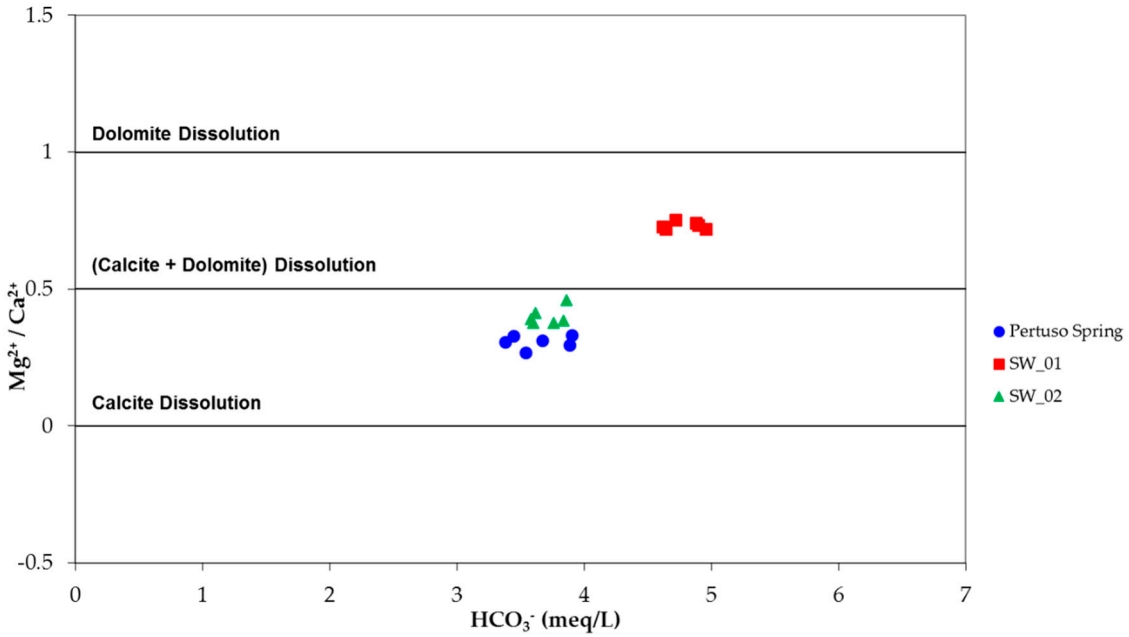

Figure 7. Mg^{2+}/Ca^{2+} ratio versus HCO_3^- in groundwater and surface water.

In regard to the Pertuso Spring groundwater, the Mg^{2+}/Ca^{2+} ratios values (~0.3) mainly depend on the residence of water in the karst system, highlighting weathering along the groundwater flow paths of low-Mg calcite. As a consequence of these properties, water samples collected downstream the Pertuso Spring (SW_02) present chemical composition typical of mixing of these two different kinds of waters (Figure 6). As a matter of fact, the highest Mg^{2+}/Ca^{2+} ratio has been recorded in water samples coming from dolomite rock masses (SW_01, ~0.7), with intermediate values at SW_02 gauging station (~0.4). On the other hand, the lowest value of this ratio in groundwater has been observed in Cretaceous limestone area (~0.3).

4.2. Discharge Experimental and Model Results

The Aniene River discharge was measured during the period July 2014–May 2016, in order to cover the range of seasonal condition characteristics of this complex hydrogeological system. Measurements by current-meter have been carried out in two gauging stations located upstream (SW_01) and downstream (SW_02) the Pertuso Spring (Table 2).

Table 2. Mean discharge values obtained by current-meter method, upstream (SW_01) and downstream (SW_02) the Pertuso Spring.

Q (m^3/s)	SW_01	SW_02
July 2014	0.540	2.450
November 2014	0.350	1.480
January 2015	0.410	1.920
May 2015	0.501	2.747
December 2015	0.278	0.931
May 2016	0.430	2.305

Table 2 shows discharge values recorded in SW_01 and SW_02 gauging stations all over the hydrological year. The source of Mg^{2+} concentration values in the Aniene River upstream the Pertuso Spring (SW_01) is the dissolution of magnesium-rich minerals in Triassic dolomites, sited in the northeast part of the Pertuso Spring basin. Along the Aniene River, this decrease in Mg^{2+} concentration values is related to an increase in stream flow discharge. SW_02 surface water is the product of the confluence of groundwater coming from the Pertuso Spring into the Aniene River (SW_01). As a matter of fact, the Aniene River, which is characterized by water with higher magnesium concentration values, is affected in its chemical composition by the Pertuso Spring groundwater inflowing, and this influence can be measured by variability in Mg^{2+} concentration values along the river downstream. The karst aquifer system has been studied in order to evaluate factors which modify the Aniene River flow due to groundwater–surface water interactions.

The *n* parameter (i.e., the percentage of the Pertuso Spring groundwater contribution to total discharge measured at the SW_02) has been calculated according to Equation (4) and reported in Table 3.

Table 3. Values of *n* as percentage contribution of the Pertuso Spring groundwater to total discharge measured at the SW_02 gauging station.

Date	*n*	*n* (%)
July 2014	0.780	78.0
November 2014	0.752	75.2
January 2015	0.794	79.4
May 2015	0.812	81.2
December 2015	0.709	70.9
May 2016	0.810	81.0

Table 4 summarizes the values of discharges evaluated. In particular, this table presents values of the Pertuso Spring discharge obtained by the difference between the values measured with the current-meter in SW_01 and SW_02 and the Pertuso Spring discharge obtained by magnesium tracer method. It is easy to see how discharge values obtained with both methods are very similar.

Table 4. Magnesium content and discharge values obtained by current-meter and magnesium tracer method (Q *: discharge values obtained by current-meter method; Q **: discharge values obtained by the difference between the values measured with the current-meter in SW_01 and SW_02).

Date	SW_01		Pertuso Spring			SW_02		
	Q *	Mg^{2+}	Q **	Q_{Mg}	Mg^{2+}	Q *	Q_{Mg}	Mg^{2+}
	(m^3/s)	(meq/L)	(m^3/s)	(m^3/s)	(meq/L)	(m^3/s)	(m^3/s)	(meq/L)
July 2014	0.54	1.94	1.91	1.92	0.80	2.45	2.46	1.05
November 2014	0.35	1.93	1.13	1.06	0.68	1.48	1.41	0.99
January 2015	0.41	2.07	1.51	1.58	0.81	1.92	1.99	1.07
May 2015	0.50	2.02	2.23	2.16	0.77	2.75	2.66	1.00
December 2015	0.28	2.07	0.67	0.68	0.86	0.93	0.96	1.21
May 2016	0.43	2.07	1.87	1.84	0.78	2.30	2.29	1.03

5. Discussion

The results of hydrogeochemical analysis and current discharge measurements confirm the groundwater–surface water mixing due to the presence of the Pertuso Spring, highlighting the key role of Mg^{2+} content to identify different feeding areas, depending on different water–rock interaction processes, and water flow paths within this karst setting.

Several previous studies used different conservative solute tracers to evaluate quantification of discharge in stream confluences starting from chemical mass balance techniques [15–17].

In this work, assessing the conservative behavior of Mg^{2+} for this specific system, it was possible to propose an inverse model for the Pertuso Spring discharge evaluation based only on Mg^{2+} concentration data.

The dilution mechanism, due to the groundwater and surface water interaction at the Pertuso confluence point, is the only mechanism responsible of the Mg^{2+} concentration change along the Aniene River (Figure 8).

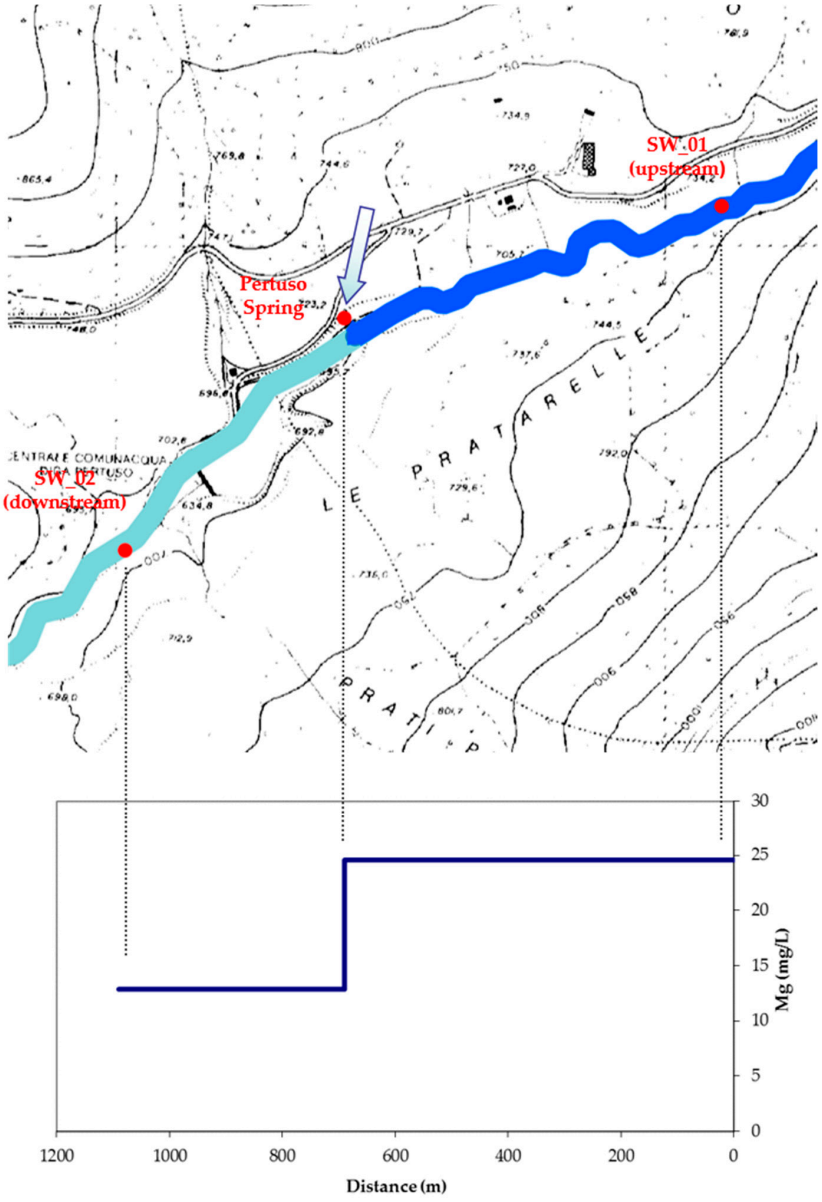

Figure 8. Schematic dilution mechanism in Mg^{2+} concentration along Aniene River.

The box plot graphically highlights the main characteristics of Mg^{2+} content (Figure 9) for the utilization in the chemical mass balance technique, whereas Ca^{2+} does not show the same adaptability (Figure 10). The two main characteristics are:

- the concentration difference between the two inflows must be significant;
- the concentration difference between the two inflows also must be greater than the uncertainty in the concentration data.

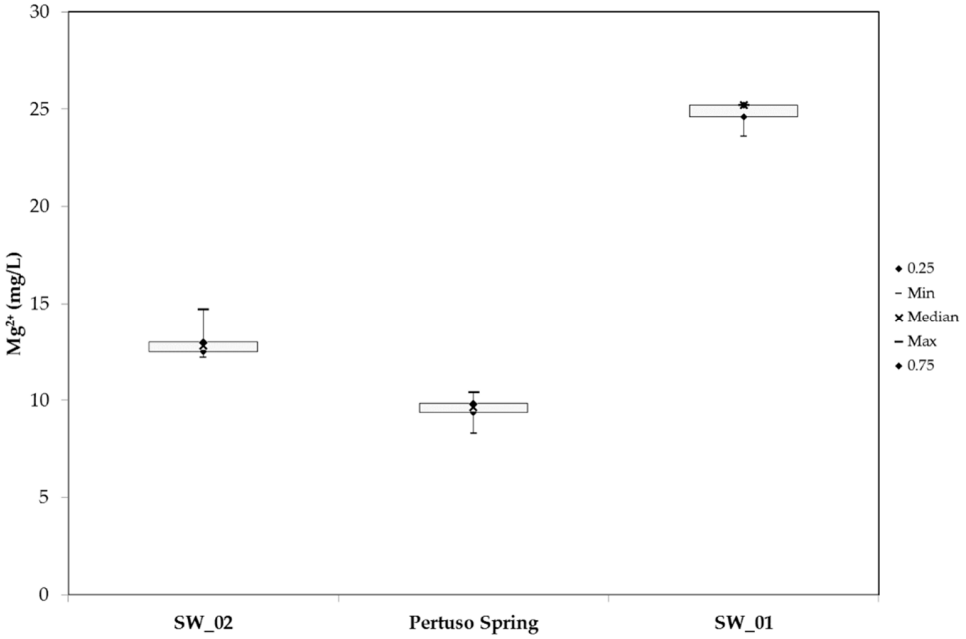

Figure 9. Box plot of mean, median, maximum, and minimum values of magnesium distribution.

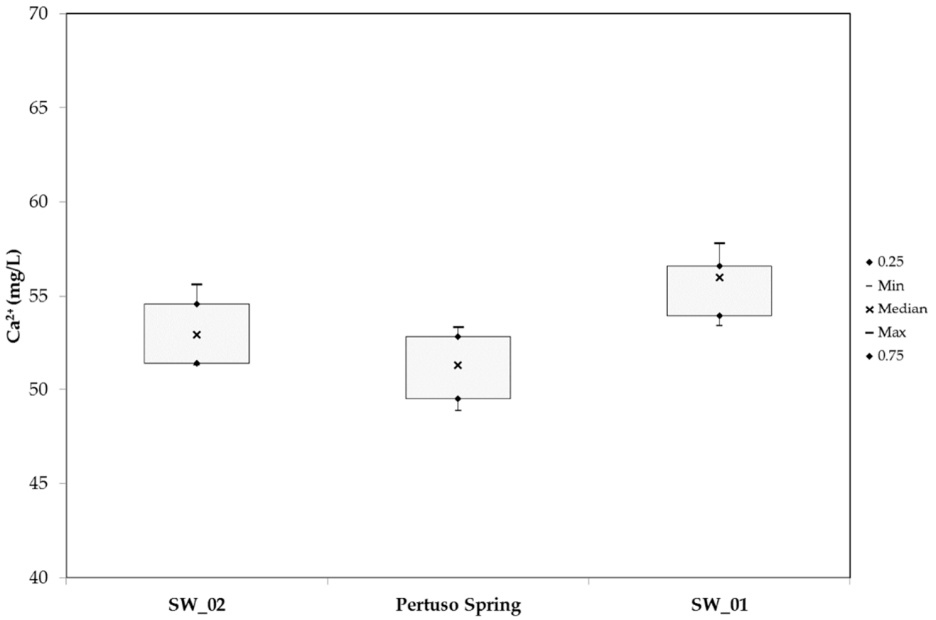

Figure 10. Box plot of mean, median, maximum, and minimum values of calcium distribution.

As a matter of fact, different from Ca^{2+}, Mg^{2+} concentration data shows a very low variability in each sampling point and a high difference between the Pertuso Spring and SW_01, due to the water transit in different geological formations (calcareous and dolomitic rocks).

These properties lead to the correct evaluation of the "*n*" parameter in the mass balance and, consequently, to valid discharge results for the Pertuso Spring, confirmed by the comparison with conventional current-meter discharge values (Table 4).

The low variability of Mg^{2+} concentration in water samples is due to the slower process of dissolution for dolomitic rocks within the karst aquifer, resulting in a best discharge evaluation factor in base-flow conditions. On the contrary, during a storm, rainwater inflow and transit in karst conduits is too much rapid and does not allow the same dissolution process.

Hence, in this karst setting, Mg^{2+} emerges as a suitable conservative tracer only for main storage groundwater—which, however, is the most important for catchment works—involving springs. As a matter of fact, this is the part of the annual spring volume discharge, which is actually reliable for exploitation. This is especially so in karst aquifers, where there is a meaningful part of this volume, though it is discharged too quickly to be caught with effectiveness.

As a consequence, the Mg^{2+} vs Q scatterplot diagram (Figure 11) shows that all plotted points, except for November 2014 data, follow a linear trend, highlighting that the increasing base-flow contribution of the Pertuso Spring discharge rate is responsible of the decrease in Mg^{2+} concentration values. This is possible because data referred to the November 2014 monitoring campaign have to be considered as an outlier (Figure 11). In fact, the lower Mg^{2+} concentration measured in November 2014 can be related to a high precipitation rate, recorded at Trevi nel Lazio meteorological station, during five days before the sampling date. As previously said, the consequent aquifer rapid response probably influenced, by dilution, the Mg^{2+} concentration in groundwater that was no more significant for the conceptual model.

Futures discharge and Mg^{2+} concentration data will be helpful for the model validation, confirming the linear trend obtained for previous data.

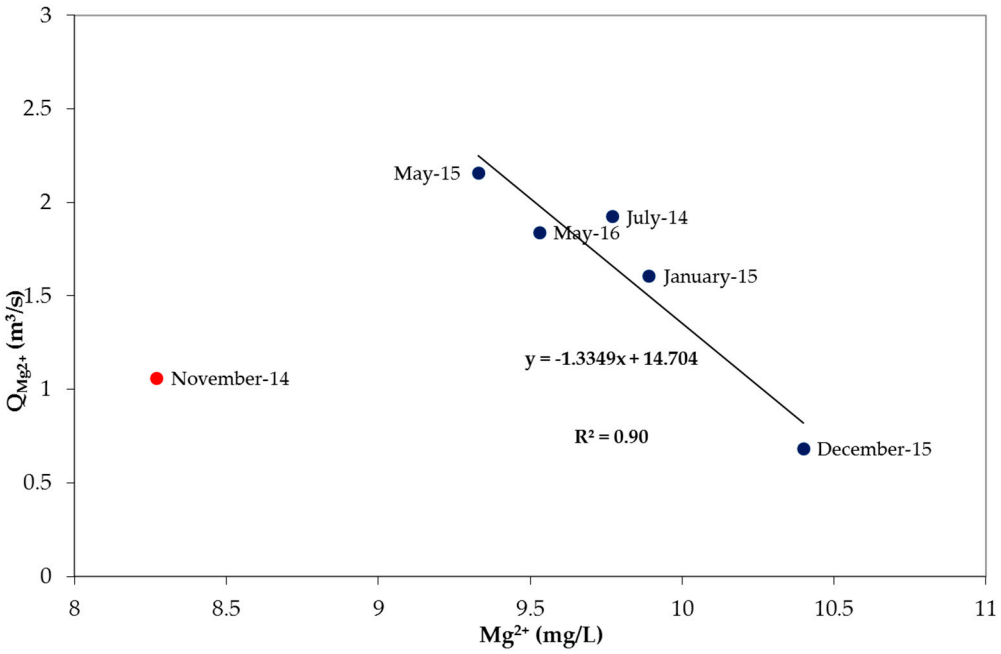

Figure 11. Relationship between the Mg^{2+} concentration and the Pertuso Spring discharge values obtained with the combined magnesium-discharge tracer approach.

6. Conclusions

This paper dealt with the assessment of the interactions between a karst aquifer feeding the Pertuso Spring and the Aniene River surface waters on the basis of stream discharge measurements and water geochemical tracers data with the aim to set up an inverse model, which allows estimation of groundwater flow coming out from the Pertuso Spring, starting from surface water discharge measurements and geochemical water characterization. These results, obtained in the area under study (sited in the karst aquifer outcropping in the Upper Valley of the Aniene River) show that it is possible to have a reliable evaluation of the Pertuso Spring discharge through the elaboration of surface water discharge measurements and Mg^{2+} concentration values, determined for groundwater, coming from the Pertuso Spring, and for both surface water samples: those collected upstream and downstream the Pertuso Spring, along the Aniene River. Although it is subject to some uncertainties, the Mg^{2+}

concentration, as an environmental tracer, provides an indirect method for discharge evaluation of the Pertuso Spring, due to the mixing of surface water and groundwater, and provides information on changes in water quantity and quality.

Acknowledgments: The research reported in this paper was supported by the Department of Civil, Building and Environmental Engineering (DICEA) of Sapienza University of Rome. The authors gratefully acknowledge the technical support of ACEA ATO2.

Author Contributions: For this research article all of the authors contributed extensively to the work. Giuseppe Sappa led this research, Francesco Maria De Filippi performed the field work, Flavia Ferranti developed the GIS analysis and compiled the figures, Giulia Cardillo participated in drafting the article and helped in manuscript correction. All the authors contributed to data analysis and to the manuscript writing.

Conflicts of Interest: The authors declare no conflict of interest.

References

1. Cozma, A.I.; Baciu, C.; Moldovan, M.; Pop, I.C. Using natural tracers to track the groundwater flow in a mining area. *Procedia Environ. Sci.* **2016**, *32*, 211–220. [CrossRef]
2. Guo, Q.; Wang, Y.; Ma, T.; Li, L. Variation of karst springs discharge in recent five decades as an indicator of global climate change: A case study at Shanxi, northern China. *Sci. China Ser. D Earth Sci.* **2005**, *48*, 2001–2010. [CrossRef]
3. Sappa, G.; Luciani, G. Groundwater management in Dar Es Salam Coastal Aquifer (Tanzania) under a difficult sustainable development. *WSEAS Trans. Environ. Dev.* **2014**, *10*, 465–477.
4. Sappa, G.; Ferranti, F.; Ergul, S.; Ioanni, G. Evaluation of the groundwater active recharge trend in the coastal plain of Dar Es Salaam (Tanzania). *J. Chem. Pharm. Res.* **2013**, *5*, 548–552.
5. Foster, S.; Hirata, R.; Andreo, B. The aquifer pollution vulnerability concept: Aid or impediment in promoting groundwater protection? *Hydrogeol. J.* **2013**, *21*, 1389–1392. [CrossRef]
6. Bakalowicz, M. Karst groundwater: A challenge for new resources. *Hydrogeol. J.* **2005**, *13*, 148–160. [CrossRef]
7. Cowie, R.; Williams, M.W.; Wireman, M.; Runkel, R.L. Use of natural and applied tracers to guide targeted remediation efforts in an acid mine drainage system, Colorado Rockies, USA. *Water* **2014**, *6*, 745–777. [CrossRef]
8. Pitty, A.F. The estimation of discharge from a karst rising by natural salt dilution. *J. Hydrol.* **1966**, *4*, 63–69. [CrossRef]
9. White, W.B. Conceptual models for carbonate aquifers. *Ground Water* **1969**, *7*, 15–22. [CrossRef]
10. Quinlan, J.F.; Ewers, R.O. Subsurface drainage in the Mammoth Cave area. In *Karst Hydrology Concepts from the Mammoth Cave Area: New York, Van Nostrand Reinhold*; White, W.B., White, E.L., Eds.; Springer: New York, NY, USA, 1989; pp. 65–104.
11. White, W.B. Karst hydrology: Recent developments and open questions. *Eng. Geol.* **2002**, *65*, 85–105. [CrossRef]
12. Sappa, G.; Ferranti, F.; de Filippi, F.M. Preliminary validation of an indirect method for discharge evaluation of Pertuso Spring (Central Italy). *WSEAS Trans. Environ. Dev.* **2016**, *12*, 214–225.
13. Lauber, U.; Goldscheider, N. Use of artificial and natural tracers to assess groundwater transit-time distribution and flow systems in a high-alpine karst system (Wetterstein Mountains, Germany). *Hydrogeol. J.* **2014**, *22*, 1807–1824. [CrossRef]
14. Ergul, S.; Ferranti, F.; Sappa, G. Arsenic in the aquifer systems of Viterbo Region, Central Italy: Distribution and Geochemistry. *Rend. Online Soc. Geol. Ital. Soc. Geol. Ital. Roma* **2013**, *24*, 116–118.
15. Alvarado, J.A.C.; Purtschert, R.; Barbecot, F.; Chabault, C.; Ruedi, J.; Schneider, V.; Aeschbach-Hertig, W.; Kipfer, R.; Loosli, H.H. Constraining the age distribution of highly mixed groundwater using ^{39}Ar: A multiple environmental tracer (^{3}H/^{3}He, ^{85}Kr, ^{39}Ar and ^{14}C) study in the semiconfined Fontainebleau Sands Aquifer (France). *Water Resour. Res.* **2007**, *43*, 1–16.
16. Troldborg, L.; Jensen, K.H.; Engesgaard, P.; Refsgaard, J.C.; Hinsby, K. Using environmental tracers in modeling flow in a complex shallow aquifer system. *J. Hydrol. Eng.* **2008**, *13*, 1037–1084. [CrossRef]
17. Lavastre, V.; La Salle, C.; Michelot, J.; Giannesini, S.; Benedetti, L.; Lancelot, J.; Lavielle, B.; Massault, M.; Thomas, B.; Gilabert, E.; et al. Establishing constraints on groundwater ages with ^{36}Cl, ^{14}C, ^{3}H, and noble gases: A case study in the eastern Paris Basin, France. *Appl. Geochem.* **2010**, *25*, 123–142. [CrossRef]

18. Caschetto, M.; Barbieri, M.; Galassi, D.M.P.; Mastrorillo, L.; Rusi, S.; Stoch, F.; Di Cioccio, A.; Petitta, M. Human alteration of groundwater-surface water interactions (Sagittario River, Central Italy): Implication for flow regime, contaminant fate and invertebrate response. *Environ. Earth Sci.* **2014**, *71*, 1791–1807. [CrossRef]
19. Kincaid-Vice, T.R. Groundwater tracing in the Woodville karst plain—Part I: An overview of groundwater tracing. *DIR Quest J. Glob. Underw. Explor.* **2003**, *4*, 31–37.
20. Aquilanti, L.; Clementi, F.; Nanni, T.; Palpacelli, S.; Tazioli, A.; Vivalda, P. DNA and fluorescein tracer tests to study the recharge, groundwater flowpath and hydraulic contact of aquifers in the Umbria-Marche limestone ridge (Central Apennines, Italy). *Environ. Earth Sci.* **2016**, *75*, 626. [CrossRef]
21. Cervi, F.; Corsini, A.; Doveri, M.; Mussi, M.; Ronchetti, F.; Tazioli, A. Characterizing the recharge of fractured aquifers: A case study in a flysch rock mass of the northern Apennines (Italy). In *Engineering Geology for Society and Territory*; Lollino, G., Arattano, M., Rinaldi, M., Giustolisi, O., Marechal, J.C., Grant, G.E., Eds.; Springer: Cham, Switzerland, 2014; Volume 3, pp. 563–567.
22. Sappa, G.; Ergul, S.; Ferranti, F. Geochemical modeling and multivariate statistical evaluation of trace elements in arsenic contaminated groundwater systems of Viterbo Area, (Central Italy). *Springerplus* **2014**, *3*, 1–19. [CrossRef] [PubMed]
23. Cook, P.G.; Favreau, G.; Dighton, J.C.; Tickell, S. Determining natural groundwater influx to a tropical river using radon, chlorofluorocarbons and ionic environmental tracers. *J. Hydrol.* **2003**, *277*, 74–88. [CrossRef]
24. Davis, S.D.; Thompson, G.M.; Bentley, H.W.; Stiles, G. Ground-water tracers—A short review. *Groundwater* **1980**, *18*, 14–23. [CrossRef]
25. Sappa, G.; Ferranti, F.; de Filippi, F.M. A proposal of conceptual model for the Pertuso Spring discharge evaluation in the Upper Valley of Aniene River. *Acque Sotter.* **2016**, *5*, 3. [CrossRef]
26. Stauffer, R.E. Use of solute tracers released by weathering to estimate groundwater inflow to Seepage Lakes. *Environ. Sci. Technol.* **1985**, *19*, 405–411. [CrossRef] [PubMed]
27. Herman, J.S.; White, W.B. Dissolution kinetics of dolomite: Effects of lithology and fluid flow velocity. *Geochim. Cosmochim. Acta* **1985**, *49*, 2017–2026. [CrossRef]
28. Bencala, K.E.; McKnight, D.M.; Zellweger, G.W. Evaluation of natural tracers in an acidic and metal-rich stream. *Water Resour. Res.* **1987**, *23*, 827–836. [CrossRef]
29. Schemel, L.E.; Cox, M.H.; Runkel, R.L.; Kimball, B.A. Multiple injected and natural conservative tracers quantify mixing in a stream confluence affected by acid mine drainage near Silverton, Colorado. *Hydrol. Process.* **2006**, *20*, 2727–2743. [CrossRef]
30. Montanari, A.; Staniscia, B. An overview of territorial resources and their users in the Rome and Chieti-Pescara Areas. In *Sustainability in the Coastal Urban Environment: Thematic Profiles of Resources and Their Users*; Khan, A.Z., Quynh, L.X., Corijn, E., Canters, F., Eds.; Sapienza Università Editrice: Rome, Italy, 2012; Volume 3, pp. 61–109.
31. Sappa, G.; Ferranti, F.; de Filippi, F.M. Environmental tracer approach to discharge evaluation of Pertuso Spring (Italy). In *Recent Advances on Energy and Environment*, Proceedings of the 10th International Conference on Energy & Environment, Budapest, Hungary, 12–14 December 2015; Bulucea, A., Ed.; World Scientific and Engineering Academy and Society (WSEAS): Budapest, Hungary, 2015; pp. 54–62.
32. Ventriglia, U. Idrogeologia II parte. In *Idrogeologia Della Provincia di Roma, IV, Regione Orientale*; Amministrazione Provinciale di Roma, Assessorato LL.PP, Viabilità e Trasporti: Roma, Italy, 1990.
33. Bono, P.; Percopo, C. Flow dynamics and erosion rate of a representative Karst Basin (Upper Aniene River, Central Italy). *Environ. Geol.* **1996**, *27*, 210–218. [CrossRef]
34. De Felice, A.M.; Dragoni, W.; Giglio, G. *Methods of Hydrological Basin Comparison*; Report No. 120; Institute of Hydrology: Roorkee, India, 1992.
35. Accordi, G.; Carbone, F. *Carta Delle Litofacies del Lazio-Abruzzo ed Aree Limitrofe*; Consiglio Nazionale Delle Ricerche: Roma, Italy, 1988.
36. Bosellini, A. *La Storia Geologica Delle Dolomiti*; Dolomiti: Trento, Italy, 1989.
37. Damiani, A.V. Studi sulla piattaforma carbonatica laziale-abruzzese. Nota I. Considerazioni e problematiche sull'assetto tettonico e sulla paleogeologia dei Monti Simbruini. Studies on the Lazio-Abruzzi carbonate platform. Note XI. Considerations and problems on tectonic and paleogeologic Simbruini Mts. In *Memorie Descrittive Carta Geologica d'Italia*; Istituto Superiore per la Protezione e la Ricerca Ambientale: Rome, Italy, 1990; Volume 38, pp. 177–206.

38. Sappa, G.; Ferranti, F. An integrated approach to the Environmental Monitoring Plan of the Pertuso Spring (Upper Valley of Aniene River). *Ital. J. Groundw.* **2014**, *3*, 47–55.
39. Sappa, G.; Ergul, S.; Ferranti, F. Vulnerability assessment of Mazzoccolo Spring Aquifer (Central Italy), combined with geo-chemical and isotope modeling. *Eng. Geol. Soc. Territ.* **2015**, *5*, 1387–1392.
40. Sappa, G.; Ergul, S.; Ferranti, F.; Sweya, L.N.; Luciani, G. Effects of seasonal change and seawater intrusion on water quality for drinking and irrigation purposes, in coastal aquifers of Dar es Salaam, Tanzania. *J. Afr. Earth Sci.* **2015**, *105*, 64–84. [CrossRef]
41. Acea Ato 2 S.p.A. Studio Idrogeologico—Proposta di Aree di Salvaguardia Della Sorgente del Pertuso "Hydrogeological Study—Proposal for Protected Areas of Pertuso Spring". Unpublished work, 2005.
42. United States Environmental Protection Agency (US EPA) Region 6. *Standard Operating Procedure for Stream Flow Measurement*; US EPA: Washington, DC, USA, 2003.
43. British, European and International Standards. *BS EN ISO 748:2007 Hydrometry—Measurement of Liquid Flow in Open Channels Using Current-Meters or Floats*; International Organization for Standardization (ISO): Geneva, Switzerland, 2007.
44. Tazioli, A. Experimental methods for river discharge measurements: Comparison among tracers and current meter. *Hydrol. Sci. J.* **2011**, *56*, 1314–1324. [CrossRef]
45. Piper, M. A graphic procedure in the geochemical interpretation of water-analyses. *Trans. Am. Geophys. Union* **1944**, *25*, 914–923. [CrossRef]
46. Edmunds, W.M.; Cook, J.M.; Darling, W.G.; Kinniburgh, D.G.; Miles, D.L.; Bath, A.H.; Morgan-Jones, M.; Andrews, J.N. Baseline geochemical conditions in the Chalk aquifer, Berkshire, UK: A basis for groundwater quality management. *Appl. Geochem.* **1987**, *2*, 251–274. [CrossRef]